ENVIRONMENTAL BACTERIOPHAGES: FROM BIOLOGICAL CONTROL APPLICATIONS TO DIRECTED BACTERIAL EVOLUTION

EDITED BY: Robert Czajkowski, Steven Earl Lindow and Robert Wilson Jackson
PUBLISHED IN: Frontiers in Microbiology

frontiers Research Topics

ISSN 1664-8714
ISBN 978-2-88963-181-0
DOI 10.3389/978-2-88963-181-0

About Frontiers

Frontiers is more than just an open-access publisher of scholarly articles: it is a pioneering approach to the world of academia, radically improving the way scholarly research is managed. The grand vision of Frontiers is a world where all people have an equal opportunity to seek, share and generate knowledge. Frontiers provides immediate and permanent online open access to all its publications, but this alone is not enough to realize our grand goals.

Frontiers Journal Series

The Frontiers Journal Series is a multi-tier and interdisciplinary set of open-access, online journals, promising a paradigm shift from the current review, selection and dissemination processes in academic publishing. All Frontiers journals are driven by researchers for researchers; therefore, they constitute a service to the scholarly community. At the same time, the Frontiers Journal Series operates on a revolutionary invention, the tiered publishing system, initially addressing specific communities of scholars, and gradually climbing up to broader public understanding, thus serving the interests of the lay society, too.

Dedication to Quality

Each Frontiers article is a landmark of the highest quality, thanks to genuinely collaborative interactions between authors and review editors, who include some of the world's best academicians. Research must be certified by peers before entering a stream of knowledge that may eventually reach the public - and shape society; therefore, Frontiers only applies the most rigorous and unbiased reviews.
Frontiers revolutionizes research publishing by freely delivering the most outstanding research, evaluated with no bias from both the academic and social point of view. By applying the most advanced information technologies, Frontiers is catapulting scholarly publishing into a new generation.

What are Frontiers Research Topics?

Frontiers Research Topics are very popular trademarks of the Frontiers Journals Series: they are collections of at least ten articles, all centered on a particular subject. With their unique mix of varied contributions from Original Research to Review Articles, Frontiers Research Topics unify the most influential researchers, the latest key findings and historical advances in a hot research area! Find out more on how to host your own Frontiers Research Topic or contribute to one as an author by contacting the Frontiers Editorial Office: researchtopics@frontiersin.org

ENVIRONMENTAL BACTERIOPHAGES: FROM BIOLOGICAL CONTROL APPLICATIONS TO DIRECTED BACTERIAL EVOLUTION

Topic Editors:
Robert Czajkowski, University of Gdansk, Poland
Steven Earl Lindow, University of California, Berkeley, United States
Robert Wilson Jackson, University of Reading, United Kingdom

Citation: Czajkowski, R., Lindow, S. E., Jackson, R. W., eds. (2019). Environmental Bacteriophages: From Biological Control Applications to Directed Bacterial Evolution. Lausanne: Frontiers Media. doi: 10.3389/978-2-88963-181-0

Table of Contents

frontiers in Microbiology

EDITORIAL
published: 07 August 2019
doi: 10.3389/fmicb.2019.01830

Editorial: Environmental Bacteriophages: From Biological Control Applications to Directed Bacterial Evolution

Robert Czajkowski[1]*, *Robert W. Jackson*[2] and *Steven E. Lindow*[3]

[1] Laboratory of Biologically Active Compounds, Intercollegiate Faculty of Biotechnology of University of Gdansk and Medical University of Gdansk, University of Gdansk, Gdansk, Poland, [2] School of Biological Sciences, University of Reading, Reading, United Kingdom, [3] Department of Plant and Microbial Biology, University of California, Berkeley, Berkeley, CA, United States

Keywords: bacterial viruses, phage cocktails, adaptation, environmental fitness, biological control, interaction, genome

OPEN ACCESS

Edited by:
Andrew S. Lang, Memorial University of Newfoundland, Canada

Reviewed by:
Ananda Shankar Bhattacharjee, Carl R. Woese Institute for Genomic Biology, University of Illinois at Urbana–Champaign, United States
Martha Josefina Vives, University of Los Andes, Colombia, Colombia

***Correspondence:**
Robert Czajkowski
robert.czajkowski@biotech.ug.edu.pl

Specialty section:
This article was submitted to Virology, a section of the journal Frontiers in Microbiology

Received: *11 June 2019*
Accepted: *25 July 2019*
Published: *07 August 2019*

Citation:
Czajkowski R, Jackson RW and Lindow SE (2019) Editorial: Environmental Bacteriophages: From Biological Control Applications to Directed Bacterial Evolution. Front. Microbiol. 10:1830. doi: 10.3389/fmicb.2019.01830

Editorial on the Research Topic

Environmental Bacteriophages: From Biological Control Applications to Directed Bacterial Evolution

The first bacterial viruses (termed bacteriophages, or phages, "*eaters of bacteria*") were discovered only at the beginning of the twentieth century, independently in England by Twort in 1915 and in France by d'Herelle in 1917 (Hadley, 1928; Abedon, 2008). Soon after their initial discovery, they have been investigated for the cure or prevention of dozens of bacterial diseases in humans and animals (Duckworth and Gulig, 2002; Buttimer et al., 2017). This therapeutic focus has however declined in the next 30 years due to the discovery of the first antibiotics and rapid development of antibiotic-based therapies in 1950s and 1960s (Sulakvelidze and Morris, 2001).

Despite the fact that phages were recognized early to be extremely abundant in the biosphere, existing in all environments where bacteria occur, only very little research was targeted to understand their ecological roles (Summers, 2012). Even today, studies about the role of bacterial viruses in most complex ecosystems are uncommon and the impact of bacterial viruses on cohabitating microorganisms is little appreciated (Rohwer et al., 2009). While knowledge of environmental bacteriophages has increased in the last 10 years (Miller, 2001; Muniesa et al., 2013), there is still much to learn about their roles in even about the most widely-studied environments such as the rhizosphere, phyllosphere, and human gut. It will be through such work that we might more wisely use phages in medical and biotechnological applications. To bolster the field, the Research Topic "Environmental Bacteriophages: from Biological Control Applications to Directed Bacterial Evolution" was developed with the aim of emphasizing the role of bacterial viruses in the spread, adaptation, evolution, and control of their bacterial hosts with an environmental perspective.

Many of the known roles of bacteriophages in natural ecosystems have been developed from studies of phage-microbial communities in both freshwater and seawater habitats (Middelboe and Brussaard, 2017). In the global ocean, lytic bacteriophages are known to be the key regulators of nutrient cycles as organic matter derived from lysed host cells are immediately consumed by heterotrophic bacteria (Fuhrman, 1999). As natural inhabitants of aquatic environments, bacteriophages have also been investigated as biological control agents of marine pathogenic bacteria (Sandaa et al., 2009). Two studies in this Research Topic targeted the use of bacterial viruses to control pathogens in aqueous systems. The paper of Jacquemot et al. describes the isolation and

characterization of the lytic bacteriophage BONAISHI. This phage was able to effectively reduce populations of *Vibrio coralliilyticus* causing bleaching of coral reefs. The results suggest that the virus can be utilized as a biological control agent to protect coral reefs against *V. coralliilyticus* pathogens. In the second study, Scarascia et al. used lytic bacteriophages isolated from a wastewater treatment plant to control *Pseudomonas aeruginosa* under saline conditions. In addition to being human pathogens, these biofilm-developing bacteria are a major problem in water-desalination systems in which they cause clogging of the membranes used in this process and consequently cause malfunctions of desalination plants. The work of Scarascia et al. provides proof-of-concept of the use of bacteriophages to decrease the size of biofilms—a process that may prove to be an environmental friendly alternative to the use of chemical and physical treatments to reduce biofilm formation in seawater systems.

Three additional papers describe the interaction of phage particles with their bacterial hosts in more complex environments. Balogh et al. and Balogh et al. assessed the potential of eight lytic bacteriophages infecting the plant pathogen *Xanthomonas perforans* to reduce population sizes of the pathogen in the phyllosphere of grapefruit and tomato plants. In these two ecosystems the effectiveness of bacteriophages in killing the pathogen was variable. A strong, positive association was only found, surprisingly, between features of the leaf surface and bacteriophage survival on the leaf. This indicates that spatial and temporally variable features of the leaf surface may have a significant impact on bacteriophage multiplication and viability, and therefore the efficacy of biological control of plant disease *in vivo*. Furthermore, these results suggest that the plant species on which the phages will be applied is an important component to be recognized in successful biological control of plant pathogens with lytic bacteriophages. The authors postulate that due to the different viral survival on different plant species, phage therapy may be more effective on some crops than on others—a concept that may revolutionize our understanding of biological control with the use of bacterial viruses in agriculture. In another report, Kabanova et al. studied the interaction of lytic bacteriophage PP35 with its host *Dickeya solani*—a necrotrophic plant pathogen causing severe damage to agricultural crops worldwide (Charkowski, 2007; Van Der Wolf et al., 2014). While assessing the host range of the virus, the authors found the saprophytic bacterium *Lelliottia* sp. strain F154, a member of the *Enterobacteriaceae* family but not closely-related to *Dickeya* spp., can serve as an alternative host for PP35. In contrast to *D. solani*, *Lelliottia* spp. is an inhabitant of surface waters, and in the experiments performed by the authors, was found not to cause disease symptoms in plants. Until this report, no alternative hosts for lytic phages capable of infecting plant pathogenic *Dickeya* spp. had been found (Czajkowski, 2016). This study, importantly, shows that such an alternative host may play a pivotal role in facilitating the dissemination of the bacteriophages in various environments (Koskella and Meaden, 2013). Furthermore, it also shows that lytic phages infecting plant pathogens may have a broader host range than initially assumed, and may commonly also be able to infect other saprophytic, non-pathogenic bacteria, suggesting that their ecological role may be larger, and potentially more elusive, than previously supposed (Hyman et al., 2010). A third report by Wandro et al. addressed the co-evolution of phage EfV12-phi1 and its host *Enterococcus faecium*. In this study the authors identified specific phage and host genes that are undergoing strong selection pressure during co-evolution in this interaction. Such experiments may help to both better understand the process of co-adaptation of viruses and their hosts (Dennehy, 2012), and also to develop engineered bacteriophages against which the host cannot easily become resistant (Pires et al., 2016).

By far, the biggest driver in interest of bacterial viruses remains that of their isolation and use for the control of diseases in humans, animals and plants (Wagner and Waldor, 2002; Karthik et al., 2014). The spread of multidrug-resistant human pathogens as well as the inability to use antibiotics in agriculture to control pathogens of important crops have led to a resurgence in interest in environmentally-sound phage therapy to replace the highly problematic antibiotic therapies. This concept is addressed by six studies in this Research Topic. Gašić et al. and Attai et al. isolated and characterized bacteriophages able to control the plant pathogenic bacterium *Xanthomonas euvesicatoria* with phage Kφ1 and *Agrobacterium tumefaciens* with phage Atu-ph07. In these two papers the authors detail the characterization of the viruses and evaluated them in proof-of-concept experiments with the pathogens. Both studies postulated that the viruses could be used to control plant pathogens *in situ* either alone or as a part of a cocktail containing several such viruses. The control of human pathogenic bacteria with the use of lytic phages is addressed in three reports. The studies of both Topka et al. and Manohar et al. targeted development of antibacterial therapies against pathogenic *Escherichia coli*, *Klebsiella pneumonia,* and *Enterobacter* spp. It is noteworthy that both studies were done using clinical isolates with confirmed virulence, and that the phages were tested under conditions resembling natural settings. Another report by Ahmadi et al. analyses the stability of two *Listeria monocytogenes* lytic bacteriophages P100 and A511 under temperature conditions expected during preparation of ready-to-use meats. *L. monocytogenes* remains one of the most important human pathogens, causing life-threatening disease with an average mortality of between 25 and 30%. The use of lytic bacteriophages of *L. monocytogenes* can reduce pathogen populations in raw meat products and is an accepted method to control the spread of this pathogen. The efficacy of such phage treatments may be, however, variable due to the high temperatures applied during processing of raw meat. Bacteriophages P100 and A511 exhibited different temperature-resistant patterns, with P100 being readily inactivated after exposure to 71°C for 30 s, whereas phage A511 was rather stable under these same conditions. The study of Ahmadi et al. indicated that when considering the use of phages for control of pathogenic bacteria in food products, the thermal stability of the virus is a particularly important consideration. The temperature component of bacteriophage fitness should remain of utmost importance also when considering using viruses to control bacterial pathogens in agriculture and/or environment. It has to be noted that probably due to the different weather conditions

(temperatures) in different parts of the globe, phage-based products may have inconsistent activity on the same pathogen.

A final study in this section describes the analysis of the lytic *Staphylococcus aureus* bacteriophage phiAGO1.3. Glowacka-Rutkowska et al. identified specific features contributing to the wide host range of this virus as well as the authors described the strategy utilized by it to co-exist with its host in the environment. The virus can modulate the response of *S. aureus* to phage infection to exhibit a carrier state (Barksdale and Arden, 1974; Abedon, 2009) in which both phage-sensitive and phage-insensitive host populations persist in the same environment.

With the development of new, high-throughput DNA sequencing methods, the significant decrease in sequencing costs is a well-recognized benefit for enhancing research (Schuster, 2007). The reduced cost of viral genome sequencing has resulted in a stunning increase in the number of available bacteriophage genomes and has facilitated associated genome-wide taxonomic and metagenomic studies (Hendrix, 2003). This new thrust is reflected in this Research Topic, in which one study characterized the genomes of newly discovered bacteriophages, while another presents a bioinformatic approach to identify genes encoding endolysins in the genomes of uncultured environmental bacteriophages. The work of Xu et al. concentrated on a phage isolated from waste water that exhibits lytic activity to multidrug-resistant *E. coli* strains. The bacteriophage vB_EcoS-B2 was considered to be virulent on the basis of genomic analyses that revealed the absence of genes putatively encoding integrase, repressor, and/or anti-repressor proteins. Likewise, Fan et al. isolated bacteriophage AJO2 from sludge that was lytic to *Acinetobacter johnsonii* and characterized it. The extensive genome analysis revealed that AJO2 possesses unique features and has low genomic similarity to other known *Acinetobacter* bacteriophages. The features of this newly characterized *A. johnsonii* bacteriophage may lead to better control strategies for this pathogen and will undoubtedly shed light on the adaptation and co-evolution of the bacterial host with its bacteriophages.

Using the available viral genomic and metagenomic data and a newly developed bioinformatic pipeline, Fernández-Ruiz et al. found new genes encoding endolysins by analyzing more than 180,000 genomes of uncultured bacteriophages. Endolysins are lytic enzymes that destroy components of host cells. They are produced by phages at the end of their replication cycle, thereby allowing the progeny (daughter) viruses to be released. While many endolysins have been characterized, the majority of the reported genes and enzymes come from cultured phages having known hosts, while uncultured bacterial viruses were identified solely from metagenomic data. The findings of Fernández-Ruiz et al. reveal that environmental phage genomes, collected from complex environments including aquatic and gut microbiomes, may be a valuable source of new lytic enzymes that can be used in medicine as well as in biotechnological applications, even if the phages carrying the genes-of-interest cannot be currently multiplied under laboratory conditions.

The future of phage research seems to be bright. With more than two thousand scientific publications related to bacteriophages appearing annually in the last 10 years (Web of Science, www.webofknowledge.com/), this field has emerged from a forgotten, peripheral research area to become a major, broad scientific topic of the twenty-first century. Bacterial viruses are now used not only as new therapies for infections caused by antibiotic-resistant pathogens or the prevention of bacterial diseases of agriculturally-important crops, but they are also being used to study the ecological fitness of their hosts and the biodiversity of complex environments.

Finally, we would like to thank all the authors for their contributions in this Research Topic, as well as acknowledge the many reviewers for their critical assessments of the submitted manuscripts.

AUTHOR CONTRIBUTIONS

All authors listed have made a substantial, direct and intellectual contribution to the work, and approved it for publication.

ACKNOWLEDGMENTS

Preparation of this manuscript was made possible by the grant NCN OPUS 13 (2017/25/B/NZ9/00036) from National Science Centre, Poland (Narodowe Centrum Nauki, Polska) given to RC.

REFERENCES

Abedon, S. T. (2008). *Bacteriophage Ecology: Population Growth, Evolution and Impact of Bacterial Viruses*. Advances in Molecular and Cellular Microbiology. Cambridge, UK: Cambridge University Press. doi: 10.1017/CBO9780511541483

Abedon, S. T. (2009). Phage evolution and ecology. *Adv. Appl. Microbiol.* 67, 1–45. doi: 10.1016/S0065-2164(08)01001-0

Barksdale, L., and Arden, S. B. (1974). Persisting bacteriophage infections, lysogeny, and phage conversions. *Annu. Rev. Microbiol.* 28, 265–300. doi: 10.1146/annurev.mi.28.100174.001405

Buttimer, C., Mcauliffe, O., Ross, R. P., Hill, C., O'mahony, J., and Coffey, A. (2017). Bacteriophages and bacterial plant diseases. *Front. Microbiol.* 8:34. doi: 10.3389/fmicb.2017.00034

Charkowski, A. O. (2007). The soft rot erwinia. *Plant Assoc. Bacteria* 3, 423–505. doi: 10.1007/978-1-4020-4538-7_13

Czajkowski, R. (2016). Bacteriophages of soft rot Enterobacteriaceae – a mini-review. *FEMS Microbiol. Lett.* 363, 1–6. doi: 10.1093/femsle/fnv230

Dennehy, J. J. (2012). What can phages tell us about host-pathogen coevolution? *Int. J. Evol. Biol.* 2012, 1–12. doi: 10.1155/2012/396165

Duckworth, D. H., and Gulig, P. A. (2002). Bacteriophages. *BioDrugs* 16, 57–62. doi: 10.2165/00063030-200216010-00006

Fuhrman, J. A. (1999). Marine viruses and their biogeochemical and ecological effects. *Nature* 399, 541–548. doi: 10.1038/21119

Hadley, P. (1928). The Twort-D'Herelle phenomenon: a critical review and presentation of a new conception (homogamic theory) of bacteriophage action. *J. Infect. Dis.* 42, 263–434. doi: 10.1093/infdis/42.4.263

Hendrix, R. W. (2003). Bacteriophage genomics. *Curr. Opin. Microbiol.* 6, 506–511. doi: 10.1016/j.mib.2003.09.004

Hyman, P., Abedon, S. T., Allen, I. L., Sima, S., and Geoffrey, M. G. (2010). "Chapter 7 - Bacteriophage host range and bacterial resistance," in *Advances*

in Applied Microbiology, eds A. I. Laskin, S. Sariaslani, and G. M. Gadd (Amsterdam: Academic Press), 217–248. doi: 10.1016/S0065-2164(10)70007-1

Karthik, K., Muneeswaran, N. S., Manjunathachar, H. V., Gopi, M., Elamurugan, A., and Kalaiyarasu, S. (2014). Bacteriophages: effective alternative to antibiotics. *Adv. Anim. Vet. Sci* 2, 1–7. doi: 10.14737/journal.aavs/2014/2.3s.1.7

Koskella, B., and Meaden, S. (2013). Understanding bacteriophage specificity in natural microbial communities. *Viruses* 5, 806–823. doi: 10.3390/v5030806

Middelboe, M., and Brussaard, C. P. D. (2017). Marine viruses: key players in marine Ecosystems. *Viruses* 9, 302–308. doi: 10.3390/v9100302

Miller, R. V. (2001). Environmental bacteriophage-host interactions: factors contribution to natural transduction. *Antonie Van Leeuwenhoek* 79, 141–147. doi: 10.1023/A:1010278628468

Muniesa, M., Colomer-Lluch, M., and Jofre, J. (2013). Potential impact of environmental bacteriophages in spreading antibiotic resistance genes. *Future Microbiol.* 8, 739–751. doi: 10.2217/fmb.13.32

Pires, D. P., Cleto, S., Sillankorva, S., Azeredo, J., and Lu, T. K. (2016). Genetically engineered phages: a review of advances over the last decade. *Microbiol. Mol. Biol. Rev.* 80, 523–543. doi: 10.1128/MMBR.00069-15

Rohwer, F., Prangishvili, D., and Lindell, D. (2009). Roles of viruses in the environment. *Environ. Microbiol.* 11, 2771–2774. doi: 10.1111/j.1462-2920.2009.02101.x

Sandaa, R. A., Gómez-Consarnau, L., Pinhassi, J., Riemann, L., Malits, A., Weinbauer, M. G., et al. (2009). Viral control of bacterial biodiversity–evidence from a nutrient-enriched marine mesocosm experiment. *Environ. Microbiol.* 11, 2585–2597. doi: 10.1111/j.1462-2920.2009.01983.x

Schuster, S. C. (2007). Next-generation sequencing transforms today's biology. *Nat. Methods* 5, 16–18. doi: 10.1038/nmeth1156

Sulakvelidze, A., and Morris, J. G. (2001). Bacteriophages as therapeutic agents. *Ann. Med.* 33, 507–509. doi: 10.3109/07853890108995959

Summers, W. C. (2012). The strange history of phage therapy. *Bacteriophage* 2, 130–133. doi: 10.4161/bact.20757

Van Der Wolf, J. M., Nijhuis, E. H., Kowalewska, M. J., Saddler, G. S., Parkinson, N., Elphinstone, J. G., et al. (2014). *Dickeya solani* sp. nov., a pectinolytic plant pathogenic bacterium isolated from potato (*Solanum tuberosum*). *Int. J. Syst. Evol. Microbiol.* 64, 768–774. doi: 10.1099/ijs.0.052944-0

Wagner, P. L., and Waldor, M. K. (2002). Bacteriophage control of bacterial virulence. *Infect. Immun.* 70, 3985–3993. doi: 10.1128/IAI.70.8.3985-3993.2002

Conflict of Interest Statement: The authors declare that the research was conducted in the absence of any commercial or financial relationships that could be construed as a potential conflict of interest.

frontiers in Microbiology

ORIGINAL RESEARCH
published: 21 March 2019
doi: 10.3389/fmicb.2019.00574

Therapeutic Characterization and Efficacy of Bacteriophage Cocktails Infecting *Escherichia coli*, *Klebsiella pneumoniae,* and *Enterobacter* Species

Prasanth Manohar[1], Ashok J. Tamhankar[2,3], Cecilia Stalsby Lundborg[2] and Ramesh Nachimuthu[1]**

[1] Antibiotic Resistance and Phage Therapy Laboratory, Department of Biomedical Sciences, School of Bioscience and Technology, Vellore Institute of Technology, Vellore, India, [2] Global Health-Health Systems and Policy: Medicines, Focusing Antibiotics, Department of Public Health Sciences, Karolinska Institutet, Stockholm, Sweden, [3] Indian Initiative for Management of Antibiotic Resistance, Mumbai, India

OPEN ACCESS

Edited by:
Robert Czajkowski, University of Gdańsk, Poland

Reviewed by:
Hidetomo Iwano, Rakuno Gakuen University, Japan
Alicja Węgrzyn, Polish Academy of Sciences, Poland

***Correspondence:**
Ashok J. Tamhankar
ashok.tamhankar@ki.se; ejetee@gmail.com
Ramesh Nachimuthu
drpnramesh@gmail.com

Specialty section:
This article was submitted to Virology, a section of the journal Frontiers in Microbiology

Received: *21 October 2018*
Accepted: *06 March 2019*
Published: *21 March 2019*

Citation:
Manohar P, Tamhankar AJ, Lundborg CS and Nachimuthu R (2019) Therapeutic Characterization and Efficacy of Bacteriophage Cocktails Infecting Escherichia coli, Klebsiella pneumoniae, and Enterobacter Species. Front. Microbiol. 10:574. doi: 10.3389/fmicb.2019.00574

Infections due to antibiotic resistant bacteria are increasing globally and this needs immediate attention. Bacteriophages are considered an effective alternative for the treatment of bacterial infections. The aim of this study was to isolate and characterize the bacteriophages that infect *Escherichia coli*, *Klebsiella pneumoniae,* and *Enterobacter* species. For this, clinical bacterial isolates of the mentioned species were obtained from diagnostic centers located in Chennai, Tamil Nadu, India. The bacteriophages were isolated from sewage water samples collected from Tamil Nadu, India. Phage isolation was performed using enrichment method and agar overlay method was used to confirm the presence of bacteriophages. All the phages were characterized for their life cycle parameters, genome analysis, and *in vitro* phage cocktail activity. The three bacteriophages exhibited broad host range activity: *Escherichia* virus myPSH2311 infecting *E. coli* belonging to six different pathotypes, *Klebsiella* virus myPSH1235 infecting *K. pneumoniae* belonging to four different serotypes and *Enterobacter* virus myPSH1140 infecting four different species of *Enterobacter*. Morphological observations suggested that the bacteriophages belonged to, *Phieco32virus* (*Escherichia* virus myPSH2311), *Podoviridae* (*Klebsiella* virus myPSH1235), and *Myoviridae* (*Enterobacter* virus myPSH1140). The life cycles (adsorption, latent period, and cell burst) of *Escherichia* virus myPSH2311, *Klebsiella* virus myPSH1235 and *Enterobacter* virus myPSH1140 were found to be 26, 40, and 11 min, respectively. Genomic analysis revealed that *Escherichia* virus myPSH2311 is closely related to *Escherichia* phage vB_EcoP_SU10, *Klebsiella* virus myPSH1235 is closely related to *Klebsiella* phage vB_KpnP_KpV48 and *Enterobacter* virus myPSH1140 is closely related to *Enterobacter* phage PG7 and *Enterobacter* phage CC31. When phage cocktail was used against multiple bacterial mixtures, there was a reduction in bacterial load from 10^6 to 10^3 CFU/mL within 2 h. All the three characterized phages were found to have a broad host range activity and the prepared phage cocktails

were effective against mixed bacterial population that are resistant to meropenem and colistin, two last resort antibiotics. Infections caused by drug resistant bacteria will be a serious threat in the future and the use of virulent bacteriophages in therapy may offer an effective solution.

Keywords: bacteriophage genome, *E. coli*, *Klebsiella pneumoniae*, *Enterobacter cloacae*, phage cocktail, phage therapy

INTRODUCTION

Bacteriophages are the viruses of bacteria that live in the same ecological niche, where their host bacteria are present (Rohwer, 2003). Phages are generally very specific (species-specific and strain-specific) to their bacterial host but some phages are polyvalent, and can infect more than one species or strain of bacteria (Chibani-Chennoufi et al., 2004). Phage therapy largely involves the treatment of bacterial infections using bacteriophages/phages (Levin and Bull, 2004). Phages with broad host range are mostly chosen for therapy, because of their broad spectrum host-range activity against multiple bacteria. The phages belonging to the order *Caudovirales* (Family-*Myoviridae*, *Siphoviridae,* and *Podoviridae*) with proteinaceous tail, that follow only lytic pathway, are preferred for therapy (Gill and Hyman, 2010). The use of bacteriophages for therapeutic purpose is an old concept that is re-emerging after about a century (Sulakvelidze et al., 2001). Antibiotic resistance has become a human health concern globally as the infections caused by resistant bacteria are becoming difficult to cure (World Health Organization [WHO], 2014; Ventola, 2015). Phage therapy can be one of the alternatives for combating antibiotic resistant bacterial infections (Rios et al., 2016).

Escherichia coli, *Klebsiella pneumoniae,* and *Enterobacter cloacae* are Gram-negative bacteria that belong to the family *Enterobacteriaceae*. All the three are enteric pathogens causing serious opportunistic infections in humans (Morens et al., 2004; Schlossberg, 2015). They cause hospital acquired and community acquired infections such as diarrhea, meningitis, urinary tract infections (UTIs), bacteremia, pneumonia, surgical site infections, and sepsis (Schlossberg, 2015). The increasing reports of resistance to carbapenem and colistin, two last resort drugs, among *Enterobacteriaceae* world over (World Health Organization [WHO], 2014) and more particularly so in the developing countries (Ventola, 2015) is a serious threat to their therapeutic use, which prompts search for alternative treatment options. Studies using bacteriophages as an antibacterial agent have shown promising outcomes in both *in vitro* and *in vivo* studies, and therefore phage therapy is being studied as a candidate to cure bacterial infections (McVay et al., 2007; Hung et al., 2011; Cao et al., 2015; Mirzaei and Nilsson, 2015). Phage cocktails have shown broad spectrum activity against many bacterial strains (Mendes et al., 2014; Yen et al., 2017). The characterization of phages for therapeutic purpose involves isolation of potential lytic phages, multi-step *in vitro* characterization, cocktail preparation and purification, dosing and *in vivo* studies. More than 50 *Escherichia* phages belonging to families *Myoviridae*, *Siphoviridae,* and *Podoviridae* have been reported with complete genome sequences[1]. Genome sequenced phages against *Klebsiella* (≈29) and *Enterobacter* (≈10) have been reported much lesser in number[2]. Here, we report characterization of three lytic bacteriophages that showed promising ability to lyse *E. coli*, *K. pneumoniae,* and *Enterobacter* species, report their host range specificity and also efficacy of phage cocktails made using these three phages in various permutations and combinations, in effectively killing combinations of host bacteria using *in vitro* phage killing assay.

MATERIALS AND METHODS

Isolation of Clinical Bacterial Strains for the Study

This study does not include any human subjects; therefore, ethical approval was not required for this study according to national and institutional guidelines. The clinical isolates of *Escherichia coli*, *Klebsiella pneumoniae*, *Enterobacter cloacae, E. hormaechei*, *E. asburiae,* and *E. aerogenes* used in this study were collected from diagnostic centers in Chennai, Tiruchirappalli, and Madurai located in the state of Tamil Nadu in India, during December 2014- September 2016. All the isolates were preserved in 30% glycerol stocks at −20°C. The clinical samples used for bacterial isolation were urine, sputum, pus, blood, wound swab, and bronchial aspirate. Bacterial identification was performed using VITEK identification system (bioMèrieux, Inc., United States) and 16S rRNA analysis. Universal primers, 27F (5′-AGAGTTTGATCCTGGCTCAG-3′) and 1492R (5′-GGTTACCTTGTTACGACTT-3′), were adopted for gene amplification and sequences of 16S rRNA genes were deposited in GenBank. All the clinical isolates were studied for resistance against meropenem and colistin, two last resort antibiotics, using microbroth dilution method following Clinical and Laboratory Standards Institute [CLSI], 2018. For the study, a total of 150 non-repetitive, Gram-negative bacterial isolates belonging to three genera *Escherichia*, *Klebsiella,* and *Enterobacter* were used. The isolated clinical pathogens included 80 *E. coli* isolates, 44 *Klebsiella pneumoniae* isolates and in the case of *Enterobacter* isolates, there were four different species namely *E. cloacae* (n = 15), *E. hormaechei* (n = 4), *E. asburiae* (n = 4), and *E. aerogenes* (n = 3) (**Table 1**). The results for meropenem and

[1]https://www.ncbi.nlm.nih.gov/genome/?term=escherichia+phage

[2]https://www.ncbi.nlm.nih.gov/

TABLE 1 | Host range infection and efficiency of plating (EOP) of the phages *Escherichia* virus myPSH2311, *Klebsiella* virus myPSH1235, and *Enterobacter* virus myPSH1140.

Bacteria	Spot test (%)	High (EOP ≥ 0.5)	Moderate (EOP > 0.1– < 0.5)	Low (EOP ≤ 0.1)	No activity (EOP < 0.001)	Sum of EOP values
Escherichia* virus myPSH2311 lytic activity against different pathotypes of *E. coli						
EPEC (*n* = 12)	10 (83%)	5	1	1	3	5.30
EHEC (*n* = 10)	6 (60%)	2	0	1	3	1.91
ETEC (*n* = 8)	4 (50%)	3	0	0	1	3.10
EIEC (*n* = 11)	9 (82%)	5	3	0	1	5.55
EAEC (*n* = 14)	10 (71%)	6	0	2	2	5.86
UPEC (*n* = 21)	17 (81%)	11	0	1	5	10.75
Unknown (*n* = 4)	2 (50%)	2	0	0	0	1.60
Total (*n* = 80)	58 (73%)	34	4	5	15	34.07
Klebsiella* virus myPSH1235 lytic activity against different serotypes of *K. pneumoniae						
Serotype K1 (*n* = 3)	2 (67%)	1	1	0	0	1.20
Serotype K2 (*n* = 7)	5 (71%)	2	1	1	1	2.85
Serotype K5 (*n* = 9)	6 (67%)	2	0	2	2	2.10
Unknown (*n* = 25)	10 (40%)	5	1	1	3	5.85
Total (*n* = 44)	23 (52%)	10	3	4	6	12.0
Enterobacter* virus myPSH1140 lytic activity against different species of *Enterobacter						
E. cloacae (*n* = 15)	15 (100%)	7	3	1	4	8.50
E. hormaechei (*n* = 4)	3 (75%)	2	0	0	1	2.72
E. asburiae (*n* = 4)	2 (50%)	2	0	0	0	2.10
E. aerogenes (*n* = 3)	2 (67%)	2	0	0	0	1.44

Values represent the lytic activity of the respective phage against the target bacterium. EPEC (enteropathogenic E. coli), EHEC (enterohemorrhagic E. coli), ETEC (enterotoxigenic E. coli), EIEC (enteroinvasive E. coli), EAEC (enteroaggregative E. coli), UPEC (uropathogenic E. coli). EOP was calculated using double agar overlay method. EOP was deemed as 'High' if the test bacterium had at least 50% activity (EOP ≥ 0.5) compared to the host bacterium, 'Moderate' if between >10 and <50% (EOP > 0.1– < 0.5), anything < 10% (EOP ≤ 0.1) was reported as 'Low.'

colistin resistance screening of these isolates are presented in **Supplementary Table S1**.

Phage Isolation and Enrichment

Bacteriophages were isolated from water samples collected from Ganges River near Varanasi in Northern part of India and sewage water treatment plants (secondary treatment stage) from different locations in Chennai, Bangalore, Tirupathi, Vellore, Karur, and Trichy in Southern part of India. Initially, the isolated bacterial strains (one isolate at a time) were grown in Luria-Bertani broth (Himedia, India) medium and were used as a host for phage isolation. Briefly, to a 5 mL of exponentially grown bacterial culture (optical density at 600 nm = 0.6), 10 mL of phage containing water samples was added and incubated at 37°C for 24 h in shaking incubator to enrich the phages against the host bacterium. This mixture was centrifuged for 15 min at 12,000 × *g* and the supernatant was filtered in 0.22-μm pore-sized membrane syringe filters for separation of phages from other contaminants. The filtrate was used for double-agar overlay method (Li et al., 2016a). Briefly, to the exponentially grown host bacterial culture (400 μL), the phage filtrate (200 μL) was added and incubated for 15 min. To the mixture, 3 mL of molten soft agar (0.75% agar) was added and over-laid onto prepared LB agar plate (1.5% agar). The plates were incubated at 37°C for 10 h and the appearance of clear plaques indicated the presence of phages against the host bacterium. The phage plaques were picked-up from the plate for further purification and the phage titer was determined. For spot test method, the bacterial (using exponentially grown host bacterial culture) lawn was prepared in LB agar plates and 10–50 μL of phage filtrate was placed as a spot over the target bacterial lawn to evaluate the phage activity. The development of clear spots indicated the phage activity and the time taken for bacterial clearance indicated the lytic activity of phages. The bacterium initially used for phage isolation was deemed as a host bacterium against the phage. Multiplicity of infection (MOI) was calculated using the number of phage particles against the potent host bacteria (PFU/CFU).

Purification of Lytic Phages

The isolated phage lysates were prepared in high titers using phage multiplication strategy (propagation on host bacterium). Briefly, the phages were multiplied using host bacterium for 24 h (day 1) and centrifuged at 6000 × *g* for 15 min. The collected supernatant was mixed with exponentially grown host bacterium (day 2) and allowed to multiply. Similar passages were carried out for 5 days and evaluated for phage activity/ titer by spot test and double agar overlay method against *E. coli*, *K. pneumoniae,* and *Enterobacter* species. The obtained high titer phages were precipitated using 10% PEG 6000 (polyethylene glycol) and 1 M NaCl. Briefly, to the phage lysate 10% PEG 6000+1 M NaCl was added, mixed gently (did not vortex) and the mixture was stored at 4°C for 24 h. The precipitated phage particles were centrifuged at 15,000 × *g* for 45 min and the obtained pellet was resuspended in sterile SM buffer (For 1 L: 5.8 g, NaCl; 50 mL, 1 M Tris-HCl

[pH 7.5]; 2 g, $MgSO_4.7H_2O$; 5 mL, 2% gelatin). The extraction was carried out by adding equal volume of chloroform and the aqueous phase was sedimented by centrifugation at 18,000 × *g* for 80 min. The obtained phage particles were dialyzed against phosphate buffer saline (PBS) for 6 h by changing buffer every 2 h and the purified phage suspension was stored at 4°C for further analysis.

Electron Microscopic Analysis

The purified phage particles (10^5 PFU/mL) were negatively stained using phosphotungstic acid, PTA (2% [w/v], pH 7.0). Briefly, 10 μL of phage lysate was added over the copper grid and the liquid was allowed to absorb for 10 min. The remaining liquid was removed using tissue paper and the prepared 2% PTA solution (staining solution) was added. After allowing it to stain for 5 min, the excess stain was removed and the grid was washed twice with sterile water. The negatively stained phage particles in the copper grid were allowed to dry at room temperature for 20–30 min and visualized under Transmission Electron Microscopy (FEI-TECNAI G2-20 TWIN, Bionand, Spain). The phage morphology was determined and head/ tail lengths (10 measurements each) were measured using ImageJ software.

Host-Range Specificity Determination and Efficiency of Plating (EOP)

The lytic activity of isolated phages was tested against the target bacteria. Accordingly, *Escherichia* phage was tested against 80 *E. coli* isolates belonging to pathotypes: EPEC (enteropathogenic *E. coli*), EHEC (enterohemorrhagic *E. coli*), ETEC (enterotoxigenic *E. coli*), EIEC (enteroinvasive *E. coli*), EAEC (enteroaggregative *E. coli*), and UPEC (uropathogenic *E. coli*). *Klebsiella* phage was tested against 37 *K. pneumoniae* isolates that belonged to serotypes K1, K2, K5 and *Enterobacter* phage was tested against 15 *E. cloacae*, 4 *E. hormaechei*, 4 *E. asburiae,* and 3 *E. aerogenes* isolates. Spot test was carried out to assess the host-range specificity of phages against the test bacteria and the resulting positive isolates were again tested for their plaque forming ability in double agar overlay method for calculating efficiency of plating (EOP) (Mirzaei and Nilsson, 2015). EOP was calculated using the number of virus particles infecting the test bacterium against the same titer of virus particles infecting the host bacterium. Accordingly, all the test bacterial strains were grown overnight (16 h) and the concentration of 10^6–10^9 (CFU/mL) was used for double agar overlay method. For the assay, 200 μL of bacterial culture was mixed with 100 μL of phage lysate (MOI = 0.01) and EOP was determined using the formula, plaque forming units (PFUs) on the test bacterium/PFU on the host bacterium, evaluated by double agar overlay method. EOP was classified as 'High,' 'Moderate,' and 'Low' based on the productive infection on the target bacterium. EOP was deemed as 'High' only if the phage-bacterium combination against the test bacterium had a productive infection of at least 50% (EOP $\geq$ 0.5) compared to the host bacterium. EOP between >10 and <50% (EOP > 0.1− < 0.5) was considered 'Moderate' and EOP < 10% (EOP $\leq$ 0.1) was recorded as 'Low' (Mirzaei and Nilsson, 2015).

Characterization: Adsorption Rate, Latency Period, and Burst Size

Exponentially grown bacterial cells were mixed with the respective phages at a MOI of 0.001 and incubated at 37°C. Aliquots of 100 μL were removed after every 4 min interval for 40 min and diluted in 4.4 mL LB broth and 0.5 mL of chloroform was added. After incubating the mixture for 30 min at 37°C, the number of non-adsorbed phages was determined subsequently using double agar overlay method. The adsorption curve was constructed using the ratio of non-adsorbed phage particles at different time intervals to the number of initial phages. One-step growth experiment was performed to determine the latent period and burst size (14). Briefly, the bacterial cells (10^8 CFU/mL) were infected with the phage particles (MOI of 0.001) and allowed to adsorb (based on the adsorption time determined previously) at 37°C. The mixture was then centrifuged at 12,000 × *g* for 5 min and the pellet was resuspended in 10 mL of LB broth and the incubation was continued at 37°C. The samples were taken at 5 min intervals for 80 min and titrated against the host bacterium. The latent-period was calculated as the duration between the phage adsorbed until the release of phage virions. The burst size of the phage was calculated using the final number of free phage particles to the initial number of phages.

Phage Stability Studies

Stability studies were conducted at different pH and temperature. For thermal stability tests, phage lysates (10^8 PFU/mL) were incubated at 4, 20, 35, 45, 50, 55, 60, 70, and 80°C for 60 min in temperature-controlled water bath and immediately transferred to the ice cold condition (−20°C) which was further tested for phage activity using double agar overlay method. The pH stability studies were performed using SM buffer and pH was adjusted using 1N NaOH and 1N HCl. The phage lysates (10^8 PFU/mL) were incubated at pH 1–14 for 60 min and the aliquots were removed for stability analysis. The results were expressed as phage viability in terms of percentage of initial viral counts. All the stability studies were tested using *E. coli* ec311, *K. pneumoniae* kp235, and *E. cloacae* el140, and the experiments were repeated in triplicates.

DNA Isolation, Genome Sequencing, and Analysis

The phage DNA was extracted from purified phage particles using phenol-chloroform (24:1) method and precipitated using ethanol (100%). The purified phage DNA was visualized on 0.8% agarose gels and the PE libraries were prepared using Illumina TruSeq Nano DNA library Prep kit. The prepared libraries were sequenced using Illumina Nextseq 500 system (using 2 bp × 150 bp chemistry) at Eurofins Genomics, Bangalore, India. The sequenced raw data was processed to obtain high quality clean reads using Trimmomaticv 0.35 to remove adapter sequences, ambiguous reads (reads with unknown nucleotides "N" larger than 5%), and low-quality sequences [reads with more than 10% quality threshold (QV) < 20 phred score]. The sequenced high quality reads were *de novo* assembled using CLC Genomics Workbench version 9.5.2. Protein-coding

and tRNA genes were identified using the final assembly. The transfer-RNA (tRNA) genes were predicted using tRNAscan-SE 2.0 web server while the protein coding genes (CDS) were predicted using FGENESV web server. Functional annotation of the predicted proteins was performed using the amino acid sequences viaBLASTp program online against a custom database of viral proteins in NCBI. Gene ontology (GO) annotations of the genes were determined by the Blast2GO platform. Distribution of GO terms across the categories – Biological Process, Molecular Function and Cellular Component was obtained through WEGOportal[3]. The NCBI sequence was downloaded from NCBI[2] for sequence comparison and the scaffolds were then subjected to reference-based assembly via CONTIGuator2. The final assembly generated by CONTIGuator was validated based on sequence homology to known bacteriophage sequences in NCBI via BlastN.

Composition and Preparation of Phage Cocktails

Phage cocktails containing different compositions of isolated phages under study were prepared and evaluated for activity against target species. For cocktail preparation, two or three different phages were mixed together in equal proportions to obtain a concentration of 10^6 PFU/mL. Briefly, cocktail EK1 contained *Escherichia* phage plus *Klebsiella* phage; KL2 contained *Klebsiella* phage plus *Enterobacter* phage; EL3 contained *Escherichia* phage plus *Enterobacter* phage and EKL4 contained *Escherichia* phage plus *Klebsiella* phage plus *Enterobacter* phage. The prepared cocktails were tested for *in vitro* phage-killing assay against respective bacterial strains. The results were compared to the activity of phages in cocktails to the activity of phages alone, and one bacterium from each genus was used for this study. Accordingly, 1 mL of host bacterium (6×10^7 CFU/mL) was diluted in LB broth to yield a final concentration of 6×10^6 CFU/mL. For each study, 100 μL (each phage at the concentration of 10^6 PFU/mL; MOI of 1.0) of bacteriophage suspension was added and the mixture was incubated at 37°C and the aliquots (100 μL) were removed at 0, 2, 4, 6, and 24 h to calculate the reduction in bacterial count. To test the activity of phage cocktails, bacteria were also used in combination similar to phage combinations (**Supplementary Table S2**). In the case of control experiments, bacteriophage buffer alone was used with the bacterial inoculum and bacterial growth was determined. All the cocktail studies were tested using *E. coli* ec311, *K. pneumoniae* kp235, and *E. cloacae* el140, and the experiments were repeated in triplicates.

[3]http://wego.genomics.org.cn

RESULTS

Nomenclature and Morphological Characterization of Phages

The phages were named as *Escherichia* virus myPSH2311, *Klebsiella* virus myPSH1235, and *Enterobacter* virus myPSH1140 following the bacteriophage nomenclature guidelines (Krupovic et al., 2016). Examination of phage morphology by TEM analysis showed that *Escherichia* virus myPSH2311 had an icosahedral head of 33 ± 3.0 nm, a non-contractile tail length of 65 ± 2.5 nm and belonged to genus *Phieco32virus*, *Klebsiella* virus myPSH1235 had the icosahedral head of 80 ± 4.5 nm and very short non-contractile tail that showed the phage belonged to family *Podoviridae* and *Enterobacter* virus myPSH1140 had an elongated head of approximately 80 ± 2.0 nm and long contractile tail of 101 ± 3.5 nm in length indicating that it belonged to the family *Myoviridae* (**Figure 1**).

Host-Range Activity Determination and Efficiency of Plating (EOP)

The spot test assay showed that the *Escherichia* virus myPSH2311 had lytic activity against 73% of the tested *E. coli* isolates, *Klebsiella* virus myPSH1235 had activity against 52% *K. pneumoniae* isolates and *Enterobacter* virus myPSH1140 showed activity against 15 *E. cloacae* (n = 15), 3 *E. hormaechei* (n = 4), 2 *E. asburiae* (n = 4), and 2 *E. aerogenes* (n = 3) isolates. In the case of double agar overlay method, *Escherichia* virus myPSH2311 had plaques against 43/80 tested *E. coli*

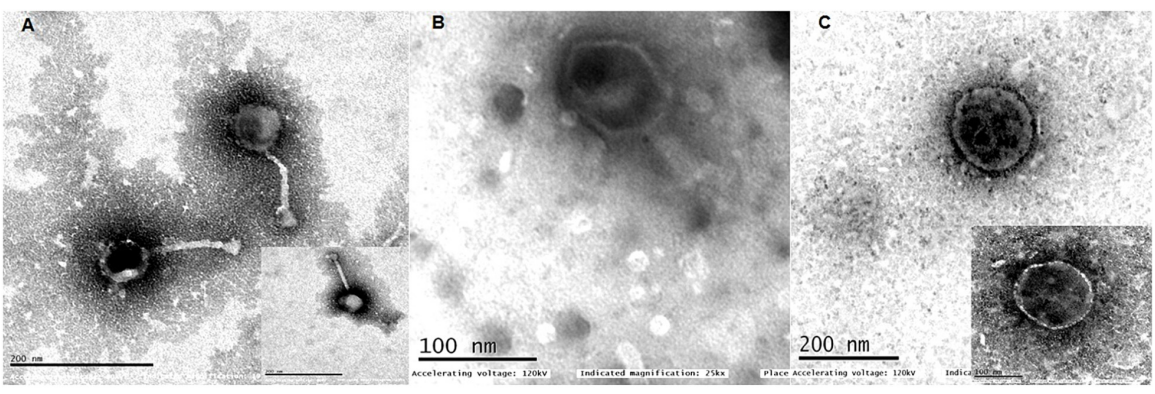

FIGURE 1 | Transmission electron microscopy (TEM) images of **(A)** *Escherichia* virus myPSH2311, **(B)** *Enterobacter* virus myPSH1140, **(C)** *Klebsiella* virus myPSH1235. The smaller images in **(A,C)** represent 100 nm.

isolates, *Klebsiella* virus myPSH1235 had plaques against 17/44 *K. pneumoniae* isolates and *Enterobacter* virus myPSH1140 had plaques against 11/15 *E. cloacae*, 2/4 *E. hormaechei*, 2/4 *E. asburiae,* and 2/3 *E. aerogenes* isolates. The percentage activity difference between the spot test and double agar overlay method was found to be 29.7% for *Escherichia* virus myPSH2311, 30% for *Klebsiella* virus myPSH1235 and for *Enterobacter* virus myPSH1140, it was 30.7% for *E. cloacae*, 40% for *E. hormaechei*, 0% for both *E. asburiae* and *E. aerogenes*. The EOP analysis that was used to differentiate the phage infectivity between spot test and double agar overlay method, showed a different scenario (**Table 1**). Though, spot test results showed that *Escherichia* virus myPSH1311 produced clear zone (spot) against 58/80 tested *E. coli* isolates; the EOP analysis showed high productive infection in 34/80 *E. coli* isolates whereas against 9 *E. coli* isolates it was moderate or low productive infection and 15/80 *E. coli* isolates had no infection. *Klebsiella* virus myPSH1235 had high productive infection against 10/44 *K. pneumoniae* isolates with 23/44 in spot test assay and the percentage difference was 78.7%. Even if all the EOP results (High + Moderate + Low) were considered for *Klebsiella* phage myPSH1235, the number of isolates producing (17/44) plaques in double agar overlay assay was still lower than the spot test (23/44) results. *Enterobacter* virus myPSH1140 had high productive infection against 7/15 tested *E. cloacae* isolates compared to 15/15 in spot test assay. The same phage showed high productive infection against 2/4 *E. hormaechei*, 2/4 *E. asburiae,* and 2/3 *E. aerogenes,* respectively (**Table 1**).

Phage Characterization: One-Step and Stability Studies

The multiplication capacity of phages was determined by one-step growth experiment to analyze the adsorption velocity, latency period and burst size (**Figure 2**). Accordingly, for *Escherichia* virus myPSH2311, the adsorption velocity was 1.1×10^{-9} mL/min with latency period of 26 min and the burst size of approximately 110 phages/infected cell. The adsorption velocity for *Klebsiella* virus myPSH1235 was 4.35×10^{-9} and the latency period was 40 min with the burst size of 120 phages/infected cell. *Enterobacter* virus myPSH1140 had an adsorption velocity of 2.8×10^{-9}, a very short latency period of 11 min and a burst size of 135 phages/infected cell (**Figure 2**). When sensitivity of phages to different pH conditions was determined by exposing them to varying range of pH from 1 to 14 for 60 min, all the three phages were found to be viable from pH 4 up to pH 11, but the phages were inactivated at pH $\leq$ 3 and $\geq$ 12 (**Figure 3**). In the case of thermal stability, all the phages were found to uphold their activity up to 55°C and reduction in activity was observed at higher temperatures (**Figure 3**). The complete characterization report is available in **Supplementary Table S3**.

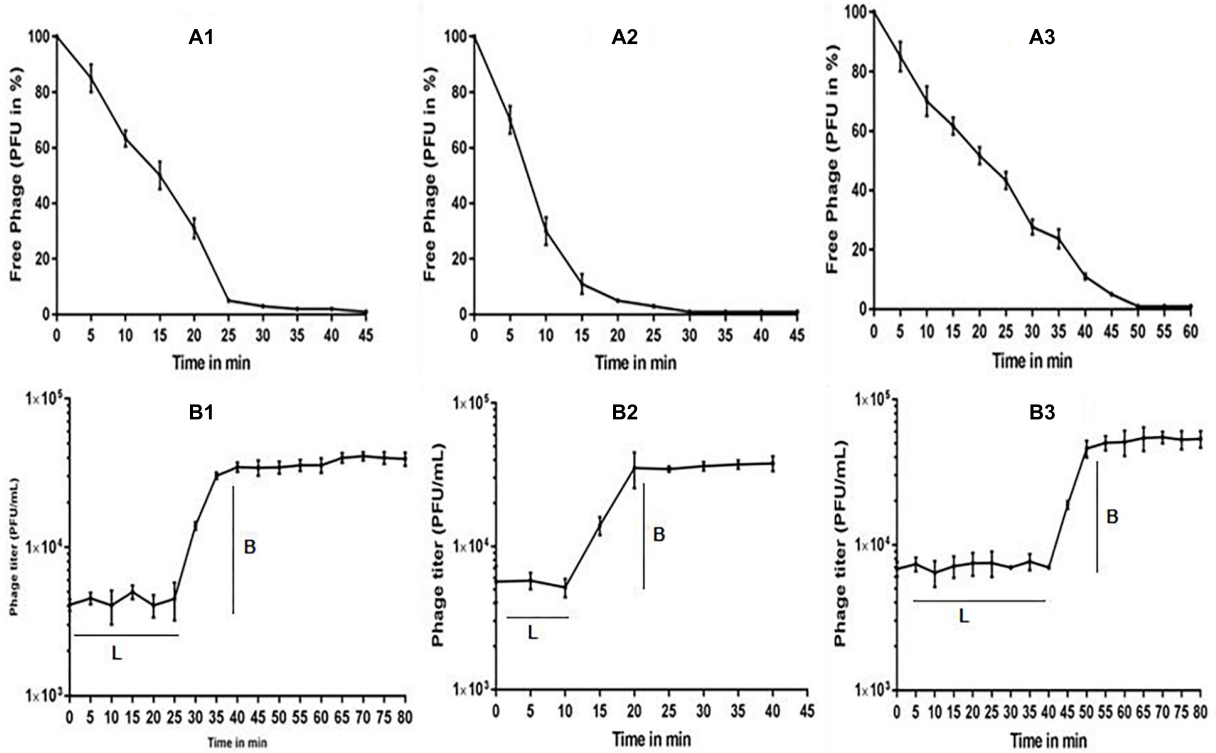

FIGURE 2 | (A) Adsorption rate of phages to their bacterial host, **(A1)** *Escherichia* virus myPSH2311, **(A2)** *Enterobacter* virus myPSH1140, **(A3)** *Klebsiella* virus myPSH1235, and **(B)** One-step growth curve experiment of phages, **(B1)** *Escherichia* virus myPSH2311, **(B2)** *Enterobacter* virus myPSH1140, **(B3)** *Klebsiella* virus myPSH1235. Legend within figure B: L-latency period; B-burst size.

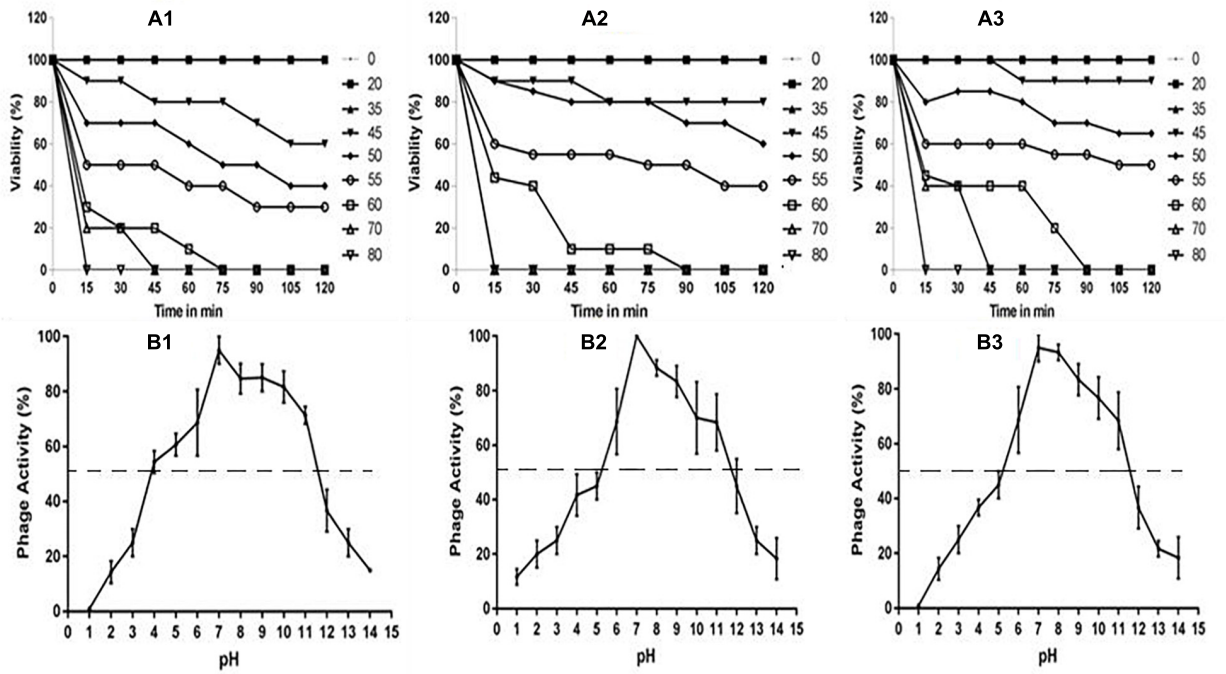

FIGURE 3 | (A) Stability of phages at varying temperatures; **(A1)** *Escherichia* virus myPSH2311, **(A2)** *Enterobacter* virus myPSH1140, **(A3)** *Klebsiella* virus myPSH1235 and **(B)** Stability of phages at varying pH at 37°C, **(B1)** *Escherichia* virus myPSH2311, **(B2)** *Enterobacter* virus myPSH1140, **(B3)** *Klebsiella* virus myPSH1235.

Genomic Analysis and Annotation

The genome of *Escherichia* virus myPSH2311 measured 68,712 bp in size with a GC content of 42.4%. The genome contains 89 proteins or coding sequences (CDS) and it includes 27 proteins of known putative function and 62 hypothetical proteins. A total of 1.01 Gb data was assembled into scaffolds using CLC workbench version 9.5.2, and the assembly size was 5,945,203 bp with the average scaffold size of 12,133 bp. The arranged complete genome of *Escherichia* virus myPSH2311 is closely related to *Escherichia* phage vB_EcoP_SU10 (88%) and *Escherichia* virus phiEco32 (72%) (**Figure 4A** and **Supplementary Figures S1**, **S2A**). The NCBI accession number for this sequence is MG976803. The complete list of all the proteins is available in **Supplementary Table S4**. *Klebsiella* virus myPSH1235 was found to have a genome size of 45,135 bp with a GC content of 53.7%. The genome contains 49 proteins or CDS, of which 21 were found to have known putative function and 28 were hypothetical proteins. The obtained 1.37 Gb data was assembled into scaffolds using CLC workbench version 9.5.2, and the assembly size was 5,740,807 bp with the average scaffold size of 1,321 bp. The genome was closely related to *Klebsiella* phage vB_KpnP_KpV48 (95%) (**Figure 4B** and **Supplementary Figures S1**, **S2B**). The complete genome of *Klebsiella* virus myPSH1235 is free of toxins or toxin-related genes, and none of the proteins representing a temperate or lysogenic lifestyle was detected (**Supplementary Table S4**). The NCBI accession number for this phage is MG972768. The complete list of all the proteins is available in **Supplementary Table S5**. *Enterobacter* virus myPSH1140 was having a genome size of 172,614 bp with a GC content of 39.9%. The gene annotation studies showed 102 proteins with known function and 138 proteins were hypothetical proteins. The obtained 1.22 Gb data was assembled into scaffolds using CLC workbench version 9.5.2, and the assembly size was 5,193,726 bp with the average scaffold size of 6,059 bp. The complete genome was having 92% similarity with *Enterobacter* phage CC31 and 90% similarity with *Enterobacter* phage PG7 (**Figure 4C** and **Supplementary Figures S1**, **S2C**). The NCBI accession number is MG999954. The complete list of all the proteins is available in **Supplementary Table S6**.

In vitro Activity of Phage Cocktail

Phage cocktails were prepared to evaluate the activity of phages against multiple bacterial strains. When the phage cocktail containing all the three phages was tested against the three meropenem and colistin resistant test bacteria, the growth declined after 2 h from 10^6 to $<10^5$ CFU/mL and at the end of 24 h the bacterial density reached to zero with no viable cells. For EK1 cocktail, >2 fold decrease in bacterial cell count (both *E. coli* and *K. pneumoniae*) was observed after 2 h, for KL2 cocktail, the bacterial cell count (both *K. pneumoniae* and *E. cloacae*) decreased from 10^6 to 10^3 CFU/mL within 2 h and for EL3 cocktail, twofold reduction of bacterial cells (both *E. coli* and *E. cloacae*) was observed after 4 h. In phage cocktail containing all the three phages, EKL4, a twofold decrease in bacterial count (*E. coli*, *K. pneumoniae*, *E. cloacae*) was observed in 2 h as comparable to the phages alone. In the

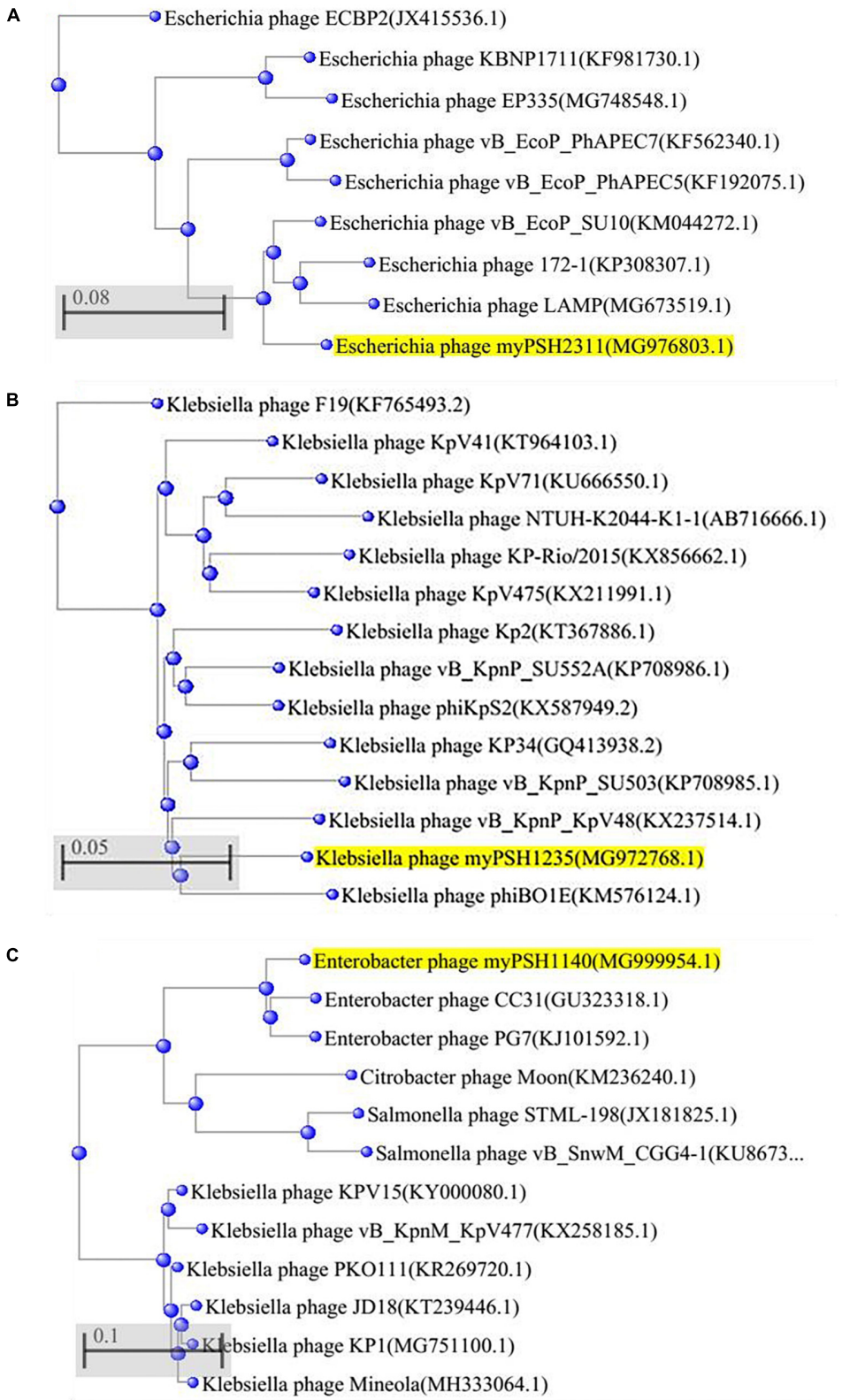

FIGURE 4 | Phylogenetic tree of **(A)** *Escherichia* virus myPSH2311, **(B)** *Klebsiella* virus myPSH1235, and **(C)** *Enterobacter* virus myPSH1140 constructed based on the complete genome sequences of selected bacteriophages in NCBI-BLAST. The tree was produced using BLAST pairwise alignment using Neighbor-Joining method. The query sequence is highlighted in yellow.

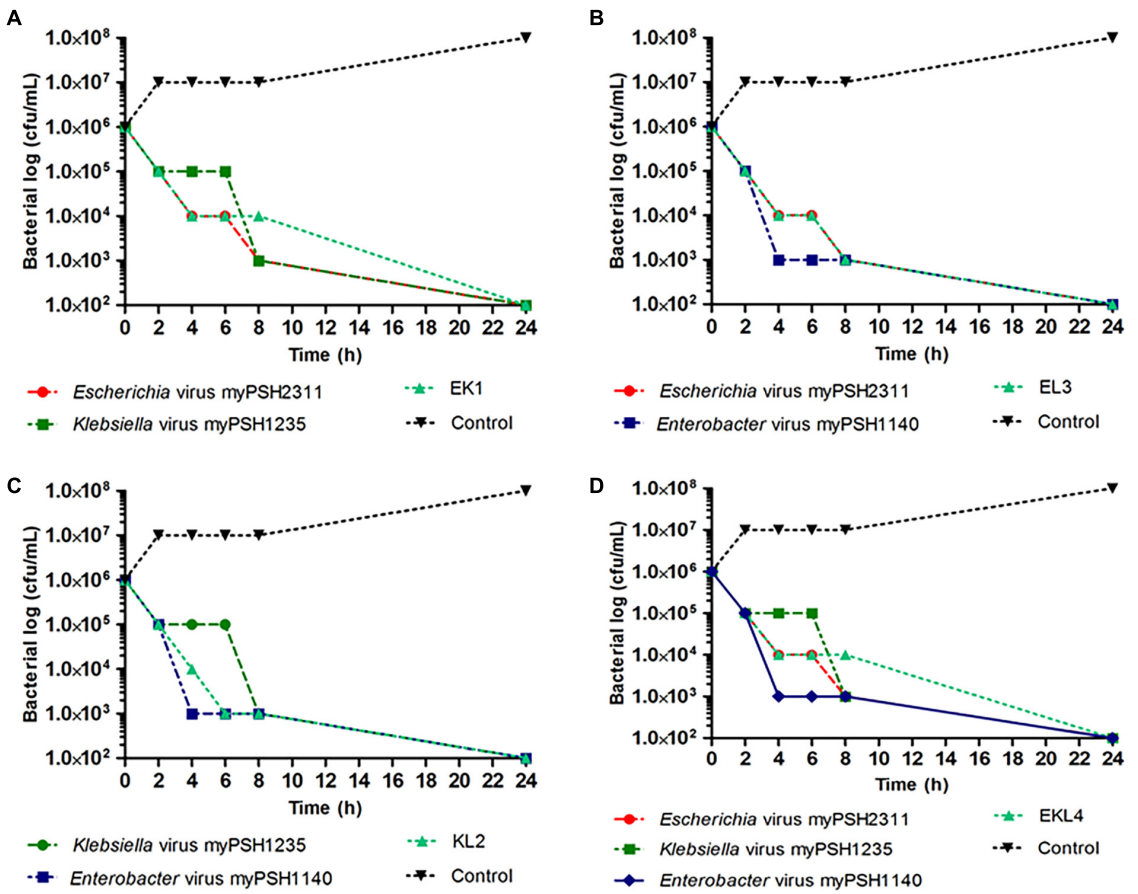

FIGURE 5 | *In vitro* phage activity of prepared phage cocktails. **(A)** activity of *Escherichia* virus myPSH2311 and *Klebsiella* virus myPSH1235 and their combination (EK1); **(B)** activity of *Klebsiella* virus myPSH1235 and *Enterobacter* virus myPSH1140 and their combination (KL2); **(C)** activity of *Escherichia* virus myPSH2311 and *Enterobacter* virus myPSH1140 and their combination (EL3); **(D)** activity of *Escherichia* virus myPSH2311, *Klebsiella* virus myPSH1235, *Enterobacter* virus myPSH1140 and their combination (EKL4) (Control for all the experiments-bacterial growth without antibacterial agents and phages).

case of prepared phage cocktails, all the combinations had similar to better activity in comparison to the phages alone (**Figure 5**). Our experiment proved the activity of prepared phage cocktails against multiple bacterial genera and showed promising results against meropenem and colistin resistant bacteria *in vitro*.

DISCUSSION

Phage therapy is currently gaining attention in clinical medicine, because the infections caused by 'superbugs – multi-drug resistant (MDR) bacteria' are almost impossible to treat, using available antibiotics (Chan et al., 2013). From clinical point-of-view, bacteriophages are likely to be used in treatment, only when the patient is infected with multi-drug resistant bacteria or during the antibiotic crisis of non-curable infections (Lin et al., 2017). The increasing studies on bacteriophages and phage therapy could put forth phage therapy as one of the alternative treatment options to treat 'superbug' infections (Rios et al., 2016). This study is one such effort to characterize bacteriophages infecting Gram-negative bacteria, *E. coli*, *K. pneumoniae,* and *Enterobacter* species.

In the present study, we characterized the phenotypic, morphological, and genomic properties of three bacteriophages that are independently specific in their activity against pathogenic *E. coli, K. pneumoniae,* and *Enterobacter* species. All the three characterized phages belong to order *Caudovirales* that are lytic phages which are generally considered for therapy (*Podoviridae* and *Myoviridae*). There are earlier studies on *Escherichia* phages that showed many of the studied phages are specific to a strain of *E. coli* (e.g., *Escherichia* phage OSYSP infecting only *E. coli* O157:H7) or had a narrow host range activity (Carter et al., 2012; Dalmasso et al., 2016; Baig et al., 2017; Lin et al., 2017). In our study, the characterized *Escherichia* virus myPSH2311 was found to have broad host range activity infecting *E. coli* isolates that belonged to six different pathotypes EPEC, EHEC, ETEC, EIEC, EAEC, and UPEC besides some unknown pathotypes. This is one of the rarest reports where an *Escherichia* phage infecting six different pathotypes of *E. coli* was characterized. But another study also report the broad host range activity of *Escherichia* phage against multiple pathotypes of *E. coli*

(Manohar et al., 2018b). The studied *Klebsiella* virus myPSH1235 showed broad host range activity against *K. pneumoniae* belonging to serotypes K1, K2, K5 besides some unknown serotypes. An earlier study showed that a multi-host *Klebsiella* phage ϕK64-1 was capable to infect *Klebsiella* capsular types K1, KN4, KN5, K11, K21, K25, K30, K35, K64, and K69. It is stated that the multi-host infectivity of the bacteriophages is due to the presence of multiple depolymerases in the tail-fibers (Pan et al., 2017). The role of polyvalent phages in phage therapy needs more detailed investigation. The studies on *Enterobacter* phage thus far are very minimal or reports of established *Enterobacter* phages capable of infecting various strains or species are scarce (Li et al., 2016a; Pereira et al., 2016). The characterized *Enterobacter* virus myPSH1140 in our study belonging to *Myoviridae* family showed activity against four species of *Enterobacter E. cloacae*, *E. hormaechei*, *E. asburiae,* and *E. aerogenes.* Our study and those of some others strongly suggest that there are bacteriophages that can have broad host range activity against different strains or species or genera of bacteria (Hamdi et al., 2017). A recent study showed that bacteriophages SH6 and SH7 were capable of infecting bacteria from different genera – *E. coli* O157:H7, *Shigella flexneri*, *Salmonella paratyphi,* and *Shigella dysenteriae* (Hamdi et al., 2017). There are studies that showed 'narrow' host range specificity of bacteriophages mainly because of the use of standard isolation procedure where single host strain of bacteria is used (Li et al., 2016b; Ross et al., 2016; Hamdi et al., 2017). Future studies should focus on testing the host range activity of bacteriophages but it is also believed that host range activity is not a fixed property of bacteriophages and can evolve overtime (Ross et al., 2016; Hamdi et al., 2017). It should also be noted that we found dissimilarities in the results obtained between spot test and plaque assay in host range activity determination, therefore plaque assay is recommended in order to obtain productive infection for the determination of host range activity of phages (Mirzaei and Nilsson, 2015).

The three characterized bacteriophages had different growth profile, which is one of the important characteristics of lytic bacteriophages. In this study, *Escherichia* virus myPSH2311 (*Podovirus*) had a growth profile with the latent period of 26 min and burst size of 110 phages/infected cell, which is beneficial for therapy. Earlier studies using *Podoviridae* phages showed latency period of ≈15–25 min and burst size of ≈50–80 phages/infected cell (Dalmasso et al., 2016). An earlier study on *Podoviridae* phages infecting *Klebsiella* species was found to have a growth profile with the latency period of 15 min and burst size of ≈50–60 phages/infected cell (Chaturongakul and Ounjai, 2014). In our study, *Klebsiella* virus myPSH1235 belonging to *Podoviridae* family was found to have a latent period of 40 min and burst size of 120 phages/infected cell, which is beneficial for therapy. It was very clear from this study that the growth profile of bacteriophages is not completely dependent on either the family or the host these bacteriophages infect. The bacteriophages belonging to *Myoviridae* family are known to have shorter life cycles and similarly the characterized *Myoviridae* phage (*Enterobacter* phage myPSH1140) had a latent period of 11 min and burst size of 135 phages/infected cell. It was also noted in this and earlier studies that the number of progeny phage particles (burst size) largely depends on the availability of host bacterial cells (Dalmasso et al., 2016). Life cycle parameters of bacteriophages will play significant role in determining both *in vitro* and *in vivo* phage activities (during therapy), because phage multiplication is directly proportional to reduction in bacteria.

The genomes of all the three characterized phages showed 70–100% similarities to the already existing phage genomes in the database. *Escherichia* virus myPSH2311 (68,712 bp) was found to have 88% sequence similarity with *Escherichia* phage vB_EcoP_SU10 (77,327 bp). The endolysin gene (ORF 12) was found to have 98% sequence similarity with *Escherichia* virus phiEco32 and 97% sequence similarity with *Escherichia* phage vB_EcoP_SU10. The DNA injection protein (ORF 17) was detected to have 98% sequence similarity with *Escherichia* phage vB_EcoP_SU10. The genome does not have toxins or toxin-related genes, and none of the genomic markers representing a temperate or lysogenic lifestyle was detected (**Supplementary Table S4**). *Escherichia* phage vB_EcoP_SU10 is a C3 morphotype phage but *Escherichia* virus myPSH2311 does not have any elongated regions in its morphological characterization (Mirzaei et al., 2014) and related to T4-phages (Petrov et al., 2010). *Klebsiella* virus myPSH1235 was found to have 80% similarity with *Klebsiella* phage vB_KpnP_KpV48. *Klebsiella* virus myPSH1235 has a genome size of 45,135 bp with 49 CDS compared to *Klebsiella* phage vB_KpnP_KpV48, which has a genome size of 44,623 bp with 57 CDS. According to the genome morphology, phylogenetic analysis and sequence similarities, the *Klebsiella* virus myPSH1235 is classified within the genus *Kp34virus*, subfamily *Autographivirinae*, family *Podoviridae*. *Klebsiella* phage vB_KpnP_KpV48 has no capsular specificity and similarly, *Klebsiella* virus myPSH1235 was also found to infect *K. pneumoniae* of capsular types K1, K2 and K5 (Solovieva et al., 2018). From clinical point of view, the *K. pneumoniae* capsular types K1 and K2 are the most virulent strains and that the infections caused by these strains can be eliminated using *Klebsiella* virus myPSH1235 is a promising result, which needs further exploration. *Enterobacter* virus myPSH1140 was found to have a large genome size of 172,614 bp with 240 CDS with 92% similarity with *Enterobacter* phage CC31 (165,540 bp and 279 CDS) and 90% similarity to *Enterobacter* phage PG7 (173,276 and 294 bp). The genome contains 240 proteins or CDS and all the identified proteins were found to have 90–100% sequence similarity with the *Enterobacter* phage CC31 and *Enterobacter* phage PG7. Similarities in the phage genome showed that there is abundance of these phages in the environment and therefore they may be isolated for therapeutic purpose.

Earlier studies on phage cocktails showed promising results in reducing the bacterial load in both *in vitro* and *in vivo* models (Lin et al., 2017; Pan et al., 2017). In our *in vitro* experiments, a phage cocktail that was prepared using the three newly isolated bacteriophages infecting three different genera of bacteria (*Escherichia* virus myPSH2311 against *E. coli*, *Klebsiella* virus myPSH1235 against *K. pneumoniae* and *Enterobacter* virus myPSH1140 against *Enterobacter* species) showed promising results in totally suppressing the bacterial load within 24 h. The phage cocktails reported in this study consisting of multiple

phage types could thus prove to be effective as clinical therapeutic agents (Chan et al., 2013; Kęsik-Szeloch et al., 2013). Ours is one of the rarest studies to use phage cocktails against different genera of bacteria. *In vivo* activity of these phage cocktails also showed promising results and the results are published elsewhere (Manohar et al., 2018a).

The strength of our study is that we established the lytic effectiveness of the phages and their cocktail against clinical bacterial isolates of three genera that are known to be pathogenic. Further we also demonstrated the lytic effectiveness of these phages and their cocktail against pathogenic bacteria that were resistant to two last resort antibiotics, meropenem, and colistin. Thus further experiments can be taken up for *in vivo* studies in search of a therapeutic treatment against bacterial infections resistant to these drugs.

CONCLUSION

The emergence of multi-drug resistant bacterial strains is a global threat which needs to be addressed by using alternative therapies, such as phage therapy. The three highlighted bacteriophages (*Escherichia* virus myPSH2311 against *E. coli*, *Klebsiella* virus myPSH1235 against *K. pneumoniae* and *Enterobacter* virus myPSH1140 against *Enterobacter* species) and their cocktails showed promising *in vitro* results that may be extended for use as biocontrol agents in some clinical applications. The development of phage cocktails could be considered for the effective treatment of bacterial infections consisting of broad targets. Hopefully, in future, availability of increased repertoire of phages may allow the development of multi-phage cocktail therapy possible.

DATA AVAILABILITY

All the data that support the findings of this study have been deposited in GenBank with the accession numbers MG976803 (*Escherichia* phage myPSH2311), MG972768 (*Klebsiella* phage myPSH1235), and MG999954 (*Enterobacter* phage myPSH1140).

AUTHOR CONTRIBUTIONS

PM and RN collected the isolates and did bacteriophage experiments, undertook the laboratory work, and wrote the initial manuscript. AT, CL, and RN interpreted the data. CL and AT revised and edited the manuscript. All authors approved the final version of the manuscript.

FUNDING

The authors would like to thank Vellore Institute of Technology (VIT) for providing research facilities to complete the work. This research was partly supported by Swedish Research Council with grants to CL (Grant Nos. 2012-02889 and 2017-01327). The authors would also like to thank Council of Scientific and Industrial Research (CSIR) for providing financial assistance (SRF) to support this research.

SUPPLEMENTARY MATERIAL

The Supplementary Material for this article can be found online at: https://www.frontiersin.org/articles/10.3389/fmicb.2019.00574/full#supplementary-material

REFERENCES

Baig, A., Colom, J., Barrow, P., Schouler, C., Moodley, A., Lavigne, R., et al. (2017). Biology and genomics of an historic therapeutic *Escherichia coli* bacteriophage collection. *Front. Microbiol.* 8:1652. doi: 10.3389/fmicb.2017.01652

Cao, F., Wang, X., Wang, L., Li, Z., Che, J., Wang, L., et al. (2015). Evaluation of the efficacy of a bacteriophage in the treatment of pneumonia induced by multidrug resistance *Klebsiella pneumoniae* in mice. *Biomed. Res. Int.* 2015:752930. doi: 10.1155/2015/752930

Carter, C. D., Parks, A., Abuladze, T., Li, M., Woolston, J., Magnone, J., et al. (2012). Bacteriophage cocktail significantly reduces *Escherichia coli* O157: H7 contamination of lettuce and beef, but does not protect against recontamination. *Bacteriophage* 2, 178–185. doi: 10.4161/bact.22825

Chan, B. K., Abedon, S. T., and Loc-Carrillo, C. (2013). Phage cocktails and the future of phage therapy. *Future Microbiol.* 8, 769–783. doi: 10.2217/fmb.13.47

Chaturongakul, S., and Ounjai, P. (2014). Phage–host interplay: examples from tailed phages and Gram-negative bacterial pathogens. *Front. Microbiol.* 5:442. doi: 10.3389/fmicb.2014.00442

Chibani-Chennoufi, S., Bruttin, A., Dillmann, M. L., and Brüssow, H. (2004). Phage-host interaction: an ecological perspective. *J. Bacteriol.* 186, 3677–3686. doi: 10.1128/JB.186.12.3677-3686.2004

Clinical and Laboratory Standards Institute [CLSI] (2018). *Performance Standards for Antimicrobial Susceptibility Testing; Twenty-Fifth Informational Supplements. Approved Standard M100-S28*. Wayne, PA: Clinical and Laboratory Standards Institute [CLSI].

Dalmasso, M., Strain, R., Neve, H., Franz, C. M., Cousin, F. J., Ross, R. P., et al. (2016). Three new *Escherichia coli* phages from the human gut show promising potential for phage therapy. *PLoS One* 11:e0156773. doi: 10.1371/journal.pone.0156773

Gill, J. J., and Hyman, P. (2010). Phage choice, isolation, and preparation for phage therapy. *Curr. Pharma. Biotechnol.* 11, 2–14. doi: 10.2174/138920110790725311

Hamdi, S., Rousseau, G. M., Labrie, S. J., Tremblay, D. M., Kourda, R. S., Slama, K. B., et al. (2017). Characterization of two polyvalent phages infecting *Enterobacteriaceae*. *Sci. Rep.* 7:40349. doi: 10.1038/srep40349

Hung, C. H., Kuo, C. F., Wang, C. H., Wu, C. M., and Tsao, N. (2011). Experimental phage therapy in treating *Klebsiella pneumoniae*-mediated liver abscesses and bacteremia in mice. *Antimicrob. Agents Chemother.* 55, 1358–1365. doi: 10.1128/AAC.01123-10

Kęsik-Szeloch, A., Drulis-Kawa, Z., Weber-Dąbrowska, B., Kassner, J., Majkowska-Skrobek, G., Augustyniak, D., et al. (2013). Characterising the biology of novel lytic bacteriophages infecting multidrug resistant *Klebsiella pneumoniae*. *Virol. J.* 10:100. doi: 10.1186/1743-422X-10-100

Krupovic, M., Dutilh, B. E., Adriaenssens, E. M., Wittmann, J., Vogensen, F. K., Sullivan, M. B., et al. (2016). Taxonomy of prokaryotic viruses: update from the ICTV bacterial and archaeal viruses subcommittee. *Arch. Virol.* 161, 1095–1099. doi: 10.1007/s00705-015-2728-0

Levin, B. R., and Bull, J. J. (2004). Population and evolutionary dynamics of phage therapy. *Nat. Rev. Microbiol.* 2, 166–73. doi: 10.1038/nrmicro822

Li, E., Wei, X., Ma, Y., Yin, Z., Li, H., Lin, W., et al. (2016a). Isolation and characterization of a bacteriophage phiEap-2 infecting multidrug resistant *Enterobacter aerogenes*. *Sci. Rep.* 6:28338. doi: 10.1038/srep28338

Li, E., Zhao, J., Ma, Y., Wei, X., Li, H., Lin, W., et al. (2016b). Characterization of a novel *Achromobacter* xylosoxidans specific siphoviruse: phiAxp-1. *Sci. Rep.* 6:21943. doi: 10.1038/srep21943

Lin, D. M., Koskella, B., and Lin, H. C. (2017). Phage therapy: an alternative to antibiotics in the age of multi-drug resistance. *World J. Gastrointest. Pharmacol. Therapeut.* 8:162. doi: 10.4292/wjgpt.v8.i3.162

Manohar, P., Nachimuthu, R., and Lopes, B. S. (2018a). The therapeutic potential of bacteriophages targeting gram-negative bacteria using *Galleria mellonella* infection model. *BMC Microbiol.* 18:97. doi: 10.1186/s12866-018-1234-4

Manohar, P., Tamhankar, A. J., Lundborg, C. S., and Ramesh, N. (2018b). Isolation, characterization and in vivo efficacy of *Escherichia* phage myPSH1131. *PLoS One* 13:e0206278. doi: 10.1371/journal.pone.0206278

McVay, C. S., Velásquez, M., and Fralick, J. A. (2007). Phage therapy of *Pseudomonas aeruginosa* infection in a mouse burn wound model. *Antimicrob. Agents Chemother.* 51, 1934–1938. doi: 10.1128/AAC.01028-06

Mendes, J. J., Leandro, C., Mottola, C., Barbosa, R., Silva, F. A., Oliveira, M., et al. (2014). *In vitro* design of a novel lytic bacteriophage cocktail with therapeutic potential against organisms causing diabetic foot infections. *J. Med. Microbiol.* 63, 1055–1065. doi: 10.1099/jmm.0.071753-0

Mirzaei, M. K., Eriksson, H., Kasuga, K., Haggård-Ljungquist, E., and Nilsson, A. S. (2014). Genomic, proteomic, morphological, and phylogenetic analyses of vB_EcoP_SU10, a podoviridae phage with C3 morphology. *PLoS One* 9:e116294. doi: 10.1371/journal.pone.0116294

Mirzaei, M. K., and Nilsson, A. S. (2015). Isolation of phages for phage therapy: a comparison of spot tests and efficiency of plating analyses for determination of host range and efficacy. *PLoS One* 10:e0118557. doi: 10.1371/journal.pone.0118557

Morens, D. M., Folkers, G. K., and Fauci, A. S. (2004). The challenge of emerging and re-emerging infectious diseases. *Nature* 430, 242–249. doi: 10.1038/nature02759

Pan, Y. J., Lin, T. L., Chen, C. C., Tsai, Y. T., Cheng, Y. H., Chen, Y. Y., et al. (2017). *Klebsiella* phage ΦK64-1 encodes multiple depolymerases for multiple host capsular types. *J. Virol.* 91:e2457–6. doi: 10.1128/JVI.02457-16

Pereira, S., Pereira, C., Santos, L., Klumpp, J., and Almeida, A. (2016). Potential of phage cocktails in the inactivation of *Enterobacter cloacae*-an in vitro study in a buffer solution and in urine samples. *Virus Res.* 211, 199–208. doi: 10.1016/j.virusres.2015.10.025

Petrov, V. M., Ratnayaka, S., Nolan, J. M., Miller, E. S., and Karam, J. D. (2010). Genomes of the T4-related bacteriophages as windows on microbial genome evolution. *Virol. J.* 7:292. doi: 10.1186/1743-422X-7-292

Rios, A. C., Moutinho, C. G., Pinto, F. C., Del Fiol, F. S., Jozala, A., Chaud, M. V., et al. (2016). Alternatives to overcoming bacterial resistances: state-of-the-art. *Microbiol. Res.* 191, 51–80. doi: 10.1016/j.micres.2016.04.008

Rohwer, F. (2003). Global phage diversity. *Cell* 113:141. doi: 10.1016/S0092-8674(03)00276-9

Ross, A., Ward, S., and Hyman, P. (2016). More is better: selecting for broad host range bacteriophages. *Front. Microbiol.* 7:1352. doi: 10.3389/fmicb.2016.01352

Schlossberg, D. (ed.) (2015). *Clinical Infectious Disease*. Cambridge: Cambridge University Press. doi: 10.1017/CBO9781139855952

Solovieva, E. V., Myakinina, V. P., Kislichkina, A. A., Krasilnikova, V. M., Verevkin, V. V., Mochalov, V. V., et al. (2018). Comparative genome analysis of novel podoviruses lytic for hypermucoviscous *Klebsiella pneumoniae* of K1, K2, and K57 capsular types. *Virus Res.* 243, 10–18. doi: 10.1016/j.virusres.2017.09.026

Sulakvelidze, A., Alavidze, Z., and Morris, J. G. (2001). Bacteriophage therapy. *Antimicrob. Agents Chemother.* 45, 649–659. doi: 10.1128/AAC.45.3.649-659.2001

Ventola, C. L. (2015). The antibiotic resistance crisis: part 1: causes and threats. *Pharm. Therapeut.* 40, 277–283.

World Health Organization [WHO] (2014). *Antimicrobial Resistance: Global Report on Surveillance 2014*. Available at: http://www.who.int/drugresistance/documents/surveillancereport/en/

Yen, M., Cairns, L. S., and Camilli, A. (2017). A cocktail of three virulent bacteriophages prevents *Vibrio cholerae* infection in animal models. *Nat. Commun.* 8:14187. doi: 10.1038/ncomms14187

Conflict of Interest Statement: The authors declare that the research was conducted in the absence of any commercial or financial relationships that could be construed as a potential conflict of interest.

frontiers in Microbiology

ORIGINAL RESEARCH
published: 20 February 2019
doi: 10.3389/fmicb.2019.00266

Isolation and Genomic Characterization of an *Acinetobacter johnsonii* Bacteriophage AJO2 From Bulking Activated Sludge

*Niansi Fan[1,2], Min Yang[2], Rencun Jin[1] and Rong Qi[2]**

[1] College of Life and Environmental Sciences, Hangzhou Normal University, Hangzhou, China, [2] State Key Laboratory of Environmental Aquatic Chemistry, Research Center for Eco-Environmental Sciences, University of Chinese Academy of Sciences, Beijing, China

A novel *Podoviridae* lytic phage AJO2, specifically infecting *Acinetobacter johnsonii*, was isolated from bulking activated sludge. The one-step growth experiment showed that the latent period and burst size of AJO2 were estimated to be 30 min and 78.1 phages per infected cell, respectively. The viability test indicated that neutral conditions (pH 6–8) were table for AJO2 survival, while it was sensitive to high temperature (≥60°C) and ultraviolet treatment (254 nm). Genomic sequencing revealed that the AJO2 had a linearly permuted, double-stranded (ds) DNA consisting of 38,124 bp, with the G+C content of 41 mol%. A total of 58 putative open reading frames (ORFs), 11 pairs of repeats and 11 promoters were identified. The AJO2 genome had a modular gene structure which shared some similarities to those of *A. baumanii* phages. However, genomic comparative analysis revealed many differences among them, and novel genes were identified in the AJO2 genome. These results contribute to subsequent researches on the interaction between bacteriophages and hosts in wastewater treatment, especially during the bulking period. Additionally, the newly isolated phage could be a good candidate as a therapeutic agent to control nosocomial infections caused by *A. johnsonii.*

Keywords: *Acinetobacter johnsonii*, bacteriophage, phage AJO2, activated sludge, genome sequence

OPEN ACCESS

Edited by:
Robert Czajkowski,
University of Gdańsk, Poland

Reviewed by:
Zhongjing Lu,
Kennesaw State University, United States
Paul Hyman,
Ashland University, United States

****Correspondence:***
Rong Qi
fns0219@aliyun.com

Specialty section:
This article was submitted to Virology, a section of the journal Frontiers in Microbiology

Received: *15 November 2018*
Accepted: *01 February 2019*
Published: *20 February 2019*

Citation:
Fan N, Yang M, Jin R and Qi R (2019) Isolation and Genomic Characterization of an Acinetobacter johnsonii Bacteriophage AJO2 From Bulking Activated Sludge. Front. Microbiol. 10:266. doi: 10.3389/fmicb.2019.00266

INTRODUCTION

As a common problem in activated sludge systems, sludge bulking draws extensive attention worldwide because of its serious consequences, such as poor sludge settle ability, water quality deterioration, sludge loss, or even system failure (Wagner, 1982; Madoni et al., 2000; Martins et al., 2004). Most sludge bulking events are caused by the overgrowth of filamentous bacteria, such as *Microthrix parvicella*, *Nostocoida limicola,* and *Nocardia nova* (Jenkins et al., 2004; Wang et al., 2014). In addition, non-filamentous bacteria also play a vital role in system function maintenance, such as *Nitrospira*, *Nitrosomonas*, polyphosphate-accumulating organisms (PAOs) and glycogen-accumulating organisms (GAOs) (Levantesi et al., 2010; Nielsen et al., 2012). The dynamic equilibrium of the microbial community is an important prerequisite for the operational stability of wastewater treatment plants (WWTPs).

Bacteriophages are the most abundant biological entities in the environment (Chibani-Chennoufi et al., 2004; Mann, 2005). Phages appear to be active components of activated sludge systems and phage-mediated bacterial mortality has the potential to influence treatment performance by influencing the bacterial abundance (Withey et al., 2005). On the one hand, analyzing the dynamic changes of bacteriophages that infect key functional groups contributes to understanding the malfunctions in WWTPs. On the other hand, the host specificity of phages makes them a potentially efficient tool to eliminate bulking-related filamentous bacteria. For example, the HHY-phage lysing *Haliscomenobacter hydrossis* (Kotay et al., 2011), SNP-phage lysing *Sphaerotilus natans* (Kotay et al., 2010) and THE1 lysing *Tetrasphaera jenkinsii* (Petrovski et al., 2012) have been isolated from activated sludge with the goal of filamentous bulking control. However, the physiological and genomic characterization of phages is incomplete and phage-host interaction mechanisms are still unclear. The main reason is that only a few phages have been isolated and sequenced, limiting its characterization and further application of "phage therapy." Therefore, it is urgent to isolate and genetically characterize more phages in activated sludge, especially during the bulking period.

In this study, phage AJO2 specific to *A. johnsonii* was isolated from bulking activated sludge. Its biological characteristics and genome sequence were also determined. Comparative analyses of AJO2, the previously-isolated phage AJO1 (Fan et al., 2017) and other phages with closely phylogenetic relationships were conducted on the basis of their morphologies, host ranges, burst sizes and genomic features. Results showed that AJO1 and AJO2 shared some similarity, but their DNA sequences and annotations revealed many differences and novel attributes. The new phage provides a valuable resource for further investigations on its physiochemical properties and relationships between phages and hosts.

MATERIALS AND METHODS

Bacterial Strains and Culture Conditions

A total of 44 strains were isolated from a large municipal WWTP in Beijing during a bulking period (SVI = 180 mL g^{-1}). 16s rRNA gene amplification and sequencing were performed for their precise identification. As one of the dominant cultivatable microorganisms, *A. johnsonii* strain Pt405 was selected as the host bacterium for phage isolation, enrichment and characterization. This strain could form 0.5 to 2.0 mm in diameter, milk-white, opaque, round colonies on LB agar at 30°C. Another 17 strains were used for host range determination in the study (**Supplementary Table S1**). Nine strains from different phyla, such as *Kocuria rosea*, *Bacillus thuringiensis*, *Flavobacterium*, *Delftia tsuruhatensis* strain M6 etc., were also isolated from the bulking sludge in the same period. Eight strains within *Acinetobacter* were obtained from China General Microbiological Culture Collection Center (CGMCC), including *A. tandoii*, *A. lwoffii*, *A. junii*, *A. haemolyticus*, *A. calcoaceticus*, *A. baumannii*, *A. radioresistens*, and *A. bouvetii*. These strains were cultured on nutrient agar at 30°C. The turbidimetric method was adopted to monitor bacterial growth through measuring optical density at 600 nm (OD_{600}). All strains were stored at −20°C for the short term and at −80°C with the equivalent 30% glycerol for the long term.

Phage Isolation and Transmission Electron Microscopy (TEM)

The isolated *A. johnsonii* strain Pt405 was used for the isolation of a lytic bacteriophage. A volume of 20 L fresh sludge sample was centrifuged at 8000 × *g* for 20 min and filtered in turn through 0.45 and 0.22 μm pore size syringe filter (Millipore, United States) to remove bacterial debris. For further enrichment, tangential flow ultrafiltration (Vivaflow 200, Sartorius, Germany) was performed and the final volume of filtrate was 150 mL. Fresh host strain was propagated in LB broth for 4−−6 h at 30°C. Subsequently, 50 mL bacterial suspension and 1 mL filtrate were gently mixed, and allow to stand for at least 1 h at room temperature with the aim of better absorption between phage and host. Afterward, the mixture was cultured by shaking (100 rpm) at 30°C for 6 h. Modified double-layer agar (DLA) assays (Adams, 1959) were performed to confirm the plaques. In brief, equal volumes of bacterial suspension and enriched filtrate were added into warm LB agar (containing 0.7% agar), and poured on a prepared LB agar plate (containing 1.5% agar). Bacteriophage plaques could be observed after incubating at 30°C overnight, and single plaque purification was performed six times according to Fan et al. (2017). The purified phages were stored in SM buffer (10 mM Tris-HCl, pH 7.5, 10 mM $MgSO_4{\cdot}7H_2O$ and 100 mM NaCl) at 4°C for short periods.

Phage particles were precipitated according to the NaCl/PEG protocol (Petrovski et al., 2012), and observed using transmission election microscopy (H7500, Hitachi, Japan) at 100 kV as described by Fan et al. (2017). The morphological features of phages were observed, and the family to which they belong could be determined.

General Characteristics of Phage

The one-step growth curve was determined at the multiplicity of infection (MOI) of 0.001 according to a previous description (Fan et al., 2017). Spectrophotometry (Jing Dan et al., 2013) and the spot-test method (Chopin et al., 1976) were performed to determine the host range. Briefly, bacterial suspensions (OD_{600}∼0.2) were mixed with 100 μL phage stock, and OD_{600} of each mixture was measured using spectrophotometer after 40 min incubation at 30°C. In the spot-test assay, 50 μL phage stock ($>10^7$ PFU mL^{-1}) was spotted on prepared agar plates spread with the tested stains.

Resistance to Various Environmental Factors

Considering the application prospects, the phage susceptibility to environmental changes was evaluated, including temperature, pH and ultraviolet (UV) light. In the thermal treatment experiment, 1.5 mL phage stock was incubated at 55, 60, and 70°C water bath for 5, 10, 15, and 20 min, respectively. In the pH test, phage stocks were incubated in media with pH of 2.0–11.0 (1.0 interval)

at 30°C. Advanced oxidation processes like UV photolysis have been widely used in wastewater treatment (De la Cruz et al., 2013; Deng and Zhao, 2015), thus UV light was selected as one of the environmental factors in this study. In the UV inactivation experiments, phage stocks were exposed under a vertical UV light (254 nm, 15W) for 10, 30, 60, 120, and 180 s, respectively. Phage titers of each set were determined using the double-layer method.

Genomic Sequencing and Annotation

Phage DNA was extracted using SDS/proteinase K as previously described by Petrovski et al. (2011). DNase I (Sigma), RNase A (Sigma) and Mung Bean Nuclease (Takara) were used to determine the nucleic acid type with the working concentration of 1 unit μL^{-1} at 37°C for 1 h. Mung Bean Nuclease is a single-strand-specific nuclease. Enzyme *Spe*I (37°C for 3 h) was also used to determine whether the genome was linear or circular.

Genomic DNA was sequenced at Novogene Company (Beijing, China). Reads were assembled using SOAP *de novo* software. Open reading frames (ORFs) were predicted using ORF Finder[1] and the GeneMarkS interface[2]. Sequence similarity was analyzed using the BLAST X interface against a non-redundant database. Putative functions were predicted based on the BLAST P algorithm (Parsley et al., 2010; Jebri et al., 2016). The conserved motifs were identified using the conserved domain database (CDD)[3], and the Pfam database[4] was used for predicted protein family allocation (Finn et al., 2010). The putative rRNA, tRNA, transfer mRNA (tmRNA) and sRNA were screened using RNAmmer (Lagesen et al., 2007), rRNAscan-SE (Lowe and Eddy, 1997; Schattner et al., 2005) and Rfam (Burge et al., 2012). Putative promoters and terminators were predicted by neural network promoter prediction and the FindTerm web tool[5] with an energy threshold value of −15. In addition, putative restriction enzyme cutting sites were predicted by NEBcutter V2.0 program[6] (Vincze et al., 2003). Phylogenetic analysis was performed using MEGA7 via the neighbor-joining method (Kumar et al., 2016). Based on the annotated phage genome, GenBank files were created with Sequin[7], and the sequences of several fragments from phage genome were deposited in the GenBank database.

[1] www.ncbi.nlm.nih.gov/projects/gorf
[2] http://topaz.gatech.edu/
[3] http://www.ncbi.nlm.nih.gov/Structure/cdd/cdd.shtml
[4] http://pfam.sanger.ac.uk

RESULTS AND DISCUSSION

Isolation and General Features of Bacteriophage AJO2

Phage AJO2 was isolated from a bulking sludge sample as a clear-plaque former against *A. johnsonii* strain Pt405. TEM observations (**Figure 1**) revealed that AJO2 had a collar and tail structure, appearing to belong to the order Caudovirales (Ackermann, 1998). Its icosahedral head (50 ± 2 nm) and

[5] http://linux1.softberry.com/berry.phtml
[6] http://nc2.neb.com/NEBcutter2/
[7] www.ncbi.nlm.nih.gov/projects/Sequin/

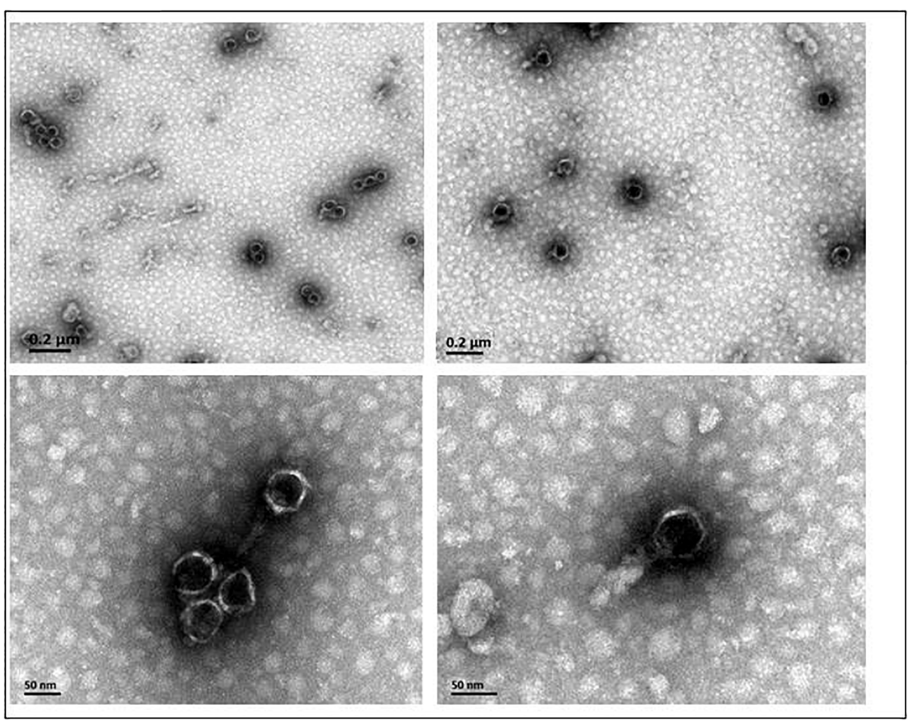

FIGURE 1 | The morphology of phage AJO2 observed by TEM.

short tail (6 ± 2 nm) is a typical morphology of the family *Podoviridae*. Compared with other *Podoviridae* phages, AJO2 was relatively smaller than Acibel007 (60 nm head and 10 nm tail) (Merabishvili et al., 2014), ϕAB6 (60 nm head and 11 nm tail) (Lai et al., 2016) and Abp1 (55 nm head and 15 nm tail) (Huang et al., 2013).

The one-step growth curve (**Supplementary Figure S1**) indicated that the latent period of AJO2 was around 30 min, and the rise period was completed at 80 min. The burst size was calculated to be 78.1 phages per infected cell. Both spot assay (**Supplementary Table S2**) and spectrophotometry results (**Supplementary Figure S2**).

Viability of AJO2 Under Various Conditions

The effects of pH, thermal and UV light on phage AJO2 were evaluated in this study. In the pH tests (**Figure 2A**), the survival rate of AJO2 maintained a level above 70% over a pH range of 6.0–8.0 and the optimal pH was 7.0. Compared with alkaline conditions (pH > 8.0), the activity of AJO2 was less affected under weakly acidic conditions (5.0–6.0). Pre-experiments showed that AJO2 was still infective after incubation at 46°C for 30 min, so higher temperatures were chosen in the thermal tests (**Figure 2B**). AJO2 could maintain a relatively high level of titer at 55°C, but its survival rate dramatically decreased below 5% at 60°C for 15 min. When the temperature increased to 70°C, AJO2 almost lost viability, indicating that the survival rate of AJO2 decreased with increasing temperature and exposure time. Similarly, AJO2 was also sensitive to UV light of 254 nm (**Figure 2C**). The survival rate of AJO2 quickly decreased from 100 to 14.63% within 30 s, and only 0.01% of phages remained infective after 3 min treatment. Although, this is a rough evaluation on the effect of UV light, it could reflect the AJO2 sensitivity to UV light to a certain extent, which provides valuable information for its practical application in the future. Therefore, neutral conditions were suitable for AJO2 survival, and it could tolerate relatively high temperatures (<60°C) and a short-term exposure to the UV light.

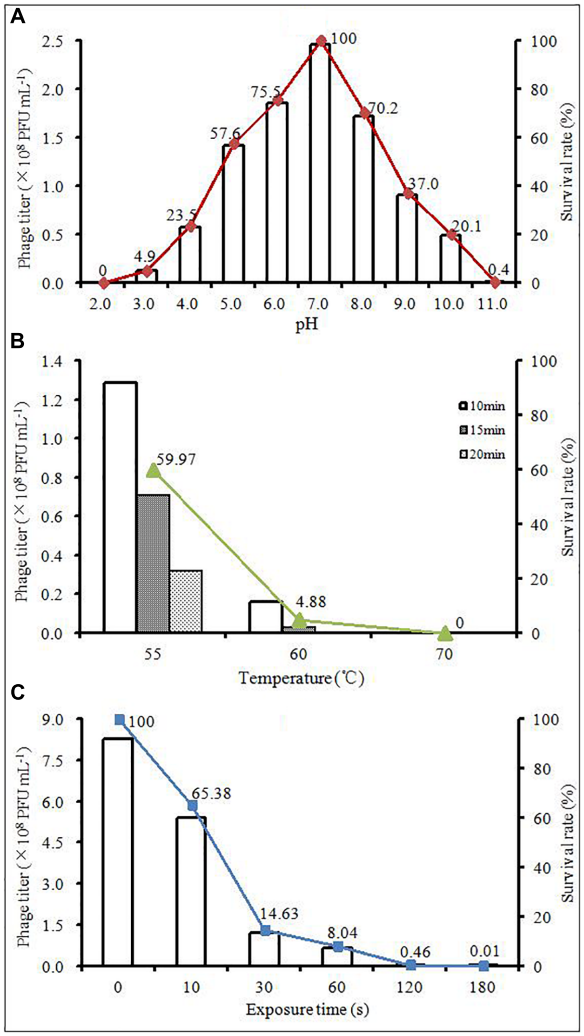

FIGURE 2 | Changes in the titer of AJO2 under different **(A)** temperature, **(B)** pH, and **(C)** time of exposure to UV light at 254 nm.

Genome Analysis and Annotation

According to the gel electrophoresis results, the nucleic acid of AJO2 was degraded by DNase I, but undegraded by RNase A and mung bean nuclease, illustrating that the nucleic acid of AJO2 was double-strand DNA (dsDNA). Restriction endonuclease experiments showed that the genome had one *Spe*I restriction site. Therefore, genome digestion with *Spe*I would produce two fragments if it was linear and only one fragment if circular. The genome of AJO2 was confirmed to be linear by *Spe*I digestion with two bands produced (data not shown). The nucleotide sequence of AJO2 genome was determined with an average of 50× DNA sequencing coverage, and has been deposited in GenBank under accession numbers MH814913-MH814931. The genome of AJO2 consisted of 38,124 bp, with an average G+C content of 41 mol % (**Figure 3**). This was similar to the G+C content of host bacteria (41.4 mol %), suggesting that AJO2 was adapted to its host (Petrovski et al., 2011). Over 90% of AJO2 genome was represented by coding sequences. In total, 58 ORFs longer than 90 nucleotides were identified, including 18 ORFs on the positive strand and 40 ORFs on the opposite strand (**Table 1**). All ORFs were numbered consecutively. Thirty ORFs could be assigned predicted functions and 28 ORFs exhibited no significant identity to any hypothetical protein.

The genome of AJO2 was modularly organized into five categories, including DNA modification and regulation, RNA metabolism, cell lysis, structure morphogenesis and other potential functions. The first module (*orf* 21, *orf* 41, *orf* 47–49, *orf* 51, and *orf* 54) encoded proteins involved in phage head, tail and membrane morphogenesis. Interestingly, most of these genes were continuously distributed between 30,000 and 35,000 bp. A similar phenomenon has been reported that structure-related genes in tailed-phage genomes are generally

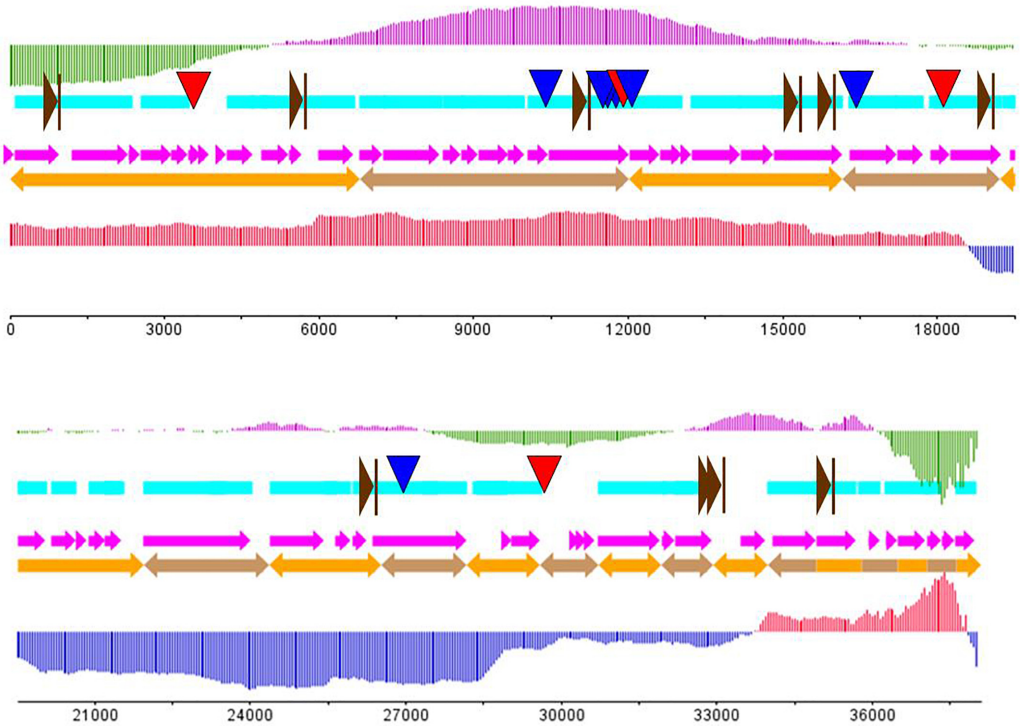

FIGURE 3 | The putative genome draft of phage AJO2. Sky-blue band indicates gene-encoding regions in the AJO1 genome; orange arrows indicate assembled scaffolds and pink arrows represent predicted ORFs in the AJO1 genome. The GC skew is calculated as (G-C)/(G+C) and the GC plot shows GC% content. The upper vertical line with fixed intervals represents the GC skew (purple for positive and green for negative); the lower vertical lines represent the GC plot (red for above-average and blue for below-average). The downward arrows give the locations of repeats (blue for LINE and red for SINE). The rightward brown arrows indicate the putative promoters.

clustered together and located behind the head protein genes (Brüssow and Desiere, 2001).

The region between *orf* 4 and *orf* 6 was predicted to participate in DNA replication. Two ORFs (*orf* 4 and *orf* 6) putatively encoded a DnaG-like primase (PHA02031), while *orf* 5 encoded a topoisomerase (PF01751). The Toprim (topoisomerase-primase) domain is a structurally conserved domain of ∼100 amino acids with two conserved motifs, one of which centers at a glutamate and the other at two aspartates (DxD). The glutamate is probably involved in catalysis, whereas the DxD motif is involved in the co-ordination of Mg (2+) required for the enzyme activity (Aravind et al., 1998). Deoxynucleoside monophosphate kinase (*orf* 27), DNA polymerase (*orf* 37), NTPases (*orf* 3) and recombination endonuclease (*orf* 23) were also revealed in the genome. The former three enzymes were related to DNA replication or repair, and the last one was related to DNA recombination. The *orf* 55 gene encoded a DNA breaking-rejoining enzyme, which was a phage integrase that mediated unidirectional site-specific recombination between two DNA recognition sequences, the phage attachment site (attP) and the bacterial attachment site (attB) (Groth and Calos, 2004). DNA-directed RNA polymerases were predicted to be encoded by *orf* 27 and *orf* 31. The N-terminal domain of DNA-directed RNA polymerase plays a role in the interactions with regions of upstream promoter DNA and nascent RNA chain, ensuring the processivity of the enzyme (Jeruzalmi and Steitz, 1998). The HTH_Tnp_4 super family putatively encoded by *orf* 14 might be a family of helix-turn-helix (HTH) motif, which has been found in all known DNA binding proteins that regulate gene expression. The HTH motif is highly similar in sequence and structure to repressor proteins, but it needs glycine to avoid steric interference (Brennan and Matthews, 1989). Such enzymes might be involved in the modification of the phage DNA.

Phage lysis modules typically consist of endolysin and holin genes that together are responsible for bacterial lysis and release of phage progeny (Daniel et al., 2007). In the AJO2 genome only the T4-type lysozyme was identified. The T4-type lysozyme processes a similar function to endolysins, which helps to release mature phage particles from the cell wall by hydrolyzing the 1,4-beta linkages between N-acetyl-D-glucosamine and N-acetylmuramic acid in peptidoglycan heteropolymers of prokaryotic cell walls. However, no ORF displaying identity to any known holin was detected within the AJO2 genome, suggesting that the presence of lysozyme may be sufficient for cell lysis, or that its functional mechanism is significantly different from previously identified lysin proteins. Mycobacteriophages have been reported to encode a novel mycolylarabinogalactan esterase (Lysin B), which facilitates lysis by compromising the integrity of the mycobacterial outer

TABLE 1 | Summary of ORFs and corresponding products in AJO2.

ORF[a]	Location[b]	Gene coordinate		Gene length (bp)	Protein function (conserved motif)[c]	*E*−value[d]
		Start	End			
1	−	2	100	99	Unknown	
2	−	102	971	870	Unknown	
3	−	1190	2305	1116	NTPases (cl17233)	1.00E-07
4	−	2308	2535	228	Putative DnaG-like primase (PHA02031)	9.00E-24
5	−	2537	3145	609	TOPRIM_primases (cl01029)	5.00E-06
6	−	3120	3470	351	Putative DnaG-like primase (PHA02031)	4.00E-07
7	−	3460	3723	264	Unknown	
8	−	3723	3866	144	Unknown	
9	−	4061	4204	144	Unknown	
10	−	4216	4731	516	Unknown	
11	−	4875	5414	540	Unknown	
12	−	5425	5680	256	Thioredoxin (cl00388)	3.00E-03
13	−	5984	6688	705	Unknown	
14	−	6777	7253	477	HTH_Tnp_4 super family (cl16321)	1.90E-03
15	−	7253	8341	1089	Unknown	
16	−	8397	8753	357	PHA 02046 super family (cl10354)	4.30E-11
17	−	8756	9088	333	Unknown	
18	−	9091	9675	585	T4-type Lysozyme (cl00222)	1.60E-15
19	−	9662	9988	327	BenE/Involved in benzoate metabolism (COG3135)	6.30E-04
20	−	10035	10460	426	Unknown	
21	−	10450	12030	1581	Collar/Phage tail collar domain (pfam07484)	7.30E-06
22	+	12029	12625	597	Unknown	
23	+	12618	13067	450	Recombination endonuclease VII (cl03794)	3.00E-10
24	+	13051	13242	192	Unknown	
25	+	13242	14177	936	Calcineurin-like phosphoesterase (pfam00149)	2.00E-05
26	+	14180	14824	645	Deoxynucleoside monophosphate kinase (cl14713)	2.20E-11
27	+	14829	16169	1341	DNA-directed RNA polymerase N-terminal (pfam14700)	5.00E-33
28	+	16290	17225	936	Unknown	
29	+	17228	17743	516	Calcineurin-like phosphoesterase (pfam00149)	4.00E-05
30	+	17876	18256	381	Unknown	
31	+	18259	19257	999	DNA-directed RNA polymerase N-terminal (cl20638)	5.00E-06
32	−	19403	20059	657	Unknown	5.30E-20
33	−	20144	20641	498	Unknown	
34	−	20649	20858	210	Unknown	
35	−	20875	21204	330	Hypothetical protein (cl10333)	
36	−	21176	21526	351	Hypothetical protein (cl10333)	4.20E-22
37	−	21943	24024	2082	DNA polymerase (cl02626)	7.40E-24
38	+	24378	25439	1062	Unknown	3.02E-21
39	+	25643	25939	297	Unknown	
40	+	25959	26258	300	Unknown	
41	+	26365	28189	1825	Phage_T7_tail super family (cl04321)	
42	−	28902	29045	144	Unknown	1.30E-06
43	−	29039	29587	548	DNA-dependent RNA polymerase (cl20211)	
44	−	30184	30381	198	Unknown	1.00E-38
45	−	30368	30487	120	Unknown	
46	−	30484	30654	171	Unknown	
47	−	30701	31900	1200	Head-tail connecting protein (cl19541)	
48	−	31926	32192	267	Tail fiber protein (cl04321)	8.00E-54
49	−	32195	32917	723	Putative internal core protein (cl20177)	6.00E-03
50	−	33462	33644	183	Hypothetical protein (PHA02030)	1.00E-16
51	+	33991	34921	930	Putative internal core protein (cl20177)	1.30E-04

(Continued)

TABLE 1 | Continued

ORF[a]	Location[b]	Gene coordinate		Gene length (bp)	Protein function (conserved motif)[c]	*E*-value[d]
		Start	End			
52	+	34924	35682	758	Hypothetical protein (PHA02030)	1.70E-41
53	+	35913	36158	246	DUF1522 super family (cl06491)	1.70E-03
54	+	36270	36488	218	Putative membrane protein (cl01069)	3.00E-03
55	–	36489	37025	536	DNA breaking-rejoining enzymes (cl00213)	6.00E-24
56	–	37066	37329	263	Unknown	
57	–	37345	37605	261	Unknown	
58	–	37602	37973	372	uPA receptor	2.30E-03

[a]ORFs were numbered consecutively. [b]+, positive strand; -, negative strand. [c]Predicted function was based on amino acid identity, conserved motifs, and gene location within functional modules. [d]The probability of obtaining a match by chance as determined by BLAST analysis. Only values of less than 10^{-3} were considered significant.

membrane linkage to the arabinogalactan–peptidoglycan layer (Payne et al., 2009).

Thioredoxin encoded by *orf* 12 is a small disulfide-containing redox protein that widely exists in all living organisms and helps to maintain a stable redox state (Holmgren, 1985). The putative gene *orf* 19 appeared to encode "BenE" protein, which possesses benzoate transmembrane transporter activity and was identified as a novel type of benzoate transporter (Saier, 2000). The last gene *orf* 58 encoded urokinase-type plasminogen activator (uPA) receptor, belonging to glycosyl-phosphatidylinositol (GPI)-linked cell-surface glycoproteins (Behrendt et al., 1991). In addition, some ORFs encoded functional proteins that were unusual in phage genomes. For example, calcineurin-like phosphoesterases (*orf* 25 and *orf* 29) contained motifs characteristic of a variety of enzymatically active phosphoesterases, but had previously only been identified in two human genes (Klabunde et al., 1996; Schwartz and Ota, 1997). The function of DFU1522 domain (*orf* 53) was unknown, and all of these proteins were from *Bradyrhizobium japonicum*.

Most putative genes were located close to each other with few intergenic spacer regions present. Regulatory sequences like promoters and terminators usually disperse in the space between genes (Lu et al., 2013). Eleven putative promoters were encoded in the AJO2 genome (**Supplementary Table S3**), and no terminators were identified using the FindTerm tool. No sequence homologs to excisionases or transposases were detected, further supporting the supposition that AJO2 is a virulent phage.

Eleven repeat structures were observed in the AJO2 genome, and these were designated R1–R11 (**Table 2**), including four long interspersed repeated sequences (LINES: R1, R2, R6, and R7), three long terminal repeats (LTR: R3–R5), three terminal repeats (TR: R8–R10) and a minisatellite DNA (also called variable number tandem repeat, VNTR). The repeat sequences occurred within genes or in intergenic regions. Two of these (R3 and R7) were located on one strand, and the rests were located on the opposite strand. All these sequences showed no similarity to any other and their functional role remains to be experimentally determined. In addition, no gene associated with pathogenicity was detected in the AJO2 genome, suggesting that AJO2 could be a potential candidate for phage therapy or control strategy against *A. johnsonii*.

Phylogenetic and Similarity Analysis

According to the genomic comparative analysis using the BLASTn algorithm, 17 Acinetobacter phages were detected with BLASTn scores above 100 (**Supplementary Table S4**). In particular, phage vB_AbaP_Acibel007 showed a high identity score of 91%, with a query coverage of 77%. As expected, AJO2 also had a relatively close relationship with vB_AbaP_Acibel007 in phylogenetic analysis (**Figure 4**). Among the 33 matches between vB_AbaP_Acibel007 and AJO2, the match with the highest score of 4774 bits located at 17,410–20,953 bp, which putatively encoded DNA-directed RNA polymerase. The highest identity similarity of 97% appeared between 23375 bp and 24592 bp, which region probably involved in encoding DNA polymerase. Screening 8 highly similar matches (score >1000, similarity >90%), most of them participated in DNA or RNA metabolism, and structure construction (**Supplementary Table S5**). The AJO2 genome sequence was also compared to that of vB_AbaP_Acibel007 using Artemis Comparison Tool (ACT) (**Figure 5A**). Although the extents of conserved regions between both phages were difficult to visualize by ACT, mainly because of multiple chromosomal rearrangements, their genomes still appeared quite different from each other.

It was notable that these phages with closer phylogenetic relationships shared a common host bacterium (*A. baumanii*), except for AJO2. The identification and adsorption between phage and host are mainly determined by phage tail structures (Lu et al., 2013). Generally, phylogenetically related phages have similar head structures, and cluster according to their capsid proteins (Bamford et al., 2005). However, three tail-related ORFs (*orf* 21, *orf* 41, and *orf* 48) in the AJO2 genome were unmatched or showed low similarity with other phages, suggesting that there could be differences among their host ranges. This was also in accordance with the previous host-range test result. In addition, the basic characteristics of phage vB_AbaP_Acibel007 and AJO2 were also different, such as host range and burst size (**Table 3**). Based on the above comparative analysis, both phages might descend from a common ancestor, but gradually diverged during evolution.

TABLE 2 | Repeats identified within the AJO2 genome.

Repeats	Type[a]	Scaffold	Coordinates		Content (%)	ORF(s)	Location[b]
			Start	End			
R1	LINE	2	10750	10810	0.1574	21	+
R2	LINE	2	11571	11622	0.1338	21	+
R3	LTR	2	11623	11670	0.1233	21	–
R4	LTR	2	11724	11806	0.2151	21	+
R5	LTR	2	11967	12008	0.1075	21	+
R6	LINE	4	16375	16438	0.1653	28	+
R7	LINE	8	26774	26826	0.1364	41	–
R8	TR	1	3616	4287	1.7600	7–10	+
R9	TR	4	18145	18297	0.3987	30–31	+
R10	TR	10	29691	29715	0.0630	44	+
R11	VNTR	2	11671	11723	0.1364	21	+

[a] *LINES, long interspersed repeated sequences; LTR, long terminal repeats; TR, terminal repeats; VNTR, variable number tandem repeat or minisatellite DNA.* [b] *+, positive strand; -, negative strand.*

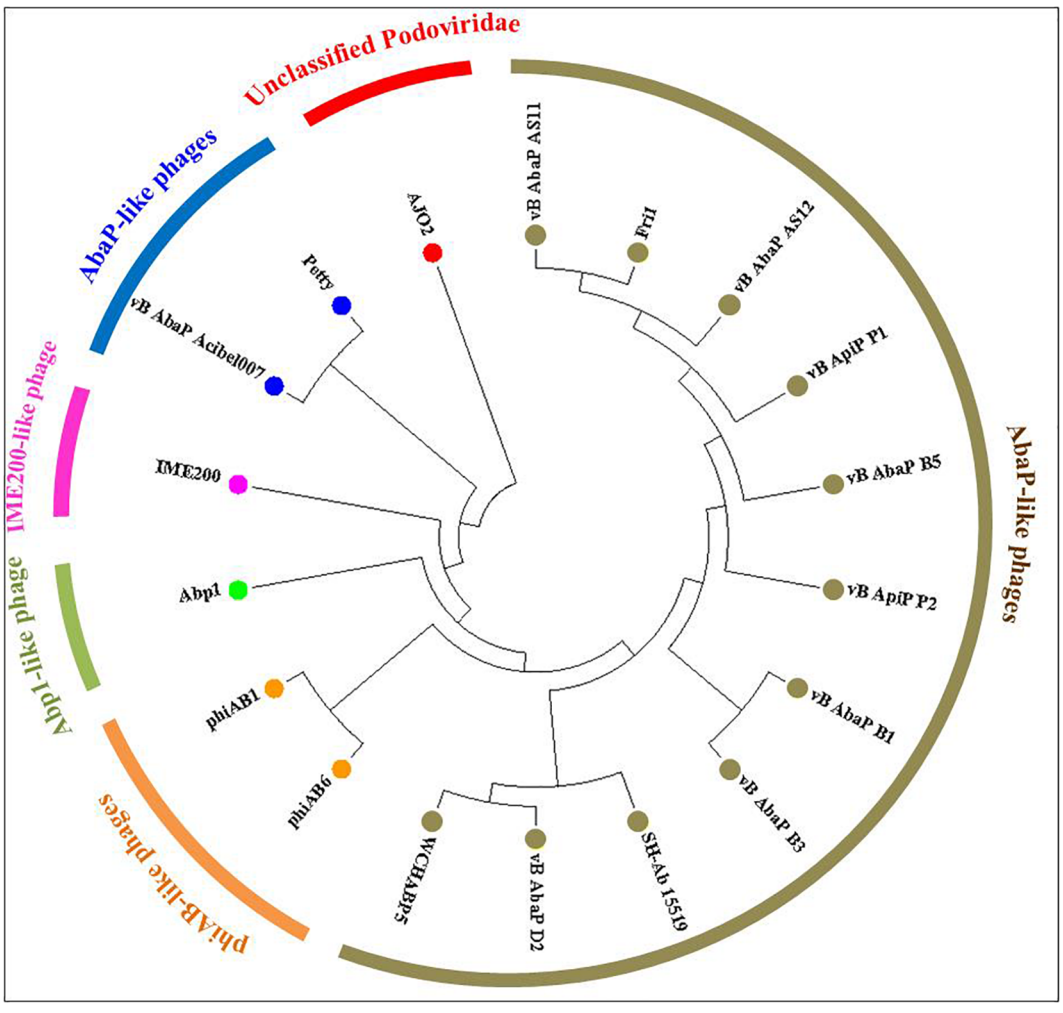

FIGURE 4 | Phylogenetic relationships between phage AJO2 and 17 representative Acinetobacter phages with relatively close relationships according to BLASTn comparative results. The diagram was constructed by MEGA7 using the neighbor-joining method, and the different colors represent different phylogenetic branches, and phages with the same color show a close relationship.

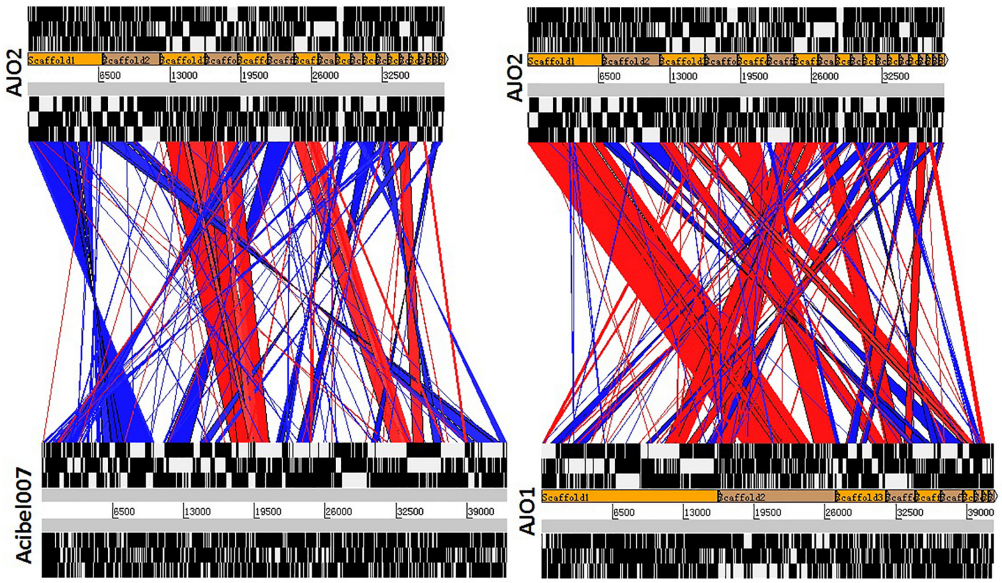

FIGURE 5 | Comparative genome alignments of **(A)** phage AJO2 and Vb_AbaP_Acibel007, and **(B)** phage AJO2 and AJO1. Visual representation of the alignments (using tBLASTX) was carried out with the Artemis Comparison Tool (ACT, http://www.sanger.ac.uk/Software/ACT). The red bars spanning between the genomes represent individual tBLASTX matches, with inverted matches colored blue.

TABLE 3 | Comparisons of phage AJO1, AJO2, and vB_AbaP_ Acibel007.

Features		AJO2	AJO1	Acibel007
Latent period (min)		~30	30	21
Rise period (min)		50	40	30
Burst size		78.1	51.3	145
Classification		*Podoviridea*	*Podoviridea*	*Podoviridea*
Isolated host		*A. johnsonii* strain Pt405	*A. johnsonii* strain JN-11	*A. baumanii*
Genome size (bp)		38124	41437	42654
G+C %		41	41.15	41.2
Predicted genes		58	54	53
No. of genes with	Putative functions	27	22	23
	Unknown functions	31	32	30

sThe AJO2 genome displayed a higher similarity with that of the previously isolated phage AJO1 than vB_AbaP_Acibel007 (**Figure 5B**), thus differences in phage AJO2 and AJO1 were evaluated at multiple levels. By genomic comparison using the BLASTn algorithm, 13 matches were detected and distributed on 9 scaffolds with the total length of 17,772 bp (**Supplementary Table S6**). Although the identities were higher than 97%, query scores were quite low (≤11%). Most of these matched sequences putatively encoded structural proteins and RNA polymerases, which explained the similar morphology of both phages. As mentioned before, phages with similar tail structures might infect the same host. Further verifications of host range were performed and results showed that both phages were virulent to *A. johnsonii* strain Pt405 and *A. johnsonii* strain JN-11. However, their physiological features differed from each other, such as optimal MOI and burst size (**Table 3**). The genome size of AJO2 was smaller, but the content of genes with putative functions (46.6%) was higher than that of AJO1 (40.7%). Besides, plaques formed by the two phages were obviously different on DLA plates. AJO1 plaques were relatively smaller (2–4 mm) with clear edges, while AJO2 formed larger plaques (4–6 mm) with blurry edges (**Supplementary Figure S3**). Based on the above genomic and comparative analyses, AJO2 is a new member of the *Podoviridae* family. The comparative genomic analysis illustrated that bacteriophages are the most abundant and diverse biological entities, and it is hard to find homologous bacteriophages in the natural environment. Such successful evolutions of bacteriophages not only contribute to their diversity and survival, but also provide an advantage in infecting various host bacteria.

CONCLUSION

This study describes the physiological characteristics and genome sequence of an *A. johnsonii* phage from bulking sludge.

Bioinformatic analysis and comparison reveal that AJO2 is a novel lytic phage, with unique genomic features and relatively low similarity to other *Acinetobacter* phages. Moreover, this phage is highly specific to *A. johnsonii*. Therefore, it may be applied for the biocontrol of *A. johnsonii*-caused infection or other environmental problems.

It is known that bacteriophages play an important role in controlling their host bacteria, but the impact on the community structure in complex systems like activated sludge is still unclear. Since the genomic database of phages is extremely limited, isolation and sequencing of more phages from various environments are essential parts of further investigations. The newly isolated phage with genome sequence described here not only enriches the database of activated sludge phages, but also expands our understanding of various genomic features of phages. With the sequence data, it will be possible to develop specific primers and qPCR assays which could be used to follow their population dynamics in mixed systems. Based on the dynamic changes of both phages and host bacteria, their interaction mechanism and the function that AJO2 might have in sludge bulking may be uncovered. The evidence presented in this study contributes to a better understanding of the phages in activated sludge, but the complete genomes of more activated sludge phages clearly need to be analyzed before their ecological roles can be elucidated.

AUTHOR CONTRIBUTIONS

NF experimental design and operation and wrote the manuscript. MY revised the manuscript. RJ revised the manuscript. RQ helped to solve the problems during process operation, funding.

FUNDING

This work was supported by the Free Exchange Programs between the University of Chinese Academy of Sciences and the Italian National Research Council.

ACKNOWLEDGMENTS

We are grateful for the financial support from the National Science and Technology Major Project on Water Pollution Control and Treatment (No. 2015ZX07203-005-03) and the Social Development Program of Hangzhou (No. 20191203B11).

SUPPLEMENTARY MATERIAL

The Supplementary Material for this article can be found online at: https://www.frontiersin.org/articles/10.3389/fmicb.2019.00266/full#supplementary-material

REFERENCES

Ackermann, H.-W. (1998). Tailed bacteriophages: the order caudovirales. *Adv. Virus. Res.* 51, 135–201. doi: 10.1016/S0065-3527(08)60785-X

Adams, M. H. (1959). "Methods of study of bacterial viruses," in *Bacteriophages*, ed. M. H. Adams (New York, NY: Interscience Publication), 443–457.

Aravind, L., Leipe, D. D., and Koonin, E. V. (1998). Toprim–a conserved catalytic domain in type IA and II topoisomerases, DnaG-type primases, OLD family nucleases and RecR proteins. *Nucleic Acids Res.* 26, 4205–4213. doi: 10.1093/nar/26.18.4205

Bamford, D. H., Grimes, J. M., and Stuart, D. I. (2005). What does structure tell us about virus evolution? *Curr. Opin. Struct. Biol.* 15, 655–663. doi: 10.1016/j.sbi.2005.10.012

Behrendt, N., Ploug, M., Patthy, L., Houen, G., Blasi, F., and Danø, K. (1991). The ligand-binding domain of the cell surface receptor for urokinase-type plasminogen activator. *J. Biol. Chem.* 266, 7842–7847.

Brennan, R. G., and Matthews, B. W. (1989). The helix-turn-helix DNA binding motif. *J. Biol. Chem.* 264, 1903–1906.

Brüssow, H., and Desiere, F. (2001). Comparative phage genomics and the evolution of Siphoviridae: insights from dairy phages. *Mol. Microbiol.* 39, 213–223. doi: 10.1046/j.1365-2958.2001.02228.x

Burge, S. W., Daub, J., Eberhardt, R., Tate, J., Barquist, L., Nawrocki, E. P., et al. (2012). Rfam 11.0: 10 years of RNA families. *Nucleic Acids Res.* 41, D226–D232. doi: 10.1093/nar/gks1005

Chibani-Chennoufi, S., Bruttin, A., Dillmann, M. L., and Brüssow, H. (2004). Phage-host interaction: an ecological perspective. *J. Bacteriol.* 186, 3677–3686. doi: 10.1128/JB.186.12.3677-3686.2004

Chopin, M., Chopin, A., and Roux, C. (1976). Definition of bacteriophage groups according to their lytic action on mesophilic lactic streptococci. *Appl. Environ. Microbiol.* 32, 741–746.

Daniel, A., Bonnen, P. E., and Fischetti, V. A. (2007). First complete genome sequence of two *Staphylococcus epidermidis* bacteriophages. *J. Bacteriol.* 189, 2086–2100. doi: 10.1128/JB.01637-06

De la Cruz, N., Esquius, L., Grandjean, D., Magnet, A., Tungler, A., De Alencastro, L. F., et al. (2013). Degradation of emergent contaminants by UV, UV/H2O2 and neutral photo-Fenton at pilot scale in a domestic wastewater treatment plant. *Water Res.* 47, 5836–5845. doi: 10.1016/j.watres.2013.07.005

Deng, Y., and Zhao, R. (2015). Advanced Oxidation Processes (AOPs) in wastewater treatment. *Curr. Poll. Rep.* 1, 167–176. doi: 10.1007/s40726-015-0015-z

Fan, N., Qi, R., and Yang, M. (2017). Isolation and characterization of a virulent bacteriophage infecting *Acinetobacter johnsonii* from activated sludge. *Res. Microbiol.* 168, 472–481. doi: 10.1016/j.resmic.2017.01.006

Finn, R. D., Mistry, J., Tate, J., Coggill, P., Heger, A., Pollington, J. E., et al. (2010). The Pfam protein families database. *Nucleic Acids Res.* 38(Suppl. 1), 211–222. doi: 10.1093/nar/gkp985

Groth, A. C., and Calos, M. P. (2004). Phage integrases: biology and applications. *J. Mol. Biol.* 335, 667–678. doi: 10.1016/j.jmb.2003.09.082

Holmgren, A. (1985). Thioredoxin. *Annu. Rev. Biochem.* 54, 237–271. doi: 10.1146/annurev.bi.54.070185.001321

Huang, G., Le, S., Peng, Y., Zhao, Y., Yin, S., Zhang, L., et al. (2013). Characterization and genome sequencing of phage Abp1, a new phiKMV-like virus infecting multidrug-resistant *Acinetobacter baumannii*. *Curr. Microbiol.* 66, 535–543. doi: 10.1007/s00284-013-0308-7

Jebri, S., Hmaied, F., Yahya, M., Ammar, A. B., and Hamdi, M. (2016). Total coliphages removal by activated sludge process and their morphological diversity by transmission electronic microscopy. *Water Sci. Technol.* 74, 318–323. doi: 10.2166/wst.2016.178

Jenkins, D., Richard, M. G., and Daigger, G. T. (2004). *Manual on the Causes and Control of Activated Sludge Bulking, Foaming and other Solids Separation Problems*. Washington, DC: Lewis Publishers.

Jeruzalmi, D., and Steitz, T. A. (1998). Structure of T7 RNA polymerase complexed to the transcriptional inhibitor T7 lysozyme. *EMBO J.* 17, 4101–4113. doi: 10.1093/emboj/17.14.4101

Jing Dan, Y. U., Shi, H. Y., Wang, D., Hua, X. U., and Sun, Y. B. (2013). Biologic characteristics of Bacteriophages specific to *Acinetobacter*

baumannii. *J. Microbiol.* 33, 17–23. doi: 10.1186/1471-2164-15-793

Klabunde, T., Sträter, N., Fröhlich, R., Witzel, H., and Krebs, B. (1996). Mechanism of Fe(III)-Zn(II) purple acid phosphatase based on crystal structures. *J. Mol. Biol.* 259, 737–748. doi: 10.1006/jmbi.1996.0354

Kotay, S. M., Choi, J., and Goel, R. (2010). "Phage therapy for sludge bulking using a novel bacteriophage infecting filamentous bacterium, *Sphaerotilus Natans*" in *Proceedings of the Water Environment Federation, WEFTEC 2010* (Alexandria, VA: Water Environ Federation), 5586–5594.

Kotay, S. M., Datta, T., Choi, J., and Goel, R. (2011). Biocontrol of biomass bulking caused by Haliscomenobacter hydrossis using a newly isolated lytic bacteriophage. *Water Res.* 45, 694–704. doi: 10.1016/j.watres.2010.08.038

Kumar, S., Stecher, G., and Tamura, K. (2016). MEGA7: molecular evolutionary genetics analysis version 7.0 for bigger datasets. *Mol. Biol. Evol.* 33, 1870–1874. doi: 10.1093/molbev/msw054

Lagesen, K., Hallin, P., Rødland, E., Stærfeldt, H., Rognes, T., and Ussery, D. (2007). RNammer: consistent annotation of rRNA genes in genomic sequences. *Nucleic Acids Res.* 35, 3100–3108. doi: 10.1093/nar/gkm160

Lai, M. J., Chang, K. C., Huang, S. W., Luo, C. H., Chiou, P. Y., Wu, C. C., et al. (2016). The tail associated protein of *Acinetobacter baumannii* phage ΦAB6 is the host specificity determinant possessing exopolysaccharide depolymerase activity. *PLoS One* 11:e0153361. doi: 10.1371/journal.pone.0153361

Levantesi, C., Serafim, L. S., Crocetti, G. R., Lemos, P. C., Rossetti, S., Blackall, L. L., et al. (2010). Analysis of the microbial community structure and function of a laboratory scale enhanced biological phosphorus removal reactor. *Environ. Microbiol.* 4, 559–569. doi: 10.1046/j.1462-2920.2002.00339.x

Lowe, T. M., and Eddy, S. R. (1997). tRNAscan-SE: a program for improved detection of transfer RNA genes in genomic sequence. *Nucleic Acids Res.* 25, 955–964. doi: 10.1093/nar/25.5.955

Lu, S., Le, S., Tan, Y., Zhu, J., Li, M., Rao, X., et al. (2013). Genomic and proteomic analyses of the terminally redundant genome of the *Pseudomonas aeruginosa* phage PaP1: establishment of genus PaP1-like phages. *PLoS One* 8:e62933. doi: 10.1371/journal.pone.0062933

Madoni, P., Davoli, D., and Gibin, G. (2000). Survey of filamentous microorganisms from bulking and foaming activated-sludge plants in Italy. *Water Res.* 34, 1767–1772. doi: 10.1016/S0043-1354(99)00352-8

Mann, N. H. (2005). The third age of phage. *PLoS Biol.* 3:e182. doi: 10.1371/journal.pbio.0030182

Martins, A. M., Pagilla, K., Heijnen, J. J., and van Loosdrecht, M. C. (2004). Filamentous bulking sludge—a critical review. *Water Res.* 38, 793–817. doi: 10.1016/j.watres.2003.11.005

Merabishvili, M., Vandenheuvel, D., Kropinski, A. M., Mast, J., De Vos, D., Verbeken, G., et al. (2014). Characterization of newly isolated lytic bacteriophages active against *Acinetobacter baumannii*. *PLoS One* 9:e104853. doi: 10.1371/journal.pone.0104853

Nielsen, P. H., Saunders, A. M., Hansen, A. A., Larsen, P., and Nielsen, J. L. (2012). Microbial communities involved in enhanced biological phosphorus removal from wastewater—a model system in environmental biotechnology. *Curr. Opin. Biotechnol.* 23, 452–459. doi: 10.1016/j.copbio.2011.11.027

Parsley, L. C., Consuegra, E. J., Thomas, S. J., Bhavsar, J., Land, A. M., Bhuiyan, N. N., et al. (2010). Census of the viral metagenome within an activated sludge microbial assemblage. *Appl. Environ. Microbiol.* 76, 2673–2677. doi: 10.1128/AEM.02520-09

Payne, K., Sun, Q., Sacchettini, J., and Hatfull, G. F. (2009). Mycobacteriophage Lysin B is a novel mycolylarabinogalactan esterase. *Mol. Microbiol.* 73, 367–381. doi: 10.1111/j.1365-2958.2009.06775.x

Petrovski, S., Seviour, R. J., and Tillett, D. (2011). Genome sequence and characterization of the Tsukamurella bacteriophage TPA2. *Appl. Environ. Microbiol.* 77, 1389–1398. doi: 10.1128/AEM.01938-10

Petrovski, S., Tillett, D., and Seviour, R. J. (2012). Isolation and complete genome sequence of a bacteriophage lysing *Tetrasphaera jenkinsii*, a filamentous bacteria responsible for bulking in activated sludge. *Virus Genes* 45, 380–388. doi: 10.1007/s11262-012-0771-4

Saier, M. H. (2000). A functional-phylogenetic classification system for transmembrane solute transporters. *Microbiol. Mol. Biol. Rev.* 64, 354–411. doi: 10.1128/MMBR.64.2.354-411.2000

Schattner, P., Brooks, A. N., and Lowe, T. M. (2005). The tRNAscan-SE, snoscan and snoGPS web servers for the detection of tRNAs and snoRNAs. *Nucleic Acids Res.* 33(Suppl._2), W686–W689. doi: 10.1093/nar/gki366

Schwartz, F., and Ota, T. (1997). The 239AB gene on chromosome 22: a novel member of an ancient gene family. *Gene* 194, 57–62. doi: 10.1016/S0378-1119(97)00149-2

Vincze, T., Posfai, J., and Roberts, R. J. (2003). NEBcutter: a program to cleave DNA with restriction enzymes. *Nucleic Acids Res.* 31, 3688–3691. doi: 10.1093/nar/gkg526

Wagner, F. (1982). "Study of the causes and prevention of sludge bulking in Germany," in *Bulking of Activated Sludge: Preventative and Remedial Methods*, eds B. Chambers and E. K. Tomlinson (Chichester: Ellis Horwood Ltd), 29–46.

Wang, J., Li, Q., Qi, R., Tandoi, V., and Yang, M. (2014). Sludge bulking impact on relevant bacterial populations in a full-scale municipal wastewater treatment plant. *Process Biochem.* 49, 2258–2265. doi: 10.1016/j.procbio.2014.08.005

Withey, S., Cartmell, E., Avery, L., and Stephenson, T. (2005). Bacteriophages—potential for application in wastewater treatment processes. *Sci. Total Environ.* 339, 1–18. doi: 10.1016/j.scitotenv.2004.09.021

Conflict of Interest Statement: The authors declare that the research was conducted in the absence of any commercial or financial relationships that could be construed as a potential conflict of interest.

frontiers in Microbiology

ORIGINAL RESEARCH
published: 31 January 2019
doi: 10.3389/fmicb.2018.03192

Predictable Molecular Adaptation of Coevolving *Enterococcus faecium* and Lytic Phage EfV12-phi1

*Stephen Wandro[1], Andrew Oliver[1], Tara Gallagher[1], Claudia Weihe[2], Whitney England[1,3], Jennifer B. H. Martiny[2] and Katrine Whiteson[1]**

[1] Department of Molecular Biology and Biochemistry, University of California, Irvine, Irvine, CA, United States, [2] Department of Ecology and Evolutionary Biology, University of California, Irvine, Irvine, CA, United States, [3] Department of Pharmaceutical Sciences, University of California, Irvine, Irvine, CA, United States

Bacteriophages are highly abundant in human microbiota where they coevolve with resident bacteria. Phage predation can drive the evolution of bacterial resistance, which can then drive reciprocal evolution in the phage to overcome that resistance. Such coevolutionary dynamics have not been extensively studied in human gut bacteria, and are of particular interest for both understanding and eventually manipulating the human gut microbiome. We performed experimental evolution of an *Enterococcus faecium* isolate from healthy human stool in the absence and presence of a single infecting Myoviridae bacteriophage, EfV12-phi1. Four replicates of *E. faecium* and phage were grown with twice daily serial transfers for 8 days. Genome sequencing revealed that *E. faecium* evolved resistance to phage through mutations in the *yqwD2* gene involved in exopolysaccharide biogenesis and export, and the *rpoC* gene which encodes the RNA polymerase β' subunit. In response to bacterial resistance, phage EfV12-phi1 evolved varying numbers of 1.8 kb tandem duplications within a putative tail fiber gene. Host range assays indicated that coevolution of this phage-host pair resulted in arms race dynamics in which bacterial resistance and phage infectivity increased over time. Tracking mutations from population sequencing of experimental coevolution can quickly illuminate phage entry points along with resistance strategies in both phage and host – critical information for using phage to manipulate microbial communities.

Keywords: phage (bacteriophage), *Enterococcus*, experimental evolution, phage therapy, tail fiber, exopolysaccharide, coevolution

OPEN ACCESS

Edited by:
Robert Czajkowski, University of Gdańsk, Poland

Reviewed by:
Beatriz Martínez, Spanish National Research Council (CSIC), Spain
Ana-Belen Martin-Cuadrado, University of Alicante, Spain

***Correspondence:**
Katrine Whiteson
katrine@uci.edu

Specialty section:
This article was submitted to Virology, a section of the journal Frontiers in Microbiology

Received: *02 October 2018*
Accepted: *10 December 2018*
Published: *31 January 2019*

Citation:
Wandro S, Oliver A, Gallagher T, Weihe C, England W, Martiny JBH and Whiteson K (2019) Predictable Molecular Adaptation of Coevolving Enterococcus faecium and Lytic Phage EfV12-phi1. Front. Microbiol. 9:3192. doi: 10.3389/fmicb.2018.03192

INTRODUCTION

Bacteriophages (phages) drive microbial diversity and function at both broad (Bouvier and Giorgio, 2007) and fine scales (Mcshan et al., 2016) through their influences on bacterial community composition (Stern et al., 2012) and bacterial pathogenesis (Davis et al., 2000). Phages are estimated to be present at 10^9 virions per gram in the gut (Kim et al., 2011) and are therefore likely to have major influences on beneficial and pathogenic gut bacteria. Phages that lyse their host (lytic phages) or alter host virulence gene expression (some temperate phages) present a potentially rich pool of new therapies against antibiotic resistant pathogens (Wright et al., 2009; Oechslin et al., 2016). Recently, the clinical application of phages against highly antibiotic resistant bacteria (Viertel et al., 2014; Chan et al., 2016; Schooley et al., 2017) has highlighted the need for well-controlled

experiments that investigate the molecular interactions between phage and bacteria. Before phage-based therapies can be developed, we must have a solid understanding of how a targeted bacterial pathogen may evolve resistance to a treatment phage, and how the treatment phage responds to host resistance.

Reciprocal evolution of bacteria and phage, or coevolution (Thompson, 1999), has been well-studied (Koskella and Brockhurst, 2014; Martiny et al., 2014; Scanlan, 2017) in two model systems: *Pseudomonas fluorescens* and *Escherichia coli* (Bohannan and Lenski, 2000; Hall et al., 2011; Koskella and Brockhurst, 2014). Although we can learn broad principles from these model systems, their study cannot replace experiments with more clinically relevant organisms to understand human associated phage-bacterial interactions. We aimed to investigate coevolution in *Enterococcus faecium*, a common, but low-abundance member of the human gut microbiome that is also an important opportunistic pathogen. The World Health Organization classifies vancomycin-resistant *E. faecium* as a Priority 2 level pathogen in need of new antibiotic therapies (Lawe-Davies and Bennett, 2017). Common enterococci infections include endocarditis, blood/wound infections, and urinary tract infections (Koch et al., 2004). Enterococci can also become dominating members of the gut community following antibiotic perturbation (Hendrickx et al., 2015), leading to dysbiosis and increased likelihood of infection (Van Tyne and Gilmore, 2014). Developing a coevolution model using lytic phage and *Enterococcus* could therefore be a useful step toward addressing this global health threat. Coevolution experiments can quickly reveal candidates for the molecular basis of *Enterococcus*-phage interactions so that optimal cocktails of phages can be constructed. Indeed, cocktails of multiple phages with orthogonal infection mechanisms hold great promise as therapeutics (Yen et al., 2017; Nale et al., 2018).

The evolution of resistance to phage infection has been well documented and can happen through many routes. These include blocking phage adsorption through mutation, restriction-modification systems, CRISPR-Cas systems, and abortive infection (Dy et al., 2014). In addition, new mechanisms of phage resistance are still being discovered (Doron et al., 2018), which highlights the potential for discovery in the interactions between bacteria and phages. Coevolution between *Enterococcus* and its phages remains poorly studied, but resistance to one *Enterococcus* phage has been shown to evolve through mutation of an integral membrane protein to prevent phage adsorption (Duerkop et al., 2016). This remains one example, and *Enterococcus* may utilize an entirely different resistance mechanism during coevolution with a different phage.

We experimentally coevolved *E. faecium* with a lytic phage (EfV12-phi1) to characterize the genomic and phenotypic outcomes of their interaction. Phage EfV12-phi1 was isolated from sewage and has been previously referred to as "1" or "Φ1" (Jarvis et al., 1993). It is a member of the Twort-like family of Myoviridae phages, a group of strictly lytic phages that infect Firmicutes and generally demonstrate a broad host range. Closely related Twort-like phages have been previously employed for phage therapy and have demonstrated lethality against a long list of clinically relevant bacterial strains, including vancomycin-resistant enterococci (VRE); Group B, C, E, G *Streptococcus*; *Staphylococcus aureus*, and others (Klumpp et al., 2010; Khalifa et al., 2015, 2018). The lysin of phage EfV12-phi1 has been previously shown to kill species of *Enterococcus* (including VRE), *Streptococcus*, and *Staphylococcus* (Yoong et al., 2004).

We conducted four coevolution experiments where phage EfV12-phi1 was grown with *E. faecium* with 1:10 serial transfers twice daily, so that a large fraction of the population is carried over. To differentiate between genomic changes associated with coevolution versus those that might be due to laboratory adaptation, we compared these experiments to parallel control experiments where *E. faecium* was grown alone or phage EfV12-phi1 was propagated on a naïve host. Based on phage-host experiments in model systems, we expected to see mutations arise in the phage tail fibers that allow phage to recognize and bind their hosts and in bacterial surface receptors where phage often enter their hosts (Silva et al., 2016).

MATERIALS AND METHODS

Bacterial Strains and Phage

The bacteria used in this study was *Enterococcus faecium* strain TX1330 (BEI HM-204), was isolated from healthy human feces and obtained through BEI Resources, NIAID, NIH as part of the Human Microbiome Project. The phage used for this study was *Enterococcus* Phage EfV12-phi1, isolated on *Enterococcus faecalis,* from Canadian sewage in 1975 (HER number 339; d'Herelle collection, Laval University, Quebec, QC, Canada).

Coevolution of *Enterococcus* Bacteria and Phage

A culture of *E. faecium* TX1330 growing exponentially (OD600 = 0.3) in brain heart infusion (BHI) broth was split into twelve replicates of 10 mL culture in 15 mL Falcon tubes. Four replicates were designated bacterial host control, four were phage control, and four were coevolution. Phage EfV12-phi1 was added to the coevolution and phage control cultures at an MOI of approximately 0.003. Cultures were incubated shaking with loose caps at 37°C. Every 12 h for 8 days, 1 mL of the replicate host control and coevolution tubes were inoculated into 9 mL of new BHI broth. For the phage control, 1 mL of phages was separated from bacteria by syringe filtration through a 0.2 um polyethersulfone filter (GE Healthcare Life Sciences) and mixed with 1 mL of the contemporary host control in 8 mL of new BHI broth. Performing 1:10 dilutions at each passage, we estimate 3.5 generations (doublings) are required to reach stationary phase again, resulting in approximately 56 generations total. After each dilution, 900 uL of 12-h culture containing the population of bacteria and phages was added to 600 uL of 50% glycerol and stored at −80°C. Transfer numbers 1, 4, 8, 12, and 16 were chosen for sequencing. At each timepoint (after 12 h of growth), the OD600 of each culture was measured.

Host Range Assay

Host range of phage and bacterial isolates from *E. faecium* were determined with streak assays as described before (Harcombe and Bull, 2005). Bacteria and phage were isolated from the first and last timepoints of the host control and coevolution replicate populations one and two. Bacteria were isolated by streak plating and picking single colonies. Phages were isolated by performing a double agar overlay with 100 uL of the raw population and then picking plaques (so that phages are growing on contemporary hosts from the same replicate population). Phages were amplified by performing plaque assays on ancestral hosts and harvested by soaking plates in 5 mL SM buffer followed by filtration of collected SM buffer through a 0.2 um syringe filter. 20 uL of each bacterial isolate and 20 uL of each phage isolate was streaked perpendicularly across an agar plate. The intersection of the bacteria and phage was examined and scored for lysis. In total, three ancestral hosts and 12 coevolved hosts were crossed against six ancestral phages and 16 coevolved phages.

DNA Extraction, Library Preparation, and Sequencing

DNA was extracted from the populations of bacteria and phages in the chosen timepoints with the Zymo Universal DNA extraction kit using the recommended protocol provided by the manufacturer. Sequencing libraries were prepared with Illumina's Nextera kit using methods outlined in Baym et al. (2015). The libraries were loaded onto an Illumina Next-Seq at 1.8 picomolar concentration using Illumina's mid-output kit for 75 bp paired end sequencing.

A more complete bacterial reference genome was assembled using Oxford Nanopore's 1D Genomic DNA Ligation kit (Goodwin et al., 2017). Briefly, DNA was repaired using the FFPE DNA repair kit (New England Biolabs) and cleaned up using AMPure XP beads (Beckman Coulter). The repaired DNA was dA-tailed using NEBNext Ultra End Repair (New England Biolabs) and sequence adapters were ligated using Blunt TA ligase master mix (New England Biolabs). The MinION sequencer was primed, per manufacturer's instructions, and 700 ng of DNA was loaded onto the sequencer. The run was allowed to generate data for 48 h. Sequence data from the MinION and Illumina sequence data from timepoint one of the host control were used together to generate a host reference genome using the MIRA assembler (Chevreux et al., 1999).

Genome Assembly and Annotation

The reference genome for *E. faecium* TX1330 was assembled using reads from time point 1 of the host control. Reads were assembled using the PATRIC smart assembler (Wattam et al., 2017), which combines the two best assemblies from SPAdes (Bankevich et al., 2012), IDBA (Peng et al., 2010), and Velvet (Zerbino and Birney, 2008) assemblers. The phage was assembled using SPAdes (Bankevich et al., 2012). The resulting contigs were annotated using PATRIC's annotation pipeline, which uses RASTtk for gene calls (Wattam et al., 2017). The sequenced genome of *E. faecium* TX1330 can be found at GenBank: GCA_003583905.1, and the EfV12-phi1 genome can be found at GenBank: MH880817.

Genomic Mutation Analysis

Paired-end reads were run through Breseq (Deatherage and Barrick, 2014) once using the ancestral phage EfV12-phi1 as the reference genome and once using the ancestral *E. faecium* TX1330 with default parameters. Briefly, Breseq uses Bowtie2 (Langmead and Salzberg, 2012) to align reads to a reference genome and creates a SAM file which SAMtools converts to a pileup file. Custom R scripts were then used to parse through the resulting alignments and detect mutations at greater than 10% frequency. Mutations were labeled as synonymous or non-synonymous by Breseq, and all predicted non-synonymous mutations were manually investigated using Geneious (Biomatters v9.0). All bacterial mutations were visualized using Geneious and phage mutations using Geneious and ggplot2 in R.

Tail Fiber PCR

Phage populations from the final timepoint of all four replicates were grown by adding 10 uL of the frozen timepoint 16 cultures to 10 mL BHI and grown overnight shaking at 37°C. Cultures were then spun down and the supernatant was syringe filtered through a 0.2 um polyethersulfone filter. Phages were then concentrated down to 1 mL using Amicon 100 kDa centrifugal filter units. DNA was extracted from concentrated phages using Zymo Universal DNA extraction kit.

Primers were designed outside the duplicated region of the tail fiber gene so that the amplicon would be longer if the region was duplicated. The primers used were F: 5′ TGTTGCACCAGA AAACGCAG 3′ and R: 5′ AGGTCTGTACGAGCCGTGTA 3′. PCR was run using Phusion polymerase with the following protocol: 98°C: 30 s (98°C 10 s, 53°C 30 s, 72°C 10 min) x 35, 72°C 10 min. Amplicons were visualized on a 1% agarose gel using Invitrogen SYBR gel stain.

Location of Mutations in RNA Polymerase B' Structure

The structure of the *E. coli* RNA polymerase B' subunit was downloaded from Protein Data Bank (4JK1, DOI: 10.2210/pdb4JK1/pdb). The amino acid sequence of the *E. faecium* TX1330 RNA polymerase B' subunit was aligned to the *E. coli* sequence to find the corresponding locations. The structure and locations of mutations were visualized using PyMOL (Schrödinger, 2015).

MinION Sequencing of Tail Fiber Duplication

The Oxford Nanopore MinION sequencer was used to sequence a phage isolate that contained the tail fiber duplication. The phage was isolated by picking a plaque from timepoint 16 of replicate 4 (directly plating 100 uL of the population). The phage isolate was propagated on a contemporary (final timepoint) *Enterococcus* isolate from population 4 to get enough phage DNA for sequencing. DNA was extracted using a Zymo Quick-DNA

micro kit. DNA was prepared for MinION sequencing according to manufacturer's recommendations using the 1D Genomic DNA by ligation protocol as described above. A total of 199,734 reads were generated with a median sequence length of 3,057 bp. Bowtie2 was used to extract the 57% of reads that aligned to the phage genome; the remaining reads aligning to the bacterial genome were discarded. The data was analyzed in Geneious to determine the number of duplications in the tail fiber gene. A total of 5,400 reads aligned to the tail fiber gene and were over 3 kb so could span the length of a single duplication (1.8 kb).

RESULTS

E. faecium and Phage EfV12-phi1 Display Arms-Race Coevolution Dynamics

We coevolved *E. faecium* with lytic phage EfV12-phi1 as four replicate microcosms, passaging 16 times in 8 days (every 12 h), allowing for approximately 53 generations (**Figure 1**). Bacterial host control cultures were also set up in quadruplicate with identical conditions minus the phage. Quadruplicate phage controls were established by growing the phage on a naïve host, separating the phage from the host during each passage, and then adding the phage lysate to an independent aliquot of the naïve host control culture. Bacterial growth was monitored daily by optical density readings, which decrease when bacterial cells are lysed by phage. Phage infection initially reduced the density of all four bacterial cultures during the first day. This was followed by increased optical density after six to seven transfers (depending on the replicate), indicative of the evolution of resistance to phage (**Figure 2A**). In two replicate cultures, optical densities did not decline again after initial resistance arose, whereas in the other two replicate cultures, optical densities oscillated for the duration of the experiment.

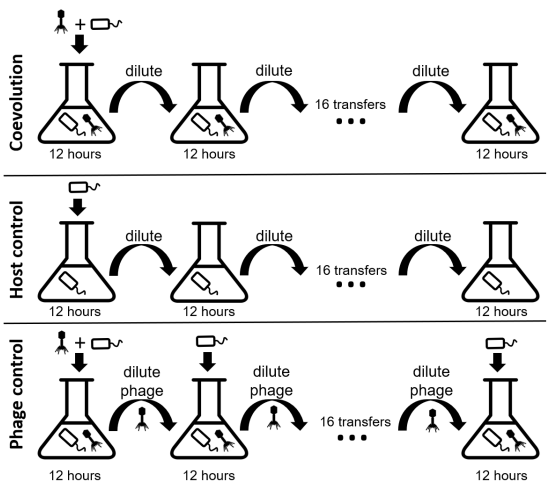

FIGURE 1 | Experimental design of the three branches of the study. In each branch, phage and bacteria or only bacteria were added to a microcosm and allowed to grow for 12 h before being diluted 10-fold. The phage control filtered out the bacteria during each dilution, preventing bacterial coevolution. Each branch was done in quadruplicate. Icon credit: thenounproject.com.

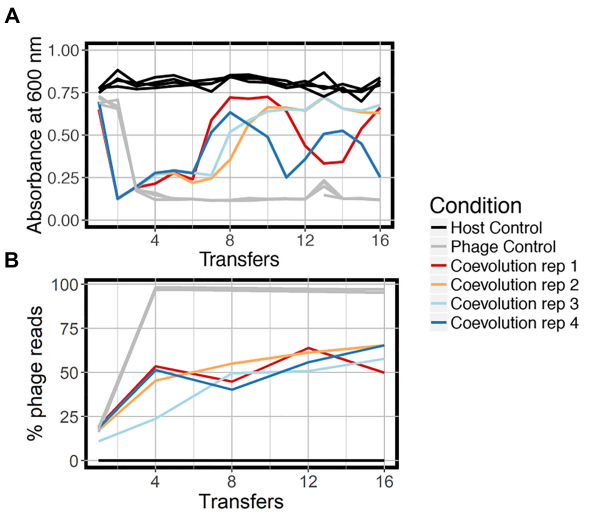

FIGURE 2 | Growth dynamics of experimental coevolution. **(A)** Optical density of the bacteria for each branch of the experiment, measured at the end of 12 h prior to diluting back 10-fold in fresh BHI media. All replicates of the host control and phage control are shown in the same color because there was little variation. **(B)** Proportion of total sequenced reads mapping to phage EfV12-phi1 indicates the relative abundance of this phage at each timepoint. Reads that did not map to phage mapped to *E. faecium*.

At the final timepoint, bacterial populations in three of four replicates remained at a high optical density, despite relatively high concentrations of phage DNA (an approximation of phage abundance; **Figure 2B**). As expected, optical densities in the phage control cultures with naïve bacteria were consistently reduced upon infection by EfV12-phi1, and host control cultures (with no infecting phage) showed no reductions in optical density.

Ancestral and coevolved bacterial isolates were challenged with infection by ancestral and coevolved phages and bacterial lysis was scored using a plate-based assay (see Methods). These experiments showed that coevolved bacterial isolates (from the final coevolution timepoint) were resistant to ancestral phage isolates, and the coevolved phage isolates infected ancestral bacterial isolates (**Figure 3**). In most cases, coevolved phages infected coevolved bacteria, suggesting that at least one round of coevolution had occurred (*E. faecium* evolved resistance, EfV12-phi1 in turn evolved an expanded host range to overcome this resistance). These results are consistent with arms race coevolutionary dynamics in which bacterial resistance and phage infectivity increase over time.

Resistance to Phage Evolves Though Exopolysaccharide and RNA Polymerase Mutations

To identify the bacterial mutations that led to resistance, and the phage mutations that enable infection of the freshly evolved host, we sequenced the populations from replicate microcosms at five

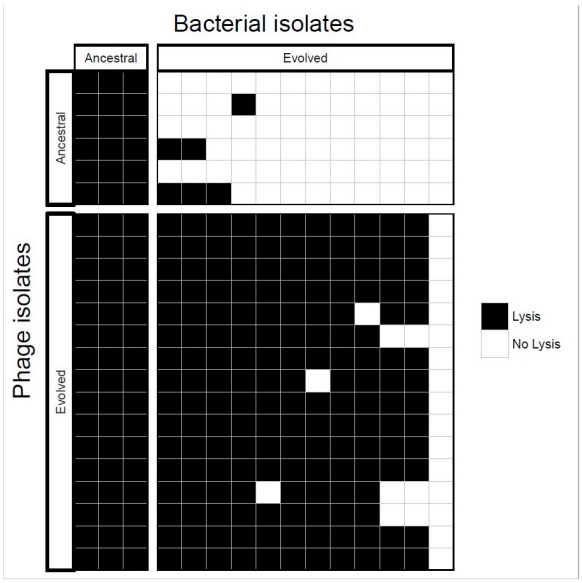

FIGURE 3 | Host range analysis of phage and bacterial isolates. Bacteria and phage isolated from the initial and final timepoints were tested for infectivity. Each box represents whether lysis occurred when a single phage isolate crossed with a single bacterial isolate.

timepoints (1, 4, 8, 12, and 16 transfers) from the coevolution treatment, three phage control timepoints (1, 4, and 16) and two host control timepoints (1 and 16). These population reads were mapped to the ancestral *E. faecium* genome that was sequenced by both Illumina NextSeq and Oxford Nanopore MinION, yielding a high-quality reference genome in three contigs and one plasmid contig. Mutation frequencies for the population were calculated based on the percentage of reads supporting the mutant base divided by the total coverage. Non-synonymous mutations were not observed in host control bacteria but were observed in seven genes in coevolving populations. Many of these genes encode hydrolases and transferases (**Table 1**). Two genes were mutated in all four replicates: putative tyrosine kinase *yqwD2* and RNA polymerase B' subunit *rpoC*.

The putative tyrosine kinase, *yqwD2*, is involved in capsule exopolysaccharide production (**Figure 4A**). Replicates had different non-synonymous mutations within this gene: three occurred on neighboring amino acid residues (P58H, P58L, and G59V), while the fourth occurred twenty residues away (K89H) (**Figure 4A**). Mutations in the *yqwD2* gene were first detected at timepoint eight and became more frequent in the coevolving bacterial populations over time. The increasing frequencies of different mutations in the same gene suggest convergent evolution toward a single mechanism for resisting phage infection.

The second bacterial gene observed to mutate when coevolving with phage EfV12-phi1 was the *rpoC* gene encoding RNA polymerase β' subunit (**Figure 4B**). A total of five different non-synonymous mutations were observed at high frequency in one or more replicates. The positions of mutations were mapped to the 3D structure of *E. coli's* RpoC, showing that all five mutations are located near each other on the interior portion of the protein near the active site (**Supplementary Figure S1**).

Phage EfV12-phi1 Combats Resistance Through Tandem Tail Fiber Duplications

Mutations in the phage genome were also tracked over time as the phage coevolved with the host bacteria. Four phage genes mutated throughout the experiment. Three of these mutations also occurred in all replicates of the phage controls, indicating that they are likely to generally increase infectivity for this specific host and are not a response to the evolution of bacterial

TABLE 1 | All mutations present in *E. faecium* TX1330 at the final timepoint.

Replicate	Gene/predicted function	Type	AA change	Frequency (%)
1	*RpoC*	Non-synonymous snp	H419R	38.2
1	*RpoC*	Non-synonymous snp	S926T	21.1
1	*RpoC*	Non-synonymous snp	L800V	14.8
1	Hypothetical protein in capsule synthesis locus	Non-synonymous snp	M29I	30
1	*yqwD2*	Non-synonymous snp	P58L	37.6
1	*yqwD2*	Non-synonymous snp	P58H	19.2
2	Malonate decarboxylase beta subunit/malonate decarboxylase gamma subunit CDS	Non-synonymous snp	G148V	45.5
2	Predicted hydrolase of the HAD superfamily CDS	Nonsense	S191stop	33.3
2	murA – UDP-N-acetylglucosamine 1-carboxyvinyltransferase	Non-synonymous snp	G20C	40
2	*yqwD2*	Non-synonymous snp	P58H	100
3	*RpoC*	Non-synonymous snp	H419R	79.2
3	*yqwD2*	Non-synonymous snp	K89N	72.2
3	hydrolase, haloacid dehalogenase-like family CDS	Nonsense	E68stop	50
4	*yqwD2*	Non-synonymous snp	P58H	92.5

All bacterial mutations are from timepoint 16 of coevolution replicates. No mutations were seen in the host controls. Locus tags for each gene can be found in ***Supplementary Table S1****.*

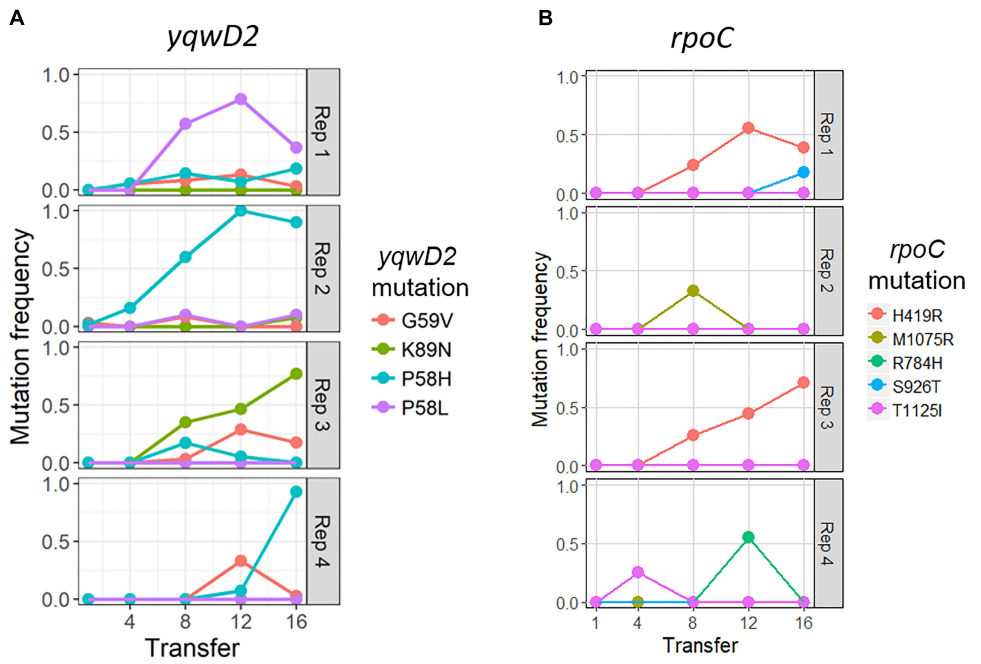

FIGURE 4 | Frequency of common bacterial mutations over time. Population frequency of mutations in **(A)** capsule biosynthesis tyrosine protein kinase *yqwD2* and **(B)** RNA polymerase B' subunit gene *rpoC*. All mutations present at a frequency of 10% in one timepoint in one replicate shown.

resistance. One of the phage-control mutations occurred in a putative structural capsid gene and resulted in a change from asparagine to lysine. In all replicates, this mutation started at a low frequency at transfer 4 (the first sequenced time point) and increased in frequency over time (**Table 2**). The other two genes encoded hypothetical proteins that were deleted from the genome between timepoints 8 and 12 (**Table 2**). These genes are located next to each other and are near the several terminally redundant repeats EfV12-phi1 uses to circularly permute its genome, suggesting a likely mechanism for excision of these genes.

The coevolution-specific phage mutation occurred in a gene encoding a putative tail fiber. Partial duplications of this gene occurred in all four coevolution replicates and never in the phage controls. Specifically, a 1.8 kb segment of a 6.6 kb putative tail fiber gene underwent in-frame tandem duplications (**Figure 5**). Over time, replicates acquired varying numbers of duplications 400 bp upstream of a predicted carbohydrate-binding domain. The duplication was initially observed as an increase in sequencing coverage present in all four populations beginning between transfers four and eight and persisting until the end of the experiment (**Figures 5A,C**). PCR was performed with primers were flanking the entire duplication so that the amplicon would increase in size if duplications occurred. For coevolved phage populations (**Figure 5B**) and isolates (data not shown), multiple amplicons of increasing size were observed that represent the size of the original tail fiber gene as well as larger tail fiber genes that contain duplications.

MinION long-read sequencing was performed on a phage isolate from the final timepoint of population 4 to resolve the duplication. Of the 1,021 reads spanning the entire tail fiber gene, 134 reads had no duplication (the original tail fiber gene), 852 reads had one duplication (two tandem copies of the duplicated sequence), 32 reads had two duplications, two reads had three duplications, and one read had four duplications. Thirty-four reads were found to consist of only tandem copies of the duplicated 1.8 kb sequence, ranging from 4 to 11 copies (7 to 20 kb in length). The mechanism by which these tandem duplications altered phage infectivity is currently not known; the duplication did not appear to be a diversity-generating mechanism, as only a single replicate acquired a SNP within the duplicated region (**Table 2**). The duplications were first detected at transfer eight, after a dramatic increase in bacterial abundance, which we attribute to the evolution of resistance to phage infection. The timing and exclusive occurrence in the coevolution treatment suggests that these tail fiber duplications were a phage response to the bacterial evolution of resistance.

DISCUSSION

To our knowledge, this represents the first effort to characterize phage-bacteria coevolution in *Enterococcus* – a common commensal in the gut microbiome that is also an important opportunistic pathogen. Similar to other well characterized systems, the experiments revealed coevolutionary arms race dynamics between *E. faecium* and its phage involving mutations in phage tail fibers and bacterial surface structures. They further demonstrated parallel coevolution among replicates and therefore predictable molecular adaptation. In particular, we

TABLE 2 | All mutations present in phage EfV12-phi1 at the final timepoint.

Replicate	Condition	Gene/predicted function	Locus tag	Type	AA change	Frequency
1	Coevolution	Hypothetical protein 8	EFV12PHI1_123	Whole gene deletion	–	−375× coverage
1	Coevolution	Hypothetical protein 9	EFV12PHI1_126	Whole gene deletion	–	−545× coverage
1	Coevolution	Tail fiber	EFV12PHI1_98	Tandem duplication	–	+3× coverage
1	Coevolution	Capsid and scaffold	EFV12PHI1_97	Non-synonymous snp	N306K	99%
2	Coevolution	Hypothetical protein 8	EFV12PHI1_123	Whole gene deletion	–	−250× coverage
2	Coevolution	Hypothetical protein 9	EFV12PHI1_126	Whole gene deletion	–	−58× coverage
2	Coevolution	Tail fiber	EFV12PHI1_98	Tandem duplication	–	+5× coverage
2	Coevolution	Capsid and scaffold	EFV12PHI1_97	Non-synonymous snp	N306K	99%
3	Coevolution	Hypothetical protein 8	EFV12PHI1_123	Whole gene deletion	–	−33× coverage
3	Coevolution	Hypothetical protein 9	EFV12PHI1_126	Whole gene deletion	–	−30× coverage
3	Coevolution	Tail fiber	EFV12PHI1_98	Tandem duplication	–	+3× coverage
3	Coevolution	Capsid and scaffold	EFV12PHI1_97	Non-synonymous snp	N306K	77.5%
4	Coevolution	Hypothetical protein 8	EFV12PHI1_123	Whole gene deletion	–	−896× coverage
4	Coevolution	Hypothetical protein 9	EFV12PHI1_126	Whole gene deletion	–	−896× coverage
4	Coevolution	Tail fiber	EFV12PHI1_98	Tandem duplication	–	+5× coverage
4	Coevolution	Tail fiber	EFV12PHI1_98	Non-synonymous snp	R1460H	23.9%
4	Coevolution	Capsid and scaffold	EFV12PHI1_97	Non-synonymous snp	N306K	93.5%
1	Phage control	Capsid and scaffold	EFV12PHI1_97	Non-synonymous snp	N306K	81.3%
1	Phage control	Hypothetical protein 8	EFV12PHI1_123	Whole gene deletion	–	−5× coverage
1	Phage control	Hypothetical protein 9	EFV12PHI1_126	Whole gene deletion	–	−5× coverage
2	Phage control	Capsid and scaffold	EFV12PHI1_97	Non-synonymous snp	N306K	90.3%
2	Phage control	Hypothetical protein 8	EFV12PHI1_123	Whole gene deletion	–	−50× coverage
2	Phage control	Hypothetical protein 9	EFV12PHI1_126	Whole gene deletion	–	−48× coverage
3	Phage control	Capsid and scaffold	EFV12PHI1_97	Non-synonymous snp	N306K	92.1%
3	Phage control	Hypothetical protein 8	EFV12PHI1_123	Whole gene deletion	–	−14× coverage
3	Phage control	Hypothetical protein 9	EFV12PHI1_126	Whole gene deletion	–	−12× coverage
4	Phage control	Capsid and scaffold	EFV12PHI1_97	Non-synonymous snp	N306K	86.8%
4	Phage control	Hypothetical protein 8	EFV12PHI1_123	Whole gene deletion	–	−20× coverage
4	Phage control	Hypothetical protein 9	EFV12PHI1_126	Whole gene deletion	–	−18× coverage

All phage mutations are from timepoint 16 in the coevolution and phage control populations. Frequencies given as population frequency for snps and fold coverage increases/decreases in the population for duplications and deletions. Locus tags correspond to GenBank record MH880817.

identified bacterial exopolysaccharide mutations suggestive of hindering phage adsorption and RNA polymerase β' subunit mutations with the potential to disrupt the phage replication cycle. However, we also identified what appears to be an unknown phage escape strategy involving large tandem repeats in the tail fiber gene. While some of the basic dynamics and molecular mechanisms of coevolution appear to be similar across many phage-host pairs (Labrie et al., 2010; Samson et al., 2013), experimental coevolution in this understudied system allowed us to quickly identify unique adaptation strategies.

Coevolving bacteria acquired mutations in the *yqwD2* gene, and we hypothesize that these mutations are at least partially responsible for the resistance phenotype seen in *E. faecium* coevolving with phage EfV12-phi1. The *yqwD2* gene is part of a capsule production operon that is well conserved among Firmicutes; it is known as Yqw in *Bacillus subtilis*, in *Streptococcus pneumoniae*, and Eps in *Streptococcus thermophilus* (Stingele et al., 1996; Bentley et al., 2006; Palmer et al., 2012). In *Streptococcus thermophilus*, the *epsD* gene (35% amino acid identity to *E. faecium yqwD2*) encodes a cytoplasmic tyrosine kinase that regulates the activity of EpsE, a phosphogalactosyltransferase. Disruption of either *epsD* or *epsE* abolished extracellular polysaccharide synthesis (Minic et al., 2007). Mutations in exopolysaccharide production genes have been shown to inhibit phage infection in *E. faecalis* (Teng et al., 2009) and *Lactococcus lactis* (Forde and Fitzgerald, 1999). Interestingly, two of these mutations occurred at residue 58 and one at residue 59 which are the beginning of a conserved nucleotide binding motif (GEGKS) (Stingele et al., 1996). A homologous protein structure within the conserved domain database (CDD) shows that this region of the protein is highly accessible. In line with protein models previously proposed (Stingele et al., 1996), perhaps these mutations interfere with the function of YqwD2, subsequently altering the structure, length, or quantity of exported exopolysaccharides (Bastin et al., 1993; Morona et al., 1995; Minic et al., 2007). While the phage receptor of phage EfV12-phi1 is unknown, distantly related phages *Staphylococcus* phage K and Bacillus phage SP01 bind to cell wall teichoic acids (Yasbin et al., 1976; Estrella et al., 2016). Similarly, phage EfV12-phi1 may bind to certain motifs of exopolysaccharides, so that modification of exopolysaccharides hinders phage adsorption. Further, several

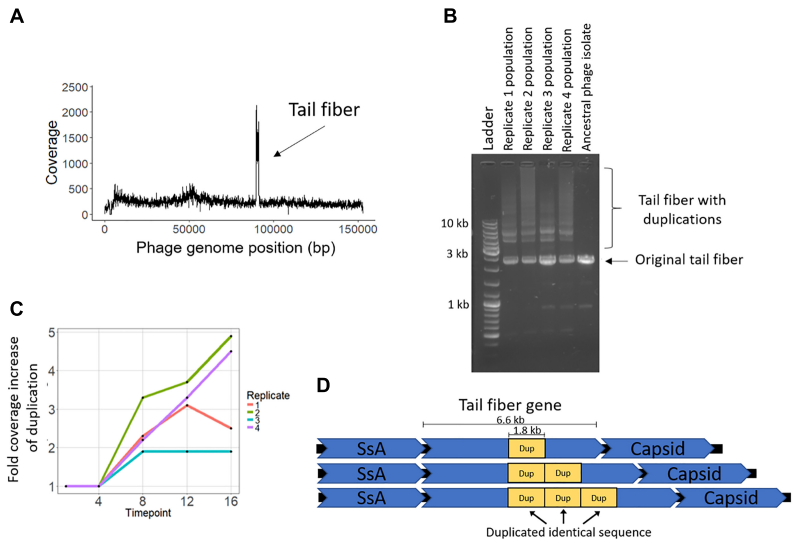

FIGURE 5 | Phage EfV12-phi1 evolved tandem duplications in the tail fiber gene to increase its infectivity. **(A)** Average coverage along the phage genome for the phage population of replicate 2 at the final timepoint. Duplication was first noticed by this spike in sequencing coverage. Reads were mapped to the original phage genome so the duplication in the tail fiber appears as a spike in coverage. **(B)** Duplications in the tail fiber visualized by PCR using primers that flank the tail fiber. Duplications resulted in a larger amplicon. Each replicate population at the final timepoint is shown as well as the ancestral phage. **(C)** Presence of tail fiber duplications over time shown by the fold coverage increase in the duplicated region divided by the average coverage of the rest of the phage genome. **(D)** Schematic of the phage tail fiber tandem duplication within the gene. Reads spanning the tail fiber gene containing up to three duplications (four total copies of duplicated sequence) were seen with MinION long read sequencing.

bacterial mutations that were not conserved among all replicates encoded sugar metabolism and modification functions which could also alter the structure and modifications present on exopolysaccharides. Future genetic knockout experiments will be useful in determining the degree to which these mutations confer resistance.

Coevolving bacteria also acquired mutations in the *rpoC* gene, which encodes the RNA polymerase β' subunit. Phage EfV12-phi1 does not encode its own RNA polymerase, so it needs to interact with the host RNA polymerase both to shut down transcription of host genes and to transcribe phage genes. Mutations in the RNA polymerase *rpoC* gene could be a mechanism to resist phage infection by disrupting RNA polymerase activity. Phages produce proteins to bind or modify host RNA polymerase subunits, including the β' subunit, to shut down host transcription and increase affinity for phage DNA (Mailhammer et al., 1975; Hesselbach and Nakada, 1977; Hodgson et al., 1985; Nechaev and Severinov, 2003). The mutation of residues that are modified or bound by phage proteins during infection could be a mechanism by which *E. faecium* can resist infection by phage EfV12-phi1. Five of the six different *rpoC* mutations observed were unique to single replicates, but all are located near each other in the 3D structure of RpoC, which suggests they all provide resistance to phage EfV12-phi1 through a common mechanism. The mutations in RpoC are localized similarly as the mutations that arise with the genetic suppressors of a protein, DksA that regulates *Escherichia coli* RpoC in response to nutrient availability (Rutherford et al., 2009). This suggests that the bacterial resistance arises through a general RpoC suppression mechanism that reduces phage success although it may not be driven by direct interaction with between phage proteins and RpoC.

The only phage mutations unique to coevolution (and not present in the evolution of phage EfV12-phi1 to naive host) were tandem duplications within a putative tail fiber gene. Myoviruses have short and long tail fibers, the latter of which are responsible for scanning the host cell surface and identifying the receptor. This gene has been confirmed to be the long tail fiber in a closely related phage, phiEF24C (Uchiyama et al., 2011). A point mutation in the homologous tail fiber of phiEF24C was seen to increase adsorption to several strains of *E. faecalis*. The duplication observed in this experiment occurs in a region of the gene that differs between EfV12-phi1 and phiEF24C. Protein homology analysis of the gene indicates a predicted carbohydrate-binding domain 100 nucleotides downstream from the duplicated region, but no conserved domains were predicted within the duplication itself. The duplicated region does not appear to generate sequence diversity which might allow recognition to different bacterial surface receptors, as has been observed in phage λ (Meyer et al., 2012). The timing of EfV12-phi1 tandem duplications suggests that they are a response to the evolution of bacterial resistance to phage infection. Overall, we speculate that phage may respond to bacterial capsule changes through modifications in the tail fiber. Although mutations in the tail fibers are common mechanisms by which phages adapt to modified bacterial receptors (Tétart et al., 1996; Scanlan et al., 2011), examples of duplications as large as the one seen in this study (1.8 kb per duplication) have not been seen before.

Phage therapy has long been a proposed solution to the growing problem of antibiotic resistant bacteria, with recent successful cases of phage therapy in the United States following a compassionate use exemption. However, phage therapy is limited by a lack of well characterized phages infecting human pathogens (Duplessis et al., 2017; Schooley et al., 2017; Zhvania et al., 2017). Phage therapy utilizes phage cocktails, which include a mix of different phages with orthogonal targets to counter the evolution of bacterial resistance. Understanding the dynamics and outcomes of bacteria-phage interactions using experimental coevolution would facilitate phage cocktail design. For example, EfV12-phi1 has broad host-range and selects for *E. faecium* mutations related to exopolysaccharide synthesis, suggesting that a cocktail including EfV12-phi1 would be most effective if the other cocktail phages targeted host structures other than exopolysaccharide.

Phage EfV12-phi1 may have therapeutic potential, given that it is widespread and the host range was previously (Yoong et al., 2004) found to include a wide range of pathogens. Predictability of phage-host interactions is desirable to ensure safety of phages and for phage cocktail design. In this phage-host pair, we observed consistent outcomes from all four replicates, despite the stochasticity of mutations that lead to those outcomes. Nine of the eleven observed bacterial mutations were not shared among all replicates, but the functions encoded by these genes shared similar features (hydrolases, transferases, sugar metabolism/modification).

In these experiments, in just 8 days, we quickly identified phage and host genes that are under selection during coevolution. Experimental manipulation of phage-host interactions, and periodic tracking of their mutational trajectories, offers exceptional insight into the mutational arms race – beyond traditional sequencing and annotation efforts. While coevolution in artificial laboratory conditions may not be reflective of coevolution that happens in a natural environment, learning about the potential outcomes of coevolution provide useful information. As microbial culturing and enumeration becomes increasingly automated, a large number of phage-host interactions can be tested in order to thoroughly investigate the mechanism of phage-host co-evolution in a diversity of clinically relevant hosts. Such insights are critical to the eventual development of phage therapies for clinical use.

DATA AVAILABILITY

All sequencing data has been deposited to the SRA at PRJNA490385. The genome for phage EfV12-phi1 can be found at GenBank: MH880817 and our assembly of *Enterococcus faecium* TX1330 can be found at GenBank assembly accession: GCA_003583905.1.

AUTHOR CONTRIBUTIONS

KW and JM conceptualized and designed the experiments. SW, TG, and CW performed the experiments. SW, AO, and WE did the sequencing analysis. SW, AO, KW, and JM wrote the paper. All authors edited the paper.

FUNDING

This work was supported by a UC Irvine Seed Grant entitled "The evolutionary ecology of the human virome". Stephen Wandro was supported by an NIH T32 training grant (#5T32AI007319-27) from UC Irvine's Center for Viral Research.

ACKNOWLEDGMENTS

We would like to acknowledge Dr. Heather Maughn for thoughtful comments and edits, Dr. Ali Mortazavi and his laboratory for allowing us to use their NextSeq, and Dr. Rich Puxty for guidance on analyzing our sequencing data. Thanks to all the members of the Whiteson Laboratory for providing advice and feedback throughout this project. Thanks to Clark Hendrickson and Cyril Samillano for helping with the final experiments.

SUPPLEMENTARY MATERIAL

The Supplementary Material for this article can be found online at: https://www.frontiersin.org/articles/10.3389/fmicb.2018.03192/full#supplementary-material

REFERENCES

Bankevich, A., Nurk, S., Antipov, D., Gurevich, A. A., Dvorkin, M., Kulikov, A. S., et al. (2012). SPAdes: a new genome assembly algorithm and its applications to single-cell sequencing. *J. Comput. Biol.* 19, 455–477. doi: 10.1089/cmb.2012.0021

Bastin, D. A., Stevenson, G., Brown, P. K., Haase, A., and Reeves, P. R. (1993). Repeat unit polysaccharides of bacteria: a model for polymerization resembling that of ribosomes and fatty acid synthetase, with a novel mechanism for determining chain length. *Mol. Microbiol.* 7, 725–734. doi: 10.1111/j.1365-2958.1993.tb01163.x

Baym, M., Kryazhimskiy, S., Lieberman, T. D., Chung, H., Desai, M. M., and Kishony, R. K. (2015). Inexpensive multiplexed library preparation for megabase-sized genomes. *PLoS One* 10:e0128036. doi: 10.1371/journal.pone.0128036

Bentley, S. D., Aanensen, D. M., Mavroidi, A., Saunders, D., Rabbinowitsch, E., Collins, M., et al. (2006). Genetic analysis of the capsular biosynthetic locus from all 90 pneumococcal serotypes. *PLoS Genet.* 2:e31. doi: 10.1371/journal.pgen.0020031

Bohannan, B. J. M., and Lenski, R. E. (2000). Linking genetic change to community evolution: insights from studies of bacteria and bacteriophage. *Ecol. Lett.* 3, 362–377. doi: 10.1046/j.1461-0248.2000.00161.x

Bouvier, T., and Giorgio, P. A. (2007). Key role of selective viral-induced mortality in determining marine bacterial community composition. *Environ. Microbiol.* 9, 287–297. doi: 10.1111/j.1462-2920.2006.01137.x

Chan, B. K., Sistrom, M., Wertz, J. E., Kortright, K. E., Narayan, D., and Turner, P. E. (2016). Phage selection restores antibiotic sensitivity in MDR *Pseudomonas aeruginosa*. *Sci. Rep.* 6:26717. doi: 10.1038/srep26717

Chevreux, B., Wetter, T., and Suhai, S. (1999). Genome sequence assembly using trace signals and additional sequence information. *Ger. Conf. Bioinformation* 99, 45–56.

Davis, B. M., Lawson, E. H., Sandkvist, M., Ali, A., Sozhamannan, S., and Waldor, M. K. (2000). Convergence of the secretory pathways for cholera toxin and the filamentous phage, CTXphi. *Science* 288, 333–335. doi: 10.1126/science.288.5464.333

Deatherage, D. E., and Barrick, J. E. (2014). Identification of mutations in laboratory-evolved microbes from next-generation sequencing data using breseq. *Methods Mol. Biol.* 1151, 165–188. doi: 10.1007/978-1-4939-0554-6_12

Doron, S., Melamed, S., Ofir, G., Leavitt, A., Lopatina, A., Keren, M., et al. (2018). Systematic discovery of antiphage defense systems in the microbial pangenome. *Science* 359:eaar4120. doi: 10.1126/science.aar4120

Duerkop, B. A., Huo, W., Bhardwaj, P., Palmer, K. L., and Hooper, L. V. (2016). Molecular basis for lytic bacteriophage resistance in enterococci. *mBio* 7:e01304-16. doi: 10.1128/mBio.01304-16.

Duplessis, C., Biswas, B., Hanisch, B., Perkins, M., Henry, M., Quinones, J., et al. (2017). Refractory *Pseudomonas* Bacteremia in a 2-Year-Old sterilized by bacteriophage therapy. *J. Pediatric Infect. Dis. Soc.* 7, 253–256. doi: 10.1093/jpids/pix056

Dy, R. L., Richter, C., Salmond, G. P. C., and Fineran, P. C. (2014). Remarkable mechanisms in microbes to resist phage infections. *Annu. Rev. Virol.* 1, 307–331. doi: 10.1146/annurev-virology-031413-085500

Estrella, L. A., Quinones, J., Henry, M., Hannah, R. M., Pope, R. K., Hamilton, T., et al. (2016). Characterization of novel *Staphylococcus aureus* lytic phage and defining their combinatorial virulence using the OmniLog system. *Bacteriophage* 6:e1219440. doi: 10.1080/21597081.2016.1219440

Forde, A., and Fitzgerald, G. F. (1999). Analysis of exopolysaccharide (EPS) production mediated by the bacteriophage adsorption blocking plasmid, pCI658, isolated from *Lactococcus lactis* ssp. cremoris HO2. *Int. Dairy J.* 9, 465–472. doi: 10.1016/S0958-6946(99)00115-6

Goodwin, S., Wappel, R., and McCombie, W. R. (2017). 1D genome sequencing on the oxford nanopore MinION. *Curr. Protoc. Hum. Genet*. 94, 18.11.1–18.11.14. doi: 10.1002/cphg.39

Hall, A. R., Scanlan, P. D., Morgan, A. D., and Buckling, A. (2011). Host-parasite coevolutionary arms races give way to fluctuating selection. *Ecol. Lett.* 14, 635–642. doi: 10.1111/j.1461-0248.2011.01624.x

Harcombe, W. R., and Bull, J. J. (2005). Impact of phages on two-species bacterial communities. *Appl. Environ. Microbiol.* 71, 5254–5259. doi: 10.1128/AEM.71.9.5254-5259.2005

Hendrickx, A. P. A., Top, J., Bayjanov, J. R., Kemperman, H., Rogers, M. R. C., Paganelli, F. L., et al. (2015). Antibiotic-driven dysbiosis mediates intraluminal agglutination and alternative segregation of *Enterococcus faecium* from the intestinal epithelium. *mBio* 6:e01346-15. doi: 10.1128/mBio.01346-15

Hesselbach, B. A., and Nakada, D. (1977). "Host shutoff" function of bacteriophage T7: involvement of T7 gene 2 and gene 0.7 in the inactivation of *Escherichia coli* RNA polymerase. *J. Virol.* 24, 736–745.

Hodgson, D., Shapiro, L., and Amemiya, K. (1985). Phosphorylation of the beta' Subunit of RNA polymerase and other host proteins upon phicd1 infection of caulobacter crescentus. *J. Virol.* 55, 238–241.

Jarvis, A. W., Collins, L. J., and Ackermann, H. W. (1993). A study of five bacteriophages of the Myoviridae family which replicate on different gram-positive bacteria. *Arch. Virol.* 133, 75–84. doi: 10.1007/BF01309745

Khalifa, L., Brosh, Y., Gelman, D., Coppenhagen-Glazer, S., Beyth, S., Poradosu-Cohen, R., et al. (2015). Targeting *Enterococcus faecalis* biofilms with phage therapy. *Appl. Environ. Microbiol.* 81, 2696–2705. doi: 10.1128/AEM.00096-15

Khalifa, L., Gelman, D., Shlezinger, M., Dessal, A. L., Coppenhagen-Glazer, S., Beyth, N., et al. (2018). Defeating antibiotic- and phage-resistant enterococcus faecalis using a phage cocktail in vitro and in a clot model. *Front. Microbiol.* 9:326. doi: 10.3389/fmicb.2018.00326

Kim, M.-S., Park, E.-J., Roh, S. W., and Bae, J.-W. (2011). Diversity and abundance of single-stranded DNA viruses in human feces. *Appl. Environ. Microbiol.* 77, 8062–8070. doi: 10.1128/AEM.06331-11

Klumpp, J., Lavigne, R., Loessner, M. J., and Ackermann, H.-W. (2010). The SPO1-related bacteriophages. *Arch. Virol.* 155, 1547–1561. doi: 10.1007/s00705-010-0783-0

Koch, S., Hufnagel, M., Theilacker, C., and Huebner, J. (2004). Enterococcal infections: host response, therapeutic, and prophylactic possibilities. *Vaccine* 22, 822–830. doi: 10.1016/j.vaccine.2003.11.027

Koskella, B., and Brockhurst, M. A. (2014). Bacteria-phage coevolution as a driver of ecological and evolutionary processes in microbial communities. *FEMS Microbiol. Rev.* 38, 916–931. doi: 10.1111/1574-6976.12072

Labrie, S. J., Samson, J. E., and Moineau, S. (2010). Bacteriophage resistance mechanisms. *Nat. Rev. Microbiol.* 8, 317–327. doi: 10.1038/nrmicro2315

Langmead, B., and Salzberg, S. L. (2012). Fast gapped-read alignment with Bowtie 2. *Nat. Methods* 9, 357–359. doi: 10.1038/nmeth.1923

Lawe-Davies, O., and Bennett, S. (2017). *WHO Publishes list of Bacteria for Which New Antibiotics are Urgently Needed. Who, 1*. Available at: http://www.who.int/mediacentre/news/releases/2017/bacteria-antibiotics-needed/en/

Mailhammer, R., Yang, H. L., Reiness, G., and Zubay, G. (1975). Effects of bacteriophage T4-induced modification of *Escherichia coli* RNA polymerase on gene expression in vitro. *Proc. Natl. Acad. Sci. U.S.A.* 72, 4928–4932. doi: 10.1073/pnas.72.12.4928

Martiny, J. B. H., Riemann, L., Marston, M. F., and Middelboe, M. (2014). Antagonistic coevolution of marine planktonic viruses and their hosts. *Ann. Rev. Mar. Sci.* 6, 393–414. doi: 10.1146/annurev-marine-010213-135108

Mcshan, W. M., Altermann, E., Hyman, P., Ross, A., and Ward, S. (2016). More is better: selecting for broad host range bacteriophages. *Front. Microbiol* 7:1352. doi: 10.3389/fmicb.2016.01352

Meyer, J. R., Dobias, D. T., Weitz, J. S., Barrick, J. E., Quick, R. T., and Lenski, R. E. (2012). Repeatability and contingency in the evolution of a key innovation in phage lambda. *Science* 335, 428–432. doi: 10.1126/science.1214449

Minic, Z., Marie, C., Delorme, C., Faurie, J. M., Mercier, G., Ehrlich, D., et al. (2007). Control of EpsE, the phosphoglycosyltransferase initiating exopolysaccharide synthesis in Streptococcus thermophilus, by EpsD tyrosine kinase. *J. Bacteriol.* 189, 1351–1357. doi: 10.1128/JB.01122-06

Morona, R., Van den Bosch, L., and Manning, P. A. (1995). Molecular, genetic, and topological characterization of O-antigen chain length regulation in *Shigella flexneri*. *J. Bacteriol.* 177, 1059–1068. doi: 10.1128/jb.177.4.1059-1068.1995

Nale, J., Redgwell, T., Millard, A., and Clokie, M. (2018). Efficacy of an optimised bacteriophage cocktail to clear clostridium difficile in a batch fermentation model. *Antibiotics* 7:13. doi: 10.3390/antibiotics7010013

Nechaev, S., and Severinov, K. (2003). Bacteriophage-induced modifications of host RNA Polymerase. *Annu. Rev. Microbiol.* 57, 301–322. doi: 10.1146/annurev.micro.57.030502.090942

Oechslin, F., Piccardi, P., Mancini, S., Gabard, J., Moreillon, P., Entenza, J. M., et al. (2016). Synergistic interaction between phage therapy and antibiotics clears *Pseudomonas aeruginosa* infection in endocarditis and reduces virulence. *J. Infect. Dis.* 215, 703–712. doi: 10.1093/infdis/jiw632

Palmer, K. L., Godfrey, P., Griggs, A., Kos, V. N., Zucker, J., Desjardins, C., et al. (2012). Comparative Genomics of Enterococci: variation in *Enterococcus faecalis*, Clade Structure in *E. faecium*, and Defining Characteristics of *E. gallinarum* and *E. casseliflavus*. *mBio* 3:e00318-11. doi: 10.1128/mBio.00318-11

Peng, Y., Leung, H. C. M., Yiu, S. M., and Chin, F. Y. L. (2010). "IDBA – A Practical Iterative de Bruijn Graph De Novo Assembler," in *Lecture Notes in Computer Science (including subseries Lecture Notes in Artificial Intelligence and Lecture Notes in Bioinformatics)*, ed. Berger B (Berlin: Springer), 426–440. doi: 10.1007/978-3-642-12683-3_28

Rutherford, S. T., Villers, C. L., Lee, J.-H., Ross, W., and Gourse, R. L. (2009). Allosteric control of *Escherichia coli* rRNA promoter complexes by DksA. *Genes Dev.* 23, 236–248. doi: 10.1101/gad.1745409

Samson, J. E., Magadán, A. H., Sabri, M., and Moineau, S. (2013). Revenge of the phages: defeating bacterial defences. *Nat. Rev. Microbiol.* 11, 675–687. doi: 10.1038/nrmicro3096

Scanlan, P. D. (2017). Bacteria–bacteriophage coevolution in the human gut: implications for microbial diversity and functionality. *Trends Microbiol.* 25, 614–623. doi: 10.1016/j.tim.2017.02.012

Scanlan, P. D., Hall, A. R., Lopez-Pascua, L. D. C., and Buckling, A. (2011). Genetic basis of infectivity evolution in a bacteriophage. *Mol. Ecol.* 20, 981–989. doi: 10.1111/j.1365-294X.2010.04903.x

Schooley, R. T., Biswas, B., Gill, J. J., Hernandez-Morales, A., Lancaster, J., Lessor, L., et al. (2017). Development and use of personalized bacteriophage-based therapeutic cocktails to treat a patient with a disseminated resistant *Acinetobacter baumannii* infection. *Antimicrob. Agents Chemother.* 61:e00954-17. doi: 10.1128/AAC.00954-17

Schrödinger, L. L. C. (2015). *The {PyMOL} Molecular Graphics System, Version∼1.8*. New York, NY: Schrödinger, LLC.

Silva, J. B., Storms, Z., and Sauvageau, D. (2016). Host receptors for bacteriophage adsorption. *FEMS Microbiol. Lett* 363:fnw002. doi: 10.1093/femsle/fnw002

Stern, A., Mick, E., Tirosh, I., Sagy, O., and Sorek, R. (2012). CRISPR targeting reveals a reservoir of common phages associated with the human gut microbiome. *Genome Res.* 22, 1985–1994. doi: 10.1101/gr.138297.112

Stingele, F., Neeser, J. R., Mollet, B., Stingele, F., and Neeser, J. (1996). Identification and characterization of the eps (Exopolysaccharide) gene cluster from Streptococcus thermophilus Sfi6. Identification and Characterization of the eps (Exopolysaccharide) Gene Cluster from *Streptococcus thermophilus* Sfi6. *J. Bacteriol.* 178, 1680–1690. doi: 10.1128/jb.178.6.1680-1690.1996

Teng, F., Singh, K. V., Bourgogne, A., Zeng, J., and Murray, B. E. (2009). Further Characterization of the epa Gene Cluster and Epa Polysaccharides of Enterococcus faecalis. *Infect. Immun.* 77, 3759–3767. doi: 10.1128/IAI.00149-09

Tétart, F., Repoila, F., Monod, C., and Krisch, H. M. (1996). Bacteriophage T4 host range is expanded by duplications of a small domain of the tail fiber adhesin. *J. Mol. Biol.* 258, 726–731. doi: 10.1006/jmbi.1996.0281

Thompson, J. N. (1999). Specific hypotheses on the geographic mosaic of coevolution. *Am. Nat.* 153, S1–S14. doi: 10.1086/303208

Uchiyama, J., Takemura, I., Satoh, M., Kato, S., Ujihara, T., Akechi, K., et al. (2011). Improved adsorption of an *Enterococcus faecalis* Bacteriophage ΦEF24C with a spontaneous point mutation. *PLoS One* 6:e26648. doi: 10.1371/journal.pone.0026648

Van Tyne, D., and Gilmore, M. S. (2014). A delicate balance: maintaining mutualism to prevent disease. *Cell Host Microbe* 16, 425–427. doi: 10.1016/J.CHOM.2014.09.019

Viertel, T. M., Ritter, K., and Horz, H. P. (2014). Viruses versus bacteria-novel approaches to phage therapy as a tool against multidrug-resistant pathogens. *J. Antimicrob. Chemother.* 69, 2326–2336. doi: 10.1093/jac/dku173

Wattam, A. R., Davis, J. J., Assaf, R., Boisvert, S., Brettin, T., Bun, C., et al. (2017). Improvements to PATRIC, the all-bacterial bioinformatics database and analysis resource center. *Nucleic Acids Res.* 45, D535–D542. doi: 10.1093/nar/gkw1017

Wright, A., Hawkins, C. H., Änggård, E. E., and Harper, D. R. (2009). A controlled clinical trial of a therapeutic bacteriophage preparation in chronic otitis due to antibiotic-resistant *Pseudomonas aeruginosa*; A preliminary report of efficacy. *Clin. Otolaryngol.* 34, 349–357. doi: 10.1111/j.1749-4486.2009.01973.x

Yasbin, R. E., Maino, V. C., and Young, F. E. (1976). Bacteriophage resistance in Bacillus subtilis 168, W23, and interstrain transformants. *J. Bacteriol.* 125, 1120–1126.

Yen, M., Cairns, L. S., and Camilli, A. (2017). A cocktail of three virulent bacteriophages prevents *Vibrio cholerae* infection in animal models. *Nat. Commun.* 8:14187. doi: 10.1038/ncomms14187

Yoong, P., Schuch, R., Nelson, D., and Fischetti, V. A. (2004). Identification of a broadly active phage lytic enzyme with lethal activity against antibiotic-resistant *Enterococcus faecalis* and *Enterococcus faecium*. *J. Bacteriol.* 186, 4808–4812. doi: 10.1128/JB.186.14.4808-4812.2004

Zerbino, D. R., and Birney, E. (2008). Velvet: algorithms for de novo short read assembly using de Bruijn graphs. *Genome Res.* 18, 821–829. doi: 10.1101/gr.074492.107

Zhvania, P., Hoyle, N. S., Nadareishvili, L., Nizharadze, D., and Kutateladze, M. (2017). Phage therapy in a 16-year-old boy with netherton syndrome. *Front. Med.* 4:94. doi: 10.3389/fmed.2017.00094

Conflict of Interest Statement: The authors declare that the research was conducted in the absence of any commercial or financial relationships that could be construed as a potential conflict of interest.

frontiers in Microbiology

ORIGINAL RESEARCH
published: 18 January 2019
doi: 10.3389/fmicb.2018.03227

The Ability of Lytic Staphylococcal Podovirus vB_SauP_phiAGO1.3 to Coexist in Equilibrium With Its Host Facilitates the Selection of Host Mutants of Attenuated Virulence but Does Not Preclude the Phage Antistaphylococcal Activity in a Nematode Infection Model

*Aleksandra Głowacka-Rutkowska[1], Agnieszka Gozdek[1], Joanna Empel[2], Jan Gawor[3], Karolina Żuchniewicz[3], Aleksandra Kozińska[2†], Janusz Dębski[4], Robert Gromadka[3] and Małgorzata Łobocka[1,5]**

[1] Department of Microbial Biochemistry, Institute of Biochemistry and Biophysics, Polish Academy of Sciences, Warsaw, Poland, [2] Department of Epidemiology and Clinical Microbiology, National Medicines Institute, Warsaw, Poland, [3] Laboratory of DNA Sequencing and Oligonucleotide Synthesis, Institute of Biochemistry and Biophysics, Polish Academy of Sciences, Warsaw, Poland, [4] Laboratory of Mass Spectrometry, Institute of Biochemistry and Biophysics, Polish Academy of Sciences, Warsaw, Poland, [5] Autonomous Department of Microbial Biology, Faculty of Agriculture and Biology, Warsaw University of Life Sciences, Warsaw, Poland

OPEN ACCESS

Edited by:
Robert Czajkowski,
University of Gdańsk, Poland

Reviewed by:
Simon Roux,
Joint Genome Institute (JGI), United States
Konstantin Anatolievich Miroshnikov,
Institute of Bioorganic Chemistry (RAS), Russia

***Correspondence:**
Małgorzata Łobocka
lobocka@ibb.waw.pl

†Present address:
Aleksandra Kozińska,
Department of Drug Biotechnology and Bioinformatics, National Medicines Institute, Warsaw, Poland

Specialty section:
This article was submitted to Virology, a section of the journal Frontiers in Microbiology

Received: 30 September 2018
Accepted: 12 December 2018
Published: 18 January 2019

Citation:
Głowacka-Rutkowska A, Gozdek A, Empel J, Gawor J, Żuchniewicz K, Kozińska A, Dębski J, Gromadka R and Łobocka M (2019) The Ability of Lytic Staphylococcal Podovirus vB_SauP_phiAGO1.3 to Coexist in Equilibrium With Its Host Facilitates the Selection of Host Mutants of Attenuated Virulence but Does Not Preclude the Phage Antistaphylococcal Activity in a Nematode Infection Model. Front. Microbiol. 9:3227. doi: 10.3389/fmicb.2018.03227

Phage vB_SauP_phiAGO1.3 (phiAGO1.3) is a polyvalent *Staphylococcus* lytic podovirus with a 17.6-kb genome (Gozdek et al., 2018). It can infect most of the *Staphylococcus aureus* human isolates of dominant clonal complexes. We show that a major factor contributing to the wide host range of phiAGO1.3 is a lack or sparcity of target sites for certain restriction-modification systems of types I and II in its genome. Phage phiAGO1.3 requires for adsorption β-*O*-GlcNAcylated cell wall teichoic acid, which is also essential for the expression of methicillin resistance. Under certain conditions an exposure of *S. aureus* to phiAGO1.3 can lead to the establishment of a mixed population in which the bacteria and phages remain in equilibrium over multiple generations. This is reminiscent of the so called phage carrier state enabling the co-existence of phage-resistant and phage-sensitive cells supporting a continuous growth of the bacterial and phage populations. The stable co-existence of bacteria and phage favors the emergence of phage-resistant variants of the bacterium. All phiAGO1.3-resistant cells isolated from the phage-carrier-state cultures contained a mutation inactivating the two-component regulatory system ArlRS, essential for efficient expression of numerous *S. aureus* virulence-associated traits. Moreover, the mutants were unaffected in their susceptibility to infection with an unrelated, polyvalent *S. aureus* phage of the genus *Kayvirus*. The ability of phiAGO1.3 to establish phage-carrier-state cultures did not

preclude its antistaphylococcal activity *in vivo* in an *S. aureus* nematode infection model. Taken together our results suggest that phiAGO1.3 could be suitable for the therapeutic application in humans and animals, alone or in cocktails with *Kayvirus* phages. It might be especially useful in the treatment of infections with the majority of methicillin-resistant *S. aureus* strains.

Keywords: ArlRS, bacteriophage carrier state, bacteriophage host range, biofilm, *Caenorhabditis elegans* infection model, phage therapy, restriction-modification systems, *Staphylococcus Rosenblumvirus* genus phage

INTRODUCTION

Staphylococcus aureus is among the most challenging bacterial pathogens that cause various types of infections mainly in humans but also in animals (Springer et al., 2009; Otto, 2012). It has developed resistance to virtually all categories of antibiotic available for clinical use, but only methicillin-resistant *S. aureus* (MRSA) has reached epidemic proportions globally and has become a major worldwide problem (Mandell et al., 2010). MRSA strains are common both in nosocomial and in community settings (Bal et al., 2016). The limitation of effective MRSA treatment options with antibiotics often leads to the development of chronic infections and is a cause of increased mortality, longer hospital stays and higher health care costs as compared to methicillin-sensitive *S. aureus* (MSSA) strains (Cosgrove et al., 2003; de Kraker et al., 2011).

One of the alternative approaches to curing infections with antibiotic-resistant *S. aureus* strains is the use of lytic bacteriophages (Borysowski et al., 2011; Kaźmierczak et al., 2014). These are natural parasites of bacteria that can specifically infect and kill their host but are harmless to eukaryotic cells. Numerous cases of successful treatment of *S. aureus* infections with bacteriophages in animals (Iwano et al., 2018; reviewed by Barrera-Rivas et al., 2017) and in humans (d'Herelle, 1931a,b; MacNeal and Frisbee, 1936a,b; Sauve, 1936; Międzybrodzki et al., 2012; Fadlallah et al., 2015; Fish et al., 2016; reviewed by Kaźmierczak et al., 2014) have been described.

Several phages from the order *Caudovirales,* of a complex virion structure comprising head and tail, are obligatorily lytic on *S. aureus* hosts and cannot transfer bacterial DNA by transduction. Thus, they can potentially be used in therapy (reviewed by Łobocka et al., 2012). Most of them have a long, contractile tail and have been currently classified to the family *Herelleviridae* (Barylski et al., 2018). Some, less numerous and including only 14 isolates of sequenced genomes have a short tail (Vybiral et al., 2003; Kwan et al., 2005; Son et al., 2010; Kraushaar et al., 2013; Swift and Nelson, 2014; Wang et al., 2016; Gozdek et al., 2018). They belong to the *Picovirinae* subfamily of family *Podoviridae* (Lavigne et al., 2008). Those that infect *S. aureus* are much alike, despite being isolated in different geographical regions (Kraushaar et al., 2013), and have been affiliated to the *Rosenblumvirus* genus, subfamily *Picovirinae* (formerly 44AHJD-like phages or 68-like phages) (Lavigne et al., 2008; Gozdek et al., 2018).

The best known representative of *Picovirinae* is a model *Bacillus* phage phi29. However, the similarities between phi29 and the staphylococcal *Picovirinae* are limited to a similar genome size (17–20 kb) and tail morphology, partially conserved synteny between the genomes and the presence of terminal DNA repeats, protein-primed DNA replication and also structural homologies between certain proteins (Vybiral et al., 2003; Lavigne et al., 2008; Kraushaar et al., 2013). Functions of about half of the proteins encoded by the staphylococcal phages could be predicted based on their homology. The major head protein, receptor binding protein (RBP) and two virion proteins of unknown function were identified by proteomic studies (Uchiyama et al., 2017; Štveráková et al., 2018).

The interactions of the staphylococcal *Picovirinae* phages with their host cells are only beginning to be understood. Their adsorption to the cell surface requires a specific glycosylation pattern of the wall teichoic acid (WTA), which depends on the activity of *tarM*- or *tarS*-encoded glycosyltransferases catalyzing α-*O*-GlcNAcylation and β-*O*-GlcNAcylation of WTA, respectively (Li et al., 2015). Studies on the adsorption requirements of various *Rosenblumvirus* phages and the results of phylogenetic analysis of their RBPs allowed distinguishing two subgroups: phages that require β-*O*-GlcNAcylation of WTA for adsorption (SAP-2, SLPW, S13′, SCH1, Psa3, GRCS, 44AHJD, P68 and 66), and phages that adsorb to α-*O*-GlcNAcylated as well as β-*O*-GlcNAcylated WTA (S24-1 and BP39) (Li et al., 2015; Uchiyama et al., 2017). Consistent with the adsorption-promoting TarS-mediated WTA modification and adsorption-inhibiting TarM-mediated WTA modification some phages of subgroup I have also been shown to infect strains of *Staphylococcus xylosus* and *Staphylococcus equorum*, which encode homologs of *S. aureus* TarS but lack genes encoding homologs of TarM (Li et al., 2015). A phage tail lysin contributes to the penetration of phage DNA into the host cell. Another protein is associated with the DNA ends (Vybiral et al., 2003). Based on the homologies between DNA polymerases and between certain structural proteins of phi29 and *Rosenblumvirus* phages the lytic development of the latter is assumed to be similar to that of phi29, albeit it has not been studied. Cell lysis allowing phage release depends on phage endolysin, whose gene is located within a cluster of morphogenesis genes, unlike in phi29 (Lavigne et al., 2008).

Studies on the antistaphylococcal activity of *Rosenblumvirus* genus phages *in vivo* are sparce. One of these phages, S13', was demonstrated to have a life-prolonging effect on *S. aureus*-infected silkworm larvae and protected about 40–50% of mice infected with *S. aureus* from death, including the death from lung-derived septicemia (Takemura-Uchiyama et al., 2013, 2014). Endolysin of another phage, SAP-2, was active in decreasing the biofilm mass of various *S. aureus* and *S. epidermidis* strains,

as estimated in visual assay experiments (Son et al., 2010). Its lytic activity against various strains was wider than that of the parental phage. Little is known about the phage–bacteria interactions leading to severe limitation of bacterial growth without, however, threatening the phage with extinction due to elimination of its host. To fill in this gap we characterized here an additional phage of this genus, phiAGO1.3. We have identified its properties contributing to the wide host-strain range, and show its atypical strategy of co-existence with the host. Additionally, we demonstrate that this strategy not only does not preclude the antistaphylococcal activity of phiAGO1.3 *in vivo* but even leads to the selection of bacterial mutants of attenuated virulence.

MATERIALS AND METHODS

Phage, Bacterial, and Nematode Strains and Culture Conditions

Staphylococcus aureus podovirus vB_SauP_phiAGO1.3 (phiAGO1.3) used in this study was isolated earlier by us from Warsaw sewage (Golec et al., 2011; Gozdek et al., 2018). However, using primers specific for temperate phages of various integrase types (Goerke et al., 2009) we identified a prophage/phage of Φ55 integrase type in the bacterial strain used for phiAGO1.3 propagation (2064/05), and in the phiAGO1.3-derived lysates of this strain (data not shown). To avoid contamination with this phage, strain 80wphwpl, which had been cured of active prophages and plasmids and whose genomic sequence had been determined (Łobocka et al., 2016) was used for phiAGO1.3 propagation in the present study. The monoclonality of the starting phiAGO1.3 preparations obtained from 80wphwpl cells was confirmed by negative results of PCR with a primer pair specific for the 2064/05-derived prophage (data not shown). Another phage used in this study, A5W, is a representative of *Kayvirus* genus and was described previously (Łobocka et al., 2012). The list of *Staphylococcus* spp. reference strains and *S. aureus* strains used in this study is given in **Supplementary Table 1** and **Figure 1**, respectively. Of 75 *S. aureus* strains used, 74 strains came from the MICROBANK collection of the National Medicines Institute (NMI), Warsaw, Poland. Sixty six of them comprised clinical strains isolated from inpatients between 1999 and 2011. Eight of them were from nasal colonization in human (n = 5), from environmental samples (n = 2), and from bovine mastitis (n = 1). The isolates were characterized, at the phenotypic and molecular level; they represented 14 genetic lineages (MLST-Clonal Compexes [CCs]: CC1, CC5, CC7, CC8, CC8/239, CC9, CC15, CC22, CC30, CC45, CC59, CC97, CC121, and CC398). Thirty five isolates resistant to methicillin (MRSA) were assigned to 27 MRSA clones. They included hospital-, community- or livestock-associated representatives of 10 CCs (CC1, CC5, CC7, CC8, CC8/239, CC22, CC30, CC45, CC59, and CC398). Methicillin-susceptible *S. aureus* (MSSA) isolates (n = 39) belonged to all CCs with the exception of CC8/239. *S. aureus* strain RN4220 (CC8) is a restriction-modification deficient and prophage-free derivative of NCTC8325 described previously (Kreiswirth et al., 1983; Nair et al., 2011). Bacteria were grown at 37°C with constant shaking (200 rpm) in Luria-Bertani broth (LB; Difco), in brain heart infusion broth (BHI; Oxoid) or in trypticase soy broth (TSB; Difco), as indicated.

A standard laboratory *Caenorhabditis elegans* strain Bristol N2 (wild-type) was used as a model host for *S. aureus* infection in all experiments. It was obtained from the Caenorhabditis Genetics Center (CGC), University of Minnesota. The nematodes were maintained on NGM agar medium and fed *E. coli* strain OP50 as described elsewhere (Sulston and Hodgkin, 1988).

Phage Propagation

To ensure the lack of contamination of phiAGO1.3-containing cell lysates with temperate phages or plasmid DNA the phage that was originally obtained by propagation in *S. aureus* 2064/05 (Gozdek et al., 2018) was passaged several times from a single plaque through *S. aureus* 80wphwpl, and lysates were verified for the absence of 2064/05-derived phage DNA by PCR with 2064/05-prophage (integrase type Φ55) specific primer pair (Goerke et al., 2009). Only confirmed monoclonal lysates were used for phiAGO1.3 propagation on a larger scale in 80wphwpl cells.

Phage Purification

Cell lysate containing phages (50 ml, 10^{11} PFU/ml) was filtered through 0.22-μm pore size membrane (MILLEX® GS) and treated with RNase A (PureLink RNase, Invitrogen) and DNase (Turbo DNase, Ambion) (final concentration 20 μg/ml of each) at 37°C for 2 h. Next, the lysate was supplemented with polyethylene glycol (PEG6000) and NaCl to final concentrations of 10% and 1 M, respectively, and incubated on ice for 24 h. Samples were centrifuged (10,000 × g, 30 min, 4°C) and the pellet was resuspended in phosphate buffered saline (PBS: 10 mM Na_2HPO_4, 137 mM NaCl, 2.7 mM KCl, 2 mM KH_2PO_4 at pH 7.4).

Determination of Bacteriophage Host Range With a Spot Test

Overnight cultures of various *S. aureus* strains in LB medium (0.2 ml) were supplemented with $CaCl_2$ and $MgSO_4$ to the final concentration of 2.5 mM each, mixed with 1 ml LB and 8 ml molten LCA (55°C), overlaid on LB agar medium in Petri dishes, and left to solidify. Lysates containing phages were standardized by diluting in LB to obtain the titer of 10^8, 10^6, and 10^4 PFU/ml. Ten microliters of each lysate at each dilution was spotted on the cell layer of each strain. Plates were incubated overnight at 37°C, and the number and morphology of plaques were determined.

Assays of Bacteriophage Lytic Activity in Liquid Cultures of *S. aureus*

Overnight cultures of various *S. aureus* strains were diluted 1:100 in fresh LB medium supplemented with $CaCl_2$ and $MgSO_4$ (2.5 mM each). Aliquots of each culture (190 μl) were added to wells of sterilized honeycomb plates and incubated in a Bioscreen C Microbiology Plate Reader (Growth Curves USA, Piscataway Township, NJ, United States) at 37°C until the optical density (OD_{600}) reached ca. 0.2. The cultures were then supplemented

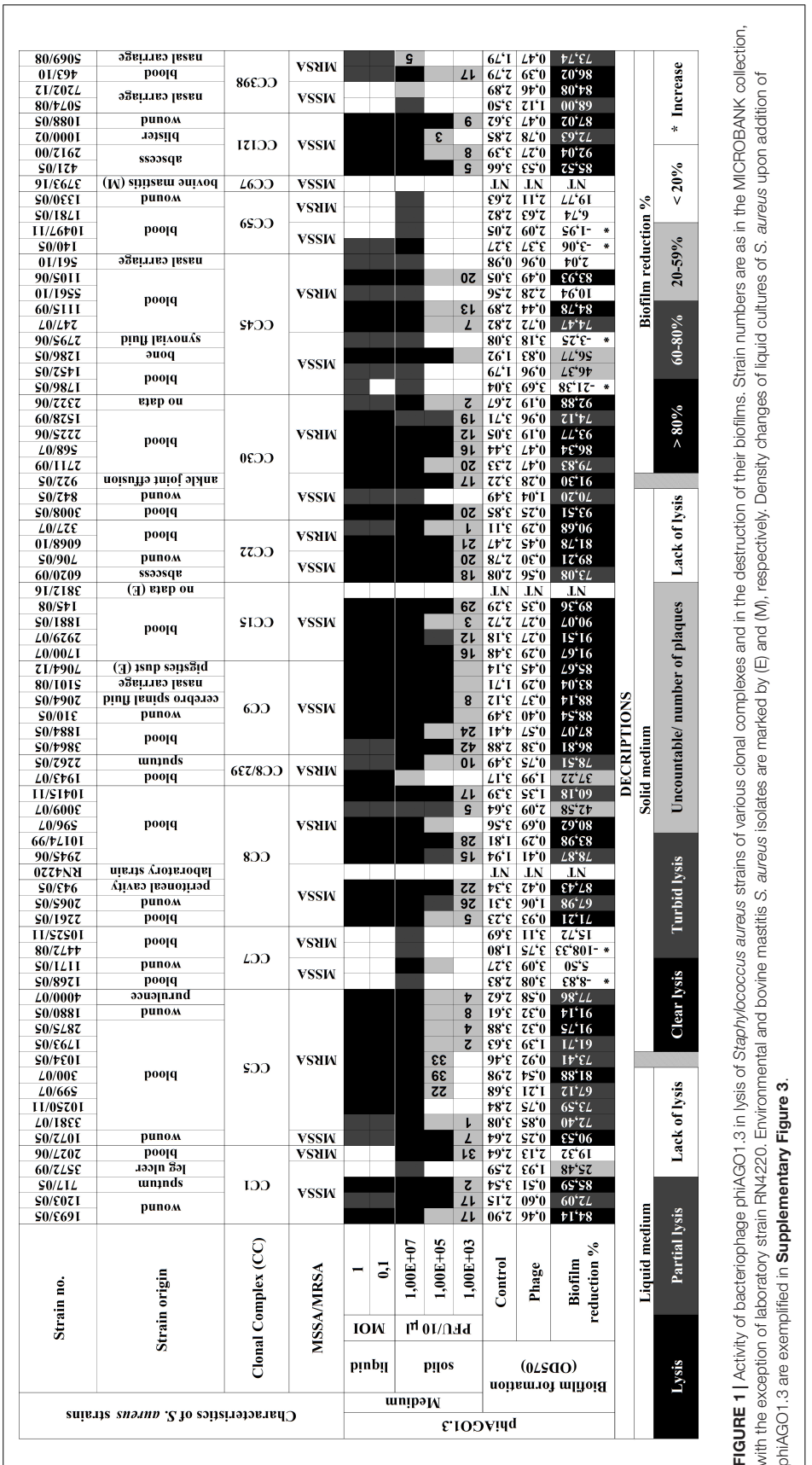

FIGURE 1 | Activity of bacteriophage phiAGO1.3 in lysis of *Staphylococcus aureus* strains of various clonal complexes and in the destruction of their biofilms. Strain numbers are as in the MICROBANK collection, with the exception of laboratory strain RN4220. Environmental and bovine mastitis *S. aureus* isolates are marked by (E) and (M), respectively. Density changes of liquid cultures of *S. aureus* upon addition of phiAGO1.3 are exemplified in **Supplementary Figure 3**.

with the phage at MOI of about 0.1 and 1 by the addition of 10 μl of an appropriately diluted lysate or LB (control samples). The cultures were left for 10 min at room temperature (RT) without shaking to allow for phage adsorption, and then were incubated as above with medium intensity shaking for 24 h. The optical density of the cultures was measured during the whole experiment in 15-min intervals.

Assay of Bacteriophage Influence on Preformed *S. aureus* Biofilms

The ability of phiAGO1.3 to disrupt preformed *S. aureus* biofilm was assayed as described previously (Stepanovic et al., 2000), with some modifications. *S. aureus* scraped from fresh LB agar plate was inoculated in 1 ml of BHI containing 2% sucrose, incubated overnight at 37°C without shaking and diluted 1:100 in fresh medium. Aliquots of bacterial suspension (100 μl) were transferred to wells of sterile 96-well flat-bottom polystyrene plates (Greiner Bio-One, Germany) containing a preformed fibrinogen layer (50 μg fibrinogen in 100 μl of water per well, incubated for 24 h at 4°C and carefully aspirated). Bacterial biofilm was allowed to form for 24 h at 37°C without agitation. The wells were then carefully washed twice with 200 μl of phosphate buffered saline (PBS). Next, 100 μl of diluted bacterial lysate containing phage (10^8 PFU/ml) or LB (control) was added, the plates were incubated for 24 h as above and washed twice with PBS. The biofilm was fixed with 200 μl of 99% methanol for 15 min, drained, left to dry at 50°C for 1 h, and then stained with 0.01% crystal violet (CV; 200 μl) for 15 min. Excess CV was removed by washing three times with water and the wells were air-dried. The amount of CV bound by the biofilm was quantified by solubilizing in 200 μl of 33% acetic acid for 10 min followed by determination of the optical density of the obtained solution at 570 nm using a microplate reader (Bio-tek Synergy^{TM} HT).

Killing Assay

The fraction of bacteria surviving phage infection was determined by killing assay, as described previously (Carlson, 2004; Abedon, 2017), with some modifications. Briefly, 80wphwpl culture (10 ml, OD_{600} of about 0.4) was infected with phiAGO1.3 at MOI 1 and 10 and left for 15 min at RT to allow for phage adsorption. The same volume of uninfected culture was used as a control. Samples were placed on ice, immediately serially diluted 10-fold in cold LB and spread on LB agar plates. The plates were incubated at 37°C for 24 h and bacterial colonies formed were counted. The fraction of surviving cells was calculated based on the ratio between the number of colonies formed by cells from infected and uninfected cultures.

Identification of Phage-Releasing Colonies

Single *S. aureus* colonies recovered following phage infection described as above, were transferred onto a top agar overlay of strain 80wphwpl, incubated overnight at 37°C and checked for the presence of a lysis zone – a hallmark of spontaneous phage release. The presence of phiAGO1.3 was additionally verified by PCR with phage-specific primers. Briefly, candidate colonies were suspended in 100 μl of ice-cold water, and 1 μl of the suspension was used as a source of template for the DNA amplification with primers OMLO707 5′-TGCATGGCTTGTTTTGCTAAAGC-3′ and OMLO708 5′-ACAAGCWGGACAACCGTCTTGGT-3′. PCR conditions were as follows: 95°C for 15 min (95°C for 30 s, 55°C for 30 s, 75°C for 1 min) × 30, 75°C for 7 min.

Determination of Phage Carrier State Stability

To evaluate the stability of the phage carrier state the fraction of cells retaining phiAGO1.3 following consecutive cell divisions was determined. Briefly, phage-releasing colony (designated as FTpt further in this manuscript) identified as above was suspended in 100 μl of cold water, placed on ice, immediately serially diluted 10-fold in cold LB and spread on LB agar plates. The plates were incubated at 37°C for 24 h, and colonies formed (designated as first generation: G_1) were transferred onto a top agar overlay of strain 80wphwpl. After overnight incubation at 37°C, the percentage of phage-producing colonies (FTpt) in G_1 population was determined. The procedure was repeated six times starting each time from cells of one phage-producing colony.

Evaluation of phiAGO1.3 Efficacy in Curing *S. aureus*-Infected Nematodes

The ability of phiAGO1.3 to cure nematodes infected with *S. aureus* 80wphwpl was assayed as previously described (Łobocka et al., 2014b), with some modifications. An overnight tryptic soy broth (TSB) bacterial culture was diluted 1:100 in fresh medium and 100 μl was spread on a 5.5-cm diameter tryptic soy agar (TSA) plate and incubated at 37°C for 24 h. *C. elegans* larvae at T4 stage taken from a synchronized culture were transferred to a lawn of *S. aureus* cells and incubated at 25°C for 24 h. The infected nematodes were then rinsed from the plates, placed on a nylon mesh (CellMicroSieves, BioDesign) with 10-μm pores, washed twice with 5 ml of LB medium, and transferred onto a TSA plate. Then, they were covered with 5 ml of phage lysate (10^9 PFU/ml) or LB medium (control), and incubated at RT for 1 h. The nematodes were then washed on a nylon mesh as above, transferred onto a TSA plate and left to dry. Twenty worms were picked randomly using a platinum wire pick and transferred to a fresh TSA plate. The plates were incubated at 25°C and scored for live and dead worms in 24-h intervals.

Isolation of *S. aureus* DNA

Bacteria were harvested from overnight cultures (3 ml) by centrifugation (10,000 × *g* for 10 min) and resuspended in 200 μl of TE buffer (10 mM Tris-HCl, 1 mM EDTA, pH 8.0). Lysostaphine (Sigma) and RNase (Invitrogen) was added to 200 and 10 μg/ml, respectively, the sample was shaked vigorously and incubated at 37°C until the culture lysed. DNA was extracted using the EXTRACTME kit for genomic DNA isolation from bacteria (Blirt DNA-Gdańsk, Poland), according to manufacturer's guidelines. DNA quality and quantity was checked by agarose gel electrophoresis.

S. aureus Genomic DNA Sequencing, and Sequence Assembly and Analysis

Staphylococcus aureus genomic DNA was sheared mechanically to ∼600–700 bp and used for Paired-End TruSeq-like library construction using a KAPA Library preparation kit (KAPA/Roche, Basel, Switzerland) following manufacturer's instructions. The library was sequenced in the paired-end mode (v3, 600 cycle chemistry kit) on a MiSeq instrument (Illumina, San Diego, CA, United States). Sequence reads were filtered by quality using the ultra-fast FASTQ preprocessing toolkit, fastp version 0.14.1 (Chen et al., 2018[1]). As an additional stage, performed only for the clone of control 80wphwpl strain used in this study (designated as 80wphwpl_v1), long reads were generated to aid genome assembly using a MinION nanopore sequencing instrument (Oxford Nanopore Technologies, Oxford, United Kingdom). Approximately 1 μg of unsheared DNA was used for library preparation using the ONT Rapid Barcoding sequencing kit (SQK-RBK004). Nanopore sequencing was performed using the NC_48h_Sequencing_Run_FLO-MIN106_SQK-RBK004 protocol (MinKnow version 2.2) and R9.4.1 MinION flowcell. Raw nanopore data was basecalled using Albacore v2.3.1 (Oxford Nanopore Technologies, Oxford, United Kingdom). Following quality filtering and sequencing adapter removal using Porechop[2] 17,527 barcoded reads remained. The median read length of the obtained dataset (132,564,821 of bases in total) was 5,649 bases. Long nanopore reads were assembled in a hybrid mode with the Illumina data using Unicycler v.0.4.6 (Wick et al., 2017). Genome hybrid assembly resulted in a single circular replicon. The suspected errors in the genome assembly, especially in genes containing tandem repeats, were verified by PCR amplification of relevant DNA fragments followed by Sanger sequencing on an ABI3730xl Genetic Analyzer (Life Technologies, United States) using BigDye Terminator Mix v. 3.1 chemistry (Life Technologies, United States). Missassemblies were further corrected using Seqman software (DNAStar, United States) to obtain the complete nucleotide sequence of 80wphwpl_v1 (2,732,618 bp). This newly generated consensus sequence of the parent strain genome was used as a template for the genomic sequence assembly of the *S. aureus* isolates resistant to infection with phiAGO1.3. Desktop software Geneious 11.0.4 (Biomatters, Ltd., Auckland, New Zealand) was used for the assembly. The alignments obtained served for the detection of differences between the mutants and the parental strain. Additional inspection of the sequence reads in the alignments served to exclude the ambiguities in the consensus sequence of the reference and mutant strains in the regions of detected mutations.

RESULTS

Basic Characteristics of phiAGO1.3

Bacteriophage phAGO1.3 was originally isolated from sewage as an obligatorily lytic phage capable of infecting most *S. aureus* strains from a small collection of clinical isolates (Gozdek et al., 2018).

Measurement of typical phage growth parameters revealed that phiAGO1.3 could be a potential candidate for therapeutic applications. It can adsorb quickly to its host cells and has a short latent period (∼30 min) (**Supplementary Figure 1**). Its burst size was estimated to be about 35. Additionally, its titer in the lysate did not change significantly after 1 h of incubation at 37 or 50°C or at pH from 5 to 9 (**Supplementary Figure 2**). Only incubation at temperatures of 60°C or higher or at pH below four or above 10 caused a drastic decrease of the phage activity. The optimal MOI for phiAGO1.3 propagation in *S. aureus* 80wphwpl was determined to be 0.01 (data not shown).

Coding Potential of phiAGO1.3 and Analysis of Its Structural Proteome

The genome of phiAGO1.3 encodes 20 proteins (Gozdek et al., 2018). Their homologs are found in various *Picovirinae* that infect *S. aureus*. Phages GRCS and PSa3, which, respectively, encode eight and seven of them, appear to be the closest relatives of phiAGO1.3 at the protein sequence level (**Supplementary Table 2**). Close homologs of all phiAGO1.3 proteins are also encoded by prototypical *Rosenblumvirus* phages 44AHJD or 68. Eleven of the phiAGO1.3 proteins are virion components, as identified by a mass spectrometry analysis of tryptic peptides of whole virions (**Supplementary Table 3**). Homologs of nine of them, including the major capsid protein, two tail proteins, lower and upper collar protein, RBP and tail amidase, have been identified or predicted previously as virion proteins of related phages (Vybiral et al., 2003; Takemura-Uchiyama et al., 2013; Uchiyama et al., 2014; Štveráková et al., 2018). The two additional virion proteins of phiAGO1.3 identified in this work (ORF01 and ORF07) are present in virions in a small amount as suggested by the small number of their peptides in analyzed samples (**Supplementary Table 3**). They have counterparts in related staphylococcal phages, but do not have apparent homologies to proteins of known function. One of them could act as the terminal protein priming the phage DNA replication, by analogy to phi29. DNA termini of phage 68, closely related to phiAGO1.3, have been shown to be covalently bound to a protein (Vybiral et al., 2003). A virion protein of phiAGO1.3 that might somehow contribute to the host specificity is ORF20. It appears to be, besides the tail fiber protein (ORF13), the most variable part of *S. aureus Rosenblumvirus* phages' virions. It is a highly acidic protein, which in phiAGO1.3 contains six repeats of ES/LTE amino acid sequence motif. The variability of ORF20 and its homologs in *S. aureus* phages results partly from the differences in the number of these repeats.

Determination of phiAGO1.3 Lytic Spectrum

Certain polyvalent staphylococcal phages infect representatives of various *Staphylococcus* sp. Thus, we tested the sensitivity of 12 selected type strains of *Staphylococcus* spp. other than *S. aureus* to phiAGO1.3 (**Supplementary Table 1**). The phage infected productively one of the two tested strains of *Staphylococcus*

[1]http://dx.doi.org/10.1101/274100

[2]https://github.com/rrwick/Porechop

hyicus, which like *S. aureus* belongs to coagulase-positive staphylococci, and, surprisingly, a type strain of a coagulase-negative *Staphylococcus–Staphylococcus lugdunensis* (DSM No. 4804, data not shown).

To evaluate the potential of phiAGO1.3 to control *S. aureus* we tested its lytic activity against agar-embedded cells, planctonic cells and biofilms of 75 *S. aureus* clinical isolates from a diversified collection (**Figure 1**). The phage infected productively 55 (73%) of those strains when tested by a spot test, as indicated by the formation of a lysis zone at high phage doses (10^7–10^5 PFU/10 μl), and single plaques or confluent plaques with some borders between them visible at lower phage doses. In the assays of the phage lytic activity in liquid culture a significant decrease of the culture density was observed for 61 (81%) of strains upon addition of phiAGO1.3 (**Figure 1** and **Supplementary Figure 3**). This difference in the number of susceptible strains is likely caused by the low efficiency of infection of some of them (e.g., 10250/11) resulting from the action of their restriction systems. Conceivably, the initial infection required some population phages to break the restriction barrier of the infected strain. This in turn could lead to the lytic development of the phage and the release of appropriately modified progeny phages able to infect cells of this strain efficiently. Such effect of a lack of strain-specific DNA modifications in the phage DNA has been observed previously for other staphylococcal obligatorily lytic phages (see, e.g., Pantůček et al., 1998).

The pattern of the culture density changes upon addition of phiAGO1.3 differed for different *S. aureus* strains. In the case of 44 strains all or nearly all cells in the culture underwent lysis (**Supplementary Figure 3A**). For the remaining 17 strains the drop in culture density, even at MOI 1, was small and followed by a plateau (**Supplementary Figure 3B**) suggesting that productive infection of some cells may be accompanied by the continuous growth of uninfected or resistant cells.

Fourteen of 75 strains tested did not lyse in liquid cultures upon addition of phiAGO1.3 (**Figure 1** and **Supplementary Figure 3C**). Additionally, we could not obtain single plaques in the spot test with those strains at any phage dose, despite the presence of lysis zones at high phage doses. Notably, for the latter strains similar lysis zones were obtained using suspensions of purified phage, indicating that they are not caused by free lysins or bacteriocins but by the phage itself. The observed effect could be caused by so called "lysis from without" or by the activity of bacterial phage defense systems causing death of infected cells to stop the phage spread. Apparently, phiAGO1.3 can adsorb to cells of those strains and penetrate their cell envelopes, but the infection is not productive.

Only three *S. aureus* strains of the entire set tested (RN4220, 3812/16, and 3793/16) appeared to be insensitive to phiAGO1.3 as indicated by the lack of any lysis in the spot tests and in liquid culture treated with the phage. Conceivably, their resistance is due to a lack of appropriate phage receptors.

In the majority of cases *S. aureus* forms biofilms at the site of infection (Moormeier and Bayles, 2017). Thus, we determined the effect of phiAGO1.3 on the biofilm mass of the strains tested (**Table 1** and **Supplementary Figure 4**). In the case of the strains which could not be infected productively in the former assays, phage addition to the preformed biofilm did not influence the biofilm biomass or caused an increase (from 21% to as much as 108%) or a slight decrease of the biofilm biomass. For all the strains that were productively infected with phiAGO1.3, a significant decrease of biofilm biomass (mostly by over 80%) was observed (see **Figure 1** and **Supplementary Figure 4**).

Properties of phiAGO1.3 Contributing to Its Wide *S. aureus* Strain Range

Staphylococcus aureus protection from invading foreign DNA and from horizontal gene transfer between different lineages is provided mainly by Type I DNA restriction-modification (R-M) systems, which were generally designated as *Sau1* although their methylation specificity varies between different CCs (Waldron and Lindsay, 2006). The ability of phiAGO1.3 to infect productively strains of at least 12 CCs implies that either it lacks the relevant target sequences in its DNA or encodes a potent antirestriction system. The target sequences of certain *S. aureus* R-M systems have been identified (McCarthy and Lindsay, 2010, 2012; McCarthy et al., 2012; Roberts et al., 2013; Monk et al., 2015; Chen et al., 2016; Cooper et al., 2017). The phiAGO1.3 genome carries no recognition sequences for CC1-2, CC8, CC30, CC45, CC51, CC72-2, CC75-2, CC93-3, CC97 and CC133-2 *Sau1* R-M systems, and only single recognition sequences for CC1-1, CC59, CC72-1, CC93-2, and CC133-1 *Sau1* R-M systems (**Table 1**). The DNA cleavage by restriction endonucleases of classical Type I R-M systems requires a collision of two enzymes translocating toward each other (Studier and Bandyopadhyay, 1988; Dreier et al., 1996; Jindrova et al., 2005; Šišáková et al., 2013). Thus, a single site does not suffice for the digestion of infecting linear phage DNA. In addition to Type I R-M systems several *S. aureus* strains encode Type II R-M systems such as Sau3A, Sau96I, and isoschizomers of SmlI that recognize 5′-GATC, 5′-GGNCC, and 5′-CTYRAG sequences, respectively, and cleave them if they are not methylated (Sussenbach et al., 1976, 1978; Stobberingh et al., 1977; Szilák et al., 1990; Godány et al., 2004). The genome of phiAGO1.3 contains only two GATC sequences and no GGNCC sequences. Taken together these results indicate that the elimination of certain restriction enzyme recognition sites is the dominant phiAGO1.3 strategy to avoid the activity of host R-M systems.

Killing Efficacy of Its Bacterial Host by phiAGO1.3 and the Establishment of Phage Carrier State

The efficacy of a given phage to kill the infected bacteria, so called killing efficacy, is a critical parameter in the evaluation of phage therapeutic potential (Carlson, 2004; Łobocka et al., 2014a; Abedon, 2017). The killing efficacy reflects a sum of the bacteria killed as a result of productive phage propagation and those killed without the productive propagation, e.g., by the induction of bacterial apoptosis. Infection of *S. aureus* 80wphwpl with phiAGO1.3 at MOI 1 caused killing of about 74% of cells, whereas the infection at MOI 10 caused killing of 93% of cells.

Irrespective of the MOI used for the infection, the bacteria that survived the infection formed colonies of two morphological

TABLE 1 | Number of target sites for the *Staphylococcus aureus* R-M systems of Type I and Type II of known specificities in phiAGO1.3 genome.

Clonal complex	HsdS subunit name in REBASE	Generic name	Recognition sequence	Number of targets in phiAGO1.3 DNA	I/T*
CC1	S. SauMW2I	CC1-1	CCAY-5-TTAA	1	4/5
	S. SauMW2II	CC1-2 (CC8-2)	CCAY-6-TGT	0	
CC5	S.SauN315II	CC5-2	CCAY-6-GTA	3	10/10
	S.SauN315I	CC5-1 (CC8-2)	AGG-5-GAT	0	
CC8#				0	7/8
CC15	S.SauL3150RFAP	CC15-1	CAAC-5-RTGA	0	4/5
CC22	S.Sau5096I	CC22-1	AGG-6-TGAR	5	4/4
CC30	S.SauMRSII	CC30-1	GWAG-5-GAT	0	8/8
	S.SauMRSI	CC30-2	GGA-7-TCG	0	
CC45	S.Sau347I	CC45-1	GWAG-6-TAAA	0	9/9
CC51	S.SauL30RFAP	CC51-1	GGA-6-CCT	0	NT
CC59	S.SauSA40ORF370P	CC59-1	GGA-6-RTGT	1	1/4
CC72	S.SauCN10RF415P	CC72-1	GARA-6-RTGT	1	NT
	S.SauCN10RF1757P	CC72-2	GGA-7-TGC	0	
CC75	S.SauII32ORF3780P	CC75-1	CAAG-5-RTC	2	NT
	S.SauII32ORF16570P	CC75-2	CNGA-7-TTYG	0	
CC93	S.SauJKDIII	CC93-3	GAAG-5-TAC	0	NT
	S.SauJKDII	CC93-2	or complement	3	
	S.SauJKDI	CC93-1	GGHA-7-TCG	1	
			CAG-6-TTC	3	
CC97	S.SauC01791ORFAP	CC97-1	CCAY-6-RTC	0	0/1
CC133	S.SauI330RF451P	CC133-1	CAG-5-RTGA	1	NT
	S.SauI330RF1794P	CC133-2	GGA-7-TTRG	0	
CC398	S.SauSTORF499PCC398-I CC398-1		ACC-5-RTGA	5	3/4
CC873	S.Sau323260RFAP	CC873-1	GAG-6-GAT	5	NT
Sau3A	R-M Type II enzymes		GATC	2	
Sau96I			GGNCC	0	

**I/T indicates the number of infected strains as compared to the number of tested strains. # indicates that the sequences are the same as CC8-2.*

types: those resembling colonies of non-infected cells (designated here as WTpt, wild-type colonies after phage treatment) and small, transparent colonies (designated as FTpt, frail type colonies after phage treatment) (**Figure 2A**). The fraction of the latter varied from 20 to 40%. While the transfer of cells from the WTpt colonies to a layer of 80wphwpl cells embedded in soft agar did not cause any effect, the transfer of cells from the FTpt colonies caused the formation of lysis zones of indicator bacteria (**Figure 2B**). The lysis was observed even after the FTpt cells were washed several times before plating. Colony PCR of FTpt bacteria with primers specific for phiAGO1.3 revealed the expected 353-bp product, indicative of the presence of phiAGO1.3 (**Figure 2C**). No product was obtained with WTpt colonies. Clearly, the phenotype of FTpt colonies is associated with the presence of phiAGO1.3 phage or phiAGO1.3 DNA.

The Establishment of Equilibrium Between Host Bacteria and phiAGO1.3 in Liquid Cultures

The optical density of 80wphwpl cultures infected with phiAGO1.3 (10^7 PFU/ml) began to decrease after 7 h and reached the lowest value (OD_{600} of about 0.2) at 15 h, and then increased to reach a plateau (OD_{600} of about 0.9) at about 25 h (**Figure 3**). The pattern of density changes in the culture of cells derived from WTpt colonies and infected with phiAGO1.3 was similar, consistent with the sensitivity of these cells to phiAGO1.3 (**Figure 3Bd**). In contrast, cultures derived from FTpt colonies behaved differently. In the absence of externally added phiAGO1.3 they grew poorly for the first few hours, then increased the optical density for the next 6 h up to OD_{600} ca. 1.2 and then decreased the optical density to reach a plateau (OD_{600} of about 0.6) at about 26 h (**Figure 3A**, empty circles). A similar pattern of density changes was observed in the FTpt-derived cultures when phiAGO1.3 (10^7 PFU/ml) was added to the cultures at the beginning of the experiment. This lack of an effect of external phage suggested that either the bacteria in the culture were not accessible to the newly added phages or that the infection by the newly added phages was prevented by other means (**Figure 3A**, black circles). Cells of FTpt-derived cultures taken at the 19-th hour, when a significant decrease of culture density was observed (OD_{600} of about 0.9), formed colonies of WTpt and FTpt types, at ratios varying between apparently identical experiment repetitions (1:1, 2:1, 1:2) despite similar curves of culture optical density changes. The total number of cells in the culture at that time, as calculated from the sum of WTpt and FTpt colonies formed, was 10^8 CFU/ml, while the total

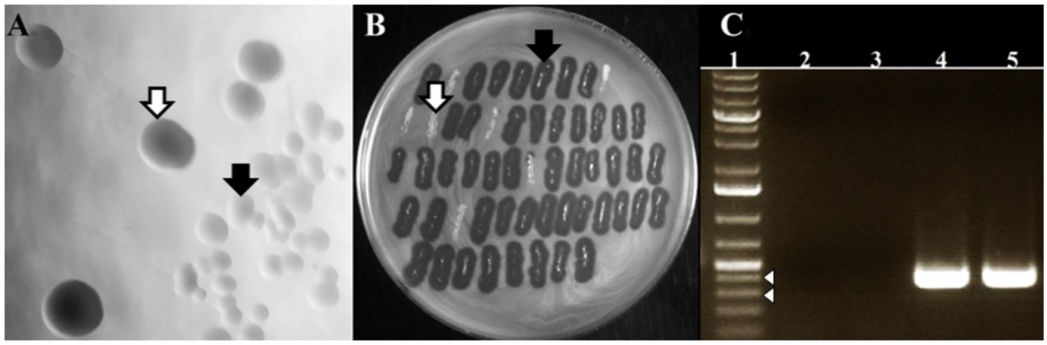

FIGURE 2 | Differentiation of colonies formed by phiAGO1.3-infected cells of *S. aureus* 80wphwpl. **(A)** Different colony morphotypes recovered following phiAGO1.3 infection: wild-type colonies, designated as WTpt (white arrow) and small, transparent colonies designated as FTpt (black arrow). **(B)** Identification of phage-releasing colonies. Single *S. aureus* colonies recovered following phage infection were picked onto a layer of 80wphwpl cells in top soft LB agar, incubated overnight at 37°C, and checked for the presence of a lysis zone (WTpt, white arrow; FTpt, black arrow). **(C)** Presence of phiAGO1.3 in colonies surviving phage infection. PCR with phage-specific primers was used to identify phage DNA. Lanes represent: (1) 1-Kb Plus DNA Ladder (Invitrogen), (2) PCR with no template, (3 and 4) Colony PCR with WTpt and FTpt colonies as a source of template, respectively, (5) PCR with phiAGO1.3 as template. White arrowheads indicate 400- and 300-bp marker.

number of phages, as calculated by titration, was 10^9 PFU/ml. In a sample taken at the 32-nd hour the total number of cells was 10^7 CFU/ml and of phages – 10^9 PFU/ml. Apparently, the phage and the bacteria can reach a kind of equilibrium in which they can stably coexist with each other.

We reasoned that the FTpt colonies could not increase in size and could not give rise to a growing liquid culture if they did not contain at least a fraction of cells able to grow and divide. Thus, we tested what kind of cells contribute to the formation of FTpt colonies. Single FTpt colonies (designated as G0 generation) were used as the starting material in these experiments. To decrease the probability of phage release and infection of new cells during cell handling and to slow down cell division, suspensions of cells of single FTpt colonies and dilutions were prepared in ice-cold water and the cells were immediately spread on LB plates (the whole procedure did not exceed 3 min). The FTpt progeny cells formed colonies of both the FTpt and WTpt types. To test whether and to what extent the segregation phenotype is inheritable the whole procedure of cell washing, dilutions and plating was repeated with each next passage of cells of FTpt colonies up to seven rounds. Regardless of the passage the fraction of cells forming FTpt colonies varied between 40 and 90% and did not show any tendency to decrease with subsequent passages. Colonies from all the passages studied were tested for the ability to release phiAGO1.3 by their application on a layer of 80wphwpl cells in soft LCA. All FTpt colonies released the phage, while no WTpt colonies did. Taken together our results demonstrate that FTpt colonies are a mixture of two types of bacterial cells and that the phage carrier state is inheritable. The recurrent segregation of FTpt colonies into phage-releasing cells and phage-free cells sensitive to phage infection ensures a stable co-existence of bacteriophage and its host bacteria.

Isolation of Cells Resistant to Infection With phiAGO1.3

When cells of FTpt colonies were suspended in molten LCA medium and poured onto solid LB medium, as is commonly done in the double-layer-agar assay of bacteriophage activity, they formed a lysis zone. However, throughout the lysis zone one could observe single bacterial colonies of various sizes (**Figure 4A**), similarly as in the case of the lysis zones obtained during phiAGO1.3 titration on a layer of 80wphwpl cells with the use of high-titer lysates.

To test whether these colonies release the phage like the FTpt colonies did, cells from the top of the colonies were transferred on a layer of 80wphwpl cells embedded in soft agar. Similarly, like as for the FTpt colonies, lysis zones of the indicator cells were formed around the cells of tested colonies. However, opposite to the test with the FTpt colonies, the intensive growth of bacteria was observed in the center of the lysis zones (compare **Figures 2B** and **4B**). To distinguish these cells from cells of the parental FTpt colonies they were designated RevFT (reverse colonies of FTpt).

All or some WTpt or RevFT cells could potentially represent phage resistant clones. To verify this possibility they were tested for the sensitivity to infection with phiAGO1.3. Cells from WTpt turned out to be sensitive to phiAGO1.3, as indicated by the ability of phiAGO1.3 to form lysis zones on a layer of these cells in LCA (compare **Figures 3Bd** and **3Bb**) and by the optical density drop of their cell cultures upon addition of phiAGO1.3 (**Figure 3A**). Most likely, WTpt represent the progeny of cells that avoided the encounter with phiAGO1.3, as happens in killing assay experiments (Łobocka et al., 2014a). The results were different for the RevFT colony-derived cells, as they did not lyse upon phiAGO1.3 application (**Figure 5Ba**). Clearly, RevFT are cells that have acquired resistance to phiAGO1.3 (**Figure 5**).

To check whether the resistance phenotype is stable, RevFT cells were purified by passaging through fresh medium, re-isolated from single colonies and tested for sensitivity to phiAGO1.3 by spotting diluted cell suspension on a layer of LCA soft agar containing phiAGO1.3 (10^9 PFU/ml). The RevFT-derived cells formed colonies and their number was comparable to that formed by a phiAGO1.3 resistant strain, RN4220 (data not shown). Clearly, the resistance of RevFT cells to phiAGO1.3

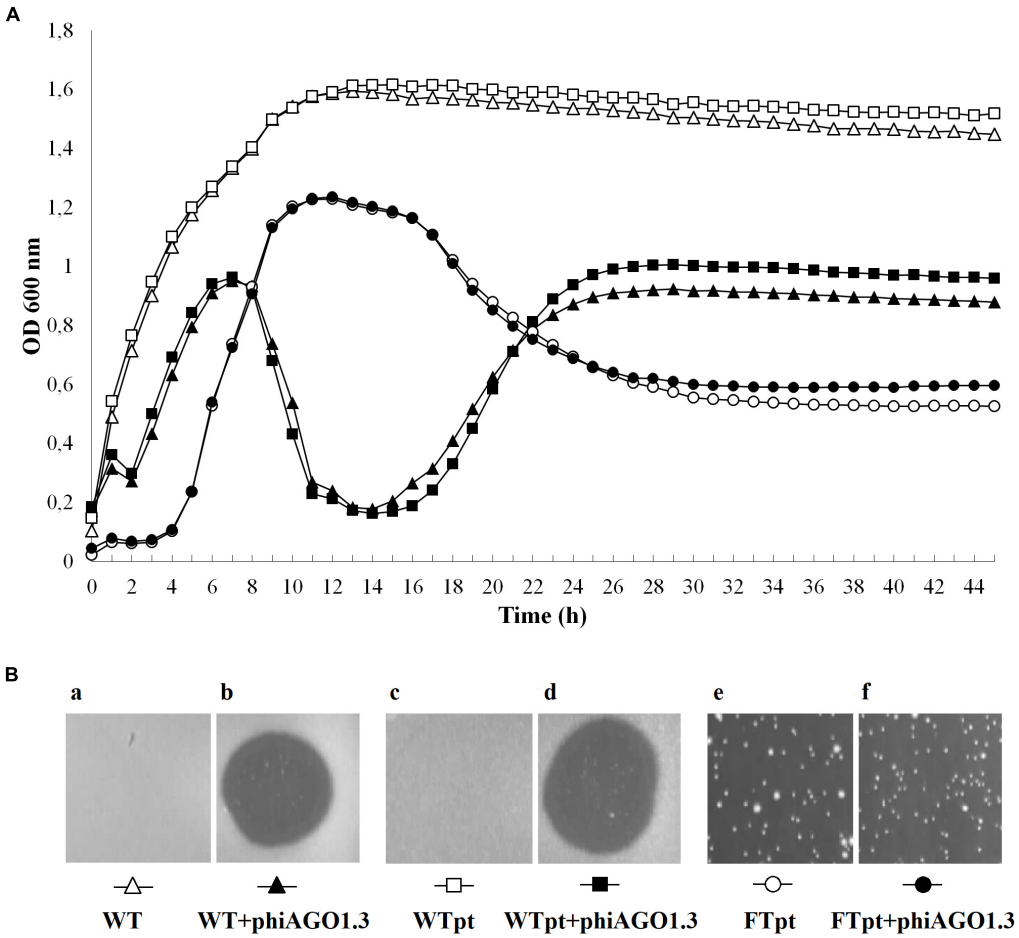

FIGURE 3 | Properties of *S. aureus* 80wphwpl (WT) and its derivatives recovered from phiAGO1.3-treated cultures (WTpt and FTpt). **(A)** Optical density changes of liquid cell cultures of WT (empty triangles), WTpt (empty squares) and FTpt (empty circles) colonies grown without phiAGO1.3 added and upon addition of phiAGO1.3 (filled triangles, squares, and circles, respectively). Portions of LB medium (190 μl) in duplicate were inoculated with appropriate colonies to OD_{600} of about 0.1–0.2. One culture of each pair was supplemented with 10 μl of phiAGO1.3 suspension in LB (10^9 PFU/ml) and one (control) with 10 μl LB. Cultures were grown in Bioscreen C at 37°C with shaking. **(Ba-f)** Sensitivity of WT and WTpt- and FTpt-derived *S. aureus* to phiAGO1.3, as measured by a spot test. FTpt-derived cells lysed spontaneously in the top agar (Be) and thus the site of phiAGO1.3 application in Bf is not visible.

is maintained even when their contact with the phage is interrupted.

Certain phages of the genus *Rosenblumvirus* require WTA for adsorption, similarly to the *Kayvirus* genus phages. However, the RevFT cells, despite being resistant to phiAGO1.3 remained sensitive to infection with the *Kayvirus* phage A5W, as indicated by the assays in solid as well as in liquid medium (**Figures 5A** [black squares] and 5Bb). Clearly, their resistance is not associated with a change of any surface or internal cell structure of *S. aureus* that could be essential for the sensitivity to A5W.

Identification of RevFT Mutation Associated With the Resistance to phiAGO1.3

The stable inheritance of phiAGO1.3 resistance by the progeny of cells forming FTpt colonies prompted us to determine the genomic sequence of several RevFT clones and compare it with the sequence of the parental 80wphwpl strain (80wphwpl_v1 control clone). All nine RevFT isolates sequenced had the substitution of G by T at position 1252 of the *arl* gene. This substitution is a nonsense mutation changing a glycine codon (GGA) to a STOP codon (TGA), which results in the production of the ArlS protein depleted of 34 C-terminal amino acid residues. ArlS is a sensory histidine kinase of the two component *S. aureus* regulatory system ArlRS (Fournier and Hooper, 2000[3]). The premature termination of translation in the mutant occurs exactly prior to the conserved GLGL motif which is an essential part of the dimerization and phospho-acceptor domain of ArlS protein (pfam HATPase_c domain) – one of the essential units of the two-component transduction system (Fournier and Hooper, 2000; West and Stock, 2001). Consistently, the ArlRS system cannot be functional in the mutant.

[3]http://www.ncbi.nlm.nih.gov/Complete_Genomes/SignalCensus.html

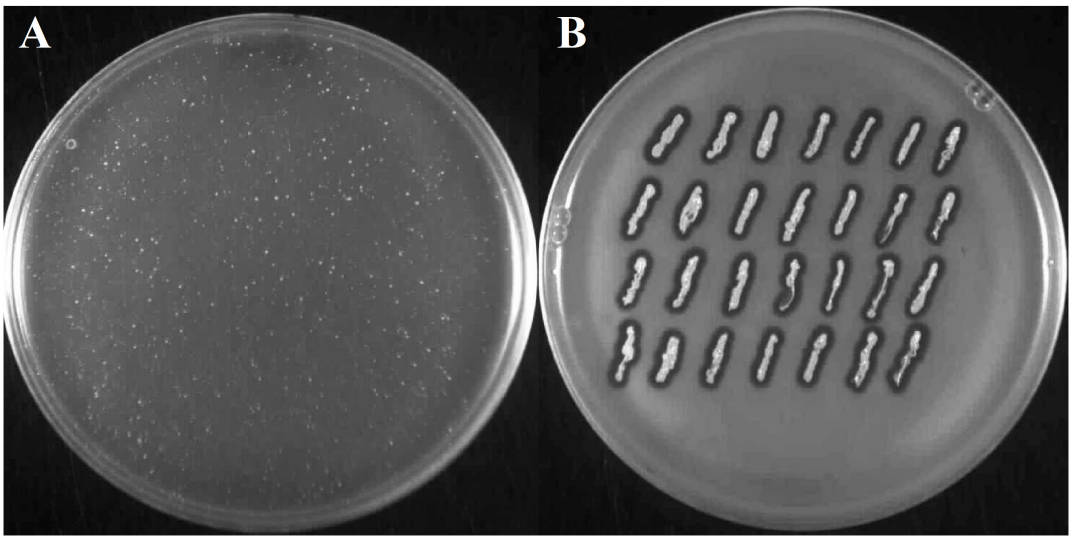

FIGURE 4 | Emergence of phiAGO1.3-resistant clones among bacteria derived from FTpt colonies. **(A)** Growth of single FTpt-derived colonies on a layer of lysed FTpt-derived cells in soft agar. Single FTpt colony was suspended in LCA and spread on LB agar. Plates were incubated for 24 h at 37°C. Colonies formed were designated RevFT. **(B)** Identification of phiAGO1.3-releasing isolates among RevFT-derived bacteria.

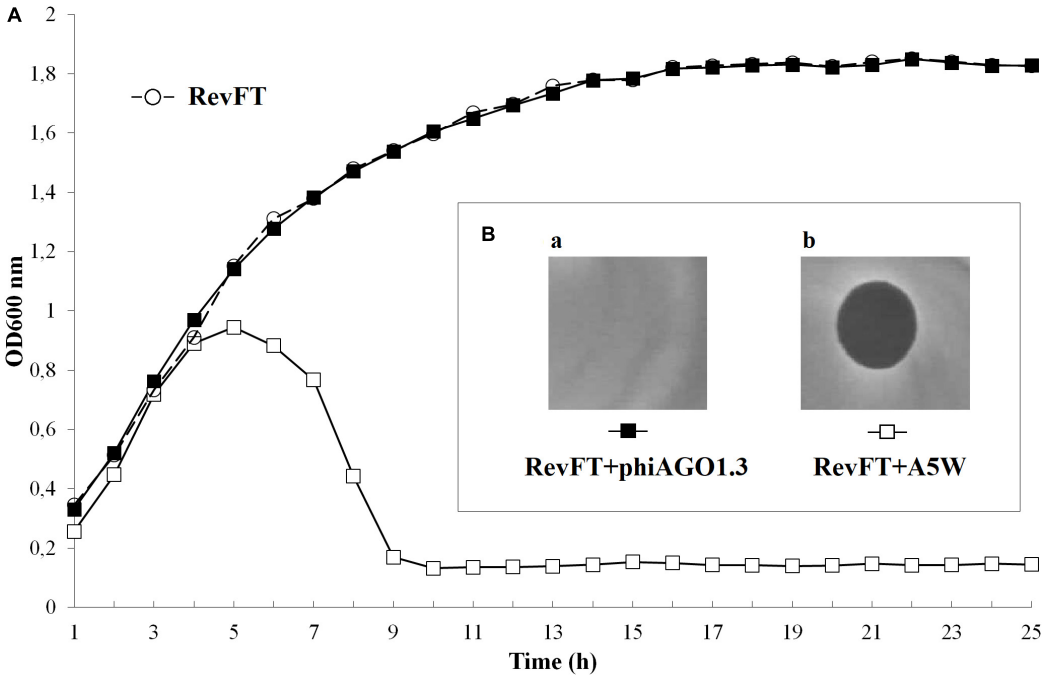

FIGURE 5 | (A) Sensitivity of RevFT-derived bacteria to two unrelated phages, phiAGO1.3 and A5W of *Kayvirus* genus. Optical density changes of RevFT culture cells (white circles) upon addition of phage phiAGO1.3 (black squares) or phage A5W (white squares). **(Ba,b)** Sensitivity of RevFT cells to phiAGO1.3 and A5W, as measured by a spot test.

Therapeutic Potential of phiAGO1.3 to Cure Nematode Infection With *S. aureus* 80wphwpl

If an equilibrium between a phage and its host bacteria similar to that observed in liquid cultures could be also established in *S. aureus*-infected humans or animals during phage therapy it might preclude the use of phiAGO1.3 for therapeutic purposes. Thus, we tested whether phiAGO1.3 can rescue from death *C. elegans* infected with *S. aureus* 80wphwpl. **Figure 6** show that 80wphwpl is pathogenic to *C. elegans,* causing gradual death of

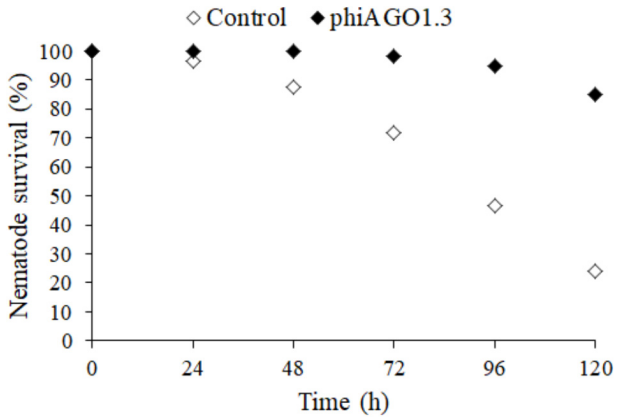

FIGURE 6 | Antistaphylococcal activity of phiAGO1.3 *in vivo*. Percentage of surviving worms fed *S. aureus* 80wphwpl (untreated control, white diamonds) and treated with phiAGO1.3 (black diamonds). Each value is the mean of six samples from three experiments where the total number of worms was 120. The differences between experiments did not exceed 4% for untreated worms and 1% for phiAGO1.3-treated ones.

more and more nematodes each day so that only about 20% of them survived at 120 h post-infection. Additionally, none of them produced progeny. Opposite to that over 80% of the nematodes survived when they were treated with just one dose of phiAGO1.3 (10^9 PFU/ml) 24 h after the infection. Moreover, ca. 100 h after the treatment with phiAGO1.3 they started to produce progeny, indicating the recovery of reproductive potential and thereby prompting us to stop the experiment. Taken together our results demonstrate that the ability of phiAGO1.3 to establish a stable mixed population with its bacterial host and to exist in equilibrium with the host under *in vitro* conditions does not negatively influence the therapeutic potential of phiAGO1.3.

Nucleotide Sequence Accession Number

The genomic sequence of the *S. aureus* 80wphwpl WT, control clone (80wphwpl_v1) has been deposited in the GenBank under the Accession No. CP034098.

DISCUSSION

Carefully selected obligatorily lytic bacteriophages that efficiently kill bacterial pathogens may become the option of choice in the treatment of infections with antibiotic-resistant bacterial strains. However, safe introduction of a phage to therapy requires its biology and outcomes of interactions with its host bacteria *in vitro* and *in vivo* to be examined to the widest extent possible.

Here, we show that the polyvalent staphylococcal lytic podovirus phiAGO1.3 has properties that make it a potential candidate for therapeutic applications, identify factors that contribute to its wide strain range, and prove its therapeutic efficacy in curing a staphylococcal infection of a model nematode, *Caenorhabditis elegans*. Additionally, we demonstrate for the first time for any staphylococcal lytic phage, that phiAGO1.3 and its host bacteria can co-exist in a stable equilibrium which can be maintained owing to the presence in such mixed population of phage-carrier state cells. The ability to form phage-carrier state cells with its host not only does not cause the lack of efficacy of phiAGO1.3 as an antistaphylococcal agent *in vivo*, but also leads to the emergence of phage-resistant host mutants impaired in virulence.

The phiAGO1.3 virion morphology, genomic features and proteome place this phage among typical *Rosenblumvirus* phages, which infect *S. aureus* (**Supplementary Table 2**; Vybiral et al., 2003; Kwan et al., 2005; Son et al., 2010; Kraushaar et al., 2013; Takemura-Uchiyama et al., 2013; Swift and Nelson, 2014; Wang et al., 2016; Gozdek et al., 2018). The host range of only some of them has been studied and varied between 50 and 90% of the *S. aureus* strains tested (Son et al., 2010; Kraushaar et al., 2013; Takemura-Uchiyama et al., 2013; Wang et al., 2016). However, none of these host-range tests were conducted using the phage propagated in a prophage-free host. Thus, one cannot exclude that the plaques observed with certain strains could represent plaques of a prophage-derived temperate phage. To avoid this ambiguity, we determined the host range of phiAGO1.3 with various representatives of the genus *Staphylococcus* and representatives of 14 *S. aureus* clonal complexes using a prophage-free host for phage propagation. Of 75 *S. aureus* strains tested only some human isolates of CC1, CC59 and CC398, a bovine mastitis isolate of CC97 and isolates of CC7 were resistant to phiAGO1.3. However, despite the lack of productive infection of the majority of these resistant strains, phiAGO1.3 could cause their lysis from without, indicating that the resistance in not caused by a lack of appropriate phage receptors.

The ability of phiAGO1.3 to infect representatives of most of the *S. aureus* CCs requires bypassing of staphylococcal Type I R-M systems (*Sau1*) of different specificities. We show here that the main strategy of phiAGO1.3 to overcome the action of R-M systems of Type I and also Type II is the avoidance or sparcity of DNA sequences recognized by these systems in its genome. This strategy appears to be common to all *Rosenblumvirus* phages. They all lack in their genomes the GGNCC sequences (targets of Sau96I) and usually lack or only have single copies of sequences recognized by certain CC-specific variants of *Sau1* (data not shown).

The absence of the recognition sequences for the *Sau1* R-M systems of certain CCs could in principle be used as a predictor of the strain-range of a phage. Our results indicate that it is often, but not always, true. Some CC22 and CC15 strains tested were infected productively by phiAGO1.3 despite the presence of five recognition sequences for each of the respective *Sau1* systems in the phiAGO1.3 genome. Some phages encode antirestriction proteins protecting phage DNA from the host Type I R-M systems (Labrie et al., 2010; Samson et al., 2013; Iyer et al., 2017). Although phiAGO1.3 does not encode homologs of known antirestriction proteins, a role of one of its proteins of unassigned function in antirestriction cannot be excluded (**Supplementary Table 3**, Vybiral et al., 2003).

Some of the CC1 and CC59 strains tested were susceptible to lysis from without but still could not be infected productively

by phiAGO1.3, despite a lack or the presence of only a single copy of recognition sequences for the respective *Sau1* systems in the phage DNA (**Table 1**). A likely reason for this could be the action of other R-M systems in these strains. Several *S. aureus* strains encode two related Type I R-M systems (Waldron and Lindsay, 2006; McCarthy and Lindsay, 2010; Monk et al., 2012; Lindsay, 2014) or contain additional R-M system genes on mobile elements, such as prophages, pathogenicity islands, or *SCC-mec* cassettes (Ito et al., 2004; Dempsey et al., 2005; Noto et al., 2008). Additionally, one cannot exclude a protective activity of CRISPR-Cas systems or abortive infection systems (Abi) (Chopin et al., 2005; Labrie et al., 2010), which also have been found in some strains of *S. aureus* (Yang et al., 2015; Cao et al., 2016; Depardieu et al., 2016). The staphylococcal Abi system involves the serine/threonine kinase Stk2 which is activated by phage proteins during lytic development and causes cell death by phosphorylating essential proteins. Stk2 protects the bacteria from the infection with all siphoviruses tested. Its influence on the sensitivity to podoviruses has not been studied.

Productive infection as well as lysis from without can serve as an indicator of successful phage adsorption to a bacterial cell. Accordingly, phiAGO1.3 could adsorb to all but three *S. aureus* strains tested. One of them is RN4220 whose WTA is modified by the TarM-mediated α-*O*-GlcNAcylation (Li et al., 2015). The inability of phiAGO1.3 to adsorb to RN4220 cells and the high homology of phiAGO1.3 RBP to the RBPs of subgroup I *Rosenblumvirus* phages (**Supplementary Table 2**) implies the requirement of WTA β-*O*-GlcNAcylation for phiAGO1.3 adsorption. What causes the sensitivity of certain *S. hyicus* and *S. lugdunensis* strains to phiAGO1.3 is unclear. We detected proteins of only partial homology to the *S. aureus* TarS (which mediates WTA β-*O*-GlcNAcylation) among predicted gene products of both infected strains (data not shown).

The β-*O*-GlcNAcylation of WTA is essential for the expression of methicillin-resistance in *S. aureus* and requires the function of TarS protein (Brown et al., 2012). This implies that MRSA strains are likely to adsorb *Rosenbslumvirus* genus phages of subgroup I. In support of that, all three strains that did not adsorb phiAGO1.3 in our tests are MSSA (**Figure 1**).

We show here that under certain conditions the exposure of *S. aureus* cells to phiAGO1.3 can lead to the establishment of a mixed population in which bacteria and bacteriophages are in an equilibrium, and remain in a stable ratio even following several serial passages – an equivalent of multiple generations. This interaction is reminiscent of so called phage carrier state cultures (PCSCs) (Lwoff, 1953). In the PCSC, phage-resistant and phage-sensitive cells co-exist in an equilibrium supporting a continuous growth of the bacterial as well as the phage population (Lwoff, 1953; Abedon, 2009). The bacteriophage carrier state has been described for over a dozen of bacteria (Hooton et al., 2016, and references therein), but as far as we know this is the first report of such a relation between staphylococci and their lytic phage.

In PCSCs phage resistance can be determined genetically and associated with the emergence of phage sensitive cells or it can be determined by phenotypic traits only. At least two phage-dependent mechanisms may be responsible for the latter. In the first case, exemplified by P22 PCSC, proteins that determine superinfection immunity of some cells in the population are inherited cytoplasmically by progeny cells despite the loss of P22 resulting from asymmetric cell division (Cenens et al., 2015). When the phage is removed from the PCSC (e.g., with anti-phage serum) the proportion of cells resistant to superinfection decreases with cell divisions and finally they disappear altogether due to dilution of the immunity factor in the cells. In the second case, uninfected bacteria are modified by soluble factors released from the phage-infected bacteria (Abedon, 2009). For instance lysin released from T7-infected *S. dysenteriae* cells at phage release inactivates the phage receptors of uninfected cells and thus induces a stable equilibrium between infected and non-infected cells (Li et al., 1961). Its concentration decreases with the increasing proportion of modified uninfected cells, until a threshold is reached below which cells recover phage sensitivity (Abedon, 2009). Some bacteria can modify the display of phage receptors or the specificity of their Type I or Type II R-M in the population in a phage-independent manner, e.g., by phase variation (Abedon, 2009; Seed et al., 2012; Cota et al., 2015; Anjum et al., 2016; Aidley et al., 2017; De Ste Croix et al., 2017). The phage population in this case would be maintained solely by infecting those bacteria in the population that currently display the receptor or do not restrict a given phage DNA. Phase variation is also a cause of intra-populational diversity of certain surface properties in *S. aureus*. For instance the adhesive properties and the ability to form biofilm may be diversified among the cells of a population as a result of reversible insertion/excision of IS256 or the expansion/contraction of a tandem repeat in *icaC* – a gene involved in the synthesis of poly-*N*-acetylglucosamine (PNAG) which is a major component of the biofilm matrix (Kiem et al., 2004; Arciola et al., 2015).

The maintenance of PCSCs can be advantageous to bacterial populations. For instance PCSCs of *Campylobacter jejuni* could serve as phage delivery vectors to new target hosts within pre-colonized chicken, facilitating the acquisition of new environment for the bacteria and for its phage (Šišáková et al., 2013). Here, we show that the ability of bacteriophage phiAGO1.3 to be maintained in the form of a phage carrier state population with its host *S. aureus* strain in laboratory cultures does not preclude its ability to cure *C. elegans* from infection with the same *S. aureus* strain. A few reasons for this discrepancy are possible: (i) the phage carrier state could be limited to certain conditions only and cannot be maintained *in vivo,* (ii) limitation of the bacterial load by phages killing the sensitive fraction of cells suffices for the natural antimicrobial defense of the nematode to combat the infection, (iii) the phage carrier state somehow interferes with the bacterial virulence.

In certain bacterial pathogens phase-variation-dependent phage resistance phenotypes are associated with changes that abolish virulence (Seed et al., 2012; Cota et al., 2015). The maintenance of the subpopulation of phage susceptible cells may be a temporal cost overweighted by the increased fitness of these pathogens upon infection of a human or animal. We found here that the mutation emerging in the population of 80wphwpl cells infected with phiAGO1.3 and causing the resistance to phiAGO1.3 leads to the synthesis of a truncated inactive version

of ArlS protein. ArlS is a part of the two-component ArlR-ArlS system known to affect several functions associated with *S. aureus* virulence and surface properties, either directly or through other regulatory systems, *agr* among them (Fournier and Hooper, 2000; Fournier et al., 2001; Liang et al., 2005; Luong and Lee, 2006). The ArlRS system is involved in catheter colonization and in endothelial cell damage by *S. aureus* (Burgui et al., 2018; Seidl et al., 2018). It is required for establishing invasive *S. aureus* infection and resistance to calprotectin-mediated Mn starvation *in vivo* and has been shown to be essential for pathogenesis in a rabbit model of sepsis and infective endocarditis (Walker et al., 2013; Radin et al., 2016). Mutations that abolish ArlRS functioning cause, among other defects, the inability of cells to agglutinate, decrease protein A expression in certain media, capsule production and intercellular adhesion, and lead to a serious deficit in the PNAG production (Luong and Lee, 2006; Burgui et al., 2018; Villanueva et al., 2018).

Certain virulence factors that are down-regulated in the ArlRS-deficient mutant, e.g., the Ser-Asp-rich bone fibronectin-binding proteins SdrC, SdrD, and SdrE (Liang et al., 2005) require sortase A (SrtA) to be covalently anchored to the cell wall peptidoglycan (Mazmanian et al., 2001). *S. aureus srtA* deletion mutants have been shown to be resistant to infection with phiAGO1.3-related phages 44AHJD, 66 and 68 (Li et al., 2015). It seems plausible that the cell surface change that causes the phiAGO1.3 resistance of *arlS* mutants concerns a sortase-dependent protein. One of the Sdr proteins is a candidate.

A common feature of the *srtA* deletion mutant studied by Li et al. (2015) and our *arlS* mutant is their sensitivity to a polyvalent *Kayvirus* phage, K and A5W, respectively. Phage K requires only the WTA backbone for adsorption, independently of WTA modifications (Xia et al., 2010, 2011; Li et al., 2015). Another *Kayvirus,* ϕSA012, contains two RBPs of which one, gp103, binds to α-*O*-GlcNAc substituted WTA and the other, gp105, to the WTA backbone (Takeuchi et al., 2016). Of the two RBPs of A5W (gpORF094 [ACB89087] and gpORF96 [ACB89089.1) one is identical with a phage K RBP, while the other is 98% identical to ϕSA012 gp103, implying that phage A5W can use both the WTA backbone and the α-*O*-GlcNAc substituted WTA for adsorption, unlike phiAGO1.3. Thus, phiAGO1.3 appears to be not only a good candidate for a therapeutic use itself but also as a component of therapeutic phage cocktails with A5W and other *Kayvirus* genus phages.

AUTHOR CONTRIBUTIONS

AG-R contributed to the study design, the performance of most of the experimental work and data analysis, and significantly contributed to the drafting and revising of the manuscript. AG contributed to the initial experimental work. JE contributed to the selection and characterization of *S. aureus* strains, contributed to the drafting, and revising of the manuscript. JG, KŻ, and RG contributed to the sequencing and assembly of bacterial genomes. AK contributed to the characterization of S. *aureus* strains. JD performed the proteomic analysis. ML participated in the study design and data analysis and interpretation, the supervision of the study, *in silico* sequence analysis, drafting and revising of the manuscript, and preparation of final version of the manuscript.

FUNDING

The major part of this work was supported by the National Science Centre (PRELUDIUM) (Grant No. UMO2012/07/N/NZ2/01596). The collection and characteristic of *S. aureus* strains performed at the National Medicines Institute was partially supported by the MIKROBANK 2 Program from the Ministry of Science and Higher Education, Poland. Preliminary characterization of phiAGO1.3 to initiate these studies was supported by the Polish Ministry of Science and Higher Education (Poland) (Grant No. PBZ-MNiSW-04/I/2007). A part of this study was presented at the Fifth International EMBO Congress on Viruses of Microbes in Wrocław, Poland, 2018.

SUPPLEMENTARY MATERIAL

The Supplementary Material for this article can be found online at: https://www.frontiersin.org/articles/10.3389/fmicb.2018.03227/full#supplementary-material

REFERENCES

Abedon, S. T. (2009). "Disambiguating bacteriophage pseudolysogeny: an historical analysis of lysogeny, pseudolysogeny, and the phage carrier state," in *Contemporary Trends in Bacteriophage Research*, ed. H. T. Adams (New York, NY: Nova Science Publishers), 285–307.

Abedon, S. T. (2017). *Expected Efficacy: Applying Killing Titer Estimations to Phage Therapy Experiments*. Available at: http://www.phage-therapy.org/writings/killing_titers.html

Aidley, J., Sørensen, M. C. H., Bayliss, C. D., and Brøndsted, L. (2017). Phage exposure causes dynamic shifts in the expression states of specific phase-variable genes of *Campylobacter jejuni*. *Microbiology* 163, 911–919. doi: 10.1099/mic.0.000470

Anjum, A., Brathwaite, K. J., Aidley, J., Connerton, P. L., Cummings, N. J., Parkhill, J., et al. (2016). Phase variation of a Type IIG restriction-modification enzyme alters site-specific methylation patterns and gene expression in *Campylobacter jejuni* strain NCTC11168. *Nucleic Acids Res.* 44, 4581–4594. doi: 10.1093/nar/gkw019

Arciola, C. R., Campoccia, D., Ravaioli, S., and Montanaro, L. (2015). Polysaccharide intercellular adhesin in biofilm: structural and regulatory aspects. *Front. Cell Infect. Microbiol.* 5:7. doi: 10.3389/fcimb.2015.00007

Bal, A. M., Coombs, G. W., Holden, M. T. G., Lindsay, J. A., Nimmo, G. R., Tattevin, P., et al. (2016). Genomic insights into the emergence and spread of international clones of healthcare-, community- and livestock-associated meticillin-resistant *Staphylococcus aureus*: blurring of the traditional definitions. *J. Glob. Antimicrob. Resist.* 6, 95–101. doi: 10.1016/j.jgar.2016.04.004

Barrera-Rivas, C. I., Valle-Hurtado, N. A., González-Lugo, G. M., Baizabal-Aguirre, V. M., Bravo-Patiño, A., Cajero-Juárez, M., et al. (2017). "Bacteriophage

therapy: an alternative for the treatment of *Staphylococcus aureus* infections in animals and animal models," in *Frontiers in Staphylococcus aureus*, eds S. M. E. Enany, and L. E. Crotty-Alexander (London: IntechOpen), 179–201.

Barylski, J., Enault, F., Dutilh, B. E., Schuller, M. P. B., Edwards, R. A., Gillis, A., et al. (2018). Analysis of spounaviruses as a case study for the overdue reclassification of tailed bacteriophages. *bioRxiv* [Preprint]. doi: 10.1101/220434

Borysowski, J., Łobocka, M. B., Międzybrodzki, R., Weber-Dabrowska, B., and Górski., A. (2011). Potential of bacteriophages and their lysins in the treatment of MRSA: current status and future perspectives. *BioDrugs* 25, 347–355. doi: 10.2165/11595610-000000000-00000

Brown, S., Xia, G., Luhachack, L. G., Campbell, J., Meredith, T. C., Chen, C., et al. (2012). Methicillin resistance in *Staphylococcus aureus* requires glycosylated wall teichoic acids. *Proc. Natl. Acad. Sci. U.S.A.* 109, 18909–18914. doi: 10.1073/pnas.1209126109

Burgui, S., Gil, C., Solano, C., Lasa, I., and Valle, J. (2018). A systematic evaluation of the two-component systems network reveals that ArlRS is a key regulator of catheter colonization by *Staphylococcus aureus*. *Front. Microbiol.* 9:342. doi: 10.3389/fmicb.2018.00342

Cao, L., Gao, C. H., Zhu, J., Zhao, L., Wu, Q., Li, M., et al. (2016). Identification and functional study of type III-A CRISPR-Cas systems in clinical isolates of *Staphylococcus aureus*. *Int. J. Med. Microbiol.* 306, 686–696. doi: 10.1016/j.ijmm.2016.08.005

Carlson, K. (2004). "Working with bacteriophages: common techniques and methodological approaches," in *Bacteriophages Biology and Applications*, eds E. Kutter and A. Sulakvelidze (Boca Raton, FL: CRC Press), 437–494. doi: 10.1201/9780203491751.ax1

Cenens, W., Makumi, A., Govers, S. K., Lavigne, R., and Aertsen, A. (2015). Viral transmission dynamics at single-cell resolution reveal Transiently immune subpopulations caused by a carrier state association. *PLoS Genet.* 11:e1005770. doi: 10.1371/journal.pgen.1005770

Chen, K., Stephanou, A. S., Roberts, G. A., White, J. H., Cooper, L. P., Houston, P. J., et al. (2016). The Type I restriction enzymes as barriers to horizontal gene transfer: Determination of the DNA target sequences recognised by livestock-associated methicillin-resistant *Staphylococcus aureus* clonal complexes 133/ST771 and 398. *Adv. Exp. Med. Biol.* 915, 81–97. doi: 10.1007/978-3-319-32189-9_7

Chen, S., Zhou, Y., Chen, Y., and Gu, J. (2018). fastp: an ultra-fast all-in-one FASTQ preprocessor. *Bioinformatics* 34, i884–i890. doi: 10.1093/bioinformatics/bty560

Chopin, M. C., Chopin, A., and Bidnenko, E. (2005). Phage abortive infection in lactococci: variations on a theme. *Curr. Opin. Microbiol.* 8, 473–479. doi: 10.1016/j.mib.2005.06.006

Cooper, L. P., Roberts, G. A., White, J. H., Luyten, Y. A., Bower, E. K. M., Morgan, R. D., et al. (2017). DNA target recognition domains in the Type I restriction and modification systems of *Staphylococcus aureus*. *Nucleic Acids Res.* 45, 3395–3406. doi: 10.1093/nar/gkx067

Cosgrove, S. E., Sakoulas, G., Perencevich, E. N., Schwaber, M. J., Karchmer, A. W., and Carmeli, Y. (2003). Comparison of mortality associated with methicillin-resistant and methicillin-susceptible *Staphylococcus aureus* bacteremia: a meta-analysis. *Clin. Infect. Dis* 36, 53–59. doi: 10.1086/345476

Cota, I., Sánchez-Romero, M. A., Hernández, S. B., Pucciarelli, M. G., García-Del Portillo, F., and Casadesús, J. (2015). Epigenetic control of *Salmonella enterica* O-Antigen Chain Length: a tradeoff between virulence and bacteriophage resistance. *PLoS Genet.* 11:e1005667. doi: 10.1371/journal.pgen.1005667

de Kraker, M. E. A., Peter, G., Davey, P. G., and Grundmann, H. (2011). Mortality and hospital stay associated with resistant *Staphylococcus aureus* and *Escherichia coli* bacteremia: estimating the burden of antibiotic resistance in Europe. *PLoS Med.* 8:e1001104. doi: 10.1371/journal.pmed.1001104

De Ste Croix, M., Vacca, I., Kwun, M. J., Ralph, J. D., Bentley, S. D., Haigh, R., et al. (2017). Phase-variable methylation and epigenetic regulation by type I restriction-modification systems. *FEMS Microbiol. Rev.* 41(Suppl._1), S3–S15. doi: 10.1093/femsre/fux025

Dempsey, R. M., Carroll, D., Kong, H., Higgins, L., Keane, C. T., and Coleman, D. C. (2005). Sau42I, a BcgI-like restriction-modification system encoded by the *Staphylococcus aureus* quadruple-converting phage Phi42. *Microbiology* 151, 1301–1311. doi: 10.1099/mic.0.27646-0

Depardieu, F., Didier, J. P., Bernheim, A., Sherlock, A., Molina, H., Duclos, B., et al. (2016). A eukaryotic-like serine/threonine kinase protects staphylococci against phages. *Cell Host Microbe.* 20, 471–481. doi: 10.1016/j.chom.2016.08.010

d'Herelle, F. (1931a). An address on bacteriophagy and recovery from infectious diseases. *Can. Med. Assoc. J.* 24, 619–628.

d'Herelle, F. (1931b). Bacteriophage as a treatment in acute medical and surgical infections. *Bull. N. Y. Acad. Med.* 7, 329–348.

Dreier, J., MacWilliams, M. P., and Bickle, T. A. (1996). DNA cleavage by the type IC restriction-modification enzyme EcoR124II. *J. Mol. Biol.* 264, 722–733. doi: 10.1006/jmbi.1996.0672

Fadlallah, A., Chelala, E., and Legeais, J. M. (2015). Corneal infection therapy with topical bacteriophage administration. *Open Ophthalmol. J.* 9, 167–168. doi: 10.2174/1874364101509010167

Fish, R., Kutter, E., Wheat, G., Blasdel, B., Kutateladze, M., and Kuhl, S. (2016). Bacteriophage treatment of intransigent diabetic toe ulcers: a case series. *J. Wound Care* 25(Suppl. 7), S27–S33. doi: 10.12968/jowc.2016.25.7.S27

Fournier, B., and Hooper, D. C. (2000). A new two-component regulatory system involved in adhesion, autolysis, and extracellular proteolytic activity of *Staphylococcus aureus*. *J. Bacteriol.* 182, 3955–3964. doi: 10.1128/JB.182.14.3955-3964.2000

Fournier, B., Klier, A., and Rapoport, G. (2001). The two-component system ArlS-ArlR is a regulator of virulence gene expression in *Staphylococcus aureus*. *Mol. Microbiol.* 41, 247–261. doi: 10.1046/j.1365-2958.2001.02515.x

Godány, A., Bukovská, G., Farkasovská, J., Brnáková, Z., Dmitriev, A., Tkáciková, E., et al. (2004). Characterization of a complex restriction-modification system detected in *Staphylococcus aureus* and *Streptococcus agalactiae* strains isolated from infections of domestic animals. *Folia Microbiol.* 49, 307–314. doi: 10.1007/BF02931048

Goerke, C., Pantůček, R., Holtfreter, S., Schulte, B., Zink, M., Grumann, D., et al. (2009). Diversity of prophages in dominant *Staphylococcus aureus* clonal lineages. *J. Bacteriol.* 191, 3462–3468. doi: 10.1128/JB.01804-08

Golec, P., Dąbrowski, K., Hejnowicz, M. S., Gozdek, A., Łoś, J. M., Wegrzyn, G., et al. (2011). A reliable method for storage of tailed phages. *J. Microbiol. Methods* 84, 486–489. doi: 10.1016/j.mimet.2011.01.007

Gozdek, A., Głowacka-Rutkowska, A., Gawor, J., Empel, J., Gromadka, R., and Łobocka, M. B. (2018). Complete genome sequences of two novel *Staphylococcus aureus* podoviruses of potential therapeutic use, vB_SauP_phiAGO1.3 and vB_SauP_phiAGO1.9. *Genome Announc.* 6, 4–5. doi: 10.1128/genomeA.00048-18

Hooton, S. P., Brathwaite, K. J., and Connerton, I. F. (2016). The bacteriophage carrier state of *Campylobacter jejuni* features changes in host non-coding RNAs and the acquisition of new host-derived CRISPR spacer sequences. *Front. Microbiol.* 7:355. doi: 10.3389/fmicb.2016.00355

Ito, T., Ma, X. X., Takeuchi, F., Okuma, K., Yuzawa, H., and Hiramatsu, K. (2004). Novel type V staphylococcal cassette chromosome *mec* driven by a novel cassette chromosome recombinase, *ccrC*. *Antimicrob. Agents Chemother.* 48, 2637–2651. doi: 10.1128/AAC.48.7.2637-2651.2004

Iwano, H., Inoue, Y., Takasago, T., Kobayashi, H., Furusawa, T., Taniguchi, K., et al. (2018). Bacteriophage ΦSA012 has a broad host range against *Staphylococcus aureus* and effective lytic capacity in a mouse mastitis model. *Biology* 7:E8. doi: 10.3390/biology7010008

Iyer, L. M., Burroughs, A. M., Anand, S., de Souza, R. F., and Aravind, L. (2017). Polyvalent proteins, a pervasive theme in the intergenomic biological conflicts of bacteriophages and conjugative elements. *J. Bacteriol* 199:e00245-17. doi: 10.1128/JB.00245-17

Jindrova, E., Schmid-Nuoffer, S., Hamburger, F., Janscak, P., and Bickle, T. A. (2005). On the DNA cleavage mechanism of Type I restriction enzymes. *Nucleic Acids Res.* 33, 1760–1766. doi: 10.1093/nar/gki322

Kaźmierczak, Z., Górski, A., and Dąbrowska, K. (2014). Facing antibiotic resistance: *Staphylococcus aureus* phages as a medical tool. *Viruses* 6, 2551–2570. doi: 10.3390/v6072551

Kiem, S., Oh, W. S., Peck, K. R., Lee, N. Y., Lee, J. Y., Song, J. H., et al. (2004). Phase variation of biofilm formation in *Staphylococcus aureus* by IS 256 insertion and its impact on the capacity adhering to polyurethane surface. *J. Korean Med. Sci.* 19, 779–782. doi: 10.3346/jkms.2004.19.6.779

Kraushaar, B., Thanh, M. D., Hammerl, J. A., Reetz, J., Fetsch, A., and Hertwig, S. (2013). Isolation and characterization of phages with lytic activity against methicillin-resistant *Staphylococcus aureus* strains belonging

to clonal complex 398. *Arch. Virol.* 158, 2341–2350. doi: 10.1007/s00705-013-1707-6

Kreiswirth, B. N., Löfdahl, S., Betley, M. J., O'Reilly, M., Schlievert, P. M., Bergdoll, M. S., et al. (1983). The toxic shock syndrome exotoxin structural gene is not detectably transmitted by a prophage. *Nature* 305, 709–712. doi: 10.1038/305709a0

Kwan, T., Liu, J., DuBow, M., Gros, P., and Pelletier, J. (2005). The complete genomes and proteomes of 27 *Staphylococcus aureus* bacteriophages. *Proc. Natl. Acad. Sci. U.S.A.* 102, 5174–5179. doi: 10.1073/pnas.0501140102

Labrie, S. J., Samson, J. E., and Moineau, S. (2010). Bacteriophage resistance mechanisms. *Nat. Rev. Microbiol.* 8, 317–327. doi: 10.1038/nrmicro2315

Lavigne, R., Seto, D., Mahadevan, P., Ackermann, H. W., and Kropinski, A. M. (2008). Unifying classical and molecular taxonomic classification: analysis of the Podoviridae using BLASTP-based tools. *Res. Microbiol.* 159, 406–414. doi: 10.1016/j.resmic.2008.03.005

Li, K., Barksdale, L., and Garmise, L. (1961). Phenotypic alterations associated with the bacteriophage carrier state of *Shigella* dysenteriae. *J. Gen. Microbiol.* 24, 355–367. doi: 10.1099/00221287-24-3-355

Li, X., Gerlach, D., Du, X., Larsen, J., Stegger, M., Kühner, P., et al. (2015). An accessory wall teichoic acid glycosyltransferase protects *Staphylococcus aureus* from the lytic activity of Podoviridae. *Sci Rep.* 5:17219. doi: 10.1038/srep17219

Liang, X., Zheng, L., Landwehr, C., Lunsford, D., Holmes, D., and Ji, Y. (2005). Global regulation of gene expression by ArlRS, a two-component signal transduction regulatory system of *Staphylococcus aureus*. *J. Bacteriol.* 187, 5486–5492. doi: 10.1128/JB.187.15.5486-5492.2005

Lindsay, J. A. (2014). *Staphylococcus aureus* genomics and the impact of horizontal gene transfer. *Intl. J. Med. Microbiol.* 304, 103–109. doi: 10.1016/j.ijmm.2013.11.010

Łobocka, M., Hejnowicz, M. S., Gągała, U., Weber-Dąbrowska, B., Wêgrzyn, G., Dadlez, M., et al. (2014a). "The First Step to Bacteriophage Therapy - How to Choose the Correct Phage," in *Phage Therapy: Current Research and Applications*, eds J. Borysowski, R. Międzybrodzki, and A. Górski (Poole: Caister Academic Press), 23–69.

Łobocka, M. B., Głowacka, A., Dąbrowski, K., Hejnowicz, M. S., Gozdek, A., Weber-Dąbrowska, B., et al. (2014b). *A Method of Evaluating the Therapeutic Efficacy of Bacteriophages*. *Pat. UPRP PL*219654 B1, Pat. EP2872156 B1; Pat. US 9678063 B2, WO2014/012872 A1.

Łobocka, M. B., Hejnowicz, M. S., Dąbrowski, K., Gozdek, A., Kosakowski, J., Witkowska, M., et al. (2012). Genomics of staphylococcal Twort-like phages: potential therapeutics of the post-antibiotic era. *Adv. Virus Res.* 83, 143–216. doi: 10.1016/B978-0-12-394438-2.00005-0

Łobocka, M. B., Hejnowicz, M. S., Dąbrowski, K., Izak, D., Gozdek, A., Głowacka, A., et al. (2016). *Staphylococcus aureus* strains for the production of monoclonal bacteriophage preparations deprived of plasmid DNA. WO 2016/030871 A1. U.S. Patent. 2016 Mar 16.

Luong, T. T., and Lee, C. Y. (2006). The arl locus positively regulates *Staphylococcus aureus* type 5 capsule via an mgrA-dependent pathway. *Microbiology* 152, 3123–3131. doi: 10.1099/mic.0.29177-0

Lwoff, A. (1953). Lysogeny. *Bacteriol. Rev.* 17, 269–337.

MacNeal, W. J., and Frisbee, F. C. (1936a). Bacteriophage service to patients with Staphylococcus septicemia. *Am. J. Med. Sci.* 191, 170–178. doi: 10.1097/00000441-193602000-00003

MacNeal, W. J., and Frisbee, F. C. (1936b). One hundred patients with *Staphylococcus septicemia* receiving bacteriophage service. *Am. J. Med. Sci.* 191, 179–195. doi: 10.1097/00000441-193602000-00004

Mandell, G. L., Bennett, J. E., and Dolin, R. (2010). *Mandell, Douglas, and Bennett's Principles and Practice of Infectious Diseases, Churchill Livingstone*. Philadelphia, PA: Elsevier.

Mazmanian, S. K., Ton-That, H., and Schneewind, O. (2001). Sortase-catalysed anchoring of surface proteins to the cell wall of *Staphylococcus aureus*. *Mol. Microbiol.* 40, 1049–1057. doi: 10.1046/j.1365-2958.2001.02411.x

McCarthy, A. J., and Lindsay, J. A. (2010). Genetic variation in *Staphylococcus aureus* surface and immune evasion genes is lineage associated: implications for vaccine design and host-pathogen interactions. *BMC Microbiol.* 10:173. doi: 10.1186/1471-2180-10-173

McCarthy, A. J., and Lindsay, J. A. (2012). The distribution of plasmids that carry virulence and resistance genes in *Staphylococcus aureus* is lineage associated. *BMC Microbiol.* 12:104. doi: 10.1186/1471-2180-12-104

McCarthy, A. J., Witney, A. A., and Lindsay, J. A. (2012). *Staphylococcus aureus* temperate bacteriophage: carriage and horizontal gene transfer (HGT) is lineage associated. *Front. Cell Infect. Microbiol.* 2:6. doi: 10.3389/fcimb.2012.00006

Międzybrodzki, R., Borysowski, J., Weber-Dąbrowska, B., Fortuna, W., Letkiewicz, S., Szufnarowski, K., et al. (2012). Clinical aspects of phage therapy. *Adv. Virus Res.* 83, 73–121. doi: 10.1016/B978-0-12-394438-2.00003-7

Monk, I. R., Shah, I. M., Xu, M., Tan, M. W., and Foster, T. J. (2012). Transforming the untransformable: application of direct transformation to manipulate genetically *Staphylococcus aureus* and *Staphylococcus epidermidis*. *mBio* 3:e00277-11. doi: 10.1128/mBio.00277-11

Monk, I. R., Tree, J. J., Howden, B. P., Stinear, T. P., and Foster, T. J. (2015). Complete bypass of restriction systems for major *Staphylococcus aureus* lineages. *mBio* 6:e00308-15. doi: 10.1128/mBio.00308-15

Moormeier, D. E., and Bayles, K. W. (2017). *Staphylococcus aureus* biofilm: a complex developmental organism. *Mol. Microbiol.* 104, 365–376. doi: 10.1111/mmi.13634

Nair, D., Memmi, G., Hernandez, D., Bard, J., Beaume, M., Gill, S., et al. (2011). Whole-genome sequencing of *Staphylococcus aureus* strain RN4220, a key laboratory strain used in virulence research, identifies mutations that affect not only virulence factors but also the fitness of the strain. *J. Bacteriol.* 193, 2332–2335. doi: 10.1128/JB.00027-11

Noto, M. J., Kreiswirth, B. N., Monk, A. B., and Archer, G. L. (2008). Gene acquisition at the insertion site for SCCmec, the genomic island conferring methicillin resistance in *Staphylococcus aureus*. *J. Bacteriol.* 190, 1276–1283. doi: 10.1128/JB.01128-07

Otto, M. (2012). MRSA virulence and spread. *Cell Microbiol* 14, 1513–1521. doi: 10.1111/j.1462-5822.2012.01832.x

Pantůček, R., Rosypalová, A., Doskar, J., Kailerová, J., Růzicková, V., Borecká, P., et al. (1998). The polyvalent staphylococcal phage phi 812: its host-range mutants and related phages. *Virology* 246, 241–252. doi: 10.1006/viro.1998.9203

Radin, J. N., Kelliher, J. L., Párraga Solórzano, P. K., and Kehl-Fie, T. E. (2016). The two-component system ArlRS and alterations in metabolism enable *Staphylococcus aureus* to resist calprotectin-induced manganese starvation. *PLoS Pathog.* 12:e1006040. doi: 10.1371/journal.ppat.1006040

Roberts, G. A., Houston, P. J., White, J. H., Chen, K., Stephanou, A. S., Cooper, L. P., et al. (2013). Impact of target site distribution for Type I restriction enzymes on the evolution of methicillin-resistant *Staphylococcus aureus* (MRSA) populations. *Nucleic Acids Res.* 41, 7472–7484. doi: 10.1093/nar/gkt535

Samson, J. E., Magadán, A. H., Sabri, M., and Moineau, S. (2013). Revenge of the phages: defeating bacterial defences. *Nat. Rev. Microbiol.* 11, 675–687. doi: 10.1038/nrmicro3096

Sauve, L. (1936). Le bacteìriophage in chirurgie. *La Med.* 17, 49–54. doi: 10.1371/journal.ppat.1002917

Seed, K. D., Faruque, S. M., Mekalanos, J. J., Calderwood, S. B., Qadri, F., and Camilli, A. (2012). Phase variable O antigen biosynthetic genes control expression of the major protective antigen and bacteriophage receptor in *Vibrio cholerae* O1. *PLoS Pathog.* 8:e1002917. doi: 10.1371/journal.ppat.1002917

Seidl, K., Leemann, M., and Zinkernagel, A. S. (2018). The ArlRS two-component system is a regulator of *Staphylococcus aureus*-induced endothelial cell damage. *Eur. J. Clin. Microbiol. Infect. Dis.* 37, 289–292. doi: 10.1007/s10096-017-3130-5

Siringan, P., Connerton, P. L., Cummings, N. J., and Connerton, I. F. (2014). Alternative bacteriophage life cycles: the carrier state of *Campylobacter jejuni*. *Open Biol.* 4:130200. doi: 10.1098/rsob.130200

Šišáková, E., van Aelst, K., Diffin, F. M., and Szczelkun, M. D. (2013). The type ISP restriction-modification enzymes LlaBIII and LlaGI use a translocation-collision mechanism to cleave non-specific DNA distant from their recognition sites. *Nucleic Acids Res.* 41, 1071–1080. doi: 10.1093/nar/gks1209

Son, J. S., Lee, S. J., Jun, S. Y., Yoon, S. J., Kang, S. H., Paik, H. R., et al. (2010). Antibacterial and biofilm removal activity of a Podoviridae *Staphylococcus aureus* bacteriophage SAP-2 and a derived recombinant cell-wall-degrading enzyme. *Appl. Microbiol. Biotechnol.* 86, 1439–1449. doi: 10.1007/s00253-009-2386-9

Springer, B., Orendi, U., Much, P., Höger, G., Ruppitsch, W., Krziwanek, K., et al. (2009). Methicillin-resistant *Staphylococcus aureus*: a new zoonotic agent? *Wien. Klein. Wochenschr.* 121, 86–90. doi: 10.1007/s00508-008-1126-y

Stepanovic, S., Vukovic, D., Dakic, I., Savic, B., and Svabic-Vlahovic, M. (2000). A modified microtiter-plate test for quantification of staphylococcal biofilm formation. *J. Microbiol. Methods* 40, 175–179. doi: 10.1016/S0167-7012(00)00122-6

Stobberingh, E. E., Schiphof, R., and Sussenbach, J. S. (1977). Occurrence of a class II restriction endonuclease in *Staphylococcus aureus*. *J. Bacteriol.* 131, 645–649.

Studier, F. W., and Bandyopadhyay, P. K. (1988). Model for how type I restriction enzymes select cleavage sites in DNA. *Proc. Natl. Acad. Sci. U.S.A.* 85, 4677–4681.

Štveráková, D., Šedo, O., Benešík, M., Zdráhal, Z., Doškař, J., and Pantůček, R. (2018). Rapid identification of intact staphylococcal bacteriophages using matrix-assisted laser desorption ionization-time-of-flight mass spectrometry. *Viruses* 10, 1–19. doi: 10.3390/v10040176

Sulston, J. E., and Hodgkin, J. (1988). "Methods," in *The Nematode Caenorhabditis elegans*, ed. W. B. Wood (Cold Spring Harbor, NY: Cold Spring Harbor Laboratory Press), 587–606.

Sussenbach, J. S., Monfoort, C. H., Schiphof, R., and Stobberingh, E. E. (1976). A restriction endonuclease from *Staphylococcus aureus*. *Nucleic Acids Res.* 3, 3193–3202. doi: 10.1093/nar/3.11.3193

Sussenbach, J. S., Steenbergh, P. H., Rost, J. A., van Leeuwen, W. J., and van Embden, J. D. (1978). A second site-specific restriction endonuclease from Staphylococcus aureus. *Nucleic Acids Res.* 5, 1153–1163. doi: 10.1093/nar/5.4.1153

Swift, S. M., and Nelson, D. C. (2014). Complete genome sequence of *Staphylococcus aureus* phage GRCS. *Genome Announc.* 2:e00209-14. doi: 10.1128/genomeA.00209-14

Szilák, L., Venetianer, P., and Kiss, A. (1990). Cloning and nucleotide sequence of the genes coding for the Sau96I restriction and modification enzymes. *Nucleic Acids Res.* 18, 4659–4664. doi: 10.1093/nar/18.16.4659

Takemura-Uchiyama, I., Uchiyama, J., Kato, S., Inoue, T., Ujihara, T., Ohara, N., et al. (2013). Evaluating efficacy of bacteriophage therapy against *Staphylococcus aureus* infections using a silkworm larval infection model. *FEMS Microbiol. Lett.* 347, 52–60. doi: 10.1111/1574-6968.12220

Takemura-Uchiyama, I., Uchiyama, J., Osanai, M., Morimoto, N., Asagiri, T., Ujihara, T., et al. (2014). Experimental phage therapy against lethal lung-derived septicemia caused by *Staphylococcus aureus* in mice. *Microbes Infect.* 16, 512–517. doi: 10.1016/j.micinf.2014.02.011

Takeuchi, I., Osada, K., Azam, A. H., Asakawa, H., Miyanaga, K., and Tanji, Y. (2016). The presence of two receptor-binding proteins contributes to the wide host range of staphylococcal Twort-like phages. *Appl. Environ. Microbiol.* 82, 5763–5774. doi: 10.1128/AEM.01385-16

Uchiyama, J., Takemura-Uchiyama, I., Kato, S., Sato, M., Ujihara, T., Matsui, H., et al. (2014). In silico analysis of AHJD-like viruses, *Staphylococcus aureus* phages S24-1 and S13', and study of phage S24-1 adsorption. *Microbiologyopen* 3, 257–270. doi: 10.1002/mbo3.166

Uchiyama, J., Taniguchi, M., Kurokawa, K., Takemura-Uchiyama, I., Ujihara, T., Shimakura, H., et al. (2017). Adsorption of Staphylococcus viruses S13' and S24-1 on *Staphylococcus aureus* strains with different glycosidic linkage patterns of wall teichoic acids. *J. Gen. Virol.* 98, 2171–2180. doi: 10.1099/jgv.0.000865

Villanueva, M., García, B., Valle, J., Rapún, B., Ruiz de Los Mozos, I., Solano, C., et al. (2018). Sensory deprivation in *Staphylococcus aureus*. *Nat. Commun.* 9:523. doi: 10.1038/s41467-018-02949-y

Vybiral, D., Takác, M., Loessner, M., Witte, A., von Ahsen, U., and Bläsi, U. (2003). Complete nucleotide sequence and molecular characterization of two lytic *Staphylococcus aureus* phages: 44AHJD and P68. *FEMS Microbiol. Lett.* 219, 275–283. doi: 10.1016/S0378-1097(03)00028-4

Waldron, D. E., and Lindsay, J. A. (2006). Sau1: a novel lineage-specific type I restriction-modification system that blocks horizontal gene transfer into *Staphylococcus aureus* and between *S. aureus* isolates of different lineages. *J. Bacteriol.* 188, 5578–5585. doi: 10.1128/JB.00418-06

Walker, J. N., Crosby, H. A., Spaulding, A. R., Salgado-Pabón, W., Malone, C. L., Rosenthal, C. B., et al. (2013). The *Staphylococcus aureus* ArlRS two-component system is a novel regulator of agglutination and pathogenesis. *PLoS Pathog.* 9:e1003819. doi: 10.1371/journal.ppat.1003819

Wang, Z., Zheng, P., Ji, W., Fu, Q., Wang, H., Yan, Y., et al. (2016). SLPW: A virulent bacteriophage targeting methicillin-resistant *Staphylococcus aureus* in vitro and in vivo. *Front. Microbiol.* 7:934. doi: 10.3389/fmicb.2016.00934

West, A. H., and Stock, A. M. (2001). Histidine kinases and response regulator proteins in two-component signaling systems. *Trends Biochem. Sci.* 26, 369–376. doi: 10.1016/S0968-0004(01)01852-7

Wick, R. R., Judd, L. M., Gorrie, C. L., and Holt, K. E. (2017). Unicycler: resolving bacterial genome assemblies from short and long sequencing reads. *PLoS Comput. Biol.* 13:e1005595. doi: 10.1371/journal.pcbi.1005595

Xia, G., Corrigan, R. M., Winstel, V., Goerke, C., Gründling, A., and Peschel, A. (2011). Wall teichoic acid-dependent adsorption of staphylococcal siphovirus and myovirus. *J. Bacteriol.* 193, 4006–4009. doi: 10.1128/JB.01412-10

Xia, G., Maier, L., Sanchez-Carballo, P., Li, M., Otto, M., Holst, O., et al. (2010). Glycosylation of wall teichoic acid in *Staphylococcus aureus* by TarM. *J. Biol. Chem.* 285, 13405–13415. doi: 10.1074/jbc.M109.096172

Yang, S., Liu, J., Shao, F., Wang, P., Duan, G., and Yang, H. (2015). Analysis of the features of 45 identified CRISPR loci in 32 *Staphylococcus aureus*. *Biochem. Biophys. Res. Commun.* 464, 894–900. doi: 10.1016/j.bbrc.2015.07.062

Conflict of Interest Statement: AG-R, JE, and MŁ are joint authors of a patent for a method of phage therapeutic activity testing with the use of nematode. AG, AG-R, JG, MŁ, and RG have filed a patent application for *S. aureus* phage propagator strains.

The remaining authors declare that the research was conducted in the absence of any commercial or financial relationships that could be construed as a potential conflict of interest.

frontiers in Microbiology

ORIGINAL RESEARCH
published: 15 January 2019
doi: 10.3389/fmicb.2018.03326

Characterization of Bacteriophage vB-EcoS-95, Isolated From Urban Sewage and Revealing Extremely Rapid Lytic Development

*Gracja Topka[1], Sylwia Bloch[1], Bożena Nejman-Faleńczyk[1], Tomasz Gąsior[2], Agata Jurczak-Kurek[3], Agnieszka Necel[1], Aleksandra Dydecka[1], Malwina Richert[4], Grzegorz Węgrzyn[1] and Alicja Węgrzyn[2]**

[1] Department of Molecular Biology, University of Gdańsk, Gdańsk, Poland, [2] Laboratory of Molecular Biology, Institute of Biochemistry and Biophysics, Polish Academy of Sciences, Gdańsk, Poland, [3] Department of Molecular Evolution, University of Gdańsk, Gdańsk, Poland, [4] Laboratory of Electron Microscopy, University of Gdańsk, Gdańsk, Poland

Morphological, biological, and genetic characteristics of a virulent *Siphoviridae* phage, named vB-EcoS-95, is reported. This phage was isolated from urban sewage. It was found to infect some *Escherichia coli* strains giving clear plaques. The genome of this phage is composed of 50,910 bp and contains 89 ORFs. Importantly, none of the predicted ORFs shows any similarity with known pathogenic factors that would prevent its use in medicine. Genome sequence analysis of vB-EcoS-95 revealed 74% similarity to genomic sequence of *Shigella* phage pSf-1. Compared to pSf-1, phage vb-EcoS-95 does not infect *Shigella* strains and has an efficient bacteriolytic activity against some *E. coli* strains. One-step growth analysis revealed that this phage has a very short latent period (4 min), and average burst size of 115 plaque forming units per cell, which points to its high infectivity of host cells and strong lytic activity. The bacteriolytic effect of vB-EcoS-95 was tested also on biofilm-producing strains. These results indicate that vB-EcoS-95 is a newly discovered *E. coli* phage that may be potentially used to control the formation of biofilms.

Keywords: bacteriophage, coliphage, lytic development, genomic analysis, biofilm

OPEN ACCESS

Edited by:
Robert Wilson Jackson, University of Reading, United Kingdom

Reviewed by:
Ananda Shankar Bhattacharjee, Bigelow Laboratory for Ocean Sciences, United States
Rolf Lood, Lund University, Sweden

***Correspondence:**
Alicja Węgrzyn
alicja.wegrzyn@biol.ug.edu.pl

Specialty section:
This article was submitted to Virology, a section of the journal Frontiers in Microbiology

Received: *29 June 2018*
Accepted: *21 December 2018*
Published: *15 January 2019*

Citation:
Topka G, Bloch S, Nejman-Faleńczyk B, Gąsior T, Jurczak-Kurek A, Necel A, Dydecka A, Richert M, Węgrzyn G and Węgrzyn A (2019) Characterization of Bacteriophage vB-EcoS-95, Isolated From Urban Sewage and Revealing Extremely Rapid Lytic Development. Front. Microbiol. 9:3326. doi: 10.3389/fmicb.2018.03326

INTRODUCTION

Bacteriophages (or phages), i.e., viruses infecting bacterial cells, represent the most abundant biological creatures on Earth (Clokie et al., 2011). Number of phage virions is estimated at the level of 10^{31} (Weitz et al., 2012). These viruses have been discovered over 100 years ago (Twort, 1915; summarized by Wegrzyn and Wegrzyn, 2015). Some of them have played an extremely important role in development of molecular biology, serving as model organisms in studies on basic cellular processes, including gene expression, replication of genetic material, developmental regulation, environmental stress responses, and others (Wegrzyn and Wegrzyn, 2005; Krisch and Comeau, 2008; Casjens and Hendrix, 2015). Moreover, bacteriophages have been extensively used in genetic engineering and biotechnology, serving as cloning vectors and providing genetic elements used in construction of strictly regulated gene expression systems, phage display systems, and others (Onodera, 2010).

The idea of the use of bacteriophages to combat bacterial infections appeared shortly after discovery of these viruses (for a review, see Wegrzyn and Wegrzyn, 2015). Early experimental phage therapy was promising, however, discovery of penicillin led to the believe that every bacterial infection can be eliminated by the use of antibiotics, and the idea of phage therapy has been largely abandoned (Kakasis and Panitsa, 2019). Recently, the return to the use of bacteriophages to combat bacterial infections is evident. In the era of the antibiotic crisis, phage therapy appears to be one of alternatives to treat infections with bacterial strains resistant to most, if not all, known antibiotics (Kutter et al., 2015; Domingo-Calap et al., 2016; Gorski et al., 2018a). Phage therapy is based on the simple expectation that viruses which can destroy bacterial cells can be an excellent tool to eliminate specific infection agents in human (or animal) body. The major advantage of this kind of therapy is its specificity [bacteriophages are usually specific to single bacterial species, and often to particular strain(s)], auto-control (phages should propagate only if their host bacteria are available), and safety (phages do not infect eukaryotic cells) (Górski et al., 2018b). However, some potential problems must also be considered, including possibility to lysogenize host cells by a phage instead of lysing it (thus, temperate phages should not be used in phage therapy), the presence of toxin genes in genomes of some bacteriophages (such phages must be avoided in phage therapy), and possibility of development of phage resistance by bacteria (Kakasis and Panitsa, 2019). Nevertheless, antibacterial activities of bacteriophages are so attractive that the use of these viruses has been extended to food protection (Gutiérrez et al., 2016), agriculture and industry (Domingo-Calap and Delgado-Martínez, 2018), i.e., in every area of human action where bacteria may cause unwanted effects.

In the light of the extremely large population of bacteriophages (10^{31} virions on Earth, as mentioned above), a huge variability of these viruses (Hatful, 2015) is perhaps not a surprise. What is the surprise, is the relatively poor knowledge on this variability and relatively low number of characterized bacteriophages relative to other organisms (discussed by Jurczak-Kurek et al., 2016). Our previous studies indicated that even if bacteriophages are isolated from a single habitat, their diversity is huge (Jurczak-Kurek et al., 2016). Moreover, many phages isolated from environmental samples reveal properties that are very promising from the point of view of their applications in biotechnology or medicine (Jurczak-Kurek et al., 2016).

In this report, we describe detailed characterization of bacteriophage vB-EcoS-95, isolated from urban sewage, including virion morphology, host range, developmental kinetics, and genome analysis. Specific features of this bacteriophage, infecting *Escherichia coli* strains, particularly an extremely short latent period and ability to destroy bacterial biofilm, suggest that it can be used in further studies on development of novel biotechnological tools and/or its use in food protection/medicine.

MATERIALS AND METHODS

Bacterial Strains and Growth Conditions

Bacterial strains used in this study are listed in **Table 1**. *E. coli* strains and *Pseudomonas* bacteria were cultured in liquid Luria–Bertani broth (LB) or plated on solid LB medium with 1.5% agar (LA medium; Lab Empire). For *Enterococcus* and *Shigella,* special Tryptic Soy Broth (TSB) and Tryptic Soy Agar (TSA) were used (BTL). The liquid cultures were grown with aeration at 37°C in a shaking incubator (200 rpm; Eppendorf). The plates with solid medium were incubated at 37°C for 24 h. The phage infection processes were studied at 37°C, under aerobic conditions in a shaking incubator (200 rpm; Eppendorf). Biofilm studies were performed by using *E. coli* MG1655 strain bearing pUC18 plasmid and F′ plasmid from *E. coli* ER2738 strain. These bacteria were grown at 37°C without shaking in 12-well polystyrene plate with M9 medium containing 0.2% glucose (POCH).

Isolation of Bacteriophage vB_Ecos-95 From Urban Sewage

Bacteriophage vB_EcoS-95 was isolated from urban sewages, according to protocols described by Jurczak-Kurek et al. (2016). Water samples were collected from Gdansk Wastewater Treatment Plant in Poland. In the first stage of the procedure, 10 ml of the sewage sample were mixed with 1 ml of the *E. coli* MG1655 overnight culture and cultivated for a few hours at 37°C with shaking. The obtained phage lysate was clarified by centrifugation (10,000 × g, 30 min, 4°C) and extracted several times with chloroform (POCH). To obtain visible plaques, formed by phages, 50 μl of the supernatant were added to 2 ml of the overnight host bacterial culture and plated using the agar double layer method (Sambrook and Russell, 2001). Next day, a single plaque was scraped with a sterile bacteriological loop and transferred to a flask with mid-log phase *E. coli* MG1655 strain. After the lysis of bacterial culture occurred, chloroform extraction was carried out and phages were re-plated on a lawn of *E. coli* MG1655 strain. Serial dilutions of the phage lysate in TM buffer (10 mM Tris-HCl, 10 mM $MgSO_4$; pH 7.2) were prepared. Then, appropriate volume of each dilution was spotted onto double agar layer to obtain single phage plaques that were propagated three times by this method to obtain purified vB_EcoS-95 lysate. For further analysis, the required amount of vB_EcoS-95 lysate was prepared by adding phage particles to the exponentially growing *E. coli* MG1655 bacteria which were then cultivated with shaking at 37°C (200 rpm; Eppendorf) until lysis occurred. In the next step, phage particles, released during lysis, were purified by centrifugation and extracted with chloroform. Phage activity was determined using a conventional double-layer agar technique (Sambrook and Russell, 2001).

Host Range Determination

The phage host range spectrum was determined using different bacterial strains which are listed in **Table 2**. The spot lysis assay was prepared onto a double layer agar plate, following the protocol described by Jurczak-Kurek et al. (2016). Briefly,

TABLE 1 | Bacterial strains and plasmid used in the study.

Bacterial strain	Source or references	Relevant genotype or other characteristics
***E. coli* LABORATORY STRAINS**		
MG1655	Jensen, 1993	F- λ– *ilvG rfb-50 rph-1*
MG1655 producing biofilm	This study	[pUC18] F^+ Amp^R, Tet^R
C600	Appleyard, 1954	F- *tonA21 thi-1 thr-1 leuB6 lacY1 glnV44 rfbC1 fhuA1* λ –
Hfr3000	Bachmann, 1972	
Tap90	Patterson and Dean, 1987	F- *recD1903::mini-tet supE44 supF58 lacY1 pro leuB6 hsdR rpsL tonA1 thi-1* lambda-
ER2738	Gough and Murray, 1983	F'*proA*$^+$*B*$^+$ *lacI*^{q} *Δ(lacZ)M15 zzf::Tn*10(Tet^R)*/ fhuA2 glnV Δ(lac-proAB) thi-1 Δ(hsdS-mcrB)5*
MC1061	Casadaban and Cohen, 1980	
DH5α	Grant et al., 1990	*F Δ(ara-leu)7697 [araD139]B/r Δ(codB-lacI)3 galK16 galE15* λ- *e14- mcrA0 relA1 rpsL150(strR) spoT1 mcrB1 hsdR2(r-m+)*
ATCC® 25922™	ATCC: The Global Bioresource Center	*F- endA1 glnV44 thi-1 recA1 gyrA96 deoR nupG Φ80dlacZΔM15 Δ(lacZYA-argF)U169, hsdR17(rK- mK+),* λ- Serotype O6
***E. coli* CLINICAL STRAINS**		
EPEC-A 129	Specialist Hospital of St. Wojciech in Gdansk (Poland)	Stool isolate; EspA
EPEC-B 21950		Stool isolate; EspB
EPEC-C 22032	Griffin et al., 1988	Stool isolate; EspC
EHEC O157:H7 ST2-8624	Beutin et al., 1989	Stool isolate; Stx1 and Stx2
EHEC O157:H7 CB571	Beutin et al., 1989; Perna et al., 2001	Stool isolate; Stx1 and Stx2
EHEC O157:H7 EDL933	Specialist Hospital of St. Wojciech in Gdansk (Poland)	Stool isolate; Stx1 and Stx2
3250		Stool isolate
23580		Stool isolate
23581		Stool isolate
OTHERS STRAINS		
Enterococcus faecalis 230	Department of Water and Waste-Water Technology of Gdansk University of Technology	Urban sewage isolate
Pseudomonas aeruginosa 575/2003	National Medicines Institute in Warsaw (Poland)	Decubitus ulcer isolate
Pseudomonas aeruginosa 1947/2003	National Medicines Institute in Warsaw (Poland)	Wound isolate
Salmonella enterica Anatum	National Salmonella Center at Medical University of Gdansk (Poland)	-
Salmonella enterica Heidelberg	National Salmonella Center at Medical University of Gdansk (Poland)	-
Salmonella enterica Panama	National Salmonella Center at Medical University of Gdansk (Poland)	-
Salmonella enterica Reading	National Salmonella Center at Medical University of Gdansk (Poland)	-
Shigella flexneri 12022	ATCC: The Global Bioresource Center	-
Staphylococcus sciuri IO	Institute of Oceanology of Polish Academy of Sciences in Sopot (Poland)	Urban sewage isolate
PLASMID		
pUC18	Thermo Fisher Scientific	ori pMB1 (pBR322 derivative), *bla*, Amp^R

EHEC, Enterohemorrhagic E. coli; EPEC, Enteropathogenic E. coli; Stx, Shiga toxin; Esp, E. coli secretion protein.

standard Petri dishes were filled with 25 ml of LA (*E. coli* and *Pseudomonas* strains) or TSA (*Enterococcus* and *Shigella* strains) medium. Then, 3 ml of LB (*E. coli* and *Pseudomonas* strains) or TSB (*Enterococcus* and *Shigella* strains) medium, supplemented with 0.7% agar/0.4% agarose, were mixed with 1 ml of the overnight bacterial culture and poured onto LA or TSA bottom agar, respectively. Ten-fold dilutions of vB_EcoS-95 lysate were prepared in TM buffer (10 mM Tris-HCl, 10 mM $MgSO_4$; pH 7.2) and spotted onto the surface of the double-layer agar plates with a tested host. Plates were incubated at 37°C for 24 h. Productive interaction of the bacteriophage with the host bacterium was revealed as the presence of plaque formation. According to the degree of clarity, the observed results were differentiated into three

TABLE 2 | Host spectrum of bacteriophage vB_EcoS-95.

Bacterial strain	Plaques
Escherichia coli MG1655	++
Escherichia coli C600	++
Escherichia coli TAP90	++
Escherichia coli Hfr3000	++
Escherichia coli MC1061	++
Escherichia coli DH5α	++
Escherichia coli ATCC 25922	–
Shigella flexneri (12022)	–
Salmonella enterica (Anatum)	–
Salmonella enterica (Heidelberg)	–
Salmonella enterica (Reading)	–
*Salmonella enterica (*Panama)	–
Pseudomonas aeruginosa (575)	–
Pseudomonas aeruginosa (1947)	–
Enterococcus faecelis (230)	–
Staphylococcus sciuri	–
Escherichia coli EPEC-A	–
Escherichia coli EPEC-B	–
Escherichia coli EPEC-C	–
Escherichia coli EHEC O157:H7	–
E. coli EHEC O157:H7 ST2-8624	–
E. coli EHEC O157:H7 CB571	–
E. coli EHEC O157:H7 EDL933	–
Clinical isolate of *E. coli* 3250	++
Clinical isolate of *E. coli* 23580	++
Clinical isolate of *E. coli* 23581	+

Symbols: (++) clear plaques, (+) turbid plaques or (–) no plaques after infection with phage.

classes: (++) clear plaques, (+) turbid plaques, and (−) no plaques.

Microscopic Analyses

Virions were purified from the phage lysate (2.1×10^{10} PFU/ml) obtained after infection of the host strain *E. coli* C600 with phage vB_EcoS-95. Purification was performed using cesium chloride density gradient centrifugation method, described by Sambrook and Russell (2001). Electron microscopic analyses of phage particles were performed employing the Philips CM 100 electron microscope (Philips, Eindhoven, The Netherlands), by using negative staining with uranyl acetate (Czajkowski et al., 2015). Dimensions of virions were measured on micrographs at magnification of 39,000 times, with analySIS Pro (iTEM) software. The Tomocube holographic 3D microscope (Perlan Technologies, Poland) was used to evaluate the structure of *E. coli* biofilms after 4 h incubation with phage vB_EcoS-95 lysate (2.1×10^{10} PFU/ml).

Determination of Plaque Morphology

Plaque morphology of phage vB_EcoS-95 was tested on the *E. coli* C600 strain. To determine plaque size, serial dilutions of phage lysate in TM Buffer (10 mM Tris-HCl, 10 mM $MgSO_4$) were prepared. Next, 1 ml of the host strain culture was mixed with 10 μl of each dilution of phage lysate and added to 3 ml of top LB with 0.7% agar. The mixture was spread onto LA plate. Diameters of plaques were measured manually and pictures were taken using the digital scanner HP Scanjet G4050 and assigned software.

The Influence of the External Factors on Phage Particles Stability

Phage stability tests were performed according to protocols described by Jurczak-Kurek et al. (2016). To determine the sensitivity of phage lysate, the following external factors were tested: temperature (−20, 20, 30, 37, 40, 62, and 95°C), pH (2, 4, 10, and 12), organic solvents (ethanol, chloroform, DMSO, and acetone), and detergents (SDS, sarkosyl, and CTAB). The survival of phages during osmotic shock conditions was also analyzed.

Efficiency of Bacteriophage Adsorption

Bacteria were grown in LB medium at 37°C to OD_{600} = 0.3. Samples of 6 ml were centrifuged and pellets were washed with 1 ml of 0.85% NaCl (Chempur). After centrifugation, each pellet was suspended in 1.3 ml of LB medium and incubated at 37°C for 15 min. Then, bacteriophage lysate was added to m.o.i. = 0.1. During the incubation, samples were withdrawn at indicated times and centrifuged (6000 × g for 1 min at room temperature). In the next step, the supernatants were titrated. Plates were incubated at 37 °C overnight. A sample withdrawn immediately after addition of phage lysate to the bacterial host strain (time zero) was considered as 100% non-adsorbed phages. Other values were calculated relative to this value.

One-Step Growth Analysis

Intracellular lytic development of phage vB_EcoS-95 was studied in one-step growth experiment, according to the procedure described by Bloch et al. (2013), with minor modifications. Briefly, *E. coli* MG1655 host cells were grown with shaking in LB medium at 37°C to OD_{600} = 0.2. Then, 10 ml of culture sample were harvested by centrifugation (4,000 × g, 10 min, 4°C). The supernatant was discarded, and the pellet was resuspended in 1 ml of fresh LB medium with 3 mM sodium azide (Sigma-Aldrich). Following 5-min incubation at 37°C, bacteriophage vB_EcoS-95 was added to *E. coli* MG1655 to m.o.i. = 0.01. After 10 min incubation at 37°C, non-adsorbed phage particles were removed by three times washing with 1 ml of LB medium containing 3 mM sodium azide (4,000 × g, 10 min, 4°C). In the next step, 25 μl of the suspension was added to 25 ml of LB medium (time 0), and aerated in an incubator shaker at 37°C. The number of phage-infected bacterial cells was determined at time 1 min after infection by mixing 5 μl of the culture sample with 0.995 ml of an overnight *E. coli* MG1655 culture and 2 ml of top agar (LB with 0.7% agar), prewarmed to 45°C. Next, the mixture was poured onto LA plate (infected bacteria were named "infection centers" because they were sources of new phage particles, which were released from host cells during one lytic cycle, and following infection of neighboring cells could form plaques). Two sets of samples were collected every 1 min during first 10 min, and then every

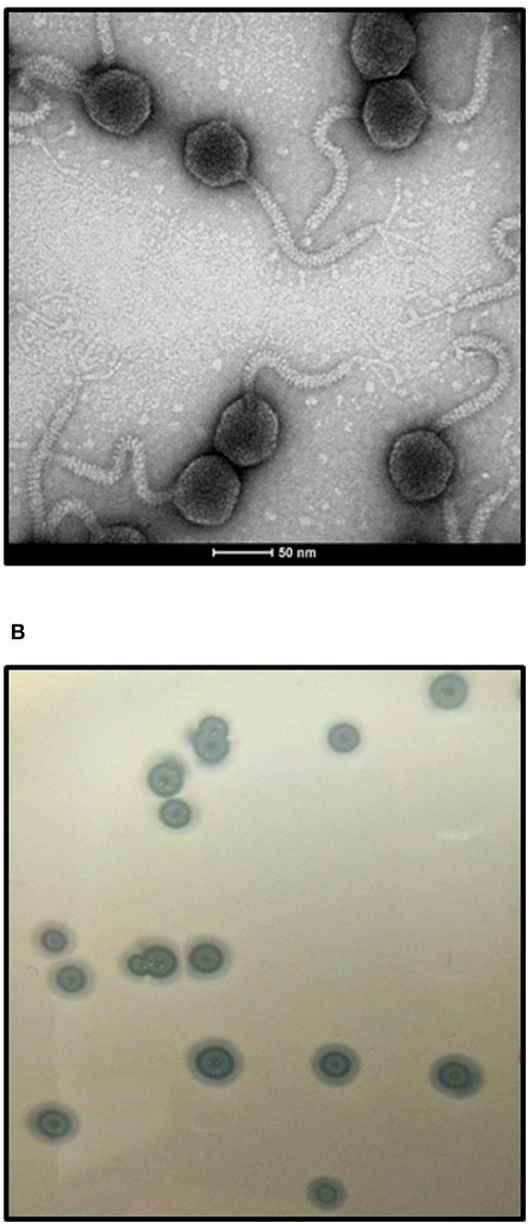

FIGURE 1 | Electron micrograph of phage vB_EcoS-95 **(A)** and its plaques formed in double-layer agar plates with *E. coli* MG1655 strain **(B)**. The bar corresponds to 50 nm.

2.5 min. The samples were serially diluted (10-fold each) in TM buffer (10 mM Tris-HCl, 10 mM $MgSO_4$) and titrated under permissive conditions. Before the titration, the second set of samples was treated with 1% chloroform (final concentration) to release the intracellular phage particles to determine the eclipse period. Based on the number of PFU/ml, the latent period and burst size were determined (the burst size was estimated as the ratio of the phage titer to the titer of infection centers).

Lysis Profile Assay

Host culture was grown to OD_{600} = 0.2 at 37°C. Phage lysate was add to m.o.i. = 0.05 to the flask. Bacteria were incubated with shaking at 37°C, and their density was monitored by OD_{600} measurement in the same time intervals (every 5 min). During this experiment, survival of host bacteria after phage infection (CFU/ml) and phage titer (PFU/ml) were also analyzed. To estimate the number of surviving cells after the vB_EcoS-95 infection, 100 µl samples were collected at times indicated above, and their serial 10-fold dilutions were prepared in LB. Forty µl of each dilution were spread onto LB agar plates. The number of viable bacterial cells was calculated on the basis of counted colonies. To determine the number of phages per ml, samples were taken every 5 min and their serial 10-fold dilutions were prepared in TM buffer. Next, 2.5 µl of each dilution were spotted onto double agar layer, and then plates were incubated overnight at 37°C. The phage titer was calculated on the basis of counted plaques.

Development of Bacterial Resistance

The emergence of bacterial resistance was measured for the combination of phage vB_EcoS-95/antibiotic rifampicin (Lab Empire) and the *E. coli* MG1655 strain. Host bacteria were cultured to OD_{600} = 0.2 at 37°C. Next, the culture was divided into three aliquots. Phage lysate was added to one of the flasks to m.o.i. of 0.01. The second one was treated with rifampicin to a final concentration of 25 µg/ml. The last one was a control. The cultivation was continued at 37°C. After 3 h of shaking, 10 µl of each samples were withdrawn. Serial dilutions in LB medium were prepared and 90 µl of each dilution was spread on LB agar plates. After overnight incubation at 37°C, percentage of surviving *E. coli* bacteria after phage infection or rifampicin treatment was calculated relative to bacterial control. To estimate the percent of bacterial colonies resistant to phage vB_EcoS-95 infection, 300 colonies were passaged in each well of a 24-well plate with 2 ml of LB medium and shaken at 37°C to OD_{600} = 0.1. Next, the phage lysate was added to each well to m.o.i. of 1. The lack of bacterial cell lysis indicated the emergence of bacterial resistance to phage vB_EcoS-95 infection. To calculate the percent of bacteria resistant to tested antibiotic, the same number of bacterial colonies was passaged onto LB agar plates supplemented with rifampicin to final concentration of 25 µg/ml, and incubated for 24 h at 37°C.

Quantification of Biofilm Density After Phage Infection

Biofilm cell density after phage infection was determined according to the protocols described by Sung et al. (2006) and Vianney et al. (2005), with some modifications. For biofilm cell culture, *E. coli* MG1655/pUC18 F′ strain was grown at 37°C in 12-well polystyrene plate with M9 medium containing 0.2% glucose. After 48 h of growth, the liquid medium containing planktonic cells was removed. The surface-attached cells in the biofilm were washed with 1 ml of 1 × PBS. In the next step, phage lysate was added to each well, except for controls, to the final titer of 10^2, 10^4, 10^5, 10^7 or 10^{10} PFU/well,

TABLE 3 | Morphological characteristic of bacteriophage vB_EcoS-95.

Phage name	Head lenght [nm]	Head diameter [nm]	Tail lenght [nm]	Tail diameter [nm]	Tail fiber lenght [nm]	Tail fiber diameter [nm]	Phage family	Plaque morphology
vB_EcoS-95	54	53	127	10	39	2.5	Siphoviridae	Clear; ø 2–3 mm

TABLE 4 | Resistance of phage virion to physical and chemical agents.

Phage name	Lysis at 4°C	-20°C	20°C	30°C	37°C	40°C	62 °C	95°C	pH 2	pH 4	pH 10	pH 12	Osmotic shock	0.09% SDS	0.1% CTAB	0.1% Sarkosyl	63% Ehtanol	90% Acetone	50% DMSO	Chloroform
vB_EcoS-95	+/–	92	100	82	82	44	4.1	0	0	0.43	93	0.27	86	0	67	14.7	0.8	0.3	71	87

Comparison of effects of physical and chemical agents on phage vB_EcoS-95. Percent of surviving phages under certain conditions is shown.

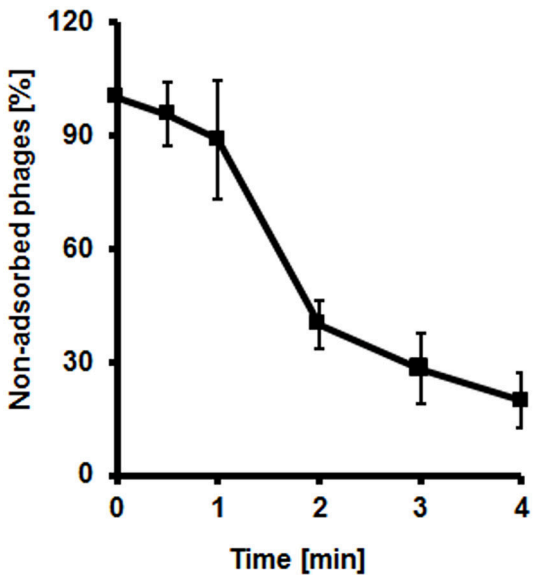

FIGURE 2 | Kinetics of vB_EcoS-95 phage adsorption on host cells. Results are presented as mean values ± SD from three independent experiments.

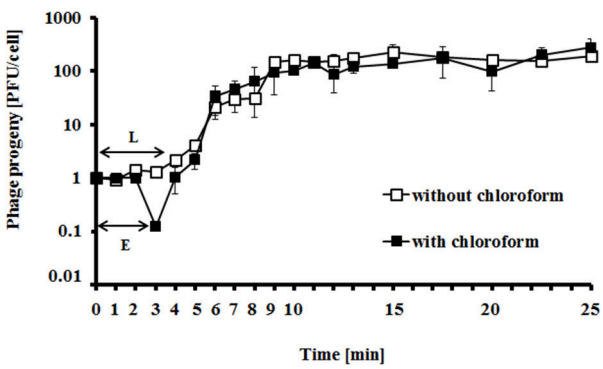

FIGURE 3 | Kinetics of progeny production by vB_EcoS-95 phage in the single life cycle. Closed squares, chloroform-treated sample; open squares, non-chloroform-treated sample. E, eclipse period; L, latent period. Results are presented as mean values ± SD from three independent experiments, and shown as PFU (plaque-forming units) per 1 cell.

and then plates were incubated at 37°C for 4 h. In the case of control wells, the medium was added instead of phage lysate. Fallowing the incubation, phage lysate was removed and surface-attached cells were resuspended in 1 ml of 1 × PBS. The biomasses of bacterial biofilm were estimated by measuring the optical density (OD) with a plate reader (EnSpire Multimode Plate Reader) at wavelength 600 nm. In order to take photos of biofilms for densitometry analyses, phage lysate was removed and surface-attached cells were dried at 37°C for 15 min. Biofilm area intensities were quantified from the performed images by densitometry, using QuantityOne software (Bio Rad®).

Assessment of Biofilm Biomass by Crystal Violet (CV) Staining

Biofilm cells were prepared according to the procedure described above. After the incubation with phage lysate (added to final titer of 10^2,10^4,10^5,10^7, or 10^{10} PFU/well), the liquid medium containing planktonic bacteria was carefully removed and surface-attached cells were treated with 0.5 ml of 0.1% crystal violet (Sigma-Aldrich). Plates were incubated in the dark for 30 min at room temperature. In the next step, crystal violet was carefully removed and biofilms were washed 5 times with 1 ml of 1 × PBS. Then, biofilms were fixed by incubating the plates at 60°C for 30 min. Following the incubation, crystal violet was dissolved by the addition of 1 ml of 96% ethanol. To determine the biomass of bacterial biofilm, absorbance was measured in a plate reader at 570 nm (EnSpire Multimode Plate Reader). Biofilm area after fixation was also photographed to visualize the differences in biofilm biomass after phage lysate treatment.

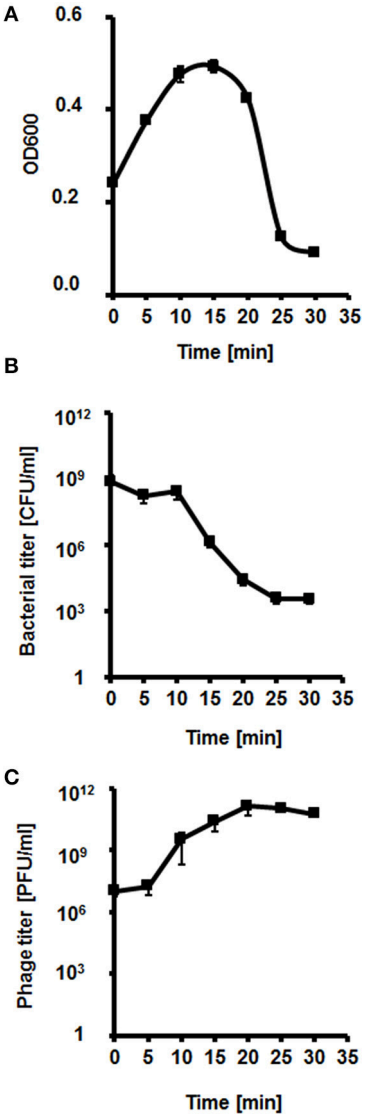

FIGURE 4 | Kinetics of lytic development of bacteriophage vB_EcoS-95 in *E. coli* MG1655 bacteria. Results are shown as **(A)** bacterial culture density measured at OD_{600}, **(B)** a number of surviving cells after the vB_EcoS-95 infection per 1 ml (CFU/ml), and **(C)** a number of phages per 1 ml (PFU/ml). Results are presented as mean values ± SD from three independent experiments. Please note that in some cases, the bars are smaller than sizes of symbols.

Assessment of Metabolic Activity of Biofilm Cells by Resazurin

Biofilms were prepared in the same way as described above. Briefly, after incubation with phage lysate (added to final titer of 10^2,10^4,10^5,10^7,10^{10} PFU/well), the liquid medium was removed. The biofilms were suspended in 1 ml of 1 × PBS. In the next step, resazurin was diluted in PBS buffer and added to each well to a final concentration of 6 μg/ml. Plates were gently shaken and incubated for 150 min at room temperature. The fluorescence of the produced resorufin ($\lambda_{exc} = 570$ and $\lambda_{em} = 590$ nm) was measured every 15 min in a plate reader (EnSpire Multimode Plate Reader). Results are presented in Fluorescent Units (FU).

Phage DNA Isolation

The phage lysate was treated with DNase I (1 U/μl; Thermo Fisher Scientific) and RNase A (5 ug/μl; Thermo Fisher Scientific) to degrade bacterial nucleic acids. To digest the exogenous DNA and RNA, the mixture was incubated for 30 min at 37°C. Then, DNase I and RNase A were inactivated by heating to 95°C and the genomic DNA of phage vB_EcoS-95 was isolated with a MasterPure™ Complete DNA and RNA Purification Kit (Epicenter). The DNA concentration was determined spectrophotometrically at 260 nm.

Sequencing of vB_EcoS-95 Genome

Phage genomes were sequenced in the Genomed company involving Next Generation Sequencing (NGS) and MiSeq (Illumina) genome sequencer. Assembly of the sequences was accomplished by the experts from the Genomed bioinformatics group. The quality of vB_EcoS-95 reads was controlled using FastQC (https://www.bioinformatics.babraham.ac.uk/projects/fastqc/), with following parameters: $-q = 20$ and $-m = 36$. The raw data (792,164 raw reads) were filtered using a Cutadapt program (http://code.google.com/p/cutadapt/) to remove the adapters, N bases, and low-quality reads. *De novo* assembly (99.97% of raw reads) was conducted using CLC Genomics Workbench. Finally, the assembly generated a single contig, corresponding to the entire phage vB-EcoS-95 genome with an average coverage of 2,629 x. Additionally, the obtained sequencing results, were analyzed for any errors in contigs assembly using following programs: BLAST (http://blast.ncbi.nlm.nih.gov/Blast.cgi), Progressive MAUVE (http://darlinglab.org/mauve/mauve.html) and Serial Cloner software (http://serialbasics.free.fr/Serial_Cloner.html).

Bioinformatic Analysis of vB_EcoS-95 Genome

The fully assembled genome of phage vB_EcoS-9 was annotated using myRAST software (Caldeira and Peabody, 2007) and UGENE bioinformatics software (http://ugene.net/) (Essoh et al., 2015). The identification of the putative protein-coding genes was based on the presence of a plausible ribosome binding site, and both the start and stop codons. Furthermore, genome annotation was verified and curated by BLAST analysis, HMMER software (http://www.hmmer.org/), Phobious webserver (http://phobius.binf.ku.dk/) and TMHMM program (http://www.cbs.dtu.dk/services/TMHMM/). Circular map of vB_EcoS-95 phage genome was generated using BLAST Ring Image Generator (BRIG) platform (https://sourceforge.net/projects/brig/) and CGView was used to perform GC skew and GC content analyses (Stothard and Wishart, 2005). A linear visualization of alignments of vB_EcoS-95 and pSf-1 (accession number KC710998) genomes was generated by Easyfig program (http://mjsull.github.io/Easyfig/files.html). The Neural Network Promoter Prediction NNPP method (http://www.

TABLE 5 | Appearance of *E. coli* MG1655 resistance to phage vB_EcoS-95 and to rifampicin.

Factor	Surviving bacteria (% of control) after 3 h of incubation	% of resistant bacteria among survivors
Phage (m.o.i. = 0.01)	<0.01	97.22 ± 2.40
Rifampicin (25 μg/ml)	3.80 ± 1.49	99.65 ± 0.60

fruitfly.org/seq_tools/promoter.html) was used to find phage-specific promoters in a DNA sequence. The positions of Rho-independent transcriptional terminators were determined using FindTerm tool (http://www.softberry.com/berry.phtml). Finally the genome sequence of the *E. coli* phage vB_EcoS-95 with annotations was deposited in the GenBank database under the accession number MF564201.

Construction of Phylogenetic Tree

Based on the predicted amino acid sequences, obtained from the genome analysis, phylogenetic analysis for the phage was made. To construct the phylogenetic tree, the sequence for the terminase large subunit (TerL), which is universally used genetic marker for the order *Caudovirales,* was selected. The terminase sequence of the vB_EcoS-95 phage was aligned with those of other reference bacteriophages within the order *Caudovirales*, which were collected from the NCBI database, using MUSCLE implanted in the MEGA (http://www.megasoftware.net/). A neighbor-joining phylogenetic tree for terminase large subunit amino acid sequences was constructed using the Poisson model. The robustness of the tree topology was assessed by bootstrap analyses based on 1,000 random resamplings.

Phage Protein Extraction

All protein analyses were carried out at the Institute of Bioorganic Chemistry of Polish Academy of Sciences. In the first step, the phage suspension in TM buffer (10 mM Tris-HCl, 10 mM $MgSO_4$) was treated with 4 volumes of ice-cold acetone and incubated at −20°C for 30 min. Then, the sample was centrifuged (13,000 × g, 5 min, 4°C) and the supernatant was discarded. The pellet was dried in laminar flow hood at room temperature. Then, the pellet was reconstituted in 50 mM ammonium bicarbonate in the initial sample volume. The total concentration of phage proteins was measured by using BCA colorimetric assay (Thermo Fisher Scientific).

In-Solution Tryptic Digestion

An aliquot of phage proteins was treated with 5.6 mM dithiothreitol (DTT) in 50 mM ammonium bicarbonate prior to heating at 95°C for 5 min. The sample was allowed to cool to room temperature and then was alkylated with 5 mM iodoacetamide. The mixture was incubated in the dark, at room temperature for 20 min. In the next step, phage proteins were digested with 0.2 μg of sequencing-grade trypsin (Promega). After overnight incubation at 37°C, the trypsin activity was suppressed by adding trifluoroacetic acid (TFA) to a final concentration of 0.1%. Then, the mixture was transferred to HPLC conical vial.

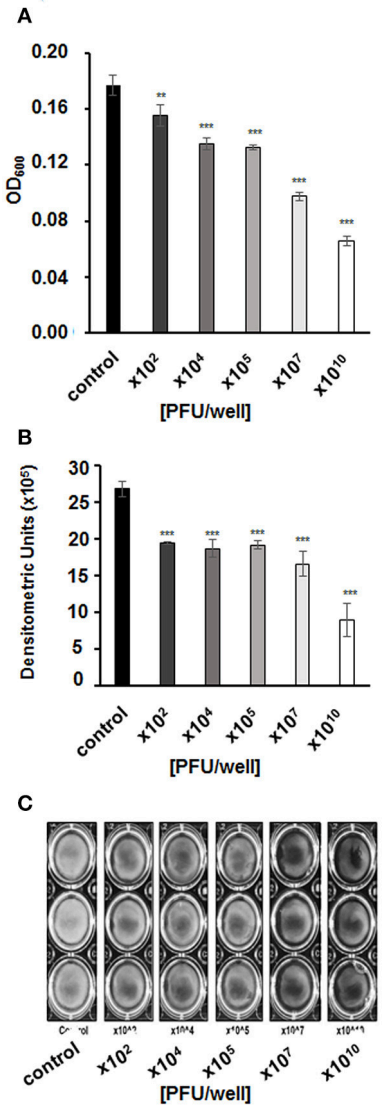

FIGURE 5 | Biofilm density after a 4-h incubation with vB_EcoS-95 phage added to final titer of 10^2,10^4,10^5,10^7, or 10^{10} PFU/well. Results were **(A)** estimated by measuring the optical density at wave length 600 nm of the resuspended biofilms or **(B)** quantified densitometrically using Quantity One program from bacterial biofilms pictures **(C)**. Results are presented as mean values ± SD from three independent experiments. Statistical analyses were performed by *t*-test. The significance of differences between control (no infection) and particular variants of phage infection are observed and marked by asterisks $P < 0.01$ (**) or $P < 0.001$ (***).

Mass Spectrometry Analysis of Proteins

The analysis of phage proteins was performed by using Dionex UltiMate 3000 RSLC nanoLC System connected to QExactive Orbitrap mass spectrometer (Thermo Fisher Scientific). Peptides derived from in-solution digestion were separated on a reverse phase Acclaim PepMap RSLC nanoViper C18 column (75 μm × 25 cm, 2 μm granulation) by using acetonitrile gradient (from 4 to 60%, in 0.1% formic acid) at 30°C and a flow rate of 300 nL/min (for 185 min). Mass spectra were acquired on the

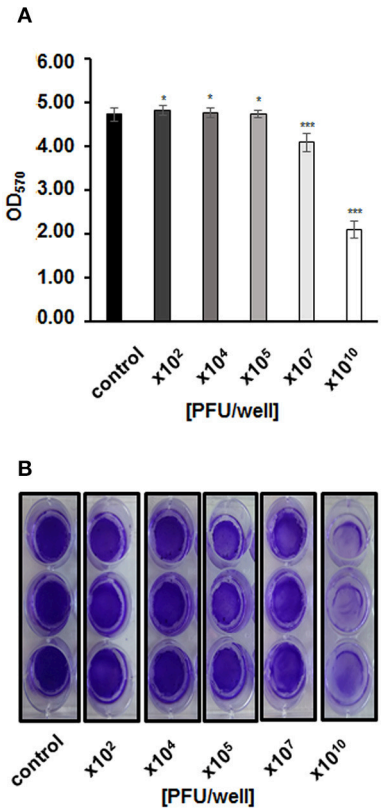

FIGURE 6 | Biofilm biomass after infection with phage vB_EcoS-95, estimated by crystal violet staining method and **(A)** presented as optical density values measured at wave length 570 nm or **(B)** photographed. Phage was added to final titer of 10^2,10^4,10^5,10^7, or 10^{10} PFU/well and incubated with bacteria in biofilm for 4 h. Error bars indicate standard deviations of triplicate experiments. Statistical analysis (*t*-test) was performed between control and analyzed variants of phage infection. Statistical differences are marked by asterisks $P < 0.05$ (*) or $P < 0.001$ (***).

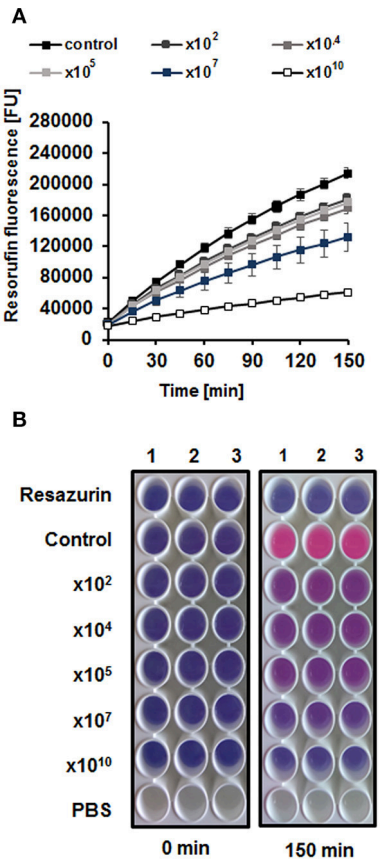

FIGURE 7 | Metabolic activity / viability of cells in the biofilm, incubated for 4 h with different numbers of vB_EcoS-95 virions (10^2,10^4,10^5,10^7, or 10^{10} PFU/well), determined by resazurin assay in which the non-fluorescent blue resazurin is converted to the fluorescent pink resorufin. Bacterial cells viability is presented as fluorescence emitted by resorufin **(A)** and pink color of the bacterial culture in the wells **(B)**. Results are presented as mean values ± SD from three independent experiments. Please note that in some cases, the bars are smaller than sizes of symbols.

Q Exactive in a data-dependent mode by using top 10 data-dependent MS/MS scans. Target value for the full scan MS spectra was set to 1e6 with a maximum injection time of 100 ms and a resolution of 70,000 at m/z 400. The 10 most intense ions charged two or more were selected with an isolation window of 2 Da and fragmented by higher energy collisional dissociation with NCE 27. The ion target value for MS/MS was set to 5e4 with a maximum injection time of 100 ms and a resolution of 17.500 at m/z 400.

Analysis of Proteomic Data

Identification of proteins was performed by using database created from translated open reading frames that have been found in the genome of phage vB_EcoS-9 (the precision of tolerance for peptide and fragment of ion masses was 10 ppm and 0.8 DA, respectively). All raw data obtained for each dataset were imported into Proteome Discoverer 1.4 software (Thermo Scientific). Protein was considered as positively identified if at least two peptide spectral matches per protein were found by Sequest search engine, and a peptide score reached the significance threshold FDR = 0.05.

Statistical Analyses

Statistical significances were determined using *t*-test**.** The significance of differences between compared experimental variants were marked by asterisks $P < 0.05$ (*), $P < 0.01$ (**) or $P < 0.001$ (***).

RESULTS

Isolation of vB-EcoS-95 and Host Range

The vB-EcoS-95 bacteriophage was isolated as a virus infecting *E. coli* from samples of urban sewage. The isolation procedure was based on the one-host enrichment method in which a raw urban sewage sample was mixed with a culture of *E. coli* MG1655 strain to obtain the lysate of vB-EcoS-95 bacteriophage, as described in the Material and Methods section.

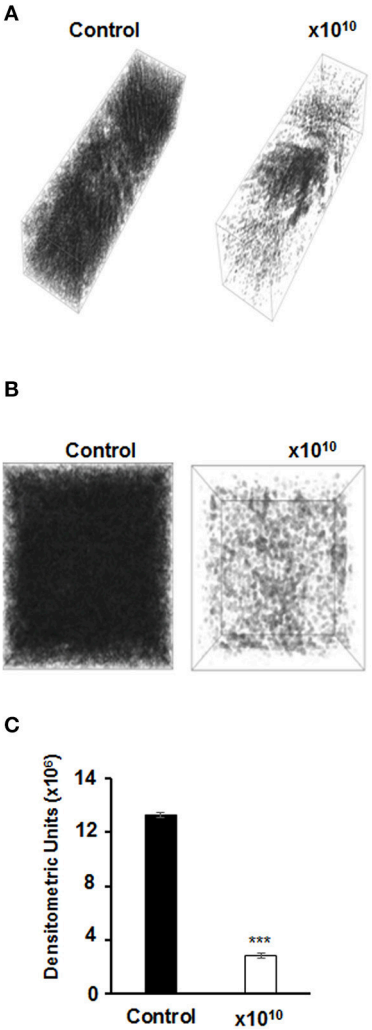

FIGURE 8 | Images of bacterial biofilms untreated and treated for 4 h with vB_EcoS-95 phage lysate added to a final titer of 10^{10}, performed by holographic 3D microscopy **(A,B)** and densitometry analysis of the obtained microscopic data **(C)**. Statistical analyses were performed by *t*-test. The significance of differences between compared experimental variants were marked by asterisks $P < 0.001$ (***).

We found that this bacteriophage is able to efficiently infect different *E. coli* strains, including those lysogenic with various lambdoid phages. However, Shiga toxin-producing *E. coli* serotype O157:H7 was resistant to vB-EcoS-95 (**Table 2**). Moreover, vB-EcoS-95 is not able to infect other bacterial species, including other species from *Enterobacteriaceae*, like *Shigella flexneri* or *Salmonella enterica* (**Table 2**).

Plaque and Virion Morphology

Bacteriophage vB-EcoS-95 forms clear plaques (diameter 2.5 ± 0.5 mm), with a halo, on *E. coli* lawn (**Figure 1**). Electron microscopic studies indicated that the virion of this phage consists of a head (diameter 53 nm), flexible, non-contractile tail (127 nm length, 10 nm width), and 3 tail fibers (about 39 nm length, 2.5 nm width). Therefore, taking into account the morphological characteristics of phage vB-EcoS-95, we conclude that this bacterial virus belongs to the *Siphoviridae* family (**Table 3**).

Sensitivity of Virions to Physical and Chemical Factors

We have tested sensitivity of vB-EcoS-95 virions to physical and chemical factors. The results, presented in **Table 4**, indicate that this phage is particularly sensitive to high temperature, low pH, the presence of SDS (ionic detergent) and organic solvents, like ethanol and acetone. It is, however, resistant to freezing, osmotic shock, and chloroform (**Table 4**).

Kinetics of Adsorption on Host Cells and Intracellular Development

We have determined that bacteriophage vB-EcoS-95 adsorbs rapidly on *E. coli* cells, with 50% phages already adsorbed within 2 min after mixing phage lysate with bacterial culture (**Figure 2**).

Intracellular phage development appeared extremely rapid, with the eclipse and latent periods 3 min and 4 min, respectively (**Figure 3**). The average bust size in *E. coli* grown at 37°C in LB medium has been estimated to be 115 PFU (plaque forming units) per cell, indicating efficient lytic development of the phage (**Figure 3**).

Lysis Profile Assay and Development of Bacterial Resistance

We have analyzed the lysis profile of phage vB-EcoS-95, taking account the bacterial density after addition of phage particles, the number of surviving host bacteria after phage infection, and the increase of the phage titer during this process (**Figure 4**). We observed that the lysis of host culture was very rapid and complete within 20–25 min. Interestingly, the emergence of resistance of *E. coli* bacteria against phage vB-EcoS-95 was similar to that against antibiotic rifampicin (**Table 5**). However, the percentage of surviving host cells after phage infection was considerably lower than that observed in antibiotic-treated bacteria (**Table 5**).

Ability of vB-EcoS-95 to Destroy Bacterial Biofims

We asked whether vB-EcoS-95 is able to destroy biofilms formed by *E. coli* cells. Thus, we have tested biofilm density (by measuring the optical density at λ600 nm of the resuspended biofilm), biofilm biomass (using the crystal violet assay), and metabolic activity of cells in the biofilm (using the resazurin assay) after administration of different numbers of vB-EcoS-95 virions. In all these tests, we have observed deleterious effects of the tested bacteriophage on bacterial biofilm: its density (**Figure 5**), biomass (**Figure 6**), and metabolic activity (**Figure 7**). In all tests, the effects of the bacteriophage on the biofilm depended on number of virions used in the experiments, with the most pronounced effects at the highest number of administered virions. We are aware that the results obtained in various kinds of experiments differ in details. This is perhaps due to various sensitivities of different methods. Nevertheless, the general trend

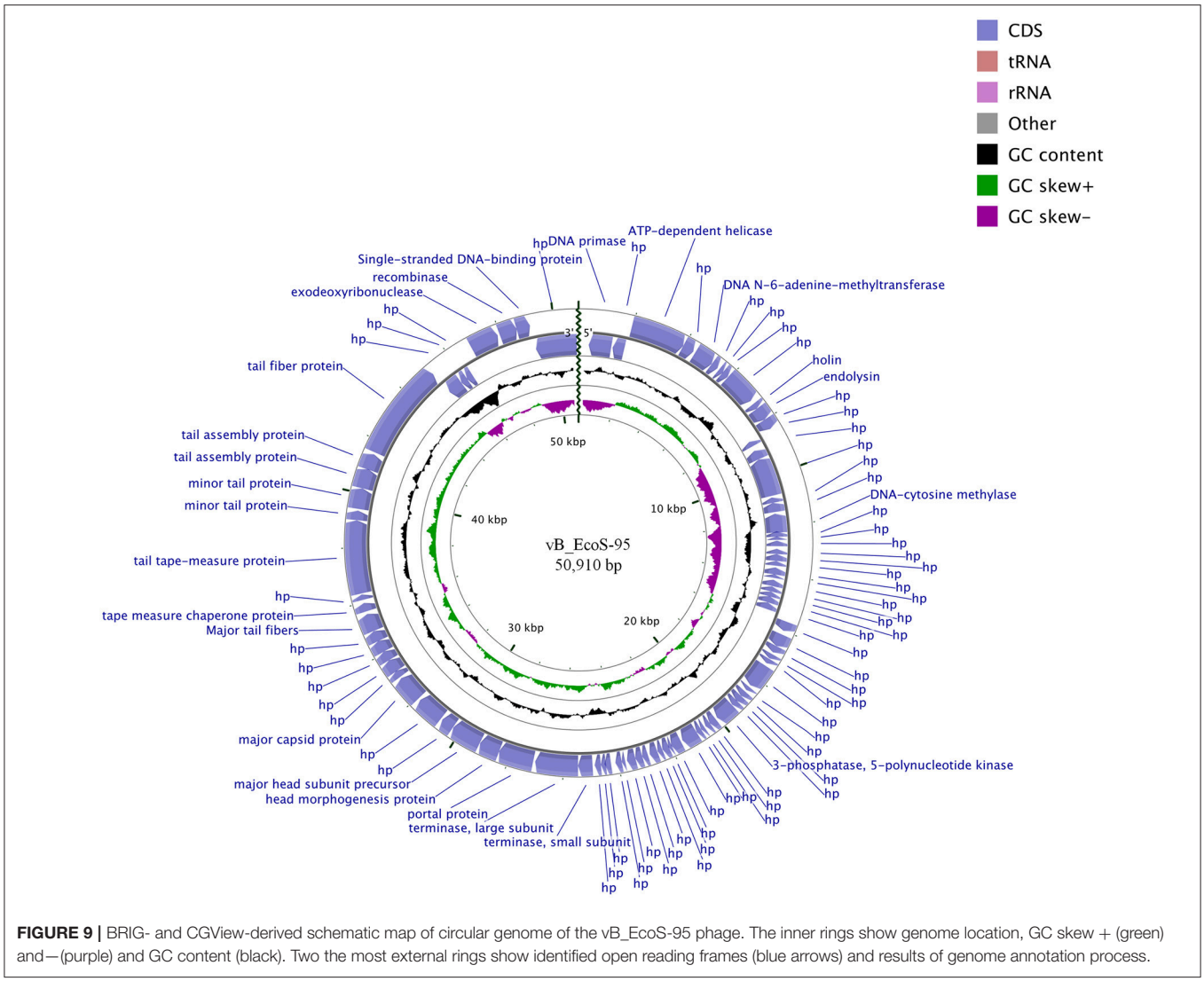

FIGURE 9 | BRIG- and CGView-derived schematic map of circular genome of the vB_EcoS-95 phage. The inner rings show genome location, GC skew + (green) and−(purple) and GC content (black). Two the most external rings show identified open reading frames (blue arrows) and results of genome annotation process.

of the effects of phage vB-EcoS-95 on the bacterial biofilm is the same in all performed tests.

The effects of vB-EcoS-95 on the biofilm destruction have been confirmed in experiments with holographic 3D microscopy. Significant lowering of the biofilm density could be observed after addition of phage vB-EcoS-95 lysate to *E. coli*-formed biofilm (**Figure 8**).

Characterization of the vB-EcoS-95 Genome

The whole genome of vB-EcoS-95 has been sequenced. It consists of 50,910 bp and is deposited in GenBank (accession number: MF564201). The map of this genome is presented in **Figure 9**. Analysis of the vB-EcoS-95 genome indicated that it is a double-stranded DNA, with a 45% total G+C content. This analysis has shown 45 putative promoters, 30 putative transcription terminators and 89 open reading frames (ORFs). Among all identified coding regions, only 24 ORFs were predicted to be functional genes. As showed in **Figure 10**, the large terminase subunit of vB-EcoS-95 bacteriophage presents the highest identity with large terminase subunit of other virulent *Siphoviridae* phage, pSf-1, that infects *Shigella flexneri* (Jun et al., 2013). Sequence similarity searches revealed that vB-EcoS-95 presents ∼74% nucleotide sequence identity with phage pSf-1. Besides, these two phages are highly similar in gene inventory. As indicated in **Figure 11**, both phage genomes contain blocks of genes in which genes are clustered by function and encode products that operate in similar way, such as proteins responsible for DNA replication, modification, recombination etc. Interestingly, in both cases, genes coding for products participating in DNA packaging and morphogenesis are located at the middle and the end of the genome.

Mass-Spectrometric Identification of Phage Proteins

The proteins of phage vB-EcoS-95 detected by MS are listed in **Table 6** with their observed molecular mass, the number of identified peptides in each protein and the corresponding

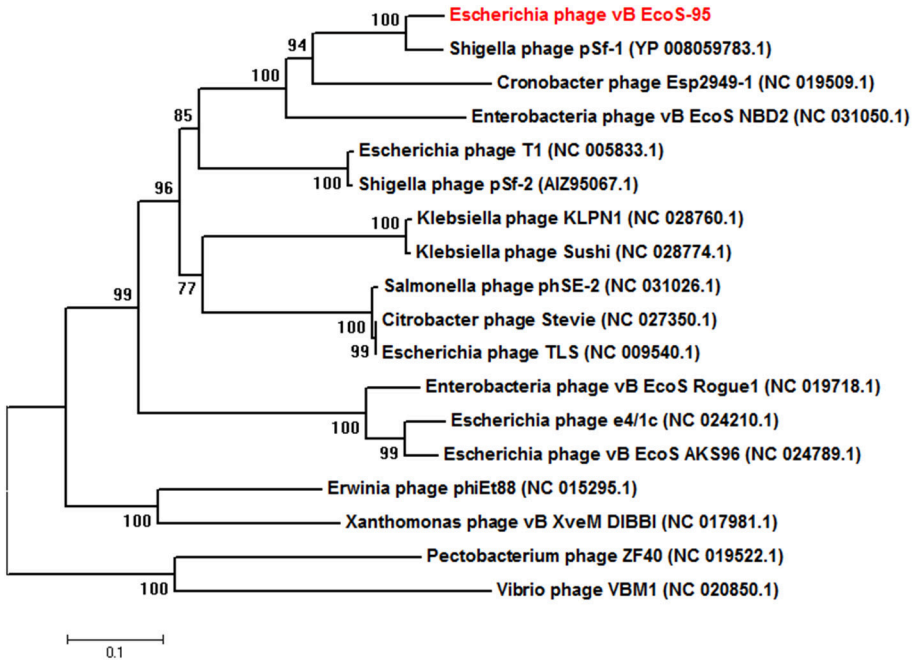

FIGURE 10 | Neighbor-joining phylogenetic tree of the terminase large subunit (TerL) amino acid sequences showing the phylogenetic position of phage vB_EcoS-95 (in red color). The reference sequences were collected from the NCBI database. The tree was constructed using MEGA 7 after performing a sequence alignment using MUSCLE. Bootstrap values, calculated based on 1,000 resamplings, are shown at the nodes.

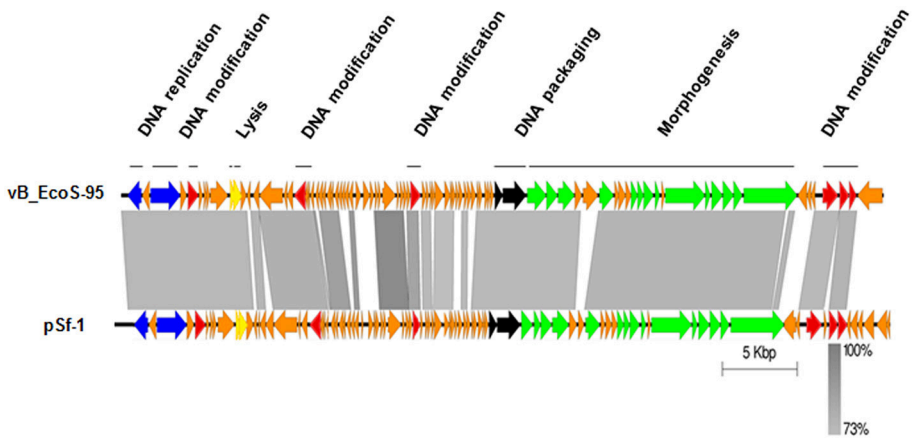

FIGURE 11 | Easyfig output image of the genomic comparison between phage vB_EcoS-95 and the most related phage pSf-1. Phage genomes are presented by linear visualization with coding regions shown as arrows. Selected open reading frames are colored in relation to their functions. The percentage of sequence similarity is indicated by the intensity of the gray color. Vertical blocks between analyzed sequences indicate regions with at least 73% of similarity.

protein sequence coverage. For all proteins, the identification was based on fragmentation patterns of unique peptides. The data analysis allowed us to assign 16 vB-EcoS-95 phage proteins to annotated open reading frames (ORFs). In this manner, protein annotation of 10 *in silico*-predicted structural proteins was confirmed. In addition, 6 gene products having little or no similarity to known phage proteins could be classified as proteins of unknown function. The identification analyses of the proteins can be verified in the **Supplementary Tables** of data available with the online version of this paper (**Supplementary Material** – MS identification data).

DISCUSSION

A newly isolated bacteriophage, vB-EcoS-95, infecting *E. coli* strains, has been characterized. It infects various *E. coli* strains, including those lysogenized with different lambdoid phages and

TABLE 6 | Mass spectrometry analysis of bacteriophage vB_EcoS-95 virion.

Detected protein	Predicted function	Molecular mass (kDa)	Number of peptides	Sequence coverage (%)	Protein Score
vB_EcoS-95_0064	Portal protein	48.5	12	40.7	127.57
vB_EcoS-95_0065	Head morphogenesis protein	28.7	12	43.43	57.75
vB_EcoS-95_0066	Major head subunit precursor	40.5	5	20.49	1.73
vB_EcoS-95_0067	Unknown protein	17.1	7	55.35	83.22
vB_EcoS-95_0068	Unknown protein	34.9	12	46.29	693.13
vB_EcoS-95_0069	Major capsid protein	36.0	17	59.44	815.89
vB_EcoS-95_0073	Unknown protein	16.3	2	13.61	3.83
vB_EcoS-95_0075	Major tail fibers	24.4	8	38.18	195.94
vB_EcoS-95_0078	Tail tape-measure protein	98.1	56	53.30	1479.50
vB_EcoS-95_0079	Minor tail protein	12.9	2	24.14	15.08
vB_EcoS-95_0080	Minor tail protein	28.4	5	25.69	3.41
vB_EcoS-95_0082	Tail assembly protein	20.7	2	8.59	99.97
vB_EcoS-95_0083	Tail fiber protein	132.4	44	42.70	1095.31
vB_EcoS-95_0084	Unknown protein	22.0	2	13.24	24.36
vB_EcoS-95_0085	Unknown protein	10.0	3	55.43	9.69
vB_EcoS-95_0090	Unknown protein	60.1	22	43.65	910.97

clinical isolates, however, *E. coli* O157:H7 bacteria are resistant to this phage.

The most intriguing property of this phage is its extremely rapid development in *E. coli* cells. Under standard laboratory conditions, i.e., growth of host bacteria at 37°C in LB medium, the latent period was as short as 4 min, and the lysis of host culture was complete within 20-25 min. This was accompanied with relative high average burst size of 115 pfu/cell. For comparison, one-step growth experiment of phage pSf-1 (the most closely related phage to vB-EcoS-95, reported to date; however, note that the level of similarity of pSf-1 and vB-EcoS-95 genomes, 74%, is still moderate) and other closely related phage pSf-2 showed that the latent period was longer (10 and 30 min, respectively) and burst size was lower (around 87 and 16 PFU/cell, respectively) (Jun et al., 2013, 2016). Another interesting feature of this phage is its ability to destroy bacterial biofilm which was demonstrated by using various methods, including crystal violet and resazurin assays, as well as holographic 3D microscopy.

Genome of vB-EcoS-95 revealed 74% similarity to previously described phage pSf-1, infecting Shigella *flexneri* (Jun et al., 2013). However, unlike that phage, vB-EcoS-95 does not infect *S. flexneri*. In fact, only some *E. coli* strains could be effectively infected by the newly isolated phage. Moreover, contrary to pSf-1, phage vB-EcoS-95 reveals an extremely short latent period (about 4 min) after infection of the *E. coli* host (see above). It is unclear what causes such a rapid lytic development of vB-EcoS-95. Genome analysis indicated that this phage does not encode its own DNA polymerase, therefore, it is unlikely that extremely quick phage DNA synthesis is responsible for this phenomenon, though one cannot exclude that initiation of this process is particularly efficient. On the other hand, it appears that vB-EcoS-95 encodes an untypical lytic protein (**Supplementary Material**—genome annotation) which might potentially contribute to rapid lysis of the host cell.

All the properties of vB-EcoS-95 make it a potentially attractive phage in further studies on its use in biotechnological applications and/or as a factor for food protection or therapeutic agent (in phage therapy). Particularly, very rapid lytic development, accompanied with a relatively high burst size indicate that this phage can destroy host cells very rapidly, which is beneficial in both phage therapy and protection of food or various materials against bacterial colonization. Effective destruction of bacterial biofilm may be of particular importance, as formation of such a structure by bacteria protects them against various antibacterial agents, including antibiotics. On the other hand, vB-EcoS-95 effectively infects only some *E. coli* strains, including some clinical isolates, but excluding *E. coli* O157:H7. This might be a potential limitation in the medical use of vB-EcoS-95, though one must note that specificity of phages to certain strains is a commonly occurring feature of these viruses. The vB-EcoS-95 phage survives well at relatively low temperatures, but <50% virions could retain infectivity at 40°C. This might suggest a potential limitation in phage therapy, as bacterial infections usually cause fever in patients. On the other hand, in phage therapy procedures, a large excess of bacteriophages is usually applied, therefore, such a survival rate should not significantly influence efficacy of the therapy.

Finally, although appearance of bacteria resistant to vB-EcoS-95 was as frequent as appearance of bacteria resistant to antibiotic, survival of *E. coli* cells after administration of the phage was significantly lower than that after administration of rifampicin. This suggest an advantage of the use of vB-EcoS-95 in phage therapy or protection of food or various materials.

In summary, the newly isolated vB-EcoS-95 phage, infecting *E. coli* cells, reveals various specific features, particularly, rapid development and cell lysis, ability to destroy bacterial biofilm, and untypical lytic protein, which suggest that further studies on its use in biotechnological and/or medical applications are desired.

DATA AVAILABILITY STATEMENT

The genome sequence is available at GenBank (accession number: MF564201). Raw data are available from authors on request.

AUTHOR CONTRIBUTIONS

GT performed most of the experiments on characterization of bacteriophage development and its ability to destroy bacterial biofilms, participated in data analysis and helped to draft methodology chapter. SB designed the experimental work, helped to perform some of the experiments and to analyse obtained data. BN-F participated in the planning of experiments and genomic analyses, helped in data analysis and drafting the manuscript. TG analyzed sequence of phage genome. AJ-K isolated vB_EcoS-95 phage from urban sewage sample and participated in genomic analyses. AN and AD performed a part of experimental work on phage biology. MR performed electron microscopic analyses of the phage. GW participated in analysis of the results and drafting the manuscript. AW was the principal investigator of the project, supervised the work, and participated in drafting the manuscript.

FUNDING

This work was supported by National Science Center (Poland) (project grant no. 2015/17/B/NZ9/01724).

ACKNOWLEDGMENTS

We would like to thank the Perlan Technologies company (Poland) for providing the Tomocube holographic 3D microscope.

SUPPLEMENTARY MATERIAL

The Supplementary Material for this article can be found online at: https://www.frontiersin.org/articles/10.3389/fmicb.2018.03326/full#supplementary-material

Table S1 | Bacteriophage vB_EcoM-95 genome annotations.

Table S2 | Mass spectrometry analysis of bacteriophage vB_EcoS-95 virion.

REFERENCES

Appleyard, R. K. (1954). Segregation of new lysogenic types during growth of a doubly lysogenic strain derived from *Escherichia coli* K12. *Genetics* 39, 440–452.

Bachmann, B. J. (1972). Pedigrees of some mutant strains of *Escherichia coli* K-12. *Bacteriol. Rev.* 36, 525–557.

Beutin, L., Montenegro, M. A., and Orskov, I. (1989). Close association of verotoxin (Shiga-like toxin) production with enterohemolysin production in strains of *Escherichia coli*. *J. Clin. Microbiol.* 27, 2559–2564.

Bloch, S., Nejman-Falenczyk, J., Lo's, J. M., Baranska, S., Lepek, K., Felczykowska, A., et al. (2013). Genes from the *exo-xis* region of λ and Shiga toxin-converting bacteriophages influence lysogenization and prophage induction. *Arch. Microbiol.*. 195, 693–703. doi: 10.1007/s00203-013-0920-8

Caldeira, J. C., and Peabody, D. S. (2007). Stability and assembly *in vitro* of bacteriophage PP7 virus-like particles. *J. Nanobiotechnol.* 5:10. doi: 10.1186/1477-3155-5-10

Casadaban, M. J., and Cohen, S. N. (1980). Analysis of gene control signals by DNA fusion and cloning in *Escherichia coli*. *J. Mol. Biol.* 138, 179–207.

Casjens, S. R., and Hendrix, R. W. (2015). Bacteriophage lambda: early pioneer and still relevant. *Virology* 479–480, 310–330. doi: 10.1016/j.virol.2015.02.010

Clokie, M. R. J., Millard, A. D., Letarov, A. V., and Heaphy, S. (2011). Phages in nature. *Bacteriophage* 1, 31–45. doi: 10.4161/bact.1.1.14942

Czajkowski, R., Ozymko, Z., De Jager, V., Siwinska, J., Smolarska, A., Ossowicki, A., et al. (2015). Genomic, proteomic and morphological characterization of two novel broad host lytic bacteriophages ΦPD10.3 and ΦPD23.1 infecting pectinolytic *Pectobacterium.* spp. and *Dickeya.* spp. *PLoS ONE* 10:e0119812. doi: 10.1371/journal.pone.0119812

Domingo-Calap, P., and Delgado-Martínez, J. (2018). Bacteriophages: protagonists of a post-antibiotic era. *Antibiotics* 7:66. doi: 10.3390/antibiotics7030066

Domingo-Calap, P., Georgel, P., and Bahram, S. (2016). Back to the future: bacteriophages as promising therapeutic tools. *HLA* 87, 133–140. doi: 10.1111/tan.12742

Essoh, C., Latino, L., Midoux, C., Blouin, Y., Loukou, G., Nguetta, S. P., et al. (2015). Investigation of a large collection of *Pseudomonas aeruginosa* bacteriophages collected from a single environmental source in Abidjan, Côte d'Ivoire. *PLoS ONE* 10:e0130548. doi: 10.1371/journal.pone.0130548

Gorski, A., Jonczyk-Matysiak, E., Miedzybrodzki, R., Weber-Dabrowska, B., Lusiak-Szelachowska, M., Baginska, N., et al. (2018a). Phage therapy: beyond antibacterial action. *Front. Med.* 5:146. doi: 10.3389/fmed.2018.00146

Górski, A., Miedzybrodzki, R., Łobocka, M., Głowacka-Rutkowska, A., Bednarek, A., Borysowski, J., et al. (2018b). Phage therapy: what have we learned? *Viruses* 10:288. doi: 10.3390/v10060288

Gough, J. A., and Murray, N. E. (1983). Sequence diversity among related genes for recognition of specific targets in DNA molecules. *J. Mol. Biol.* 166, 1–19. doi: 10.1016/S0022-2836(83)80047-3

Grant, S. G., Jessee, J., Bloom, F. R., and Hanahan, D. (1990). Differential plasmid rescue from transgenic mouse DNAs into *Escherichia coli* methylation-restriction mutants. *Proc. Natl. Acad. Sci. U.S.A.* 87:4645–4649.

Griffin, P. M., Ostroff, S. M., Tauxe, R. V., Greene, K. D., Wells, J. G., Lewis, J. H., et al. (1988). Illnesses associated with *Escherichia coli* O157:H7 infections. A broad clinical spectrum. *Ann. Intern Med.* 109, 705–712. doi: 10.7326/0003-4819-109-9-705

Gutiérrez, D., Rodríguez-Rubio, L., Martínez, B., Rodríguez, A., and García, P. (2016). Bacteriophages as weapons against bacterial biofilms in the food industry. *Front. Microbiol.* 7:825. doi: 10.3389/fmicb.2016.00825

Hatful, G. F. (2015). Dark matter of the biosphere: the amazing world of bacteriophage diversity. *J. Virol.* 89, 8107–8110. doi: 10.1128/JVI.01340-15

Jensen, K. F. (1993). The *Escherichia coli* K-12 wild types W3110 and MG1655 have an *rph* frameshift mutation that leads to pyrimidine

starvation due to low *pyrE* expression levels. *J. Bact*. 175, 3401–3407. doi: 10.1128/jb.175.11.3401-3407.1993

Jun, J. W., Kim, H. J., Yun, S. K., Chai, J. Y., Lee, B. C., and Park, S. C. (2016). Isolation and comparative genomic analysis of T1-Like *Shigella* bacteriophage pSf-2. *Curr. Microbiol.* 72, 235–241. doi: 10.1007/s00284-015-0935-2.

Jun, J. W., Kim, J. H., Shin, S. P., Han, J. E., Chai, J. Y., and Park, S. C. (2013). Characterization and complete genome sequence of the *Shigella* bacteriophage pSf-1. *Res. Microbiol.* 164, 979–986. doi: 10.1016/j.resmic.2013.08.007

Jurczak-Kurek, A., Gasior, T., Nejman- Falenczyk, B., Bloch, S., Dydecka, A., Topka, G., et al. (2016). Biodiversity of bacteriophages: morphological and biological properties of a large group of phages isolated from urban sewage. *Sci. Rep*. 6:34338. doi: 10.1038/srep34338

Kakasis, A., and Panitsa, G. (2019). Bacteriophage therapy as an alternative treatment for human infections. A comprehensive review. *Int. J Antimicrob. Agents* 53, 16–21. doi: 10.1016/j.ijantimicag.2018.09.004

Krisch, H. M., and Comeau, A. M. (2008). The immense journey of bacteriophage T4 - from d'Hérelle to Delbrück and then to Darwin and beyond. *Res. Microbiol.* 159, 314–324. doi: 10.1016/j.resmic.2008.04.014

Kutter, E. M., Kuhl, S. J., and Abedon, S. (2015). T. Re-establishing a place for phage therapy in western medicine. *Future Microbiol.* 10, 685–688. doi: 10.2217/fmb.15.28

Onodera, K. (2010). Molecular biology and biotechnology of bacteriophage. *Adv. Biochem. Eng. Biotechnol.* 119, 17–43. doi: 10.1007/10_2008_46

Patterson, T. A., and Dean, M. (1987). Preparation of high titer lambda phage lysates. *Nucleic Acids Res.* 15:6298.

Perna, N. T., Plunkett, G., Burland, V., Mau, B., Glasner, J. D., Rose, D. J., et al. (2001). Genome sequence of enterohaemorrhagic *Escherichia coli* O157:H7. *Nature* 409, 529–533. doi: 10.1038/35054089

Sambrook, J., and Russell, D. W. (2001). *Molecular Cloning: A Laboratory Manual, 3rd Edn*. New York, NY: Cold Spring Harbor Laboratory Press.

Stothard, P., and Wishart, D. S. (2005). Circular genome visualization and exploration using CGView. *Bioinformatics* 21, 537–539. doi: 10.1093/bioinformatics/bti054

Sung, B. H., Lee, C. H., Yu, B. J., Lee, J. H., Lee, J. Y., Kim, M. S., et al. (2006). Development of a biofilm production-deficient *Escherichia coli* strain as a host for biotechnological applications. *Appl. Environ. Microbiol.* 72, 3336–3342. doi: 10.1128/AEM.72.5.3336-3342.2006

Twort, F. W. (1915). An investigation on the nature of ultra-microscopic viruses. *Lancet* 186, 1241–1243. doi: 10.1016/S0140-6736(01)20383-3

Vianney, A., G., Jubelin, S., Renault, C., Dorel, P., Lejeune, and Lazzaroni, J. C. (2005). *Escherichia coli tol* and *rcs* genes participate in the complex network affecting curli synthesis. *Microbiology* 151, 2487–2497. doi: 10.1099/mic.0.27913-0

Wegrzyn, A., and Wegrzyn, G. (2015). Bacteriophages: 100 years of the history of studies on model viruses in molecular biology. *Edorium J. Mol. Biol.* 1, 6–9. doi: 10.5348/M11-2015-2-ED-2

Wegrzyn, G., and Wegrzyn, A. (2005). Genetic switches during bacteriophage lambda development. *Prog. Nucleic Acid Res. Mol. Biol.* 79, 1–48. doi: 10.1016/S0079-6603(04)79001-7

Weitz, J. S., Poisot, T., Meyer, J., R., Flores, C., O., Valverde, S., Sullivan, M. B., et al. (2012). Phage-bacteria infection networks. *Trends Microbiol.* 21, 82–91. doi: 10.1016/j.tim.2012.11.003

Conflict of Interest Statement: The authors declare that the research was conducted in the absence of any commercial or financial relationships that could be construed as a potential conflict of interest.

frontiers in Microbiology

ORIGINAL RESEARCH
published: 11 January 2019
doi: 10.3389/fmicb.2018.03288

Host Specificity of the *Dickeya* Bacteriophage PP35 Is Directed by a Tail Spike Interaction With Bacterial *O*-Antigen, Enabling the Infection of Alternative Non-pathogenic Bacterial Host

*Anastasia P. Kabanova[1,2], Mikhail M. Shneider[1], Aleksei A. Korzhenkov[3], Eugenia N. Bugaeva[2], Kirill K. Miroshnikov[4], Evelina L. Zdorovenko[5], Eugene E. Kulikov[4], Stepan V. Toschakov[3,4], Alexander N. Ignatov[2], Yuriy A. Knirel[5] and Konstantin A. Miroshnikov[1,2]**

[1] Shemyakin-Ovchinnikov Institute of Bioorganic Chemistry, Russian Academy of Sciences, Moscow, Russia, [2] Research Center "PhytoEngineering" Ltd., Rogachevo, Russia, [3] Immanuel Kant Baltic Federal University, Kaliningrad, Russia, [4] Winogradsky Institute of Microbiology, Federal Research Center "Fundamentals of Biotechnology", Russian Academy of Sciences, Moscow, Russia, [5] Zelinsky Institute of Organic Chemistry, Russian Academy of Sciences, Moscow, Russia

OPEN ACCESS

Edited by:
Robert Czajkowski,
University of Gdańsk, Poland

Reviewed by:
Adelaide Almeida,
University of Aveiro, Portugal
Leticia Veronica Bentancor,
Universidad Nacional de Quilmes (UNQ), Argentina

***Correspondence:**
Konstantin A. Miroshnikov
kmi@ibch.ru

Specialty section:
This article was submitted to Virology, a section of the journal Frontiers in Microbiology

Received: 15 October 2018
Accepted: 18 December 2018
Published: 11 January 2019

Citation:
Kabanova AP, Shneider MM, Korzhenkov AA, Bugaeva EN, Miroshnikov KK, Zdorovenko EL, Kulikov EE, Toschakov SV, Ignatov AN, Knirel YA and Miroshnikov KA (2019) Host Specificity of the Dickeya Bacteriophage PP35 Is Directed by a Tail Spike Interaction With Bacterial O-Antigen, Enabling the Infection of Alternative Non-pathogenic Bacterial Host. Front. Microbiol. 9:3288. doi: 10.3389/fmicb.2018.03288

Dickeya solani is a recently emerged virulent bacterial potato pathogen that poses a major threat to world agriculture. Because of increasing antibiotic resistance and growing limitations in antibiotic use, alternative antibacterials such as bacteriophages are being developed. *Myoviridae* bacteriophages recently re-ranked as a separate *Ackermannviridae* family, such as phage PP35 described in this work, are the attractive candidates for this bacterial biocontrol. PP35 has a very specific host range due to the presence of tail spike protein PP35 gp156, which can depolymerize the *O*-polysaccharide (OPS) of *D. solani*. The *D. solani* OPS structure, →2)-β-D-6-deoxy-D-altrose-(1→, is so far unique among soft-rot *Pectobacteriaceae*, though it may exist in non-virulent environmental *Enterobacteriaceae*. The phage tail spike depolymerase degrades the shielding polysaccharide, and launches the cell infection process. We hypothesize that non-pathogenic commensal bacteria may maintain the population of the phage in soil environment.

Keywords: bacteriophage, *Dickeya solani*, *Lelliottia*, genomics, tail spike protein, polysaccharide, depolymerase

INTRODUCTION

Soft-rot *Pectobacteriaceae* (SRP) include phytopathogenic bacterial species from the genera *Pectobacterium* and *Dickeya* that cause economic losses in potato crops, as well as other vegetables and ornamental plants worldwide (Pérombelon, 2002). *Dickeya* spp. were mostly associated with plant diseases in tropical climates (Toth et al., 2011). A new virulent species named *D. solani* emerged in the early 2010s (Laurila et al., 2010; van der Wolf et al., 2014) and rapidly spread throughout Europe, including Russia (Ignatov et al., 2014). No potato cultivars is resistant to *D. solani*, and the spread of the disease is mostly contained by quarantining and controlling seed

stocks (Mansfield et al., 2012). Treating seeds and harvested tubers with bacteriophages – viruses specific to particular bacterial pathogens – is considered a promising and environmentally safe strategy to protect plants and harvested crops from bacterial diseases (Frampton et al., 2012). A number of isolated bacteriophages infect *D. solani* (Adriaenssens et al., 2012b; Day et al., 2017) and some can also infect other *Dickeya* spp. (Czajkowski et al., 2014b, 2015). They have been thoroughly characterized and used to protect and control soft rot caused by *D. solani*. The primary goal of the present study was an investigation of the *D. solani* – specific bacteriophage newly isolated in Russia and the molecular details of its interaction with the bacterial host.

MATERIALS AND METHODS

Isolation and Purification of Phage PP35

Bacteriophage PP35 was isolated in 2014 from sewage water near an outbreak of soft rot in harvested potatoes caused by *D. solani* (Moscow region, Russia). Phage was propagated on *D. solani* strain F012 in LB at 26°C following a published general protocol (Clokie and Kropinski, 2009). After chloroform treatment, removal of cell debris by centrifugation (8000 *g*, 20 min), filtration through a 0.22-μm-pore size membrane filter (Millipore), and treatment with DNase I (0.5 mg/mL, 60 min), the phage was purified by ultracentrifugation (22,000 *g*, 120 min, 4°C, Beckman SW28 rotor) in a CsCl step gradient with densities of 0.5 to 1.7 g/mL. The resulting suspension of PP35 was dialyzed overnight against phage buffer (10 mM Tris–HCl, pH 7.4, 10 mM $MgSO_4$) to remove CsCl. Purified phage was stored at 4°C in phage buffer.

Host Range and General Characterization of Phage PP35

The host range of phage PP35 was tested by standard plaque assays and by spotting phage suspensions (10^6 pfu/ml) onto a bacterial lawn. Bacterial strains listed in **Supplementary Table S1** were grown on LB agar at 26°C. In adsorption experiments, the host strains F012 or F154 were grown to an $OD_{600} \sim 0.4$ and infected with PP35 at a multiplicity of infection of 0.1. Every 3 min after infection, 100 μl aliquots were taken and transferred into 800 μl LB medium supplied with 50 μl chloroform. After bacterial lysis the mixtures were centrifuged and the supernatant was titrated to determine the amount of non-adsorbed or reversibly adsorbed phages. One-step-growth assays were performed according to Adriaenssens et al. (2012b). To assay a lytic activity of phage PP35, an exponentially growing culture of F012 or F154 (10^6 cfu/ml) was mixed with phage PP35 (MOI of 0.1). The mixture was then incubated with shaking at 26°C. Every 10 min, aliquots were taken, and the appropriate dilutions were spread on LB agar plates, and incubated overnight at 26°C. The next day, colonies were counted. Phage stability was studied by incubating a 10^7 pfu/ml phage suspension at different temperatures or in a range of buffer solutions (20 mM Tris–HCl/20 mM Na citrate/20 mM Na phosphate) adjusted with NaOH to pH range 4–9. All experiments were performed independently 3–4 times, and the results were averaged. Plots were generated with Microsoft Excel.

TABLE 1 | Genome assembly properties.

Genome	Contig (scaffold) count	Assembly length, bp	Mean coverage
PP35 (phage)	1 (1)	152 048	245
Dickeya F012	27 (25)	4 879 104	52.3
Lelliottia F154	23 (23)	4 457 928	54.3

Electron Microscopy

Purified phage particles were applied to grids and stained with 1% uranyl acetate aqueous solution (Ackermann, 2009). The specimens were observed in a JEOL JEM-CX100 electron microscope at 100 kV accelerating voltage.

Genome Sequencing and Annotation

Bacterial and phage DNA was extracted using the phenol-chloroform method and fragmented with a Bioruptor sonicator (Diagenode). Paired-end libraries were constructed using Nebnext Ultra DNA library prep kit (New England Biolabs) and sequenced on the Illumina MiSeq^{TM} platform (Illumina) using paired 150 bp reads. After filtering with CLC Genomics Workbench 8.5 (Qiagen), overlapping paired-end library reads were merged with the SeqPrep tool[1]. Reads from bacteriophage PP35 were assembled in CLC Genomic workbench v. 7.5; reads from F012 and F154 bacterial strains were assembled using SPAdes 3.6.1 (Bankevich et al., 2012). Contig count, assembly length and mean coverage are displayed in **Table 1**.

Bacterial genomes were annotated with the RAST automated pipeline[2] (Aziz et al., 2008). Phage genome was annotated by first calling ORFs with GeneMarkS (Besemer et al., 2001). ORF functions were predicted using Psi-BLAST alignment against the NCBI nr database (Altschul et al., 1997) and Pfam domain prediction using HMMER (Finn et al., 2011). tRNA coding regions were identified with tRNAscan-SE (Schattner et al., 2005), search of other non-coding RNA was performed using SEED. Putative phage promoters were predicted by PHIRE (Lavigne et al., 2004) and phiSITE (Klucar et al., 2009). CRISPR arrays were detected using CRISPRfinder[3]. ANI were calculated using the ani.rb script[4]. Genome sequences were clustered by ANI value within R.

Phage Genome Comparison and Taxonomy

A phylogeny for the phage was constructed using the VICTOR server (Meier-Kolthoff and Göker, 2017). All pairwise comparisons of the amino acid sequences were conducted using the Genome-BLAST Distance Phylogeny (GBDP) method (Meier-Kolthoff et al., 2013) with settings recommended for

[1]https://github.com/jstjohn/SeqPrep
[2]http://rast.nmpdr.org/
[3]http://crispr.i2bc.paris-saclay.fr/Server/
[4]https://github.com/lmrodriguezr/enveomics

prokaryotic viruses (Meier-Kolthoff and Göker, 2017). The resulting intergenomic distances were used to infer a balanced minimum evolution tree with branch support via FASTME including SPR post-processing for each of the formulas D0, D4, and D6, respectively (Lefort et al., 2015). Branch support was inferred from 100 pseudo-bootstrap replicates each. Trees were rooted at the midpoint (Farris, 1972) and visualized with FigTree (Rambaut, 2016). Taxon boundaries at the species, genus, and family level were estimated with the OPTSIL program, the recommended clustering thresholds (Meier-Kolthoff and Göker, 2017) and an *F* value (fraction of links required for cluster fusion) of 0.5.

Sequences were uploaded into the ANI calculator package[5] in order to perform pairwise genome calculations of the ANI using the default conditions. The ANI calculator estimates the average nucleotide identity using reciprocal best hits (two-way ANI) between two genomic datasets.

Tail Spike Protein Cloning, Expression and Purification

Nucleotide sequence representing phage PP35 ORF156 (120600–122246) was PCR-amplified using primers 5′-TATTTCCAGGGC AGCGGATCCAACTCGCAATTCTCACAGCCG (forward) and 5′-GCTCGAGTGCGGCCGCAAGCTTACCCCAATTTGTACC AGG (reverse) bearing BamHI and HindIII restriction sites. An amplicon was cloned to vector pTSL (Taylor et al., 2016) using NEBuilder HiFi DNA Assembly kit (New England Biolabs). Clones with inserts were selected by PCR, restriction analysis, and verified by sequencing. Preparative gene expression was performed in *E. coli* B834(DE3) by induction with 1 mM IPTG at 16°C overnight. Cells were pelleted at 4,000 g, lysed by sonication in lysis buffer (20 mM Tris–HCl (pH 8.0), 200 mM NaCl), and centrifuged (13,000 *g*) to remove debris. Recombinant tail spike protein (PP35gp156) was purified on a Ni-NTA Sepharose column (GE Healthcare, 5 mL) by a stepwise gradient from 0 to 200 mM imidazole in 20 mM Tris–HCl (pH 8.0), 200 mM NaCl. Purified fractions were dialyzed against 20 mM Tris–HCl (pH 8.0) to remove imidazole, and treated with TEV protease for 12 h at 20°C. The target protein was purified on a 5 mL SourceQ 15 (GE Healthcare) column by a linear gradient of 0–600 mM NaCl in 20 mM Tris–HCl (pH 8.0). Protein concentration was determined spectrophotometrically at 280 nm using a theoretical absorption coefficient of 65,320 M^{-1} cm^{-1}. PP35 gp156 oligomeric state was assessed by gel filtration on Superdex 200 10 × 300 column (GE Healthcare).

Isolation of the *O*-Polysaccharides

Bacterial LPS was isolated by extraction of bacterial cells (∼2 g) with hot phenol-water (Westphal and Jann, 1965) followed by removal of nucleic acids and proteins by precipitation with 50% trichloroacetic acid at 4°C. A LPS sample (70 mg) was hydrolyzed with aqueous 2% HOAc at 100°C for 1 h, a lipid precipitate was removed by centrifugation (13,000 *g*, 20 min), and the carbohydrate portion was fractionated by gel-permeation chromatography on a Sephadex G-50 Superfine (GE Healthcare) column (56 × 2.6 cm) in 0.05 M pyridinium acetate buffer (pH 4.5) monitored with a Knauer differential refractometer to yield a high-molecular-mass OPS preparation (7 mg).

[5]http://enve-omics.ce.gatech.edu/ani/index

Treatment of the *O*-Polysaccharides With Bacteriophage PP35 Recombinant Tail Spike Protein

Dried sample of F012 or F154 *O*-polysaccharide was solubilized in 20 mM Tris–HCl (pH 8.0), then purified PP35 gp156 recombinant protein was added to 1/100 (*w*/*w*), and the reaction mixture was incubated overnight at 20°C.

NMR Spectroscopy of *O*-Polysaccharides

Samples were deuterium-exchanged by freeze-drying twice from 99.9% D_2O and then examined as solutions in 99.9% D_2O. ^1H and ^{13}C NMR spectra were recorded on a Bruker Avance II 600 MHz spectrometer (Germany) at 50°C using sodium 3-trimethylsilylpropanoate-2,2,3,3-d_4 (δ_H 0.0, δ_C −1.6) as internal reference for calibration. Assignments of the ^1H and ^{13}C NMR signals were measured using two-dimensional ^1H,^1H COSY, ^1H,^1H TOCSY, and ^1H,^{13}C HSQC experiments, which were done by standard Bruker software. The Bruker TopSpin 2.1 program was used to acquire and process the NMR data. Spin-lock time of 60 ms was used in the ^1H,^1H TOCSY experiment.

Mass Spectrometry of Products of OPS Degradation With Recombinant PP35 gp156

Negative ion mode HR ESI MS was performed on a Bruker micrOTOF II instrument. Interface capillary voltage was 3200 V, mass range from *m/z* 50 to 3000 Da. Samples were dissolved in a 1:1:0.1 acetonitrile/water/triethylamine mixture, and the solution was injected with a syringe at a flow rate of 3 μL/min. Nitrogen was applied as drying gas; interface temperature was set at 180°C. Internal calibration was done with Electrospray Calibrant Solution (Fluka).

RESULTS

Basic Properties of Phage PP35

Bacteriophage PP35 was isolated in 2014 from sewage water in a potato storage warehouse (Moscow region, Russia) with a soft rot infection caused by *D. solani*. Pathogenic strain F156 was identified as *D. solani* by PCR amplification and DNA sequencing of the 16S rRNA region (van Vaerenbergh et al., 2012). The better characterized *D. solani* lab strain, F012, was used as a host for phage propagation. Phage PP35 forms small clear plaques 1–2 mm in diameter on strains of *D. solani* including strain F012. We obtained a high phage titer for further purification, genomic DNA extraction, and electron microscopy. Phage PP35 is stable in solution between a pH of 5–10, and temperatures between 4 and 40°C. Freezing without cryoprotectors or heating above 50°C causes phage particles to rapidly lose infectivity.

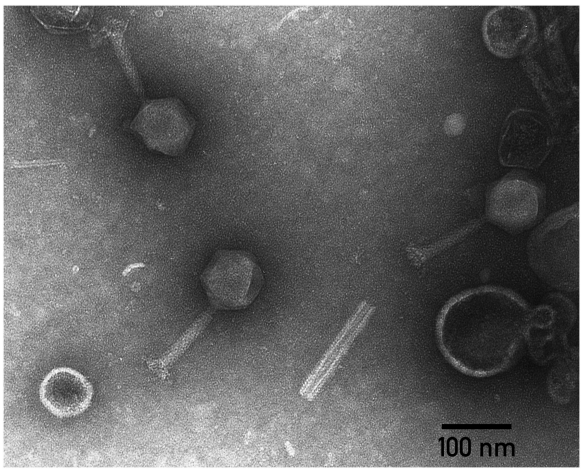

FIGURE 1 | Electron micrograph of PP35 virions. Specimens were stained with 1% uranyl acetate.

Transmission electron microscopy shows that the phage PP35 particle has a contractile tail (∼ 130 nm long), isometric icosahedral head (∼95 nm in diameter), and a pronounced baseplate complex with approximately 10 nm-long tail spikes (**Figure 1**). The morphology of PP35 is similar to that of *Salmonella* phage Vi1 (Pickard et al., 2010) and other phages assigned to the Vi1-like group. This large group of phages was previously referred as the *Vi1virus* genus of the family *Myoviridae* (Adriaenssens et al., 2012a). However, Vi1-like viruses were reclassified recently as the taxonomic family *Ackermannviridae,* where *Dickeya* viruses related to phage Limestone are grouped as the *Limestonevirus* genus of subfamily *Aglimvirinae* (Adriaenssens et al., 2017). Therefore, dependent on the ratification of the proposal, the unified naming of PP35 should be either vB_DsoM_PP35 or vB_DsoA_PP35.

Phage Host Range Determination

Among 36 strains representing various *Pectobacterium* and *Dickeya* spp. causing black leg and soft rot in potato, phage PP35 only infects nine strains determined as *D. solani*, and not *D. dianthicola*, *P. atrosepticum*, *P. parmentieri*, *P. carotovorum* subsp. *carotovorum* and *P.c.* subsp. *brasilense* (**Supplementary Table S1**). This corresponds to previous observations concerning this phage group: The host range of phages Limestone1 (Adriaenssens et al., 2012b), ϕD3 (Czajkowski et al., 2015), XF4, and JA15 (Day et al., 2017) is also limited to *D. solani*.

Phage PP35 also can infect at least one non-virulent *Enterobacteriaceae* isolate associated with soft rot pathogenesis. This strain, F154, yielded a positive signal from the PCR diagnostic test for *Pectobacterium* based on primer set EXPCC (Kang et al., 2003). Further sequencing and bioinformatic analysis of strain F154 genome referred it as a representative of the genus *Lelliottia*. The *Lelliottia* genus was reclassified from *Enterobacter* spp. and divided into two species, *L. nimipressuralis* and *L. amnigena* (previously *Enterobacter nimipressuralis* and *E. amnigenus*, respectively) (Brady et al., 2013), based on genomic MLST analysis and biochemical properties. Two other species of *Lelliottia* were proposed, based on genomic identity and with very slight differences in biochemical properties – *L. jeotgali* (Yuk et al., 2018) and *L. aquatilis* (Kämpfer et al., 2018). *Lelliottia* spp. are environmental bacteria (optimum growth temperature ca. 30°C) that can be isolated from natural water sources, and little is known about their ecological role. They are reportedly associated with food spoilage and phytopathogenesis, including soft rot (Kõiv et al., 2015), and, rarely, with human infections (Kim et al., 2010).

Infectious Properties of PP35 With Respect to *Dickeya* and *Lelliottia* Strains

Phage infection parameters were determined with adsorption, one-step-growth, and bacterial elimination assays for phage PP35 on strains *D. solani* F012 and *Lelliottia* sp. F154. Infection kinetics were similar in both cases, with fast (∼ 2 min) and complete adsorption of phages to host bacteria with MOI = 0.1 (**Figure 2A**). One-step-growth assays also shows similar curves, with a somewhat longer latent period (80 vs. 65 min) and smaller burst size (90 vs. 150 released particles per cell) for F154 (**Figure 2B**). Within 3 h no substantial secondary growth of bacteria was observed (**Figure 2C**). Therefore, it is possible to conclude that the lytic infection cycle is realized equally effectively in both bacterial hosts.

Phage Genome Comparison

The annotated genome sequence of phage PP35 was deposited in the GenBank database with accession number MG266157.1. Double stranded DNA genome contains 152,048 bp with an average GC content of 49.30%. The genome follows the bidirectional and clustered organization typical for T-even bacteriophages. BLASTN alignment of full-length genomes shows very close relations between PP35 and a number of previously described *Dickeya* phages: Limestone (HE600015.1) (Adriaenssens et al., 2012b), ϕXF4 (KY942057.1), ϕJA15 (KY942056.1) (Day et al., 2017), RC-2014 (KJ716335.1) (Czajkowski et al., 2014b), ϕD3 (Czajkowski et al., 2015). Sequence similarity (**Table 2**) identified them as belonging to a single species of the genus *Limestonevirus* (Adriaenssens et al., 2017). By transferring annotations from the well described genome and proteome of Limestone, the type phage of the genus (Adriaenssens et al., 2012b), we assigned putative functions to ∼30% of 198 predicted ORFs (**Supplementary Table S2**). Taxonomic analysis using the VICTOR server (Meier-Kolthoff and Göker, 2017) clusters phage PP35 with the newly proposed family *Ackermannviridae* (**Figure 3**). Sequences and genome locations of predicted promotors as well as metabolically and structurally essential genes are conserved not only among *Dickeya* -specific Limestone-like phages, but also throughout the genomes of other phages in this family: *Shigella* phage Ag3, *Salmonella* phages SKML-39, Sh19 (Hooton et al., 2011), vB_SalM_SJ3 (Zhang et al., 2014), Vi01 (Pickard et al., 2010), and Maynard (Tatsch et al., 2013) (50–80% pairwise identity) (**Table 2**). For example, the genome of phage Vi1 was shown to bear hypermodified pyrimidines derived from

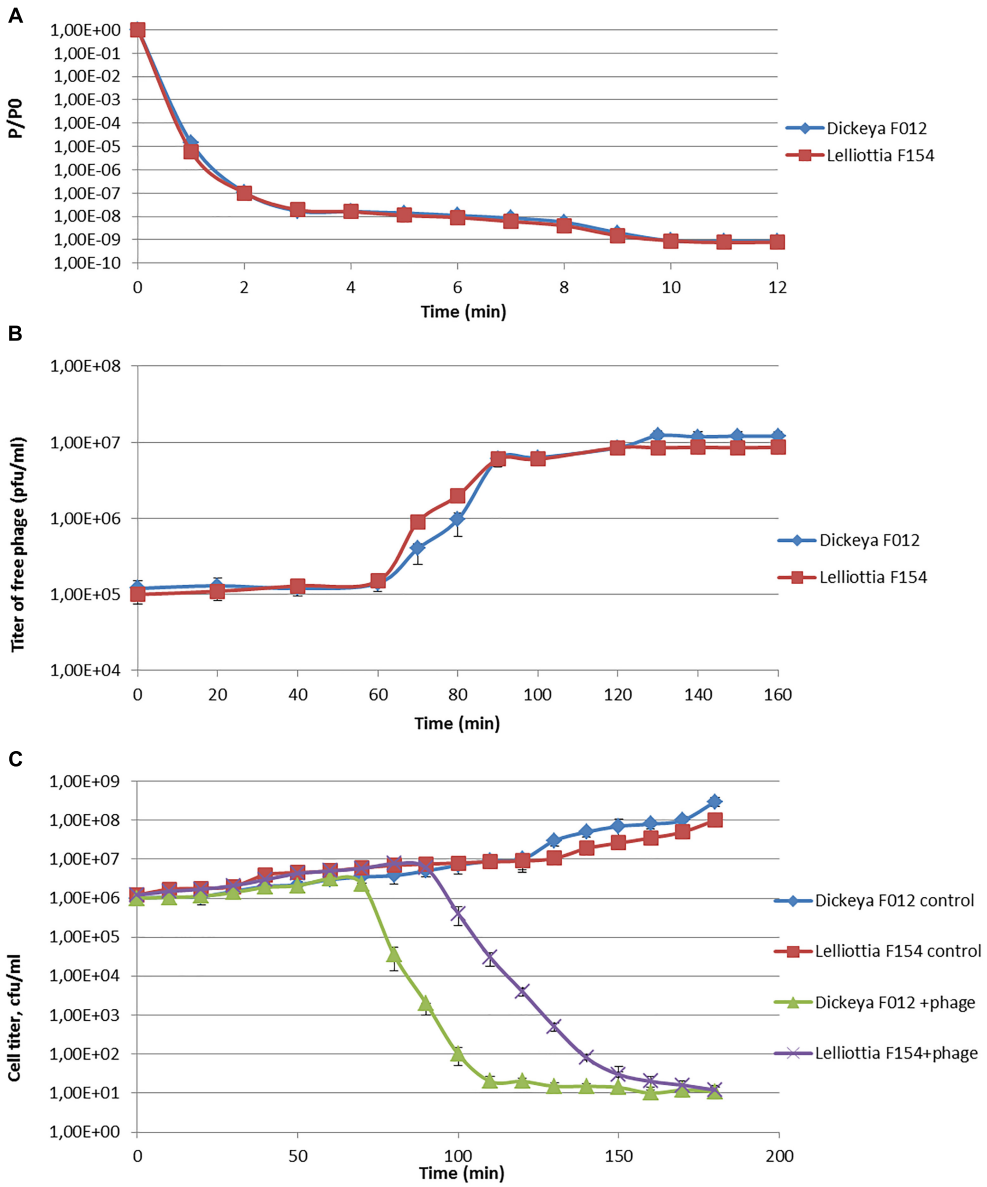

FIGURE 2 | (A) Adsorption of phage PP35 on host surface. **(B)** One-step growth curves of PP35 using *D. solani* F012 and *Lelliottia* F154 as hosts. **(C)** Multistep bacterial killing curve in the life cycle of phage PP35. Intact growing *D. solani* F012 and *Lelliottia* F154 cells were used as controls. (MOI = 0.1 in all experiments).

5-hydroxymethyl-2'-deoxyuridine (5-hmdU) (Lee et al., 2018). The exact structure of DNA modification in PP35 and the ratio of non-canonical residues are yet to be determined, but the genes responsible for 5-hmdU transformation are conserved in all *Ackermannviridae* phages, and correspond to ORF43 (dUMP hydroxymethyltransferase), ORF44 and ORF183 (kinases), ORF169 (PLP enzyme), ORF113 and ORF187 (alpha-glutamyl/putrescinyl thymidine pyrophosphorylases) in PP35 genome (**Supplementary Table S2**). Another example of conserved gene clusters is the region located at bp 114,315–128,300 in the PP35 genome. This operon includes 10 ORFs encoding components of the phage baseplate and the adsorption apparatus (**Supplementary Table S2**). The predicted tail spike sequence encoded by PP35 ORF 156, is identical to the corresponding tail spike sequences of the *Dickeya* phages listed above. The N-terminal domain of ORF156 that is responsible for the attachment of the spike to the phage particle is conserved among all *Ackermannviridae*. Most PP35 genes with unidentified functions are homologous and syntenous with genes in other Limestone-like phages. There are only three unique genes in the PP35 genome, and few indels and duplications (**Supplementary Table S2** and **Figure 4**). Most of these ORFs are hypothetical proteins presumably related to homing endonucleases. No integrases, excisionases, or repressors indicative of lysogenic infection cycle, and no genes encoding toxins or antibiotic resistance mechanisms were detected.

TABLE 2 | Genome properties of *Ackermannviridae* phages.

Phage	NCBI #	Genome (kbp)	GC%	ORFs	tRNA	ANI%	Reference
PP35	MG266157.1	152.0	49.3	198	1	100	This work
Limestone	HE600015.1	152.4	49.3	201	1	98.78	Adriaenssens et al., 2012b
ϕD3	KM209228	152.3	49.4	190	1	99.09	Czajkowski et al., 2015
RC2014	KJ716335.1	155.4	49.6	196	1	98.28	Czajkowski et al., 2014b
ϕJA15	KY942056.1	153.8	49.3	198	1	99.16	Day et al., 2017
ϕXF4	KY942057.1	151.5	49.4	195	1	98.90	Day et al., 2017
Ag3	NC_013693.1	158.0	50.4	216	4	87.67	Direct submission
SKML-39	NC_019910.1	159.6	50.2	208	7	87.66	Hooton et al., 2011
Sh19	NC_019530.1	157.8	44.7	166	5	77.45	Hooton et al., 2011
SJ3	KJ174318	162.9	44.4	210	4	77.36	Zhang et al., 2014
Vi01	NC_015296.1	157.7	45.2	208	6	76.45	Pickard et al., 2010
Maynard	KF669654.1	154.7	45.6	200	4	79.71	Tatsch et al., 2013

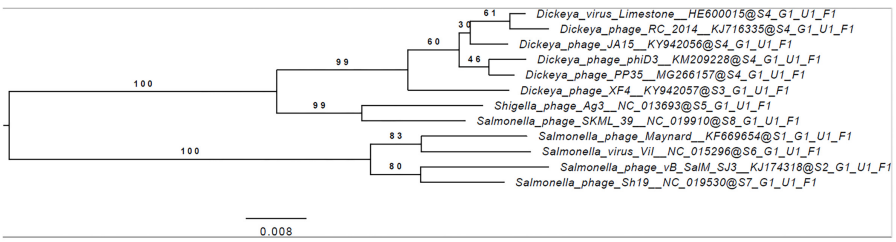

FIGURE 3 | Phylogenomic genome-BLAST distance phylogeny trees inferred using the formula, D4 and yielding average support of 35, 73, and 48%, respectively. The numbers above branches are GBDP pseudo-bootstrap support values from 100 replications.

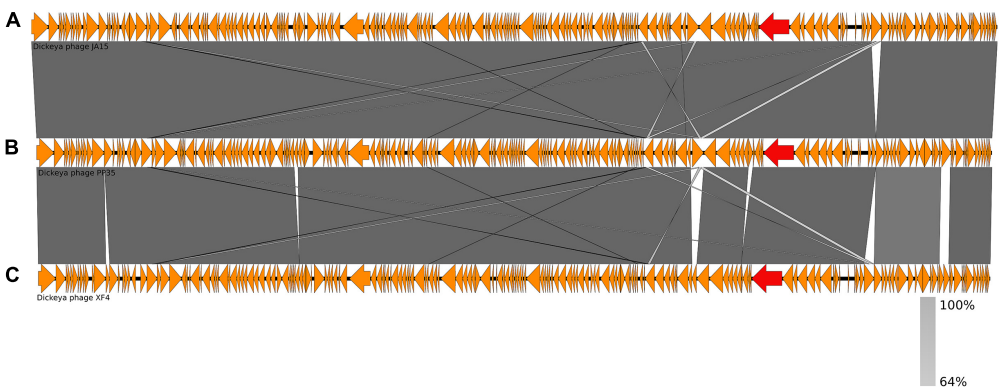

FIGURE 4 | Genome comparison of *Dickeya* phages: **(A)** Limestone, **(B)** PP35, **(C)** ϕD3. Genes encoding tail spike proteins are marked red.

Host Genome Comparison

The *D. solani* strain F012 (the PP35 host) genome (NCBI accession numbers PGOJ00000000.1) is similar to other *D. solani* genomes deposited in the public nucleotide databases. IPO2222^T is the nearest relative of the *Dickeya* strain F012, with 100% ANI (which is not the same as 100% nucleotide similarity) (**Table 3**). Homogeneity among *D. solani* strains is thought to reflect the recent evolution of this species (Pritchard et al., 2013). There are only 17 SNPs and InDels between the F012 and IPO2222^T genomes. Two putative small CRISPR arrays in contigs PGOJ01000008.1 and PGOJ01000012.1 were identified. Identical CRISPR spacers from those arrays were also found in *Dickeya* spp., *Pantoea vagans*, and *Pectobacterium polaris* genomes.

The *Lelliottia* strain F154 genome (accession number PKFV00000000.1) is most similar to the draft genome of *Lelliottia sp.* WB101 (GCA_003051885.1) isolated from a denitrifying woodchip bioreactor (98.23% ANI). There is no species designation for F154 and WB101 yet. Genome assemblies of *Lelliottia* strain F153 (draft genome accession number PKFT00000000.1) and F159 (PKFU00000000.1) are included in the same cluster as genomes of F154 and WB101 (ANI > 98.2%). These strains were also isolated in 2014 in the Moscow region, Russia, and are associated with soft rot pathogenesis in

TABLE 3 | Genomic features of Dickeya F012 and type strain IPO2222^T.

	Dickeya solani IPO2222^T	*Dickeya solani* F012
Genome, bp	4919833	4878843
#genes	4208	4309
CDS	4059	4234
RNA	104	75
tRNA	75	62
ncRNA	7	7
Pseudogenes	45	110

potato, however, they are resistant to phage PP35. ANI values between genome assemblies from this cluster and other *Lelliottia* assemblies are not greater than 88.6%, suggesting that these four strains form a distinct species of *Lelliottia* (**Figure 5**). The newly formed species *L. aquatilis* (which includes *Lelliottia* sp. 7254-16) and *Lelliottia jeotgalii* (PFL01) are most similar to the F154-like cluster, but distinct enough that F154 doesn't belong to either species (**Figure 5**). Our findings show the necessity for subsequent phylogenomic research to refine *Lelliottia* strains taxonomy after a thorough study and comparison of their physiological and biochemical properties.

Properties of the Tail Spike Protein of PP35

Earlier studies suggest that the host range of tailed phages is largely determined by the interaction of their baseplate structures (tail fibers and tail spikes) with molecules on the bacterial surface (Fokine and Rossmann, 2014). Surface polysaccharides, including the *O*-antigens of lipopolysaccharides (LPS), are obvious candidates for receptor interaction with phages (Steinbacher et al., 1996). Tail spikes contain enzymatic domains (Leiman and Molineux, 2008) that depolymerize (Barbirz et al., 2008) or deacetylate (Prokhorov et al., 2017) OPS to allow a phage to attach to the cell surface. Recombinant tail spike proteins of phages infecting *Enterobacteria* (Steinbacher et al., 1996; Barbirz et al., 2008), *Pseudomonas* (Olszak et al., 2017), and *Acinetobacter* (Lee et al., 2017) have been extensively studied functionally and structurally. They were shown to have uniform trimeric β-helical architecture, and enzymatic active sites are located either on the surface of the resulting trimeric prism or within the loops protruding from the prism (Leiman and Molineux, 2008). Recombinant PP35 gp156 tail spike protein forms trimers spontaneously, and can be purified to electrophoretic homogeneity. The protein tends to aggregate at high concentrations, so its crystallization and further detailed structural investigation is impossible at present. In dilute solution (<2 mg/mL) PP35 gp156 is stable for several weeks at 4°C.

Identification of Surface Polysaccharides of *Dickeya* F012 and *Lelliottia* F154

^{13}C NMR spectroscopy (**Figure 6**) showed that the OPS of *D. solani* F012 is composed of 6-deoxy-D-altrose repeating units and is identical to the polysaccharides of five other strains of

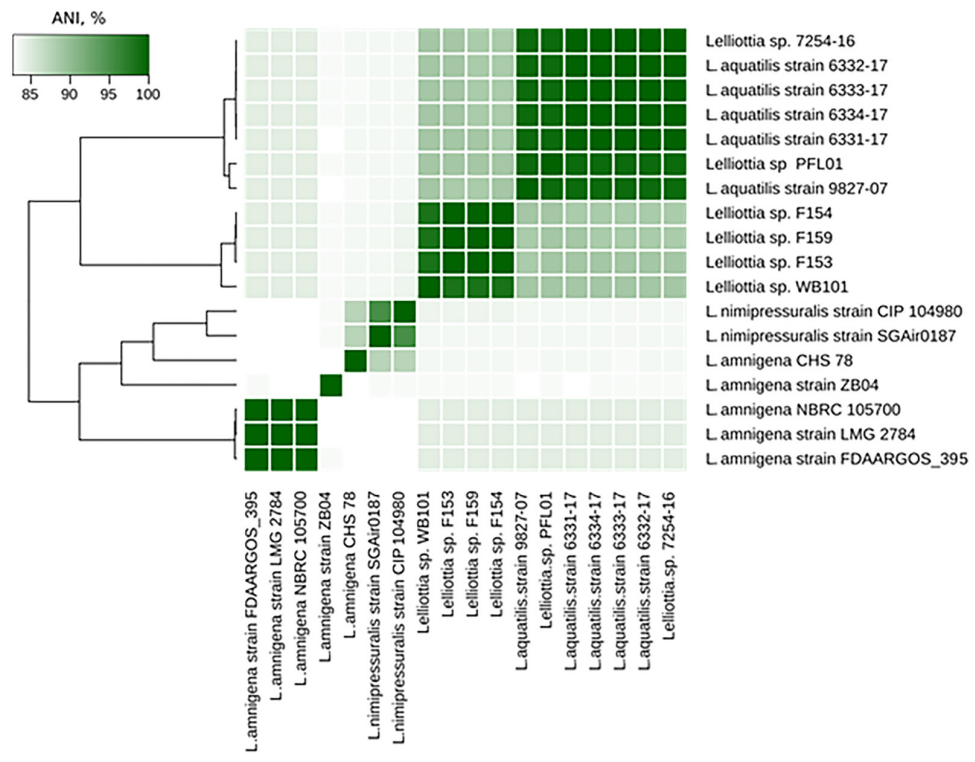

FIGURE 5 | *Lelliottia* genome clusters inferred by ANI between genome assemblies.

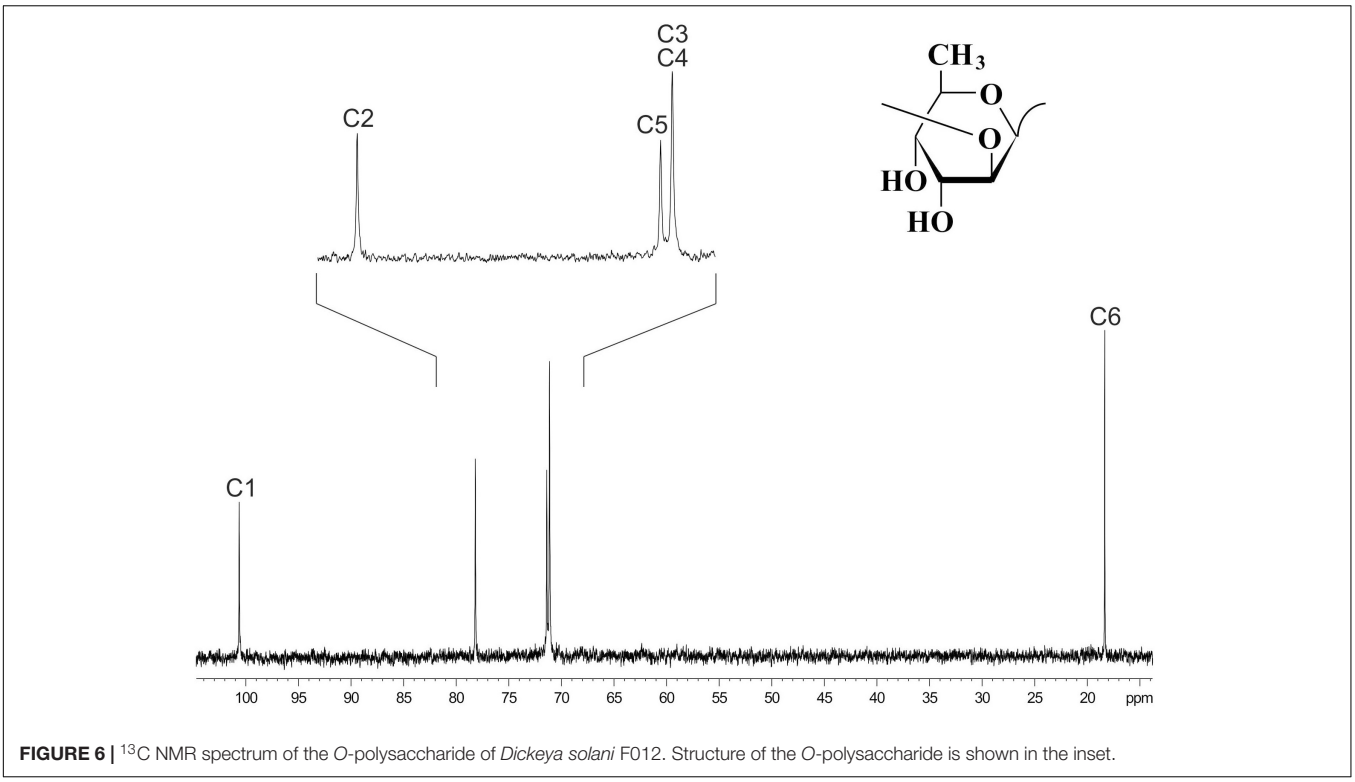

FIGURE 6 | ^{13}C NMR spectrum of the *O*-polysaccharide of *Dickeya solani* F012. Structure of the *O*-polysaccharide is shown in the inset.

D. solani and *D. dadantii* 3937 reported previously (Ossowska et al., 2017). Analysis of the OPS of *Lelliottia* sp. F154 revealed the same structure with the units →2)- 6-deoxy- β-D-altrose-(1→ (**Figure 6**). Thus, we hypothesize that the indistinguishable OPS homolog on the surface of the bacterial cells susceptible to phage PP35 is the primary receptor for the PP35 tail spike protein.

Depolymerization of the *O*-antigen launches the phage infection process, and the metabolic differences between *Dickeya* and *Lelliottia* do not prevent the infection. To test the hypothesis that PP35 tail spike protein depolymerizes the OPS of strains from these genera, we incubated OPS purified from representative strains with recombinant PP35 gp156. We measured the formation of 6-deoxy-D-altrose oligomers in the range of 4–13 monosaccharide units (degradation products) with high-resolution electrospray ionization mass spectrometry (HR ESI MS). The degradation of *Dickeya* F012 OPS resulted in mostly octa- and nonamers, while the products of *Lelliottia* F154 OPS degradation are distributed more evenly (**Figure 7**). Therefore, gp156 can hydrolyze 6-deoxy- β-D-altrose-(1→2)-6-deoxy-D-altrose linkage.

We sought the genomic loci responsible for the synthesis and secretion of *O*-antigen. The ORFs involved to lipopolysaccharide synthesis listed in Ossowska et al. (2017) are conserved in *Dickeya* genomes, and most other enterobacterial genomes. They catalyze the formation of lipid A and the linkage between lipid and sugar moieties common for *Enterobacteriaceae* (Knirel and Valvano, 2011). We hypothesized that the ABC transporter-dependent OPS biosynthesis pathway was responsible for *D. solani* OPS production (Greenfield and Whitfield, 2012), because *D. solani* OPS consists of the single repetitive carbohydrate GDP-6-deoxyaltrose. We identified the operon of eight ORFs that fits this model. The annotated ORFs of this operon include: (i) manC (protein accession number WP_022634985.1 in the case of F012 genome), manB (WP_022634986.1), and GDP-mannose 4,6-dehydratase (WP_022634987.1) that isomerizes and activates mannose substrate; (ii) GDP-fucose synthetase (WP_022634990.1) some alleles of which produce GDP-6-deoxyaltrose (Lau and Tanner, 2008); (iii) wzm (WP_026594546.1) permease and wzt

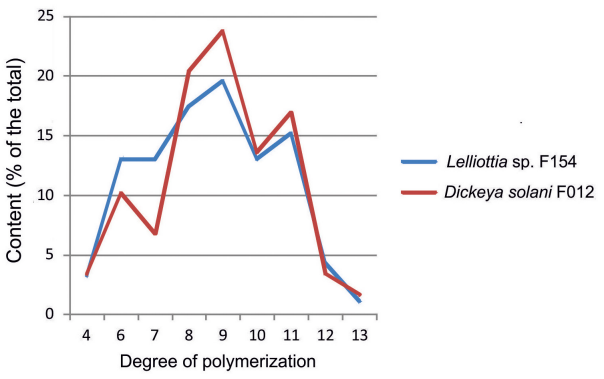

FIGURE 7 | Distribution of oligomers of 6-deoxy-D-altrose derived from the *O*-polysaccharides of *D. solani* F012 and *Lelliottia* sp. F154 by depolymerization with bacteriophage PP35 recombinant tail-spike protein gp156 based on HR ESI MS analysis data.

(WP_022634989.1) ATP-binding protein that are responsible for the transport of the nascent polysaccharide chain; and (iv) two glycosyltransferases responsible for GDP-6-deoxyaltrose chain initiation, and subsequent polymerization. Homologs of these genes from all *D. solani* genomes present in NCBI GenBank are identical. Distant homologs of some of these ORFs can be found in the genome of *Lelliottia* F154 genome, but they are members of a more complicated cascade of genes. Therefore, we were unable to identify all *Lelliottia* F154 ORFs involved in the 6-deoxy-D-altrose OPS production. Further research is required to identify and characterize those ORFs.

DISCUSSION

In this work, we characterize the interaction of *Dickeya solani* bacteriophage PP35 with its host. This interaction is believed to be the same as for *sensu stricto* Limestone and ϕD3 phages because they share a host range limited to *D. solani* strains and identical tail spike protein sequences. Attachment of the tail spike to the OPS on the bacterial surface and enzymatic depolymerization of the polysaccharide are key initial events in phage infection. The structure of the OPS is the same for all *D. solani* strains (Ossowska et al., 2016), as well as some other *Pectobacteriaceae* and *Enterobacteriaceae*. We present an example of *Enterobacteriaceae* phage host *Lelliottia* F154. This bacterial strain is evolutionarily distantly related to *Dickeya* sp., shows no virulence to potatoes, and lacks the genetic loci essential for pectate degradation associated with pathogenesis. However, it is infected by phage PP35 effectively, and we'd propose that such a bacterium may be an environmental reservoir for phage PP35.

Investigation of *D. solani* emergence and spread in Europe suggested that the pathogen arose from a single recent evolutionary event (van der Wolf et al., 2014). *D. solani* isolates from different locations in Europe (Belgium, Netherlands, Great Britain, Finland, Israel, Poland, and Russia) that are very closely related according to ANI. Attempts to isolate *D. solani* –specific bacteriophages in samples where the pathogen was detected resulted in the characterization of very similar Myoviruses resembling phage Limestone, the first isolated type representative of the species. Thus, we hypothesize two routes for natural phage infection of the plant pathogen *D. solani*: (i) Phages travel from a single source together with the bacterial population via transfer of seed potatoes, and (ii) a population of bacteriophages propagating on an endemic non- *D. solani* bacterium cross-infects *D. solani*.

There are numerous reports about phages that infect multiple bacterial hosts, especially *Enterobacteriaceae* (Hyman and Abedon, 2010). However, differences in metabolism between environmental and pathogenic bacteria and, especially, the possibility of generalized transduction reported for Limestone-like phages (Day et al., 2017) should lead to greater genetic diversity than is observed (**Table 2**). On the other hand, Limestone-like phages isolated in nearby locations and using the same *D. solani* strain for enrichment are not identical (Adriaenssens et al., 2012b; Czajkowski et al., 2014a; Day et al., 2017). Phages of this type retain viability on the surface of potato tubers for several weeks (Czajkowski et al., 2017), so the distribution of different phages via seed potato distribution is also possible. Further monitoring and assessment of the diversity of SRP-specific phages is necessary to model the geographic distribution and temporal dynamics of these phages more quantitatively.

The discovery of alternative hosts for SRP-specific phages is useful for phage control applications in addition to its ecological implications. It is desirable to use a well characterized non-pathogenic host for large-scale phage production (Gill and Hyman, 2010). Non-virulent *Lelliottia* strain F154 had similar infection parameters compared to the target pathogenic host and can be a valid choice for industrial propagation of *Limestonevirus.* Limestone-like phages also were shown to be effective for preventive and curative treatment of *D. solani* in field applications (Adriaenssens et al., 2012b). The infection properties of phage PP35 are like those previously described for phages belonging to this species. These properties indicate that it is a promising candidate to include in a phage cocktail for soft rot treatment and prevention.

DATA AVAILABILITY STATEMENT

The complete genome sequence of phage PP35 has been deposited in the NCBI database under the GenBank accession number MG266157.1. Draft genome assemblies of strains F012 and F154, and related information can be found in the NCBI database under the GenBank Accession numbers PGOJ00000000.1, and PKFV00000000.1, correspondingly.

AUTHOR CONTRIBUTIONS

MS, AI, and KAM designed the experiments. APK, MS, AAK, EB, EZ, and EK planned and performed the experiments. AAK, KKM, ST, AI, YK, and KAM performed the data analysis. APK, MS, AI, and KAM wrote the manuscript.

FUNDING

This research was supported by Russian Science Foundation grant #16-16-00073.

ACKNOWLEDGMENTS

We thank Prof. A. S. Shashkov and Dr. A. O. Chizhov for help with NMR spectroscopy and mass spectrometry, respectively. We express our gratitude to Dr. N. M. Brown for thorough proofreading and discussion of the manuscript.

SUPPLEMENTARY MATERIAL

The Supplementary Material for this article can be found online at: https://www.frontiersin.org/articles/10.3389/fmicb.2018.03288/full#supplementary-material

REFERENCES

Ackermann, H.-W. (2009). Basic phage electron microscopy. *Methods Mol. Protocols* 501, 113–126. doi: 10.1007/978-1-60327-164-6

Adriaenssens, E. M., Ackermann, H. W., Anany, H., Blasdel, B., Connerton, I. F., Goulding, D., et al. (2012a). A suggested new bacteriophage genus: "Viunalikevirus.". *Arch. Virol.* 157, 2035–2046. doi: 10.1007/s00705-012-1360-5

Adriaenssens, E. M., Krupovic, M., Knezevic, P., Ackermann, H. W., Barylski, J., Brister, J. R., et al. (2017). Taxonomy of prokaryotic viruses: 2016 update from the ICTV bacterial and archaeal viruses subcommittee. *Arch. Virol.* 162, 1153–1157. doi: 10.1007/s00705-016-3173-4

Adriaenssens, E. M., van Vaerenbergh, J., Vandenheuvel, D., Dunon, V., Ceyssens, P. J., de Proft, M., et al. (2012b). T4-related bacteriophage LIMEstone isolates for the control of soft rot on potato caused by "*Dickeya solani*.". *PLoS One* 7:e33227. doi: 10.1371/journal.pone.0033227

Altschul, S. F., Madden, T. L., Schäffer, A. A., Zhang, J., Zhang, Z., Miller, W., et al. (1997). Gapped BLAST and PSI-BLAST: a new generation of protein database search programs. *Nucleic Acids Res.* 25, 3389–3402. doi: 10.1093/nar/25.17.3389

Aziz, R. K., Bartels, D., Best, A. A., DeJongh, M., Disz, T., Edwards, R. A., et al. (2008). The RAST Server: rapid annotations using subsystems technology. *BMC Genom.* 9:75. doi: 10.1186/1471-2164-9-75

Bankevich, A., Nurk, S., Antipov, D., Gurevich, A. A., Dvorkin, M., Kulikov, A. S., et al. (2012). SPAdes: a new genome assembly algorithm and its applications to single-cell sequencing. *J. Comput. Biol.* 19, 455–477. doi: 10.1089/cmb.2012.0021

Barbirz, S., Müller, J. J., Uetrecht, C., Clark, A. J., Heinemann, U., and Seckler, R. (2008). Crystal structure of *Escherichia coli* phage HK620 tailspike: Podoviral tailspike endoglycosidase modules are evolutionarily related. *Mol. Microbiol.* 69, 303–316. doi: 10.1111/j.1365-2958.2008.06311.x

Besemer, J., Lomsadze, A., and Borodovsky, M. (2001). GeneMarkS: a self-training method for prediction of gene starts in microbial genomes. Implications for finding sequence motifs in regulatory regions. *Nucleic Acids Res.* 29, 2607–2618. doi: 10.1093/nar/29.12.2607

Brady, C., Cleenwerck, I., Venter, S., Coutinho, T., and De Vos, P. (2013). Taxonomic evaluation of the genus *Enterobacter* based on multilocus sequence analysis (MLSA): proposal to reclassify *E. nimipressuralis* and *E. amnigenus* into *Lelliottia* gen. nov. as *Lelliottia nimipressuralis* comb. nov. and *Lelliottia amnigena* comb. nov.,. *Syst. Appl. Microbiol.* 36, 309–319. doi: 10.1016/j.syapm.2013.03.005

Clokie, M. R. J., and Kropinski, A. M. (2009). *Bacteriophages?: Methods and Protocols: Isolation, Characterization, and Interactions*, Vol. 1. New York, NY: Humana Press. doi: 10.1007/978-1-60327-164-6

Czajkowski, R., Ozymko, Z., and Lojkowska, E. (2014a). Isolation and characterization of novel soilborne lytic bacteriophages infecting *Dickeya* spp. biovar 3 (' *D. solani* '). *Plant Pathol.* 63, 758–772. doi: 10.1111/ppa.12157

Czajkowski, R., Ozymko, Z., Siwinska, J., Ossowicki, A., de Jager, V., Narajczyk, M., et al. (2015). The complete genome, structural proteome, comparative genomics and phylogenetic analysis of a broad host lytic bacteriophage ϕD3 infecting pectinolytic *Dickeya* spp. *Stand. Genomic Sci.* 10:68. doi: 10.1186/s40793-015-0068-z

Czajkowski, R., Ozymko, Z., Zwirowski, S., and Lojkowska, E. (2014b). Complete genome sequence of a broad-host-range lytic *Dickeya* spp. bacteriophage ϕD5. *Arch. Virol.* 159, 3153–3155. doi: 10.1007/s00705-014-2170-8

Czajkowski, R., Smolarska, A., and Ozymko, Z. (2017). The viability of lytic bacteriophage ΦD5 in potato-associated environments and its effect on *Dickeya solani* in potato (*Solanum tuberosum* L.) plants. *PLoS One* 12:e0183200. doi: 10.1371/journal.pone.0183200

Day, A., Ahn, J., Fang, X., and Salmond, G. P. C. (2017). Environmental bacteriophages of the emerging *Enterobacterial* phytopathogen, *Dickeya solani*, show genomic conservation and capacity for horizontal gene transfer between their bacterial hosts. *Front. Microbiol.* 8:1654. doi: 10.3389/fmicb.2017.01654

Farris, J. S. (1972). Estimating phylogenetic trees from distance matrices. *Am. Nat.* 106, 645–668. doi: 10.1086/282802

Finn, R. D., Clements, J., and Eddy, S. R. (2011). HMMER web server: interactive sequence similarity searching. *Nucleic Acids Res.* 39, W29–W37. doi: 10.1093/nar/gkr367

Fokine, A., and Rossmann, M. G. (2014). Molecular architecture of tailed double-stranded DNA phages. *Bacteriophage* 4:e28281. doi: 10.4161/bact.28281

Frampton, R. A., Pitman, A. R., and Fineran, P. C. (2012). Advances in bacteriophage-mediated control of plant pathogens. *Int. J. Microbiol.* 2012:326452. doi: 10.1155/2012/326452

Gill, J. J., and Hyman, P. (2010). Phage choice, isolation, and preparation for phage therapy. *Curr. Pharm. Biotechnol.* 11, 2–14. doi: 10.2174/138920110790725311

Greenfield, L. K., and Whitfield, C. (2012). Synthesis of lipopolysaccharide *O*-antigens by ABC transporter-dependent pathways. *Carbohydr. Res.* 356, 12–24. doi: 10.1016/j.carres.2012.02.027

Hooton, S. P. T., Timms, A. R., Rowsell, J., Wilson, R., and Connerton, I. F. (2011). *Salmonella typhimurium*-specific bacteriophage ΦSH19 and the origins of species specificity in the Vi01-like phage family. *Virol. J.* 8:498. doi: 10.1186/1743-422X-8-498

Hyman, P., and Abedon, S. T. (2010). Bacteriophage host range and bacterial resistance. *Adv. Appl. Microbiol.* 70, 217–248. doi: 10.1016/S0065-2164(10)70007-1

Ignatov, A. N., Karlov, A. N., and Dzhalilov, F. S. (2014). Spreading of the blackleg of potatoes in Russia caused by bacteria of Dickeya genus. *Zaschita Karantin Rastenij* 11, 41–43.

Kämpfer, P., Glaeser, S. P., Packroff, G., Behringer, K., Exner, M., Chakraborty, T., et al. (2018). *Lelliottia aquatilis* sp. nov., isolated from drinking water. *Int. J. Syst. Evol. Microbiol.* 68, 2454–2461. doi: 10.1099/ijsem.0.002854

Kang, H. W., Kwon, S. W., and Go, S. J. (2003). PCR-based specific and sensitive detection of *Pectobacterium carotovorum* ssp. carotovorum by primers generated from a URP-PCR fingerprinting-derived polymorphic band. *Plant Pathol.* 52, 127–133. doi: 10.1046/j.1365-3059.2003.00822.x

Kim, D. M., Jang, S. J., Neupane, G. P., Jang, M. S., Kwon, S. H., Kim, S. W., et al. (2010). *Enterobacter nimipressuralis* as a cause of pseudobacteremia. *BMC Infect. Dis.* 10:315. doi: 10.1186/1471-2334-10-315

Klucar, L., Stano, M., and Hajduk, M. (2009). PhiSITE: database of gene regulation in bacteriophages. *Nucleic Acids Res.* 38, D366–D370. doi: 10.1093/nar/gkp911

Knirel, Y. A., and Valvano, M. A. (2011). *Bacterial Lipopolysaccharides?: Structure, Chemical Synthesis, Biogenesis and Interaction with Host Cells*. Berlin: Springer-Verlag. doi: 10.1007/978-3-7091-0733-1

Kõiv, V., Roosaare, M., Vedler, E., Ann Kivistik, P., Toppi, K., Schryer, D. W., et al. (2015). Microbial population dynamics in response to *Pectobacterium atrosepticum* infection in potato tubers. *Sci. Rep.* 5:11606. doi: 10.1038/srep11606

Lau, S. T. B., and Tanner, M. E. (2008). Mechanism and active site residues of GDP-fucose synthase. *J. Am. Chem. Soc.* 130, 17593–17602. doi: 10.1021/ja807799k

Laurila, J., Hannukkala, A., Nykyri, J., Pasanen, M., Hélias, V., Garlant, L., et al. (2010). Symptoms and yield reduction caused by *Dickeya* spp. strains isolated from potato and river water in Finland. *Eur. J. Plant Pathol.* 126, 249–262. doi: 10.1007/s10658-009-9537-9

Lavigne, R., Sun, W. D., and Volckaert, G. (2004). PHIRE, a deterministic approach to reveal regulatory elements in bacteriophage genomes. *Bioinformatics* 20, 629–635. doi: 10.1093/bioinformatics/btg456

Lee, I. M., Tu, I. F., Yang, F. L., Ko, T. P., Liao, J. H., Lin, N. T., et al. (2017). Structural basis for fragmenting the exopolysaccharide of *Acinetobacter baumannii* by bacteriophage ϕaB6 tailspike protein. *Sci. Rep.* 7:42711. doi: 10.1038/srep42711

Lee, Y.-J., Dai, N., Walsh, S. E., Müller, S., Fraser, M. E., Kauffman, K. M., et al. (2018). Identification and biosynthesis of thymidine hypermodifications in the genomic DNA of widespread bacterial viruses. *Proc. Natl. Acad. Sci. U.S.A.* 115, E3116–E3125. doi: 10.1073/pnas.1714812115

Lefort, V., Desper, R., and Gascuel, O. (2015). FastME 2.0: a comprehensive, accurate, and fast distance-based phylogeny inference program. *Mol. Biol. Evol.* 32, 2798–2800. doi: 10.1093/molbev/msv150

Leiman, P. G., and Molineux, I. J. (2008). Evolution of a new enzyme activity from the same motif fold. *Mol. Microbiol.* 69, 287–290. doi: 10.1111/j.1365-2958.2008.06241.x

Mansfield, J., Genin, S., Magori, S., Citovsky, V., Sriariyanum, M., Ronald, P., et al. (2012). Top 10 plant pathogenic bacteria in molecular plant pathology. *Mol. Plant Pathol.* 13, 614–629. doi: 10.1111/j.1364-3703.2012.00804.x

Meier-Kolthoff, J. P., Auch, A. F., Klenk, H.-P. P., and Göker, M. (2013). Genome sequence-based species delimitation with confidence intervals and improved distance functions. *BMC Bioinformatics* 14:60. doi: 10.1186/1471-2105-14-60

Meier-Kolthoff, J. P., and Göker, M. (2017). VICTOR: genome-based phylogeny and classification of prokaryotic viruses. *Bioinformatics* 33, 3396–3404. doi: 10.1093/bioinformatics/btx440

Olszak, T., Shneider, M. M., Latka, A., Maciejewska, B., Browning, C., Sycheva, L. V., et al. (2017). The *O*-specific polysaccharide lyase from the phage LKA1 tailspike reduces *Pseudomonas* virulence. *Sci. Rep.* 7:16302. doi: 10.1038/s41598-017-16411-4

Ossowska, K., Czerwicka, M., Sledz, W., Zoledowska, S., Motyka, A., Golanowska, M., et al. (2017). The uniform structure of *O*-polysaccharides isolated from *Dickeya solani* strains of different origin. *Carbohydr. Res.* 445, 40–43. doi: 10.1016/j.carres.2017.04.001

Ossowska, K., Czerwicka, M., Sledz, W., Zoledowska, S., Motyka, A., Szulta, S., et al. (2016). The structure of *O*-polysaccharides isolated from plant pathogenic bacteria *Pectobacterium wasabiae* IFB5408 and IFB5427. *Carbohydr. Res.* 426, 46–49. doi: 10.1016/j.carres.2016.03.017

Pérombelon, M. C. M. (2002). Potato diseases caused by soft rot erwinias: an overview of pathogenesis. *Plant Pathol.* 51, 1–12. doi: 10.1046/j.0032-0862.2001.Shorttitle.doc.x

Pickard, D., Toribio, A. L., Petty, N. K., van Tonder, A., Yu, L., Goulding, D., et al. (2010). A conserved acetyl esterase domain targets diverse bacteriophages to the Vi capsular receptor of *Salmonella enterica* serovar typhi. *J. Bacteriol.* 192, 5746–5754. doi: 10.1128/JB.00659-10

Pritchard, L., Humphris, S., Saddler, G. S., Parkinson, N. M., Bertrand, V., Elphinstone, J. G., et al. (2013). Detection of phytopathogens of the genus Dickeya using a PCR primer prediction pipeline for draft bacterial genome sequences. *Plant Pathol.* 62, 587–596. doi: 10.1111/j.1365-3059.2012.02678.x

Prokhorov, N. S., Riccio, C., Zdorovenko, E. L., Shneider, M. M., Browning, C., Knirel, Y. A., et al. (2017). Function of bacteriophage G7C esterase tailspike in host cell adsorption. *Mol. Microbiol.* 105, 385–398. doi: 10.1111/mmi.13710

Rambaut, A. (2016). *FigTree v1.4.3. Molecular Evolution, Phylogenet ics and Epidemiology*. Available at: http://tree.bio.ed.ac.uk/software/figtree/

Schattner, P., Brooks, A. N., and Lowe, T. M. (2005). The tRNAscan-SE, snoscan and snoGPS web servers for the detection of tRNAs and snoRNAs. *Nucleic Acids Res.* 33, W686–W689. doi: 10.1093/nar/gki366

Steinbacher, S., Baxa, U., Miller, S., Weintraub, A., Seckler, R., and Huber, R. (1996). Crystal structure of phage P22 tailspike protein complexed with *Salmonella* sp. *O*-antigen receptors. *Proc. Natl. Acad. Sci. U.S.A.* 93, 10584–10588. doi: 10.1073/pnas.93.20.10584

Tatsch, C. O., Wood, T. L., Chamakura, K. R., and Kuty Everett, G. F. (2013). Complete Genome of *Salmonella enterica* serovar typhimurium myophage maynard. *Genome Announc.* 1:e00866-13. doi: 10.1128/genomeA.00866-13 e00866-13,

Taylor, N. M. I., Prokhorov, N. S., Guerrero-Ferreira, R. C., Shneider, M. M., Browning, C., Goldie, K. N., et al. (2016). Structure of the T4 baseplate and its function in triggering sheath contraction. *Nature* 533, 346–352. doi: 10.1038/nature17971

Toth, I. K., van der Wolf, J. M., Saddler, G., Lojkowska, E., Hélias, V., Pirhonen, M., et al. (2011). Dickeya species: an emerging problem for potato production in Europe. *Plant Pathol.* 60, 385–399. doi: 10.1111/j.1365-3059.2011.02427.x

van der Wolf, J. M., Nijhuis, E. H., Kowalewska, M. J., Saddler, G. S., Parkinson, N., Elphinstone, J. G., et al. (2014). *Dickeya solani* sp. nov., a pectinolytic plant-pathogenic bacterium isolated from potato (*Solanum tuberosum*). *Int. J. Syst. Evol. Microbiol.* 64, 768–774. doi: 10.1099/ijs.0.052944-0

van Vaerenbergh, J., Baeyen, S., de Vos, P., and Maes, M. (2012). Sequence diversity in the Dickeya flic gene: phylogeny of the Dickeya genus and taqman PCR for "D. *solani", new biovar* 3 variant on potato in Europe. *PLoS One* 7:e35738. doi: 10.1371/journal.pone.0035738

Westphal, O., and Jann, K. (1965). Bacterial lipopolysaccharides: extraction with phenol-water and further applications of procedure. *Methods Carbohydr. Chem.* 5, 83–91.

Yuk, K.-J., Kim, Y.-T., Huh, C.-S., and Lee, J.-H. (2018). *Lelliottia jeotgali* sp. nov., isolated from a traditional Korean fermented clam. *Int. J. Syst. Evol. Microbiol.* 68, 1725–1731. doi: 10.1099/ijsem.0.002737

Zhang, J., Hong, Y., Harman, N. J., Das, A., and Ebner, P. D. (2014). Genome sequence of a salmonella phage used to control *Salmonella* transmission in Swine. *Genome Announc.* 2:e00521-14. doi: 10.1128/genomeA.00521-14

Conflict of Interest Statement: The authors declare that the research was conducted in the absence of any commercial or financial relationships that could be construed as a potential conflict of interest.

frontiers in Microbiology

ORIGINAL RESEARCH
published: 24 October 2018
doi: 10.3389/fmicb.2018.02501

Therapeutic Potential of a New Jumbo Phage That Infects *Vibrio coralliilyticus*, a Widespread Coral Pathogen

Loïc Jacquemot[1†], *Yvan Bettarel*[2], *Joanne Monjol*[1], *Erwan Corre*[3], *Sébastien Halary*[4], *Christelle Desnues*[4], *Thierry Bouvier*[2], *Christine Ferrier-Pagès*[5] *and Anne-Claire Baudoux*[1*]

[1] *Sorbonne Universités UPMC Paris 06, CNRS, UMR7144 Adaptation et Diversité en Milieu Marin, Station Biologique de Roscoff, Roscoff, France,* [2] *MARBEC, Université Montpellier, IRD, CNRS, Ifremer, Montpellier, France,* [3] *Sorbonne Universités UPMC Paris 06, CNRS, FR2424 Fédération de Recherche, Station Biologique de Roscoff, Roscoff, France,* [4] *Aix Marseille Université, Microbes, Evolution Phylogeny and infection (MEPHI), CNRS FRE2013, IRD 198, AP-HM, IHU - Méditerranée Infection, Marseille, France,* [5] *Centre Scientifique de Monaco, Equipe Ecophysiologie Coralienne, Monaco, Monaco*

OPEN ACCESS

Edited by:
Robert Czajkowski, University of Gdansk, Poland

Reviewed by:
Inmaculada Garcia-Heredia, University of Alicante, Spain
Simon Roux, Joint Genome Institute (JGI), United States
Ahmed Askora, Zagazig University, Egypt

***Correspondence:**
Anne-Claire Baudoux
acbaudoux@sb-roscoff.fr

†Present Address:
Loïc Jacquemot, Département de Biologie, Institut de Biologie Intégrative et des Systèmes (IBIS), Université Laval, Québec, QC, Canada

Specialty section:
This article was submitted to Virology, a section of the journal Frontiers in Microbiology

Received: *26 July 2018*
Accepted: *01 October 2018*
Published: *24 October 2018*

Citation:
Jacquemot L, Bettarel Y, Monjol J, Corre E, Halary S, Desnues C, Bouvier T, Ferrier-Pagès C and Baudoux A-C (2018) Therapeutic Potential of a New Jumbo Phage That Infects Vibrio coralliilyticus, a Widespread Coral Pathogen. Front. Microbiol. 9:2501. doi: 10.3389/fmicb.2018.02501

Biological control using bacteriophages is a promising approach for mitigating the devastating effects of coral diseases. Several phages that infect *Vibrio coralliilyticus*, a widespread coral pathogen, have been isolated, suggesting that this bacterium is permissive to viral infection and is, therefore, a suitable candidate for treatment by phage therapy. In this study, we combined functional and genomic approaches to evaluate the therapeutic potential of BONAISHI, a novel *V. coralliilyticus* phage, which was isolated from the coral reef in Van Phong Bay (Vietnam). BONAISHI appears to be strictly lytic for several pathogenic strains of *V. coralliilyticus* and remains infectious over a broad range of environmental conditions. This candidate has an unusually large dsDNA genome (303 kb), with no genes that encode known toxins or implicated in lysogeny control. We identified several proteins involved in host lysis, which may offer an interesting alternative to the use of whole bacteriophages for controlling *V. coralliilyticus*. A preliminary therapy test showed that adding BONAISHI to an infected culture of *Symbiodinium* sp. cells reduced the impact of *V. coralliilyticus* on *Symbiodinium* sp. photosynthetic activity. This study showed that BONAISHI is able to mitigate *V. coralliilyticus* infections, making it a good candidate for phage therapy for coral disease.

Keywords: phage therapy, coral disease, *Vibrio coralliilyticus*, viral genomics, phage–host interactions

INTRODUCTION

Coral reefs are one of the most productive and diversified ecosystems on the planet (Connell, 1978) and they provide a wealth of ecological services as well as being economically important, supporting fisheries, tourism, and medical applications (Moberg and Folke, 1999; Hughes et al., 2003; Cooper et al., 2014). The health of these ecosystems is severely threatened by the combined effect of local anthropogenic pressures and global changes (Jackson et al., 2001; Hughes et al., 2003; Pandolfi et al., 2003; Bellwood et al., 2004). Over-exploitation of marine species, pollution, and increased sea surface temperature are associated with the emergence of coral diseases, which are contributing to the decline of coral reefs worldwide.

Several studies have identified *Vibrio* spp. (ϒ-Proteobacteria) as causative agents of coral bleaching for multiple coral species and in multiple locations (Ushijima et al., 2014; reviewed in Mera and Bourne, 2018). *Vibrio coralliilyticus* (*V. coralliilyticus*) has emeregd as an important bacterial pathogen model for understanding the establishement and propagation of coral disease (Sussman et al., 2008; O'Santos et al., 2011; Garren et al., 2014; Pollock et al., 2015). Studies have shown that V. *coralliilyticus* infection is temperature dependent and infects the coral endosymbiont *Symbiodinum* through the production of proteases that inhibit photosynthesis. This results in the loss of the endosymbiont from the coral tissues and ultimately leads to coral bleaching (Ben-Haim et al., 2003; Sussman et al., 2008, 2009; Cohen et al., 2013). With the increasing devastation of coral reefs, the development of new tools and strategies to control pathogens and treat diseased corals is becoming a major issue. Currently, biocontrol strategies, such as phage therapy, are being seriously evaluated for mitigating coral diseases (Efrony et al., 2009; Teplitski and Ritchie, 2009; Atad et al., 2012; Cohen et al., 2013).

The potential of viruses (more specifically bacteria viruses also referred to as bacteriophages or phages) as therapeutic agents to treat infectious diseases has been known for a long time (d'Herelle, 1926; Duckworth, 1976; Duckworth and Gulig, 2002). The idea of phage therapy arose from the early discovery that a given virus usually infects a single host species, leaving the rest of the microbial community untouched. Moreover, viruses are obligate intracellular organisms and, therefore, their production is self-regulated and limited by the availability of suitable hosts. Over the past decade, there have been promising *in vitro* and *in situ* trials of phage therapy for corals. One used BA3, a virulent bacteriophage that infect the causative agent of white plague disease (Efrony et al., 2007, 2009), to inhibit the progression of the disease and its transmission to healthy corals (Atad et al., 2012). Although this research is still at an early stage, this promising result in the open sea suggest that *in situ* phage therapy for coral diseases is achievable (Atad et al., 2012). The isolation and characterization of new bacteriophages is, therefore, essential to increase the collection of potential candidates for therapeutic assays.

The therapeutic value of a candidate bacteriophage relies on the characterization of viral properties such as the virion stability, growth kinetics, viral yield, and host range. Understanding the lifestyle of the candidate phage is probably the key to their use in therapy. Only virulent bacteriophages, which replicate through a lytic cycle and kill their host after infection, will be suitable candidates. Temperate bacteriophages, which replicate using a lysogenic cycle, may improve host fitness through gene transfer. It is, however, difficult to distinguish between virulent and temperate phage because temperate viruses can switch to a lytic cycle in response to environmental changes, such as temperature, pH salinity, UV, pollution, or nutrient availability (Jiang and Paul, 1996; Williamson and Paul, 2006, reviewed in Howard-Varona et al., 2017). Furthermore, infection dynamics can be highly variable, even between two closely related hosts (Holmfeld et al., 2014; Dang et al., 2015). Over the past decade, genomics has greatly improved our understanding of host—virus interactions, and is the key to establishing whether a candidate is an obligate lytic bacteriophage (Howard-Varona et al., 2017). Bacteriophage genome sequencing is also essential for evaluating the safety of a candidate (absence of toxins and temperate phage hallmarks), and to provide information on the candidate's evolution history and ecology (Lobocka et al., 2014).

In this study, we report a novel bacteriophage, hereafter referred to as *Vibrio* phage BONAISHI that infects the model coral pathogen *V. coralliilyticus.* We studied it using a combination of functional, genomic, and metagenomic approaches to evaluate the potential of this phage for mitigating disease caused by *V. coralliilyticus*.

MATERIAL AND METHODS

Virus Isolation

Seawater samples were collected from coral surrounding water off Whale Island (Van Phong Bay, Vietnam). A 50 mL aliquot was supplemented with 10% (v/v) Marine Broth (MB, Difco) and the mixture was enriched with 1 mL *Vibrio coralliilyticus* LMG20984 (YB1) culture and incubated for 48 h at 25°C (Brussaard et al., 2016). The sample was clarified (7,000 g, 15 min) and the supernatant was filtered through 0.2 μm PES filters to separate the viral community. A 100 μL aliquot of the filtrate was added to 900 μL YB1 culture and incubated for 30 min at 25°C. The mixture was included in molten agar (Marine Broth supplemented with 0.6% noble agar) and spread on a Marine Agar plate. After 48 h incubation, a translucent plaque indicating host lysis was removed from the bacterial lawn, eluted in 0.22 μm filtered Salt Marine (SM) buffer (100 mM NaCl, 8 mM MgSO4, 50 mM Tris-HCl pH 8.0) and combined with a host culture in a plaque assay (Brussaard et al., 2016). This procedure was repeated twice to ensure the clonality of the bacteriophage. Finally, the clonal phage suspension and host culture were used in a plaque assay giving confluent lysis. The plaques were eluted in SM buffer, the eluent was clarified by centrifugation (7,000 g, 30 min, 4°C), and the supernatant was filtered through 0.22 μm and stored at 4°C until use.

Transmission Electronic Microscopy

A 10 μL aliquot of the phage suspension was loaded onto a Formvar/carbon film coated 400 mesh copper grid (Euromedex). After 5 min incubation, the grid was blotted with filter paper and stained with 2% uranyl acetate for 30 s, blotted again to remove excess dye and air dried for 30 min (Ackermann and Heldal, 2010). The specimen was imaged using JEOL 1400 transmission electron microscope operating at 120 keV at a magnification of 80,000X.

Environmental Range of Infectivity

The tolerance of BONAISHI to temperature and pH ranges was evaluated by monitoring the loss of infectivity of a freshly produced suspension by spot test. For evaluating the temperature range, 100 μL of viral suspension (5 x 10^8 PFU/mL) was incubated at temperatures from 4 to 70°C for 30 min in a dry bath. The samples were then cooled for 5 min at 4°C and virus infectivity was assessed by spot test. Briefly, 5 μL of the treated

viral suspension was spotted on a host lawn obtained by plating a 1:4 mixture of host culture in molten agar onto a marine agar plate. For evaluating the pH range, 100 μL of viral suspension were added to 900 μL SM buffer adjusted at pH ranging from 2 to 10. The samples were incubated for 24 h at 4°C and then spot-tested as described above.

Host Range

A selection of 43 bacterial strains (**Table S1**) related to the original host *V. coralliilyticus* YB1 were used to determine the host specificities of BONAISHI. The ability of BONAISHI phage to infect these strains was determined by pairwise infection. The bacterial strains were grown in Marine Broth media (DIFCO) overnight. Each culture was included in molten agar (Marine Broth supplemented with 0.6% noble agar) and spread on a Marine Agar plate. A freshly produced suspension of BONAISHI was serially diluted in SM buffer and a 5 μL drop of each dilution was spotted on a bacterial lawn. After 24–48h incubation at 25°C, the formation of translucent spots, indicative of host lysis, was recorded.

Life Strategy

The growth cycle of BONAISHI was tested on two *V. coralliilyticus* strains including the original host LMG 20984 (YB1) and the alternate host LMG 23696 (P1) (Middelboe et al., 2010). Both host cultures were grown in MB and divided into four 25 mL sub-cultures. One sub-culture served as control and the remaining 3 were inoculated with a freshly produced BONAISHI suspension at multiplicity of infection (MOI) of 0.1 as determined by flow cytometry (see below). All cultures were incubated at 25°C for 48 h. Samples for viral and bacterial counts were taken every hour for 10 h, and then every 4 h for 48 h. Samples were immediately fixed with glutaraldehyde (0.5% final concentration) for 10 min at 4°C, flash frozen in liquid nitrogen, and stored at −80°C until flow cytometry analysis (see below). Bacterial host and virus counts were used to calculate the phage latent period and burst size. The latent period corresponds to the time elapsed between the viral inoculation and the release of virions. The burst-size, which corresponds to the number of virions produced per infected host cell, was determined by the ratio of the net increase in virus concentration over the net decrease in host concentration during the first burst.

Flow Cytometry

For determining the bacterial abundance, samples were diluted in autoclaved 0.2 μm filtered TE buffer (10 mM Tris-HCl, 1 mM EDTA, pH 8.0) and stained with a SYBR Green (10,000-fold dilution of commercial solution) for 15 min in the dark at ambient temperature. For determining the viral abundance, 100–1,000-fold diluted samples were stained with SYBR Green (20,000-fold dilution of commercial solution) for 10 min in the dark at 80°C. Analyses were performed using a FACS Canto II equipped with an argon-laser (455 nm). The trigger was set on the green fluorescence and the sample was delivered at a rate of 0.06 mL min^{-1} and analyzed for 1 min (Brussaard, 2004). Viral and bacterial counts were corrected for a blank consisting of TE-buffer with autoclaved 0.2 μm filtered seawater at the corresponding dilution.

Genome Extraction and Sequencing

A 1 L viral suspension was concentrated by ultrafiltration using a 30 kDa PES membrane (Vivaflow 50, Vivascience) and centrifugal concentrator (Vivaspin 20, 30 kDa, PES) to a final volume of 2 mL. The concentrate was subsequently purified on linear sucrose gradient (10–40 % in 0.2 μm SM) by ultracentrifugation (SW41.Ti rotor, 96,808 g, 30 min at 4°C). The BONAISHI particles formed a well resolved band that was extracted, dialyzed against SM buffer using a centrifugal concentrator (Vivaspin 20, 30 kDa, PES) and stored at 4°C until use. The genome of the purified phage suspension was extracted using a DNAeasy Blood and Tissue kit (QUIAGEN, Valencia, CA) according to the manufacturer's protocol. Samples were sent to GATC Biotech, and sequenced using PACBIO RS II (17,131 mean read length). Raw read sequences assembled as a single contig using HGAP software (Chin et al., 2013). The final draft assembly was 303, 340 bp with an average coverage of 1,720x and an average base quality score of 86%.

Bioinformatic Analysis

Phage Genome Annotation

Putative coding DNA sequences (CDS) in the BONAISHI genome were predicted using Glimmer (Delcher et al., 1999) and Genemark (Besemer et al., 2001). The coordinates of each translated open reading frames (ORF) were also inspected manually. ORF smaller than 200 base pairs (bp) were removed from the analysis. The predicted amino acid sequences were assigned manually by BLASTP and PSI-BLAST (cutoff e-value $<10^{-5}$) against the NCBI non-redundant database (January 2018) and InterProScan 5 (Jones et al., 2014), as well as the fully automated RAST server annotation service (Aziz et al., 2008). BLASTP was used to search for putative toxins in the databases MvirDB (Zhou et al., 2006), VirulenceFinder (Chen et al., 2005), Vibrio-base (Choo et al., 2014), and t3DB (Lim et al., 2009; Wishart et al., 2015) toxin databases. The IntegrallDB (Moura et al., 2009) and ACLAME (Leplae et al., 2006) databases were used to check for prophage-like sequences. tRNAScanSE (Lowe and Eddy, 1997) and Aragorn (Laslett and Canback, 2004) were used to check for tRNA. The genome map was produced using Artemis (Rutherford et al., 2000) and DNA Plotter (Carver et al., 2009). The BONAISHI genome sequence has been submitted to the GenBank database under accession number MH595538.

Terminase Large Subunit (TerL) Protein Phylogeny

The amino acids sequence of the terminase large subunit from 63 jumbo phages including BONAISHI were used for phylogenetic analysis. Sequences were trimmed to 406 bp, the minimum sequence length of *Aeromonas* phage px29, using BioEdit (Hall, 1999). Sequences were aligned by Muscle and the tree was constructed by Maximum Likelihood with 1,000 bootstrap iterations using Mega 6.06 (Tamura et al., 2013).

Host Genome Analysis

The clustered regularly interspaced short palindromic repeats (CRISPR), in the pathogenic *V. coralliilyticus* strains P1 and YB1 genome, were searched for genetic signatures of viral resistance mechanisms using CRISPRfinder (Grissa et al., 2007). Genetic exchange between the phage BONAISHI and its bacterial hosts was checked by homology between the phage ORFs and the ORFs of *V. coralliilyticus* P1 (AEQS00000000) and YB1 (ACZN00000000) using BLASTP.

Metagenomic Analysis

To determine the distribution of BONAISHI, the genome was used to recruit homologous reads from 56 coral-associated virome in Metavir (Roux et al., 2011), and 137 CAMERA Broad Phage metagenomes (Seshadri et al., 2007) and viral contigs in IMG/VR (Paez-Espino et al., 2017, **Table S2**). These samples comprised a wide range of marine environments including tropical and temperate pelagic ecosystems, healthy and diseased coral reefs including slurry from individual coral colonies, coral mucus, and the water from coral reefs. We also carried out recruitments in prokaryote metagenome from 4 coral atolls (Dinsdale et al., 2008) to check whether BONAISHI genome sequences were inserted into prokaryote genomes. Each reads served as a query and was assigned to a (single) best-matching hit by BLASTN and TBLASTX if the alignments met the following criteria: e-value $< 10^{-3}$, alignment length > 50, bitscore > 40. BLASTN parameters were set to: open gap cost $= 8$, extend gap cost $= 6$, match reward $= 5$, mismatch penalty $= -4$, word size $= 8$. Reads were recruited from each metagenome in order to determine the fraction of recruited reads that can be assigned to BONAISHI.

Preliminary Treatment of Diseased Symbiodinium

Culture of *Symbiodinium* sp. cells (Clade A1) originally extracted from the scleractinian coral *Galaxea fascicularis* (Goiran et al., 1996) were maintained in the laboratory in F/2 medium (Guillard and Ryther, 1962) prepared from Guillard's Marine Water Enrichment Solution (Sigma-Aldrich G9903). Cultures were maintained at 25°C under 100 µmol photons m^{-2} s^{-1} of white light provided by fluorescent tubes (Mazda 18WJr/865) using a 12:12 light:dark cycle. One day prior to the therapy assay, exponentially growing *Symbiodinium* sp. cultures were transferred to 30°C under the same light conditions. A 20 mL aliquot was concentrated at 5,000 g for 10 min at 30°C (VIVASPIN 20, PES, 30 kDa). The retentate was gently resuspended in 20 ml EDTA free F/2 medium and the procedure was repeated twice to wash the culture. The *Symbiodinium sp.* abundance was determined by flow cytometry and adjusted to 10^4 cells mL^{-1}. *V. coralliilyticus YB1* was cultured overnight in MB and then purified in the same way. Bacterial abundance was determined by flow cytometry and adjusted to 10^7 cells mL^{-1}. A freshly produced suspension of BONAISHI was purified by sucrose gradient and diluted in SM buffer. The viral abundance was determined by flow cytometry.

For the therapy assay, the algal culture was split into 3 equal sub-cultures. One sub-culture served as control, while two of the subcultures were inoculated with an equal volume of *V. coralliilyticus YB1*. Of these, one was also inoculated with 10^8 phages mL^{-1}. All three treatments were sampled at 0, 5, 20, and 60 min to determine the photosystem II quantum yield of *Symbiodinium* sp. cells using a pulse amplitude modulated fluorimeter (Phyto-PAM, Walz) connected to a chart recorder (Labpro, Vernier). After 5 min relaxation in darkness, the non-actinic modulated light (450 nm) was turned on in order to measure the fluorescence basal level, F_0. A saturating red light pulse (655 nm, 4 000 µmol quanta m^{-2} s^{-1}, 400 ms) was applied to determine the maximum fluorescence level in the dark adapted sample, F_M. The maximal photosystem II fluorescence quantum yield of photochemical energy conversion, F_V/F_M, was calculated using the following formula:

$$\frac{F_V}{F_M} = \frac{(F_M - F_0)}{F_M} \quad (1)$$

RESULTS

Morphology

The *Vibrio* phage BONAISHI formed relatively large, round plaques on *V. coralliilyticus YB1* and produced high titer suspension. TEM microscopy showed that BONAISHI has an isometric capsid of 120 nm in diameter connected to a 190 nm long, contractile tail (**Figure 1**). This indicates that BONAISHI belongs to the order of the *Caudovirales* and the family of the *Myoviridae*.

Tolerance to Environmental Factors

The incubations showed that BONAISHI can tolerate a pH ranging from 3 to 10 and temperatures ranging from 4 to 50°C without loss of infectivity (**Table 1**). This high tolerance suggests that the phage is very stable in the environment.

Host Specificities

Spot tests using a broad range of potential hosts indicated that BONAISHI was able to infect and lyse several strains of

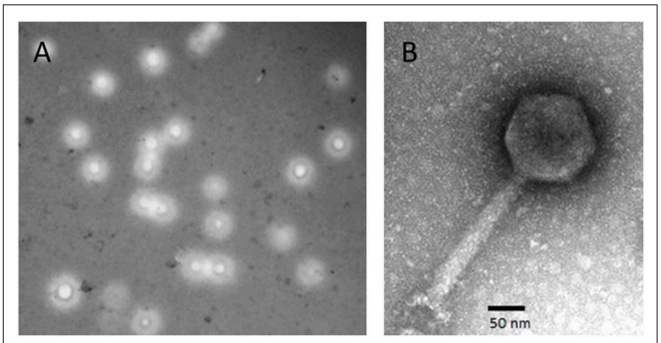

FIGURE 1 | Morphology of Vibrio phage BONAISHI. **(A)** BONAISHI forms large, round plaque on a lawn of *V. coralliilyticus YB1 on* 0.6% soft agar. **(B)** Transmission electron micrographs of a negatively stained particle of bacteriophage BONAISHI. The icosahedral head (120 nm in diameter) and the long, contractile tail (190 nm in length) suggest that BONAISHI belongs to the *Myoviridae* family.

TABLE 1 | Tolerance of *Vibrio* phage BONAISHI to temperature and pH.

Treatments	Infectivity
TEMPERATURE (°C)	
4	+
15	+
20	+
25	+
30	+
35	+
40	+
45	+
50	+
60	-
70	-
pH	
2	-
3	+
4	+
5	+
6	+
7	+
8	+
9	+
10	+

V. coralliilyticus of interest (**Table S1**). Besides *V. coralliilyticus* YB1, BONAISHI can infect another known coral pathogen, *V. coralliilyticus* P1, as well as *V. coralliilyticus* LMG21348, isolated from a bleached coral colony (*Pocillopora damicornis*), and *V. coralliilyticus* 1H13, isolated from the mucus of a *Fungia* specimen. This phage did not lyse of any of the closely related species in the test, suggesting that it is species-specific.

Life Cycle

One-step growth experiments showed that the phage readily propagated on each of its hosts with a latent period of 2–3 h (strains P1 and YB1) and burst size of 8 (P1) and 19 (YB1) (**Figure 2**). Nearly all the virions produced (96%) were infectious virions per infected cell. The infected host culture collapsed rapidly and there was total lysis 10 h after inoculation.

General Features of BONAISHI Genome

The genome of BONAISHI consists of a large double-stranded circularly permuted DNA sequence of 303,340 base-pair (bp) with a % G+C content of 42.5% (**Figure 3**). Terminal duplications at the extremities of the assembled sequence are 14,373 bp, giving a non-redundant genome of 288,967 bp. Glimmer and Genemark predicted 301 putative ORFs, which comprised 93.8% of the total sequence and were mostly oriented in a single direction. Most ORFs initiate translation at an ATG start codon except for 6 ORFs, 4 of which have a GTG start codon and the other 2 a TTG start codon. We did not find any tRNA in the genome. Of the 301 predicted ORFs, 110 ORFs (36.4%) had significant homologs in public databases and a biochemical function could be assigned for 62 of these (**Table 2**, **Figure 3**). Blast searches revealed that most of the ORFs (66/110) with significant homologs were closely related to other *Myoviridae* (**Table 2**). Most best-hits corresponded to members of the genus *Phikzvirus,* which comprises myoviruses with a large genome (> 200 kb), including *Pseudomonas* phages Phikz and PhiPA3, *Erwinia* phage *Ea35-70, Ralstonia* phage RSF1 and RSL2 and *Vibrio* phage pVa21, VP4B, pTD1, Phabio, and Noxifer. Although many gene functions could be assigned, most of the predicted genes are ORFans that are unique to BONAISHI.

Gene Annotation

Proteins Involved in Virion Structure and Assembly

The predicted proteins involved in the virion structure and assembly included a major and an accessory capsid protein (ORF 101 and 113), several tail components including a tail tube (ORF 36), a tail shealth (ORF 37), and an accessory tail protein (ORF 300), as well as several conserved structural proteins (ORFs 7, 15, 30, 39, 40, 97, 99, 100, 102, 108, 110, 119, 120, 121, and 301). We also identified a terminase large subunit (ORF 41) involved in DNA packaging. All these structural components shared strong homologies with proteins encoded by other members of *Phikzvirus* genus (**Table 1**, **Figure S1**). Phylogenetic analyses based on the amino acid sequence of the terminase large subunit classified BONAISHI as a singleton (**Figure 4**). The closest sequences belong to *Vibrio* phage pVa-21 and a cluster with *Cronobacter* phage CR5, *Erwinia* phage vB EamM, phiEaH2 and *Salmonella* phage SPN3US. The second closest cluster comprised *Phikzvirus Pseudomonas* phage KTN4, Phikz, Noxifer, PA3, Phabio, and 201 phi2-1.

Proteins Involved in DNA Replication, Recombination and Repair

The BONAISHI genome encoded at least 10 proteins involved in DNA replication, recombination, and repair. These included a DNA polymerase B (ORF 96), putative DnaB, and DEAD-like helicases (ORF 85 and 111), NAD-dependent DNA ligase (ORF 198), SbcC-like nucleases (ORF2 and 76), a ribonuclease H (ORF 10), Holliday junction resolvase (ORF 118), uvsx recombinase (ORF12). ORF 235 corresponded to the HNH family of homing endonuclease located between genes encoding β subunits of ribonucleotide diphosphate reductase.

Proteins Involved in Nucleotide Metabolism and DNA Modification

We were able to assign a putative function to 10 enzymes involved into nucleotide metabolism. Predicted proteins included two ribonucleotide diphosphate reductase (RDR) α subunits (ORFs 232 and 233) and two RDR β subunits (ORFs 234 and 236), 4 proteins of the pyridine nucleotide salvage pathway corresponding to a nicotinamide riboside transporter (ORF 181), a nicotinamide phosphoribosyltransferase (ORF 177) as well as nicotinamide mononucleotide adenylyltransferases (ORF 172 and 176). BONAISHI also encodes 2 proteins involved in thymidine biosynthesis one of which is a thymidylate synthase complementing protein (ORF 269) and the other a thymidylate

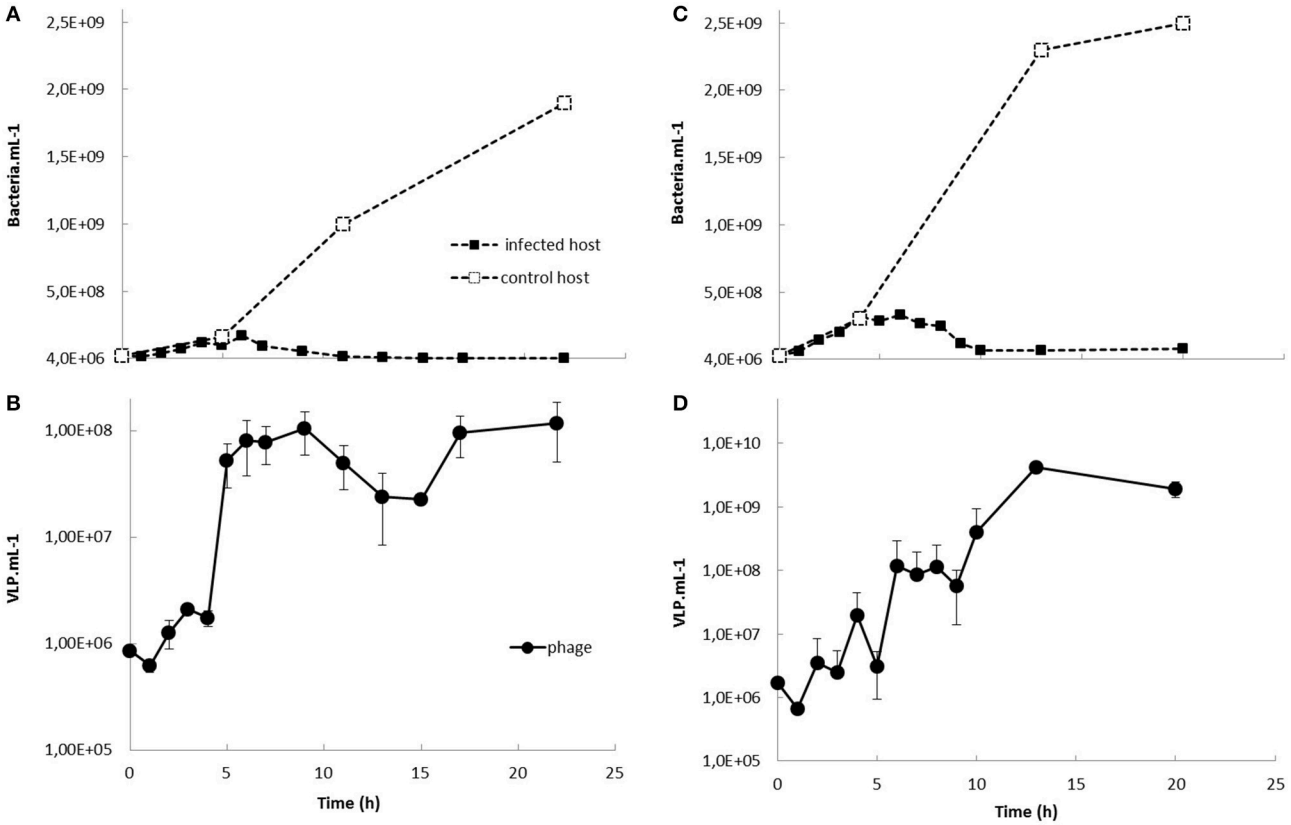

FIGURE 2 | One-step growth experiments of BONAISHI on *Vibrio coralliilyticus* strain P1 **(A,B)** and YB1 **(C,D)**. Bacteria and bacteriophage counts were assessed by flow cytometry upon staining with the nucleic acid dye SYBR Green (Life technology) according to Brussaard (2004).

kinase (ORF 231). We did not identify any gene for protein involved in DNA modification.

Proteins Involved in DNA Transcription

A transcription regulator related to the PadR family (ORF 212) was found as well as two sets of multisubunit RNA polymerase genes (β- and β'- RNAP subunits). ORFs 24, 25, 26, 92 corresponded to the Phikz virion-associated RNAP and ORFs 72, 83, 84 shared significant homologies with the Phikz genes encoding the early expressed RNAP (**Table 2**, **Figure S1**). No homologs of the early expressed Phikz β- RNAP subunits were found in BONAISHI genome. ORF 49 was assigned to an RNA binding protein.

Lysis, Host-Phage Interaction, and Lysogeny

We were able to annotate two proteins (ORFs 23 and 138) involved into host-virus interactions. There were good blastp hits on proteins of unknown function in the NCBI nr database that could be expanded to known glycoside hydrolases (GH) in the expert database CAZY (Carbohydrate Active enZYmes db, http://www.cazy.org). These included a glycoside hydrolase with a conserved endopeptidase domain (ORF 23) affiliated to the GH23 family, which mostly include lysozymes. The protein encoded by ORF 138 belongs to the glycoside hydrolase family GH19, which comprises chitinases and lysozymes. Both enzyme groups catalyze the hydrolysis of polysaccharides containing N-Acetylglucosamine, but the gene sequence does not discriminate between the two. No genes implicated in lysogeny establishment or control (integrase/excisionase, transposases, ParA/ParB genes, attachment sites, transcription repressor, etc.) were detected in the BONAISHI genome, even using prophage expert databases, which confirms that it is exclusively lytic. In addition, blastp searches using BONAISHI hosts genome did not find evidence of the presence of BONAISHI as prophage. Only three genes involved in DNA replication and recombination (ORF 225), nucleotide metabolism (ORF 192) and gene encoding for a phosphate starvation protein showed high score but the similarity was relatively low (<77%).

Miscellaneous Proteins

We identified a phosphate starvation protein PhoH (ORF 261). This protein has been reported in many other *Myoviridae*. For therapeutic applications of this phage, we also looked for potential toxin encoding genes using BLASTP on 4 toxin expert databases. No homologs to currently known toxins were detected.

Metagenomic Analysis

The global distribution of BONAISHI was investigated using marine viromes from various waters including coral mucus and the water from coral reefs (**Table S2**). The highest number of

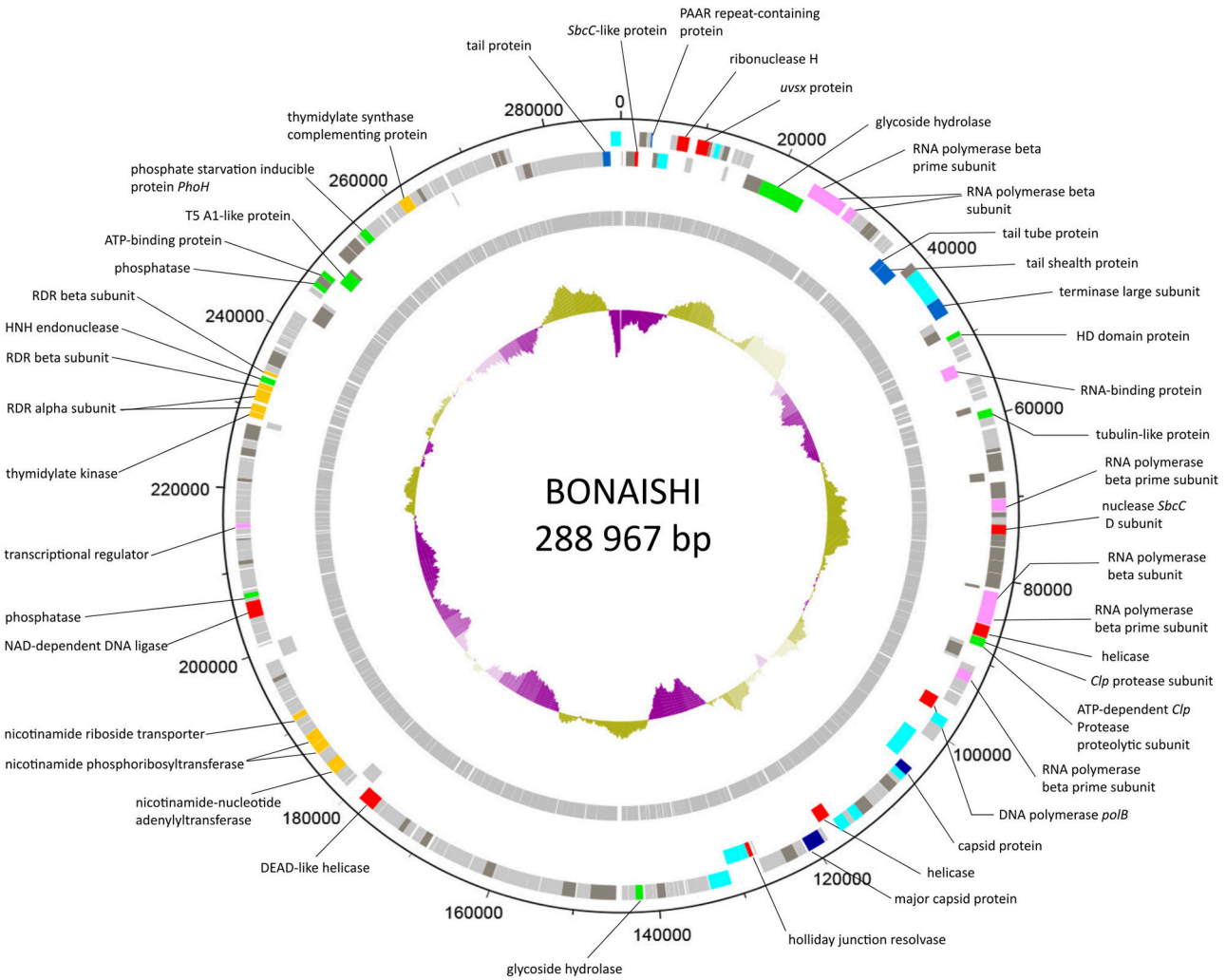

FIGURE 3 | Genome map of BONAISHI. The 110 protein-coding genes are shown as colored blocks. Protein-coding genes that are transcribed in the forward and reverse direction are located on the external and internal circle, respectively. The functional assignments of the protein-coding genes are derived from blastp matches in NCBI nr and expert databases. We confidently discriminated proteins involved in general virion structure (light blue), head, and tail structure and assembly (dark blue), DNA replication,recombination and repair (red), nucleotide metabolism (orange), DNA transcription (pink), and host phage interactions (green). Genes marked "h.p." made strong matches to hypothetical protein sequences in the database with no identified functions (dark gray). The GC content of the genome sequence is indicated by the internal purple or green histograms.

recruited reads was from the virome collected at ALOHA station in the North Pacific subtropical gyre (CAM_SMPL_00823): BONAISHI recruited 1.04% of the reads with a mean identity of 58.23%. None of the recruited reads exceeded 85% identity. We also used prokaryotic metagenomes to test whether the BONAISHI genome is found as a prophage in bacterial hosts. No bacterial reads were recruited.

Preliminary Therapy Assays of Diseased Symbiodinium

Symbiodinium sp. control culture showed optimal photosynthetic activity with the quantum yield Fv/Fm between 0.57 and 0.59 during the course of the experiment. As expected, inoculation with *V. coralliilyticus* caused a rapid photoinhibition with a 50% decrease in the quantum yield 60 min after inoculation (**Figure 5**). BONAISHI was able to significantly counteract the bacterial algicidal activity (*t*-test, $p < 0.001$) as, with both *V. coralliilyticus* and BONAISHI, the quantum yield was only 14% lower than the control 60 min after inoculation.

DISCUSSION

In recent years, *Vibrio coralliilyticus* has been used as a model pathogen to gain insights into the establishement and propagation of coral diseases (Sussman et al., 2008; O'Santos et al., 2011; Garren et al., 2014; Pollock et al., 2015). The use of phages to control *V. coralliilyticus* has been reported recently

TABLE 2 | Summary table of *Vibrio* phage BONAISHI predicted proteins that contained relevant annotation information as determined from significant BLASTP hits (*e*-value < e-3) against the GenBank non-redundant and CAZY databases.

	Predicted function	START	STOP	Size (n)	Best-hit	Classification	E-value	Score (bits)	N° accession
ORF01c	hypothetical protein	653	1753	1100	*Pseudocercospora musae*	Fungi	2.00E-07	66.00	KNG49823.1
ORF02c	SbcC-like protein	1750	2184	435	*Pseudomonas phage 201phi2-1*	Myoviridae	1.00E-17	88.00	YP_001956973
ORF03	conserved hypothetical protein	2241	3119	879	*Pseudomonas phage Phikz*	Myoviridae	2.00E-32	130.00	NP_803730
ORF05	PaaR repeat-containing protein	3722	4018	297	*Vibrio cholerae*	ϒ-proteobacteria	3.00E-21	89.00	WP_057643503
ORF06c	conserved hypothetical protein	4055	4657	603	*Pseudomonas phage Phikz*	Myoviridae	1.00E-25	203.00	AAL83062
ORF07c	virion structural protein	4667	5962	1296	*Pseudomonas phage KTN4*	Myoviridae	7.00E-32	147.00	ANM44952.1
ORF10	ribonuclease H	6889	8271	1383	*Pseudomonas phage 201phi2-1*	Myoviridae	3.00E-25	117.00	YP_001956963
ORF12	*uvsx* protein	9269	10744	1476	*Pseudomonas phage 201phi2-1*	Myoviridae	1.00E-89	290.00	YP_001956960
ORF13	conserved hypothetical protein	10746	11108	363	*Pseudomonas phage phiPA3*	Myoviridae	3.00E-28	108.00	AEH03597
ORF15	virion structural protein	11460	12125	666	*Pseudomonas phage phiPA3*	Myoviridae	2.00E-27	113.00	AEH03595
ORF17	hypothetical protein	12558	13256	699	*Erwinia phage Ea35-70*	Myoviridae	8.00E-09	64.00	YP_009004948
ORF22c	conserved hypothetical protein	16270	18384	2115	*Ralstonia phage RSL2*	Myoviridae	3.00E-74	261.00	BAQ02568
ORF23c	glycoside hydrolase	18393	24110	5718	*Ralstonia phage RP31*	Myoviridae	2.00E-70	277.00	BAW19303.1
ORF24	RNA polymerase beta prime subunit	24183	25850	1668	*Pseudomonas phage OBP*	Myoviridae	1.00E-110	346.00	YP_004958184
ORF25	RNA polymerase beta subunit	25847	28741	2895	*Ralstonia phage RSF1*	Myoviridae	1.00E-102	358.00	BAS04832
ORF26	RNA polymerase beta subunit	29242	30369	1128	*Pseudomonas phage 201phi2-1*	Myoviridae	2.00E-61	223.00	YP_001956996
ORF29	conserved hypothetical protein	32135	32860	726	*Pseudomonas phage Noxifer*	Myoviridae	3.00E-21	110.00	ARV77361.1
ORF30	virion structural protein	32871	33641	771	*Ralstonia phage RSF1*	Myoviridae	3.00E-31	124.00	BAS04828
ORF36c	tail tube protein	36168	37040	873	*Pseudomonas phage 201phi2-1*	Myoviridae	2.00E-24	108.00	YP_001956757
ORF37c	tail sheath protein	37089	39137	2049	*Erwinia phage Ea35-70*	Myoviridae	2.00E-83	286.00	YP_009004971
ORF38	hypothetical protein	39208	40278	1071	*Erwinia phage Ea35-70*	Myoviridae	3.00E-09	67.00	YP_009004972
ORF39	virion structural protein	40288	42819	2532	*Pseudomonas phage 201 phi2-1*	Myoviridae	2.00E-55	226.00	YP_001956754.1
ORF40	virion structural protein	42831	44483	1653	*Pseudomonas phage 201phi2-1*	Myoviridae	3.00E-27	125.00	YP_001956753
ORF41	terminase large subunit	44535	46691	2157	*Pseudomonas phage 201phi2-1*	Myoviridae	1.00E-142	442.00	YP_001956731
ORF43c	conserved hypothetical protein	47798	49027	1230	*Pseudomonas phage Noxifer*	Myoviridae	4.00E-37	164.00	ARV77197.1
ORF44	HD domain protein	49121	49720	600	*Salmonella phage SPN3US*	Myoviridae	3.00E-23	101.00	AEP84084
ORF49c	RNA-binding protein	52606	54225	1620	*Actinomyces massiliensis*	Actinobacteria	2.00E-73	251.00	WP_017194325

(Continued)

TABLE 2 | Continued

	Predicted function	START	STOP	Size (n)	Best-hit	Classification	E-value	Score (bits)	N° accession
ORF58c	conserved hypothetical protein	58317	59075	759	*Erwinia phage Ea35-70*	Myoviridae	1.00E-22	102.00	YP_009005001
ORF59	tubulin-like protein	59178	60167	990	*Erwinia phage Ea35-70*	Myoviridae	3.00E-21	101.00	YP_009005002
ORF68	hypothetical protein	64017	64424	408	*Ralstonia phage RSL2*	Myoviridae	7.00E-06	52.00	BAQ02532
ORF69	conserved hypothetical protein	64596	66782	2187	*Erwinia phage Ea35-70*	Myoviridae	1.00E-105	345.00	YP_009005012
ORF70c	hypothetical protein	66814	67875	1062	*Ralstonia phage RSF1*	Myoviridae	9.00E-08	63.00	BAS05022
ORF71	hypothetical protein	68148	70115	1967	*ϒ-protebacteria bacterium*	ϒ-proteobacteria	1.00E-15	94.00	OUV32520.1
ORF72	RNA polymerase beta prime subunit	70204	71697	1494	*Erwinia phage Ea35-70*	Myoviridae	3.00E-44	171.00	YP_009005015
ORF73	conserved hypothetical protein	71795	72433	639	*Erwinia phage Ea35-70*	Myoviridae	9.00E-15	79.00	YP_009005021
ORF76	nuclease SbcC subunit	73326	74498	1173	*Pseudomonas phage PhipA3*	Myoviridae	1.00E-46	172.00	AEH03486
ORF77	conserved hypothetical protein	74495	75289	795	*Erwinia phage PhiEaH1*	Siphoviridae	9.00E-23	103.00	YP_009010069
ORF78	hypothetical protein	75301	75972	672	*Uncultured bacterium*	Bacteria	2.00E-06	56.00	EKD22589
ORF79	hypothetical protein	76106	77656	1551	*Pseudomonas phage phiPA3*	Myoviridae	9.00E-06	59.00	AEH03489
ORF80	conserved hypothetical protein	77691	79211	1521	*Pseudomonas phage phiPA3*	Myoviridae	1.00E-16	93.00	AEH03490
ORF81	hypothetical protein	79251	81056	1806	*Gossypium arboreum*	Magnoliopsida	1.00E-06	63.00	KHG21929
ORF82c	hypothetical protein	81109	81456	348	*Pseudomonas phage PA7*	Myoviridae	5.00E-09	59.00	AFO71119
ORF83	RNA polymerase beta subunit	81518	83584	2067	*Pseudomonas phage Phabio*	Myoviridae	8.00E-66	260.00	ARV76743.1
ORF84	RNA polymerase beta prime subunit	83584	85557	1974	*Ralstonia phage RSF1*	Myoviridae	1.00E-50	196.00	BAS05006
ORF85	helicase	85657	87198	1542	*Pseudomonas phage OBP*	Myoviridae	1.00E-40	176.00	AEV89521.1
ORF86	Clp protease subunit	87276	87848	573	*Bacillus cereus*	Bacilli	5.00E-05	52.00	WP_048520069
ORF87	ATP-dependent Clp protease proteolytic subunit	87848	88339	492	*Dactylosporangium aurantiacum*	Actinobacteria	1.00E-27	110.00	WP_033356707
ORF89c	conserved hypothetical protein	88833	90389	1557	*Pseudomonas phage PA7*	Myoviridae	2.00E-15	89.00	AFO71110
ORF92	RNA polymerase beta prime subunit	91656	92915	1260	*Ralstonia phage RSF1*	Myoviridae	8.00E-49	180.00	BAS04991
ORF96c	DNA polymerase *polB*	96090	97820	1731	*Ralstonia phape RP12*	Unclassified virus	6.00E-107	343.00	BAW19225.1
ORF97	virion structural protein	97895	99190	1296	*Erwinia phage PhiEaH1*	Siphoviridae	2.00E-23	111.00	YP_009010288
ORF99c	virion structural protein	101147	104005	2859	*Pseudomonas phage 201phi2-1*	Myoviridae	1.00E-93	327.00	YP_001956873
ORF100c	virion structural protein	104007	105122	1116	*Ralstonia phage RSL2*	Myoviridae	2.00E-49	180.00	BAQ02702
ORF101	capsid protein*	105166	106242	1077	*Ralstonia phage RSF1*	Myoviridae	3.00E-22	105.00	BAS04975
ORF102	virion structural protein	106257	107141	885	*Ralstonia phage RSF1*	Myoviridae	4.00E-07	60.00	BAS04974

(Continued)

TABLE 2 | Continued

	Predicted function	START	STOP	Size (n)	Best-hit	Classification	E-value	Score (bits)	N° accession
ORF104	hypothetical protein	107713	109107	1394	*ϒ-protebacteria bacterium*	ϒ-proteobacteria	1.00E-12	83.00	OUV32343.1
ORF107	conserved hypothetical protein	111644	113257	1614	*Ralstonia phage RSF1*	Myoviridae	8.00E-22	108.00	BAS04969
ORF108	virion structural protein	113257	114459	1203	*Pseudomonas phage PhiPA3*	Myoviridae	8.00E-12	77.00	AEH03528
ORF110	virion structural protein	115149	116531	1383	*Pseudomonas phage PhiPA3*	Myoviridae	2.00E-28	126.00	AEH03530
ORF111c	helicase	116571	118181	1611	*Pseudomonas phage 201phi2-1*	Myoviridae	2.00E-48	1884.00	YP_001956921
ORF113	major capsid protein	118843	121035	2193	*Erwinia phage Ea35-70*	Myoviridae	2.00E-23	116.00	YP_009005109
ORF115	conserved hypothetical protein	122460	124031	1572	*Ralstonia phage RSL2*	Myoviridae	1.00E-46	179.00	BAQ02643
ORF118c	holliday-junction resolvase	127427	127987	561	*Pseudomonas phage Phabio*	Myoviridae	4.00E-18	99.00	ARV76843.1
ORF119c	virion structural protein	128029	128865	837	*Pseudomonas phage 201phi2-1*	Myoviridae	8.00E-44	159.00	YP_001956947
ORF120c	virion structural protein	128878	130947	2070	*Pseudomonas phage phiPA3*	Myoviridae	7.00E-72	256.00	AEH03570
ORF121	virion structural protein	131049	133649	2601	*Pseudomonas phage phabio*	Myoviridae	4.00E-61	245.00	ARV76832.1
ORF133	hypothetical protein	139060	140100	1041	*Vibrio tasmaniensis*	ϒ-proteobacteria	2.00E-11	73.00	WP_017112059
ORF138	glycoside hydrolase	141805	142716	912	*Aureimonas altamirensis*	α-proteobacteria	2.00E-49	174.00	BAT26087
ORF141	hypothetical protein	145070	148201	3132	*Psychromonas ingrahamii*	ϒ-proteobacteria	1.00E-08	72.00	WP_011768462.1
ORF143	hypothetical protein	150013	151644	1631	*Vibrio phage s4-7*	Unclassified virus	2.00E-06	63.00	AOQ26845.1
ORF151	hypothetical protein	160192	161433	1242	*Colwellia phage 9A*	Siphoviridae	4.00E-08	66.00	YP_006489231
ORF159	hypothetical protein	168857	169801	945	*Escherichia phage phAPEC8*	Myoviridae	4.00E-10	68.00	YP_007348452
ORF163	hypothetical protein	172164	172847	684	*Ruegeria halocynthiae*	α-proteobactérie	1.00E-19	91.00	WP_037312174
ORF167	dead-like helicase	176707	178806	2100	*Erwinia phage Ea35-70*	Myoviridae	1.00E-114	367.00	YP_009004923
ORF172	nicotinamide-nucleotide adenylyltransferase	182827	184476	1650	*Vibrio phage 11895-B1*	Myoviridae	1.00E-106	331.00	YP_007673553
ORF176	nicotinamide-nucleotide adenylyltransferase	185996	187114	1119	*Thiorhodococcus drewsii*	ϒ-proteobacteria	3.00E-46	170.00	WP_007039048
ORF177	nicotinamide phosphoribosyltransferase	187169	188668	1500	*Vibrio nigripulchritudo*	ϒ-proteobacteria	3.00E-59	210.00	WP_022562194
ORF181	nicotinamide riboside transporter	190786	191502	717	*Vibrio phage 11895-B1*	Myoviridae	3.00E-76	238.00	YP_007673552
ORF189	hypothetical protein	196049	196543	717	*Kaistia granuli*	α-proteobacteria	1.00E-08	57.00	WP_018183972
ORF198	NAD-dependent DNA ligase	204242	206257	2016	*Vibrio maritimus*	ϒ-proteobacteria	0.00E+00	608.00	WP_042496716
ORF200	phosphatase	206698	207330	633	*Vibrio phage VH7D*	Myoviridae	6.00E-19	89.00	YP_009006310
ORF206	hypothetical protein	210803	211318	516	*Psychromonas aquimarina*	ϒ-proteobacteria	7.00E-34	126.00	WP_028862581

(Continued)

TABLE 2 | Continued

	Predicted function	START	STOP	Size (n)	Best-hit	Classification	E-value	Score (bits)	N° accession
ORF209	hypothetical protein	213895	214209	315	*Enterovibrio calviensis*	ϒ-proteobacteria	6.00E-07	52.00	WP_017007757
ORF212	transcriptional regulator	215240	215764	525	*Leptolyngbya sp. PCC 7375*	cyanobacteria	1.00E-05	53.00	EKV01169
ORF220	hypothetical protein	220875	221303	429	*Shewanella sp. phage 1/4*	Myoviridae	6.00E-11	64.00	YP_009100318
ORF227	hypothetical protein	224066	224998	933	*Pseudomonas phage PhiPA3*	Myoviridae	9.00E-06	57.00	AEH03433
ORF229	hypothetical protein	226086	227921	1835	*Vibrio phage RYC*	Unclassified virus	7.00E-70	243.00	BAV81012.1
ORF231	thymidylate kinase	228796	229458	663	*Desulfosporosinus acidiphilus*	Clostridia	8.00E-42	150.00	WP_014828008
ORF232	ribonucleotide-diphosphate reductase subunit alpha	229535	230446	912	*Aeromonas molluscorum 848*	ϒ-proteobacteria	1.00E-132	385.00	EOD53957
ORF233	ribonucleotide-diphosphate reductase subunit alpha	230844	232277	1434	*Neisseria meningitidis*	β-proteobacteria	0.00E+00	635.00	WP_049227356
ORF234	ribonucleotide-diphosphate reductase subunit beta	232355	233062	708	*Thiomicrospira sp. Kp2*	ϒ-proteobacteria	3.00E-96	294.00	WP_040727751
ORF235	HNH endonuclease	233205	233927	723	*Bacillus pumilus*	Bacilli	7.00E-32	123.00	WP_051149989
ORF236	ribonucleotide-diphosphate reductase subunit beta	234231	234617	387	*Shigella sonnei*	ϒ-proteobacteria	2.00E-36	129.00	CSE34793
ORF238	hypothetical protein	235508	237232	1725	*Polyangium brachysporum*	β-proteobacteria	2.00E-23	114.00	WP_047195109
ORF249c	hypothetical protein	242652	244886	2235	*Vibrio mimicus*	ϒ-proteobacteria	4.00E-08	67.00	WP_001015571
ORF253	phosphatase	246359	247015	657	*Verrucomicrobium spinosum*	verucomicrobia	2.00E-22	97.00	WP_009962909
ORF254	hypothetical protein	247012	247842	831	*Shewanella sp.*	ϒ-proteobacteria	6.00E-06	57.00	WP101034114.1
ORF255	ATP-binding protein	247870	248553	684	*Vibrio phage RYC*	Unclassified virus	1.00E-36	137.00	BAV81012.1
ORF256c	T5 A1-like protein	248608	250479	1872	*Caulobacter phage phiCbK*	Siphoviridae	3.00E-83	281.00	YP_006988022
ORF257c	hypothetical protein	250484	250927	444	*Pseudoalteromonas (multispecies)*	ϒ-proteobacteria	9.00E-19	86.00	WP_024591352
ORF258	conserved hypothetical protein	251087	252592	1506	*Campylobacter phage CP30A*	Myoviridae	3.00E-20	102.00	YP_006908082
ORF259	conserved hypothetical protein	252655	253968	1314	*Campylobacter phage CP30A*	Myoviridae	2.00E-18	96.00	YP_006908082
ORF261	phosphate starvation protein PhoH	254632	255627	996	*Corynebacterium glucuronolyticum*	Actinobacteria	6.00E-49	175.00	WP_005389286
ORF269	thymidylate synthase-complementing protein	260653	262095	1443	*Parcubacteria*	Parcubacteria	5.00E-62	217.00	KKR42866
ORF272	conserved hypothetical protein	263205	263723	519	*Cronobacter phage vB_CsaM_GAP32*	Myoviridae	9.00E-15	77.00	YP_006987447
ORF289	conserved hypothetical protein	273177	273917	740	*Vibrio phage vB_VhaS-a*	Unclassified virus	4.00E-18	100.00	ANO57550.1
ORF290	conserved hypothetical protein	273997	274665	668	*Vibrio phage vB_VhaS-a*	Unclassified virus	1.00E-14	88.00	ANO57549.1
ORF295c	hypothetical protein	276639	277370	731	*Ralstonia phage RP12*	Myoviridae	9.00E-10	73.00	BAW19047.1
ORF300	hypothetical tail protein	286648	287631	983	*Pseudomonas phage Phabio*	Myoviridae	7.00E-15	90.00	ARV76834.1
ORF301	virion structural protein	287726	288967	1241	*Pseudomonas phage Noxifer*	Myoviridae	3.00E-07	65.00	ARV77324.1

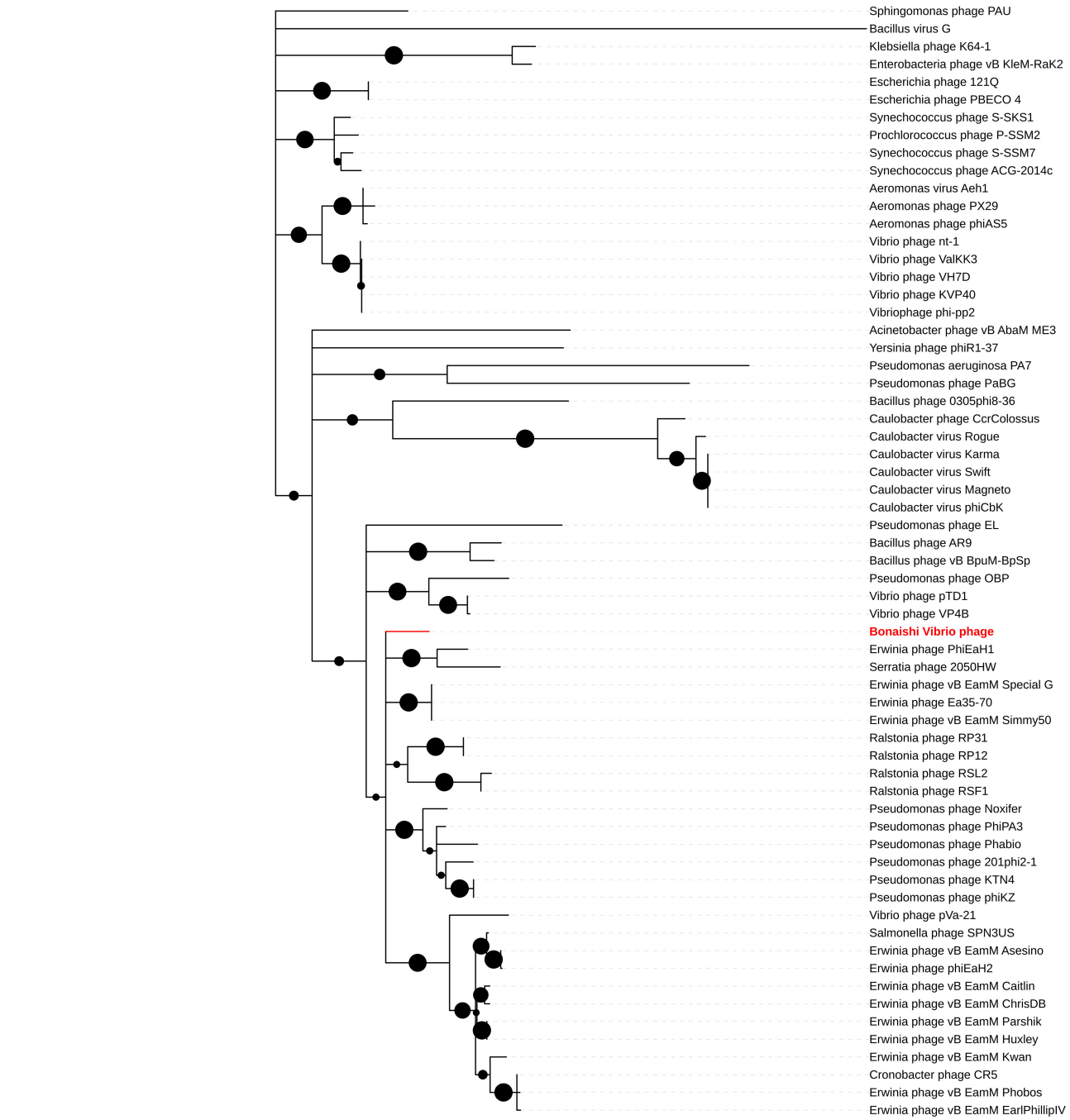

FIGURE 4 | Phylogenetic analysis of 63 Jumbo phages based on the amino acids sequence of the terminase large subunit. Sequences were aligned by Muscle and the tree was constructed by Maximum Likelihood method with a bootstrap of 1,000 using Mega 6.0 (Tamura et al., 2013) as in Yuan and Gao (2017). Bootstrap values higher than 0.5 are represented by black circles, ranging from 0.5 (smaller circle) to 1 (bigger circle).

(Efrony et al., 2007; Cohen et al., 2013) but if phage therapy is to become a practical approach, fundamental knowledge on pathogen-virus interactions must be investigated in detail to evaluate, on the one hand, the therapeutic potential of the candidate phage and, on the other hand, the suitability of the host for phage therapy.

The detection of virus-derived genes in the *Vibrio coralliilyticus* P1 and YB1 genomes (Weynberg et al., 2015) shows that these pathogenic strains have interacted with phages during the course of their evolutionary history. Past interactions events with viruses can lead to the development of resistance mechanisms to escape phage infection, which may, in turn,

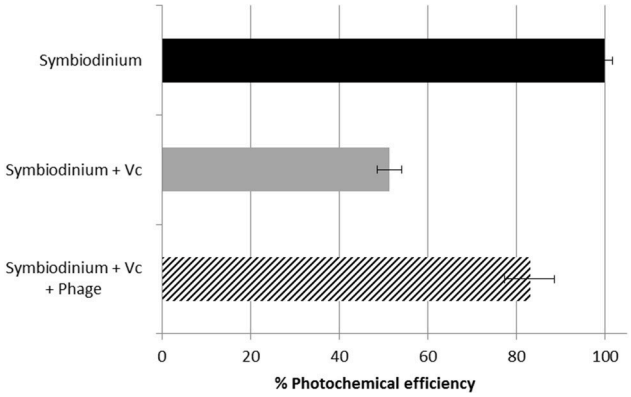

FIGURE 5 | Quantum yield (Fv/Fm) of the photosystem II of control *Symbiodinium* sp. culture (black), *Symbiodinium* sp. inoculated with *V. coralliilyticus* YB1 pathogen (gray), and *Symbiodinium* sp. co-inoculated with *V. coralliilyticus* YB1 pathogen and *Vibrio* phage BONAISHI (hashed) after 60 min incubation. Results are expressed as the % of Fv/Fm in the control culture. As reported in previous study, the inoculation of *V. coralliilyticus* YB1 pathogen induced a rapid decline in *Symbiodinium* sp. photochemical efficiency. The addition of BONAISHI rapidly counteracted the impact of *V. coralliilyticus* YB1 on the efficiency of *Symbiodinium* photochemical activity.

limit the application of phage therapy. We, however, did not detect any of the distinctive genetic signatures of viral resistance mechanisms, such as the insertion of short palindromic sequences (CRISPR, data not shown) in *V. coralliilyticus* P1 and YB1. Although other resistance mechanisms exist, the recurrent isolation of phages that infect *V. coralliilyticus* YB1 and/or P1 (Efrony et al., 2007; Cohen et al., 2013; Ramphul et al., 2017) supports the idea that *V. coralliilyticus* pathogens are permissive to viral infection and are suitable candidates for treatment by phage therapy.

The *Vibrio* phage BONAISHI isolated from coastal waters in the South China Sea is distinct from the known *V. coralliiltyicus* phages YB2, YC, CKB-S1, CKB-S2, RYC (Efrony et al., 2007; Cohen et al., 2013; Ramphul et al., 2017). Although all these phages belong to the order of *Caudovirales* (tailed bacteriophages), BONAISHI has an unusually large genome, 303 kbp, rather than 11 kbp to 158 kbp. With such a large genome, BONAISHI is a novel jumbo phage (or giant phage). These are tailed phages with a dsDNA genome larger than 200 kb (Hendrix, 2009; Yuan and Gao, 2017). Jumbo phages have often been isolated in recent years and they mostly infect Gram-negative bacteria, including the genera *Synechoccocus*, *Vibrio*, *Pseudomonas*, *Caulobacter*, *Erwinia*, and *Aeromonas* (Yuan and Gao, 2017). As observed for most jumbo phages, the large genome of BONAISHI is packaged in a large head connected to a long, contractile tail. The genome of jumbo phages typically includes core genes involved in virion structure and assembly, DNA replication, and nucleotide metabolism, including several genes encoding multisubunit RNAP. In BONAISHI, the core genes are scattered throughout the genome sequence and most of them share significant homology with other jumbo phages affiliated to the *Phikzvirus* genus. BONAISHI is the first marine representative of this divergent group within the *Myoviridae*. Interestingly, many Phikzviruses are considered to be promising biocontrol agents for plant-pathogenic bacteria (*Ralstonia solanacearum, Erwinia amylovora*) and some of them are already found in commercial products for phage therapy (Fujiwara et al., 2011; Bhunchoth et al., 2016).

The life history traits and genomic analysis showed that *Vibrio* phage BONAISHI is a good candidate for biological control of *V. coralliilyticus*. Firstly, BONAISHI appears to be structurally stable as it can withstand a wider range of pH (3–10) and temperature (4–45°C) than in the environment where it would be used. Second, it readily infects and lyses several pathogenic strains of *V. coralliilyticus* but no related species. Thirdly incubation experiments showed that the replication cycle is fast (latent period < 3 h). The presence of genes encoding virion-associated RNAP (ORFs 24, 25, 26, and 92) and early-expressed RNAP (ORFs 72, 83, and 84) in the BONAISHI genome may, at least partly, explain the rapid cycle (Ceyssens et al., 2014). In Phikzviruses, these two sets of RNAP may operate in concert during the replication cycle (Ceyssens et al., 2014; Yuan and Gao, 2017). The virion-associated RNAP may be injected into the host cell to start immediate gene expression whereas the early expressed RNAP may function during the middle and late phases of phage gene expression. The consecutive action of these enzymes, unique to Phikzviruses, confers the ability to produce viral progeny independently of the host transcription apparatus (Ceyssens et al., 2014; Yuan and Gao, 2017). In addition, the absence of detectable tRNA in BONAISHI genome suggests that it is well adapted to the translation machinery of its hosts, which is a critical process for efficient phage propagation. Finally, the genomic analysis did not identify any temperate phage hallmarks such as integration mediating enzymes, or genome architecture or sequence similarity with known temperate phages. Furthermore, the absence of homology between BONAISHI gene sequences and bacteria reads from coral metagenomes supports the idea that this phage does not integrate into the host genome. These results suggest very strongly that the *Vibrio* phage BONAISHI is a strictly lytic phage that is species specific and stable, although it appears to be relatively rare in the environment.

Another important issue for therapeutic applications of phages is to ensure that the candidate does not perform specialized or generalized transduction (Duckworth and Gulig, 2002). Given that BONAISHI appears to be strictly lytic based on the growth experiments and the genome analysis, it is unlikely that this candidate will perform specialized transduction of host DNA. Specialized transduction is restricted to temperate phages and occurs when the prophage is not cleanly excised during induction and includes the flanking bacterial genes which are then packaged in the viral progeny. Our candidate, however, may be able to perform generalized transduction. In this type of transduction, random segments of degraded host chromosome are mistakenly packaged instead of the phage DNA and may be transmitted by horizontal gene transfer. Phages that use a headful DNA packaging mechanism, such as many jumbo phages including BONAISHI, may be able to perform generalized transduction. However, it is, to the

best of our knowledge, impossible to predict the frequency of generalized transduction based purely on the genome analysis. For example, giant bacteriophages with similar headful DNA packaging mechanisms can have very different transduction rates as, for example, the T4 and T4G bacteriophages (Young et al., 1982; Young and Edlin, 1983). The ability of BONAISHI to perform generalized transduction would, therefore, require proper laboratory investigation.

An alternative to avoid potential issue with phage-mediated gene transfer is, rather than using whole bacetriophages, to use bacteriolytic proteins encoded by phages, among which the most notable are phage-encoded peptidoglycan hydrolases (PGH, see review by Roach and Debarbieux, 2017). PGHs, also called endolysins, degrade the cell peptidoglycan from within and contribute to the release of progeny and cell burst. A second type of PGH can be associated with the virion and initiate cell wall penetration through localized peptidoglycan or lipopolysaccharide degradation during the infection process. Both types of PGH are already used as bacteriocins in animal models of human infection and disease (see Roach and Debarbieux, 2017 and references therein). Jumbo phages typically encode more proteins for the lysis of the host cell wall including endolysin, glycoside hydrolase and chitinase, which are often bound to the virion than small genome phages (Yuan and Gao, 2017). In BONAISHI genome, we identified two glycoside hydrolases distantly related to known enzymes that belong to the families GH19 and GH23 using the expert database CAZY. Although the catalytic activities of these molecules cannot be determined based solely on the genome analysis, their overexpression and characterization might provide interesting tools for controlling *V. coralliilyticus* infection.

A preliminary assay suggests that BONAISHI is a promising candidate for treating *V. coralliilyticus* infection. Studies investigating the action of *V. coralliilyticus* on coral symbionts showed that photosynthesis was inactivated by the expression of a Zn-metalloprotease (Sussman et al., 2009). Our experiments on *Symbiodinum* cultures infected by *V. coralliilyticus* showed that BONAISHI phage treatment was effective: adding the phage to the infected cultures rapidly reduced *Symbiodinium* PSII inactivation. As reported in previous studies, phage addition probably lysed the bacterial pathogen, stopping Zn-metalloprotease production and further damage to *Symbiodinium* sp. cells (Cohen et al., 2013). Future studies should now focus on the effectiveness of the treatment either under realistic field conditions or in mesocosms to start including bacteriophages (and/or derived compounds) in an integrated management program to mitigate the damage caused by the infectious agents responsible for coral diseases. We recommend genome sequencing and analysis of any future phage candidate as a prerequisite to any field test to ensure safe environmental applications as this provides essential information on the phage replication cycle and host-virus interactions.

AUTHOR CONTRIBUTIONS

A-CB, YB, and TB, designed the study. LJ, JM, and A-CB performed the experiments and analyzed the results. LJ, SH, CD, and EC performed the bioinformatics analyses. CF-P provided and helped with the diseased *Symbiodium* cultures. LJ and A-CB wrote the manuscript.

ACKNOWLEDGMENTS

This work was supported jointly by the EC2CO PATRICIA Project, the TOTAL Foundation, and the ANR CALYPSO (ANR-15-CE01-0009). We would like to thank Andrew Millard for discussion on phage transduction, Simon Roux for his help with metagenomic analysis, Gurvan Michel for his assistance with CAZYmes annotation, Pei Ge for her technical assistance, and Tony Tebby for the manuscript editing. We would also like thank the three reviewers for their constructive comments on a previous version of this manuscript. We are also very grateful to Michel Galey, Alexandre Portier, and all the staff from Whale Island Resort for their hospitality and help during our stay.

SUPPLEMENTARY MATERIAL

The Supplementary Material for this article can be found online at: https://www.frontiersin.org/articles/10.3389/fmicb.2018.02501/full#supplementary-material

REFERENCES

Ackermann, H.-W., and Heldal, M. (2010). "Basic electron microscopy of aquatic viruses," in *Manual of Aquatic Viral Ecology,* eds S. W. Wilhelm, M. G.Weinbauer, and C. A. Suttle (Waco, TX: ASLO), 182–192.

Atad, I., Zvuloni, A., Loya, Y., and Rosenberg, E. (2012). Phage therapy of the white plague-like disease of Favia favus in the Red Sea. *Coral Reefs* 31, 665–670. doi: 10.1007/s00338-012-0900-5

Aziz, R. K., Bartels, D., Best, A. A., Dejongh, M., Disz, T., Edwards, R. A., et al. (2008). The RAST server: rapid annotations using subsystems technology. *BMC Genomics* 9:75. doi: 10.1186/1471-2164-9-75

Bellwood, D. R., Hughes, T. P., and Folke, C., Nyström, M. (2004). Confronting the coral reef crisis. *Nature* 429, 827–833. doi: 10.1038/nature02691

Ben-Haim, Y., Thompson, F. L., Thompson, C. C., Cnockaert, M. C., Hoste, B., Swings, J., et al. (2003). *Vibrio coralliilyticus* sp. nov. a temperature-dependent pathogen of the coral Pocillopora damicornis. *Int. J. Syst. Evol. Microbiol.* 53, 309–315. doi: 10.1099/ijs.0.02402-0

Besemer, J., Lomsadze, A., and Borodovsky, M. (2001). GeneMarkS: a self-training method for prediction of gene starts in microbial genomes. Implications for finding sequence motifs in regulatory region. *Nucleic Acids Res.* 29, 2607–2618. doi: 10.1093/nar/29.12.2607

Bhunchoth, A., Blanc-Mathieu, R., Mihara, T., Nishimura, Y., Askora, A., Phironrit, N., et al. (2016). Two asian jumbo phages, ϕRSL2 and ϕRSF1, infect *Ralstonia solanacearum* and show common features of ϕKZ-related phages. *Virology* 494, 56–66. doi: 10.1016/j.virol.2016.03.028

Brussaard, C. P. D. (2004). Optimization of procedures for counting viruses by flow cytometry. *Appl Environ Microbiol* 70, 1506–1513. doi: 10.1128/AEM.70.3.1506-1513.2004

Brussaard, C. P. D., Baudoux, A.-C., and Rodriguez-Varela, F. (2016). "Marine viruses," in *The Marine Microbiome–an Untold Resource of Biodiversity and Biotechnological Potential.* eds. L. J. Stal and S. M. Cretoiu (Springer International Publishing), 305–32.

Carver, T., Thomson, N., Bleasby, A., Berriman, M., and Parkhill, J. (2009). DNAPlotter: circular and linear interactive genome visualization. *Bioinformatics* 25, 119–120. doi: 10.1093/bioinformatics/btn578

Ceyssens, P. J., Minakhin, L., Van den Bossche, A., Yakunina, M., Klimuk, E., Blasdel, B., et al. (2014). Development of giant bacteriophage phi KZ is independent of the host transcription apparatus. *J. Virol.* 88:105010. doi: 10.1128/JVI.01347-14

Chen, L. H., Yang, J., Yu, J., Yao, Z. J., Sun, L. L., Shen, Y., et al. (2005). VFDB: a reference database for bacterial virulence factors. *Nucleic Acids Res.* 33:D325–D328. doi: 10.1093/nar/gki008

Chin, C. S., Alexander, D. H., Marks, P., Klammer, A. A., Drake, J., Heiner, C., et al. (2013). Nonhybrid, finished microbial genome assemblies from long-read SMRT sequencing data. *Nat Methods* 10, 563–569 doi: 10.1038/nmeth.2474

Choo, S. W., Heydari, H., Tan, T. K., Siow, C. C., Beh, C. Y., Wee, W. Y., et al. (2014) VibrioBase: a model for next-generation genome and annotation database development. *Sci. World J.* 2014:569324. doi: 10.1155/2014/569324

Cohen, Y., Joseph Pollock, F., Rosenberg, E., and Bourne, D. G. (2013). Phage therapy treatment of the coral pathogen *Vibrio coralliilyticus*. *Microbiol. Open* 2, 64–74. doi: 10.1002/mbo3.52

Connell, J. H. (1978). Diversity in tropical rain forests and coral reefs. *Science* 199, 1302–1310. doi: 10.1126/science.199.4335.1302

Cooper, E. L., Hirabayashi, K., Strychar, K. B., and Sammarco, P. W. (2014). Corals and their potential applications to integrative medicine. *Evid. Based Complement. Alternat. Med.* 2014:184959. doi: 10.1155/2014/184959

Dang, V. T., Howard-Varona, C., Schwenck, S., and Sullivan, M. B. (2015). Variably lytic infection dynamics of large B acteroidetes podovirus phi38: 1 against two *Cellulophaga baltica* host strains. *Environ. Microbiol.* 17, 4659–4671. doi: 10.1111/1462-2920.13009

Delcher, A. L., Harmon, D., Kasif, S., White, O., and Salzberg, S. L. (1999). Improved microbial gene identification with GLIMMER. *Nucleic Acids Res.* 27, 4636–4641. doi: 10.1093/nar/27.23.4636

d'Herelle, F. (1926). *The Bacteriophage and Its Behavior*. Baltimore, MD: Williams & Wilkins, 490–497.

Dinsdale, E. A., Pantos, O., Smriga, S., Edwards, R. A., Angly, F., Wegley, L., et al. (2008). Microbial ecology of four coral atolls in the Northern Line Islands. *PLoS ONE* 3:e1584. doi: 10.1371/journal.pone.0001584

Duckworth, D. H. (1976). Who discovered bacteriophage? *Bacteriol. Rev.* 40:793.

Duckworth, D. H., and Gulig, P. A. (2002). Bacteriophages. *BioDrugs* 16, 57–62. doi: 10.2165/00063030-200216010-00006

Efrony, R., Atad, I., and Rosenberg, E. (2009). Phage therapy of coral white plague disease: properties of phage BA3. *Curr. Microbiol.* 58, 139–145. doi: 10.1007/s00284-008-9290-x

Efrony, R., Loya, Y., Bacharach, E., and Rosenberg, E. (2007). Phage therapy of coral disease. *Coral Reefs* 26, 7–13. doi: 10.1007/s00338-006-0170-1

Fujiwara, A., Fujisawa, M., Hamasaki, R., Kawasaki, T., Fujie, M., Yamada, T. (2011). Biocontrol of Ralstonia solanacearum by treatment with lytic bacteriophages. *Appl. Environ. Microbiol.* 77, 4155–4162. doi: 10.1128/AEM.02847-10

Garren, M., Son, K., Raina, J.-B., Rusconi, R., Menolascina, F., Shapiro, O. H., et al. (2014). A bacterial pathogen uses dimethylsulfoniopropionate as a cue to target heat-stressed corals. *ISME J.* 8, 999–1007. doi: 10.1038/ismej.2013.210

Goiran, C., Al-Moghrabi, S., Allemand, D., and Jaubert, J. (1996). Inorganic carbon uptake for photosynthesis by the symbiotic coral/dinoflagellate association I. Photosynthetic performances of symbionts and dependence on sea water bicarbonate. *J. Exp. Mar. Biol. Ecol.* 199, 207–225. doi: 10.1016/0022-0981(95)00201-4

Grissa, I., Vergnaud, G., and Pourcel, C. (2007). CRISPRfinder: A web tool to identify clustered regularly interspaced short palindromic repeats. *Nucleic Acids Res.* 35(Suppl. 2), W52–7. doi: 10.1093/nar/gkm360

Guillard, R., and Ryther, J. (1962). Studies of marine planktonic diatoms. I. *Cyclotella nana* Hustedt, and *Detonula confervacea*. *Can. J. Microbiol.* 8, 229–239. doi: 10.1139/m62-029

Hall, T. A. (1999). BioEdit: a user-friendly biological sequence alignment editor and analysis. *Nucleic Acids Symp. Ser.* 41, 95–98.

Hendrix, R. W. (2009). Jumbo Bacteriophages. *Curr. Top. Microbiol. Immunol.* 328, 229–240. doi: 10.1007/978-3-540-68618-7_7

Holmfeld, K., Howard-Varona, C., Solonenko, N., and Sullivan, M. B. (2014). Contrasting genomic patterns and infection strategies of two co-existing Bacteroidetes podovirus genera. *Environ. Microbiol.* 16, 2501–13. doi: 10.1111/1462-2920.12391

Howard-Varona, C., Hargreaves, K. R., Abedon, S. T., Sullivan, M. B. (2017). Lysogeny in nature: mechanisms, impact and ecology of temperate phages. *ISME J.* 11, 1511–1520. doi: 10.1038/ismej.2017.16

Hughes, T. P., Baird, A. H., Bellwood, D. R., Card, M., Connolly, S. R., Folke, C., et al. (2003). Climate change, human impacts, and the resilience of coral reefs. *Science* 301, 929–33. doi: 10.1126/science.1085046

Jackson, J. B. C., Kirby, M. X., Berger, W. H., Bjorndal, K. A., Botsford, L. W., Bourque, B. J., et al. (2001). Historical overfishing and the recent collapse of coastal ecosystems. *Science* 293, 629–637. doi: 10.1126/science.1059199

Jiang, S. C., and Paul, J. H. (1996). Occurrence of lysogenic bacteria in marine microbial communities as determined by prophage induction. *Mar. Ecol. Prog. Ser.* 142, 27–38. doi: 10.3354/meps142027

Jones, P., Binns, D., Chang, H.-Y., Fraser, M., Li, W., McAnulla, C., et al. (2014). InterProScan 5: genome-sclae protein function classification. *Bioinformatics* 30, 1236–1240. doi: 10.1093/bioinformatics/btu031

Laslett, D., and Canback, B. (2004) ARAGORN, a program to detect tRNA genes and tmRNA genes in nucleotide sequences. *Nucleic Acids Res* 32, 11–16. doi: 10.1093/nar/gkh152

Leplae, R., Lima-Mendez, G., Toussaint, A. (2006). A first global analysis of plasmid encoded proteins in the ACLAME database. *FEMS Microbiol. Rev.* 30, 980–994. doi: 10.1111/j.1574-6976.2006.00044.x

Lim, E., Pon, A., Djoumbou, Y., Knox, C., Shrivastava, S., Guo, A. C., et al. (2009). T3DB: a comprehensively annotated database of common toxins and their targets. *Nucleic Acids Res.* 38(suppl. 1), D781–D786. doi: 10.1093/nar/gkp934

Lobocka, M., Hejnowicz, M. S., Gagala, U., Weber-Dabrowska, B., Wegrzyn, G., Dadlez, M. (2014). "The first step to bacteriophage therapy: how to choose the correct phage," in *Phage Therapy: Current Research and Applications*, eds J. Borysowski, R. Miedzybrodsky, and A. Gorski (Norfolk, UK: Caister Academic Press), 23–67.

Lowe, T. M., and Eddy, S. R. (1997). rRNAscan-SE: A program for improved detection of transfer RNA genes in genomic sequence. *Nucleic Acids Res.* 25, 955–964.

Mera, H., and Bourne, D. G. (2018). Disentangling causation: complex roles of coral associated microorganisms in disease. *Environ. Microbiol.* 20, 431–449. doi: 10.1111/1462-2920.13958

Middelboe, M., Chan, A. M., Bertelsen, S. K. (2010) "Isolation and life cycle characterization of lytic viruses infecting heterotrophic bacteria and cyanobacteria," in *Manual of Aquatic Viral Ecology*, eds S. W. Wilhelm, and M. G. Weinbauer, and C. A. Suttle (Waco, TX: ASLO), 118–133.

Moberg, F., and Folke, C. (1999). Ecological goods and services of coral reef ecosystems. *Ecol. Econ.* 29, 215–233. doi: 10.1016/S0921-8009(99)00009-9

Moura, A., Soares, M., Pereira, C., Leitão, N., Henriques, I., Correia, A. (2009). INTEGRALL: a database and search engine for integrons, integrases and gene cassettes. *Bioinformatics* 25, 1096–1098. doi: 10.1093/bioinformatics/btp105

O'Santos, E., Alves, N., Dias, G. M., Mazotto, A. M., Vermelho, A., Vora, G. J., et al. (2011). Genomic and proteomic analyses of the coral pathogen Vibrio coralliilyticus reveal a diverse virulence repertoire. *ISME J.* 5, 1471–83. doi: 10.1038/ismej.2011.19

Paez-Espino, P., Chen, I.-M. A., Palaniappan, K., Ratner, A., Chu, K., Szeto, E., et al. (2017). IMG/VR: a database of cultured and uncultured DNA Viruses and retroviruses. *Nucleic Acids Res.* 45, D457–D465. doi: 10.1093/nar/gkw1030

Pandolfi, J. M., Bradbury, R. H., Sala, E., Hughes, T. P., Bjorndal, K. A., Cooke, R. G., et al. (2003). Global trajectories of the long-term decline of coral reef ecosystems. *Science* 301, 955–958. doi: 10.1126/science.1085706

Pollock, F. J., Krediet, C. J., Garren, M., Stocker, R., Winn, K., Wilson, B., et al. (2015). Visualization of coral host–pathogen interactions using a stable GFP-labeled Vibrio coralliilyticus strain. *Coral Reefs* 34, 655–662. doi: 10.1007/s00338-015-1273-3

Ramphul, C., Estela, B., Dohra, H., Suzuki, T., Yoshimatsu, K., Yoshinaga, K., et al. (2017). Marine genomics genome analysis of three novel lytic *Vibrio coralliilyticus* phages isolated from seawater, Okinawa, Japan. *Mar. Genomics* 35, 69–75. doi: 10.1016/j.margen.2017.06.005

Roach, D. R., and Debarbieux, L. (2017). Phage therapy: awakening a sleeping giant. *Emerg. Topics Life Sci.* 1, 93–103. doi: 10.1042/ETLS20170002

Roux, S., Faubladier, M., Mahul, A., Paulhe, N., Bernard, A., et al. (2011) Metavir: a web server dedicated to virome analysis. *Bioinformatics* 27, 3074–3075. doi: 10.1093/bioinformatics/btr519

Rutherford, K., Parkhill, J., Crook, J., Horsnell, T., Rice, P., Rajandream, M. A., et al. (2000) Artemis: sequence visualization and annotation. *Bioinformatics* 16, 944–945. doi: 10.1093/bioinformatics/16.10.944

Seshadri, R., Kravitz, S. A., Smarr, L., Gilna, P., Frazier, M. (2007) CAMERA: a community resource for metagenomics. *PLoS Biol* 5:e75. doi: 10.1371/journal.pbio.0050075

Sussman, M., Mieog, J. C., Doyle, J., Victor, S., Willis, B. L., Bourne, D. G. (2009). Vibrio zinc-metalloprotease causes photoinactivation of coral endosymbionts and coral tissue lesions. *PLoS ONE* 4:e4511. doi: 10.1371/journal.pone.0004511

Sussman, M., Willis, B. L., Victor, S., Bourne, D. G. (2008). Coral pathogens identified for White Syndrome (WS) epizootics in the Indo-Pacific. *PLoS ONE* 3:e2393. doi: 10.1371/journal.pone.0002393

Tamura, K., Stecher, G., Peterson, D., Filipski, A., and Kumar, S. (2013). MEGA6: molecular evolutionary genetics analysis version 6.0. *Mol. Biol. Evol.* 30, 2725–2729. doi: 10.1093/molbev/mst197

Teplitski, M., and Ritchie, K. (2009). How feasible is the biological control of coral diseases? *Trends Ecol. Evol.* 24, 378–385. doi: 10.1016/j.tree.2009.02.008

Ushijima, B., Videau, P., Burger, A. H., Shore-Maggio, A., Runyon, C. M., Sudek, M., et al. (2014). Vibrio coralliilyticus strain OCN008 is an etiological agent of acute Montipora white syndrome. *Appl. Environ. Microbiol.* 80, 2102–2109. doi: 10.1128/AEM.03463-13

Weynberg, K. D., Voolstra, C. R., Neave, M. J., Buerger, P., van Oppen, M. J. H. (2015) From cholera to corals: viruses as drivers of virulence in a major coral bacterial pathogen. *Sci. Rep.* 5:17889. doi: 10.1038/srep17889

Williamson, S. J., and Paul, J. H. (2006). Environmental factors that influence the transition from lysogenic to lytic existence in the φHSIC/Listonella pelagia marine phage–host system. *Microbial Ecol.* 52, 217–225. doi: 10.1007/s00248-006-9113-1

Wishart, D., Arndt, D., Pon, A., Sajed, T., Guo, A. C., Djoumbou, Y., et al. (2015). T3DB: the toxic exposome database. *Nucleic Acids Res.* 43, D928–D934. doi: 10.1093/nar/gku1004

Young, K. K., Edlin, G. (1983). Physical and genetic analysis of bacteriophage T4: generalized transduction. *Mol. Gen. Genet.* 192, 241–246. doi: 10.1007/BF00327673

Young, K. K., Edlin, G., and Wilson, G. G. (1982). Genetic analysis of bacteriophage T4: transducing bacteriophages. *J. Virol.* 41, 345–347.

Yuan, Y., and Gao, M. (2017). Jumbo bacteriophages: an overview. *Front. Microbiol.* 8, 1–9. doi: 10.3389/fmicb.2017.00403

Zhou, C. E., Smith, J., Lam, M., Zemla, A., Dyer, M. D., and Slezak, T. (2006). MvirDB—a microbial database of protein toxins, virulence factors and antibiotic resistance genes for bio-defence applications. *Nucleic Acids Res.* 35(suppl. 1), D391–D394. doi: 10.1093/nar/gkl791

Conflict of Interest Statement: The authors declare that the research was conducted in the absence of any commercial or financial relationships that could be construed as a potential conflict of interest.

frontiers in Microbiology

ORIGINAL RESEARCH
published: 18 September 2018
doi: 10.3389/fmicb.2018.02176

Relative Level of Bacteriophage Multiplication *in vitro* or in Phyllosphere May Not Predict *in planta* Efficacy for Controlling Bacterial Leaf Spot on Tomato Caused by *Xanthomonas perforans*

Botond Balogh[1†], Nguyen Thi Thu Nga[2] and Jeffrey B. Jones[1]*

[1] Plant Pathology Department, University of Florida, Gainesville, FL, United States, [2] Department of Plant Protection, Can Tho University, Can Tho, Vietnam

OPEN ACCESS

Edited by:
Robert Czajkowski,
University of Gdańsk, Poland

Reviewed by:
Leticia Veronica Bentancor,
Universidad Nacional de Quilmes (UNQ), Argentina
Grzegorz Wegrzyn,
University of Gdańsk, Poland

***Correspondence:**
Jeffrey B. Jones
jbjones@ufl.edu

†Present address:
Botond Balogh,
Nichino Europe, Co., Ltd.,
Cambridge, United Kingdom

Specialty section:
This article was submitted to Virology, a section of the journal Frontiers in Microbiology

Received: 30 June 2018
Accepted: 24 August 2018
Published: 18 September 2018

Citation:
Balogh B, Nga NTT and Jones JB (2018) Relative Level of Bacteriophage Multiplication in vitro or in Phyllosphere May Not Predict in planta Efficacy for Controlling Bacterial Leaf Spot on Tomato Caused by Xanthomonas perforans. Front. Microbiol. 9:2176. doi: 10.3389/fmicb.2018.02176

Following analysis of eight phages under *in vitro*, growth chamber and greenhouse conditions with the bacterial spot of tomato pathogen *Xanthomonas perforans,* there was no correlation between disease control efficacy and *in vitro* phage multiplication, *in vitro* bacterial suppression, or *in vivo* phage multiplication in the presence of the host, but there was a low correlation between phage persistence on the leaf surface and disease control. Two of the 8 virulent phages (ΦXv3-21 and ΦXp06-02) were selected for in depth analysis with two *X. perforans* (Xp06-2-1 and Xp17-12) strains. In *in vitro* experiments, phage ΦXv3-21 was equally effective in infecting the two bacterial strains based on efficiency of plating (EOP). Phage ΦXp06-02, on the other hand, had a high EOP on strain Xp06-2-1 but a lower EOP on strain Xp17-12. In several growth chamber experiments, ΦXv3-21 was less effective than phage ΦXp06-02 in reducing disease caused by strain Xp06-2-1, but provided little or no disease control against strain Xp17-12. Interestingly, ΦXp06-02 could multiply to significantly higher levels on the tomato leaf surface than phage ΦXv3-21. The leaf surface appears to be important in terms of the ability of certain bacteriophages to multiply in the presence of the bacterial host. ΦXv3-21, when applied to grapefruit leaves in combination with a bacterial host, was unable to multiply to high levels, whereas on tomato leaflets the phage multiplied exponentially. One plausible explanation is that the leaf surface may be an important factor for attachment of certain phages to their bacterial host.

Keywords: bacterial spot of tomato, *Xanthomonas perforans*, *Xanthomonas citri*, citrus canker, biological control

INTRODUCTION

Bacterial diseases are a major problem on crops in temperate, sub-tropical and tropical environments. Although disease control strategies are available for many bacterial-incited diseases, challenges exist that minimize the ability to control many bacterial pathogens. For most bacterial incited diseases, an integrated management strategy is used and includes plant resistance, biological

control, chemical control and various cultural practices to minimize inoculum (Obradovic et al., 2004, 2005).

In Florida, copper based compounds and antibiotics have been used to control bacterial spot of tomato and pepper. Streptomycin, an aminoglycoside antibiotic, was used extensively in the 1950s (Thayer and Stall, 1961). Following its initial use, in a matter of years, strains quickly developed resistance (Thayer and Stall, 1961). As a result, streptomycin no longer was effective in controlling bacterial spot of tomato and pepper and growers returned to using copper based bactericides. Management strategies for fire blight of apple and pear relied on streptomycin for many years (Cooksey, 1990; Manulis et al., 1998). Resistance to this antibiotic was detected in *Erwinia amylovora* strains and was determined to be associated with a plasmid, unlike in the bacterial spot pathogen *Xanthomonas euvesicatoria* in which resistance was associated with spontaneous mutation.

Although copper bactericides have been used extensively, copper resistance was not observed in *X. euvesicatoria* strains until 1983 (Marco and Stall, 1983) and the copper resistance was determined to be associated with a plasmid (Stall et al., 1986). Copper resistance has been found in diverse plant pathogens (Bender and Cooksey, 1986, 1987; Stall et al., 1986; Bender et al., 1990; Lee et al., 1994; Manulis et al., 1998; Basim et al., 1999; Canteros, 1999; Behlau et al., 2011). In most cases, copper resistance has been associated with plasmids (Bender and Cooksey, 1986, 1987; Stall et al., 1986; Bender et al., 1990; Behlau et al., 2011) and to a lesser extent copper resistance genes are associated with the chromosome (Lee et al., 1994; Basim et al., 1999; Behlau et al., 2017). Copper-tolerant strains of *X. euvesicatoria* were shown to be sensitive to copper bactericides when mixed with ethylene-bis-dithiocarbamates (Marco and Stall, 1983); unfortunately, during optimal disease conditions, copper-mancozeb has not been consistently effective in controlling bacterial spot nor in increasing yield (Jones and Jones, 1985; Obradovic et al., 2004).

Biological control as an alternative disease control strategy for bacterial diseases on tomato has focused extensively on using non-pathogenic microorganisms including Hrp-strains (pathogenic strains mutated in the Hrp-region and rendered non-pathogenic) of pathogens to suppress foliar or root pathogens in order to reduce disease (Frey et al., 1994; Liu, 1998; Wilson et al., 2002; Byrne et al., 2005; Ji et al., 2006; Hert, 2007; Jones et al., 2007; Obradovic et al., 2008; Iriarte et al., 2012). Plant growth-promoting rhizobacteria (PGPR) have been extensively tested for suppressing disease as a result of induction of plant defense responses in the plant (Obradovic et al., 2005; Ji et al., 2006). These approaches have achieved varying levels of success. Another approach consisted of using bacteriocin-producing strains that are inhibitory to pathogenic strains of a closely related organism (Chen and Echandi, 1984; Hert, 2007; Hert et al., 2009).

Bacteriophages have also been used as biological control agents (Jones et al., 2007). Mallmann and Hemstreet (1924) determined that liquid filtrate from black rot infected cabbage tissue inhibited growth of *X. campestris in vitro*. As research on bacteriophages progressed, their presence in other plant tissue was determined. Coons and Kotila (1925) isolated phages from various sources, such as rotting carrots, soil, and river water, that were inhibitory to *Erwinia carotovora* subsp. *carotovora* and *Agrobacterium tumefaciens*. Furthermore, they isolated phages from soil samples associated with "black leg" symptoms on potato (Kotila and Coons, 1925). The isolated phages inhibited the disease causal agent *E. carotovora* subsp. *atroseptica* and when co-inoculated with the pathogen prevented rotting of potato tubers. The first field trials were conducted by Thomas (1935) against Stewart's wilt of corn. In that study corn seeds infested with the pathogen *Pantoea stewartii* were treated with phages isolated from diseased plant material. This seed treatment was quite effective and resulted in a reduction in disease incidence. In that study treatment of *P. stewartii*-infected corn seed resulted in a reduction in disease incidence from 18 to 1.4%. Moore (1926) proposed using bacteriophages for disease control of bacterial plant pathogens. Over the years they have been used for several plant–bacterium pathosystems to demonstrate the efficacy of phages for disease control (Civerolo and Keil, 1969; Tanaka et al., 1990; Zaccardelli et al., 1992; Saccardi et al., 1993; Flaherty et al., 2000).

Bacteriophages offer an alternative to conventional management strategies for controlling plant diseases caused by bacterial pathogens (Civerolo, 1973; Tanaka et al., 1990; Gill et al., 2003; Jackson et al., 2004; Obradovic et al., 2005; Jones et al., 2006; Jones et al., 2007; Balogh et al., 2008; Obradovic et al., 2008; Fujiwara et al., 2011; Gašic et al., 2011; Murugaiyan et al., 2011). Although various studies showed that phage-therapy was plausible for controlling plant pathogenic bacteria associated with several systems, Okabe and Goto (1963) concluded that phages were not an effective control strategy. Various concerns as to their limitations have been discussed. Their narrow spectrum of activity against specific bacterial species is a concern in comparison to antibacterial materials, such as antibiotics, which have broad spectrum activity (Summers, 2005). Along with the narrow spectrum of activity, the probability that bacteria become resistant to individual phages via mutation is a real concern. Katznelson (1937) observed this, as well as Okabe and Goto (1963), and Vidaver (1976). The latter two viewed the possibility of mutation as a major impediment for use as a control strategy.

The environment in the phyllosphere is deleterious to phage resulting in precipitous declines in bacteriophage population (Civerolo and Keil, 1969; McNeil et al., 2001; Balogh, 2002; Balogh et al., 2003). This short-lived persistence on plant leaf surfaces is the major limiting factor for phage therapy in the phyllosphere. In the phyllosphere phages are exposed to deleterious factors, with their viability plummeting in a very short period of time. These factors include sunlight irradiation, especially in the UV-A and -B regions, ambient temperature, desiccation and exposure to certain chemical pesticides, such as copper-based bactericides that are commonly used for bacterial disease management (Iriarte et al., 2007). Of these factors, UV was found to be the most deleterious factor, especially in the early afternoon hours.

In biological control, maintaining high populations of biocontrol agents in relatively close proximity to the target bacterium is critical to their success (Johnson, 1994). Persistence of phage in the phyllosphere and rhizosphere has been a major

concern, given that phage therapy necessitates high densities of phage exist in close proximity to the target pathogen (Gill and Abedon, 2003). Phages must be present at a certain titer (i.e., threshold titer) relative to the target bacterium; at concentrations below this, phages will have a minimal impact on disease control. Balogh (2002) demonstrated that a threshold of 10^6 or 10^8 PFU/ml of *X. perforans* specific phage provided similar control of bacterial spot on tomatoes inoculated with 10^8 cfu/ml of *Xanthomonas perforans*, but phage applied at 10^4 PFU/ml was ineffective. Given the inability to persist for long periods on leaf surfaces and the requirement for high phage populations, long-term survival of phage on leaf surfaces requires different strategies for maintaining high phage concentrations.

Various approaches have been used to increase persistence in the phyllosphere. One approach, which involved applying phage to plants in the evening, was effective for maintaining high phage concentrations on the leaf surface for an extended period of time and was associated with improved disease control (Balogh et al., 2003). A second approach used was to mix phage suspensions with various compounds (formulations) to extend bacteriophage persistence on leaf surfaces (Balogh et al., 2003; Iriarte et al., 2007). Although formulations were identified and shown to be effective, phage levels still plummeted below detectable levels on leaves that were free of the target bacterium (Balogh, 2002; Balogh et al., 2003).

A third approach tested for enhancing persistence was to increase phage populations in the phyllosphere by multiplying on bacterial hosts that are not pathogens or pathogens that are impaired in virulence. This ability could potentially be used if phages are applied into an environment where a phage-sensitive bacterium is present, or where the phages and bacterial host are delivered together. On leaf surfaces, phages persist at high populations on infected leaves where there are high concentrations of the bacterial pathogen (phage host) than on leaf surfaces without the host (Iriarte et al., 2012). Boulè et al. (2011) and Svircev et al. (2005) utilized a different strategy in which a non-pathogen (*Pantoea agglomerans*) host to the phage was applied to apple flower blossoms to enhance phage populations that in turn would be present to infect and reduce population of *Erwinia amylovora*.

We have observed that bacteriophages behave differently on leaf surfaces than *in vitro*. Therefore, we present information that predicting the ability to control the bacterial pathogen on leaf surfaces based solely on *in vitro* results is not sufficient to predict efficacy *in planta*. In this study our goal was to monitor the population dynamics of bacteriophages and their interaction with their host bacterium in the phyllosphere. More specifically, we wanted to answer the following questions: Is there a difference between the ability of different phages to multiply in the phyllosphere? If so, is there a connection between success in *in planta* multiplication and disease control ability? Does the nature of the phyllosphere itself influence phage-bacterium interaction (i.e., do some plants support phage multiplication better than others)? And lastly, can we learn something from these studies that could be used for improving phage therapy for plant protection?

MATERIALS AND METHODS

Bacterial Strains and Bacteriophages

Bacterial strains and bacteriophages used in this study are listed in **Supplementary Table 2**.

Interaction of *Xanthomonas citri* subsp. *citri* and Its Bacteriophages on Grapefruit Foliage in the Greenhouse

Disease Control Studies

Two experiments were carried out at the greenhouse of the Department of Agriculture & Consumer Services, Division of Plant Industry, citrus canker 84 quarantine facility. Duncan grapefruit plants were heavily pruned and fertilized to induce the simultaneous production of a new flush that is susceptible to citrus canker infection. Three weeks later, uniform, new foliage emerged and was treated with one of three different single-phage suspensions (ΦXV3-21, ΦXaacF1, or ccΦ19-1, 5×10^9 PFU/mL, at 50 mL/plant) or with sterilized tap water. The treatments were applied in the evening using a hand-held sprayer, and then the plants were placed in white plastic bags. The following morning the bags were removed from the plants, and the plants were spray-inoculated with a bacterial suspension of *X. citri* strain Xac65 adjusted to 1×10^6 CFU/mL at the rate of 50 mL/plant. After inoculation the plants were placed inside the bags for an additional 24 h of high moisture. After removal from the bags and after the foliage was allowed to dry the plants were arranged in a completely randomized pattern on a greenhouse bench. The disease was assessed 3–4 weeks after inoculation. In the first experiment the phage suspensions were prepared by diluting high titer lysates, but because of concerns that the presence of nutrient broth in the phage lysate may contribute to increased disease severity, in the second experiment the phage lysates were concentrated in order to remove nutrient broth. The ratio of diseased leaf surface area was estimated using the Horsfall-Barratt (HB) scale (12). The HB values were converted to estimated mean percentages by using the Elanco Conversion Tables for Horsfall-Barratt Rating Numbers (Elanco Products Co., Indianapolis, IN, United States). Analysis of variance (ANOVA) and subsequent separation of sample means by Student-Newman-Keuls means comparison test ($P = 0.05$) was carried out using the software package ARM Revision 2018.3.

Population Dynamics Studies on Grapefruit and Tomato

In order to determine if bacteriophages ΦXV3-21, ΦXaacF1, and ccΦ19-1 are able to multiply on the grapefruit foliage in the presence of their host, Xac65, "Duncan" grapefruit plants were sprayed with a mixture of the three phages at low concentration (5×10^6 PFU/mL; 50 mL/plant), immediately followed by application of the bacterial suspension at a much higher concentration (1×10^8 cfu/mL) or with sterilized tap water. Phage populations were monitored by removing three leaves 9 h after application, recovering the phages from the leaves and determining concentrations. In

order to determine populations of the individual phages, the leaf washes were plated on three Xac strains that specifically detected each of the three phages. Each strain was only sensitive to one of three phages. Strain Xac41 was used for specific detection of ΦXaacF1, Xac15 for ccΦ19-1 and Xac30 for ΦXv3-21. Tomato trials were conducted using the same methodology, using "Bonny Best" tomato cultivar.

Interaction of *Xanthomonas perforans* and Its Phages *in vitro* and *in planta*

Greenhouse Disease Control Trials

The objective of these trials was to evaluate the efficacy of 8 individual phages to reduce tomato bacterial spot disease caused by *X. perforans* strain Xp06-2-1. Young "Bonny Best" tomato plants were dipped in phage suspension (5×10^7 PFU/mL), and 2 h later spray-inoculated with Xp06-2-1 (5×10^6 CFU/mL). After inoculation the plants were placed in plastic bags, and kept in a growth chamber for 36 h. Afterward, they were transported into a greenhouse and taken out of the bags. Disease severity was assessed 10–14 days after inoculation.

In planta Phage Persistence and Multiplication Assay

Eight *Xanthomonas perforans* phages were evaluated for their ability to persist and to multiply on the tomato phyllosphere. Plants were dipped in phage suspensions (5×10^6 PFU/ml) and then spayed with water or a bacterial suspension of *X. perforans* strain Xp06-2-1 adjusted to 10^8 CFU/mL. Phage titer was determined at the beginning and after overnight incubation (16 h). Plants were bagged throughout this experiment.

In vitro Phage Multiplication and Bacterial-Growth-Suppression Assays

Individual phages, at 10^7 PFU/mL were incubated for 16 h with a bacterial suspension of *X. perforans* strain Xp06-2-1 adjusted to 10^8 CFU/mL. The final and original phage titers were compared to determine the amount of phage multiplication. The final bacterial concentrations were compared between phage-infected and non-infected bacterial cultures to determine the effect of individual phages in reducing bacterial populations.

RESULTS

Disease Control Trials on Grapefruit

Three bacteriophages, ΦXv3-21, ccΦ19-1, and ΦXaacF1, all able to lyse *X. citri* subsp. *citri* strain Xac65, were evaluated for their ability to reduce citrus canker incited by Xac65 in grapefruit in two greenhouse trials. Of the three phages, only ΦXaacF1 resulted in significant disease reduction: 58 and 69% reduction in the two experiments (**Table 1**). Plants treated with ccΦ19-1 had a slight but non-significant disease reduction in both trials (10 and 31%), whereas ΦXv3-21 appeared to increase the disease severity slightly (−31 and −21%).

Interaction of Three Bacteriophages and Their Host, *X. citri* subsp. *citri* Strain Xac65 in the Grapefruit Phyllosphere

A mixture of the above mentioned three bacteriophages was sprayed on grapefruit plants, which were immediately sprayed with a suspension of Xac65 or tap water, and the phage populations were monitored over the next 9 h. All three bacteriophages declined rapidly after application to the grapefruit leaves without host bacterium being present with more than a 95% reduction in their populations over the 9 h period (**Table 2**). However, in the presence of the host, Xac65, all three phages showed some signs of multiplication in at least one of the two experiments, based on their ability to maintain higher populations after a 9 h period compared to phages without a bacterial host. However, their responses varied greatly. ΦXv3-21 and ccΦ19-1 populations dropped even in the presence of Xac65, although not as quickly as without their host (80% reduction with host vs. 99% without it for ΦXv3-21 in experiment 2, and 89 vs. 97% for ccΦ19-1). ΦXaacF1, on the other hand, actually increased in numbers in the presence of its host: 95% reduction vs. 30% increase in exp. 1, and 94% reduction vs. 239% increase in exp. 2. Altogether, ΦXaacF1 persisted better than the other two phages without a host and multiplied to a limited extent in the presence of the host.

Phages were applied in equal concentration, so the original ratio of the three phages was 33/33/33. In the absence of the host,

TABLE 1 | Comparative efficacy of three bacteriophages, applied as foliar preventative sprays, on citrus canker disease development, incited by phage-sensitive *Xanthomonas citri* subsp. *citri* strain Xac65, as measured by disease severity.

	Mean citrus canker severity [%]				Reduction in severity - Abbott [%]	
	Trial 1 – 25 DAT[x,y]		Trial 2 – 16 DAT		Trial 1 – 25 DAT	Trial 2 – 16 DAT
Untreated	44.5	a	21.7	ab	0.0	0.0
ΦXv3-21	58.4	a	26.2	a	−31.2	−20.6
ccΦ19-1	40.0	a	14.9	ab	10.1	31.4
ΦXaacF1	18.8	b	6.8	b	57.9	68.8
p(F)[z]	0.0200		0.0395			

[z] *p(F) = Probability that there are no differences in treatment means according to analysis of variance.*
[y] *Means within the same column followed by the same letter are not significantly different (P = 0.05, Student-Newman-Keuls).*
[x] *DAT = days after treatment.*

TABLE 2 | Population dynamics of three citriphages in the grapefruit phyllosphere in the presence or absence of their host bacterium, *Xanthomonas citri* subsp. *citri* strain Xac65.

Grapefruit												
	Experiment 1						**Experiment 2**					
Bacteriophage populations on grapefruit	ccΦ19-1[z] [Xac15]		ΦXv3-21 [Xac30]		ΦXaacF1 [Xac41]		ccΦ19-1 [Xac15]		ΦXv3-21 [Xac30]		ΦXaacF1 [Xac41]	
Phage populations recovered from the leaves [log10 pfu/leaf][y]												
0 h	3.23	a	3.91	a	4.29	a	3.90	a	4.83	a	4.21	b
9 h| without host	0.38	b	2.14	b	2.91	b	1.51	b	2.66	c	2.93	c
9 h| with host	0.00	b	1.4	b	4.19	a	3.09	a	3.78	b	4.72	a
Relative changes in phage populations over time [% increase vs. 0 h]												
9 h| without host	−100		−98		−95		−99		−97		−94	
9 h| with host	−100		−99		30		−80		−89		239	
Relative frequency in residual phage population mixture [%]												
9 h| without host	4		29		67		12		13		75	
9 h| with host	0		1		99		7		4		89	

[z] *Bacteriophages were exclusively detected on the bacterial stains shown in parentheses.*
[y] *Means within the same column followed by the same letter are not significantly different (P = 0.05, Student-Newman-Keuls).*

ΦXaacF1 came to dominate the declining phage population and made up 67–75% of the recoverable phage population after 9 h of incubation (**Table 2**). In the presence of the host, ΦXaacF1 dominated even more constituting 89–99% of the total phage population. Of these three phages, only ΦXaacF1, which was most successful in multiplying on its host bacterium on the plant surface, was able to control citrus canker disease progress (**Table 1**).

Interaction of Three Bacteriophages With *Xanthomonas citri* subsp. *citri* Strain Xac65 in the Tomato Phyllosphere

We speculated that the waxy grapefruit leaf provides a less than ideal environment for the bacteriophages. Thus we decided to look at the interaction of the same three phages and their bacterial host in a different environment, the phyllosphere of the incompatible host, tomato.

Without the host all three phages deteriorated in a 9-h period, but to a much lesser degree than in the grapefruit leaves, 24–66% population reduction (**Table 3**). ΦXaacF1 suffered the worst decline on tomato in both experiments, but still 34 and 43% of its populations were recovered after 9 h (**Table 3**). Additionally, in tomato all three phages actually increased in numbers in the presence Xac65. ΦXv3-21 produced the slightest (and non-significant) increase: 23 and 78% increase in two experiments. ccΦ19-1 populations increased by 82 and 327%. ΦXaacF1 had a spectacular 169 and 301-fold population increase in experiments 1 and 2, respectively. These results suggest that tomato provides a much better environment for the phages. As for the composition of the phage mixture: in the absence of the hosts, the ratio stayed close to the originally applied 33:33:33 ratio. But due to the unequal capacities for multiplication in the presence of the host, ΦXaacF1 came to dominate the population providing 97 and 99% of the total in the two experiments.

Interaction of Bacteriophages and Their Host, *Xanthomonas perforans*, *in vitro* and in the Phyllosphere

Two phages, ΦXp06-02 and ΦXv3-21, were chosen for the following experiments. ΦXp06-02 is a narrow host-range phage isolated from tomato bacterial spot lesions (**Supplementary Table 1**). Phage ΦXv3-21, on the other hand, has broad host range, and is able to lyse a number of *X. perforans* strains (**Supplementary Table 1**) as well as other xanthomonads, such as *X. citri* subsp. *citri* strains (**Table 1**). In greenhouse tests, ΦXp06-02 was more effective in controlling tomato bacterial spot than ΦXv3-21 (**Table 5**). Our aim was to set up a situation in which the two phages are interacting with a strain that both can lyse; and a strain on which ΦXp06-02 is compromised. Xp06-2-1 was chosen as the sensitive strain and Xp17-12 as the strain on which ΦXv3-21 was only effective based on *in vitro* activity. Phage ΦXv3-21 had similar efficiency of plating (EOP) on both bacterial strains (meaning that they were equally successful in infecting both strains). ΦXp06-02 on the other hand, had about a 5% EOP on Xp17-12 compared to on Xp06-2-1 (meaning that it was largely unsuccessful in infecting/lysing this strain).

TABLE 3 | Population dynamics of three citriphages in the tomato phyllosphere in the presence or absence of their host bacterium *Xanthomonas citri* subsp. *citri* strain Xac65.

Tomato												
	Experiment 1						**Experiment 2**					
Bacteriophage populations on tomato	ccΦ19-1[z] [Xac15]		ΦXv3-21 [Xac30]		ΦXaacF1 [Xac41]		ccΦ19-1 [Xac15]		ΦXv3-21 [Xac30]		ΦXaacF1 [Xac41]	
Phage populations recovered from the leaves [log10 pfu/leaflet][y]												
0 h	6.10	b	5.69	ab	5.29	b	6.28	ab	5.73	–	5.35	b
9 h| without host	5.98	b	5.29	b	4.82	b	5.99	b	5.50	–	4.98	c
9 h| with host	6.73	a	5.94	a	7.52	a	6.54	a	5.82	–	7.83	a
Relative changes in phage populations over time [% increase vs. 0 h]												
9 h| without host	−24		−60		−66		−49		−41		−57	
9 h| with host	327		78		16,882		82		23		30,100	
Relative frequency in residual phage population mixture [%]												
9 h| without host	49		27		24		33		38		28	
9 h| with host	2		1		97		1		0		99	

[z]Bacteriophages were exclusively detected on the bacterial stains shown in parentheses.
[y]Means within the same column followed by the same letter are not significantly different (P = 0.05, Student-Newman-Keuls).

ΦXv3-21 provided slight, but mostly a significant level of control against both strains, Xp06-2-1 and Xp17-12, whereas ΦXp06-02 provided excellent control of Xp06-2-1 and slight-to-no control of Xp17-12 (**Table 4**). The fact that ΦXp06-02 was effective against Xp06-2-1, but not Xp17-12, was similar to the EOP results.

The interaction of these two phages with these two *X. perforans* strains in the phyllosphere was also assessed (**Figure 1**). ΦXp06-02 populations increased to significantly higher numbers in the tomato phyllosphere in the presence of Xp06-2-1 cells. However, in the presence of Xp17-12 its populations plummeted, suggesting that it was not able to multiply on this strain. ΦXv3-21 populations were intermediate, but this phage had slightly higher populations on Xp06-2-1 than on Xp17-12. In essence, in this system, the phage population size correlated with disease control efficacy: the ΦXp06-02/Xp06-2-1 interaction resulted in the highest phage population on tomato, and this was also the interaction with the lowest disease severity. On the other hand, the ΦXp06-02/Xp17-12 had the lowest phage populations and the worst disease control.

Xanthomonas perforans Phages – Correlation of Disease Control Efficacy and *in vitro*/*in vivo* Properties

The objective of the next set of experiments was to determine if some measurable *in vitro* or *in vivo* phage properties could be used to predict the actual disease control capacity of individual phages. Eight phages were evaluated for their ability to control tomato bacterial spot disease on "Bonny Best" tomato plants caused by *X. perforans* strain Xp06-2-1 under greenhouse conditions (**Table 5**). The following four properties were determined for each phage: (1) the efficacy of multiplying *in vitro* on Xp06-2-1 in liquid culture (i.e., how easy is it to grow the phage on the target bacterium); (2) the efficacy of suppressing Xp06-2-1 growth *in vitro* in liquid culture; (3) the ability to persist *in planta* on "Bonny Best" plants without the presence of a host bacterium; and (4) the ability to multiply *in planta* on "Bonny Best" plants in the presence of Xp06-2-1. These properties were correlated with the measured disease control efficacy (**Figure 2**), and all but ability to persist on the leaf surface showed any apparent correlation with it (i.e., none of these properties had predictive power for the actual disease control activity of the phage). Persistence on the leaf surface had a low correlation with ability to control disease.

DISCUSSION

In a previous study we demonstrated that disease control efficacy increases if phages persist longer in the target environment, the phyllosphere (Balogh et al., 2003). Several approaches were used to increase longevity including the use of protective formulations, sunlight avoidance or use of propagating hosts (Balogh, 2002; Balogh et al., 2003; Iriarte et al., 2007, 2012). Basically the net change in phage populations is the product

TABLE 4 | Effect of phage treatments on tomato bacterial spot disease severity, caused by *Xanthomonas perforans* strains (Xp06-2-1 or Xp17-12), as measured by the Horsfall-Barratt scale.

	Horsfall-Barratt Ratings [1–12]					
	Experiment 1		Experiment 2		Experiment 3	
Treatment\pathogen	Xp06-2-1[z]	Xp17-12	Xp06-2-1	Xp17-12	Xp06-2-1	Xp17-12
Untreated	4.03 a	4.00 a	4.57 a	4.69 a	4.35 a	4.89 a
ΦXv3-21	3.33 ab	3.00 b	3.61 b	4.03 b	3.42 b	3.72 b
ΦXp06-02	3.00 b	3.81 ab	2.42 c	3.95 b	2.36 c	4.22 ab

[z]*Means within the same column followed by the same letter are not significantly different (P = 0.05, Student-Newman-Keuls).*

TABLE 5 | Efficacy of 8 *Xanthomonas perforans*-specific bacteriophages in reducing disease severity of bacterial spot on tomato caused by *X. perforans* strain Xp06-2-1.

	Disease control [Abbott %]			
	Trial 1	Trial 2	Trial 3	*Average*
ΦXv3-1	17	48	–2	***21***
ΦXp06-01	5	40	30	***25***
ΦXv3-3	29	48	36	***38***
ΦXv3-21	43	49	27	***40***
ΦXacm2004-11	40	41	na	***41***
ΦXp06-04	58	52	44	***51***
ΦXp06-02	53	62	47	***54***
ΦXv3-16-1h	54	60	53	***56***

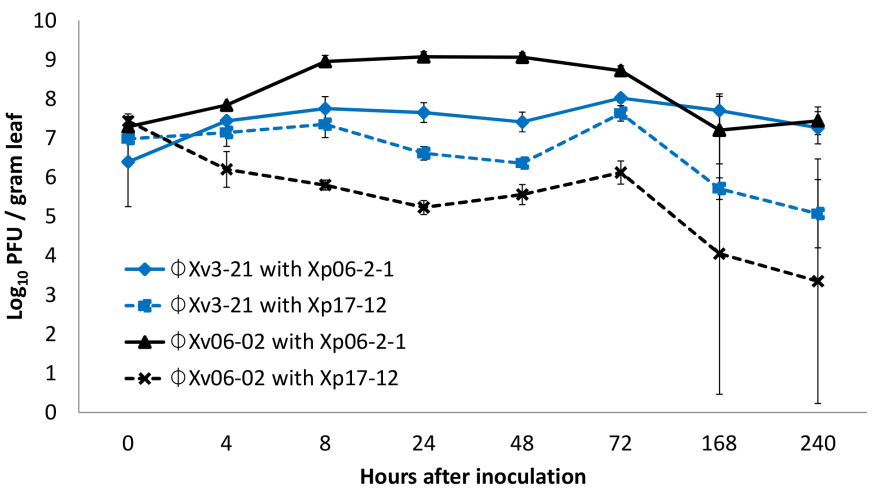

FIGURE 1 | Populations of phages ΦXv3-21 and ΦXp06-02 in the tomato phyllosphere in the presence of *Xanthomonas perforans* strains Xp06-21 or Xp17-12.

of two opposing forces: an increase due to multiplication on host bacterium and a decrease due to many different factors including sunlight irradiation, desiccation and rain-leaching (Balogh et al., 2003; Iriarte et al., 2007). Thus, increasing overall longevity of phages requires protecting the bacteriophage against harmful factors and helping in multiplication.

Our intent was to demonstrate that multiplication on leaf surfaces is important for disease control and that the traditional *in vitro* plaque assays are not sufficient in determining what phages need to be used, because they represent an ideal situation for phage attachment that does not exist in the harsh reality of plant surfaces. We demonstrated that EOP is not the only factor that is required for determining the ability of phage to persist on leaf surfaces when the bacterial host is present. We also showed with two different phages which had similar high EOPs, only one multiplied to high concentrations on tomato leaves while the other dropped to low levels (**Figure 1**). Therefore, predicting the ability to multiply on leaf surfaces cannot be determined strictly based on EOP as it is only a good predictor

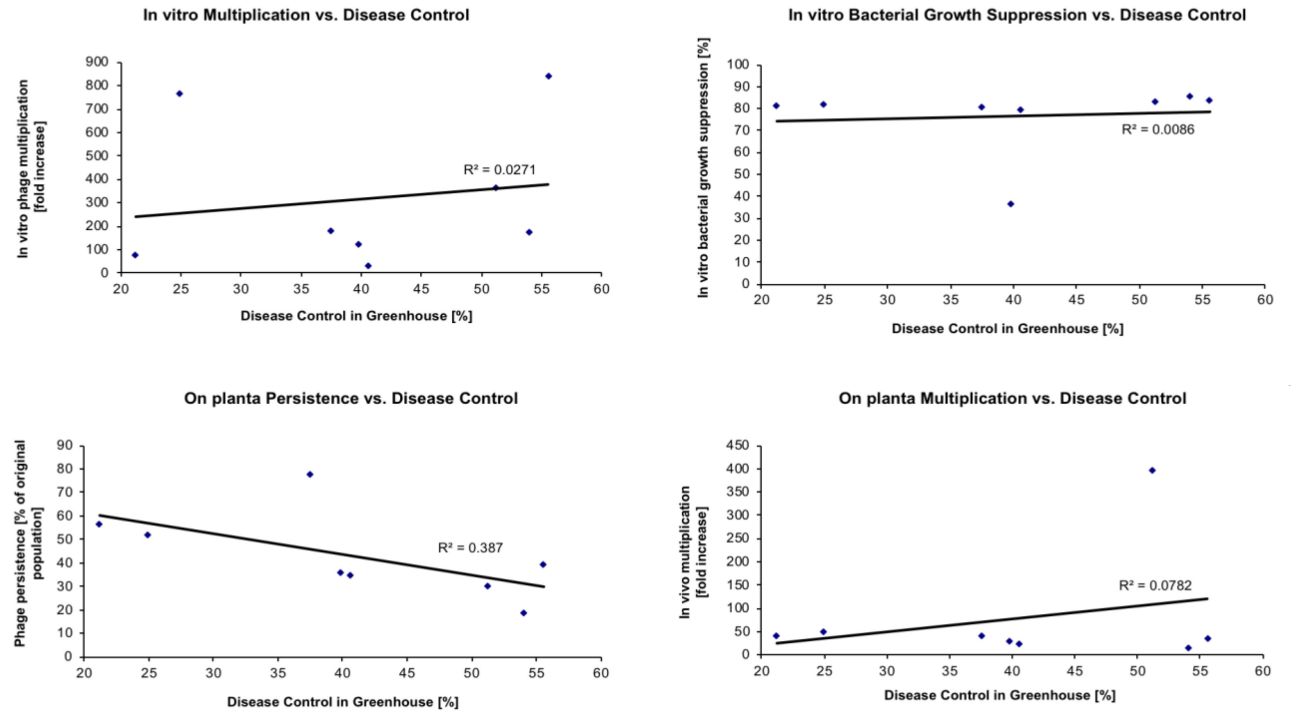

FIGURE 2 | Relationship between phage characteristics and their disease control efficacy in greenhouse. Phages listed in **Table 5** were used in this study with *X. perforans* strain Xp06-2-1. The identity of the specific phage can be determined based on the disease control values in **Table 5**.

for those phages-bacterial host combinations where the EOP is low.

We also similarly demonstrated on grapefruit leaves that phage populations increased with certain phage-host combinations and not with others. Interestingly ΦXv-3-21 multiplied on tomato leaflets when the bacterial host was present, but gradually declined on grapefruit leaves with or without a bacterial host. Possibly the leaf surface may be a factor for multiplication of certain phages or perhaps the bacterial host was the contributing factor. Neither one can be ruled out as two different bacterial hosts were used.

We demonstrated that if host bacterium is present on leaves some phages can persist much better. Furthermore, based on these limited tests, it appears that phages that are more successful in multiplying in the phyllosphere environment and are able to keep up higher populations and persist longer as long as their host is present, are able to provide effective disease suppression (**Table 4**). It was also apparent based on these studies that bacterial populations were not affected by the presence of the phage. So using propagating bacteria to maintain phages in the phyllosphere appears to be a promising approach that is worth pursuing further. Actually, it is possible to imagine that future phage therapy products will not only include a mixture of phages, but also one or more propagating bacteria.

And what kind of bacterium would be feasible to maintain phages in the phyllosphere? It should be able to colonize the target plant well enough to build up and maintain sufficient populations, while not causing any adverse effects on plant development. It could be an avirulent strain of the target pathogen (as explored by Tanaka et al. (1990) with *Ralstonia solanacearum*) or a non-pathogenic relative of the target organism (as explored by Svircev et al. with *Erwinia amylovora* and *Pantoea agglomerans*). In case of *Xanthomonas* spp., however, these approaches may not work: although avirulent mutants of *X. perforans* are able to colonize tomato plants successfully (Iriarte et al., 2007) phages are not able to persist at high concentrations. Furthermore, non-pathogenic xanthomonads are not found frequently as epiphytes (personal observations).

It is also interesting to consider if bacterial populations were not affected by the presence of the phage, how does phage therapy reduce disease? In the case of the citrus canker pathosystem, the only one of these three phages that could control citrus canker disease progress, ΦXaacF1, was most successful in multiplying on its host bacterium on the plant surface, and was the only one able to actually increase its populations in the phyllosphere. Interestingly, it appeared during electron microscopic studies that ΦXaacF1 was able to attach to Xac65 in deionized water, while ΦXv3-21 and ccΦ19-1 could only do it in nutrient broth, a complex medium (Balogh, personal observation). Consequently, it seems possible that ΦXaacF1 does not require any metal ion cofactors for attachment as many other phages do (including ΦXv3-21 and ccΦ19-1), and because of this it is readily able to multiply in the low ionic phyllosphere environment. And this would not be a surprise, since ΦXaacF1 was isolated from citrus

leaf lesions (Balogh, 2006), and so it probably had an evolutionary pressure to be less needy.

Whatever the reason for a phage's ability to successfully multiply in the phyllosphere, it is likely that phages originating from the phyllosphere will be in general better adapted to this environment. And if the above connection is true, meaning better phyllosphere multiplication translates to better disease control, then phyllosphere phages are likely to be better biocontrol agents than other phages. Also, if multiplication is important for disease control then the traditional *in vitro* plaque assays are not sufficient in determining what phages need to be used, because they represent an ideal situation for phage attachment that does not exist in the harsh reality of plant surfaces. Our results also showed that the success of phage multiplication depends on the plant, as well. In this case two phages that were unable to multiply on grapefruit sufficiently to at least maintain current population levels were able to do so on tomato. And the third phage, which increased in numbers on grapefruit, produced a much bigger population increase on tomato (single vs. triple digit increase in grapefruit and tomato, respectively). This finding implies that phage therapy will be more successful on some plants than on others.

AUTHOR CONTRIBUTIONS

BB and JJ conceived the project. All authors oversaw the experiments, performed data analyses and interpreted them, and wrote and approved the final manuscript.

ACKNOWLEDGMENTS

This research was supported by the USDA special grant (JJ, R. E. Stall, and X. Sun, USDA 2001-34446-10781-S).

SUPPLEMENTARY MATERIAL

The Supplementary Material for this article can be found online at: https://www.frontiersin.org/articles/10.3389/fmicb.2018.02176/full#supplementary-material

REFERENCES

Balogh, B. (2002). *Strategies of Improving the Efficacy of Bacteriophages for Controlling Bacterial Spot of Tomato*. MS thesis, University of Florida, Gainesville, FL.

Balogh, B. (2006). *Characterization and Use of Bacteriophages Associated with Citrus Bacterial Pathogens for Disease Control*. Ph.D. Dissertation. Gainesville, FL: University of Florida.

Balogh, B., Canteros, B. I., Stall, K. E., and Jones, J. B. (2008). Control of citrus canker and citrus bacterial spot with bacteriophages. *Plant Dis.* 92, 1048–1052. doi: 10.1094/PDIS-92-7-1048

Balogh, B., Jones, J. B., Momol, M. T., Olson, S. M., Obradovic, A. O., King, P., et al. (2003). Improved efficacy of newly formulated bacteriophages for management of bacterial spot on tomato. *Plant Dis.* 87, 949–954. doi: 10.1094/PDIS.2003.87.8.949

Basim, H., Stall, R. E., Minsavage, G. V., and Jones, J. B. (1999). Chromosomal gene transfer by conjugation in the plant pathogen *Xanthomonas axonopodis* pv. *vesicatoria*. *Phytopathology* 1999, 1044–1049. doi: 10.1094/PHYTO.1999.89.11.1044

Behlau, F., Canteros, B. I., Minsavage, G. V., Jones, J. B., and Graham, J. H. (2011). Molecular characterization of copper resistance genes from *Xanthomonas citri* subsp. *citri* and *Xanthomonas alfalfae* subsp. *citrumelonis*. *Appl. Environ. Microbiol.* 77, 4089–4096. doi: 10.1128/AEM.03043-10

Behlau, F., Gochez, A. M., Lugo, A. J., Elibox, W., Minsavage, G. V., Potnis, N., et al. (2017). Characterization of a unique copper resistance gene cluster in *Xanthomonas campestris* pv. *campestris* isolated in Trinidad, West Indies. *Eur. J. Plant Pathol.* 147, 671–681. doi: 10.1007/s10658-016-1035-2

Bender, C. L., and Cooksey, D. A. (1986). Indigenous plasmids in *Pseudomonas syringae* pv. *tomato*: conjugative transfer and role in copper resistance. *J. Bacteriol.* 165, 534–541. doi: 10.1128/jb.165.2.534-541.1986

Bender, C. L., and Cooksey, D. A. (1987). Molecular cloning of copper resistance genes from *Pseudomonas syringae* pv. *tomato*. *J. Bacteriol.* 169, 470–474. doi: 10.1128/jb.169.2.470-474.1987

Bender, C. L., Malvick, D. K., Conway, K. E., George, S., and Pratt, P. (1990). Characterization of pXV10A, a copper resistance plasmid in *Xanthomonas campestris* pv. *vesicatoria*. *Appl. Environ. Microbiol.* 56, 170–175.

Boulè, J., Sholberg, P. L., Lehman, S. M., O'Gorman, D. T., and Svircev, A. M. (2011). Isolation and characterization of eight bacteriophages infecting *Erwinia amylovora* and their potential as biological control agents in British Columbia, Canada. *Can. J. Plant Pathol.* 33, 308–317. doi: 10.1080/07060661.2011.588250

Byrne, J. M., Dianese, A. C., Ji, P., Campbell, H. L., Cuppels, D. A., Louws, F. J., et al. (2005). Biological control of bacterial spot of tomato under field conditions at several locations in North America. *Biol. Control* 32, 408–418. doi: 10.1016/j.biocontrol.2004.12.001

Canteros, B. I. (1999). "Copper resistance in *Xanthomonas campestris* pv. *citri*. Plant pathogenicbacteria," in *Proceedings of the International Society of Bacteriology*, ed. A. Mahadevan (Chennai: Centre for Advanced Study in Botany, University of Madras), 455–459.

Chen, W. Y., and Echandi, E. (1984). Effects of avirulent bacteriocin-producing strains of *Pseudomonas solanacearum* on the control of bacterial wilt of tobacco. *Plant Pathol.* 33, 245–253. doi: 10.1111/j.1365-3059.1984.tb02646.x

Civerolo, E. L., and Keil, H. L. (1969). Inhibition of bacterial spot of peach foliage by *Xanthomonas pruni* bacteriophage. *Phytopathology* 59, 1966–1967.

Civerolo, E. L. (1973). Relationship of *Xanthomonas pruni* bacteriophages to bacterial spot disease in prunus. *Phytopathology* 63, 1279–1284.

Cooksey, D. A. (1990). Genetics of bactericide resistance in plant pathogenic bacteria. *Annu. Rev. Phytopathol.* 28, 201–219. doi: 10.1146/annurev.py.28.090190.001221

Coons, G. H., and Kotila, J. E. (1925). The transmissible lytic principle (bacteriophage) in relation to plant pathogens. *Phytopathology* 15, 357–370.

Flaherty, J. E., Jones, J. B., Harbaugh, B. K., Somodi, G. C., and Jackson, L. E. (2000). Control of bacterial spot on tomato in the greenhouse and field with h-mutant bacteriophages. *HortScience* 35, 882–884.

Frey, P., Prior, P., Marie, C., Kotoujansky, A., Trigalet-Demery, D., and Trigalet, A. (1994). Hrp- mutants of *Pseudomonas solanacearum* as potential biocontrol agents of tomato bacterial wilt. *Appl. Environ. Microbiol.* 60, 3175–3181.

Fujiwara, A., Fujisawa, M., Hamasaki, R., Kawasaki, T., Fujie, M., and Yamada, T. (2011). Biocontrol of *Ralstonia solanacearum* by treatment with lytic bacteriophages. *Appl. Environ. Microbiol.* 77, 4155–4162. doi: 10.1128/AEM.02847-10

Gašic, K., Ivanovic, M. M., Ignjatov, M., Calic, A., and Obradovic, A. (2011). Isolation and characterization of *Xanthomonas euvesicatoria* bacteriophages. *J. Plant Pathol.* 93, 415–423. doi: 10.4454/jpp.v93i2.1197

Gill, J. J., and Abedon, S. T. (2003). *Bacteriophage Ecology and Plants*. doi: 10.1094/APSnetFeature-2003-1103

Gill, J. J., Svircev, A. M., Smith, R., and Castle, A. J. (2003). Bacteriophages of *Erwinia amylovora*. *Appl. Environ. Microbiol.* 69, 2133–2138.

Hert, A. P. (2007). *Evaluation of Bacteriocins in Xanthomonas perforans for Use in Biological Control of Xanthomonas euvesicatoria*. Ph.D. thesis, University of Florida, Gainesville, FL.

Hert, A. P., Marutani, M., Momol, M. T., Roberts, P. D., Olson, S. M., and Jones, J. B. (2009). Suppression of the bacterial spot pathogen *Xanthomonas euvesicatoria* on tomato leaves by an attenuated mutant of *Xanthomonas perforans*. *Appl. Environ. Microbiol.* 75, 3323–3330. doi: 10.1128/AEM.02399-08

Iriarte, F. B., Balogh, B., Momol, M. T., Smith, L. M., Wilson, M., and Jones, J. B. (2007). Factors affecting survival of bacteriophage on tomato leaf surfaces. *Appl. Environ. Microbiol.* 73, 1704–1711. doi: 10.1128/AEM.02118-06

Iriarte, F. B., Obradovic, A., Wernsing, M. H., Jackson, L. E., Balogh, B., Hong, J. A., et al. (2012). Soil-based systemic delivery and phyllosphere in vivo propagation of bacteriophages:two possible strategies for improving bacteriophage efficacy for plant disease control. *Bacteriophage* 2, 215–224. doi: 10.4161/bact.23530

Jackson, L. E., Jones, J. B., Momol, M. T., and Ji, P. (2004). "Bacteriophage: a viable bacteria control solution," in *Proceedings of the. First Internat Symposiums Tomato Diseases Orlando*, Orlando, FL, 21–24.

Ji, P., Campbell, H. L., Kloepper, J. W., Jones, J. B., Suslow, T. V., and Wilson, M. (2006). Integrated biological control of bacterial speck and spot of tomato under field conditions using foliar biological control agents and plant growth-promoting rhizobacteria. *Biol. Control.* 36, 358–367. doi: 10.1016/j.biocontrol.2005.09.003

Johnson, K. B. (1994). Dose–response relationships and inundative biological control. *Phytopathology* 84, 780–784. doi: 10.1094/Phyto-84-780

Jones, J. B., Jackson, L. E., Balogh, B., Obradovic, A., Iriarte, F. B., and Momol, M. T. (2007). Bacteriophages for plant disease control. *Annu. Rev. Phytopathol.* 45, 245–262. doi: 10.1146/annurev.phyto.45.062806.094411

Jones, J. B., Iriarte, F. B., Obradovic, A., Balogh, B., Momol, M. T., and Jackson, L. E. (2006). "Management of bacterial spot on tomatoes with bacteriophages," in *Procceedings of the 1st International Symposium on Biological Control of Bacterial Plant Diseases*, Darmstadt, 408:154.

Jones, J. B., and Jones, J. P. (1985). The effect of bactericides, tank mixing time and spray schedule on bacterial leaf spot of tomato. *Proc. Fla. State Hortic. Soc.* 98, 244–247.

Katznelson, H. (1937). Bacteriophage in relation to plant diseases. *Bot. Rev.* 3, 499–521. doi: 10.1007/BF02870486

Kotila, J. E., and Coons, G. H. (1925). Investigations on the blackleg disease of potato. *Mich. Agric. Exp. Stn. Tech. Bull.* 67, 3–29.

Lee, Y. A., Hendson, M., Panopoulos, N. J., and Schroth, M. N. (1994). Molecular cloning, chromosomal mapping, and sequence analysis of copper resistance genes from *Xanthomonas campestris* pv. *juglandis*: homology with small blue copper proteins and multicopper oxidase. *J. Bacteriol.* 176, 173–188. doi: 10.1128/jb.176.1.173-188.1994

Liu, T. (1998). *Biological Control with Tomato Bacterial Spot with Hrp- Mutants of Xanthomonas campestris pv. Vesicatoria*. MS thesis, University of Florida, Gainesville, FL.

Mallmann, W. L., and Hemstreet, C. J. (1924). Isolation of an inhibitory substance from plants. *J. Agric. Res.* 599–602.

Manulis, S., Zutra, D., Kleitman, F., Dror, O., David, I., Zilberstaine, M., et al. (1998). Distribution of streptomycin-resistant strains of *Erwinia amylovora* in Israel and occurrence of blossom blight in the autumn. *Phytoparasitica* 26, 223–230. doi: 10.1007/BF02981437

Marco, G. M., and Stall, R. E. (1983). Control of bacterial spot of pepper initiated by strains of *Xanthomonas campestris* pv. *vesicatoria* that differ in sensitivity to copper. *Plant Dis.* 67, 779–781. doi: 10.1094/PD-67-779

McNeil, D. L., Romero, S., Kandula, J., Stark, C., Stewart, A., and Larsen, S. (2001). Bacteriophages: a potential biocontrol agent against walnut blight (*Xanthomonas campestris* pv. *juglandis*). *N. Z. Plant Prot.* 54, 220–224.

Moore, E. S. (1926). D'Herelle's bacteriophage in relation to plant parasites. *S. Afr. J. Sci.* 23:306.

Murugaiyan, S., Bae, J. Y., Wu, J., Lee, S. D., Um, H. Y., Choi, H. K., et al. (2011). Characterization of filamentous bacteriophage PE226 infecting *Ralstonia solanacearum* strains. *J. Appl. Microbiol.* 110, 296–303. doi: 10.1111/j.1365-2672.2010.04882.x

Obradovic, A., Jones, J. B., Momol, M. T., Balogh, B., and Olson, S. M. (2004). Management of tomato bacterial spot in the field by foliar applications of bacteriophages and SAR inducers. *Plant Dis.* 88, 736–740. doi: 10.1094/PDIS.2004.88.7.736

Obradovic, A., Jones, J. B., Momol, M. T., Olson, S. M., Jackson, L. E., Balogh, B., et al. (2005). Integration of biological control agents and systemic acquired resistance inducers against bacterial spot on tomato. *Plant Dis.* 89, 712–716. doi: 10.1094/PD-89-0712

Obradovic, A., Jones, J. B., Balogh, B., and Momol, M. T. (2008). "Integrated management of tomato bacterial spot," in *Integrated Management of Plant Diseases Caused by Fungi, Phytoplasma and Bacteria*, eds A. Ciancio and G. Mukerji (Berlin: Springer Science + Business Media BV), 211–223.

Okabe, N., and Goto, M. (1963). Bacteriophages of plant pathogens. *Annu. Rev. Phytopathol.* 1963, 397–418. doi: 10.1146/annurev.py.01.090163.002145

Saccardi, A., Gambin, E., Zaccardelli, M., Barone, G., and Mazzucchi, U. (1993). *Xanthomonas campestris* pv. *pruni* control trials with phage treatments on peaches in the orchard. *Phytopathol. Mediterr.* 32, 206–210.

Stall, R. E., Loschke, D. C., and Jones, J. B. (1986). Linkage of copper resistance and avirulence loci on a self-transmissible plasmid in *Xanthomonas campestris* pv. *vesicatoria*. *Phytopathology* 76, 240–243. doi: 10.1094/Phyto-76-240

Summers, W. C. (2005). "Bacteriophage research: early history," in *Bacteriophages: Biology and Applications*, eds E. Kutter and A. Sulakvelidze (Boca Raton, FL: CRC Press), 5–27.

Svircev, A. M., Lehman, S. M., Kim, W. S., Barszcz, E., Schneider, K. E., and Castle, A. J. (2005). "Control of the fire blight pathogen with bacteriophages," in *Proceedings of the 1st International Symposiums Biology Control Bacteriology Plant Diseases*, eds W. Zeller and C. Ullrich (Berlin: Die Deutsche Bibliothek – CIP-Einheitsaufnahme), 259–261.

Tanaka, H., Negishi, H., and Maeda, H. (1990). Control of tobacco bacterial wilt by an avirulent strain of *Pseudomonas solanacearunm* M4S and its bacteriophage. *Ann. Phytopathol. Soc. Jpn.* 56, 243–246. doi: 10.3186/jjphytopath.56.243

Thayer, P. L., and Stall, R. E. (1961). A survey of *Xanthomonas vesicatoria* resistance to streptomycin. *Proc. Flo. State Hortic. Soc.* 75, 163–165.

Thomas, R. C. (1935). A bacteriophage in relation to Stewart's disease of corn. *Phytopathology* 25, 371–372.

Vidaver, A. K. (1976). Prospects for control of phytopathogenic bacteria by bacteriophages and bacteriocins. *Annu. Rev. Phytopathol.* 1976, 451–465. doi: 10.1146/annurev.py.14.090176.002315

Wilson, M., Campbell, H. L., Ji, P., Jones, J. B., and Cuppels, D. A. (2002). Biological control of bacterial speck of tomato under field conditions at several locations in North America. *Phytopathology* 92, 1284–1292. doi: 10.1094/PHYTO.2002.92.12.1284

Zaccardelli, M., Saccardi, A., Gambin, E., and Mazzucchi, U. (1992). *Xanthomonas campestris* pv. *pruni* bacteriophages on peach trees and their potential use for biological control. *Phytopathol. Mediterr.* 31, 133–140.

Conflict of Interest Statement: The authors declare that the research was conducted in the absence of any commercial or financial relationships that could be construed as a potential conflict of interest.

The reviewer GW and handling Editor declared their shared affiliation at the time of review.

frontiers in Microbiology

CORRECTION
published: 29 October 2018
doi: 10.3389/fmicb.2018.02647

Corrigendum: Relative Level of Bacteriophage Multiplication *in vitro* or in Phyllosphere May Not Predict *in planta* Efficacy for Controlling Bacterial Leaf Spot on Tomato Caused by *Xanthomonas perforans*

Botond Balogh[1†], *Nguyen Thi Thu Nga*[2] *and Jeffrey B. Jones*[1*]

[1] *Plant Pathology Department, University of Florida, Gainesville, FL, United States,* [2] *Department of Plant Protection, Can Tho University, Can Tho, Vietnam*

Keywords: bacterial spot of tomato, *Xanthomonas perforans*, *Xanthomonas citri*, citrus canker, biological control

Approved by:
Frontiers in Microbiology Editorial Office, Frontiers Media SA, Switzerland

***Correspondence:**
Jeffrey B. Jones
jbjones@ufl.edu

[†]***Present Address:***
Botond Balogh, Nichino Europe, Co., Ltd., Cambridge, United Kingdom

Specialty section:
This article was submitted to Virology, a section of the journal Frontiers in Microbiology

Received: *02 October 2018*
Accepted: *17 October 2018*
Published: *29 October 2018*

Citation:
Balogh B, Nga NTT and Jones JB (2018) Corrigendum: Relative Level of Bacteriophage Multiplication in vitro or in Phyllosphere May Not Predict in planta Efficacy for Controlling Bacterial Leaf Spot on Tomato Caused by Xanthomonas perforans. Front. Microbiol. 9:2647. doi: 10.3389/fmicb.2018.02647

A Corrigendum on

Relative Level of Bacteriophage Multiplication *in vitro* or in Phyllosphere May Not Predict *in planta* Efficacy for Controlling Bacterial Leaf Spot on Tomato Caused by *Xanthomonas perforans*

by Balogh, B., Nga, N. T. T., and Jones, J. B. (2018) Front. Microbiol. 9:2176. doi: 10.3389/fmicb.2018.02176

In the original article, there was a mistake in **Figure 1** as published. The author and the Frontiers Production Office published Figure 2 as **Figure 1** in error. The missing **Figure 1** appears below.

In addition, there was an error in the affiliations for author BB. Nichino Europe, Co., Ltd., Cambridge, United Kingdom is the author's current affiliation and not the one held at the time this research was conducted. Therefore, the affiliation list has been updated to reflect this and Nichino Europe added as the present address.

The authors and the Frontiers Production Office apologize for these errors and state that they do not change the scientific conclusions of the article in any way. The original article has been updated.

Conflict of Interest Statement: The authors declare that the research was conducted in the absence of any commercial or financial relationships that could be construed as a potential conflict of interest.

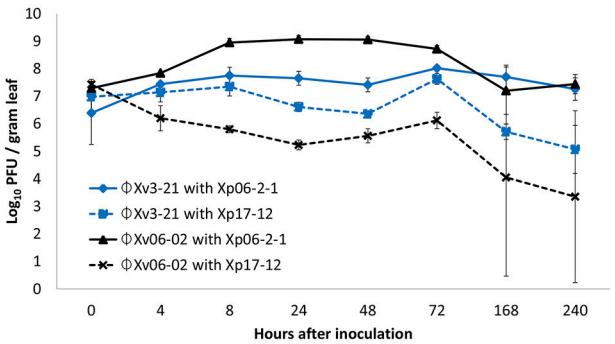

FIGURE 1 | Populations of phages ΦXv3-21 and ΦXp06-02 in the tomato phyllosphere in the presence of *Xanthomonas perforans* strains Xp06-21 or Xp17-12.

frontiers in Microbiology

ORIGINAL RESEARCH
published: 29 August 2018
doi: 10.3389/fmicb.2018.02021

Complete Genome of the *Xanthomonas euvesicatoria* Specific Bacteriophage KΦ1, Its Survival and Potential in Control of Pepper Bacterial Spot

*Katarina Gašić[1], Nemanja Kuzmanović[2], Milan Ivanović[3], Anđelka Prokić[3], Milan Šević[4] and Aleksa Obradović[3]**

[1] Institute for Plant Protection and Environment (IZBIS), Belgrade, Serbia, [2] Institute for Epidemiology and Pathogen Diagnostics, Federal Research Centre for Cultivated Plants, Julius Kühn-Institut, Braunschweig, Germany, [3] Department of Plant Pathology, Faculty of Agriculture, University of Belgrade, Belgrade, Serbia, [4] Institute of Vegetable Crops Ltd., Smederevska Palanka, Serbia

OPEN ACCESS

Edited by:
Robert Czajkowski, University of Gdańsk, Poland

Reviewed by:
Stephen Tobias Abedon, The Ohio State University, United States
Alessandro M. Varani, Universidade Estadual Paulista Júlio de Mesquita Filho (UNESP), Brazil

***Correspondence:**
Aleksa Obradović
aleksao@agrif.bg.ac.rs

Specialty section:
This article was submitted to Virology, a section of the journal Frontiers in Microbiology

Received: *06 June 2018*
Accepted: *09 August 2018*
Published: *29 August 2018*

Citation:
Gašić K, Kuzmanović N, Ivanović M, Prokić A, Šević M and Obradović A (2018) Complete Genome of the Xanthomonas euvesicatoria Specific Bacteriophage KΦ1, Its Survival and Potential in Control of Pepper Bacterial Spot. Front. Microbiol. 9:2021. doi: 10.3389/fmicb.2018.02021

Xanthomonas euvesicatoria phage KΦ1, a member of *Myoviridae* family, was isolated from the rhizosphere of pepper plants showing symptoms of bacterial spot. The phage strain expressed antibacterial activity to all *X. euvesicatoria* strains tested and did not lyse other *Xanthomonas* spp., nor other less related bacterial species. The genome of KΦ1 is double-stranded DNA of 46.077 bp including 66 open reading frames and an average GC content of 62.9%, representing the first complete genome sequence published for a phage infecting xanthomonads associated with pepper or tomato. The highest genome similarity was observed between phage KΦ1 and the *Xanthomonas oryzae* pv. *oryzae* specific phage OP2. On the other hand, when compared with other members of the genus *Bcep78virus*, the genome similarity was lower. Forty-four (67%) predicted KΦ1 proteins shared homology with *Xanthomonas* phage OP2, while 20 genes (30%) were unique to KΦ1. Phage KΦ1, which is chloroform resistant and stable in different media and in the pH range 5-11, showed a high titer storage ability for at least 2 years at +4°C. Copper-hydroxide and copper-oxychloride reduced phage activity proportionally to the used concentrations and the exposure time. UV light was detrimental to the phage strain, but skim milk plus sucrose formulation extended its survival *in vitro*. The phages survived for at least 7 days on the surface of pepper leaves in the greenhouse, showing the ability to persist on the plant tissue without the presence of the host bacterium. Results of three repeated experiments showed that foliar applications of the unformulated KΦ1 phage suspension effectively controlled pepper bacterial spot compared to the standard treatment and the untreated control. The integration of the phage KΦ1 and copper-hydroxide treatments resulted in an increased efficacy compared to the copper-hydroxide alone.

Keywords: ***Xanthomonas euvesicatoria*, bacteriophage, genome analysis, survival, phage therapy**

INTRODUCTION

Pepper (*Capsicum annuum* L.) is one of the major vegetable crops in Serbia, covering approx. 20,000 ha of open fields. Furthermore, the area in protected environment, planted with pepper, is constantly increasing (Ignjatov et al., 2012). Large areas and intensive production, both in the open field and in plastic tunnels and greenhouses, make Serbia one of the leading pepper growing countries in Europe. However, the occurrence of pepper diseases causes significant losses and occasionally limits successful production. Bacterial spot, caused by *Xanthomonas euvesicatoria* (formerly *X. campestris* pv. *vesicatoria* group A, Jones et al., 2004; Obradović et al., 2004b), is one of the most important pepper diseases in all pepper growing areas and in Serbia as well (Balaž, 1994; Obradović et al., 2000, 2001).

The limited efficacy of current disease control strategies certainly contributes to the economic importance of this disease. Cultural practices do not provide a sufficient reduction of the disease and have not been fully implemented by commercial growers. The development by the pathogen copper or streptomycin resistance (Thayer and Stall, 1961; Marco and Stall, 1983; Adaskaveg and Hine, 1985; Minsavage et al., 1990; Pernezny et al., 1995; Martin et al., 2004) and increased public concern about detrimental effects of pesticide residues initiated efforts in searching for alternatives in control of bacterial diseases.

Bacteriophages, viruses that infect bacterial cells, have regained attention as natural antimicrobial agents to fight bacterial diseases of plants. They are natural components of the biosphere, self-replicating within host cells, highly host specific and non-toxic to eukaryotic cells (Jones et al., 2007). All these attributes, including the fact that phage multiplication and storage are fairly easy and inexpensive (Greer, 2005), make them an attractive agricultural biopesticide.

Bacteriophages have been successfully used for managing several plant diseases caused by *Xanthomonas* species, including bacterial spot of peach caused by *Xanthomonas campestris* pv. *pruni* (Civerolo and Keil, 1969; Saccardi et al., 1993), walnut blight caused by *X. campestris* pv. *juglandis* (McNeil et al., 2001), geranium bacterial blight caused by *X. campestris* pv. *pelargonii* (Flaherty et al., 2001), leaf blight of onion caused by *X. axonopodis* pv. *allii* (Lang et al., 2007), tomato bacterial spot caused by *Xanthomonas* complex (Flaherty et al., 2000; Obradović et al., 2004a, 2005), and citrus canker and citrus bacterial spot caused by *X. axonopodis* pv. *citri* and *X. axonopodis* pv. *citrumelo*, respectively (Balogh et al., 2008).

However, the effectiveness of phages as biocontrol agents depends not only on the susceptibility of the target bacterium, but also on environmental factors that affect phage survival. In the phyllosphere, phages can be inactivated by various factors including extreme temperatures and pH, desiccation and sunlight irradiation (especially in the UV spectrum), or they can be washed off from leaf surfaces either by rain or overhead irrigation (Suttle and Chen, 1992; Iriarte et al., 2007; Jones et al., 2007; Svircev et al., 2010). Additionally, phage persistence in the phyllosphere can be reduced by exposure to certain pesticides, such as copper compounds (Iriarte et al., 2007).

Several strategies were tested in order to increase phage vitality on foliage, such as the use of protective formulations (Balogh et al., 2003; Obradović et al., 2004a; Iriarte et al., 2007), evening or early morning application (Flaherty et al., 2000; Balogh et al., 2003), and the use of carrier bacteria for phage propagation in the environment (Svircev et al., 2006). Although it was found that copper ions inactivate phages *in vitro* (Balogh et al., 2005), this negative effect can be avoided by application of copper-based pesticides at least 4 days before phage application in the field (Balogh et al., 2008). This information indicates a possible successful integration of bacteriophages and copper compounds for disease control.

Despite the growing interest in using phages in control of phytopathogenic bacteria, there is still little information on their genome organization and structure. So far, there have been nine published whole genome sequences of phages that lyse *Xanthomonas* spp. Among them, five belong to the family *Siphoviridae* (Gene Bank acc. nos. NC_019933, NC_007709, NC_009543, NC_004902, and NC_012742), two phages belong to family *Podoviridae* (acc. nos. NC_020205 and NC_001396), one phage belongs to *Myoviridae* (acc. no. NC_007710) and one phage is classified at the level of the order *Caudovirales*. All these phages infect either *Xanthomonas axonopodis* pv. *citri*, *Xanthomonas oryzae* pv. *oryzae*, or *Xanthomonas campestris*. Hitherto, there has not been published a phage genome for these infecting *Xanthomonas* spp. associated with pepper or tomato.

In this paper we present the genome characteristics of a phage specific to *Xanthomonas euvesicatoria* affecting pepper, isolated from the pepper rhizosphere in Serbia (Gašić, 2011). Beside the first report of its complete genome sequence, we present the effect of some environmental factors on the phage stability and its potential to control pepper bacterial spot, under controlled conditions.

MATERIALS AND METHODS

Bacterial Strains, Bacteriophage and Culture Conditions

Bacterial strains used in this study were stored at −80°C in glycerol (30% v/v) nutrient broth (NB) (Torlak, Serbia). The strains were grown on nutrient agar (NA; Torlak, Serbia) at 28°C for 24 h prior to use. For preparation of bacterial suspensions, cultures were suspended in sterile distilled water. The concentration was adjusted to 5×10^8 CFU/ml photometrically ($OD_{600} = 0.3$), and then diluted accordingly.

The phage KΦ1, belonging to the family *Myoviridae*, was isolated from the rhizosphere of pepper plants showing symptoms of bacterial spot, and was stored either at +4 or at −80°C (Gašić, 2011). For the phage detection and propagation, we used either semisolid nutrient agar yeast extract medium (NYA; 0.8% NB, 0.6% agar, and 0.2% yeast extract) (Balogh et al., 2003) or NB. Phage concentrations were determined by serial dilutions and a subsequent plaque assay on NYA medium, with *Xanthomonas euvesicatoria* strain KFB189 as a host, as previously described (Gašić, 2011). Briefly, 10-fold dilutions of the phage suspension were prepared and 100 μl of each was mixed with

100 μl of the host bacterium suspension (approx. 10^9 CFU/ml) at the bottom of a Petri dish. The NYA medium (cooled to 48°C) was poured into plates, followed by gently swirling to evenly distribute the bacteria and the phages within the medium. The plates were incubated at 27°C for 24 h to assess plaque formation. Phage concentration was estimated according to the formula for bacterial enumeration (Klement et al., 1990) and was expressed as "plaque forming units per ml" (PFU/ml).

Determination of Phage KΦ1 Host Range

Host range analysis of phage KΦ1 was performed using 19 strains of *X. euvesicatoria,* isolated during 2015 from different localities in Serbia, including the reference strain NCPPB 2968 (**Table 1**). Additionally, we studied the phage potential lytic activity to some closely related pepper- and tomato-associated xanthomonads: *X. vesicatoria*, *X. gardneri,* and *X. perforans*. Besides *Xanthomonas* spp., we tested host specificity of the phage KΦ1 to some less related bacteria as well (**Table 1**). The host range test was performed by spotting 4 μl phage suspension (conc. 10^8 PFU/ml) on the solidified NYA medium inoculated with 100 μl water suspension (conc. 10^9 CFU/ml) of each bacterial strain. Phage activity was scored based on the spot-like clearing of the bacterial growth indicating host cell lysis. The spots were categorized as clear or turbid, indicating high host sensitivity or partial lysis, respectively. The absence of spot formation indicated a non-host relationship. The host range experiment was performed in triplicate.

Bacteriophage Genomic DNA Purification

In order to obtain high phage titer for genomic DNA purification, KΦ1 phage was propagated in *X. euvesicatria* strain KFB 189 as previously described (Gašić, 2011). Following the 16 h incubation, bacterial cells were removed by centrifugation (8,000 *g* for 20 min) and the resulting phage suspension (40 ml) was filtered through a 0.22 μm membrane filter. Ten milliliter of the phage suspension was further concentrated by centrifugation (16,000 *g*, 90 min, 4°C), resuspending the phage containing pellet in 700 μl of SM buffer. The resulting phage suspension was further treated with 10 μl DNase I (1 U/μl) and 1 μl RNase A (100 mg/ml) at 37°C for 45 min to digest any bacterial nucleic acids. Phage genomic DNA was extracted by organic extraction as described by Lehman et al. (2009). DNA concentration and purity were verified using the NanoPhotometerTM Pearl (Implen GmbH, Germany). DNA integrity and absence of degradation were verified by electrophoresis on 0.8% agarose gel.

Bacteriophage Genome Sequencing and Analysis

Phage KΦ1 genomic DNA was sequenced using the Illumina HiSeq 2500 paired-end technology at Baseclear[1], Leiden, Netherlands following the manufacturer's instructions. The assembly was performed using the CLC Genomics Workbench version 8.0. The IGS Annotation Engine (Institute for Genome Sciences, University of Maryland School of Medicine automated pipeline[2]) and RAST (Rapid Annotation using Subsystem Technology[3]) were used for structural and functional annotation of the sequence. The phage genome was mapped and annotated using available phage genome sequences deposited in GenBank[4]. The analysis of the genome was done using Manatee[5] accessed via the website of the Institute for Genome Sciences, University of Maryland School of Medicine. For prediction of the phage KΦ1 lifestyle, PHACTS was used (McNair et al., 2012). In order to find potential genes coding for toxins and allergens or genes related to virulence, KΦ1 phage genome was analyzed using VirulentPred[6] (Garg and Gupta, 2008). ARAGORN[7] (Laslett and Canback, 2004) and tRNAscan-SE[8] (Lowe and Chan, 2016) were used to search for tRNA genes. Genomic comparisons were performed with Mauve (Darling et al., 2010), using a progressive alignment with the default settings, and comparisons at the proteomic level were done using CoreGenes 3.5 (Zafar et al., 2002).

Nucleotide Sequence Accession Number

The KΦ1 phage genome sequence has been deposited in the NCBI GenBank database under the accession number KY210139.

Phage Survival in Different Media

In order to determine optimal media for the phage storage and survival, we studied the stability of phage KΦ1 in NB, tap water, distilled water, 10 mM magnesium-sulfate solution and SM buffer (10 mM Tris–HCl, pH 7.5; 100 mM NaCl; and 10 mM $MgSO_4$). The media were used to prepare the phage suspension, respectively (conc. 10^{10} CFU/ml) and store it at 4°C in dark conditions. The phage concentration in each medium was checked seven times during 3 weeks, by using *X. euvesicatoria* strain KFB189 as the host, by the procedure described above. The experiment was repeated three times and the result was reported as the mean number of plaques counted (PFU/ml) for each substrate.

Phage Survival at +4 and +20°C

Two flasks, each containing 50 ml of NB KΦ1 phage suspension (conc. 10^7 PFU/ml), were incubated either at +4 or +20°C, in dark conditions for 6 months. Phage titer was checked at different time intervals. The plaque count assays were performed in triplicate and the results were reported as the mean number of plaques counted (PFU/ml).

Effect of pH on Phage Viability

In order to study the effect of different pH values on phage viability, phage KΦ1 was suspended in 1 ml SM buffer, previously adjusted to pH's 2, 5, 7, 9, 11, and 12. Phage suspensions in

[1]www.baseclear.com

[2]http://ae.igs.umaryland.edu/cgi/index.cgi

[3]http://rast.nmpdr.org/ website

[4]http://www.ncbi.nlm.nih.gov/genbank/

[5]http://manatee.sourceforge.net/

[6]http://203.92.44.117/virulent/submit.html

[7]http://130.235.46.10/ARAGORN/

[8]http://lowelab.ucsc.edu/tRNAscan-SE

TABLE 1 | The host range of bacteriophage KΦ1.

Bacterial species	Strain	Origin, host, year of isolation	Source	KΦ1 phage spot formation
Xanthomonas euvesicatoria	KBI 116, KBI 117, KBI 118, KBI 119, KBI 120, KBI 121, KBI 123, KBI 124, KBI 125, KBI 126, KBI 127, KBI 128, KBI 129, KBI 130, KBI 131, KBI 132, KBI 133, and KBI 134	Serbia, *Capsicum annuum*, 2015	KBI[a]	+
Xanthomonas euvesicatoria	NCPPB 2968	United States, *Capsicum frutescens*, 1977	NCPPB[b]	+
Xanthomonas vesicatoria	NCPPB 1423	Hungary, *Lycopersicon esculentum*, 1957	NCPPB	–
Xanthomonas gardneri	NCPPB 4321	Serbia, *Lycopersicon esculentum*, 1953	NCPPB	–
Xanthomonas perforans	NCPPB 881	United States, *Lycopersicon esculentum*, 1991	NCPPB	–
Acidovorax citrulli	NCPPB 3679	United States, *Citrullus lanatus*, year unknown	NCPPB	–
Erwinia amylovora	KBI 32	Serbia, *Cydonia oblonga*, 2013	KBI	–
	KBI 68	Serbia, *Pyrus communis,* 2014	KBI	–
	KFB 687	Serbia, *Malus domestica*, 2013	KBI	–
	CFBP 1430	France, *Pyrus communis,* 2010	CFBP[c]	–
Pectobacterium carotovorum ssp. *carotovorum*	KFB 68	Serbia, *Brassica oleracea* var. *capitata,* 1999	KFB[d]	–
	KFB 85	Serbia, *Apium graveolens*, 1998	KFB	–
Dickeya spp.	KBI 05	United Kingdom, *Solanum tuberosum*, year unknown	KBI	–
Ralstonia solanacearum	NCPPB 4156	The Nederlands, *Solanum tuberosum*, 1995	NCPPB	
Agrobacterium tumefaciens	C58	United States, *Prunus cerasus*, 1958	S. Süle	
Clavibacter michiganensis ssp. *michiganensis,*	CFBP 4999	Hungary, *Lycopersicon esculentum,* 1957	CFBP	–
Clavibacter michiganensis ssp. *sepedonicus*	CFBP 3561	Finland, *Solanum tuberosum*, 1983	CFBP	–
Pseudomonas syringae pv. *lachrymans*	KFB 214	Serbia, *Cucumis sativus*, 2007	KFB	–
Pseudomonas syringae pv. *syringae*,	GSPB 1142	Germany, *Phaseolus* sp., 1967	GSPB[e]	–
Pseudomonas fruorescens[f]	B130	Ji et al. (1996)	AU	–

+ lysis of bacterial cells (spot formation), – lack of bacterial cell lysis (no spot formation). [a]KBI – Collection of Bacteria, Institute for Plant Protection and Environment, Belgrade, Serbia. [b]NCPPB – National Collection of Plant Pathogenic Bacteria, United Kingdom. [c]CFBP – Collection Française de Bactéries Phytopathogènes, INRA, Angers, France. [d]KFB – Collection of Phytopathogenic Bacteria, University of Belgrade, Faculty of Agriculture, Serbia. [e]GSPB – Göttingen Collection (Sammlung) of Phytopathogenic Bacteria, Göttingen, Germany. [f]Originated from J. Kloepper, Auburn University (AU) originally designated as 89B61.

SM buffer were adjusted to a final concentration of 10^4 PFU/ml. After 24 h of incubation in dark conditions at room temperature, 10-fold dilutions of each sample were prepared and assayed for phage activity. The assays were carried out in duplicate and the results were reported as the mean number of plaques counted (PFU/ml).

Effect of UV Light on Phage Survival *in vitro*

The effect of UV light irradiation on KΦ1 phage survival was studied using two microtiter plates treated with 10% skim milk and dried in a flow hood for 3 h according to the slightly modified method of Iriarte et al. (2007). Two treatments were carried out on each plate: 24 wells per treatment were treated with 30 μl of the phage suspension (conc. 10^7 PFU/ml) either formulated (0.75% skim milk plus 0.5% sucrose) or non-formulated. The plates were placed inside Petri dishes (R-18 cm) and stored at room temperature either in the continuous dark or exposed to UV light 254/366 nm/dark (16 h/8 h) conditions. The phage's titer was assessed on the first day and later at different time intervals during 2 months. Three wells per treatment were assayed by adding 300 μl of tap water to each well. After 1 min, rinsates from each well were transferred into microcentrifuge tubes and titer was calculated as already described. The assays were carried out in duplicate and the results were reported as the mean number of plaques counted (PFU/ml).

Effect of Copper Compounds on Phage Survival *in vitro*

In order to study potential negative effects of some pesticides on KΦ1 phage survival, phage suspension was mixed with commercial preparations of copper-hydroxide (Kocide 2000, DuPont) and copper-oxychloride (Bakarni oksihlorid 50, Galenika-Fitofarmacija) dissolved in tap water. Two concentrations of both copper-hydroxide (0.2 and 2%) and copper-oxychloride (0.5 and 5%) were used: the first one was determined according to the manufacturer's recommendation for the plant treatment and the second was 10-fold higher. The KΦ1 phage suspension was added to 100 ml of each chemical to the final concentration 10^7 PFU/ml and incubated at 20°C in dark conditions. The results were recorded on the first day and later on at a 7-day interval, during 3 weeks. The phage titer was determined as described previously and expressed as PFU/ml.

Phage Epiphytic Survival in Greenhouse Conditions

The changes in KΦ1 phage population on plant leaves were assessed in greenhouse conditions as described by Balogh et al. (2005) with slight modifications. Pepper plants, at the 10-leaf stage, were sprayed with suspension of phage KΦ1 (conc. 10^8 PFU/ml) in the evening (7 PM) using a handheld sprayer. The phage population was monitored by sampling fully developed terminal pepper leaves in the morning during 7 days. Each sample consisted of eight terminal leaves collected from the three plants, respectively, and placed into a sterile flask. Each sample was weighed before adding 100 ml of tap water and shaken for 30 min at 400 rpm on a horizontal shaker. An amount of 1.5 ml of rinsate was transferred to microcentrifuge tubes and treated with chloroform (1:10 v/v) for 30 min. Following incubation, the chloroform was pelleted by a pulse spin and 1 ml of the supernatant was centrifuged at 10,000 *g* for 15 min in order to remove debris. Phage concentration in the resulting suspension was calculated and expressed as the number of PFU per gram of leaf tissue by the following equation: y = plaque number × 1,000/dilution ratio/weight of sample (g).

Efficacy of Bacteriophage KΦ1 in Control of Pepper Bacterial Spot in Greenhouse Conditions

High titer of phage KΦ1 (10^9 to 10^{10} PFU/ml) was produced by inoculating log phase culture of *X. euvesicatoria* strain KFB 189 (approx. 10^8 CFU/ml) in NB with a multiplicity of infection of 0.1, followed by overnight incubation at 28°C. Phage suspension was treated with 10% (v/v) chloroform and stored at 4°C until use. Phage concentration was diluted to 10^8 PFU/ml just before treatment application.

Xanthomonas euvesicatoria strain KFB 189, sensitive to copper compounds, was used for inoculation of pepper plants. The 24-h-old culture, grown on NA, was suspended in sterile distilled water, and the concentration was adjusted to approx. 5×10^8 CFU/ml photometrically (OD_{600} = 0.3), and then diluted appropriately. In the experiments 1 and 2, the concentration of inoculum was 10^8 CFU/ml, while in the experiment 3 it was 10^6 CFU/ml. Pepper plants of cv. Šorokšari (Institute of Vegetable Crops, Smederevska Palanka, Serbia) were grown in pots (R = 10 cm) containing Floradur B Fine soil (Floragard, Germany) in the greenhouse at 24–28°C. Plants were watered daily and fertilized with a soluble 18-18-18 NPK fertilizer (Navarsol IV, Timac Agro Italia) until they reached the four-leaf stage.

The treatments included single phage applications either 2 h before or 15 min after inoculation, as well as double application 2 h before and 15 min after inoculation. Integrated control was attempted by the application of copper-hydroxide (Kocide 2000, DuPont – active ingredient 53.8% copper-hydroxide) 24 h and phage 2 h before pepper inoculation. Copper-hydroxide treatment alone was used as a standard, while inoculated but untreated plants were used as a negative control. Application of treatments and inoculation were performed using a handheld sprayer. Following inoculation, plants were covered by translucent plastic bags for 48 h and arranged in a completely randomized block design in the greenhouse at 28°C.

Plants were assessed for disease severity 7 and 14 days after inoculation. The number of lesions on five leaves of each plant was evaluated. The data were analyzed by applying one-way analysis of variance (ANOVA) and Duncan's multiple range test using Statistica for Windows statistical software (Release 7.0; StatSoft Inc., Tulsa, OK, United States).

RESULTS

Host Range Analysis

Bacteriophage strain KΦ1 showed antibacterial activity against all tested *X. euvesicatoria* strains, by forming clear spots on bacterial lawns of each strain, respectively. There was not any antibacterial activity on the other tested xanthomonads affecting pepper or tomato, nor on the rest of the bacterial species used in this study (**Table 1**).

Genome Properties

The phage KΦ1 has a double-stranded 46,077 bp DNA genome with GC content of 62.9% and 66 predicted open reading frames (ORFs). The average gene length was predicted to be 632 nucleotides, and 90.6% of the genome consisted of coding regions. Out of 66 putative ORFs, 16 (24.2 %) had an assigned function, three (4.5%) ORFs had unknown function, whereas the rest of 47 ORFs were classified as hypothetical (conserved) proteins (**Figure 1** and **Supplementary Table S1**). A total of six ORFs were annotated to encode proteins involved in the nucleic acid metabolism, transcription and translation (phage helicase, DNA polymerase I, DNA-directed RNA polymerase, DNA primase, DNA methylase family protein, and endodeoxyribonuclease RusA family protein). Nine ORFs were predicted to code for proteins involved in DNA packaging (phage terminase, large subunit) or virion morphogenesis (phage capsid and scaffold, putative structural protein, head protein, tail fiber proteins, baseplate J-like protein, baseplate protein, and tail length tape measure protein). One putative ORF associated with host lysis was also identified. (**Figure 1** and **Supplementary Table S1**). The genome of phage KΦ1 did not encode any transport RNAs. The start codon for transcription was ATG in 80.3% of genes, and GTG in 19.7% of phage genes.

Comparative genomic analysis revealed that phage KΦ1 showed significant similarity only to the *Xanthomonas* phage OP2, specific to *Xanthomonas oryzae* pv. *oryzae*, a member of the genus *Bcep78virus* (ICTV, 2017). Forty-four (67%) predicted KΦ1 proteins shared homology with *Xanthomonas* phage OP2, while 20 genes (30%) were unique to KΦ1 (**Figure 2** and **Supplementary Table S1**). Lifestyle prediction by PHACTS indicated that KΦ1 was a lytic bacteriophage, which is in accordance with the observed morphology of plaques. There were no toxin genes, or genes related to virulence found in the phage genome, indicting its suitability for phage therapy.

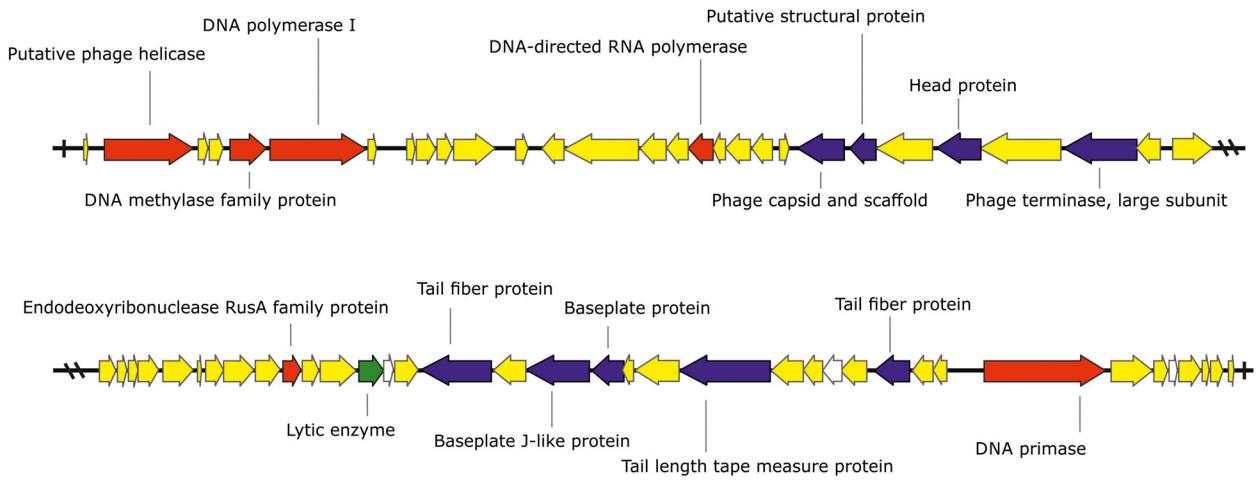

FIGURE 1 | The genome of the bacteriophage KΦ1 (46,077 bp). ORFs coding for proteins involved in DNA metabolism, transcription, and translation are marked in *red*, ORFs coding for proteins involved in phage particle assembly are marked in *blue*, and ORF coding for enzyme involved in host lysis is marked in *green*. ORFs coding for hypothetical and conserved hypothetical proteins are marked in *yellow*, while ORFs of unknown function are marked in *white*. *Arrows* indicate the direction of transcription and translation. The figure was generated using the genome visualization program SnapGenehttp://www.snapgene.com/ ver. 2.3.4.

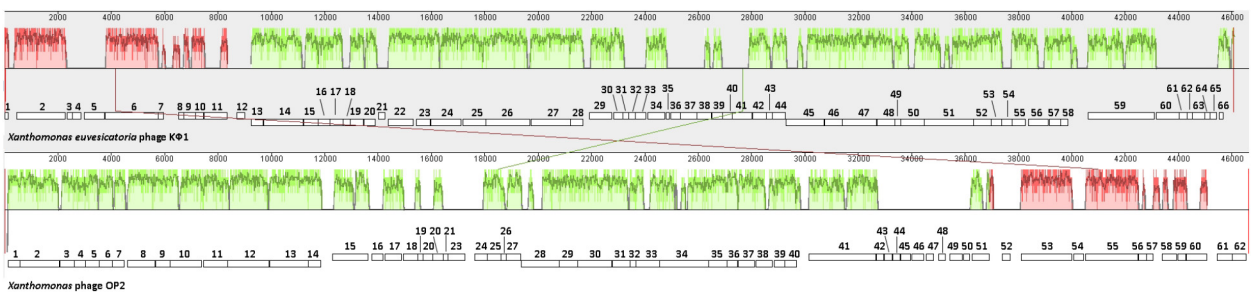

FIGURE 2 | The alignment of the annotated phage KΦ1 and *Xanthomonas* phage OP2 genome sequences using Mauve. Annotated genes are shown as *white boxes*, with genes transcribed from the reverse strand shifted downward. Numbers above boxes correspond to the ORFs in KΦ1 phage (**Supplementary Table S1**) and *Xanthomonas* phage OP2 (Gene Bank acc. no. NC_007710) genomes, respectively. The degree of sequence similarity between aligned regions is indicated by the height of the similarity profile. *Connection lines* indicate similar regions between phages KΦ1 and OP2.

Phage Survival in Different Media

Studies of phage vitality in different media showed that NB was the most favorable medium for phage survival, in which the concentration of phages decreased only by 0.06 log units during 3 weeks (**Figure 3**). A decrease of phage concentration in sterile tap water, 10 mM magnesium sulfate solution and SM buffer was 0.25, 0.35, and 0.7 log units, respectively. A reduction in phage concentration was observed in the first days of experiment, while in the next days the concentration was not significantly changed. Concentration of phage KΦ1 in sterile distilled water was reduced by 2.64 log units during 3 weeks, which makes distilled water a less favorable environment for the phage survival.

Phage Survival at +4 and +20°C

The results indicate that the storage of the phage at +4°C provided higher stability of virus particles compared with the storage at +20°C. During the 6 months of the experiment, the initial phage concentration decreased by 0.19 log units at +4°C and by 0.63 log units at +20°C (**Figure 4**).

Effect of pH on Phage Viability

Phage KΦ1 was stable in SM buffer of pH values ranging from 5 to 11, during 24 h at room temperature and in dark conditions (**Figure 5**). The phages were completely inactivated at pH values 2 and 12 during 24 h.

Effect of UV Light on Phage Vitality *in vitro*

Concentration of both formulated and non-formulated phages did not change significantly over the period of 60 days in dark conditions. Phage concentration decreased by 2.01 and 1.80 log units for the non-formulated and formulated phages, respectively (**Figure 6**). However, when phages were subjected to a 16 h UV light/8 h dark photoperiod, their population was reduced significantly compared to the initial concentration. The non-formulated phage population dropped to an undetectable level after 40 days of incubation. Formulation of phages provided the protective effect and influenced phage survival *in vitro* under UV/dark conditions. The formulated phage population dropped by 4.63 log units within 60 days.

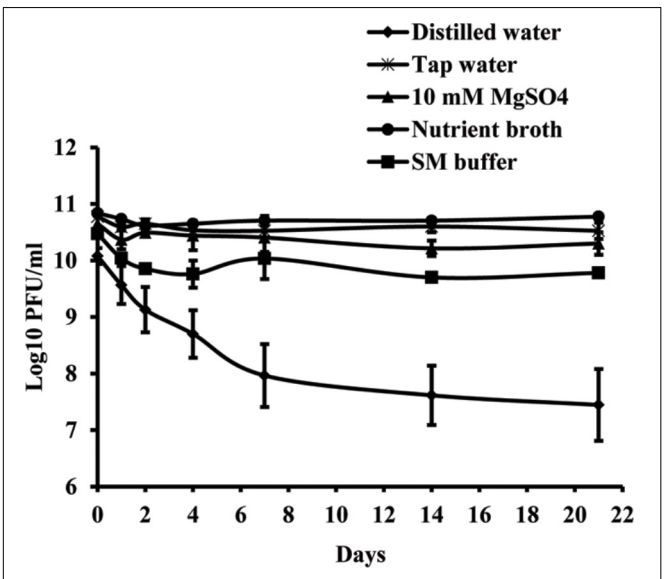

FIGURE 3 | KΦ1 phage survival in different media during 3 weeks. Error bars indicate the standard error.

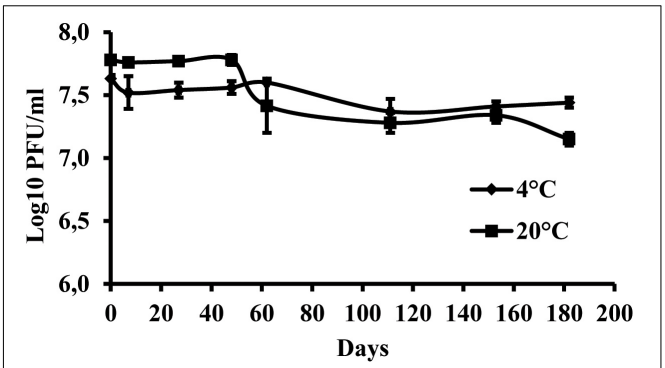

FIGURE 4 | Changes in KΦ1 phage concentration at temperatures of +4 and +20°C, during 6 months of incubation. Error bars indicate the standard error.

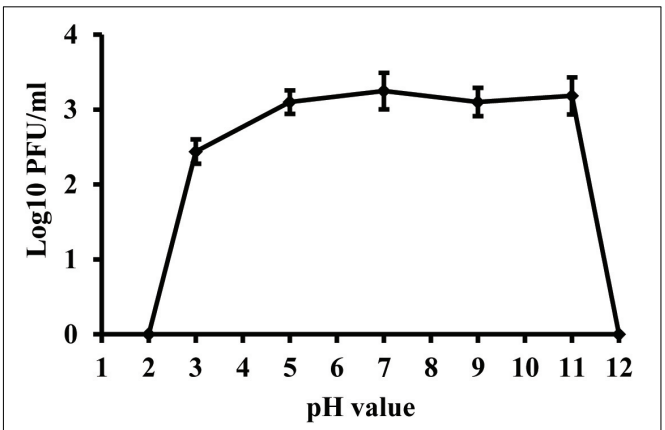

FIGURE 5 | Stability of phage KΦ1 at different pH values during 24 h. Error bars indicate the standard error.

Effect of Copper Pesticides on Phage Vitality *in vitro*

Copper compounds reduced phage activity compared to the control, during 3 weeks. A toxic effect was observed in both application rates, the one recommended by the manufacturer as well as with a concentration ten times higher. The least toxic was copper-hydroxide in the concentration of 0.2%, which is concentration of the active ingredient in the commercial product (**Figure 7**). However, the most toxic was copper-oxychloride. Its toxicity corresponded to the concentration applied. The lower concentration (0.5%) of this compound was more toxic than the higher copper-hydroxide (2%) concentration.

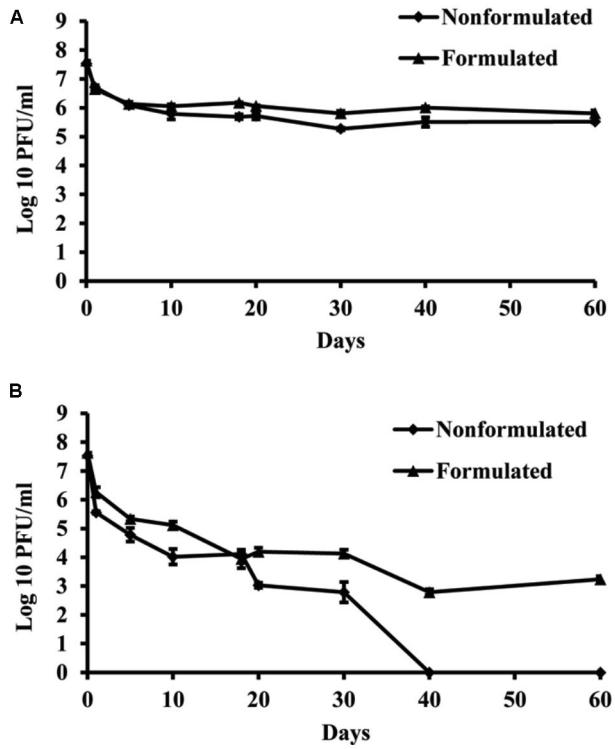

FIGURE 6 | The effect of UV light on survival of KΦ1 phage. Non-formulated and formulated (0.75% skim milk plus 0.5% sucrose) phages were stored during 2 months either in completely dark conditions **(A)** or were subjected to a 16 h UV light/8 h dark photoperiod **(B)**. Error bars indicate the standard error.

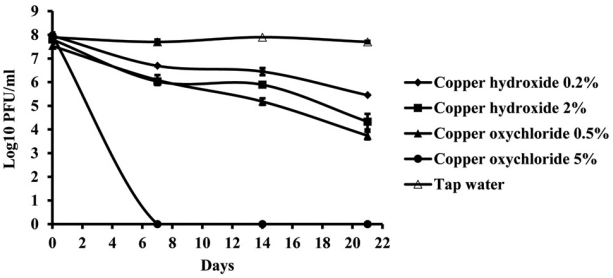

FIGURE 7 | The effect of copper compounds on phage KΦ1 survival during 3 weeks. Error bars indicate the standard error.

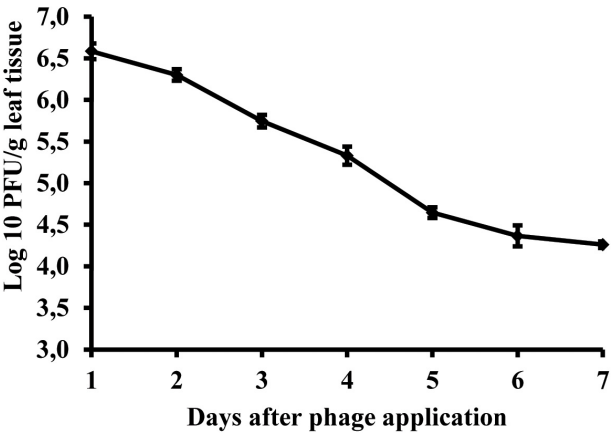

FIGURE 8 | Changes in bacteriophage KΦ1 populations on pepper foliage during 7 days in greenhouse conditions. Error bars indicate the standard error.

Phage Survival in Pepper Phyllosphere

Studies of bacteriophage KΦ1 population dynamics on pepper leaves showed that phages can persist for at least 7 days on the leaf surface in the absence of a host, under greenhouse conditions. During this period, the number of phage particles per gram leaf tissue dropped by 2.41 log units from initial concentration (**Figure 8**).

Efficacy of Phage KΦ1 in Control of Pepper Bacterial Spot in Greenhouse Conditions

In all the experiments, the application of KΦ1 phage treatments significantly reduced the lesion number on pepper leaves compared to the untreated control (**Table 2**). The double application of phages, pre- and post-inoculation, was the most effective among the three variants of the phage treatments, but not always statistically different from the single applications. In all the experiments, there was no significant difference between the phage application 2 h before or 15 min after inoculation. However, the most efficient treatment was the integrated application of the phage suspension and copper-hydroxide. Although there was no significant difference in efficacy between this integrated application and the copper-hydroxide treatment alone, the phage application contributed to the additional reduction in the number of lesions in all the experiments (**Table 2**).

DISCUSSION

According to recent publications, bacteriophages have regained researchers' attention as potential biocontrol agents in plant protection (Jones et al., 2007; Buttimer et al., 2017). Frequent occurrence of plant pathogenic bacteria, ineffective chemical control and increasing environmental concerns certainly have contributed to the increased interest in using bacteriophages for the control of bacterial infections in plants. In this research, we studied the host range, genome characteristics, survival, and biocontrol potential of bacteriophage strain KΦ1 specific to *X. euvesicatoria*, a causal agent of pepper bacterial spot.

Phage KΦ1, isolated from the pepper plant's rhizosphere, is a lytic phage, producing clear spots on the bacterial lawn of different strains of *X. euvesicatoria*. Our previous results have shown that phage KΦ1 belongs to the *Myoviridae* family, A1 morphotype, with a latent period of 20 min and the burst size of 75 ± 4 viruses per infected cell (Gašić, 2011). Since we used chloroform during phage isolation to eliminate bacterial cells,

TABLE 2 | The effect of phage KΦ1 treatment in pepper bacterial spot development in greenhouse conditions.

Treatments	Application timing	Average lesion number[y]		
		Experiment 1[x]	Experiment 2	Experiment 3
Phage KΦ1	2 h before inoculation	237 b	302 bc	280 b
Phage KΦ1	2 h before and 15 min after inoculation	157 cb	213 c	182 bc
Phage KΦ1	15 min after inoculation	229 b	358 ab	294 b
Copper-hydroxide* + phage KΦ1	24 h before inoculation; 2 h before inoculation	63 c	41 d	66c
Copper-hydroxide	24 h before inoculation	111 c	106 d	179 bc
Untreated control	None	332 a	422 a	567 a

*[x]Concentration of inoculum was 10^8 CFU/ml in experiments 1 and 2 and 10^6 CFU/ml in experiment 3. [y]Average lesion number per plant 14 days after inoculation. Means followed by different letters (a, b, c, d) within a column are significantly different according to Duncan's multiple range test, P = 0.05 level. *Kocide 2000, DuPont – active ingredient 53.8% copper-hydroxide. Concentration 0.2%, as recommended by manufacturer was used in all experiments.*

we can confirm that KΦ1 was not sensitive to this chemical. Moreover, after 24-month storage of phage KΦ1 suspension in NB containing 10% (v/v) of chloroform, the titer was not significantly changed (unpublished data). Chloroform resistance is an important factor, since the phages which are not easily cultured and maintained, or cannot be stored on a large scale, are not desirable as potential biological control agents for their use in the field (Schisler and Slininger, 1997).

Results of phage KΦ1 host range performed during current research, including the previous study (Gašić, 2011), revealed that phage KΦ1 infected only *X. euvesicatoria* strains, but not other *Xanthomonas* spp., nor *Erwinia amylovora*, *Pectobacterium carotovorum* subsp. *carotovorum, Ralstonia solanacearum, Acidovorax citrulli, Clavibacter michiganensis* subsp. *sepedonicus, Clavibacter michiganensis* subsp. *michiganensis, Agrobacterium tumefaciens, Dickeya* spp., *Pseudomonas syringae* pv. *syringae*, and *Pseudomonas syringae* pv. *lachrymans*, including the saprophytic strain *P. fluorescens.* High specificity enables the elimination of target bacteria without damaging other and possibly beneficial bacteria. Moreover, the fact that phage KΦ1 has a broad host range among *X. euvesicatoria* strains is very important for its use in biocontrol of pepper bacterial spot.

The phage genome contains a dsDNA of 46,077 bp, including 66 ORFs and an average GC content 62.9%. Based on bioinformatics analysis, the closest relative of phage KΦ1 is *Xanthomonas* phage OP2 (acc. no. NC_007710) belonging to the *Myoviridae* family, genus *Bcep78virus* (Inoue et al., 2006; ICTV, 2017). OP2 is bacteriophage that lyses *Xanthomonas oryzae* pv. *oryzae*, possesses dsDNA of 46,643 bp, and the average GC content of 60.9%. For most of the 44 proteins (67%) shared by KΦ1 and OP2, the BLASTP alignments showed 43 to 84% sequence identity. Among the shared proteins, 33 of them having additional hits beside OP2, showed homology with some of the *Burkholderia cepacia* phages within the genus *Bcep78virus* (Summer et al., 2006). However, the complementary OP2 protein was the best match in all, except four cases (**Supplementary Table S1**).

Unlike some structural protein-encoding genes of the phage KΦ1, putative genes KΦ1_45 and KΦ1_51 encoding tail fiber proteins, exhibited low degree of similarity with corresponding genes of phages OP2 and/or BcepNY3 at the amino acid level (**Supplementary Table S1**). The protein sequence comparisons revealed that tail fiber protein coded by gene KΦ1_45 displayed only 53 and 55% of identity with fiber proteins of BcepNY3 and OP2 phages, respectively. A second tail fiber protein coded by gene 51 of phage KΦ1_showed 61% of identity with corresponding protein of OP2 phage. In this respect, some previous studies reported that tail fiber proteins can be involved in host specificity of the phages (Tétart et al., 1996; Le et al., 2013). Therefore, a lack of homology between tail fiber protein sequences of KΦ1 and OP2 might suggest differences in the host range of these two phages.

A study of Lavigne et al. (2008) has proposed that phages sharing at least 40% homologs or orthologs proteins belong to the same genus. Proteomic comparison of phage KΦ1 and OP2 by using CoreGenes revealed that two phages shared 60% of their proteomes. This result is consistent with the protein-by-protein comparison using BLASTP and confirms that KΦ1 and OP2 could be classified into the same genus, *Bcep78virus.* The genomes of these phages ranged from 46 to 49 kb in size and encoded 66 to 71 proteins (Lavigne et al., 2009). Furthermore, toxin genes or virulence genes were not detected, indicating that strain KΦ1 is suitable for phage therapy. The lytic lifestyle of KΦ1 phage was predicted with PHACTS as well. To our knowledge, this is the first genome sequence reported for a phage infecting *X. euvesicatoria*. This information provides a solid base for the future, advanced molecular research interaction between KΦ1 phage and its *X. euvesicatoria* host.

In order to determine the most favorable conditions for phage storage, KΦ1 phage survival in different media was studied. NB was found as the most favorable media for phage storage, followed by sterile tap water, 10 mM magnesium sulfate solution and SM buffer. In all these media, phage titter was slightly changed during 3 weeks. On the contrary, phage concentration in sterile distilled water significantly decreased during 3 weeks. Similar results were reported by Appunu and Dhar (2008), who studied the stability of phage in distilled water, saline solution and YM broth. After 30 days at 4°C in distilled water, there were no viable phage particles, whereas in other media titer declined much more slowly. The differences in phage stability in media may be due to the interaction of phage coat proteins with cations, anions and organic molecules present in the medium (Appunu and Dhar, 2008). Temperature is an important factor affecting phage stability. KΦ1 phage was stored at +4 and +20°C in NB as

an optimal medium for 6 months. At the temperature of +20°C, KΦ1 phage concentration decreased by 0.44 log units more than the concentration of phage stored at 4°C, indicating that the lower temperature was more favorable for phage storage, as it was also observed by Ritchie and Klos (1979).

The negative effects of UV light on microorganisms has been widely known and investigated in various microbial ecology studies (Newsham et al., 1997; Paul et al., 1997). In our experiments, the detrimental effect of UV light particularly affected non-formulated KΦ1 phages that were completely inactivated after 40 days, while in conditions of constant darkness, phages survived more than 60 days. Skim milk and sucrose formulation significantly contributed to phage survival, especially in UV light/dark conditions. Similar results were obtained by Iriarte et al. (2007), where non-formulated phages were completely eliminated after 15 days under UV light/dark conditions, while the concentration of formulated phages decreased by 1.62 log units within 60 days. The formulation containing skim milk and sucrose developed by Balogh et al. (2003) effectively protects the phage particles from the negative effect of UV light and other environmental factors associated with survival on leaf surface. The high level of protein and sugar in milk has beneficial effects on survival of the viruses (Iriarte et al., 2007). The first information about the beneficial properties of milk for the survival of phage with the use of whey filtrate dates back to 1953 (Prouty, 1953). Also, it was reported that dextrose and tryptone can be used to protect phage particles (Ehrlich et al., 1964; Iriarte et al., 2007).

Copper ions are toxic to all cells because they react with sulfhydryl groups of certain amino acids and cause denaturation of proteins and enzymes (Agrios, 2005). Our experiment indicated the negative effect of copper hydroxide and copper oxychloride on the phage activity *in vitro*. During 3 weeks of incubation, the phage concentration decreased in suspensions of copper compounds of recommended concentration for commercial use. It was found that the concentration of copper oxychloride recommended for commercial use (0.5%) was significantly more toxic than the recommended (0.2%) and 10× higher (2%) concentration of copper hydroxide. Similarly, the negative effect of copper compounds on phage survival *in vitro* has been observed by Balogh et al. (2005), who studied the effect of copper oxychloride on the activity of the phage during 6 days. These results showed unsuitability of using copper compounds with non-formulated phages in the same tank before treatment.

A prerequisite for the successful use of bacteriophages to control plant pathogenic bacteria is that a phage comes in contact with its host on the leaf surface. The phyllosphere is a harsh environment and phages applied to aerial tissues degrade rapidly due to exposure to high temperature, high and low pH, sunlight, pesticides, or are dislodged by rain leaching (Gill and Abedon, 2003). Determining phage persistence on the pepper leaf surface was important for their future use as biological agents in bacterial spot control. Our results showed that KΦ1 phages may persist at least 7 days on pepper leaf surface under greenhouse conditions, without the presence of the host bacterium. This finding is significant for defining the time interval of future phage treatment in disease control. However, we should keep in mind that phage persistence in the greenhouse is probably longer than its persistence in the field, since the greenhouse protects phages from the negative effects of some environmental factors. The intensity of UV light is significantly reduced due to the passage of sunlight through a glass surface. Also, greenhouse conditions protect phages from extremely high temperatures and washing of viruses by rain, and contribute to their persistence in the phyllosphere. Similar results were obtained by Zaccardelli et al. (1992), who studied the survival of phage specific to *X. campestris* pv. *pruni* on the surface of peach leaves in the absence of a host. Phages survived for 5 days on the leaf surface in a climatic chamber, where phage concentration was decreased from an initial value of 1.12×10^7 to 2.6×10^5 PFU/g leaf tissue. Epiphytic survival of phage on the leaves in the orchard was at least 5 days, and approximately 10^4 times lower than its survival on the leaves in the climatic chamber. Balogh et al. (2005) recovered phages from the tomato canopy up to 2 and 4 days after application under field and greenhouse conditions, respectively. The reduction in phage populations occurred mainly during the daytime. One of the unique advantages of phages compared to chemical pesticides, however, is their ability to increase their concentration by multiplying on a bacterial host. Under favorable environmental conditions, in the presence of high host populations, phages persist much better than without the host (Balogh et al., 2009).

The efficacy of phage KΦ1 as a biological agent in control of pepper bacterial spot in greenhouse conditions was confirmed in all three experiments. All phage treatments significantly reduced the intensity of bacterial leaf spot of pepper compared to the untreated control. However, a single application of KΦ1 phages did not achieve a constant level of efficacy. Such results could be explained by the limited survival of non-formulated phages on the leaf surface. Similar inconsistency was observed by Obradović et al. (2005), where phage treatments were applied in control of tomato bacterial spot. Our results did not show any significant differences in disease reduction between the phage applications before and after inoculation. The most efficient treatment was the combination when copper compound was applied 1 day and phages 2 h before inoculation. Although it was reported that copper compounds may be detrimental to phages (Balogh et al., 2005; Iriarte et al., 2007), the copper-hydroxide application approximately 1 day before the application of phages did not affect the phage efficacy, based on the number of lesions counted (**Table 2**). However, the combination of these treatments contributed to the higher efficacy.

Biological control using bacteriophages as biological agents is a sustainable strategy in plant protection, since biopesticides are quickly degraded in the ecosystem. In addition, there is no phytotoxicity, resistant bacterial strains develop more slowly, and they are considered as safe for human health. Our results clearly show that phage KΦ1 possesses high specificity and lytic activity to a range of *X. euvesicatoria* strains. These findings, as well as other studied characteristics, make this phage a valuable candidate for biological control of bacterial spot of pepper. Current study provides the starting point for the future research

in order to improve phage KΦ1 stability and efficacy in disease control in field conditions.

AUTHOR CONTRIBUTIONS

KG and AO conceived and designed the experiments. KG, MI, AP, and MŠ performed the experiments. KG, NK, and AO analyzed the data. KG wrote the paper. AO revised the paper. All authors read and approved the final manuscript.

FUNDING

This research was supported by the Ministry of Education, Science and Technological Development, Serbia, project III46008.

ACKNOWLEDGMENTS

This article is based upon work from COST Action CA16107 EuroXanth, supported by COST (European Cooperation in Science and Technology). We would like to thank the Institute for Genome Sciences Annotation Engine service at the School of Medicine, University of Maryland for providing structural and functional annotation of the sequences.

SUPPLEMENTARY MATERIAL

The Supplementary Material for this article can be found online at: https://www.frontiersin.org/articles/10.3389/fmicb.2018.02021/full#supplementary-material

REFERENCES

Adaskaveg, J. E., and Hine, R. B. (1985). Copper tolerance and zinc sensitivity of Mexican strains of *Xanthomonas campestris* pv. vesicatoria causal agent of bacterial spot of pepper. *Plant Dis.* 69, 993–996. doi: 10.1094/PD-69-993

Agrios, G. N. (2005). *Plant Pathology. Elsevier*. Burlington, MA: Academic Press.

Appunu, C., and Dhar, B. (2008). Morphology and general characteristics of lytic phages infective on strains of *Bradyrhizobium japonicum*. *Curr. Microbiol.* 56, 21–27. doi: 10.1007/s00284-007-9031-6

Balaž, J. (1994). Pegavost lišća paprike prouzrokovana bakterijom *Xanthomonas campestris* pv. *vesicatoria*. *Savremena poljoprivreda* 42, 341–345.

Balogh, B., Canteros, B. I., Stall, R. E., and Jones, J. B. (2008). Control of citrus canker and citrus bacterial spot with bacteriophages. *Plant Dis.* 92, 1048–1052. doi: 10.1094/PDIS-92-7-1048

Balogh, B., Jones, J. B., Momol, M. T., and Olson, S. M. (2005). Persistence of bacteriophages as biocontrol agents in the tomato canopy. *Acta Hortic.* 695, 299–302. doi: 10.17660/ActaHortic.2005.695.34

Balogh, B., Jones, J. B., Momol, M. T., Olson, S. M., Obradović, A., King, B., et al. (2003). Improved efficacy of newly formulated bacteriophages for management of bacterial spot of tomato. *Plant Dis.* 87, 949–954. doi: 10.1094/PDIS.2003.87.8.949

Balogh, B., Momol, T., Obradović, A., and Jones, J. B. (2009). "Bacteriophages as agents for the control of plant pathogenic bacteria," in *Disease Control in Crops - Biological and Environmentally Friendly Approaches*, ed. D. Walters (Oxford: Wiley-Blackwell), 246–256.

Buttimer, C., McAuliffe, O., Ross, R. P., Hill, C., O'Mahony, J., and Coffey, A. (2017). Bacteriophages and bacterial plant diseases. *Front. Microbiol.* 8:34. doi: 10.3389/fmicb.2017.00034

Civerolo, E. L., and Keil, H. L. (1969). Inhibition of bacterial spot of peach foliage by *Xanthomonas pruni* bacteriophage. *Phytopathology* 12, 1966–1967.

Darling, A. E., Mau, B., and Perna, N. T. (2010). progressiveMauve: multiple genome alignment with gene gain, loss and rearrangement. *PLoS One* 5:e11147. doi: 10.1371/journal.pone.0011147

Ehrlich, R., Miller, S., and Idoine, L. S. (1964). Effects of environmental factors on the survival of airborne T-3 coliphage. *Appl. Microbiol.* 12, 479–482.

Flaherty, J. E., Harbaugh, B. K., Jones, J. B., Somodi, G. C., and Jackson, L. E. (2001). H-mutant bacteriophages as a potential biocontrol of bacterial blight of geranium. *HortScience* 36, 98–100.

Flaherty, J. E., Jones, J. B., Harbaugh, B. K., Somodi, G. C., and Jackson, L. E. (2000). Control of bacterial spot on tomato in the greenhouse and field with h-mutant bacteriophages. *HortScience* 35, 882–884.

Garg, A., and Gupta, D. (2008). VirulentPred: a SVM Based prediction method for virulent proteins in bacterial pathogens. *BMC Bioinformatics* 9:62. doi: 10.1186/1471-2105-9-62

Gašić, K., Ivanović, M. M., Ignjatov, M., Ćalić, A., and Obradović, A. (2011). Isolation and characterization of *Xanthomonas euvesicatoria* bacteriophages. *J. Plant Pathol.* 93, 415–423.

Gill, J., and Abedon, S. T. (2003). *Bacteriophage Ecology and Plants*. Guelph, ON: APSnet.

Greer, G. G. (2005). Bacteriophage control of foodborne bacteria. *J. Food Prot.* 68, 1102–1111. doi: 10.4315/0362-028X-68.5.1102

ICTV (2017). *Virus Taxonomy: 2017 Release, International Committee on Taxonomy of Viruses (ICTV)*. Available at: https://talk.ictvonline.org/taxonomy/

Ignjatov, M., Šević, M., Gašić, K., Jovièić, D., Nikolić, Z., Milošević, D., et al. (2012). Proučavanje osetljivosti odabranih genotipova paprike prema prouzrokovaču bakteriozne pegavosti. *Ratar. Povrt.* 49, 177–182.

Inoue, Y., Matsuura, T., Ohara, T., and Azegami, K. (2006). Sequence analysis of the genome of OP2, a lytic bacteriophage of *Xanthomonas oryzae* pv. *oryzae*. *J. Gen. Plant Pathol.* 72, 104–110. doi: 10.1007/s10327-005-0259-3

Iriarte, B. F., Balogh, B., Momol, M. T., Smith, M. L., Wilson, M., and Jones, J. B. (2007). Factors affecting survival of bacteriophage on tomato leaf surfaces. *Appl. Environ. Microbiol.* 73, 1704–1711. doi: 10.1128/AEM.02118-06

Ji, P., Kloepper, J. W., Wilson, M., and Campbell, H. L. (1996). Rhizobacterial-induced systemic resistance in tomato against bacterial speck. *Phytopathology* 86:S50.

Jones, J. B., Jackson, L. E., Balogh, B., Obradović, A., Iriarte, F. B., and Momol, M. T. (2007). Bacteriophages for plant disease control. *Annu. Rev. Phytopathol.* 45, 245–262. doi: 10.1146/annurev.phyto.45.062806.094411

Jones, J. B., Lacy, G. H., Bouzar, H., Stall, R. E., and Shaad, N. (2004). Reclassification of Xanthomonads associated with bacterial spot disease of tomato and pepper. *Syst. Appl. Microbiol.* 27, 755–762. doi: 10.1078/0723202042369884

Klement, Z., Rudolf, K., and Sands, D. C. (1990). *Methods in Phytobacteriology*. Budapest: Akadémiai Kiadó.

Lang, J. M., Gent, D. H., and Schwartz, H. F. (2007). Management of Xanthomonas leaf blight of onion with bacteriophages and a plant activator. *Plant Dis.* 91, 871–878. doi: 10.1094/PDIS-91-7-0871

Laslett, D., and Canback, B. (2004). ARAGORN, a program to detect tRNA genes and tmRNA genes in nucleotide sequences. *Nucleic Acids Res.* 32, 11–16. doi: 10.1093/nar/gkh152

Lavigne, R., Darius, P., Summer, E. J., Seto, D., Mahadevan, P., Nilsson, A. S., et al. (2009). Classification of myoviridae bacteriophages using protein sequence similarity. *BMC Microbiol.* 9:224. doi: 10.1186/1471-2180-9-224

Lavigne, R., Seto, D., Mahadevan, P., Ackermann, H. W., and Kropinski, A. M. (2008). Unifying classical and molecular taxonomic classification: analysis of the Podoviridae using BLASTP-based tools. *Res. Microbiol.* 159, 406–414. doi: 10.1016/j.resmic.2008.03.005

Le, S., He, X., Tan, Y., Huang, G., Zhang, L., and Lux, R. (2013). Mapping the tail fiber as the receptor binding protein responsible for differential host

specificity of *Pseudomonas aeruginosa* bacteriophages PaP1 and JG004. *PLoS One* 8:e68562. doi: 10.1371/journal.pone.0068562

Lehman, S. M., Kropinski, A. M., Castle, A. J., and Svircev, A. M. (2009). Complete genome of the broad-host-range *Erwinia amylovora* phage φEa21-4 and its relationship to *Salmonella* phage Felix O1. *Appl. Environ. Microbiol.* 75, 2139–2147. doi: 10.1128/AEM.02352-08

Lowe, T. M., and Chan, P. P. (2016). TRNAscan-SE on-line: integrating search and context for analysis of transfer RNA genes. *Nucleic Acids Res.* 44, W54–W57. doi: 10.1093/nar/gkw413

Marco, G. M., and Stall, R. E. (1983). Control of bacterial spot of pepper initiated by strains of *Xanthomonas campestris* pv. *vesicatoria* that differ in sensitivity to copper. *Plant Dis.* 67, 779–781. doi: 10.1094/PD-67-779

Martin, H. L., Hamilton, V. A., and Kopittke, R. A. (2004). Copper tolerance in Australian populations of *Xanthomonas campestris* pv. *vesicatoria* contributes to poor field control of bacterial spot of pepper. *Plant Dis.* 88, 921–924. doi: 10.1094/PDIS.2004.88.9.921

McNair, K., Bailey, B. A., and Edwards, R. A. (2012). PHACTS, a computational approach to classifying the lifestyle of phages. *Bioinformatics* 28, 614–618. doi: 10.1093/bioinformatics/bts014

McNeil, D. L., Romero, S., Kandula, J., Stark, C., Stewart, A., and Larsen, S. (2001). Bacteriophages: a potential biocontrol agent against walnut blight (*Xanthomonas campestris* pv. *juglandis). N. Z. Plant Prot.* 54, 220–224.

Minsavage, G. V., Canteros, B. I., and Stall, R. E. (1990). Plasmid-mediated resistance to streptomycin in *Xanthomonas campestris* pv. *vesicatoria*. *Phytopathology* 80, 719–723. doi: 10.1094/Phyto-80-719

Newsham, K. K., Low, M. N. R., McLeod, A. R., Greenslade, P. D., and Emmett, B. A. (1997). Ultraviolet-B radiation influences the abundance and distribution of phylloplane fungi on pedunculate oak (Quercus robur). *New Phytol.* 138, 287–297. doi: 10.1046/j.1469-8137.1997.00740.x

Obradović, A., Jones, J. B., Momol, M. T., Balogh, B., and Olson, S. M. (2004a). Management of tomato bacterial spot in the field by foliar applications of bacteriophages and SAR inducers. *Plant Dis.* 88, 736–740. doi: 10.1094/PDIS.2004.88.7.736

Obradović, A., Jones, J. B., Momol, M. T., Olson, S. M., Jackson, L. E., Balogh, B., et al. (2005). Integration of biological control agents and systemic acquired resistance inducers against bacterial spot on tomato. *Plant Dis.* 89, 712–716. doi: 10.1094/PD-89-0712

Obradović, A., Mavridis, A., Rudolph, K., Janse, J. D., Arsenijević, M., Jones, J. B., et al. (2004b). Characterization and PCR-based typing of *Xanthomonas campestris* pv. *vesicatoria* from peppers and tomatoes in Serbia. *Eur. J. Plant Pathol.* 110, 285–292. doi: 10.1023/B:EJPP.0000019797.27952.1d

Obradović, A., Mavridis, A., Rudolph, K., and Arsenijević, M. (2000). Bacterial spot of capsicum and tomato in Yugoslavia. *EPPO Bull.* 30, 333–336. doi: 10.1111/j.1365-2338.2000.tb00905.x

Obradović, A., Mavridis, A., Rudolph, K., Arsenijević, M., and Mijatović, M. (2001). "Bacterial diseases of pepper in Yugoslavia," in *Plant Pathogenic Bacteria*, ed. S. H. De Boer (Alphen aan den Rijn: Kluwer Academic Publishers), 255–258. doi: 10.1007/978-94-010-0003-1_59

Paul, N. D., Rasanayagam, S., Moody, S. A., Hatcher, P. E., and Ayres, P. G. (1997). The role of interactions between trophic levels in determining the effects of UV-B on terrestrial ecosystems. *Plant Ecol.* 128, 296–308. doi: 10.1023/A:1009746511767

Pernezny, K., Kudela, V., Kokoškova, B., and Hladka, I. (1995). Bacterial diseases of tomato in the Czech and Slovak Republics and lack of streptomycin resistance among copper tolerant bacterial strains. *Crop Prot.* 14, 267–270. doi: 10.1016/0261-2194(94)00010-6

Prouty, C. C. (1953). Storage of the bacteriophage of the lactic acid streptococci in the desiccated state with observations on longevity. *Appl. Microbiol.* 1, 250–251.

Ritchie, D. F., and Klos, E. J. (1979). Some properties of *Erwinia amylovora* bacteriophages. *Phytopathology* 69, 1078–1083. doi: 10.1094/Phyto-69-1078

Saccardi, A., Gambin, E., Zaccardelli, M., Barone, G., and Mazzucchi, U. (1993). *Xanthomonas campestris* pv. *pruni* control trials with phage treatments on peaches in the orchard. *Phytopathol. Mediterr.* 32, 206–210.

Schisler, D. A., and Slininger, P. J. (1997). Microbial selection strategies that enhance the likelihood of developing commercial biological control products. *J. Ind. Microbiol. Biotechnol.* 19, 172–179. doi: 10.1038/sj.jim.2900422

Summer, E. J., Gonzalez, C. F., Bomer, M., Carlile, T., Morrison, W., Embry, A., et al. (2006). Divergence and mosaicism among virulent soil phages of the *Burkholderia cepacia* complex. *J. Bacteriol.* 188, 255–268. doi: 10.1128/JB.188.1.255-268.2006

Suttle, C. A., and Chen, F. (1992). Mechanisms and rates of decay of marine viruses in seawater. *Appl. Environ. Microbiol.* 58, 3721–3729.

Svircev, A. M., Castle, A. J., and Lehman, S. M. (2010). "Bacteriophages for control of phytopathogens in food production systems," in *Bacteriophages in the Control of Food- and Waterborne Pathogens*, eds P. M. Sabour and M. W. Griffiths (Washington, DC: ASM Press), 79–96.

Svircev, A. M., Lehman, S. M., Kim, W., Barszcz, E., Schneider, K. E., and Castle, A. J. (2006). "Control of the fire blight pathogen with bacteriophages," in *Proceedings of the 1st International Symposium on Biological Control of Bacterial Plant Diseases*, eds W. Zeller and C. Ullrich (Berlin-Dahlem: Mitteilungen aus der Biologischen Bundesanstalt für Land- und Forstwirtschaft), 259–261.

Tétart, F., Repoila, F., Monod, C., and Krisch, H. M. (1996). Bacteriophage T4 host range is expanded by duplications of a small domain of the tail fiber adhesin. *J. Mol. Biol.* 258, 726–731. doi: 10.1006/jmbi.1996.0281

Thayer, P. L., and Stall, R. E. (1961). A survey of Xanthomonas vesicatoria resistance to streptomycin. *Proc. Fla. State Hort. Soc.* 75, 163–165.

Zaccardelli, M., Saccardi, A., Gambin, E., and Mazzucchi, U. (1992). *Xanthomonas campestris* pv. *pruni* bacteriophages on peach trees and their potential use for biological control. *Phytopathol. Mediterr.* 31, 133–140.

Zafar, N., Mazumder, R., and Seto, D. (2002). CoreGenes: a computational tool for identifying and cataloging "core" genes in a set of small genomes. *BMC Bioinformatics* 3:12. doi: 10.1186/1471-2105-3-12

Conflict of Interest Statement: The authors declare that the research was conducted in the absence of any commercial or financial relationships that could be construed as a potential conflict of interest.

frontiers in Microbiology

ORIGINAL RESEARCH
published: 14 August 2018
doi: 10.3389/fmicb.2018.01861

Larger Than Life: Isolation and Genomic Characterization of a Jumbo Phage That Infects the Bacterial Plant Pathogen, *Agrobacterium tumefaciens*

Hedieh Attai[1], *Maarten Boon*[2], *Kenya Phillips*[1], *Jean-Paul Noben*[3], *Rob Lavigne*[2] *and Pamela J. B. Brown*[1]*

[1] Division of Biological Sciences, University of Missouri, Columbia, MO, United States, [2] Laboratory of Gene Technology, KU Leuven, Leuven, Belgium, [3] Biomedical Research Institute and Transnational University Limburg, Hasselt University, Hasselt, Belgium

OPEN ACCESS

Edited by:
Robert Czajkowski,
University of Gdansk, Poland

Reviewed by:
Clay Fuqua,
Indiana University Bloomington, United States
Nikolai Ravin,
Research Center of Biotechnology of the Russian Academy of Sciences, Russia

***Correspondence:**
Pamela J. B. Brown
brownpb@missouri.edu

Specialty section:
This article was submitted to Virology, a section of the journal Frontiers in Microbiology

Received: 19 June 2018
Accepted: 24 July 2018
Published: 14 August 2018

Citation:
Attai H, Boon M, Phillips K, Noben J-P, Lavigne R and Brown PJB (2018) Larger Than Life: Isolation and Genomic Characterization of a Jumbo Phage That Infects the Bacterial Plant Pathogen, Agrobacterium tumefaciens. Front. Microbiol. 9:1861. doi: 10.3389/fmicb.2018.01861

Agrobacterium tumefaciens is a plant pathogen that causes crown gall disease, leading to the damage of agriculturally-important crops. As part of an effort to discover new phages that can potentially be used as biocontrol agents to prevent crown gall disease, we isolated and characterized phage Atu_ph07 from Sawyer Creek in Springfield, MO, using the virulent *Agrobacterium tumefaciens* strain C58 as a host. After surveying its host range, we found that Atu_ph07 exclusively infects *Agrobacterium tumefaciens*. Time-lapse microscopy of *A. tumefaciens* cells subjected to infection at a multiplicity of infection (MOI) of 10 with Atu_ph07 reveals that lysis occurs within 3 h. Transmission electron microscopy (TEM) of virions shows that Atu_ph07 has a typical *Myoviridae* morphology with an icosahedral head, long tail, and tail fibers. The sequenced genome of Atu_ph07 is 490 kbp, defining it as a jumbo phage. The Atu_ph07 genome contains 714 open reading frames (ORFs), including 390 ORFs with no discernable homologs in other lineages (ORFans), 214 predicted conserved hypothetical proteins with no assigned function, and 110 predicted proteins with a functional annotation based on similarity to conserved proteins. The proteins with predicted functional annotations share sequence similarity with proteins from bacteriophages and bacteria. The functionally annotated genes are predicted to encode DNA replication proteins, structural proteins, lysis proteins, proteins involved in nucleotide metabolism, and tRNAs. Characterization of the gene products reveals that Atu_ph07 encodes homologs of 16 T4 core proteins and is closely related to Rak2-like phages. Using ESI-MS/MS, the majority of predicted structural proteins could be experimentally confirmed and 112 additional virion-associated proteins were identified. The genomic characterization of Atu_ph07 suggests that this phage is lytic and the dynamics of Atu_ph07 interaction with its host indicate that this phage may be suitable for inclusion in a phage cocktail to be used as a biocontrol agent.

Keywords: *Agrobacterium*, jumbo bacteriophage, mass spectrometry, genomics, biocontrol, Atu_ph07

INTRODUCTION

Bacteriophages, or phages, are the most abundant biological entities on the planet (Clokie et al., 2011). Phages are viruses that specifically infect bacteria, often causing lysis. Phage-mediated host cell lysis of bacteria impacts environments both directly through release of dissolved organic carbon and micronutrients and indirectly by modulation of the microbial communities (Srinivasiah et al., 2008). Phages also contribute to horizontal gene transfer and host cell evolution. Bacteria-phage coevolution significantly drives gene diversity and evolution (Koskella and Brockhurst, 2014), providing both bacteria and phages with genes necessary to thrive in their environments. The diversity and vast number of phage genes coupled with limited functional characterization results in the presence of many predicted proteins of unknown function (Hatfull, 2015). Since characterization of phages and their proteins will provide biological insights, some of which can be leveraged to address current challenges in medicine and agriculture, research on phage biology, phage-host interactions, and phage-derived enzymes has recently reemerged (Santos et al., 2018).

Phage cocktails have successfully been deployed as a form of biocontrol against plant pathogens, including *Xanthomonas* species, *Ralstonia solanacearum*, *Pseudomonas syringae*, and *Dickeya solani* (Adriaenssens et al., 2012; Rombouts et al., 2016; Buttimer et al., 2017b). *Agrobacterium tumefaciens* is a Gram-negative bacterium that causes crown gall disease in flowering plants (Escobar and Dandekar, 2003) and phage cocktails may be a viable option to improve biocontrol of this phytopathogen; however, there are only three well-characterized *Agrobacterium* phages: Atu_ph02, Atu_ph03, and 7-7-1 (Kropinski et al., 2012; Attai et al., 2017). When searching for additional lytic phages with potential to serve as biocontrol agents against *A. tumefaciens*, we isolated a unique jumbo phage, Atu_ph07, with a dsDNA genome size of 490,380 bp.

Jumbo phages have genomes exceeding 200 kbp (Hendrix, 2009) and are less frequently isolated since they are often eliminated during common size-exclusion isolation methods due to their large size (Yuan and Gao, 2017). Most jumbo phages are members of the *Myoviridae* family and contain visible tails. The largest known phage genome belongs to *Bacillus* phage G at 497 kbp (Donelli et al., 1975), followed by *Salicola* phage SCTP-2 at 440 kbp, *Xanthomonas* phage XacN1 at 384 kbp (Yoshikawa et al., 2018), *Pectobacterium* phage CBB at 378 kbp (Buttimer et al., 2017a), *Cronobacter* phage vB_CsaM_GAP32 at 358 kbp (Abbasifar et al., 2014), and *Serratia* phage BF at 357 kbp (Casey et al., 2017). Recently, some of these T4-like jumbo phages (CBB, vB_CsaM_GAP32, BF, vB_KleM-Rak2, K64-1, 121Q, vB_Eco_slurp01, PBECO4) were classified into a new phylogenetic clade called "Rak2-like viruses" (Buttimer et al., 2017a; Yoshikawa et al., 2018), named after Enterobacteria phage Rak2 (Simoliunas et al., 2013).

In this work, we use phenotypic, genomic, and proteomic approaches to characterize phage Atu_ph07 (formal name according to Kropinski et al., 2009: vB_AtuM_Atu_ph07). Based upon comparative genome analysis and phylogenetic analysis, Atu_ph07 clusters just outside the Rak2-like phages. Though most Atu_ph07 ORFs encode as-yet uncharacterized hypothetical proteins, this work identifies functions for some key proteins, including experimentally validated structural proteins, and compares those proteins to homologs in related phages.

MATERIALS AND METHODS

Bacterial Strains and Culture Conditions

Strains used in this study are shown in **Table 1.** *Agrobacterium tumefaciens* strains were cultured in Lysogeny Broth (LB), with the exception of *A. tumefaciens* strain LBA4404, which was grown in yeast mannitol (YM) medium. *Agrobacterium vitis* was cultured using potato dextrose media (Difco), *Rhizobium rhizogenes* was grown in mannitol glutamate yeast (MGY) medium and *Caulobacter crescentus* was grown in peptone-yeast extract (PYE) medium (Poindexter, 1964). *Sinorhizobium meliloti* was grown in LB (Weidner et al., 2013). These strains were grown at 28°C. *Escherichia coli* was grown in LB at 37°C. Liquid cultures were grown with shaking and solid medium was prepared with 1.5% agar.

Clonal Isolation of Bacteriophage Atu_ph07

Atu_ph07 was isolated from Sawyer Creek in Springfield, MO using *Agrobacterium tumefaciens* strain C58 as the host. Atu_ph07 was isolated using an enrichment protocol (Santamaría et al., 2014) adapted as described previously (Attai et al., 2017).

Partial Purification of Virions

Virions were concentrated and partially purified from 2 L lysate by polyethylene glycol (PEG) precipitation (Yamamoto et al., 1970) and differential centrifugation. All centrifugations and incubations were performed at 4°C. The starting lysate was distributed evenly into six 500-ml centrifuge bottles and centrifuged at 5,000 rpm for 20 min to pellet bacterial cells. The supernatants were poured into fresh bottles, which were centrifuged as before to pellet residual bacterial cells. The doubly-cleared supernatants were treated with DNase I (Sigma D5025) at a final concentration of 3.5 μg/ml with stirring for 1 h at room temperature to digest bacterial DNA. Solid NaCl was added to a final concentration of 0.5 M with stirring; when the salt was fully dissolved, solid PEG 8000 (Fisher BP233-1) was added gradually to a final concentration of 10% w/w with constant stirring; stirring was continued for another 2 h. The suspension was distributed evenly into six 500–ml centrifuge bottles, which were refrigerated overnight before being centrifuged at 8,000 rpm for 10 min to pellet the virions; supernatants were decanted and discarded; the bottles were centrifuged again and residual supernatants were removed by aspiration. To each bottle, 20 ml 1 × Dulbecco's phosphate-buffered saline with magnesium and calcium (DPBS; Fisher) was added and the pellets dissolved by gentle shaking at 4°C overnight.

The six dissolved pellets were distributed evenly into four 50–ml disposable plastic conical centrifuge tubes, which were centrifuged for 10 min at 5,000 rpm to pellet insoluble material. The cleared supernatants were pooled and 1/9 vol of 5 M NaCl was added. Solid PEG 8000 was added gradually with

TABLE 1 | Bacterial strains used in this study.

Strain or plasmid	Relevant characteristics	Growth medium	Reference or source
***A. tumefaciens* STRAINS**			
C58	Nopaline type strain; pTiC58; pAtC58	LB	Watson et al., 1975
EHA105	C58 derived, succinamopine strain, T-DNA deletion derivative of pTiBo542	LB	MU plant transformation core facility
GV3101	C58 derived, nopaline strain	LB	MU plant transformation core facility
NTL4	C58 derived, nopaline-agrocinopine strain, Δ*tetRA*	LB	Luo et al., 2001
AGL-1	C58 derived, succinamopine strain, T-DNA deletion derivative of pTiBo542 ΔrecA	LB	MU plant transformation core facility
LBA4404	Ach5 derived, octopine strain, T-DNA deletion derivative of pTiAch5	YM	MU plant transformation core facility
Chry5	Succinamopine strain, pTiChry5	LB	Bush and Pueppke, 1991
LMG215	*Agrobacterium* biovar 1, genomospecies 4, isolated from hops in 1928	LB	Chang lab at Oregon State University
LMG232	*Agrobacterium* biovar 1, genomospecies 1, isolated from beet in 1963	LB	Chang lab at Oregon State University
A74a	*Agrobacterium* biovar 1, genomospecies 8, isolated from Pennsylvania lavender in 2003	LB	Chang lab at Oregon State University
06-777-2L	*Agrobacterium* biovar 1, genomospecies 7, isolated from Marguerite Daisy in 2006	LB	Chang lab at Oregon State University
OTHER BACTERIAL STRAINS			
A. vitis S4	Vitopine strain, pTiS4, pSymA, pSymB	Potato dextrose	Slater et al., 2009
Rhizobium rhizogenes D108/85	*Agrobacterium* biovar 2, isolated from Michigan blueberry 1985	MGY	Chang lab at Oregon State University
Caulobacter crescentus CB15	Alphaproteobacterium	PYE	Nierman et al., 2001
Sinorhizobium meliloti 1021	Rhizopine strain, pSymA, pSymB, pRme41a	LB	Weidner et al., 2013
Escherichia coli DH5α	Gammaproteobacterium	LB	Life Technologies

stirring to a final concentration of 10% w/w, and stirring was continued for another 1 h at room temperature. The suspension was distributed evenly into four 50–ml centrifuge tubes, which were centrifuged 20 min at 10,000 rpm to pellet virions. The supernatants were decanted and discarded, and the tubes were centrifuged again briefly. Residual supernatants were aspirated and discarded. To each tube, 15 ml DPBS was added, and the tubes were rotated overnight at 4°C to dissolve the pellets. The tubes were centrifuged for 10 min at 5,000 rpm to pellet insoluble material. The supernatants combined and 0.6 ml of sterile 10–mM phenol red (pH ∼7) was added to color the solution cherry-red. This solution was layered onto 2–ml cushions of 5% w/w sucrose in DPBS in six 14 × 89 mm Ultraclear centrifuge tubes (Beckman 331372) and centrifuged at 40,000 rpm for 20 min in a Beckman SW41Ti rotor. The clear supernatants were aspirated gently. 1 ml DPBS was added to each tube and the pellets were dissolved by periodic vortexing and standing overnight at 4°C. The dissolved pellets were transferred to six 1.5–ml microtubes, which were vortexed to complete dissolution and centrifuged at 6,000 rpm for 5 min to pellet insoluble material. The supernatants were transferred to fresh 1.5–ml microtubes, which were centrifuged at 13,000 rpm for 30 min to pellet virions. The supernatants were aspirated, the tubes were centrifuged, and the residual supernatants were aspirated. The pellets were resuspended in 1 ml DPBS by periodic vortexing and standing overnight at 4°C. Finally, the tubes were centrifuged at 6,000 rpm for 5 min to pellet insoluble material and the cleared supernatants were transferred to fresh 1.5–ml microtubes and stored at 4°C. The solutions were notably turbid. Virion concentration was estimated at 10^{12} physical particles/ml by scanning a 1/10 dilution spectrophotometrically, assuming that intact virions have about the same molar absorption coefficient at 260 nm as do naked 490,380-bp DNA molecules. The infective titer was 7×10^{10} plaque forming units (pfu)/ml.

Plaque Assays

Whole-plate plaque assays were performed with the soft agar overlay method (Attai et al., 2017). Briefly, 100 μl cells, grown at an optical density at 600 nm (OD_{600}) of ∼0.2 and diluted to OD_{600} of 0.05, were mixed with 100 μl phage for 15 min at room temperature prior to dilution to allow attachment. This mixture of cells and phage were serially diluted in LB and added to 3 ml melted 0.15 or 0.3% LB-soft agar. The solution was then overlaid onto a 1% LB-agar plate and swirled for even distribution. For host range testing, serial dilutions of phage were spotted onto a bacterial lawn. A mixture of 100 μl cells (OD_{600} of ∼0.2) and 0.3% LB-soft agar was overlaid onto a 1% LB-agar plate. Once the cells solidified, 5 μl of phage dilutions were spotted onto the soft agar. Plates were incubated for 1–2 days to allow plaque formation.

Preparation of Virion DNA

Virion DNA was prepared essentially as described (Attai et al., 2017). A 500–μl portion of partially purified virions was pipetted into a 1.5–ml microfuge tube and extracted twice with neutralized phenol (liquefied phenol equilibrated twice with 1/10 vol 1 M Tris-HCl pH 8, discarding the small upper phase each time) and once with chloroform:isoamyl alcohol (24:1 v/v) as follows: 500 μl neutralized phenol or chloroform:isoamyl alcohol was added to the microtube, the microtube was vigorously vortexed, and the phases were separated by centrifugation at 13,000 rpm for 2 min; most of the lower (organic) phase was removed and discarded, the microtube was centrifuged as before, and the upper (aqueous) phase containing the DNA was transferred to a fresh microtube, taking care to avoid residual bottom layer and interphase material. Next, 40 μl 3 M sodium acetate (pH adjusted

to 6 with acetic acid) and 1 ml 100% ethanol were mixed with the final extract to precipitate the DNA. The precipitate was pelleted by centrifugation at 13,000 rpm for 10 min and washed gently with 1 ml freezer-cold 70% ethanol. The pellet was air-dried, dissolved in 100 μl 1 mM Tris-HCl pH 7.5, 100 μM Na_2EDTA, and stored at −20°C.

Growth Curves

Growth curves were performed by growing bacteria at a starting OD_{600} of 0.05 in LB. Cells were mixed with purified Atu_ph07 in liquid media at the MOIs indicated. Cell growth was measured by the culture turbidity, represented by the absorbance at OD_{600}. Measurements were taken every 10 min for 36 h. Cells were grown at 28°C and shaken for 1 min prior to each reading. The OD_{600} was measured using a BioTek Synergy H1 Hybrid reader. Results were taken in quadruplicate and averaged. For host range testing, Atu_ph07 was added to cells at an MOI of 10.

Time-Lapse Microscopy

A. tumefaciens strain C58 cells were grown to an OD_{600} of 0.2 and infected with Atu_ph07 at an MOI of 10. Infected cells were incubated at room temperature for 15 min to allow phage attachment and 1 μl infected cells were spotted on a 1% agarose pad containing LB, as previously described (Howell et al., 2017). Cells were imaged using a 60 × oil immersion objective (1.4 numerical aperture) by differential interference microscopy every 10 min for 24 h using a Nikon Eclipse TiE equipped with a QImaging Rolera EM-C^2 1 K electron-multiplying charge-coupled-device (EMCCD) camera and Nikon Elements imaging software.

Transmission Electron Microscopy

Virion morphology was observed by applying a small volume of concentrated purified virions onto a freshly, glow-discharged carbon-coated TEM grid and negatively stained with 2% Nano-W (Nanoprobes, LLC, Brookhaven NY). Specimens were observed on a JEOL JEM-1400 transmission electron microscope at 120 kV. Capsid diameters of 100 virions were measured using ImageJ (v.2.0.0) (Schneider et al., 2012). Head lengths were measured from the top of the phage head vertex to the top of the neck ($n = 114$). Head widths were measured from the right vertex of the head to the left vertex, approximately equidistant between the top of the head vertex and top of the neck and perpendicular to the tail ($n = 118$). Tail lengths were measured from the bottom of the head vertex to the baseplate ($n = 102$). Contracted tails were also measured ($n = 12$).

Genome Sequencing and Assembly

Libraries for genome sequencing were constructed from virion DNA following the manufacturer's protocol and reagents supplied in Illumina's TruSeq DNA PCR-free sample preparation kit (FC-121-3001). Briefly, 2.4 μg of DNA was sheared using standard Covaris methods to generate average fragmented sizes of 350 bp. The resulting 3′ and 5′ overhangs were converted to blunt ends by an end repair reaction using 3′-to-5′ exonuclease and polymerase activities, followed by size selection (350 bp) and purification with magnetic sample purification beads. A single adenosine nucleotide was added to the 3′ ends of the blunt fragments followed by the ligation of Illumina indexed paired-end adapters. The adaptor-ligated library was purified twice with magnetic sample purification beads. The purified library was quantified using a KAPA library quantification kit (KK4824), and library fragment sizes were confirmed by Fragment Analyzer (Advanced Analytical Technologies, Inc.). Libraries were diluted, pooled, and sequenced using a paired-end 75-base read length according to Illumina's standard sequencing protocol for the MiSeq. Library preparation and sequencing were conducted by the University of Missouri DNA Core facility.

Genome Annotation

Protein-coding regions were annotated by RAST server (Aziz et al., 2008) and PSI-BLAST (Altschul et al., 1997) with an e-value cut-off of 1e-03. Proteins of interest were analyzed by TMHMM (Krogh et al., 2001) and SignalP 4.1 (Petersen et al., 2011). The presence of tRNAs were detected by tRNAscan-SE (version 2.0) (Lowe and Chan, 2016). Codon usage was analyzed by Geneious (v.11.0.5) (Kearse et al., 2012). Pairwise (%) nucleotide identity was determined using the Mauve plugin in Geneious (Darling et al., 2004).

16S rRNA Gene Amplification

16S rRNA gene sequences were amplified by colony PCR using One*Taq* DNA Polymerase (New England Biolabs) and universal primers, 27F and 1492R (Hogg and Lehane, 1999; Turner et al., 1999). Amplified DNA was purified using the GeneJET PCR Purification Kit (Thermo Scientific) and sequenced by the MU DNA Core facility.

Phylogenetic and Gene Product Analysis

Homologs of the major capsid protein, large terminase subunit, and portal vertex protein were identified by BLASTp using an E-value cutoff of 1e-03. Protein alignment was performed by Geneious using ClustalW (v.2.1) and the BLOSUM matrix (Larkin et al., 2007; Kearse et al., 2012). Maximum-likelihood trees based on phylogeny (PhyML) were built using a Geneious plugin with 100 bootstrap models (Guindon et al., 2010). For the 16S rRNA tree, a ClustalW nucleotide alignment and a neighbor-joining tree were created in Geneious using the Jukes-Cantor genetic distance model. These trees were imported and annotated in iTOL (v3) (Letunic and Bork, 2016).

SDS-PAGE and Electron Spray Ionization Mass Spectrometry (ESI-MS/MS)

Starting from a PEG purified phage stock of $>10^{10}$ pfu/ml, a protein pellet was obtained by chloroform:methanol extraction [1:1:0.75 (vol/vol/vol)]. The pellet was resuspended in loading buffer [40% Glycerol (vol/vol), 4% SDS (wt/vol), 200 mM Tris-HCl pH 6.8, 8 mM EDTA, 0.4% Bromophenol blue (wt/vol)] and heated at 95°C for 5 min before loading on a 12% SDS-PAGE gel. After separation by gel electrophoresis, virion proteins were visualized by staining in Gelcode™ Blue Safe Protein Stain (Thermo Scientific). Fragments covering the full lane of the gel were subsequently isolated and subjected to trypsin digestion as described by Shevchenko et al. (1996). The samples

were then analyzed by nano-liquid chromatography-electrospray ionization tandem mass spectrometry (nanoLC-ESI-MS/MS) and peptides were identified, based on a database containing all predicted phage proteins, using the search engines SEQUEST [v 1.4.0.288] (ThermoFinnigan) and Mascot [v 2.5] (Matrix Science).

Lysogen Induction and Detection Assays

To test if Atu_ph07 produces lysogens, we attempted to induce C58 cells that survived Atu_ph07 infection with mitomycin C and ultra-violet (UV) irradiation. Ten survivor strains were isolated by streak-purifying 3 times on LB-agar and were confirmed to survive Atu_ph07 infection by conducting spot assays. Survivor cells were grown to OD_{600} of 0.4–0.5 and mixed with mitomycin C (Fisher) at a final concentration of 0.5 μg/ml for 2 h at 28°C with shaking or grown to an OD_{600} of 0.6–0.7 irradiated with UV for a time ranging from 3 s to 120 s. In each case, cells were centrifuged at 7,500 rpm for 10 min. The supernatant was filtered through a 0.45 μm column and centrifuged at 4,000 rpm for 10 min. The flow-through was spotted (5 μl) on a lawn of C58 ($OD_{600} = 0.2$, 0.3% LB-agar) and incubated overnight at 28°C to be observed for plaque formation in comparison to the Atu_ph07 control.

To find prophages in the genomes of survivor strains, we attempted to PCR amplify genes from Atu_ph07 that are not present in C58 using two sets of primers, which amplified nicotinate phosphoribosyltransferase (CDS 242) and adenine-specific methyltransferase (CDS 399). Primers to amplify nicotinate phosphoribosyltransferase (1,299 bp) were 5′ ATG ATC GAT ATC GCA ACA 3′ (forward) and 5′ TTA GAC AAT TAG AGG TGC 3′ (reverse) and adenine-specific methyltransferase (759 bp) primers were 5′ATG CAA ATT GGT AAT GGG 3′ (forward) and 5′ TTA AAA TTC AAA TAG CCC 3′ (reverse). PCR was performed using One*Taq* DNA Polymerase (New England Biolabs). DNA from Atu_ph07 or *A. tumefaciens* were used as positive and negative controls, respectively.

Accession Number

The genome sequence of Atu_ph07 has been deposited in the GenBank database with the nucleotide accession number MF403008.

RESULTS AND DISCUSSION

Isolation and Characterization of Atu_ph07

Agrobacterium tumefaciens strain C58 (Watson et al., 1975) was used as a host strain to isolate phages from environmental samples. We isolated phage Atu_ph07 from a water sample from Sawyer Creek in Springfield, MO using a modified phage enrichment protocol (Santamaría et al., 2014). Following filtration of water samples, we noticed the clearing of bacterial cultures after two rounds of incubation with C58. The presence of phage was apparent after performing plaque assays. Virions were concentrated and partially purified using polyethylene glycol (PEG) precipitation and differential centrifugation. Atu_ph07 appeared to make small, turbid plaques on 0.3% soft agar (**Figure 1A**, left), and larger, clearer plaques on 0.15% soft agar (**Figure 1A**, right). Lowering the agar concentration allows propagation of jumbo phages by promoting phage diffusion through the medium. Growth curves of *A. tumefaciens* infected with Atu_ph07 at different multiplicities of infection (MOIs) show that Atu_ph07 inhibits growth of its host after 2 h (**Figure 1B**; **Supplementary Figure S1A**). Time-lapse microscopy of *A. tumefaciens* cells infected with Atu_ph07 at an MOI of 10 shows that Atu_ph07 causes cell lysis within 3 h (**Figure 1C**, **Supplementary Movie M1**). Transmission electron microscopy (TEM) of virions revealed icosahedral heads (length 146 ± 0.6 nm and width 152 ± 0.8 nm) and long tails (136 ± 0.5 nm), as shown in **Figure 1D**. Phage tails appear to be contractile, as shorter tails with an average length of 77 ± 2.6 nm were observed and some heads also appear to be empty. Lastly, the TEMs indicate the presence of tail fibers and "hairy" whiskers (**Figure 1D**, inset). Similar features have also been observed in Enterobacteria phage vB_PcaM_CBB (Buttimer et al., 2017a). While the "hairy" whiskers are tail-associated in Enterobacteria phage vB_PcaM_CBB (Buttimer et al., 2017a), these long, thin appendages appear to be primarily capsid-associated in Atu_ph07. Together, the morphology confirms that Atu_ph07 belongs to the family *Myoviridae* (Ackermann, 2009).

Host Range of Atu_ph07

Since plaque formation by Atu_ph07 is inconsistent (**Figure 1A**), growth curves in the presence or absence of Atu_ph07 at an MOI of 10 were used to assess the host range of the phage (**Supplementary Figure S1**). Susceptible test strains have a decreased growth rate and growth yield in the presence of phage when compared to growth in the absence of phage (**Figure 2**, **Supplementary Figure S1A**), and plaques are formed when an undiluted phage stock with an infective titer of 7×10^{10} pfu/ml is spotted on the test strain. In contrast, resistant strains have comparable growth curves in the presence or absence of phage (**Figure 2**, **Supplementary Figure S1B**), and no plaques develop when the phage stock is spotted on lawns of the test strain.

To determine if similarity of the bacterial strains plays a role in phage infectivity, we acquired or sequenced the 16S rRNA gene of the host strains and constructed a phylogenetic tree **(Figure 2)**. The strains of *A. tumefaciens* form a monophyletic clade consistent with the grouping of these closely related strains into Agrobacteria biovar 1 based on biochemical tests and pathogenicity assays (Keane et al., 1970; Panagopoulos and Psallidas, 1973). While it remains debated if biovar 1 comprises a single species (Sawada et al., 1993; Young et al., 2006) or a complex of related species (Mougel et al., 2002; Portier et al., 2006; Costechareyre et al., 2010), the bacterial strains in this group are heterogeneous, comprising at least nine genomospecies (G1–G9) (Mougel et al., 2002). *A. tumefaciens* C58, which was the host used to isolate Atu_ph07, belongs to the G8 genomospecies (Mougel et al., 2002) and each G8 strain tested was susceptible to Atu_ph07 **(Figure 2)**. While other Agrobacteria biovar 1 strains belonging to G1 (LBA4404 and Chry5) are susceptible to Atu_ph07, this is not a universal phenotype as G4 strain LMG215 is resistant to Atu_ph07 **(Figure 2)**. Representative isolates from biovars 2 and 3, as well as other Alphaproteobacterial strains, are not susceptible to Atu_ph07 infection **(Figure 2).** Thus, the

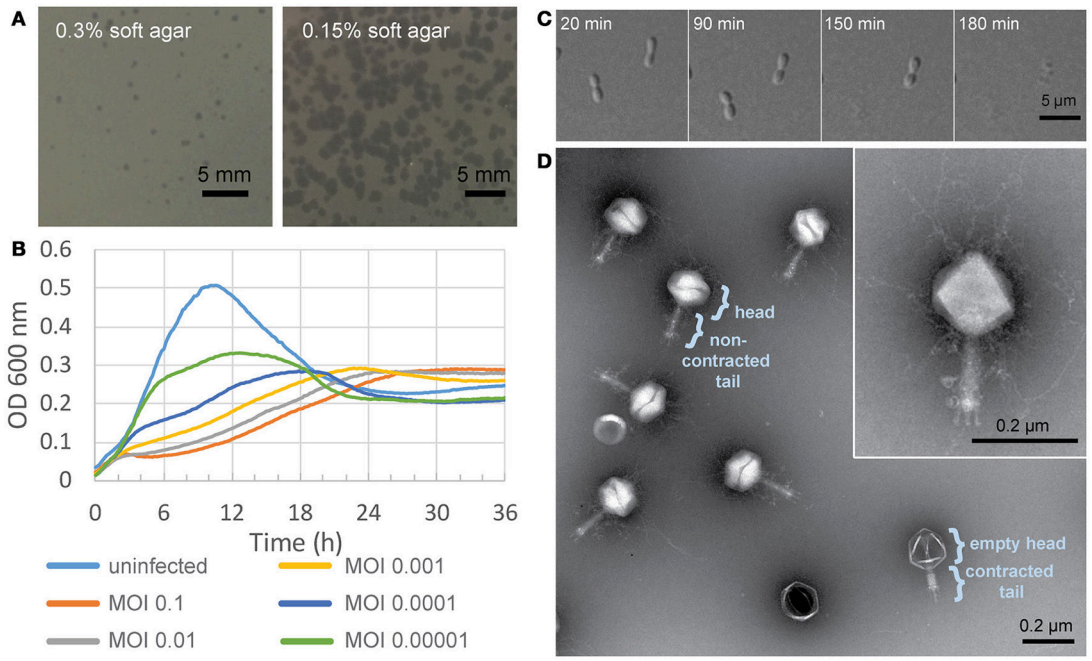

FIGURE 1 | Characterization of Atu_ph07. **(A)** Atu_ph07 forms small plaques on a lawn of *A. tumefaciens* C58 on 0.3% soft agar (left) and larger plaques on 0.15% soft agar (right). **(B)** Growth curve of *A. tumefaciens* infected with Atu_ph07 at different MOIs. **(C)** Time-lapse microscopy of *A. tumefaciens* cells infected with Atu_ph07 at an MOI of 10. **(D)** TEM image of Atu_ph07 shows the phage is in the family *Myoviridae*. Inset of a single phage particle at higher magnification is shown to emphasize the presence of tail fibers and whiskers.

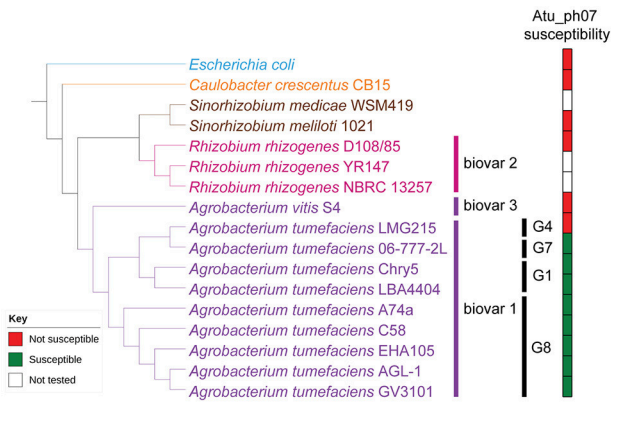

FIGURE 2 | Host range of Atu_ph07. Phylogenetic tree of Alphaproteobacteria tested for Atu_ph07 susceptibility in this study was constructed using 16S rRNA sequences. *Agrobacterium* strains are represented in purple, *Rhizobium* strains in pink, *Sinorhizobium* strains in brown, *Caulobacter* in orange, and the outgroup, *Escherichia coli*, is in blue. Agrobacteria biovars and genomospecies are indicated. Phage susceptibility (green) or resistance (red) for each strain is indicated.

host range of Atu_ph07 appears to be restricted within a subset of Agrobacteria biovar 1.

Genome Analysis and Phylogeny

The Atu_ph07 genome is 490,380 bp in length, leading to the classification of Atu_ph07 as a jumbo phage. Like other agriculturally-relevant jumbo phages, Atu_ph07 has a low G+C content (37.1%) (Almpanis et al., 2018). The genome was annotated using a combination of Rapid Annotation using Subsystem Technology (RAST) (Aziz et al., 2008) and manual annotation based on PSI-BLAST analysis (Altschul et al., 1997). Atu_ph07 contains 714 open reading frames (ORFs), including 390 ORFans (no discernable homologs in other lineages), 214 conserved hypothetical proteins with no assigned function, and 110 predicted proteins with assigned functions based on similarity to conserved proteins (**Table 2**, **Supplementary Table S1**, **Figure 3**).

Due to the high degree of divergence, comparative genome analysis of jumbo phages is challenging. Based on nucleotide identity, Atu_ph07 is most similar to *Synechococcus* phage S-SSM7 (Sullivan et al., 2010). However, the genomes are only 13.1% identical and do not share collinear blocks. Since whole genome alignments did not reveal phages similar to Atu_ph07, we next constructed phylogenetic trees using the sequence of proteins conserved in many jumbo phages. There is no universal gene present in all phages, therefore signature gene products including the major capsid protein, large terminase subunit, and portal vertex protein were selected for the phylogenetic analysis (Adriaenssens and Cowan, 2014). These phylogenies place Atu_ph07 among the jumbo phages in the T4-superfamily (**Figure 4**). Although the genome of Atu_ph07 only shares 33 homologous ORFs with the genome of bacteriophage T4 (**Supplementary Table S2**), core proteins involved in phage morphogenesis and DNA replication, recombination, and repair were identified (**Supplementary Table S3**) (Miller et al.,

TABLE 2 | Summary of key genomic features of Atu_ph07.

Genome length (bp)	G + C content (%)	Number of ORFs	Coding density (%)	Number of hypothetical proteins	Number of ORFs with predicted functions	Number of ORFans	Number of tRNAs
490,380	37.1	714	83.6	214	110	390	33

2003). The phylogenetic trees are consistent with the recent characterization of *Xanthomonas* phage XacN1 (Yoshikawa et al., 2018), which suggested that XacN1, *Salicola* phage SCTP-2 and Atu_ph07 are distantly related to the Rak2-like jumbo phages.

The ORFs in the Atu_ph07 genome were compared to those in XacN1, SCTP-2, and Rak2-like phage genomes (**Figure 5**, **Supplementary Table S2**). The genome of phage SCTP-2 has the highest number of conserved genes with 141 genes (19.7% of Atu_ph07 ORFs) in common with the Atu_ph07 genome, perhaps due to the relatively large size of these phage genomes. Overall, the gene composition of Atu_ph07 is not well conserved with the Rak2-like phages (**Figure 5**, **Supplementary Table S2**), consistent with proposal that Atu_ph07, together with SCTP-2, may belong to a new clade that comprises a sister group to the Rak2-like phages (Yoshikawa et al., 2018).

Functional Annotation

Most of the 110 Atu_ph07 ORFs that can be assigned to a functional annotation are predicted to function in DNA replication, modification, recombination or repair (**Figure 3**, light blue arrows), nucleotide metabolism (**Figure 3**, yellow arrows), translation and posttranslational proteins (**Figure 3**, pink arrows) and structural proteins (**Figure 3**, purple arrows) (**Supplementary Table S1**).

DNA Replication, Repair, and Recombination

Atu_ph07 encodes 26 enzymes involved in DNA replication, repair, and recombination (**Figure 3**, light blue arrows, **Supplementary Table S1**). The majority of these enzymes are all highly conserved in XacNI, SCTP-2, and the Rak2-like phages (**Figure 5**, **Supplementary Table S2**). These highly conserved enzymes include homologs of six of the T4 core proteins involved in DNA replication, repair, and recombination (Petrov et al., 2010). The enzymes with homology to the T4 core proteins are predicted to function as part of the DNA helicase-primase complex (gp70), DNA polymerases (gp276, gp277), sliding clamp loader (gp312), and recombination-related endonucleases (gp691, gp693) (**Supplementary Table S3**). One of the endonucleases (gp693) is directly upstream of a protein (gp694) with similarity to the RNA polymerase sigma factor for late transcription. This gene product shares similarity with corresponding proteins in XacNI, SCTP-2, T4, and most of the Rak2-like phages (**Supplementary Table S2**). The Atu_ph07 genome also encodes a predicted DNA polymerase III alpha subunit (gp316) and epsilon subunit (gp671) suggesting that the polymerase may contribute to both DNA replication and 3′-5′ exonuclease activity. The DNA polymerase III subunits are conserved in most of the Rak2-like phages (**Figure 5**, **Supplementary Table S2**). Atu_ph07 encodes three type II topoisomerase proteins involved in chromosome partitioning (gp4, gp5, gp200) (Kato et al., 1992). Gp4 is highly conserved with DNA gyrase subunit B encoded by the Rak2-like phages and gp5 encodes topoisomerase IV subunit A, also well-conserved in the Rak2-like phages (**Figure 5**). Together, the presence of these highly conserved genes suggests that Atu_ph07 encodes the proteins necessary to complete phage DNA replication and DNA-related functions including recombination and repair.

Nucleotide Metabolism

To supplement the nucleotide pool required for phage DNA and RNA synthesis, T4-like phage genomes encode enzymes for nucleotide metabolism (Petrov et al., 2010). The Atu_ph07 genome contains several enzymes predicted to contribute to nucleotide metabolism (**Figure 3**, **Supplementary Table S1**). These include both alpha and beta subunits (gp122, gp123) of ribonucleotide reductase (RNR) of class 1a (*nrdA* and *nrdB*), which are involved in oxygen-dependent nucleotide metabolism of ribonucleotides into deoxyribonucleotides, a step that is needed for DNA replication (Dwivedi et al., 2013). RNR proteins catalyze nucleotide metabolism with the help of glutaredoxin and thioredoxin (Sengupta, 2014). Two putative glutaredoxin proteins are encoded by Atu_ph07 (gp121, gp266), one of which (gp121) is directly adjacent to the alpha subunit of RNR. Thioredoxin is encoded by gp221.

T4-like phages require ATP and NADH/NAD^+ for important processes like DNA synthesis, transcription, and translation. To metabolize NAD^+, phages use nicotinamide-adenine dinucleotide pyrophosphatase (NUDIX) hydrolases (Bessman et al., 1996; Lee et al., 2017). This family of enzymes is involved in housekeeping functions of the cell, including the hydrolysis of unwanted nucleotides or removal of excess metabolites. Atu_ph07 encodes three putative members of the NUDIX hydrolase superfamily (gp257, gp303, gp557). Other putative proteins involved in nucleotide metabolism include NadR (gp587) and PnuC (gp586). NadR transcriptionally regulates NAD biosynthesis and PnuC is a membrane transporter that allows nicotinamide mononucleotide (NMN) uptake (Foster et al., 1990; Kurnasov et al., 2002).

tRNA Genes and tRNA Processing Genes

The genome of Atu_ph07 encodes 33 tRNA genes, including 32 canonical tRNAs corresponding to all amino acids except asparagine and threonine (**Figure 6**, **Supplementary Table S4**). The remaining tRNA is a suppressor with an anticodon of UCA indicating read-through of opal (UGA) stop codons. The UGA stop codon is abundant in both the phage (N = 267) and *A. tumefaciens* (N = 2,923) genomes suggesting that there are several potential genes targeted by the suppressor tRNA. With the exception of the suppressor tRNA, all of the tRNAs encoded in the Atu_ph07 genome are also found

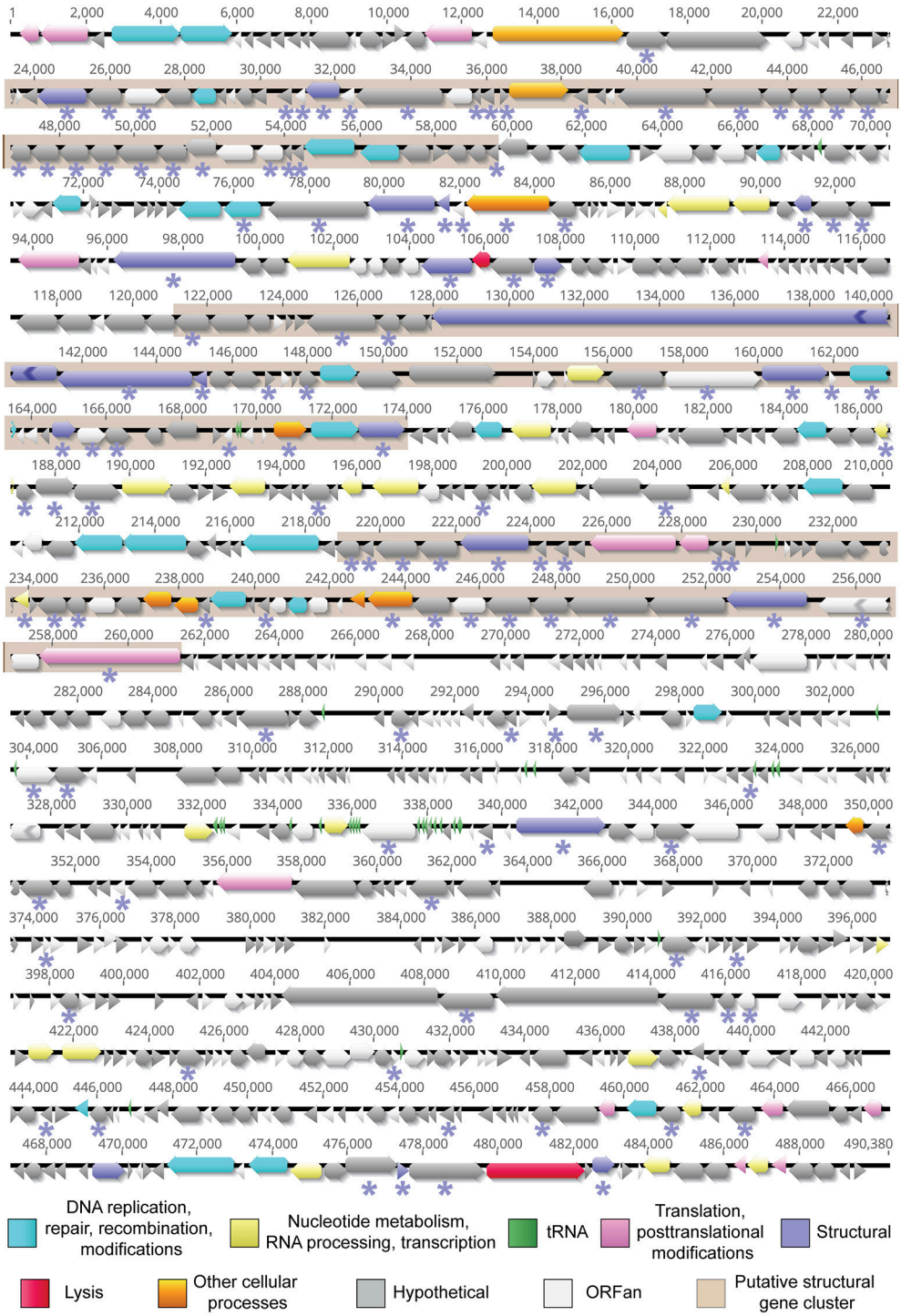

FIGURE 3 | The annotated genome of Atu_ph07. ORFs are represented by functional categories in corresponding colors. Regions shaded in beige represent putative structural protein clusters as identified using ESI-MS/MS analysis. Proteins detected by ESI-MS/MS analysis are indicated with an asterisk (*) below the corresponding ORF.

in the *A. tumefaciens* genome suggesting that the tRNAs do not improve decoding capacity; however, some of the phage tRNAs correspond to codons that are more frequently used in the phage genome **(Figure 6)**. This observation is consistent with the notion that phage-encoded tRNAs allow translation to be optimized for the codon usage of the phage genome

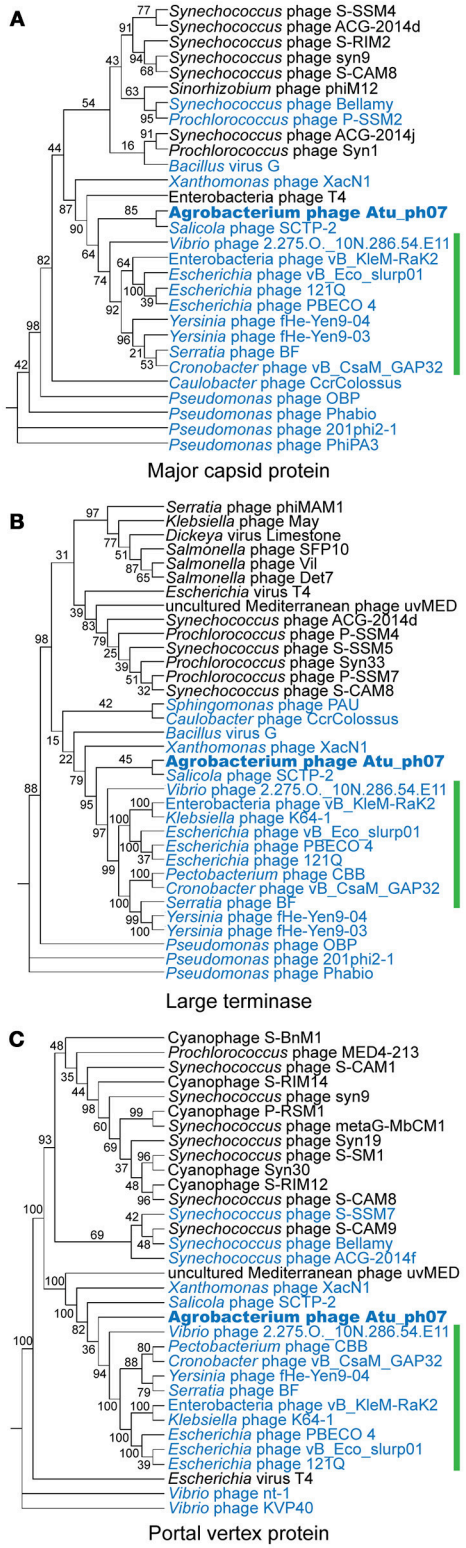

FIGURE 4 | Phylogenetic comparison of Atu_ph07 and related phages. Phylogenetic trees of phages based on alignments of the **(A)** major capsid protein, **(B)** large terminase, and **(C)** portal vertex protein. Jumbo phages are labeled in blue and Atu_ph07 is indicated with bold font. Bootstrap values of 100 replicates are indicated. Rak2-like phages are indicated by a green line.

(Bailly-Bechet et al., 2007). In addition to the tRNA genes, the Atu_ph07 genome encodes four tRNA processing proteins. These tRNA processing proteins include tRNA nucleotidyltransferase (gp18) and $tRNA^{His}$-5′-guanylyltransferase (gp227), which are involved in tRNA maturation. Putative peptidyl-tRNA hydrolases (gp680, gp256) function to decrease the pool of peptidyl-tRNAs formed throughout the initiation, elongation, and termination stages of translation.

Clp-Like Proteins

The Atu_ph07 phage genome encodes seven putative members of the Clp family of proteins that function to degrade proteins, including ClpX (gp2), a prophage Clp protease-like protein (gp128), an ATP-dependent Clp protease ATP-binding subunit (gp155), ClpA (gp292), ClpB (gp492), ATP-dependent Clp protease proteolytic subunit (gp676), and ClpS (gp708). The Clp proteases may contribute to virion assembly or have alternative functions. For example, during phage lambda DNA replication, the ClpX/ClpP protease removes the O protein from the origin of replication (Zylicz et al., 1998) and the activity of ClpX/ClpP has been associated with slowing down DNA replication of the phage under poor growth conditions (Wegrzyn et al., 2000). In the Atu_ph07 genome, *clpX* (gp2) is located in close proximity to genes predicted to encode topoisomerase proteins (gp4-5) suggesting that the ClpX protein may function in the regulation of phage DNA replication. In *E. coli*, ClpS is an adaptor protein that modifies the substrate specificity of the ClpA/ClpP protease and contributes to degradation or refolding of protein aggregates (Dougan et al., 2002). ClpA (gp292) is highly conserved in most of the Rak2-like phages (**Figure 5**). The presence of the ClpB (gp492) and DnaJ (gp293) chaperones, which also function in the removal of protein aggregates (Mogk et al., 1999), further suggests that Atu_ph07 may help its host to survive the stress of phage infection long enough for the phage replication cycle to be completed. Together, these observations suggest that Clp proteins likely contribute to diverse aspects of phage biology potentially including virion assembly, DNA replication, and proteolytic clearance of protein aggregates.

Structural Proteins

Based on homology, the genome of Atu_ph07 was predicted to encode 20 proteins involved in phage morphogenesis and structure (**Figure 3**, **Supplementary Table S1**). Candidate structural genes encode proteins for head morphogenesis and structure (gp125, gp143, gp198, gp204, gp215), baseplate (gp181, gp182, gp686, gp697), tail sheath (gp132, gp140), and tail fibers (gp31, gp288, gp327, gp472). All five of the candidate head proteins, one of the baseplate wedge subunits (gp182), and both of the tail sheath proteins share significant homology with T4 core structural proteins (**Supplementary Tables S2, S3**). The Atu_ph07 genome does not encode proteins with similarity to T4 core tail fiber proteins (**Supplementary Table S3**); however short tail fibers are evident when Atu_ph07 is observed under transmission electron microscopy (**Figure 1D**). One of the tail fiber proteins (gp472) is most closely related (51% identity) to a tail fiber protein encoded in the genome of *Agrobacterium* phage

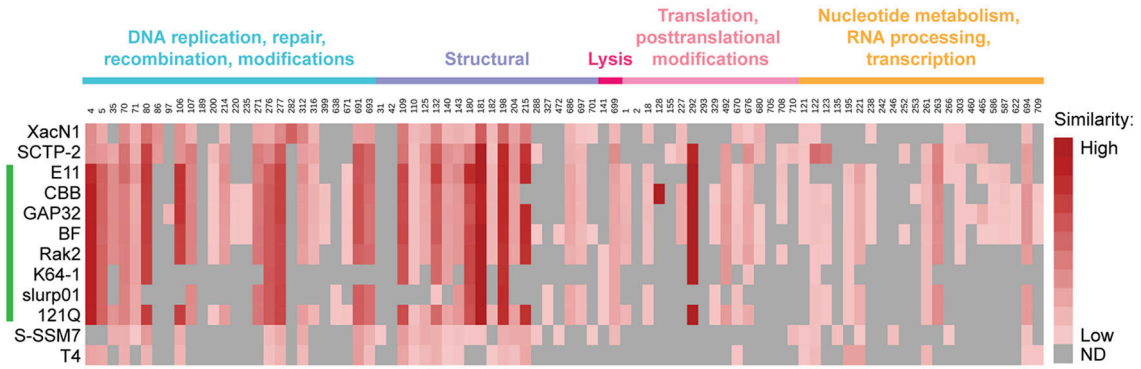

FIGURE 5 | Similarity of annotated gene products in Atu_ph07 and related phages. Heat map displaying Atu_ph07 gene products compared with homologs in 12 related phages, including members of the Rak2-like phages (indicated with a green line). Intensity of the red color indicates the degree of similarity among homologs. Gray boxes indicate that a homolog with an E-value smaller than 1e-03 was not detected (ND). Gene products are organized by functional category and Atu_ph07 gp numbers are indicated.

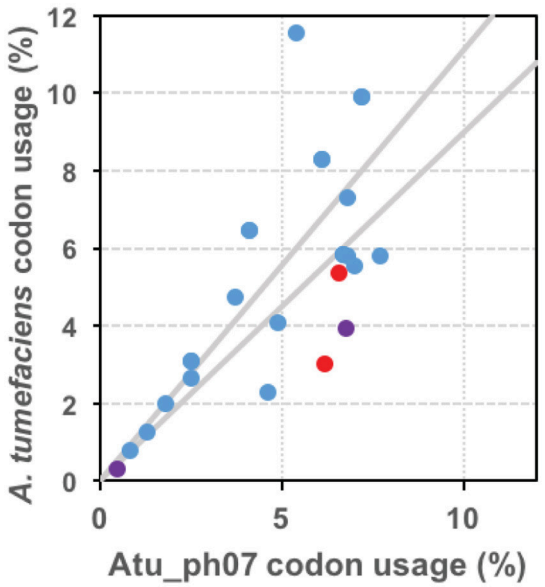

FIGURE 6 | tRNAs are encoded in the Atu_ph07 genome. Graphical representation of codon bias of phage Atu_ph07 and its host *A. tumefaciens* strain C58. Data points represent the usage of each codon in the Atu_ph07 and *A. tumefaciens* genomes. Red points represent codons only found in *A. tumefaciens*, purple points represent codons only found in Atu_ph07, and blue points represent codons found in both genomes. Gray lines outline the region in which codon usage in both genomes is similar.

Atu_ph02 (Attai et al., 2017), suggesting that these phages may share an entry route into *Agrobacterium* cells.

Based upon the complex morphology of Atu_ph07, we hypothesized that the genome annotation likely underestimates the quantity of proteins involved in phage morphogenesis and structure. To experimentally identify structural proteins, electrospray ionization mass spectrometry (ESI-MS/MS) was used (**Figure 7**, **Supplementary Table S5**). Indeed, the number of structural proteins identified by ESI-MS/MS (indicated by purple asterisks in **Figure 3**) is greater than the number of structural proteins predicted by the genome annotation (purple arrows in **Figure 3**). Overall, the proteomic analysis supported the annotation of structural proteins, as all of the head, neck, tail fiber, and most of the tail (5/7) proteins could be identified in the virion proteome. As expected, the most abundant protein observed in the particle proteome is the major capsid protein (gp215, fragment 6 in **Figure 7**). A total of 131 proteins were found among the phage virion proteins, with sequence coverages higher than 5%, or more than one identified unique peptide (**Supplementary Table S5**). About 78% (102/131) of these proteins do not have an assigned function. The majority of the virion proteins are encoded in three large clusters CDS 31-76, CDS 170-215, and CDS 284-329 (shaded in beige in **Figure 3**) that contain a high proportion of structural proteins. The remaining proteins reside in smaller clusters or as separate genes spread across the genome. Notably, CDS 31-76 contains 29 identified proteins of which only two were predicted as structural proteins in the genome, indicative of the presence of unique structural proteins in Atu_ph07. The lack of similarity with known virion proteins should not be surprising, as only a small number of jumbo phages with whisker-like structures have been described to date.

Atu_ph07 Induces Cell Lysis

The genome content is insufficient to confidently predict the phage life cycle, however the phage can induce lysis (**Figures 1B,C**). To assess the possibility of a lysogenic phase, we isolated ten variant clones of *A. tumefaciens* strain C58 that survive exposure to Atu_ph07 at high MOI. Lysogens were not induced from any of the 10 unsusceptible variant clones by exposing them to UV irradiation or mitomycin C (see Materials and Methods for experimental details). Furthermore, we were unable to PCR-amplify two distinctive Atu_ph07 genes, nicotinate phosphoribosyltransferase (CDS 242), and adenine-specific methyltransferase (CDS 399), from the unsusceptible variants. Consistent with these observations, no integrase- or Cro-like genes, which are required for lysogeny in several

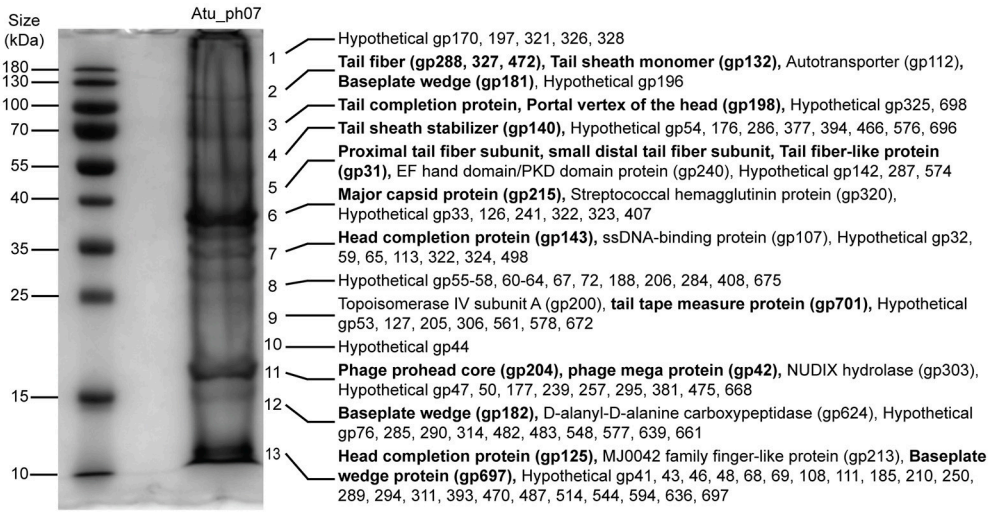

FIGURE 7 | SDS-PAGE of Atu_ph07 structural proteins as identified by ESI-MS/MS. Phage proteins were separated by size and fragments covering the full lane of the gel were excised for proteomic analysis. Numbers at the right of the gel indicate the position of fragments which were excised from the gel. Proteins identified in each fragment are listed. Bold font indicates validation of annotated structural proteins.

temperate phage species, could be identified in the Atu_ph07 genome.

Since we observe that Atu_ph07 can induce cell lysis **(Figure 1C)**, we searched for genes encoding candidate lysis proteins in the genome. Atu_ph07 contains two predicted lysozymes (gp141 and gp699). Gp141 is in close proximity to the predicted phage head completion protein and tail sheath monomer, indicating that it may be involved in phage DNA entry. Gp699 has homologes in the Rak2-like phages and is adjacent to three predicted structural proteins—the baseplate hub subunit (gp686), baseplate wedge protein (gp697), and tail tape measure protein (gp701).

To widen our search for candidate lysis proteins, we searched for transmembrane (TM) proteins which can be indicative of the presence of the canonical endolysin-holin-spanin system of host cell lysis (Young, 2014). A TMHMM analysis (Krogh et al., 2001) of the predicted proteins identified 40 predicted TM proteins, only three of which have putative functions: ribonucleotide reductase of class 1a beta subunit (gp123), ribosyl nicotinamide transporter PnuC (gp586), and peptidyl tRNA hydrolase (gp680). Eight of these encoded TM proteins (gp369-gp376) appear consecutively on the genome at ∼280 kbp, however each of these are ORFs with no detectable similarity in the database, or ORFans (Yin and Fischer, 2008), and therefore we were unable to predict their function as a unit at this time. Thus, at present, the mechanism of Atu_ph07-mediated host cell lysis remains unknown.

CONCLUSION

Several jumbo phages have been recently characterized, many encoding a large number of hypothetical proteins. Recently, a group of T4-like phages have been categorized into a new monophyletic group called "Rak2-like." While phage Atu_ph07 clusters just outside this group, many genes share homology with core genes in the Rak2-like phage genomes. Atu_ph07 infects a subset of *A. tumefaciens* strains **(Figure 2)** and its ability to infect this plant pathogen makes it a candidate for biocontrol.

The phage biology of Atu_ph07 is likely to be remarkable in its own right. While the genome encodes genes for DNA replication, transcription, translation, nucleotide metabolism, as well as over 130 experimentally confirmed structural proteins, many more molecular mechanisms remain to be unraveled. Understanding the modes through which a non-living entity can acquire, store, replicate, and express such a vast number of genes to promote its life cycle is a fascinating aspect of phage biology unique to jumbo phages. A logical assumption considering the coding density of this phage is that many of the putative hypothetical proteins have functional significance and provide jumbo phages with an evolutionary advantage in specific ecological niches. Continued exploration of jumbo phages will help elucidate the mechanisms in which diverse bacteriophages have evolved to thrive as the most abundant biological entities in the world.

AUTHOR CONTRIBUTIONS

HA, MB, KP, and J-PN conducted experiments. All authors designed experiments and analyzed data. HA, MB, RL, and PB contributed to writing and editing of the manuscript.

FUNDING

This research is supported by startup funds, a research council grant (URC 14-051), and a research board grant (3786-2) from the University of Missouri to PJBB. This work was supported in part by the Excellence in Electron Microscopy Award provided

by the University of Missouri Electron Microscopy Core and the Office of Research. HA has been supported by the National Institute of General Medical Sciences (NIGMS) of the National Institutes of Health (NIH) under award number T32GM008396 and the U.S. Department of Education Graduate Assistance in Areas of National Need (GAANN) Fellowship. KP was supported by the IMSD EXPRESS Program via grant number R25GM056901 from the NIGMS, a component of the NIH. RL and MB are supported by a GOA grant from KU Leuven and J-PN was supported by Hercules Foundation project R-3986.

ACKNOWLEDGMENTS

We thank Jeff Chang at Oregon State University for providing *Agrobacterium* and *Rhizobium* strains, as well as their 16S rRNA sequences. We thank Zhanyuan Zhang at the MU Plant Transformation Core facility for providing *Agrobacterium* strains. We thank Tommi White, DeAna Grant, and Martin Schauflinger of the MU Electron Microscopy Core for help with the transmission electron microscopy. We thank Nathan Bivens and the MU DNA Core for assistance with sequencing the bacteriophages and William Spollen and the MU Research Informatics Core for assistance with genome assembly and GenBank submission. We thank Michelle Williams and Blackman Water Labs for donating water samples from which we isolated Atu_ph07. George Smith provided valuable technical assistance during the initial purification and characterization of Atu_ph07. Finally, we thank George Smith, Linda Chapman, and members of the Brown lab for their feedback during the preparation of this manuscript.

SUPPLEMENTARY MATERIAL

The Supplementary Material for this article can be found online at: https://www.frontiersin.org/articles/10.3389/fmicb.2018.01861/full#supplementary-material

REFERENCES

Abbasifar, R., Griffiths, M. W., Sabour, P. M., Ackermann, H. W., Vandersteegen, K., Lavigne, R., et al. (2014). Supersize me: *Cronobacter sakazakii* phage GAP32. *Virology* 460–461, 138–146. doi: 10.1016/j.virol.2014.05.003

Ackermann, H. W. (2009). Phage classification and characterization. *Methods Mol. Biol.* 501, 127–140. doi: 10.1007/978-1-60327-164-6

Adriaenssens, E. M., and Cowan, D. A. (2014). Using signature genes as tools to assess environmental viral ecology and diversity. *Appl. Environ. Microbiol.* 80, 4470–4480. doi: 10.1128/AEM.00878-14

Adriaenssens, E. M., van Vaerenbergh, J., Vandenheuvel, D., Dunon, V., Ceyssens, P. J., de Proft, M., et al. (2012). T4-related bacteriophage LIMEstone isolates for the control of soft rot on potato caused by "*Dickeya solani*." *PLoS One* 7:e33227. doi: 10.1371/journal.pone.0033227

Almpanis, A., Swain, M., Gatherer, D., and Mcewan, N. (2018). Correlation between bacterial G + C content, genome size and the G + C content of associated plasmids and bacteriophages. *Microb. Genomics* 4:e000168. doi: 10.1099/mgen.0.000168

Altschul, S. F., Madden, T. L., Schäffer, A. A., Zhang, J., Zhang, Z., Miller, W., et al. (1997). Gapped BLAST and PSI-BLAST: a new generation of protein database search programs. *Nucleic Acids Res.* 25, 3389–3402. doi: 10.1093/nar/25.17.3389

Attai, H., Rimbey, J., Smith, G. P., and Brown, P. J. B. (2017). Expression of a peptidoglycan hydrolase from lytic bacteriophages Atu_ph02 and Atu_ph03 triggers lysis of *Agrobacterium tumefaciens*. *Appl. Environ. Microbiol.* 83, e01498–e01417. doi: 10.1128/AEM.01498-17

Aziz, R. K., Bartels, D., Best, A. A., DeJongh, M., Disz, T., Edwards, R. A., et al. (2008). The RAST Server: rapid annotations using subsystems technology. *BMC Genomics* 9:75. doi: 10.1186/1471-2164-9-75

Bailly-Bechet, M., Vergassola, M., and Rocha, E. (2007). Causes for the intriguing presence of tRNAs in phages. *Genome Res.* 17, 1486–1495. doi: 10.1101/gr.6649807

Bessman, M. J., Frick, D. N., and O'Handley, S. F. (1996). The MutT proteins or "Nudix" hydrolases, a family of versatile, widely distributed "housecleaning" enzymes. *J. Biol. Chem.* 271, 25059–25062. doi: 10.1074/jbc.271.41.25059

Bush, A. L., and Pueppke, S. G. (1991). Characterization of an unusual new *Agrobacterium tumefaciens* strain from *Chrysanthemum morifolium* ram. *Appl. Environ. Microbiol.* 57, 2468–2472.

Buttimer, C., Hendrix, H., Oliveira, H., Casey, A., Neve, H., McAuliffe, O., et al. (2017a). Things are getting hairy: Enterobacteria bacteriophage vB_PcaM_CBB. *Front. Microbiol.* 8:44. doi: 10.3389/fmicb.2017.00044

Buttimer, C., McAuliffe, O., Ross, R. P., Hill, C., O'Mahony, J., and Coffey, A. (2017b). Bacteriophages and bacterial plant diseases. *Front. Microbiol.* 8:34. doi: 10.3389/fmicb.2017.00034

Casey, E., Fitzgerald, B., Mahony, J., Lugli, G. A., Ventura, M., and Van Sinderen, D., (2017). Genome sequence of *Serratia marcescens* phage BF. *Genome Announc.* 5, e00211–e00217. doi: 10.1128/genomeA.00211-17

Clokie, M. R., Millard, A. D., Letarov, A. V., and Heaphy, S. (2011). Phages in nature. *Bacteriophage* 1, 31–45. doi: 10.4161/bact.1.1.14942

Costechareyre, D., Rhouma, A., Lavire, C., Portier, P., Chapulliot, D., Bertolla, F., et al. (2010). Rapid and efficient identification of *Agrobacterium* species by *recA* allele analysis. *Microb. Ecol.* 60, 862–872. doi: 10.1007/s00248-010-9685-7

Darling, A. C., Mau, B., Blattner, F. R., and Perna, N. T. (2004). Mauve: multiple alignment of conserved genomic sequence with rearrangements. *Genome Res.* 14, 1394–1403. doi: 10.1101/gr.2289704

Donelli, G., Dore, E., Frontali, C., and Grandolfo, M. E. (1975). Structure and physico-chemical properties of bacteriophage G. III. A homogeneous DNA of molecular weight 5 × 108. *J. Mol. Biol.* 94, 555–62. doi: 10.1016/0022-2836(75)90321-6

Dougan, D. A., Reid, B. G., Horwich, A. L., and Bukau, B. (2002). ClpS, a substrate modulator of the ClpAP machine. *Mol. Cell* 9, 673–683. doi: 10.1016/S1097-2765(02)00485-9

Dwivedi, B., Xue, B., Lundin, D., Edwards, R. A., and Breitbart, M. (2013). A bioinformatic analysis of ribonucleotide reductase genes in phage genomes and metagenomes. *BMC Evol Biol.* 13:33. doi: 10.1186/1471-2148-13-33

Escobar, M. A., and Dandekar, A. M. (2003). *Agrobacterium tumefaciens* as an agent of disease. *Trends Plant Sci.* 8:380–6. doi: 10.1016/S1360-1385(03)00162-6

Foster, J. W., Park, Y. K., Penfound, T., Fenger, T., and Spector, M. P. (1990). Regulation of NAD metabolism in *Salmonella typhimurium*: molecular sequence analysis of the bifunctional *nadR* regulator and the *nadA-pnuC* operon. *J. Bacteriol.* 172, 4187–4196. doi: 10.1128/jb.172.8.4187-4196.1990

Guindon, S., Dufayard, J. F., Lefort, V., Anisimova, M., Hordijk, W., and Gascuel, O. (2010). New algorithms and methods to estimate maximum-likelihood phylogenies: assessing the performance of PhyML 3.0. *Syst. Biol.* 59, 307–321. doi: 10.1093/sysbio/syq010

Hatfull, G. F. (2015). Dark matter of the biosphere: the amazing world of bacteriophage diversity. *J. Virol.* 89, 8107–8110. doi: 10.1128/JVI.01340-15

Hendrix, R. W. (2009). Jumbo bacteriophages. *Curr. Top. Microbiol. Immunol.* 328, 229–240. doi: 10.1007/978-3-540-68618-7-7

Hogg, J. C., and Lehane, M. J. (1999). Identification of bacterial species associated with the sheep scab mite (*Psoroptes ovis*) by using amplified genes coding for 16S rRNA. *Appl. Environ. Microbiol.* 65, 4227–4229.

Howell, M., Daniel, J. J., and Brown, P. J. B. (2017). Live cell fluorescence microscopy to observe essential processes during microbial cell growth. *J. Vis. Exp.*, *e*56497. doi: 10.3791/56497

Kato, J., Suzuki, H., and Ikeda, H. (1992). Purification and characterization of DNA topoisomerase IV in *Escherichia coli*. *J. Biol. Chem.* 267, 25676–25684.

Keane, B. P. J., Kerr, A., and Newt, P. B. (1970). Crown gall of stone fruit identification and nomenclature of *Agrobacterium* isolates. *Aust. J. biol. Sci.* 23, 585–596. doi: 10.1071/BI9700585

Kearse, M., Moir, R., Wilson, A., Stones-Havas, S., Cheung, M., Sturrock, S., et al. (2012). Geneious Basic: an integrated and extendable desktop software platform for the organization and analysis of sequence data. *Bioinformatics* 28, 1647–1649. doi: 10.1093/bioinformatics/bts199

Koskella, B., and Brockhurst, M. A. (2014). Bacteria-phage coevolution as a driver of ecological and evolutionary processes in microbial communities. *FEMS Microbiol. Rev.* 38, 916–931. doi: 10.1111/1574-6976.12072

Krogh, A., Larsson, B., von Heijne, G., and Sonnhammer, E. L. (2001). Predicting transmembrane protein topology with a hidden Markov model: application to complete genomes. *J. Mol. Biol.* 305, 567–580. doi: 10.1006/jmbi.2000.4315

Kropinski, A. M., Prangishvili, D., and Lavigne, R. (2009). Position paper: the creation of a rational scheme for the nomenclature of viruses of Bacteria and Archaea. *Environ. Microbiol.* 11, 2775–2777. doi: 10.1111/j.1462-2920.2009.01970.x

Kropinski, A. M., Van Den Bossche, A., Lavigne, R., Noben, J. P., Babinger, P., and Schmitt, R. (2012). Genome and proteome analysis of 7-7-1, a flagellotropic phage infecting *Agrobacterium* sp H13-3. *Virol. J.* 9:102. doi: 10.1186/1743-422X-9-102

Kurnasov, O. V., Polanuyer, B. M., Ananta, S., Sloutsky, R., Tam, A., Gerdes, S. Y., et al. (2002). Ribosylnicotinamide kinase domain of NadR protein: identification and implications in NAD biosynthesis. *J. Bacteriol.* 184, 6906–6917. doi: 10.1128/JB.184.24.6906-6917.2002

Larkin, M. A., Blackshields, G., Brown, N. P., Chenna, R., Mcgettigan, P. A., McWilliam, H., et al. (2007). Clustal W and Clustal X version 2.0. *Bioinformatics* 23, 2947–2948. doi: 10.1093/bioinformatics/btm404

Lee, J. Y., Li, Z., and Miller, E. S. (2017). *Vibrio* phage KVP40 encodes a functional NAD^+ salvage pathway. *J. Bacteriol.* 199:e00855–16. doi: 10.1128/JB.00855-16

Letunic, I., and Bork, P. (2016). Interactive tree of life (iTOL) v3: an online tool for the display and annotation of phylogenetic and other trees. *Nucleic Acids Res.* 44, W242–W245. doi: 10.1093/nar/gkw290

Lowe, T. M., and Chan, P. P. (2016). tRNAscan-SE On-line: integrating search and context for analysis of transfer RNA genes. *Nucleic Acids Res* 44, W54–W57. doi: 10.1093/nar/gkw413

Luo, Z. Q., Clemente, T. E., and Farrand, S. K. (2001). Construction of a derivative of *Agrobacterium tumefaciens* C58 that does not mutate to tetracycline resistance. *Mol. Plant. Microbe. Interact.* 14, 98–103. doi: 10.1094/MPMI.2001.14.1.98

Miller, E. S., Kutter, E., Mosig, G., Arisaka, F., Kunisawa, T., and Rüger, W. (2003). Bacteriophage T4 genome. *Microbiol. Mol. Biol. Rev.* 67, 86–156. doi: 10.1128/mmbr.67.1.86-156.2003

Mogk, A., Tomoyasu, T., Goloubinoff, P., Rüdiger, S., Röder, D., Langen, H., et al. (1999). Identification of thermolabile *Escherichia coli* proteins: prevention and reversion of aggregation by DnaK and ClpB. *EMBO J.* 18, 6934–6949. doi: 10.1093/emboj/18.24.6934

Mougel, C., Thioulouse, J., Perrière, G., and Nesme, X. (2002). A mathematical method for determining genome divergence and species delineation using AFLP. *Int. J. Syst. Evol. Microbiol.* 52, 573–586. doi: 10.1099/00207713-52-2-573

Nierman, W. C., Feldblyum, T. V., Laub, M. T., Paulsen, I. T., Nelson, K. E., Eisen, J. A., et al. (2001). Complete genome sequence of *Caulobacter crescentus*. *Proc Natl Acad Sci U.S.A.* 98, 4136–4141. doi: 10.1073/pnas.061029298

Panagopoulos, C. G., and Psallidas, P. G. (1973). Characteristics of Greek isolates of *Agrobacterium tumefaciens* (E. F. Smith & Townsend) Conn. *J. Appl. Bacteriol.* 36, 233–240. doi: 10.1111/j.1365-2672.1973.tb04096.x

Petersen, T. N., Brunak, S., von Heijne, G., and Nielsen, H. (2011). SignalP 4.0: discriminating signal peptides from transmembrane regions. *Nat Methods* 8, 785–786. doi: 10.1038/nmeth.1701

Petrov, V. M., Ratnayaka, S., Nolan, J. M., Miller, E. S., and Karam, J. D. (2010). Genomes of the T4-related bacteriophages as windows on microbial genome evolution. *Virol. J.* 7:292. doi: 10.1186/1743-422X-7-292

Poindexter, J. S. (1964). Biological properties and classification of the *Caulobacter* group. *Bacteriol. Rev.* 28, 231–295.

Portier, P., Fischer-Le Saux, M., Mougel, C., Lerondelle, C., Chapulliot, D., Thioulouse, J., et al. (2006). Identification of genomic species in *Agrobacterium* biovar 1 by AFLP genomic markers. *Appl. Environ. Microbiol.* 72, 7123–7131. doi: 10.1128/AEM.00018-06

Rombouts, S., Volckaert, A., Venneman, S., Declercq, B., Vandenheuvel, D., Allonsius, C. N., et al. (2016). Characterization of novel bacteriophages for biocontrol of bacterial blight in leek caused by *Pseudomonas syringae* pv. *porri*. *Front. Microbiol.* 7:279. doi: 10.3389/fmicb.2016.00279

Santamaría, R. I., Bustos, P., Sepúlveda-Robles, O., Lozano, L., Rodríguez, C., Fernández, J. L., et al. (2014). Narrow-host-range bacteriophages that infect *Rhizobium etli* associate with distinct genomic types. *Appl. Environ. Microbiol.* 80, 446–454. doi: 10.1128/AEM.02256-13

Santos, S. B., Costa, A. R., Carvalho, C., Nóbrega, F. L., and Azeredo, J. (2018). Exploiting bacteriophage proteomes: the hidden biotechnological potential. *Trends Biotechnol.* doi: 10.1016/j.tibtech.2018.04.006. [Epub ahead of print].

Sawada, H., Ieki, H., Oyaizu, H., and Matsumoto, S. (1993). Proposal for rejection of *Agrobacterium tumefaciens* and revised descriptions for the genus *Agrobacterium* and for *Agrobacterium radiobacter* and *Agrobacterium rhizogenes*. *Int. J. Syst. Bacteriol.* 43, 694–702. doi: 10.1099/00207713-43-4-694

Schneider, C. A., Rasband, W. S., and Eliceiri, K. W. (2012). NIH Image to ImageJ : 25 years of image analysis HISTORICAL commentary NIH Image to ImageJ : 25 years of image analysis. *Nat. Methods* 9, 671–675. doi: 10.1038/nmeth.2089

Sengupta, R. (2014). Thioredoxin and glutaredoxin-mediated redox regulation of ribonucleotide reductase. *World J. Biol. Chem.* 5:68. doi: 10.4331/wjbc.v5.i1.68

Shevchenko, A., Wilm, M., Vorm, O., and Mann, M. (1996). Mass spectrometric sequencing of proteins from silver-stained polyacrylamide gels. *Anal. Chem.* 68, 850–858. doi: 10.1021/ac950914h

Simoliunas, E., Kaliniene, L., Truncaite, L., Zajanckauskaite, A., Staniulis, J., Kaupinis, A., et al. (2013). *Klebsiella* phage vB_KleM-RaK2 - a giant singleton virus of the family Myoviridae. *PLoS ONE* 8:e60717. doi: 10.1371/journal.pone.0060717

Slater, S. C., Goldman, B. S., Goodner, B., Setubal, J. C., Farrand, S. K., Nester, E. W., et al. (2009). Genome sequences of three *Agrobacterium* biovars help elucidate the evolution of multichromosome genomes in bacteria. *J. Bacteriol.* 191, 2501–2511. doi: 10.1128/JB.01779-08

Srinivasiah, S., Bhavsar, J., Thapar, K., Liles, M., Schoenfeld, T., and Wommack, K. E. (2008). Phages across the biosphere: contrasts of viruses in soil and aquatic environments. *Res. Microbiol.* 159, 349–357. doi: 10.1016/j.resmic.2008.04.010

Sullivan, M. B., Huang, K. H., Ignacio-Espinoza, J. C., Berlin, A. M., Kelly, L., Weigele, P. R., et al. (2010). Genomic analysis of oceanic cyanobacterial myoviruses compared with T4-like myoviruses from diverse hosts and environments. *Env. Microbiol.* 12, 3035–3056. doi: 10.1111/j.1462-2920.2010.02280.x

Turner, S., Pryer, K. M., Miao, V. P., and Palmer, J. D. (1999). Investigating deep phylogenetic relationships among cyanobacteria and plastids by small subunit rRNA sequence analysis. *J. Eukaryot. Microbiol.* 46, 327–338. doi: 10.1111/j.1550-7408.1999.tb04612.x

Watson, B., Currier, T. C., Gordon, M. P., Chilton, M. D., and Nester, E. W. (1975). Plasmid required for virulance of *Agrobacterium tumefaciens*. *J. Bacteriol.* 123, 255–264

Wegrzyn, A., Czyz, A., Gabig, M., and Wegrzyn, G. (2000). ClpP/ClpX-mediated degradation of the bacteriophage λ O protein and regulation of λ phage and λ plasmid replication. *Arch. Microbiol.* 174, 89–96. doi: 10.1007/s002030000177

Weidner, S., Baumgarth, B., Göttfert, M., Jaenicke, S., Pühler, A., Schneiker-Bekel, S., et al. (2013). Genome sequence of *Sinorhizobium meliloti* Rm41. *Genome Announc.* 1, e00013–e00012. doi: 10.1128/genomeA.00013-12

Yamamoto, K. R., Alberts, B. M., Benzinger, R., Lawhorne, L., and Treiber, G. (1970). Rapid bacteriophage sedimentation in the presence of polyethylene glycol and its application to large-scale virus purification. *Virology* 40, 734–744

Yin, Y., and Fischer, D. (2008). Identification and investigation of ORFans in the viral world. *BMC Genomics* 9:24. doi: 10.1186/1471-2164-9-24

Yoshikawa, G., Askora, A., Blanc-Mathieu, R., Kawasaki, T., Li, Y., Nakano, M., et al. (2018). *Xanthomonas citri* jumbo phage XacN1 exhibits a wide host range and high complement of tRNA genes. *Sci. Rep.* 8:4486. doi: 10.1038/s41598-018-22239-3

Young, J. M., Pennycook, S. R., and Watson, D. R. (2006). Proposal that *Agrobacterium radiobacter* has priority over *Agrobacterium tumefaciens*.

Request for an Opinion. *Int. J. Syst. Evol. Microbiol.* 56, 491–493. doi: 10.1099/ijs.0.64030-0

Young, R. (2014). Phage lysis: three steps, three choices, one outcome. *J. Microbiol.* 52, 243–258. doi: 10.1007/s12275-014-4087-z

Yuan, Y., and Gao, M. (2017). Jumbo bacteriophages: an overview. *Front. Microbiol.* 8:403. doi: 10.3389/fmicb.2017.00403

Zylicz, M., Liberek, K., Wawrzynow, A., and Georgopoulos, C. (1998). Formation of the preprimosome protects lambda O from RNA transcription-dependent proteolysis by ClpP/ClpX. *Proc. Natl. Acad. Sci. U.S.A.* 95, 15259–15263. doi: 10.1073/pnas.95.26.15259

Conflict of Interest Statement: The authors declare that the research was conducted in the absence of any commercial or financial relationships that could be construed as a potential conflict of interest.

frontiers in Microbiology

ORIGINAL RESEARCH
published: 18 May 2018
doi: 10.3389/fmicb.2018.01033

Thousands of Novel Endolysins Discovered in Uncultured Phage Genomes

*Iris Fernández-Ruiz†, Felipe H. Coutinho† and Francisco Rodriguez-Valera**

Evolutionary Genomics Group, Departamento de Producción Vegetal y Microbiología, Universidad Miguel Hernández de Elche, San Juan de Alicante, Spain

Bacteriophages express endolysins toward the end of their replication cycle to degrade the microbial cell wall from within, allowing viral progeny to be released. Endolysins can also degrade the prokaryotic cell wall from the outside, thus have potential to be used for biotechnological and medical purposes. Multiple endolysins have been identified within the genomes of isolated phages, but their diversity in uncultured phages has been overlooked. We used a bioinformatics pipeline to identify novel endolysins from nearly 200,000 uncultured viruses. We report the discovery of 2,628 putative endolysins, many of which displayed novel domain architectures. In addition, several of the identified proteins are predicted to be active against genera that include pathogenic bacteria. These discoveries enhance the diversity of known endolysins and are a stepping stone for developing medical and biotechnological applications that rely on bacteriophages, the most diverse biological entities on Earth.

Keywords: bacteriophage, endolysins, metagenomics, biotechnology, protein discovery

OPEN ACCESS

Edited by:
Robert Czajkowski, University of Gdańsk, Poland

Reviewed by:
Jessica Labonté, Texas A&M University at Galveston, United States
Konstantin Anatolievich Miroshnikov, Institute of Bioorganic Chemistry (RAS), Russia

****Correspondence:***
Francisco Rodriguez-Valera
frvalera@umh.es

† These authors have contributed equally to this work.

Specialty section:
This article was submitted to Virology, a section of the journal Frontiers in Microbiology

Received: *13 March 2018*
Accepted: *01 May 2018*
Published: *18 May 2018*

Citation:
Fernández-Ruiz I, Coutinho FH and Rodriguez-Valera F (2018) Thousands of Novel Endolysins Discovered in Uncultured Phage Genomes. Front. Microbiol. 9:1033. doi: 10.3389/fmicb.2018.01033

INTRODUCTION

Bacteriophages (Phages) have evolved a multitude of endolysins for the purpose of degrading the complex cell wall structures of their bacterial hosts (Pimentel, 2014). Despite sharing a common function, endolysins are a diverse class of enzymes with a multitude of action mechanisms and protein architectures (Oliveira et al., 2013; Vidová et al., 2014). Protein domains within endolysins grant them their host specificity and efficiency (Hermoso et al., 2007). Multiple classes of endolysins have been described and classified according to the specific enzymatic activities of their catalytic domains, including glycosidases, amidases, and carboxy/endo-peptidase (Schmelcher et al., 2012). Endolysins of phages that infect Gram-positive bacteria often have a modular structure that includes one enzymatic catalytic domain (ECD) at the N-terminal and at least one cell wall binding domain (CBD) at the C-terminal portion of the protein connected by a flexible interdomain linker (Nelson et al., 2012). Meanwhile endolysins of phages that infect Gram-negative bacteria often exhibit a globular structure that contains a single catalytic domain (Pohane and Jain, 2015).

Some endolysins can degrade the cell wall from the outside, which grants them potential to be used for biotechnological and medical applications (Nelson et al., 2012; Gutiérrez et al., 2018). The ongoing crisis of antibiotic based treatments calls for alternative strategies for fighting bacterial infections (Ventola, 2015) and endolysins have multiple advantages over antibiotics: they have higher target specificity and so far no forms of resistance have been reported (Nelson et al., 2012). Furthermore, endolysins can be engineered to alter their host range and efficiency (Díez-Martínez et al., 2014; Blázquez et al., 2016). Several recombinant endolysins are now in preliminary study phase for use in human and veterinary medicine, with promising results

for the treatment against both Gram-positive and Gram-negative bacteria (Briers et al., 2014; Cooper et al., 2016). Some endolysins can even combat intracellular human pathogens (Shen et al., 2016), demonstrating that their potential applicabilities are wider than originally conceived. Finally, these enzymes can be cloned into expression vectors for large scale synthesis. Therefore the potential applications of endolysins are not only of medical but also of industrial (e.g., detecting food-borne pathogens) and agricultural relevance (e.g., treatment against phytopathogens) (Schmelcher and Loessner, 2016).

Despite the recognized diversity and potential of endolysins, our current understanding of these enzymes is limited. Analysis of sequence repositories suggests that less than 1,000 of these proteins are currently known (Oliveira et al., 2013). Although previous studies have characterized the diversity of endolysins through bioinformatic approaches, they focused on reference genomes of isolated phages and prophages, and overlooked environmental phages that have not yet been isolated or cultured (Oliveira et al., 2013; Vidová et al., 2014). Thus, currently available catalogs of endolysins do not cover the diversity of enzymes encoded in the genomes of the many uncultured phages spread across Earth's many ecosystems. Culture independent approaches have revolutionized our understanding of phage genetic diversity, revealing thousands of phage genomes and entirely novel evolutionary lineages at an unprecedented scale (Mizuno et al., 2013; Roux et al., 2015; Paez-Espino et al., 2016; Yutin et al., 2017). These novel genomes are a rich resource for the discovery of endolysins that could have unique domain architectures and target hosts for which no endolysins are currently known. Thus, we sought to screen the genomes of bacteriophages discovered through culture independent approaches to expand the known repertoire of endolysins, asses their structural diversity, and determine how this diversity changes across targeted hosts and ecosystems.

MATERIALS AND METHODS

A database of uncultured viral genomes was compiled from publications aimed at large scale discovery of phages without culturing (Mizuno et al., 2013, 2016; Roux et al., 2015, 2016; Paez-Espino et al., 2016; Coutinho et al., 2017). This dataset comprised 183,298 genomic sequences (**Supplementary File S1**) of uncultured viral genomes adding up to 2.9 Gbp of raw data (**Supplementary Table S1**). We also retrieved available metadata associated with those sequences regarding the ecosystems from which they originated, and the predicted hosts reported in the original publications. These studies used multiple strategies to assign hosts to metagenomic contigs which included: high genomic similarity to reference phage genomes; homology matches between phage and prokaryotic genomes; CRISPR spacers from prokaryotic genomes matching metagenomic contigs; similarity between phage and prokaryotic tRNAs; and co-occurrence of phage genome pairs indicative of a shared host. Prophages described by Roux et al. (2015) were assigned hosts according to the prokaryotic genomes in which they were identified.

A dataset of *bona fide* endolysin sequences encoded in genomes of double stranded DNA phages was compiled to be used as a reference database. This database comprised 629 proteins from NCBI RefSeq phages and was manually curated so to exclude structural lysins (i.e., exolysins) (Oliveira et al., 2013). Prodigal (Hyatt et al., 2010) was run in metagenomic mode to identify protein encoding genes of uncultured phage genomes. All predicted protein sequences were queried against the reference endolysin database using Diamond (Buchfink et al., 2015). Proteins that had hits to the reference database were classified as putative endolysins if matches were within the following thresholds: identity $\geq$ 50%, e-value $\leq$ 0.001, query coverage $\geq$ 30%, and alignment length $\geq$ 50 amino acids. Protein domains of putative endolysins were identified by querying sequences against the Pfam database using HMMER version v3.1b2 (Finn et al., 2015) with default parameters. Additionally, putative endolysins were analyzed through SignalIP (Petersen et al., 2011) to detect signal peptide sequences. Finally, both the putative and reference endolysins were clustered into orthologous groups (OGs) using OrthoMCL (Li et al., 2003) within the GET_HOMOLOGUES pipeline (Contreras-Moreira and Vinuesa, 2013) by setting an inflation factor of 1 and all other parameters set to default. Multiple sequence alignments were constructed through Clustal Omega (Sievers et al., 2014) for each OG represented by at least 10 proteins. Alignments were used to perform phylogenetic reconstructions through FastTree (Price et al., 2010) using default parameters (Amino acid distances BLOSUM45 and Jones-Taylor-Thorton model and support value calculation). An additional tree was built based on a multiple alignment of all proteins assigned to OGs of 10 or more proteins.

RESULTS AND DISCUSSION

A total of 2,628 putative endolysins were identified (**Supplementary File S2**). Homolog identification clustered these proteins into 297 OGs. We focused downstream analysis on 46 OGs represented by 10 or more proteins. Each of these OGs was manually validated as true endolysins by inspecting for: presence of *bona fide* endolysins from the reference database; prevalence of typical endolysins domains (e.g., Lysozyme, Amidase, and Glycosyl Hydrolase); and close phylogenetic relationship between putative and *bona fide* endolysins as assessed by inspecting phylogenetic trees generated for each OG. Considering the degree of diversity among phage genomes and the rate in which their genes evolve, we used very conservative thresholds to identify putative endolysins (identity $\geq$ 50%, e-value $\leq$ 0.001, query coverage $\geq$ 30% and alignment length $\geq$ 50 amino acids). Yet, due to high levels of structural similarities between structural lysins and endolysins, it is possible that some of the putative endolysins identified are actually structural lysins (enzymes used by phages to breach the cell wall at the beginning of the infection process). Yet, using a curated database of *bona fide* endolysins from reference phage genomes, conservative thresholds, and manual validation of the OGs should minimize the occurrence of false positives in our dataset.

Proteins assigned to the same OG often displayed identical domain architectures, although some exceptions were observed (**Figure 1** and **Supplementary File S3**). A total of 62 domains were identified across 46 OGs (**Table 1**), including 26 types of ECDs, 12 CBDs, and 24 domains of unknown function. For 27 OGs only a single catalytic domain was observed. Meanwhile, 19 OGs harbored at least one protein with both cell wall binding and ECDs. Signal peptide sequences were detected only in six OGs, suggesting that most of the discovered endolysins rely on other mechanisms for membrane translocation such as holin-dependent transportation. The most frequent domain observed in the putative endolysins was phage_lysozyme (PF00959) a Glycoside Hydrolase, followed by Peptidase_M15 (PF08291), and Amidase_2 (PF01510).

We investigated associations between OGs and predicted hosts of uncultured phages. A total of 32 OGs had at least one endolysin derived from a phage genome for which host prediction was available. Endolysins from OGs predicted to target Gram-negatives were often composed of a single ECD, while those derived from OGs predicted to target Gram-positive bacteria were often composed of both a CBD and an ECD. Often a single bacterial genus could be targeted by multiple OGs (**Figure 2**). For example, enzymes targeting *Streptococcus* were present in nine distinct OGs and those targeting *Bacillus* were found in four OGs. Most OGs are predicted to be active against multiple bacterial genera with only two exceptions: OG44 and OG26 which respectively target *Streptococcus* and *Bacillus*. In general, OGs predicted to target multiple taxa were restricted to organisms with the same gram staining patterns. Interestingly endolysins from phages predicted to infect *Mycobacterium* were all assigned to a single group (OG6), likely due to the unique cell wall composition of these organisms.

A total of 34 OGs harbor at least one endolysin predicted to be active against genera that include potentially pathogenic bacteria (e.g., *Staphylococcus*, *Clostridium,* and *Klebsiella*). Ten of those OGs have at least one protein predicted to target bacteria currently classified by the World Health Organization as critical priority for the development of alternative therapies. In addition, five OGs include proteins predicted to be active against phytopathogens (e.g., *Xylella, Erwinina,* and *Burkholderia*) (Mansfield et al., 2012; Blomme et al., 2017). *In vivo* experiments are necessary to confirm the efficiency of these proteins for fighting pathogens, since different species or strains of bacteria

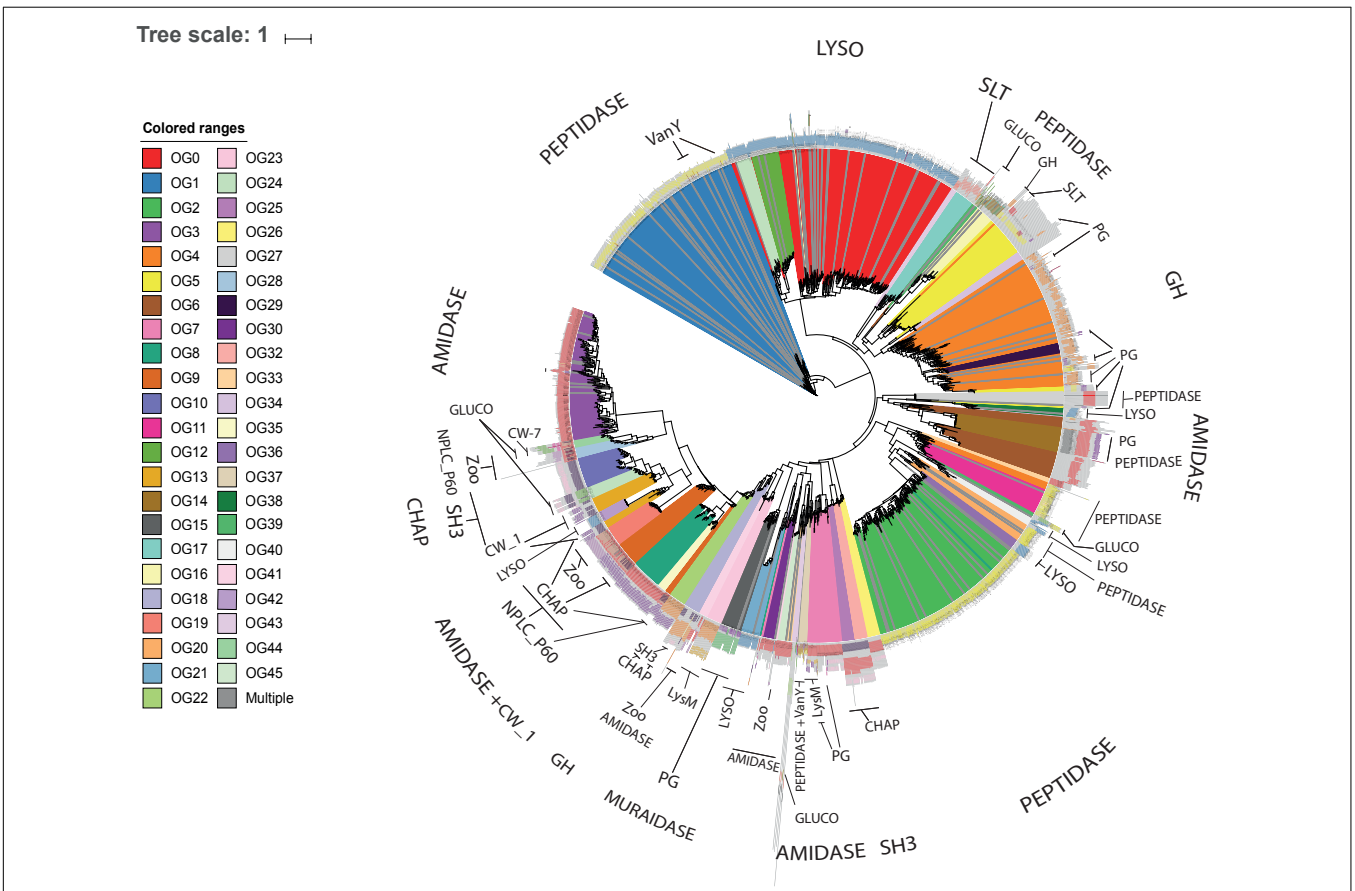

FIGURE 1 | Novel diversity of endolysins discovered in uncultured phage genomes. Cladogram displaying the phylogenetic reconstruction of endolysins assigned to the 46 OGs represented by 10 or more proteins. Branches are colored according to OG assignments. Protein architecture is displayed adjacent to each leaf, identical colors represent identical Pfam domains.

TABLE 1 | Prevalence of domains, signal peptide and inferred cell wall target of endolysin orthologous groups.[Hoja1]

	OG_#	OG0	OG1	OG2	OG3	OG4	OG5	OG6	OG7	OG8	OG9	OG10	OG11	OG12	OG13	OG14	OG15	OG16	OG17	OG18	OG19	OG20	OG21	OG22	OG23	OG24	OG25	OG26	OG27	OG28	OG29	OG30	OG31	OG32	OG33	OG34	OG35	OG36	OG37	OG38	OG39	OG40	OG41	OG42	OG43	OG44	OG45
	Number of proteins	230	210	196	163	157	58	47	43	40	39	36	34	33	31	30	27	25	24	23	23	22	22	20	19	17	17	16	16	15	15	15	15	15	14	14	12	11	11	11	11	11	11	11	10	10	10
	Signal peptide	No	No	No	No	No	No	No	No	No	No	No	No	Yes	No	No	No	Yes	Yes	No	No	No	No	No	Yes	No	No	Yes	No	No	No	No	No	No	No	No	No	Yes	No	No	No	No	No	No	No	No	No
Domain Function	Cell Wall Target type	U	U	U	U	U	U	U	G+	U	U	U	U	G-	U	U	U	U	G-	U	U	U	U	U	U	G-	U	G+	U	U	U	U	G+	U	G+	U	U	G-	U	U	U	U	U	U	G+	G+
Amidase	PF12123 | Amidase02_C (N-acetylmuramoyl-l-alanine amidase)	0	0	0	0	0	0	0	0	0	0	0	0	0	0	0	0	0	0	0	0	0	0	0	0	0	0	0	0	0	0	0	0	78.6	0	0	0	0	0	0	0	0	0	0	0	0	0
Amidase	PF01510 | Amidase_2 (N-acetylmuramoyl-L-alanine amidase)	0	1	1	93.2	0.6	0	89.4	93	90	2.6	0	0	0	0	90	0	0	0	0	0	4.5	0	0	0	5.9	0	93.8	93.8	0	6.7	93.3	0	93.3	0	0	100	0	0	0	0	0	100	0	0	0	0
Amidase	PF01520 | Amidase_3 (N-acetylmuramoyl-L-alanine amidase)	0	0	0.5	0	0	0	0	0	0	0	0	0	0	0	0	0	0	0	0	0	0	0	0	0	0	94.1	0	0	0	0	6.7	0	92.9	0	0	0	0	0	0	0	0	0	0	0	0	100
Amidase	PF05382 | Amidase_5 (Bacteriophage peptidoglycan hydrolase)	0	0	0	0	0	0	0	0	0	94.9	0	0	0	0	0	0	0	0	0	95.7	0	0	0	0	0	0	0	0	93.3	0	0	0	0	0	0	0	0	0	0	0	0	0	0	90	0
Amidase/Peptidase	PF05257 | CHAP domain	0	0	0	0	0	0	0	0	0	59	94.4	0	0	77.4	0	0	0	0	60.9	0	0	0	0	0	0	94.1	0	0	86.7	0	0	93.3	93.3	0	0	0	0	0	0	0	9.1	0	0	30	0
Carboxy/Endo-peptidase	PF11814 | DUF3335 (Peptidase_C39 like family)	0	0.5	0	0	0	0	0	0	0	0	0	0	0	0	0	0	0	0	0	0	0	0	0	0	0	0	0	0	0	0	0	0	0	0	0	0	0	0	0	0	0	0	0	0	0	0
Carboxy/Endo-peptidase	PF00877 | NLPC_P60 (NlpC/P60 family)	0	0	0	0	0	0	0	0	0	87.2	0	0	0	0	0	0	0	0	0	82.6	0	0	0	0	0	0	0	0	46.7	0	0	0	0	0	0	0	0	0	0	0	0	0	0	70	0
Carboxy/Endo-peptidase	PF13529 | Peptidase_C39_2 (Peptidase_C39 like family)	0.9	0.5	0.5	0.6	0	1.7	0	0	0	0	0	0	0	6.7	0	92	0	0	0	0	0	0	0	0	0	0	0	0	0	0	0	0	0	0	0	0	0	0	0	36.4	0	0	0	0	0
Carboxy/Endo-peptidase	PF12385 | Peptidase_C70 (Papain-like cysteine protease AvrRpt2)	0.9	0.5	0.5	0.6	0	1.7	0	0	0	0	0	0	0	3.3	0	96	0	0	0	0	0	0	0	0	0	0	0	0	0	0	0	0	0	0	0	0	0	0	0	18.2	0	0	0	0	0
Carboxy/Endo-peptidase	PF01427 | Peptidase_M15 (D-ala-D-ala dipeptidase)	0	0	0	0	0	0	0	0	0	0	0	2.9	0	0	0	0	0	0	0	0	0	0	0	0	0	0	0	0	0	0	0	0	0	0	0	0	0	0	0	0	0	0	0	0	0	0
Carboxy/Endo-peptidase	PF05951 | Peptidase_M15_2 (Bacterial protein of unknown function (DUF88))	0.9	26.9	52.8	1.9	6.5	0	0	2.3	2.5	0	2.8	61.8	0	6.5	0	0	4	0	0	0	95.5	0	0	0	0	0	0	0	0	0	0	0	0	7.1	0	0	0	0	9.1	0	0	0	0	0	0
Carboxy/Endo-peptidase	PF08291 | Peptidase_M15_3 (Peptidase M15)	2.2	2.4	93.8	1.9	9	0	2.1	4.7	5	0	2.8	97.1	0	6.5	0	0	4	0	4.3	0	95.5	0	5	0	0	0	0	0	0	0	0	0	0	7.1	0	0	0	0	36.4	0	0	0	0	0	0
Carboxy/Endo-peptidase	PF13539 | Peptidase_M15_4 (D-alanyl-D-alanine carboxypeptidase)	1.3	92.8	1.5	2.5	0.6	82.8	0	2.3	2.5	0	0	2.9	3	0	0	3.7	0	4.2	0	0	4.5	0	0	0	0	5.9	6.3	0	0	0	0	0	0	7.1	0	0	100	0	0	0	0	0	0	0	0	0
Carboxy/Endo-peptidase	PF01551 | Peptidase_M23 (Peptidase family M23)	0	0	0	0	0	2.1	0	0	0	0	0	0	0	90	0	0	0	0	0	0	4.5	0	0	0	0	0	0	0	0	0	0	0	0	0	0	0	0	0	0	0	0	0	40	0	0
Carboxy/Endo-peptidase	PF02557 | VanY (D-alanyl-D-alanine carboxypeptidase)	0	2.4	0	0.6	0	0	0	0	0	0	0	2.9	0	0	0	0	0	0	0	0	0	0	0	0	0	0	0	0	0	0	0	0	0	0	0	0	0	100	0	0	0	0	0	0	0
Glycosidase	PF01832 | Glucosaminidase (Mannosyl-glycoprotein endo-beta-N-acetylgluc)	0.4	0	0	0	0	0	0	0	0	0	0	0	0	0	0	0	0	0	0	0	0	0	0	0	0	0	0	0	0	0	0	0	86.7	0	0	0	0	0	0	81.8	0	0	0	20	100	0
Glycosidase	PF00182 | Glyco_hydro_19 (Chitinase class I)	0.9	0.5	0.5	0.6	83.2	12.1	6.4	0	0	0	0	0	0	0	0	0	0	0	0	0	0	0	0	0	5.3	0	0	0	6.3	0	93.3	0	0	0	0	0	0	0	0	0	0	0	0	0	0	0
Glycosidase	PF01183 | Glyco_hydro_25 (Glycosyl hydrolases family 25)	0	0	0	0	0	0	0	0	0	0	0	0	0	0	0	0	0	0	95.7	0	0	0	95	94.7	0	0	0	0	0	0	0	0	0	0	0	0	0	0	0	0	0	0	0	0	0	0
Glycosidase	PF11790 | Glyco_hydro_cc (Glycosyl hydrolase catalytic core)	0	0	0	0	0	0	0	0	0	0	0	0	0	0	0	0	0	0	0	0	0	0	0	0	0	0	0	0	0	0	0	0	0	7.1	0	0	0	0	0	0	0	0	0	0	0	0
Glycosidase	PF13702 | Lysozyme_like (Lysozyme-like)	0	0	0	0	0	0	0	0	0	0	0	0	0	0	0	0	0	0	0	0	0	0	0	0	0	0	0	0	0	0	0	0	0	0	0	0	0	0	0	0	0	10	0	0	0	0
Glycosidase	PF16499 | Melibiase_2 (Glycosyl hydrolases family 27)	0	0	0	0.6	0	0	0	0	0	0	0	0	0	0	0	0	0	0	0	0	0	0	0	0	0	0	0	0	0	0	0	0	0	0	0	0	0	0	0	0	0	0	0	0	0	0
Glycosidase	PF11860 | Muraidase (N-acetylmuramidase)	0	0	1	0	0	0	0	0	0	0	0	0	0	0	96.3	0	0	0	0	0	0	0	0	0	0	0	0	0	0	0	0	0	0	0	0	0	0	0	0	0	0	0	0	0	0	0
Glycosidase	PF00959 | Phage_lysozyme (Glycosyl hydrolases family 24)	95.2	2.4	1	1.9	2.6	1.7	6.4	0	0	2.6	2.8	0	97	0	3.3	0	4	0	0	4.3	0	95.5	0	0	94.1	0	0	0	6.7	0	6.7	0	6.7	0	0	0	100	0	100	0	100	0	100	0	0	0
Glycosidase	PF01464 | SLT (Soluble Lytic Transglycosylase domain)	0	0	0	0	0	10.3	0	0	0	0	0	0	0	0	0	0	0	95.8	0	0	0	0	0	0	0	0	0	0	0	0	0	0	0	0	0	0	0	0	0	0	0	0	100	0	0
Glycosidase	PF13406 | SLT_2 (Soluble Lytic Transglycosylase domain)	0	0	0	0	0	0	0	0	0	0	0	0	0	0	0	0	0	0	0	0	0	0	0	0	0	0	0	0	0	0	0	0	0	0	0	0	0	0	0	0	0	0	60	0	0	0
Glycosidase	PF06737 | Transglycosylase (Transglycosylase-like domain)	0	0	0	0	0	10.3	0	0	0	0	0	0	0	0	0	0	0	0	0	0	0	0	0	0	0	0	0	0	0	0	0	0	0	0	0	0	0	0	0	0	0	0	0	0	0	0
Cell Wall Binding	PF08230 | CW_7 (CW_7 repeat)	0	0	0	0	0	0	0	4.7	0	0	0	0	0	0	0	0	0	0	0	0	0	0	0	0	0	0	0	0	0	0	0	0	0	0	0	0	0	0	0	0	0	0	0	100	0	0
Cell Wall Binding	PF01473 | CW_binding_1 (Putative cell wall binding repeat)	0	0	0	0	0	0	0	0	90	94.9	0	0	0	74.2	0	0	0	0	0	0	0	0	95	0	0	0	0	0	0	0	0	0	0	0	0	100	0	0	0	0	0	0	0	0	0	0
Cell Wall Binding	PF03815 | LCCL (LCCL domain)	0	0	0	0	0	0	0	0	0	0	0	0	0	0	0	0	0	0	0	0	0	0	0	0	0	0	0	0	0	0	0	0	0	0	0	0	0	0	0	0	0	0	0	10	0	0
Cell Wall Binding	PF08310 | LGFP (LGFP repeat)	0	0	0	0	0	0	2.1	0	0	0	0	0	0	0	0	0	0	0	0	0	0	0	0	0	0	0	0	0	0	0	0	0	0	0	0	0	0	0	0	0	0	0	0	0	0	0
Cell Wall Binding	PF01476 | LysM (LysM domain)	0	0	0	0	0	0	0	18.6	0	0	0	0	0	0	0	0	0	0	0	0	0	0	0	94.7	0	0	0	0	0	0	0	0	0	0	0	0	0	0	0	0	0	0	0	0	0	0
Cell Wall Binding	PF01471 | PG_binding_1 (Putative peptidoglycan binding domain)	1.8	0	0.5	1.9	7.7	19	0	20.9	0	0	0	0	0	0	90	85.2	0	0	0	0	0	0	0	0	0	0	0	0	0	0	0	0	0	0	0	0	0	0	18.2	0	0	0	0	0	0	0
Cell Wall Binding	PF08823 | PG_binding_2 (Putative peptidoglycan binding domain)	0	0	0	0	0	0	0	0	0	0	0	0	0	0	3.7	0	0	0	0	0	0	0	0	0	0	0	0	0	0	0	0	0	0	0	0	0	0	0	0	0	0	0	0	0	0	0
Cell Wall Binding	PF09374 | PG_binding_3 (Predicted Peptidoglycan domain)	0	0	0.5	1.2	7.1	6.9	0	7	0	0	0	0	0	0	80	59.3	0	0	0	0	0	0	0	0	0	0	0	0	0	0	0	0	0	0	0	0	0	0	18.2	0	0	0	0	0	0	0
Cell Wall Binding	PF08239 | SH3_3 (Bacterial SH3 domain)	0	0	0	0	0	0	0	41.9	0	0	50	0	0	3.2	0	0	0	0	26.1	0	0	0	0	0	0	29.4	87.5	0	0	0	0	6.7	0	7.1	0	0	0	0	0	0	0	0	0	0	0	0	0
Cell Wall Binding	PF06347 | SH3_4 (Bacterial SH3 domain)	0	0	0	0	0	0	0	25.6	0	0	0	0	0	0	0	0	0	0	4.3	0	0	0	0	0	0	0	31.3	0	0	0	0	0	0	0	0	0	0	0	0	0	0	0	0	0	0	0
Cell Wall Binding	PF08460 | SH3_5 (Bacterial SH3 domain)	0	0	0	0	0	0	0	0	0	0	94.4	0	0	6.5	0	0	0	0	0	0	0	0	0	0	0	82.4	0	0	13.3	0	6.7	80	86.7	7.1	0	0	0	0	0	0	0	0	0	0	0	0
Cell Wall Binding	PF16775 | ZoocinA_TRD (Target recognition domain of lytic exoenzyme)	0	0	0	0	0	0	0	0	0	0	0	0	0	0	0	0	0	0	95.7	0	0	0	0	0	0	0	0	0	73.3	0	0	0	0	0	0	0	0	0	0	0	0	0	0	90.9	0	0
Unknown	PF14399 | BtrH_N (Butirosin biosynthesis protein H, N-terminal)	0	0	0	0	0	0	0	0	0	0	0	0	0	0	0	0	8	0	0	0	0	0	0	0	0	0	0	0	0	0	0	0	0	0	0	0	0	0	0	0	0	0	0	0	0	0
Unknown	PF00313 | CSD (Cold-shock' DNA-binding domain)	0	0	0	0.6	0	0	0	0	0	0	0	0	0	0	0	0	0	0	0	0	0	0	0	0	0	0	0	0	0	0	0	0	0	0	0	0	0	0	0	0	0	0	0	0	0	0
Unknown	PF07065 | D123	0	0	0	0	0	8.6	0	0	0	0	0	0	0	0	0	0	0	0	0	0	0	0	0	0	0	0	0	0	0	0	0	0	0	0	0	0	0	0	0	0	0	0	0	0	0	0
Unknown	PF06649 | DUF1161	0	0	0	0	0	0	0	0	0	0	0	0	0	0	0	0	0	0	0	0	0	0	0	0	0	0	0	0	0	0	0	0	0	0	0	0	0	0	0	0	0	0	0	0	0	20
Unknown	PF09872 | DUF2099 (Uncharacterized protein conserved in archaea)	0	0.5	0	0	0	0	0	0	0	0	0	0	0	0	0	0	0	0	0	0	0	0	0	0	0	0	0	0	0	0	0	0	0	0	0	0	0	0	0	0	0	0	0	0	0	0
Unknown	PF10721 | DUF2514	0	0	0	0	1.3	0	0	0	0	0	0	0	0	0	0	0	0	0	0	0	0	0	0	0	0	0	0	0	0	0	0	0	0	0	0	0	0	0	0	0	0	0	0	0	0	0
Unknown	PF14362 | DUF4407	0	0	0	0	0	0	0	0	0	0	0	0	0	0	0	0	0	0	0	0	0	0	0	0	0	0	0	0	0	0	0	0	0	0	0	0	0	0	0	0	0	0	0	20	0	0
Unknown	PF15762 | DUF4691	0.4	0	0	0	0	0	0	0	0	0	0	0	0	0	0	0	0	0	0	0	0	0	0	0	0	0	0	0	0	0	0	0	0	0	0	0	0	0	0	0	0	0	0	0	0	0
Unknown	PF11838 | ERAP1_C (ERAP1-like C-terminal domain)	0	0	0	0	0	0	0	0	0	0	0	0	0	0	0	0	4	0	0	0	0	0	0	0	0	0	0	0	0	0	0	0	0	0	0	0	0	0	0	0	0	0	0	0	0	0
Unknown	PF06904 | Extensin-like_C (Extensin-like protein C-terminus)	0	0	0	0	0	0	0	0	0	0	0	0	0	0	0	17.6	0	0	0	0	0	0	0	0	0	0	0	0	0	0	0	0	0	0	0	0	0	0	0	0	0	0	0	0	0	0
Unknown	PF09535 | Gmx_para_CXXCG	0	0	0	0	0	0	0	0	0	0	0	0	0	0	0	0	4	0	0	0	0	0	0	0	0	0	0	0	0	0	0	0	0	0	0	0	0	0	0	0	0	0	0	0	0	0
Unknown	PF01085 | HH_signal (Hedgehog amino-terminal signalling domain)	0	0	0	0	0	0	0	0	0	0	0	11.8	0	0	0	0	0	0	0	0	0	0	0	0	0	0	0	0	0	0	0	0	0	0	0	0	0	0	0	0	0	0	0	0	0	0
Unknown	PF12759 | HTH_Tnp_IS1 (InsA C-terminal domain)	0	0	0.5	0	0	0	0	0	0	0	0	0	0	0	0	0	0	0	0	0	0	0	0	0	0	0	0	0	0	0	0	0	0	0	0	0	0	0	0	0	0	0	0	0	0	0
Unknown	PF13403 | Hint_2 (Hint domain)	0	0	0	0	0	0	0	0	0	0	0	0	0	0	0	0	0	0	0	0	0	0	0	0	0	0	0	0	0	0	0	0	0	0	0	0	0	0	0	0	0	9.1	0	0	0	0
Unknown	PF00977 | His_biosynth (Histidine biosynthesis protein)	0	0.5	0	0	0	0	0	0	0	0	0	0	0	0	0	0	0	0	0	0	0	0	0	0	0	0	0	0	0	0	0	0	0	0	0	0	0	0	0	0	0	0	0	0	0	0
Unknown	PF14890 | Intein_splicing (Intein splicing domain)	0	0	0	0	0	0	0	0	0	0	0	0	0	0	0	0	0	0	4.3	0	0	0	0	0	0	0	0	0	0	0	0	0	0	0	0	0	0	0	0	0	0	0	0	0	0	0
Unknown	PF13418 | Kelch_4 (Galactose oxidase, central domain)	0	0	0	0	0	0	0	0	0	0	0	0	0	0	0	0	0	0	0	0	0	0	0	0	0	0	0	0	0	0	0	0	0	0	16.7	0	0	0	0	0	0	0	0	0	0	0
Unknown	PF14528 | LAGLIDADG_3 (LAGLIDADG-like domain)	0	0	0	0	0	0	0	0	0	0	0	0	0	0	0	0	0	0	8.7	0	0	0	0	0	0	0	0	0	0	0	0	0	0	0	0	0	0	0	0	0	0	0	0	0	0	0
Unknown	PF13472 | Lipase_GDSL_2 (GDSL-like Lipase/Acylhydrolase family)	0	0	0	0.6	0	0	0	0	0	2.6	0	0	0	0	0	0	0	0	0	0	0	0	0	0	0	0	0	0	0	0	0	0	0	0	0	0	0	0	0	0	0	0	0	0	0	0
Unknown	PF10294 | Methyltransf_16 (Lysine methyltransferase)	0.4	0	0	0	0	0	0	0	0	0	0	0	0	0	0	0	0	0	0	0	0	0	0	0	0	0	0	0	0	0	0	0	0	0	0	0	0	0	0	0	0	0	0	0	0	0
Unknown	PF02211 | NHase_beta (Nitrile hydratase beta subunit)	0	0	0	0	0	0	0	2.3	0	0	0	0	0	0	0	0	0	0	0	0	0	0	0	0	0	0	0	0	0	0	0	0	0	0	0	0	0	0	0	0	0	0	0	0	0	0
Unknown	PF16494 | Na_Ca_ex_C (C-terminal extension of sodium/calcium exchanger)	0	0	0	1.9	0	0	0	0	0	0	0	0	0	0	0	0	0	0	0	0	0	0	0	0	0	0	0	0	0	0	0	0	0	0	0	0	0	0	0	0	0	0	0	0	0	0
Unknown	PF10145 | PhageMin_Tail (Phage-related minor tail protein)	0	0	0	0	0	0	0	0	0	0	0	0	0	0	0	0	0	0	0	0	0	0	0	0	0	0	0	0	0	0	0	0	0	0	0	0	0	0	0	0	0	0	40	0	0	0
Unknown	PF10671 | TcpQ (Toxin co-regulated pilus biosynthesis protein)	0	0.5	0	0	0	0	0	0	0	0	0	0	0	0	0	0	0	0	0	0	0	0	0	0	0	0	0	0	0	0	0	0	0	0	0	0	0	0	0	0	0	0	0	0	0	0

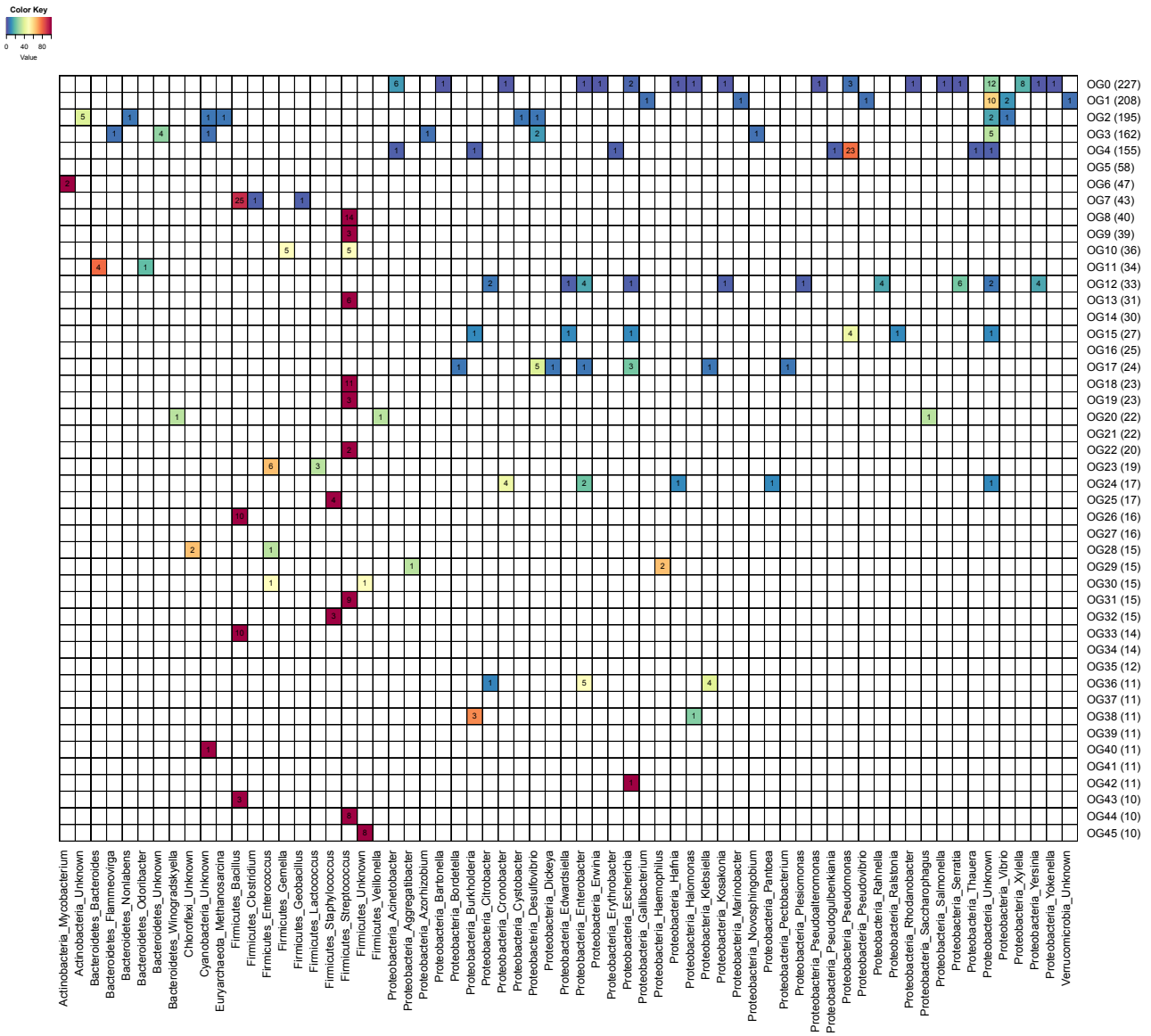

FIGURE 2 | Heatmap depicting prevalence of targeted host genus across endolysin orthologous groups (OGs). Numbers within cells represent the amount of proteins targeting each host genus (columns) among the 46 OGs (rows) represented by 10 proteins or more. Cell colors depict the percentage frequency of each host among OGs. Calculated percentages do not include proteins derived from genomic sequences without host assignments.

that belong to the same genus may differ in their pathogenic potential.

Next we investigated the frequency of associations between endolysin domains and targeted bacteria (**Figure 3**). On the one hand, some genera were targeted by few domain categories. For example, most of the enzymes that targeted *Bacillus* have amidase (PF12123/PF01510/PF01520) activity in their catalytic domain and SH3 (PF08239/PF06347) on their CBDs, suggesting that this might be the most efficient mechanism to degrade the cell wall of the members of this clade. On the other hand, genera such as *Streptococcus* were targeted by endolysins that rely on multiple types of catalytic activities such as Amidase (PF01510/PF05382), Cysteine Histidine-dependent Amidohydrolases/Peptidases (CHAP) domain (PF05257), Glucosaminidase (PF01832), Glycosyl hydrolases family 25 (PF01183), as well as multiple CBDs such as CW1 (PF01473), CW7 (PF08230), and SH3 (PF08239/PF06347). This pattern suggests that multiple domain architectures might be efficient for targeting the cell walls of *Streptococcus*. Finally, the Phage_lysozyme (PF00959) and Soluble Lytic Transglycosylase (SLT, PF01464/PF13406) domains were often detected in endolysins predicted to target Proteobacteria, demonstrating that these domains are tuned to degrade the cell walls of this diverse phylum of Gram-negatives.

Host assignments for phage genomes derived from metagenomic datasets are based on bioinformatic predictions which vary on their degree of precision and recall. These

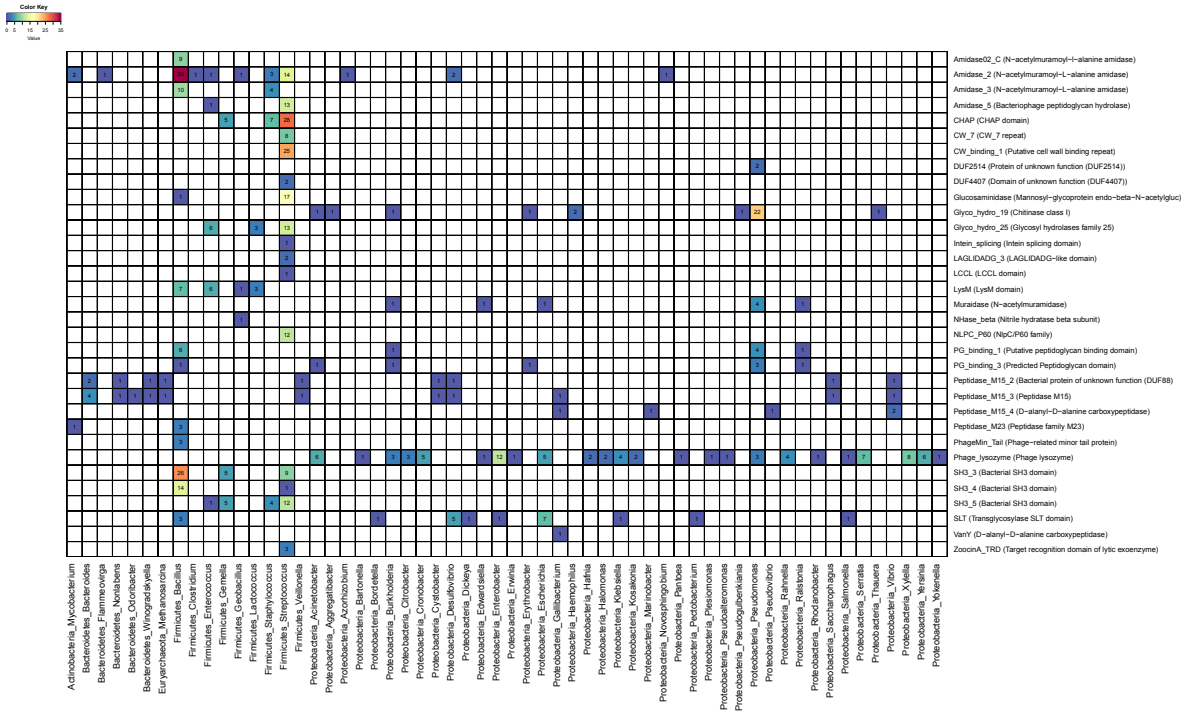

FIGURE 3 | Heatmap depicting associations between targeted host genus and endolysin domains. Numbers and colors within cells represent the frequency of protein domains (rows) among endolysins targeting each host genera (columns).

approaches have high accuracy for higher taxonomic ranks such as phylum or class but sometimes lead to incorrect predictions at the lower ranks such as genus or species (Edwards et al., 2015; Coutinho et al., 2017). Thus, the associations between OGs/domains and targeted hosts inferred from metagenomic data should be interpreted as putative and in need of experimental validation (which is currently out of our scope). Yet the validity of our findings is corroborated by: (1) Use of conservative thresholds to maximize accuracy during the host prediction analysis described in the original publications that first reported phage genomes obtained from metagenomic samples. (2) Endolysin domains identified in uncultured phages match those previously described for isolated and cultured bacteriophages (Oliveira et al., 2013). (3) Approximately, 74% of host assignments obtained for the 46 OGs analyzed in depth were derived from prophage sequences integrated into host genomes that were obtained from pure cultures (instead of metagenomic data). Thus the bulk of the host/OG and host/domain associations are based on high confidence host assignments.

Several of the identified protein domains are not typically present in endolysins from reference phage genomes. Those include domains that are likely associated with peptidoglycan lysis such as Melibiase_2 (PF16499; Glycosyl hydrolases family 27) and Glyco_hydro_cc (PF11790; Glycosyl hydrolase catalytic core), but also domains with no obvious role in this process, such as: Methyltransf_16 (PF10294; Lysine methyltransferase), Lipase_GDSL_2 (PF13472; GDSL-like Lipase/Acylhydrolase family), and PhageMin_Tail (PF10145; Phage-related minor tail protein). Presence of the latter could be either the result of protein fusions or represent novel functions or action mechanisms of endolysins. Since computational domain identification may be subjected to errors, experimental validation is necessary to corroborate the presence of these domains and to determine their molecular functions. Nevertheless, our results demonstrate that the molecular versatility of endolysins is still poorly understood considering the lack of information available for so many of the identified domains.

Finally, we explored associations between endolysin architecture and their ecosystem of origin. Most of the putative endolysins were derived from aquatic ecosystems or human microbiome samples, which are the habitats most often sampled by metagenomic studies (**Supplementary Figure S1**). This pattern highlights the potential for endolysin discovery in these sites but also the need for investigations of other ecosystems such as plant associated and terrestrial habitats, that also yielded novel endolysins. Aquatic phages appear to be a rich resource for endolysins containing amidase, peptidase and glycosidase domains, which points to them as a source of endolysins active against both Gram-positive and Gram-negative bacteria. Meanwhile, endolysins derived from phages of the human microbiome most often have amidase and peptidase domains, typical of enzymes acting on Gram-positive hosts.

CONCLUSION

We were able to notably expand the known diversity of endolysins and describe proteins with novel and often complex domain architectures, thus challenging the current understanding of the diversity of those enzymes. Our findings show that environmental phage genomes, specially those from aquatic and human associated microbiomes, are a rich resource for endolysins discovery. Since several of the identified endolysins are predicted to be effective against plant and animal pathogens, those are ideal candidates for purification and further characterization, specially those predicted to act on Gram-positive bacteria, against which endolysin therapy has showed the most promising results so far (Gerstmans et al., 2016). Our findings regarding associations between bacterial targets and domains provide insights for the engineering of recombinant proteins that have higher efficiency or an extended host spectrum. Further experimental research will be necessary to corroborate our findings regarding the endolytic activity, domain architecture, and target spectrum of these proteins and to evaluate their potential applications as antimicrobial agents. Culture independent approaches will continue to expand the genetic diversity of phages, and our strategy represents a simple, fast, and scalable approach for discovering endolysins encoded in their genomes.

AUTHOR CONTRIBUTIONS

IF-R, FC, and FR-V conceived the study and designed the experiments. IF-R and FC performed the experiments and analyzed the data. All authors contributed to writing the manuscript.

FUNDING

FC and FR-V were supported by grants "VIREVO" CGL2016-76273-P (AEI/FEDER, EU) (co-funded with FEDER funds); Acciones de Dinamización "REDES DE EXCELENCIA" CONSOLIDER- CGL2015-71523-REDC from the Spanish Ministério de Economía, Industria y Competitividad and PROMETEO II/2014/012 "AQUAMET" from Generalitat Valenciana.

SUPPLEMENTARY MATERIAL

The Supplementary Material for this article can be found online at: https://www.frontiersin.org/articles/10.3389/fmicb.2018.01033/full#supplementary-material

FIGURE S1 | Heatmap depicting associations between ecosystem sources and endolysin domains. Numbers and colors within cells represent the frequency of protein domains (rows) among endolysins identified in phage genomes from each ecosystem category (columns).

TABLE S1 | Detailed metadata of the genomic sequences of uncultured phages analyzed in this study: including sequence identifier, original dataset, sequence length, number of identified protein encoding genes, ecosystem source and host taxonomic classification.

FILE S1 | Multifasta file containing the 183,6298 genomic sequences of uncultured viruses analyzed in this study.
File can be downloaded here: https://drive.google.com/open?id=15rRJMfguPGhfiuQor7pulrIlr2J02tJQ

FILE S2 | Multifasta file containing the amino acid sequences of 2,628 putative endolysins identified in the genomes of uncultured viruses.

FILE S3 | Newick format file of the phylogenetic reconstruction of endolysin proteins displayed in **Figure 1**.

REFERENCES

Blázquez, B., Fresco-Taboada, A., Iglesias-Bexiga, M., Menéndez, M., and García, P. (2016). PL3 amidase, a tailor-made lysin constructed by domain shuffling with potent killing activity against pneumococci and related species. *Front. Microbiol.* 7:1156. doi: 10.3389/fmicb.2016.01156

Blomme, G., Dita, M., Jacobsen, K. S., Pérez Vicente, L., Molina, A., Ocimati, W., et al. (2017). Bacterial diseases of bananas and enset: current state of knowledge and integrated approaches toward sustainable management. *Front. Plant Sci.* 8:1290. doi: 10.3389/fpls.2017.01290

Briers, Y., Walmagh, M., Van Puyenbroeck, V., Cornelissen, A., Cenens, W., Aertsen, A., et al. (2014). Engineered endolysin-based "Artilysins" to combat multidrug-resistant gram-negative pathogens. *mBio* 5:e01379-14. doi: 10.1128/mBio.01379-14.Editor

Buchfink, B., Xie, C., and Huson, D. H. (2015). Fast and sensitive protein alignment using DIAMOND. *Nat. Methods* 12, 59–60. doi: 10.1038/nmeth.3176

Contreras-Moreira, B., and Vinuesa, P. (2013). GET_HOMOLOGUES, a versatile software package for scalable and robust microbial pangenome analysis. *Appl. Environ. Microbiol.* 79, 7696–7701. doi: 10.1128/AEM.02411-13

Cooper, C. J., Khan Mirzaei, M., and Nilsson, A. S. (2016). Adapting drug approval pathways for bacteriophage-based therapeutics. *Front. Microbiol.* 7:1209. doi: 10.3389/fmicb.2016.01209

Coutinho, F. H., Silveira, C. B., Gregoracci, G. B., Edwards, R. A., Brussaard, C. P. D., Dutilh, B. E., et al. (2017). Marine viruses discovered through metagenomics shed light on viral strategies throughout the oceans. *Nat. Commun.* 8, 1–12. doi: 10.1038/ncomms15955

Díez-Martínez, R., De Paz, H. D., García-Fernández, E., Bustamante, N., Euler, C. W., Fischetti, V. A., et al. (2014). A novel chimeric phage lysin with high in vitro and in vivo bactericidal activity against *Streptococcus pneumoniae*. *J. Antimicrob. Chemother.* 70, 1763–1773. doi: 10.1093/jac/dkv038

Edwards, R. A., McNair, K., Faust, K., Raes, J., and Dutilh, B. E. (2015). Computational approaches to predict bacteriophage-host relationships. *FEMS Microbiol. Rev.* 40, 258–272. doi: 10.1093/femsre/fuv048

Finn, R. D., Clements, J., Arndt, W., Miller, B. L., Wheeler, T. J., Schreiber, F., et al. (2015). HMMER web server: 2015 update. *Nucleic Acids Res.* 43, W30–W38. doi: 10.1093/nar/gkv397

Gerstmans, H., Rodriguez-Rubio, L., Lavigne, R., and Briers, Y. (2016). From endolysins to Artilysin(R)s: novel enzyme-based approaches to kill drug-resistant bacteria. *Biochem. Soc. Trans.* 44, 123–128. doi: 10.1042/BST20150192

Gutiérrez, D., Fernández, L., Rodríguez, A., and García, P. (2018). Are phage lytic proteins the secret weapon to kill *Staphylococcus aureus*? *mBio* 9, e1923-17. doi: 10.1128/mBio.01923-17

Hermoso, J. A., García, J. L., and García, P. (2007). Taking aim on bacterial pathogens: from phage therapy to enzybiotics. *Curr. Opin. Microbiol.* 10, 461–472. doi: 10.1016/j.mib.2007.08.002

Hyatt, D., Chen, G.-L., Locascio, P. F., Land, M. L., Larimer, F. W., and Hauser, L. J. (2010). Prodigal: prokaryotic gene recognition and translation initiation site identification. *BMC Bioinformatics* 11:119. doi: 10.1186/1471-2105-11-119

Li, L., Stoeckert, C. J. Jr., and Roos, D. S. (2003). OrthoMCL: identification of ortholog groups for eukaryotic genomes. *Genome Res.* 13, 2178–2189. doi: 10.1101/gr.1224503

Mansfield, J., Genin, S., Magori, S., Citovsky, V., Sriariyanum, M., Ronald, P., et al. (2012). Top 10 plant pathogenic bacteria in molecular plant pathology. *Mol. Plant Pathol.* 13, 614–629. doi: 10.1111/j.1364-3703.2012.00804.x

Mizuno, C. M., Ghai, R., Saghaï, A., López-García, P., and Rodriguez-Valera, F. (2016). Genomes of abundant and widespread viruses from the deep ocean. *mBio* 7:e00805-16. doi: 10.1128/mBio.00805-16

Mizuno, C. M., Rodriguez-Valera, F., Kimes, N. E., and Ghai, R. (2013). Expanding the marine virosphere using metagenomics. *PLoS Genet.* 9:e1003987. doi: 10.1371/journal.pgen.1003987

Nelson, D. C., Schmelcher, M., Rodriguez-Rubio, L., Klumpp, J., Pritchard, D. G., Dong, S., et al. (2012). *Endolysins as Antimicrobials*, 1st Edn. New York, NY: Elsevier Inc. doi: 10.1016/B978-0-12-394438-2.00007-4

Oliveira, H., Melo, L. D., Santos, S. B., Nobrega, F. L., Ferreira, E. C., Cerca, N., et al. (2013). Molecular aspects and comparative genomics of bacteriophage endolysins. *J. Virol.* 87, 4558–4570. doi: 10.1128/JVI.03277-12

Paez-Espino, D., Eloe-Fadrosh, E. A., Pavlopoulos, G. A., Thomas, A. D., Huntemann, M., Mikhailova, N., et al. (2016). Uncovering Earth's virome. *Nature* 536, 425–430. doi: 10.1038/nature19094

Petersen, T. N., Brunak, S., von Heijne, G., and Nielsen, H. (2011). SignalP 4.0: discriminating signal peptides from transmembrane regions. *Nat. Methods* 8:785. doi: 10.1038/nmeth.1701

Pimentel, M. (2014). "Genetics of phage lysis," in *Molecular Genetics of Mycobacteria*, 2nd Edn, eds G. F. Hatfull and W. R. Jacobs Jr. (Washington, DC: ASM Press), 121–133.

Pohane, A. A., and Jain, V. (2015). Insights into the regulation of bacteriophage endolysin: multiple means to the same end. *Microbiology* 161, 2269–2276. doi: 10.1099/mic.0.000190

Price, M. N., Dehal, P. S., and Arkin, A. P. (2010). FastTree 2 - Approximately maximum-likelihood trees for large alignments. *PLoS One* 5:e9490. doi: 10.1371/journal.pone.0009490

Roux, S., Brum, J. R., Dutilh, B. E., Sunagawa, S., Duhaime, M. B., Loy, A., et al. (2016). Ecogenomics and potential biogeochemical impacts of globally abundant ocean viruses. *Nature* 537, 689–693. doi: 10.1101/053090

Roux, S., Hallam, S. J., Woyke, T., and Sullivan, M. B. (2015). Viral dark matter and virus-host interactions resolved from publicly available microbial genomes. *Elife* 4:e08490. doi: 10.7554/eLife.08490

Schmelcher, M., Donovan, D. M., and Loessner, M. J. (2012). Bacteriophage endolysins as novel antimicrobials. *Future Microbiol.* 7, 1147–1171. doi: 10.2217/fmb.12.97

Schmelcher, M., and Loessner, M. J. (2016). Bacteriophage endolysins: applications for food safety. *Curr. Opin. Biotechnol.* 37, 76–87. doi: 10.1016/j.copbio.2015.10.005

Shen, Y., Barros, M., Vennemann, T., Gallagher, D. T., Yin, Y., Linden, S. B., et al. (2016). A bacteriophage endolysin that eliminates intracellular streptococci. *Elife* 5, 1–26. doi: 10.7554/eLife.13152

Sievers, F., Wilm, A., Dineen, D., Gibson, T. J., Karplus, K., Li, W., et al. (2014). Fast, scalable generation of high-quality protein multiple sequence alignments using Clustal Omega. *Mol. Syst. Biol.* 7, 539–539. doi: 10.1038/msb.2011.75

Ventola, C. L. (2015). The antibiotic resistance crisis: part 2: management strategies and new agents. *Pharm. Ther.* 40, 344–352.

Vidová, B., Šramková, Z., Tišáková, L., Oravkinová, M., and Godány, A. (2014). Bioinformatics analysis of bacteriophage and prophage endolysin domains. *Biologia* 69, 541–556. doi: 10.2478/s11756-014-0358-8

Yutin, N., Makarova, K. S., Gussow, A. B., Krupovic, M., Segall, A., Edwards, R. A., et al. (2017). Discovery of an expansive bacteriophage family that includes the most abundant viruses from the human gut. *Nat. Microbiol.* 3, 38–46. doi: 10.1038/s41564-017-0053-y

Conflict of Interest Statement: The authors declare that the research was conducted in the absence of any commercial or financial relationships that could be construed as a potential conflict of interest.

frontiers in Microbiology

ORIGINAL RESEARCH
published: 04 May 2018
doi: 10.3389/fmicb.2018.00793

Characterization and Genomic Study of Phage vB_EcoS-B2 Infecting Multidrug-Resistant *Escherichia coli*

Yue Xu[1,2†], *Xinyan Yu*[1,2†], *Yu Gu*[1,2], *Xu Huang*[3,4], *Genyan Liu*[3,4] *and Xiaoqiu Liu*[1,2*]

[1] *Key Laboratory of Pathogen Biology of Jiangsu Province, Nanjing Medical University, Nanjing, China,* [2] *Department of Microbiology, Nanjing Medical University, Nanjing, China,* [3] *Department of Laboratory Medicine, The First Affiliated Hospital with Nanjing Medical University, Nanjing, China,* [4] *National Key Clinical Department of Laboratory Medicine, Nanjing, China*

The potential of bacteriophage as an alternative antibacterial agent has been reconsidered for control of pathogenic bacteria due to the widespread occurrence of multi-drug resistance bacteria. More and more lytic phages have been isolated recently. In the present study, we isolated a lytic phage named vB_EcoS-B2 from waste water. VB_EcoS-B2 has an icosahedral symmetry head and a long tail without a contractile sheath, indicating that it belongs to the family *Siphoviridae*. The complete genome of vB_EcoS-B2 is composed of a circular double stranded DNA of 44,283 bp in length, with 54.77% GC content. vB_EcoS-B2 is homologous to 14 relative phages (such as *Escherichia* phage SSL-2009a, *Escherichia* phage JL1, and *Shigella* phage EP23), but most of these phages exhibit different gene arrangement. Our results serve to extend our understanding toward phage evolution of family *Siphoviridae* of coliphages. Sixty-five putative open reading frames were predicted in the complete genome of vB_EcoS-B2. Twenty-one of proteins encoded by vB_EcoS-B2 were determined in phage particles by Mass Spectrometry. Bacteriophage genome and proteome analysis confirmed the lytic nature of vB_EcoS-B2, namely, the absence of toxin-coding genes, islands of pathogenicity, or genes through lysogeny or transduction. Furthermore, vB_EcoS-B2 significantly reduced the growth of *E. coli* MG1655 and also inhibited the growth of several multi-drug resistant clinical stains of *E. coli*. Phage vB_EcoS-B2 can kill some of the MRD *E. coli* entirely, strongly indicating us that it could be one of the components of phage cocktails to treat multi-drug resistant *E. coli.* This phage could be used to interrupt or reduce the spread of multi-drug resistant *E. coli.*

Keywords: bacteriophage vB_EcoS-B2, genome sequence, multi-drug resistance, comparative genome, mass spectrometry

OPEN ACCESS

Edited by:
Robert Wilson Jackson, University of Reading, United Kingdom

Reviewed by:
Grzegorz Wegrzyn, University of Gdansk, Poland
Rui Zhang, Xiamen University, China

***Correspondence:**
Xiaoqiu Liu
xiaoqiuliu2014@126.com

†These authors have contributed equally to this work.

Specialty section:
This article was submitted to Virology, a section of the journal Frontiers in Microbiology

Received: *29 December 2017*
Accepted: *09 April 2018*
Published: *04 May 2018*

Citation:
Xu Y, Yu X, Gu Y, Huang X, Liu G and Liu X (2018) Characterization and Genomic Study of Phage vB_EcoS-B2 Infecting Multidrug-Resistant Escherichia coli. Front. Microbiol. 9:793. doi: 10.3389/fmicb.2018.00793

INTRODUCTION

Escherichia coli is a gram-negative bacterium, which can cause intestinal (diarrhea) or extraintestinal (urinary tract infection, septicaemia, pneumonia, and meningitis) diseases in humans and animals (Cabal et al., 2016). Current antibiotic treatments used to treat *E. coli often* result in a spread of multidrug resistance (MDR) of *E. coli* (Lepape and Monnet, 2009). For example, *E. coli* strains produce Extended-Spectrum Beta Lactamase and metallo-β-lactamas, enzymes which make *E. coli* become resistant to several antibiotic drugs (Peña et al., 2006; Birgy et al., 2011). Currently, carbapenems appear to be the last

available treatment for the severe infections caused by MDR *E. coli*. The recent finding of carbapenemase which hydrolyzes carbapenem may soon lead to cases with no therapeutic issue (Birgy et al., 2011). The emergence of carbapenemase and the lack of efficient antibiotics are alarming, therefore, the well-tolerated, highly effective therapeutic alternatives are urgently needed (Birgy et al., 2011; Castanheira et al., 2017). This has encouraged researchers into returning to use bacteriophages (phages) as a supplement or substitute of antibiotics to treat infection caused by bacterial (Bolocan et al., 2016).

Although phages have been discovered over a century ago, phages continue to have a major impact on modern biological sciences, especially with the growth of interests in the microbiome (Haq et al., 2012; Laanto et al., 2017) and treating multidrug-resistant bacteria (Kutateladze and Adamia, 2010; Bolocan et al., 2016). Many reports described that various pathogenic *E. coli* have been killed by lysis phages (Bourdin et al., 2014). Therapeutic bacteriophages that efficiently lyse the *E. coli* O104:H4 outbreak strain could be selected easily from a phage bank or isolated from the environment (Merabishvili et al., 2012). Phage EC200PP was able to treat sepsis and meningitis infections induced by drug-resistant *E. coli* S242 (Pouillot et al., 2012). Fitzgerald-Hughes's study proved that Extended-Spectrum Beta Lactamase producing *E. coli* strains can be killed by commercially available and laboratory-isolated bacteriophages (Fitzgerald-Hughes et al., 2014). Dufour et al. determined that bacteriophage LM33-P1 can infect β-lactams and fluoroquinolones resistant *E. coli* strains efficiently both *in vitro* and *in vivo* (Dufour et al., 2016). The study on the efficient treatment of *E. coli*-induced pneumonia with two bacteriophages (536 P1 and 536 P7) showed that a combination of antibiotic treatment and phage therapy resulted in a 100% survival rate in VAP-infected mice (Dufour et al., 2015). Therefore, bacteriophages can be used as a supplement for antibiotics to treat the infection caused by bacteria.

Phages are the most abundant biological entities present on earth, providing an unlimited resource for possible phage applications (Srinivasiah et al., 2008). Phages flourish in oceans, soil, wastewater treatment plants, hot-water springs, and animal gut (Srinivasiah et al., 2008; Williamson et al., 2017). *E. coli* phages are commonly isolated from sewage, hospital waste water, polluted rivers, and fecal samples of humans or animals (Jamalludeen et al., 2009; Dalmasso et al., 2016; Snyder et al., 2016; Amarillas et al., 2017). Selection of wide spectrum phages or phages cocktail components for therapeutic preparation are key procedures to overcome the shortage of phage therapy, such as narrow host range of phages and emergence of bacterial resistance to phages (Regeimbal et al., 2016). Constructing the "right" cocktail is essential for achieving the maximum effectiveness of phage therapy (Bourdin et al., 2014; Schooley et al., 2017). It is also essential to have a set of well-characterized phages available for constructing the "right" cocktail to infect the broad range of bacterial pathogens (Sybesma et al., 2016). Therefore, isolating new phages and unraveling their genome sequence seems to be urgently needed to accumulate sufficient phage stocks for phage therapy.

In the present study, we isolated a lytic phage named vB_EcoS-B2 from waste water. Transmission electron microscopy of vB_EcoS-B2 morphology revealed that it belongs to the *Siphoviridae* family. vB_EcoS-B2 significantly reduced the growth of *E. coli* under laboratory conditions. Prior to its application in phage therapy, we determined the genomic sequence and particle proteins of phage vB_EcoS-B2. Our results confirmed that vB_EcoS-B2 does not include virulent genes, islands of pathogenicity, or genes through lysogeny or transduction, which is a good candidate for phage therapy.

MATERIALS AND METHODS

Bacterial Strains and Culture Conditions

The bacterial strains used in this study were listed in **Table 1**. *E. coli* strains BL21 (DE3), DH5α, JM110, TOP10, BW25113, S17-1 were stocks in our lab. Thirty-five clinical isolates of *E. coli* were isolated from clinical samples of patients in the First Affiliated Hospital of Nanjing Medical University, Nanjing, China. All clinical strains which were used for phage host range determination have antibiotic resistance. Twenty-one of them are Extended-Spectrum Beta Lactamase producing stains. Five of them are metallo-β-lactamas (New Delhi metallo-β-lactamase-5) producing stains. All strains were grown in Luria–Bertani (LB) medium at 37°C.

Isolation and Propagation of Bacteriophages

E. coli MG1655 was used for isolating and enriching virulent bacteriophage from waste water in Nanjing. Sewage sample was filtered using 0.45 μm pore-size filters (Millipore, USA) to remove bacteria. Filtrates were added to *E. coli* MG1655 culture in early-log-phase at 37°C for 24 h with constant shaking to enrich the phages. Then the culture was centrifuged at 12,000 g for 10 min at 4°C to remove *E. coli* cells. The enriched phage suspension was tested for plaque formation with *E. coli* MG1655 using the double-layer agar plate method. Plaques formed on the plates after 12 h of incubation at 37°C. Single plaque was picked to start the second (and subsequent) round of amplification. The infection cycle was repeated until the plaques were homogeneous. The phages were then amplified and stored at 4°C.

Purification of Phages

Purification of vB_EcoS-B2 was carried out as described previously with slight modifications (Heo et al., 2009). Briefly, *E. coli* MG1655 culture at the early-log-phase (OD600 = 0.4) was infected by phage vB_EcoS-B2 at 37°C for 3 h with shaking. Cell debris was removed by centrifugation (14,000 g, 10 min, 4°C). The supernatant was passed through 0.45-μm-pore-size filters, yielding a crude extract of phage. Then the phage crude extract was concentrated by ultracentrifugation (100,000 g, 2h, 4°C), and the pellet containing phages was suspended in SM buffer (5.8 g/L NaCl, 2 g/L $MgSO_4 \cdot 7H_2O$, 50 ml/L 1M pH7.5 Tris-HCl). The concentrated suspension was further purified by cesium chloride gradient centrifugation (90,000 g, 20 h, 4°C). The phage zone was collected (about 1 mL) and diluted into 10 ml SM buffer, followed by participation at 200,000 g for 3 h to remove CsCl. Finally, the

TABLE 1 | Host range spectrum of thebacteriophage vB_EcoS-B2.

E. coli strain	Source	Subtype	Resistance	Lysis or not
E. coli K-12 MG1655				Clear plaque
E. coli TOP10				Clear plaque
E. coli S17-1				Clear plaque
E. coli DH5α				Clear plaque
E. coli BW25113				Clear plaque
E. coli BL21(DE3)				Clear plaque
E. coli JM110				N
25922	ATCC 25922	Non-ESBL		N
35218	ATCC 35218	ESBL		Turbid plaque
389 A6	Urine	ESBL	Aztreonam, cefazolin, ceftazidime, cefatriaxone, sulfamethoxazole, and trimethoprim	Turbid plaque
389 A9	pus and secretion	ESBL	Aztreonam, cefazolin, ceftazidime, sulfamethoxazole, and trimethoprim	N
389 D9	Urine	Non-ESBL	Sulfamethoxazole and trimethoprim	N
389 E6	Urine	Non-ESBL	Levofloxacin	N
389 G4	Urine	Non-ESBL	Amikacin, Ampicillin sulbactam, aztreonam, cefazolin, cefepime, cefotaxime, cefoxitin, ceftazidime, gentamycin, Levofloxacin,	N
389 G6	Urine	Non-ESBL	Levofloxacin	N
389 G7	Urine	ESBL	Amikacin, Ampicillin sulbactam, aztreonam, cefazolin, cefotaxime, Levofloxacin	N
389 J4	Sputum	ESBL	Aztreonam, cefazolin, cefepime, ceftazidime, cefatriaxone,	N
390 A7	Sputum	Non-ESBL	Sulfamethoxazole and trimethoprim	N
390 B6	Urine	Non-ESBL	Sulfamethoxazole and trimethoprim	N
390 G7	Urine	Non-ESBL	Ampicillin sulbactam, cefazolin, gentamycin, Levofloxacin, sulfamethoxazole, and trimethoprim	Clear plaque
390 H2	Urine	Non-ESBL	Ampicillin sulbactam, cefazolin, gentamycin, Levofloxacin, sulfamethoxazole, and trimethoprim	N
390 J2	Urine	Non-ESBL	Levofloxacin, minocycline, sulfamethoxazole, and trimethoprim	N
391 D3	Urine	Non-ESBL	Cefazolin, gentamycin, sulfamethoxazole, and trimethoprim	N
391 G4	Blood	ESBL	Aztreonam, cefazolin, cefepime, ceftazidime, cefatriaxone,	N
393 B7	Urine	ESBL	Amikacin, amoxicillin and clavulanate, Ampicillin sulbactam, aztreonam, cefazolin, cefepime, cefotaxime, cefoxitin, ceftazidime, gentamycin, Levofloxacin, minocycline, sulfamethoxazole, and trimethoprim	N
393 C1	Ascites	ESBL	Ampicillin sulbactam, aztreonam, cefazolin, cefepime, cefotaxime, ceftazidime, gentamycin, sulfamethoxazole and trimethoprim	Clear plaque
393 C8	Urine	ESBL	Cefazolin, cefepime, cefotaxime, Levofloxacin, sulfamethoxazole, and trimethoprim	N
393 D3	Urine	ESBL	Cefazolin, cefepime, cefotaxime, ceftazidime, Levofloxacin,	N
394 F7	Urine	ESBL	Amoxicillin and clavulanate, aztreonam, cefazolin, cefotaxime, cefoxitin, ceftazidime	N
394 G1	Urine	ESBL	Amoxicillin and clavulanate, cefazolin, cefoxitin, imipenem, sulfamethoxazole, and trimethoprim	N
394 H7	Urine	ESBL	Aztreonam, cefepime, cefotaxime, ceftazidime, Levofloxacin	Clear plaque
395 B5	Urine	ESBL	Ampicillin sulbactam, aztreonam, cefazolin, cefepime, cefotaxime, gentamycin, Levofloxacin, sulfamethoxazole, and trimethoprim	N
395 G6	Urine	ESBL	Aztreonam, cefazolin, cefepime, cefotaxime, ceftazidime, gentamycin	N
395 J2	Sputum	ESBL	Ampicillin, gentamycin, Levofloxacin, minocycline	N

(Continued)

TABLE 1 | Continued

E. coli strain	Source	Subtype	Resistance	Lysis or not
396 F3	Sputum	ESBL	Amikacin, ampicillin, gentamycin, Levofloxacin, minocycline	Clear plaque
396 J1	Urine	ESBL	Cefazolin, cefepime, cefotaxime, imipenem, Levofloxacin,	N
396 J5	Urine	ESBL	Aztreonam, cefazolin, cefepime, cefotaxime, imipenem, Levofloxacin	N
397 C8	Sputum	ESBL	Aztreonam, cefazolin, cefepime, ceftazidime, cefatriaxone	N
397 D3	Urine	ESBL	Ampicillin sulbactam, aztreonam, cefazolin, cefepime, cefotaxime, cefoxitin, gentamycin, Levofloxacin, sulfamethoxazole, and trimethoprim	N
37	n.d	NDM-5	Ampicillin/Sulbactam, aztreonam, imipenem, Levofloxacin, piperacillin, Cefuroxime sodium, cefuroxime axetil, sulfamethoxazole, and trimethoprim, ceftazidime, Tazobactam, Meropenem, cefotetan, cefatriaxone, cefazolin, Cefepime plaster	N
40	n.d	NDM-5	Ampicillin/Sulbactam, amikacin, aztreonam, gentamycin, imipenem, Levofloxacin, piperacillin, Cefuroxime sodium, cefuroxime axetil, sulfamethoxazole and trimethoprim, ceftazidime, Tazobactam, tobramycin, Meropenem, cefotetan, cefatriaxone, cefazolin, Cefepime plaster	N
64	n.d	NDM-5	Ampicillin/Sulbactam,gentamycin,imipenem,Levofloxacin,piperacillin,Cefuroxime sodium,cefuroxime axetil,sulfamethoxazole and trimethoprim,ceftazidime,Tazobactam,tobramycin, Meropenem,cefotetan,cefatriaxone,cefazolin,Cefepime plaster	N
69	n.d	NDM-5	Ampicillin/Sulbactam, amikacin, aztreonam, gentamycin, imipenem, Levofloxacin, piperacillin, Cefuroxime sodium, cefuroxime axetil, sulfamethoxazole and trimethoprim, ceftazidime, Tazobactam, tobramycin, Meropenem, cefotetan, cefatriaxone, cefazolin, Cefepime plaster	N
92	n.d	NDM-5	Ampicillin/Sulbactam, gentamycin,imipenem, Levofloxacin, piperacillin, Cefuroxime sodium, cefuroxime axetil, sulfamethoxazole and trimethoprim, ceftazidime, Tazobactam, tobramycin, Meropenem, cefotetan, cefatriaxone, cefazolin, Cefepime plaster	Turbid plaque

Positive results are indicated by "Clear plaque" or "Turbid plaque," and negative results are indicated by "N"; n.d., no data available; In the column "subtype," "ESBL" represent "Extended-Spectrum Beta Lactamase," "NDM-5" represent "New Delhi metallo-β-lactamase-5."

pellet was resuspended in SM buffer to yield the highly purified vB_EcoS-B2 particles.

Electron Microscopy

The purified phage particles of vB_EcoS-B2 were fixed on a copper grid with a carbon-coated film and negatively stained with 2% (w/v) phosphotungstic acid. The micrographs were taken under FEI Tecnai G2 Spirit Bio TWIN transmission electron microscope at 80 kV.

Temperature Stability

The stability of bacteriophage under different temperature conditions was determined by constant temperature water bath method, a 1.5 mL tube containing 200 μL (approximately 10^{10} pfu/mL) equal volumes of phage were incubated under different temperature (4, 25,37, 45, 50, 55, 60, and 65°C). The phage titer was determined at intervals of 30 min from 0 to180 min, then at 6 and 24 h by the double-layer method. Three independent experiments were done and the value is represented by means.

Host Range Analysis

Ability of vB_EcoS-B2 to infect *E. coli* strains was tested. A total of 10^9 cells were mixed with melted agar, and this mixture was poured on solid agar to make double-layer agar plates. After solidification, 10 μL of phage suspensions (approximately 10^{10} pfu/mL) of bacteriophage stock suspensions was spotted on plates carrying each bacterial strain. After adsorption of the spots, the plates were inverted and incubated for 24 h at 37°C before the degree of lysis was scored (Postic and Finland, 1961). All experiments were conducted according to the standard institutional guidelines of Nanjing Medical University (Nanjing, China). The study was approved by the research and ethics committee of the First Affiliated Hospital of Nanjing Medical University.

One-Step Growth Curve

One-step growth experiment was carried out as described previously with little modification (Yang et al., 2015). In brief, *E. coli* MG1655 was grown in LB medium until the early-log-phase (1×10^8 CFU/mL). Phage vB_EcoS-B2 was added to *E. coli* MG1655 culture at a multiplicity of infection (MOI) of 10 separately, and allowed to absorb for 10 min at 37°C. Then the mixture was centrifuged at 14, 000 g for 1 min to remove un-adsorbed phages. After washing twice with fresh LB medium, the pellet of infected cells was resuspended in 50 mL of LB medium and the culture was continuously incubated at 37°C. Using double-layer agar plate method, we determined the free bacteriophage count at each time point. The latency period and burst period were obtained directly from these one-step growth curves. The burst size of vB_EcoS-B2 was calculated by dividing the phage titers at plateau phase by the initial number of infective bacterial cells.

Bacterial Challenge Assay

For the bacterial challenge assay, 50 mL fresh LB broth was inoculated with an overnight culture of *E. coli* MG1655 (1% inoculum), followed by incubation at 37°C at 220 rpm until the OD600 was about 0.3. vB_EcoS-B2 stock solutions were then added (MOI = 10) to these cultures. Bacterial growth was monitored by measuring the OD600 at various time points. As a negative control, bacterial cultures were inoculated with SM buffer instead of vB_EcoS-B2. OD600 was recorded at 15 min intervals, over a period of 300 min.

Extraction and Sequencing of the vB_EcoS-B2 Genome

The purified phage sample was treated with DNase I (New England Biolabs) and RNase A (Tiangen Biotech) for 2 h at 37°C to digest the exogenous DNA and RNA. The preparation was then treated with proteinase K (Tiangen Biotech) for 15 min at 55°C. The phage genome DNA was further prepared with a TIANamp Bacteria DNA Kit (Tiangen Biotech). DNA concentration was determined using a spectrophotometer (Nanodrop Technologies, USA). The vB_EcoS-B2 genomic DNA was sequenced using an Illumina HiSeq 2500 sequencer and reads were assembled into a whole genome using SOAPdenovov2.04 software and GapCloserv1.12.

Annotation and Comparison

Putative open reading frames (ORFs) were predicted using artemis software (http://www.sanger.ac.uk/science/tools/artemis) and Glimmer 3 (Aggarwal and Ramaswamy, 2002), with a threshold of 30 amino acids (aa) as a minimum for the length of protein. Function annotation was performed using the BLAST tools at NCBI (http://blast.ncbi.nlm.nih.gov/Blast.cgi) against the non-redundant protein sequences database. Transfer RNAs (tRNAs) were identified using tRNAscan-SE (v1.23, http://lowelab.ucsc.edu/tRNAscan-SE) and ribosome RNAs (rRNAs) were determined using RNAmmer (v1.2, http://www.cbs.dtu.dk/services/RNAmmer/). DNAman was used to calculate molecular masses and isoelectric points for predicted phage proteins. The whole viral nucleotide sequence similarities between phages were determined by megablast analysis at NCBI. The global alignment of putative amino acid sequences was carried out by EMBOSS Needle tool at EMBL-EBI (European Molecular Biology Laboratory-European Bioinformatics Institute). Comparison of ORFs from relative phages was performed using EasyFig (http://mjsull.github.io/Easyfig/files.html) (Sullivan et al., 2011). Phylogenetic analyses between the genomes of related phages were performed with MEGA using the Neighbor-Joining algorithm.

Structural Protein Analysis of vB_EcoS-B2

The highly purified phage sample was subjected to sodium dodecyl sulfate polyacrylamide gel electrophoresis (SDS-PAGE) using 12% acrylamide concentration. Gels were stained with silver as described by Shevchenko et al. (1996). For protein identification by liquid chromatography electrospray ionization with tandem mass spectrometry (LC-ESI MS/MS), the phage particles were digested with trypsin, and the tryptic peptides were analyzed by Q Exactive mass spectrometer (Thermo Scientific, USA). The corresponding ORFs were searched using MASCOT engine (Matrix Science, London,

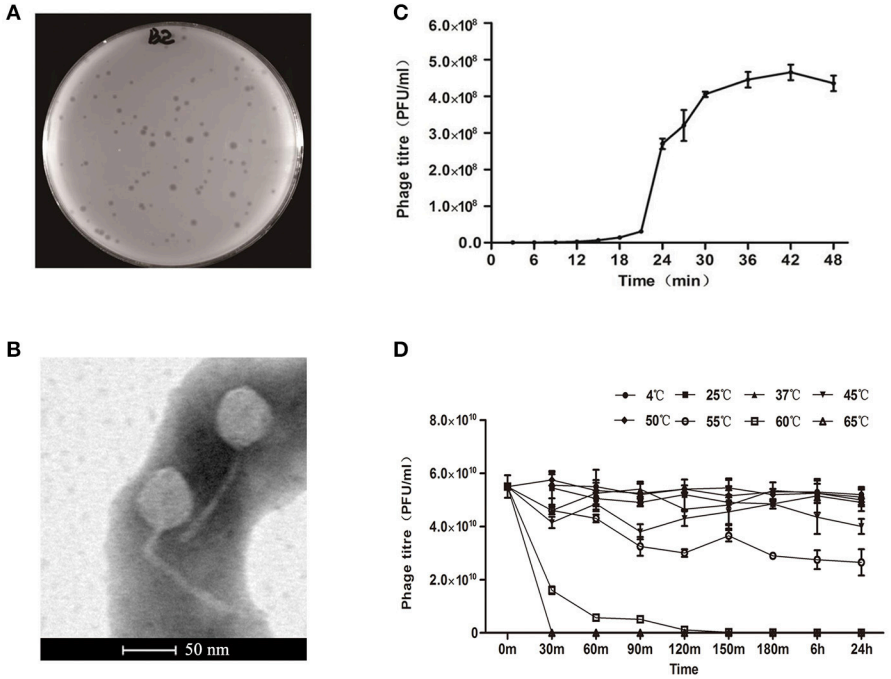

FIGURE 1 | Isolation, morphology, and biological properties of phage vB_EcoS-B2. **(A)** Plaque morphology of phage vB_EcoS-B2. **(B)** Transmission electron micrographs of *E. coli* phage vB_EcoS-B2. Bar indicates 50 nm. **(C)** One-step growth curve of vB_EcoS-B2 on *E. coli* strain MG1655 at 37°C. **(D)** Thermo stability of vB_EcoS-B2: the phages were incubated at different temperatures for 24 h. Each value is the average from three different cultures ± standard deviation in **(C,D)**.

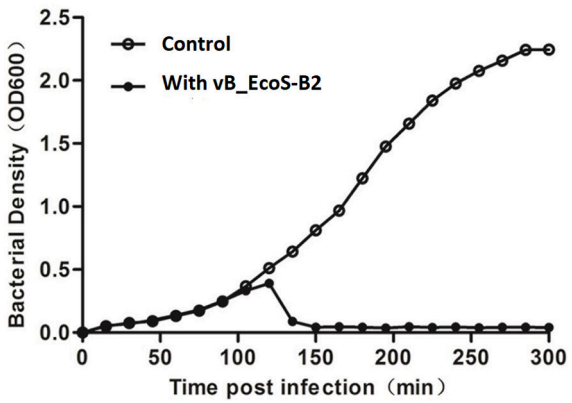

FIGURE 2 | Bacterial challenge assay with phage vB_EcoS-B2 to *E. coli* MG1655. vB_EcoS-B2 was added at an MOI of 10 to the bacterial culture after 1.5 h incubation (OD600 = 0.25) (close circles). OD600 was recorded at 15 min intervals, over a period of 300 min. A bacterial culture inoculated with SM buffer instead of vB_EcoS-B2 was used as the negative control (open circles). Each value is the average from three different cultures.

UK; version 2.2) against the protein sequence library of vB_EcoS-B2.

Nucleotide Sequence Accession Number

The genome sequence of vB_EcoS-B2 was deposited in GenBank under the accession number MG581355.

RESULTS AND DISCUSSION

Phage Morphology

A new *E. coli* phage vB_EcoS-B2 was isolated from wastewater in Nanjing. The phage formed clear round plaque (about 1–3 mm-diameter) with *E. coli* strain MG1655 after overnight culture at 37°C (**Figure 1A**). The purified phage particles of vB_EcoS-B2 were examined under the Transmission Electron Microscope. vB_EcoS-B2 has an icosahedral symmetry head and a long tail without a contractile sheath, indicating that it belongs to the family of *Siphoviridae*. The isometric head of vB_EcoS-B2 had a mean diameter of 48 nm, and the long non-contractile tail was about 143 ± 6 nm (**Figure 1B**). vB_EcoS-B2 is closely resembled to the morphology of *Enterobacteria* phage SSL-2009a (an icosahedral head 62 nm in diameter and a long, flexible tail 138 nm in length) and *Shigella* phage EP23 (head diameter 59 ± 3 nm; non-contractile, filamentous tails 142 ± 32 nm in length) (Li et al., 2010; Chang and Kim, 2011).

Phage Population Dynamics

One-step growth experiments were performed to assess the population kinetics of vB_EcoS-B2, in the presence of *E. coli* strain MG1655 (**Figure 1C**). vB_EcoS-B2 had latent period about 20 min. All phages had been released by 30 min after infection (**Figure 1C**), and had a burst size of 224.1 ± 10.7 phage particles. Latent time of vB_EcoS-B2 was shorter than that of phage EP23 which had a latent period of 45 min (Chang and Kim, 2011). Latent and burst periods of vB_EcoS-B2 were very similar to that

TABLE 2 | Predicted ORFs and genes encoded by the vB_EcoS-B2 genome.

ORFs	Start	Stop	Directions	No. of residues	MW(da)	pI	Predicted molecular function
ORF1	1	2,292	+	763	86167.7	8.56	DNA polymerase I
ORF2	2,292	2,570	+	92	10147.2	10.39	Hypothetical protein
ORF3	2,611	2,784	+	57	6825.7	10.35	Hypothetical protein
ORF4	2,822	3,046	+	74	8761.5	9.94	Hypothetical protein
ORF5	3,051	4,475	+	474	53461.8	9.55	DNA helicase
ORF6	4,472	5,167	+	231	26496.7	8.27	Putative DNA cytosine methyltransferase C5
ORF7	5,164	5,487	+	107	11695	9.14	Putative HNH endonuclease
ORF8	5,569	6,033	+	154	17882.3	8.19	Hypothetical protein
ORF9	6,020	6,505	+	161	18708.4	9.72	DNA methyltransferase
ORF10	6,486	6,710	+	74	8686.6	8.9	Hypothetical protein
ORF11	6,707	7,177	+	156	17872.8	6.25	Hypothetical protein
ORF12	7,242	7,796	+	184	20488.5	4.93	Hypothetical protein
ORF13	7,839	8,414	+	191	21491.9	6.78	Hypothetical protein
ORF14	8,442	10,265	−	607	65194.4	4.79	Putative tail tip protein
ORF15	10,346	10,630	+	94	10251.1	7.28	Hypothetical protein
ORF16	10,582	11,253	−	223	23211.6	8.18	Hypothetical protein
ORF17	11,256	11558	−	100	10216.6	8.5	Hypothetical protein
ORF18	11,596	15,015	−	1,139	125892.9	5.11	Putative tail fiber protein
ORF19	15,012	15629	−	205	21245.4	8.71	Putative tail assembly protein I
ORF20	15,620	16,360	−	246	27577.5	4.95	Tail assembly protein
ORF21	16,363	17,151	−	262	28806.3	4.88	Putative minor tail protein L
ORF22	17,148	17,747	−	199	21696.3	6.52	Putative minor tail protein
ORF23	17,784	20,426	−	880	93307.2	9.93	Putative tail length tape-measure protein 1
ORF24	20,426	20,518	−	30	3341.4	10.5	Hypothetical protein
ORF25	20,490	20,681	−	63	6931.5	8.51	Hypothetical protein
ORF26	20,821	21,051	−	76	8543.3	5.77	Hypothetical protein
ORF27	21,135	21,497	−	120	13958.5	4.78	Hypothetical protein
ORF28	21,567	22,292	−	241	25755.3	5.82	Putative major tail protein
ORF29	22,354	22,776	−	140	15087.1	4.73	Hypothetical protein
ORF30	22,776	23,369	−	197	21918	11.19	Putative tail protein
ORF31	23,371	23,730	−	119	13053.8	9.59	Putative structural protein
ORF32	23,711	23,827	−	38	3990.7	3.76	Hypothetical protein
ORF33	23,829	24,359	−	176	18924.7	3.89	Hypothetical protein
ORF34	24,388	25,488	−	366	38395.4	7.66	Major head protein
ORF35	25,586	26,287	−	233	25384.1	5.51	Hypothetical protein
ORF36	26,388	26,756	+	122	13128.6	5.65	Hypothetical protein
ORF37	26,796	27,560	+	254	28937.1	8.29	Hypothetical protein
ORF38	27,574	27,732	−	52	5739.7	4.33	Hypothetical protein
ORF39	27,686	28,015	−	109	11931.4	9.88	Hypothetical protein
ORF40	28,008	29,111	−	367	40988.6	9.94	Head morphogenesis protein
ORF41	29,095	30,615	−	506	55192.3	4.51	Phage structural protein
ORF42	30,627	32,012	−	461	52196.7	7.52	Terminase large subunit
ORF43	32,012	32,584	−	190	21084	8.05	Putative terminase small subunit
ORF44	32,694	33,836	−	380	42737.4	7.35	Putative phosphoesterase
ORF45	33,857	34,057	+	66	7221.1	8.22	Hypothetical protein
ORF46	34,074	34,241	−	55	5603.2	4.48	Hypothetical protein
ORF47	34,258	34,749	−	163	18156.3	9.41	Lysozyme
ORF48	34,736	34,981	−	81	8870	8.51	Putative holin-like class I protein
ORF49	34,978	35,268	−	96	10183.1	8.23	Putative holin-like class II protein
ORF50	35,323	35,622	−	99	11796	9.72	Hypothetical protein

(Continued)

TABLE 2 | Continued

ORFs	Start	Stop	Directions	No. of residues	MW(da)	pI	Predicted molecular function
ORF51	35,687	35,833	−	48	5626.5	11.71	Hypothetical protein
ORF52	35,830	36,363	−	177	20721.2	10.59	Hypothetical protein
ORF53	36,360	36,494	−	44	5107.7	3.43	Hypothetical protein
ORF54	36,485	36,670	−	61	7413.4	11.48	Hypothetical protein
ORF55	36,770	37,075	−	101	11091.8	10.31	Hypothetical protein
ORF56	37,072	37,206	−	44	5206.2	8.24	Hypothetical protein
ORF57	37,297	37,554	−	85	9233.9	11.49	Hypothetical protein
ORF58	37,609	39,861	−	750	82443.1	6.15	Hypothetical protein
ORF59	39,872	40,201	−	109	12545.1	8.47	DNA recombination nuclease inhibitor gamma
ORF60	40,424	41,032	+	202	23053.6	4.52	Hypothetical protein
ORF61	41,081	41,332	+	83	9953.6	9.91	Hypothetical protein
ORF62	41,333	41,521	+	62	7168	8.22	Hypothetical protein
ORF63	41,521	42,951	+	476	52319.8	8.73	Hypothetical protein
ORF64	42,944	43,186	+	80	9323.4	6.49	Hypothetical protein
ORF65	43,277	44,059	+	260	29909.5	4.55	Hypothetical protein

of phage SSL-2009a which have latent and burst periods 10–15 and 30–40 min (Li et al., 2010), respectively. Even though the burst size of vB_EcoS-B2 is less than that of SSL-2009a (about 375 PFU per infected cell) (Li et al., 2010), it is still a large burst size. As an antibacterial agent, a phage with a large burst size may indicate an easy selective advantage since phages with large burst sizes can increase the initial dose of phages several hundred-folds in short periods of time (Nilsson, 2014). The phages to be used in phage therapy must be strictly virulent and should be reproduced effectively and rapidly (Nilsson, 2014). Therefore, the large burst size and short latent time of vB_EcoS-B2 make it a good candidate for being used as the biocontrol agent against bacterial pathogens.

Thermal Stability

The thermal stability test was determined at different temperatures (4, 25, 37, 45, 50, 55, 60, and 65°C) whithin 24 h (**Figure 1D**). Results showed that the biological activity of phage vB_EcoS-B2 did not show any difference within the temperature ranging from 4 to 50°C, but decreased sharply when the temperature increasing above 55°C. Even though vB_EcoS-B2 does not like SSL-2009a which keeps activity more than 45 min over 63°C (Li et al., 2010), vB_EcoS-B2 is stable at relatively low temperature for longer time (Supplementary Figures 1, 2). The phage is stable over a range of temperatures (4–50°C) for 24 h, suggesting that it has a good thermal stability and therefore easy to be preserved.

Host Range and Effect of Phages on *E. coli* Growing Culture

The ability of newly isolated phage to lyse *E. coli* strains was assayed by the spot test. vB_EcoS-B2 can infect some of the well-known *E. coli* strains and several clinical MRD *E. coli* stains (**Table 1**). vB_EcoS-B2 is similar to SSL-2009a that is able to infect some engineered *E. coli* strains (**Table 1**). vB_EcoS-B2 can also infect the *E. coli* strain ATCC 35218, which could not be infected by SSL-2009a (Li et al., 2010). JL1 is a phage which can infect *E. coli* O157:H7 (Pan et al., 2013). EP23 can infect the three *E. coli* strains and two *S. sonnei* strains (Chang and Kim, 2011). The observations suggested that these very similar phages have different host range. Phage vB_EcoS-B2 only targeted seven MDR *E. coli* strains out of the 35 clinical isolates (**Table 1**). Therefore, Phage vB_EcoS-B2 has a relative narrow host spectrum. To overcome the narrow host range of phages, it is generally accepted that cocktails of multiple phages can be used to kill the great diversity of *E. coli* strains (Schmerer et al., 2014).

The effect of vB_EcoS-B2 alone on the growth of strain MG1655 was tested at MOI = 10 after 300 min of the phage added into the strain. vB_EcoS-B2 can efficiently reduce the growth of *E. coli* MG1655 after 30 min of infection (**Figure 2**, Supplementary Figure 3). Even though its host-range is relatively narrow, vB_EcoS-B2 has the possibility to be used as biocontrol agents against *E. coli* since it had strong lytic ability to *E. coli*. Therefore, it is essential to analyze complete sequence of vB_EcoS-B2 to ensure that the genome of vB_EcoS-B2 did not encode any genes associated with toxins, virulence factors, or lysogenic proteins.

Basic Characteristics of vB_EcoS-B2 Genome

The complete genome of vB_EcoS-B2 is composed of a circular double stranded DNA of 44,283 bp in length, with 54.77% GC content which was slightly higher than those of *E. coli* (50.6%). Sixty-five putative open reading frames (ORFs) were predicted in the complete genome of vB_EcoS-B2. The annotation of the properties of phage vB_EcoS-B2 genome, such as positions, directions, and putative functions of each gene were summarized in **Table 2**. Twenty-three ORFs were in the direct strand of the phage genome and 42 of them were in complementary strand (**Figure 3**). Only 25 ORFs (38.5%) were predicted and determined to be putative functional (different colors), whereas 40 ORFs were assigned to hypothetical proteins (black color) (**Figure 3**). The 25 predicted functional proteins were categorized into five functional groups: DNA

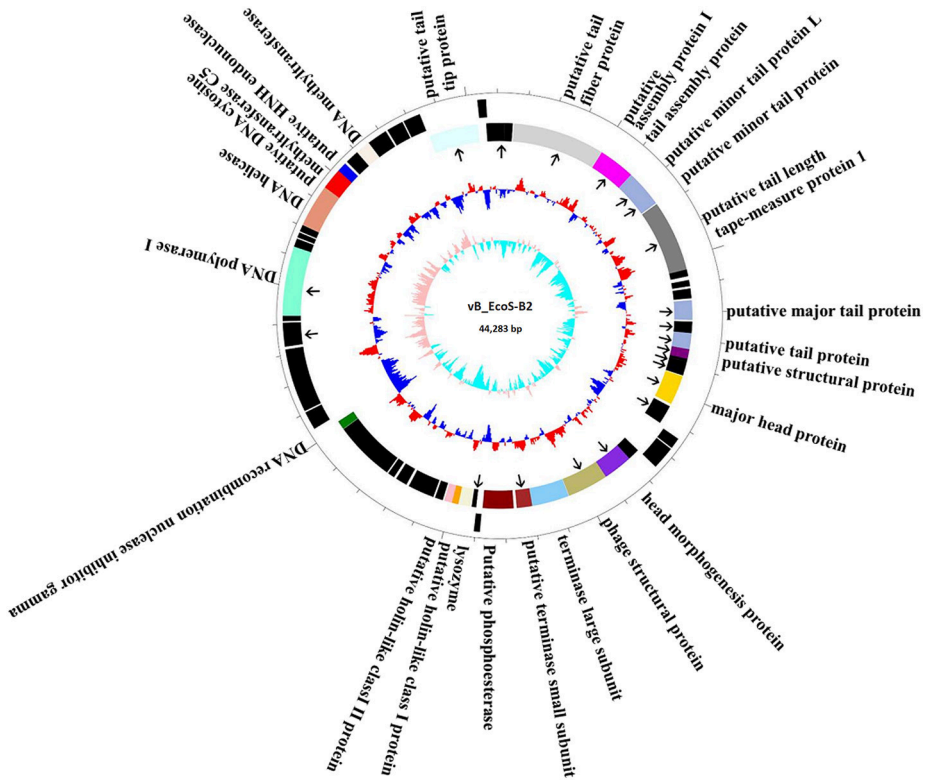

FIGURE 3 | Map of the genome organization of bacteriophage vB_EcoS-B2. The predicted ORFs are indicated as different colors in first circle. The outward showed the forward transcription genes and the inward showed the reversed transcription genes. Different colors identify ORFs with predicted molecular function. Hypothetical proteins marked by black. The second circle shows the G/C content. Red outward indicated that the G/C content of this region is higher than the average G/C content of the whole genome, and blue inward indicated G/C content of this region less than the average. The third circle shows the GC skew. Particle proteins identified by Mass spectrometry were pointed by black arrows.

replication/modification (DNA polymerase I, DNA helicase, putative DNA cytosine methyltransferase C5, putative HNH endonuclease, DNA methyltransferase, DNA recombination nuclease inhibitor gamma), host lysis (lysozyme, putative holin-like class I protein, and putative holin-like class II protein), packaging (terminase large subunit, putative terminase small subunit), structural proteins (putative tail tip protein, putative tail fiber protein, putative tail assembly protein I, tail assembly protein, putative minor tail protein L, putative minor tail protein, putative tail length tape-measure protein 1, putative major tail protein, putative tail protein, putative structural protein, major head protein, head morphogenesis protein, and phage structural protein), and additional functions (putative phosphoesterase) (**Table 2**, **Figure 3**). In addition, in vB_EcoS-B2 genome no statistically significant BLASTP similarity was identified in genes encoding integrase, recombinase, repressor, and excisionase (markers of temperate bacteriophages) (Carrias et al., 2011). Consequently, the vB_EcoS-B2 phage should be considered as a virulent bacteriophage. Genome analysis also suggests that the phage vB_EcoS-B2 does not encode genes associated with toxins or other virulence factors. Virulent characteristics and no possible pathogen factors make it feasible to be a potential candidate for therapeutic application.

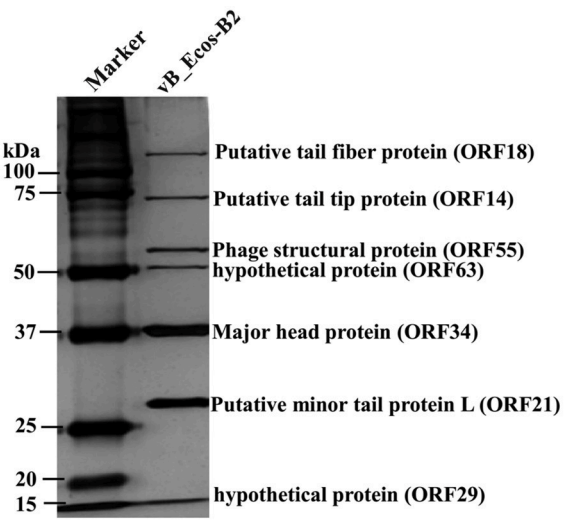

FIGURE 4 | vB_EcoS-B2 virion structural proteins. The purified vB_EcoS-B2 particles were denatured and separated by SDS-PAGE and stained with silver. The positions of seven bands corresponding to different structure proteins are indicated on the right. Molecular mass markers are shown on the left.

TABLE 3 | Mass spectrometry data for vB_EcoS-B2.

ORFs	Predicted molecular function	Peptides	Unique peptides	Unique sequence coverage [%]	MW(da)
ORF23	Putative tail length tape-measure protein 1	70	70	77.4	93307.2
ORF18	Putative tail fiber protein	52	52	59.2	125892.9
ORF34	Major head protein	40	40	86.1	38395.4
ORF14	Putative tail tip protein	36	36	56.7	65194.4
ORF41	Phage structural protein	31	31	72.7	55192.3
ORF28	Putative major tail protein	25	25	83.9	25755.3
ORF40	Head morphogenesis protein	24	24	61	40988.6
ORF21	Putative minor tail protein L	18	18	63.4	28806.3
ORF44	Putative phosphoesterase	13	13	36.6	42737.4
ORF35	Hypothetical protein	13	13	56.2	25384.1
ORF22	Putative minor tail protein	11	11	51.5	21696.3
ORF30	Putative tail protein	9	9	43.1	21918
ORF33	Hypothetical protein	7	7	54.2	18924.7
ORF31	Putative structural protein	7	7	58.7	13053.8
ORF46	Hypothetical protein	5	5	94.5	5603.2
ORF16	Hypothetical protein	5	5	38.6	23211.6
ORF63	Hypothetical protein	4	4	15.4	52319.8
ORF29	Hypothetical protein	3	3	41.1	15087.1
ORF1	DNA polymerase I	3	3	8.5	86167.7
ORF32	Hypothetical protein	2	2	22.3	3990.7
ORF19	Putative tail assembly protein I	2	2	21	21245.4

Particles proteins detected by MS are listed with their predicted functions and molecular mass. Molecular mass was calculated from the amino acid sequence of each gene. Number of identified peptides and unique peptides in each protein and the corresponding unique peptide sequence coverage are also indicated.

Structural Proteins of vB_EcoS-B2

In order to analyze the structural proteins of vB_EcoS-B2, purified phage particles were denatured by boiling with sample buffer, and then separated by SDS-PAGE. At least seven distinct protein bands, with molecular weights ranging from 28.8 to 125.9 kDa, were visualized in the SDS-PAGE gel (**Figure 4**). Five bands were identified as phage structural proteins (Major head protein, Putative minor tail protein L, Phage structural protein, Putative tail tip protein, and Putative tail fiber protein), and two bands were identified as hypothetical proteins (**Figure 4**). To determine every structural protein, phage particle proteins were identified by mass spectrometry, and results were listed in **Table 3**. Twenty-one proteins were identified in mass spectrometry, including proteins corresponding to all seven distinct bands on SDS-PAGE gel (**Table 3**, **Figure 4**). Twelve out of 13 known structural proteins were identified by mass spectrometry, and some hypothetical proteins (ORF16, ORF29, ORF32, ORF33, ORF35, ORF46, ORF63) were also identified, which may be some unknown structural proteins. Interestingly, DNA polymerase I and putative phosphoesterase were determined in our phage particles. DNA polymerase I could fill DNA gaps during DNA repair, recombination, and replication (Andraos et al., 2004). DNA polymerase I and putative phosphoesterase may play important roles in the phage early infection processes, which will be our interests in our further studies.

Comparative Genome Analysis

Based on the result of BLAST analyses, the genome sequence of vB_EcoS-B2 displays significant similarity (coverage 87–95%, identity 90–94%) to 14 phages isolated from different regions around the world, suggesting that the complex evolutionary relationships exist among these phages. The corresponding genome sequences of these phages were aligned, concatenated, and a phylogenetic tree was built using the maximum likelihood method (**Figure 5**). Phylogenetic tree of these phages has two main branches. Phylogenetic tree analysis showed that vB_EcoS-B2 is a novel bacteriophage that is closely related to phages JL1, YD-2008.s, Sloth, Envy, slur05, and lust, and relatively distant to phages SSL-2009a, HK578, EK99P-1, Sodalis phage SO-1, Shigella phage EP23, slur06, Gluttony, and Pride (**Figure 5**). The results of the comparative genomic analyses extend our understanding of the evolution and relationship between vB_EcoS-B2 and its bacteriophage relatives.

Most of the proteins from vB_EcoS-B2 and 14 relative phages are homology with each other. But some blank regions could be observed though genome comparison of these phages (**Figure 6**). The phage tail tip protein encoded by ORF14 shows a greater divergence between these phages (43–99% coverage and 68–85% identity) (**Figure 6**). The ORF14 is relatively similar to tail fiber protein of phage Envy (99% coverage and 70% identity). The tail proteins are thought to be involved in host recognition, and confer the phage host range specificity (Hashemolhosseini et al., 1994). The small differences in tail fiber proteins are often associated with significant differences in host ranges and other biological properties (Yosef et al., 2017). This putative tail tip protein of vB_EcoS-B2 is relatively different from tail tip/fiber proteins of other phages, which may make the

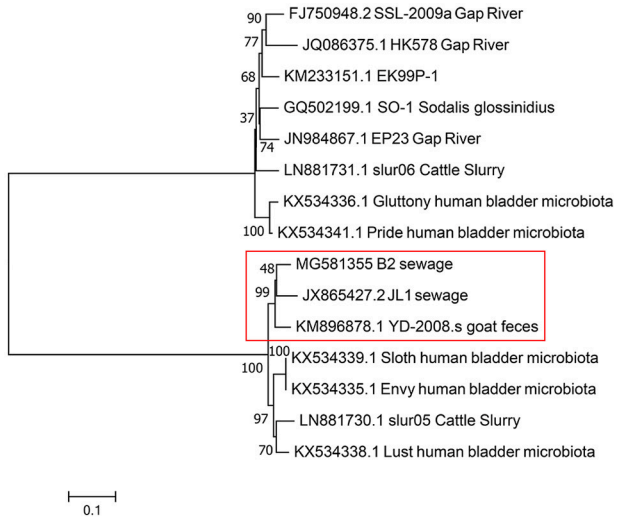

FIGURE 5 | Phylogenetic tree based on whole genome sequence comparisons of selected phages. Whole genome sequence comparison was compared using the ClustalW program, and the phylogenetic tree was generated using the neighbor-joining method with 1,000 bootstrap replicates. vB_EcoS-B2 in brief is"B2"in this phylogenetic trees.

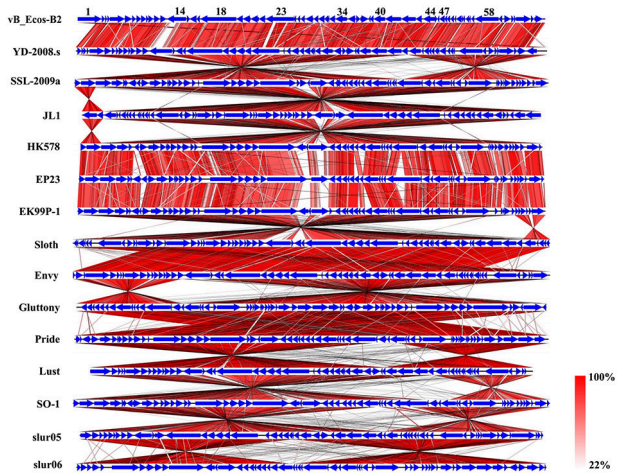

FIGURE 6 | Schematic genomic alignment of the phage vB_EcoS-B2 with other 14 homologous phages. Homologous ORFs or genes are present in blue, and the percentages of amino acid identities are shown with different colors.

host range of phage vB_EcoS-B2 different from other relative phages.

Multiple alignment of the vB_EcoS-B2 and 14 relative phages showed that most of regions are highly homologous at protein levels, but they exhibit different gene arrangement with each other (**Figure 6**). For example, DNA polymerase I and DNA helicase regions of vB_EcoS-B2 were reversely matched with phage SSL-2009a. The tail protein region of phage vB_EcoS-B2 was forwardly matched with the same regions of Enterobacteria phage SSL-2009a. But head morphogenesis protein, terminase large subunit, and lysozyme regions, were back to reversely matched with phage SSL-2009a (**Figure 6**). Pan et al. found that the gene arrangement and genome structure of phage JL1 are different from those of the other four phages, such as SSL-2009a (Pan et al., 2013). EP23 and SSL-2009a had high similarities in amino acid sequences (95.5% on average). But their gene orders were not conserved with each other (Chang and Kim, 2011). A lot of gene inversions and rearrangement were observed between these phages, such as YD-2008s and SSL-2009a, JL1 and HK578, EK99P-1 and sloth, Envy and Gluttony, Pride and lust, SO-1and slur05 (**Figure 6**). Gene recombination seems to have been occurred in high frequency in these phages (**Figure 6**). Our results convinced that topological rearrangement of genomes has lower barriers than changes of amino acid sequences during evolution of phage vB_EcoS-B2 with its phage relatives (Li et al., 2010; Chang and Kim, 2011; Pan et al., 2013). Gene order has major effects on growth rate for T7 phage even when genome entry is normal, suggesting that the consequence of altered gene order probably extends to fitness measures that are not tied to a short generation time (Cecchini et al., 2013). vB_EcoS-B2 and its relatives may be co-evoluted with their host through rearrangement of their genes under different selection pressures. Tailed bacteriophages constitute the most abundant and diverse group of dsDNA viruses, in which evolution is very complicated (Iranzo et al., 2016). Several results illustrated that phages may undergo genetic exchange by horizontal gene transfer from a large shared pool, and that horizontal gene transfer between phages is a component of evolution (Håggard-Ljungquist et al., 1992; Hendrix et al., 1999; Casjens, 2008; Dekel-Bird et al., 2013; Chen et al., 2016). In our study, both horizontal exchange and vertical gene order rearrangement may affect the organization of bacteriophage genomes and blur phylogenetic reconstructions in vB_EcoS-B2 and its relative phages.

In conclusion, we have isolated and characterized a new lytic phage vB_EcoS-B2 which belongs to family *Siphoviridae*, with lytic activity against several MDR *E. coli* isolates. vB_EcoS-B2, like JL1 and EP23, can be assigned into virulent phages because of the presence of lysis genes such as lysozyme, putative holin-like class I protein and putative holin-like class II protein, and no similarities to lysogenic genes coding integrase, repressor, and anti-repressor proteins. The genome sequence analysis of vB_EcoS-B2 provided no evidence of genes related to potential virulence factors or antibiotic resistance genes. In addition, the identification of the 21 structural proteins confirmed that the vB_EcoS-B2 is a new virulent bacteriophage of *E. coli*. It also demonstrated a high degree of identity of vB_EcoS-B2 with ORFs from some other phages. Genome and proteome analysis confirmed the lytic nature of the vB_EcoS-B2. Comparative genome analysis sheds light on the mechanisms of evolutionary changes of these phage genomes. Our results indicate that gene arrangement and genome structure of phage vB_EcoS-B2 is different from that of its phage relatives. The vB_EcoS-B2 genome encodes several putative proteins, including enzymes with antimicrobial activity for the biocontrol of pathogenic bacteria or involved in the phage infection process. The phage

genome sequence data also provide useful basic information for further research on the interaction between phages and their hosts.

AUTHOR CONTRIBUTIONS

YX, XY, YG, and XL conceived, designed and coordinated the study. YX, XY, and YG carried out the experimentation. YX, XY, YG, and XL analyzed the results. GL, XH, YX, XY, YG, and XL contributed reagents, materials, analysis tools. All authors wrote, read, and approved the final manuscript.

FUNDING

This work was supported by the National Natural Science Foundation of China (81501797) and the Natural Science Foundation of Jiangsu Province (BK20151558).

SUPPLEMENTARY MATERIAL

The Supplementary Material for this article can be found online at: https://www.frontiersin.org/articles/10.3389/fmicb.2018.00793/full#supplementary-material

REFERENCES

Aggarwal, G., and Ramaswamy, R. (2002). Ab initio gene identification: prokaryote genome annotation with GeneScan and GLIMMER. *J. Biosci*. 27, 7–14. doi: 10.1007/BF02703679

Amarillas, L., Rubí-Rangel, L., Chaidez, C., González-Robles, A., Lightbourn-Rojas, L., and León-Félix, J. (2017). Isolation and characterization of phiLLS, a novel phage with potential biocontrol agent against multidrug-resistant *Escherichia coli*. *Front. Microbiol*. 8:1355. doi: 10.3389/fmicb.2017.01355

Andraos, N., Tabor, S., and Richardson, C. C. (2004). The highly processive DNA polymerase of bacteriophage T5. Role of the unique N and C termini. *J. Biol. Chem*. 279, 50609–50618. doi: 10.1074/jbc.M408428200

Birgy, A., Doit, C., Mariani-Kurkdjian, P., Genel, N., Faye, A., Arlet, G., et al. (2011). Early detection of colonization by VIM-1-producing *Klebsiella pneumoniae* and NDM-1-producing *Escherichia coli* in two children returning to France. *J. Clin. Microbiol*. 49, 3085–3087. doi: 10.1128/JCM.00540-11

Bolocan, A. S., Callanan, J., Forde, A., Ross, P., and Hill, C. (2016). Phage therapy targeting *Escherichia coli*-a story with no end? *FEMS. Microbiol. Lett*. 363:fnw256. doi: 10.1093/femsle/fnw256

Bourdin, G., Navarro, A., Sarker, S. A., Pittet, A. C., Qadri, F., Sultana, S., et al. (2014). Coverage of diarrhoea-associated *Escherichia coli* isolates from different origins with two types of phage cocktails. *Microb. Biotechnol*. 7, 165–176. doi: 10.1111/1751-7915.12113

Cabal, A., García-Castillo, M., Cantón, R., Gortázar, C., Domínguez, L., and Álvarez, J. (2016). Prevalence of *Escherichia coli* virulence genes in patients with diarrhea and a subpopulation of healthy volunteers in Madrid, Spain. *Front. Microbiol*. 7:641. doi: 10.3389/fmicb.2016.00641

Carrias, A., Welch, T. J., Waldbieser, G. C., Mead, D. A., Terhune, J. S., and Liles, M. R. (2011). Comparative genomic analysis of bacteriophages specific to the channel catfish pathogen *Edwardsiella ictaluri*. *Virol. J*. 8:6. doi: 10.1186/1743-422X-8-6

Casjens, S. R. (2008). Diversity among the tailed-bacteriophages that infect the Enterobacteriaceae. *Res. Microbiol*. 159, 340–348. doi: 10.1016/j.resmic.2008.04.005

Castanheira, M., Mendes, R. E., and Sader, H. S. (2017). Low frequency of ceftazidime-avibactam resistance among Enterobacteriaceae isolates carrying blaKPC collected in U.S. hospitals from 2012 to 2015. *Antimicrob. Agents. Chemother*. 61:e02369-16. doi: 10.1128/AAC.02369-16

Cecchini, N., Schmerer, M., Molineux, I. J. Springman, R., and Bull, J. J. (2013). Evolutionarily stable attenuation by genome rearrangement in a virus. *G3* 3, 1389–1397. doi: 10.1534/g3.113.006403

Chang, H. W., and Kim, K. H. (2011). Comparative genomic analysis of bacteriophage EP23 infecting *Shigella sonnei* and *Escherichia coli*. *J. Microbiol*. 49, 927–934. doi: 10.1007/s12275-011-1577-0

Chen, M., Xu, J., Yao, H., Lu, C., and Zhang, W. (2016). Isolation, genome sequencing and functional analysis of two T7-like coliphages of avian pathogenic *Escherichia coli*. *Gene* 582, 47–58. doi: 10.1016/j.gene.2016.01.049

Dalmasso, M., Strain, R., Neve, H., Franz, C. M., Cousin, F. J., Ross, R. P., et al. (2016). Three new *Escherichia coli* phages from the human gut show promising potential for phage therapy. *PLoS ONE* 11:e0156773. doi: 10.1371/journal.pone.0156773

Dekel-Bird, N. P., Avrani, S., Sabehi, G., Pekarsky, I., Marston, M. F., Kirzner, S., et al. (2013). Diversity and evolutionary relationships of T7-like podoviruses infecting marine cyanobacteria. *Environ. Microbiol*. 15, 1476–1491. doi: 10.1111/1462-2920.12103

Dufour, N., Clermont, O., La Combe, B., Messika, J., Dion, S., Khanna, V., et al. (2016). Bacteriophage LM33 P1, a fast-acting weapon against the pandemic ST131- O25b:H4 *Escherichia coli* clonal complex. *J. Antimicrob. Chemother*. 71, 3072–3080. doi: 10.1093/jac/dkw253

Dufour, N., Debarbieux, L., Fromentin, M., and Ricard, J. D. (2015). Treatment of highly virulent extraintestinal pathogenic *Escherichia coli* pneumonia with bacteriophages. *Crit. Care Med*. 43, e190–e198. doi: 10.1097/CCM.0000000000000968

Fitzgerald-Hughes, D., Bolkvadze, D., Balarjishvili, N., Leshkasheli, L., Ryan, M., Burke, L., et al. (2014). Susceptibility of extended-spectrum-beta-lactamase-producing *Escherichia coli* to commercially available and laboratory-isolated bacteriophages. *J. Antimicrob. Chemother*. 69, 1148–1150. doi: 10.1093/jac/dkt453

Håggard-Ljungquist, E., Halling, C., and Calendar, R. (1992). DNA sequences of the tail fiber genes of bacteriophage P2: evidence for horizontal transfer of tail fiber genes among unrelated bacteriophages. *J. Bacteriol*. 174, 1462–1477. doi: 10.1128/jb.174.5.1462-1477.1992

Haq, I. U., Chaudhry, W. N., Akhtar, M. N., Andleeb, S., and Qadri, I. (2012). Bacteriophages and their implications on future biotechnology: a review. *Virol. J*. 9:9. doi: 10.1186/1743-422X-9-9

Hashemolhosseini, S., Montag, D., Krämer, L., and Henning, U. (1994). Determinants of receptor specificity of coliphages of the T4 family. A chaperone alters the host range. *J. Mol. Biol*. 241, 524–533. doi: 10.1006/jmbi.1994.1529

Hendrix, R. W., Smith, M. C., Burns, R. N., Ford, M. E., and Hatfull, G. F. (1999). Evolutionary relationships among diverse bacteriophages and prophages: all the world's a phage. *Proc. Natl. Acad. Sci. U.S.A*. 96, 2192–2127. doi: 10.1073/pnas.96.5.2192

Heo, Y. J., Lee, Y. R., Jung, H. H., Lee, J., Ko, G., and Cho, Y. H. (2009). Antibacterial efficacy of phages against *Pseudomonas aeruginosa* infections in mice and *Drosophila melanogaster*. *Antimicrob. Agents. Chemother*. 53, 2469–2474. doi: 10.1128/AAC.01646-08

Iranzo, J., Krupovic, M., and Koonin, E. V. (2016). The double-stranded DNA virosphere as a modular hierarchical network of gene sharing. *MBio* 7:e00978-16. doi: 10.1128/mBio.00978-16.

Jamalludeen, N., She, Y. M., Lingohr, E. J., and Griffiths, M. (2009). Isolation and characterization of virulent bacteriophages against *Escherichia coli* serogroups O1, O2, and O78. *Poult. Sci*. 88, 1694–1702. doi: 10.3382/ps.2009-00033

Kutateladze, M., and Adamia, R. (2010). Bacteriophages as potential new therapeutics to replace or supplement antibiotics. *Trends Biotechnol*. 28, 591–595. doi: 10.1016/j.tibtech.2010.08.001

Laanto, E., Hoikkala, V., Ravantti, J., and Sundberg, L. R. (2017). Long-term genomic coevolution of host-parasite interaction in the natural environment. *Nat. Commun*. 8:111. doi: 10.1038/s41467-017-00158-7

Lepape, A., and Monnet, D. L. (2009). Experience of European intensive care physicians with infections due to antibiotic-resistant bacteria. *Euro Surveill*. 14, 1–3. doi: 10.2807/ese.14.45.19393-en

Li, S., Liu, L., Zhu, J., Zou, L., Li, M., Cong, Y., et al. (2010). Characterization and genome sequencing of a novel coliphage isolated from engineered *Escherichia coli Intervirology* 53, 211–220. doi: 10.1159/000299063

Merabishvili, M., DeVos, D., Verbeken, G., Kropinski, A. M., Vandenheuvel, D., Lavigne, R., et al. (2012). Selection and characterization of a candidate therapeutic bacteriophage that lyses the *Escherichiacoli* O104:H4 strain from the 2011 outbreak in Germany. *PLoS ONE* 7:e52709. doi: 10.1371/journal.pone.0052709

Nilsson, A. S. (2014). Phage therapy–constraints and possibilities. *Ups. J. Med. Sci.* 119, 192–198. doi: 10.3109/03009734.2014.902878

Pan, F., Wu, H., Liu, J., Ai, Y., Meng, X., Meng, R., et al. (2013). Complete genome sequence of *Escherichia coli* O157:H7 lytic phage JL1. *Arch. Virol.* 158, 429–432. doi: 10.1007/s00705-013-1727-2

Peña, C., Gudi ol, C., Tubau, F., Saballs, M., Pujol, M., Dominguez, M. A., et al. (2006). Risk-factors for acquisition of extended-spectrum beta-lactamase-producing *Escherichia coli* among hospitalised patients. *Clin. Microbiol. Infect.* 12, 279–284. doi: 10.1111/j.1469-0691.2005.01358.x

Postic, B., and Finland, M. (1961). Observations on bacteriophage typing of *Pseudomonas aeruginosa*. *J. Clin. Invest*. 40, 2064–2075. doi: 10.1172/JCI104432

Pouillot, F., Chomton, M., Blois, H., Courroux, C., Noelig, J., Bidet, P., et al. (2012). Efficacy of bacteriophage therapy in experimental sepsis and meningitis caused by a clone O25b:H4-ST131 *Escherichia coli* strain producing CTX-M-15. *Antimicrob. Agents Chemother*. 56, 3568–3575. doi: 10.1128/AAC.06330-11

Regeimbal, J. M., Jacobs, A. C., Corey, B. W., Henry, M. S., Thompson, M. G., Pavlicek, R. L., et al. (2016). Personalized therapeutic cocktail of wild environmental phages rescues mice from Acinetobacter baumannii wound infections. *Antimicrob. Agents Chemother*. 60, 5806–5816. doi: 10.1128/AAC.02877-15

Schooley, R. T., Biswas, B., Gill, J. J., Hernandez-Morales, A., Lancaster, J., Lessor, L., et al. (2017). Development and use of personalized bacteriophage-based therapeutic cocktails to treat a patient with a disseminated *resistant Acinetobacter baumannii* infection. *Antimicrob. Agents Chemother*. 61:e00954–17. doi: 10.1128/AAC.00954-17

Schmerer, M., Molineux, I. J., Bull, and J. J.. (2014). Synergy as a rationale for phage therapy using phage cocktails. *PeerJ* 2:e590. doi: 10.7717/peerj.590

Shevchenko, A., Wilm, M., Vorm, O., and Mann, M. (1996). Mass spectrometric sequencing of proteins from silver-stained polyacrylamide gels. *Anal. Chem*. 68, 850–858. doi: 10.1021/ac950914h

Snyder, A. B., Perry, J. J., and Yousef, A. E. (2016). Developing and optimizing bacteriophage treatment to control enterohemorrhagic *Escherichia coli* on fresh produce. *Int. J. Food Microbiol*. 236, 90–97. doi: 10.1016/j.ijfoodmicro.2016.07.023

Srinivasiah, S., Bhavsar, J., Thapar, K., Liles, M., Schoenfeld, T., and Wommac, K. E. (2008). Phages across the biosphere: contrasts of viruses in soil and aquatic environments. *Res. Microbiol*. 159, 349–357. doi: 10.1016/j.resmic.2008.04.010

Sullivan, M. J., Petty, N. K., and Beatson, S. A. (2011). Easyfig: a genome comparison visualizer. *Bioinformatics*27, 1009–1010. doi: 10.1093/bioinformatics/btr039

Sybesma, W., Zbinden, R., Chanishvili, N., Kutateladze, M., Chkhotua, A., Ujmajuridze, A., et al. (2016). Bacteriophages as potential treatment for urinary tract infections. *Front. Microbiol*. 7:465. doi: 10.3389/fmicb.2016.00465

Williamson, K. E., Fuhrmann, J. J., Wommack, K. E., and Radosevich, M. (2017). Viruses in soil ecosystems: an unknown quantity within an unexplored territory. *Annu. Rev. Virol*. 4, 201–219. doi: 10.1146/annurev-virology-101416-041639

Yang, M., Du, C., Gong, P., Xia, F., Sun, C., Feng, X., et al. (2015). Therapeutic effect of the YH6 phage in a murine hemorrhagic pneumonia model. *Res. Microbiol*. 166, 633–643. doi: 10.1016/j.resmic.2015.07.008

Yosef, I., Goren, M. G., Globus, R., Molshanski-Mor, S., and Qimron, U. (2017). Extending the host range of bacteriophage particles for DNA transduction. *Mol. Cell* 66, 721–728. doi: 10.1016/j.molcel.2017.04.025

Conflict of Interest Statement: The authors declare that the research was conducted in the absence of any commercial or financial relationships that could be construed as a potential conflict of interest.

frontiers in Microbiology

ORIGINAL RESEARCH
published: 02 May 2018
doi: 10.3389/fmicb.2018.00875

Bacteriophage Infectivity Against *Pseudomonas aeruginosa* in Saline Conditions

Giantommaso Scarascia[1], *Scott A. Yap*[1], *Anna H. Kaksonen*[2] *and Pei-Ying Hong*[1]*

[1] *Biological and Environmental Science & Engineering Division, Water Desalination and Reuse Center, King Abdullah University of Science and Technology, Thuwal, Saudi Arabia,* [2] *Land and Water, Commonwealth Scientific and Industrial Research Organization, Canberra, ACT, Australia*

Pseudomonas aeruginosa is a ubiquitous member of marine biofilm, and reduces thiosulfate to produce toxic hydrogen sulfide gas. In this study, lytic bacteriophages were isolated and applied to inhibit the growth of *P. aeruginosa* in planktonic mode at different temperature, pH, and salinity. Bacteriophages showed optimal infectivity at a multiplicity of infection of 10 in saline conditions, and demonstrated lytic abilities over all tested temperature (25, 30, 37, and 45°C) and pH 6–9. Planktonic *P. aeruginosa* exhibited significantly longer lag phase and lower specific growth rates upon exposure to bacteriophages. Bacteriophages were subsequently applied to *P. aeruginosa*-enriched biofilm and were determined to lower the relative abundance of *Pseudomonas*-related taxa from 0.17 to 5.58% in controls to 0.01–0.61% in treated microbial communities. The relative abundance of *Alphaproteobacteria*, *Pseudoalteromonas,* and *Planococcaceae* decreased, possibly due to the phage-induced disruption of the biofilm matrix. Lastly, when applied to mitigate biofouling of ultrafiltration membranes, bacteriophages were determined to reduce the transmembrane pressure increase by 18% when utilized alone, and by 49% when used in combination with citric acid. The combined treatment was more effective compared with the citric acid treatment alone, which reported ca. 30% transmembrane pressure reduction. Collectively, the findings demonstrated that bacteriophages can be used as a biocidal agent to mitigate undesirable *P. aeruginosa*-associated problems in seawater applications.

Keywords: bacteriophage, green biocides, biofilm removal, planktonic cells, ultrafiltration membrane

OPEN ACCESS

Edited by:
Robert Czajkowski,
University of Gdansk, Poland

Reviewed by:
Antonio Mas,
Universidad de Castilla-La Mancha, Spain
Joaquin Martinez Martinez,
Bigelow Laboratory for Ocean Sciences, United States

***Correspondence:**
Pei-Ying Hong
peiying.hong@kaust.edu.sa

Specialty section:
This article was submitted to Virology, a section of the journal Frontiers in Microbiology

Received: *04 February 2018*
Accepted: *16 April 2018*
Published: *02 May 2018*

Citation:
Scarascia G, Yap SA, Kaksonen AH and Hong P-Y (2018) Bacteriophage Infectivity Against Pseudomonas aeruginosa in Saline Conditions. Front. Microbiol. 9:875. doi: 10.3389/fmicb.2018.00875

INTRODUCTION

Seawater reverse osmosis (SWRO) desalination has had a great impact on the production of drinking water in the past 40 years (Goosen et al., 2005), and is particularly relied upon by sea-bordered countries that face water scarcity issues (Peñate and García-Rodríguez, 2012). Similar to all membrane-based technologies, SWRO is affected by biofouling. Biofilm formation on membrane detrimentally lowers the flux and salt rejection capacity. In order to maintain the desired desalination performance, plant operators usually apply higher transmembrane pressure which in turn increases energy consumption and economic costs (Fritzmann et al., 2007; Matin et al., 2011).

Bacteria such as *Pseudomonas, Bacillus, Mycobacterium, Acinetobacter* are often detected on fouled RO membranes (Matin et al., 2011). In particular, *Pseudomonas* spp. and *Desulfovibrio* spp. were identified on fouled ultrafiltration (UF) and RO membranes sampled from a SWRO pilot

plant located in the Arabian Gulf (Hong et al., 2016). *Pseudomonas* spp. create an optimal niche for *Desulfovibrio* spp. and other sulfate-reducing bacteria (SRB) by depleting oxygen. In addition, SRB and *Pseudomonas aeruginosa* are able to reduce sulfate and thiosulfate, respectively, to produce hydrogen sulfide, a corrosive and toxic gas (Hong et al., 2016). The presence of *Pseudomonas* spp. and SRB in SWRO are favored by the high sulfate concentration prevalent in seawater. In addition, sodium metabisulfite applied to neutralize chlorine within the SWRO (Hong et al., 2016) further provide a source of electron acceptors for these bacterial populations.

To reduce both inorganic and organic foulants on membranes, oxidizing agents such as chlorine, permanganate, and ozone (Fritzmann et al., 2007; Gao et al., 2011) are used in large concentrations. However, the addition of these chemicals in seawater can result in the formation of carcinogenic and toxic disinfection byproducts that can result in public health concerns (Le Roux et al., 2015; Sanawar et al., 2017). Alternatively, regular cleaning of the membrane would have to be performed with acid cleaning (Greenlee et al., 2009). Citric acid cleaning is often used in the pretreatment stage of SWRO to chelate inorganic minerals and disrupt the stability of biofilm matrix attached on the pretreatment UF membranes (Lee et al., 2001; Porcelli and Judd, 2010). Despite their common usage, these biocidal agents have limited penetration through a biofilm matrix and are less effective against biofilm-associated bacteria compared to its effect on planktonic cells (Matin et al., 2011). Moreover, some chemicals e.g., chlorine, can detrimentally impact RO membrane integrity.

To address the concerns arising from conventional biocides and cleaning agents, this study evaluates the use of lytic bacteriophages (i.e., viruses that infect bacteria at high host specificity) to inhibit the growth of planktonic *P. aeruginosa* in saline conditions. In addition, bacteriophages can also induce the release of depolymerases that degrade extracellular polymeric substances (EPS) and hence disrupt biofilm matrix (Harper et al., 2014). It is therefore hypothesized that bacteriophage would be effective to disrupt *P. aeruginosa*-associated biofilms formed on seawater filtration membranes. Although bacteriophage treatment against *P. aeruginosa* biofilm has been performed in therapeutic treatments (McVay et al., 2007; Fu et al., 2010; Alemayehu et al., 2012; Olszak et al., 2015), and as antifouling agents in water and wastewater membrane filtration systems (Zhang et al., 2013; Bhattacharjee et al., 2015), the conditions at which the bacteriophages were applied in those studies differ from those experienced in a SWRO system. Understanding how environmental conditions can impact bacteriophage infectivity is crucial for an effective application of bacteriophages in SWRO systems, where the conditions vary between high pH (i.e., the usual pH of seawater) to low pH (i.e., when citric acid cleaning is performed), high salinity (i.e., in raw seawater) to low salinity (i.e., after seawater is desalinated), and from low (i.e., in the raw seawater) to high temperatures (i.e., seawater retained within the desalination unit).

In this study, the impact of various parameters, namely multiplicity of infection (MOI), pH, salinity and temperature, on the activity of seven lytic bacteriophages against planktonic *P. aeruginosa* cells was analyzed. Three bacteriophages were further applied against a *P. aeruginosa*-enriched seawater biofilm at various pH values and temperatures. Finally, a cocktail of the three bacteriophages was applied alone and in combination with citric acid cleaning to cross-flow seawater ultrafiltration setup, and the membrane modules were assessed for their transmembrane pressure and biofilm cell counts.

MATERIALS AND METHODS

Bacteriophage Isolation

Bacteriophages were isolated from an influent collected from a wastewater treatment plant located in KAUST. A 50 mL aliquot of the influent was centrifuged at 8,500 *g* for 20 min and thereafter supernatant was filtered through 0.22 μm cellulose acetate syringe filter (VWR, Radnor, PA) to remove bacterial cells. The filtrate was mixed with 50 mL Lennox broth (LB) supplemented with 35 g/L NaCl and 4 mM Ca^{2+}, and 50 mL of exponentially growing *P. aeruginosa* strain DSM1117. The mixed culture was incubated for 24 h at 37°C. Thereafter, 1% v/v chloroform was added to lyse the bacterial cells, and incubated for 2 h at room temperature with constant agitation at 100 rpm. The culture was centrifuged at 8,500 *g* for 30 min at 4°C and the supernatant was filtered through 0.22 μm syringe filter to remove bacterial cells. Several dilutions, ranging from 10^{-3} to 10^{-5} fold, were performed in sodium magnesium (SM) buffer (5.8 g/L NaCl, 0.975 g/L $MgSO_4$, 50 ml/L 50 mM Tris-Cl 7.5 pH) and 10 μL of each diluted sample was mixed with 100 μL of *P. aeruginosa* culture to detect the presence of plaques using the double layer plate method (Adams, 1959). Seven plaques were isolated with sterile inoculating loops, transferred to SM buffer and filtered through 0.22 μm syringe filter to remove bacterial cells. The bacteriophages from the seven plaques were named P1 through P7 and propagated 10 more times using the above mentioned procedure.

Infection of Planktonic Cultures With Bacteriophages at Various Conditions

All bacteriophages were tested for their infectivity against other bacterial species using the soft agar plaque assay method. All the bacteria used in this study are listed in **Table 1**. After verifying their host specificity, bacteriophage activity against *P. aeruginosa* was analyzed at various multiplicity of infection (MOI) values, namely 0.1, 1, and 10. MOI represents the ratio between the number of bacteriophage particles determine as phage forming units (PFU/mL) and bacterial cells determined as colony forming units (CFU/mL) in a mixture of 1:1 LB broth and SM buffer, pH 7. MOI was calculated for each bacteriophage based on the number of plaques formed on agar (**Figure S1**). For each MOI, one control was prepared without bacteriophages. The treated cultures and controls were incubated at 37°C with constant shaking at 200 rpm for 24 h. Growth curves of *P. aeruginosa* were obtained with and without the presence of the seven phages. The best MOI value in terms of bacterial inhibition time (in h) and specific growth rate reduction (h^{-1}) compared with the control was selected for evaluating the impact of other parameters. Subsequently, bacteriophage infectivity against *P. aeruginosa*

TABLE 1 | Name and origin of the bacteria used in this study.

Bacteria	Origin
Pseudomonas aeruginosa DSM1117	Blood culture
Pseudomonas stutzeri CE9	Chlorinated wastewater effluent (Jeddah, Saudi Arabia; Al-Jassim et al., 2015)
Pseudomonas otitidis CP2	
Pseudomonas resinovorans CE5	
Pseudomonas pseudoalcaligenes CE3	
Aeromonas hydrophila subsp. *anaerogenes* CP3	
Aeromonas veronii CP10	

cultures was evaluated at different temperatures, pH, and salinity, with the same procedure described above at a constant MOI of 10. All experiments were performed in triplicates.

Infection of Biofilm With Bacteriophages at Various Conditions

To examine the effect of bacteriophages on the biofilm structure at various temperatures (25, 30, 37, and 45°C) and pH values (5, 6, 7, 8), 28 drip flow reactors (BioSurface Technologies Corp., Bozeman, MT) were assembled. Twenty eight cellulose acetate ultrafiltration membranes (Sterilitech Corporation, Kent, WA), each with surface area of 11.25 cm^2, were secured on glass coupons and placed into the drip flow reactors to establish biofilm on the membranes. Reactors were covered with aluminum foil to avoid light exposure. Seawater from Red Sea was fed into each reactor at a continuous rate of 5 mL per minute. The feed was replaced with fresh seawater every 3 d. After 4 weeks, the feed solution was replaced with 5 L of *P. aeruginosa*-enriched seawater. Briefly, *P. aeruginosa* was cultivated overnight on *Pseudomonas* isolation agar (Sigma-Aldrich, St Louis, MO); single colonies were transferred into multiple tubes with 20 mL LB broth and grown at 37°C with constant shaking (200 rpm) to reach OD_{600} of 0.7. After centrifugation at 4,100 *g* for 30 min, bacterial pellet was resuspended in 5 L seawater to achieve a cell density of 3.5×10^7 CFU/mL of *P. aeruginosa*. This feed was also replaced every 3 d.

After 4 weeks, to calculate the starting number of *Pseudomonas* colonies, 4 membranes were removed from the reactor and washed twice in 1× phosphate-buffered saline (PBS) to remove loosely attached biofilm. Membranes were cut into 16 identical pieces and were placed individually into collection tubes containing 2 mL 1× PBS. Attached biofilm was sonicated for 5 min by a Q500 sonicator (Qsonica, Newton, CT, US) at 30% amplitude with 3 s pulsating steps to detach biomass from the membranes. The supernatant was serially diluted for spread plating on *Pseudomonas* isolation agar and incubated at 37°C for 1 d for colony counting. The remaining membranes were removed, rinsed twice in 1× PBS to remove loosely attached biofilm, and aseptically cut into four pieces for a total of 96 identical fragments. Each piece was transferred to an individual 15 mL tube containing LB broth and SM buffer (each in 50% v/v, salinity 3.5%). Bacteriophages P1, P5, and P7 were propagated as described above and were diluted with SM buffer to the adequate number of PFU/mL to attain an MOI value of 10. Each bacteriophage was then used individually to infect attached biofilm on the membrane at four different temperatures (25, 30, 37, and 45°C) and pH values (5, 6, 7, 8) for 10 h at constant shaking of 200 rpm. A control without bacteriophage inoculation was prepared for each temperature and pH condition. After 10 h of phage infection, biofilm was sonicated in 3.5 mL of 1× PBS and analyzed based on procedures as described in sections *P. aeruginosa* Colony and Bacteriophage Plaque Counts on Membranes and RNA Extraction and 16S rRNA Gene Based High-Throughput Sequencing. All experiments were conducted in triplicate.

Pseudomonas aeruginosa Colony and Bacteriophage Plaque Counts on Membranes

A 100 μL aliquot of bacterial suspension was used to evaluate the number of colony forming units (CFU)/cm^2 on *Pseudomonas* isolation agar, while 1 mL was filtered through 0.22 μm syringe filter to assess the number of plaque forming units (PFU)/cm^2 recovered from the different tested conditions.

RNA Extraction and 16S rRNA Gene Based High-Throughput Sequencing

A 2 mL aliquot of the biofilm suspension (as described in section Infection of Biofilm With Bacteriophages at Various Conditions) was utilized for RNA extraction. To avoid RNA degradation, 4 mL of RNAprotect® Cell Reagent (Qiagen, Hilden, Germany) was added to each bacterial suspension immediately after sampling. The mixture was incubated at room temperature for 5 min and then centrifuged for 10 min at 5,400 *g*. After centrifugation, the supernatant was removed and the pellet was stored at −80°C for ∼2 weeks until RNA extraction.

RNA extraction from the biomass pellet was performed using the RNeasy® Midi Kit (Qiagen, Hilden, Germany) following manufacturer's protocol and RNA concentration was measured with the Invitrogen RNA HS Qubit® 2.0 assay kit (Thermo Fisher Scientific, Carlsbad, CA). Extracted RNA was reverse transcribed into first-strand complementary DNA (cDNA) using the Invitrogen SuperScript™ First-Strand Synthesis System (Thermo Fisher Scientific, Carlsbad, CA). The cDNA was then used as template to amplify for 16S rRNA genes with primer pair 515F (5′- Illumina overhang- GTG YCA GCM GCC GCG GTA A-3′) and 907R (5′- Illumina overhang- CCC CGY CAA TTC MTT TRA GT-3′) based on the procedure described earlier (Scarascia et al., 2017). Purified amplicons were submitted to KAUST Genomic Core lab for amplicon sequencing on Illumina MiSeq platform. All high-throughput sequencing files used in this study are deposited in the European Nucleotide Archive (ENA) and are accessible via accession number PRJEB23782.

Biofilm Microbial Community Data Analysis

Amplicon sequences were sorted on a Phred score >30 and primers, adaptors, and index sequences were removed. After removing any sequences longer than 280 nt, sequence chimeras were identified and removed by UCHIME (Edgar et al., 2011). Chimera-free sequences were split and a subset containing

100,000 sequences were further analyzed for each sample. Taxonomical assignment was obtained at 95% classification reliability level with copy number adjustment using the Ribosomal Database Project (RDP) Classifier (Wang et al., 2007). Relative abundance at genus and phylum level was calculated for each sample. Special emphasis was made to determine the relative abundance of *Pseudomonas*-related taxa in the presence of bacteriophages compared to the control. Chimera-removed sequence files were also sorted for unique operational taxonomic units (OTUs) at 97% 16S rRNA gene similarity [27]. Similarity percentages (SIMPER) analysis was performed using Primer-E version 7 to identify OTUs that showed a significant difference in their relative abundance between infected and non-infected biofilm (Clarke, 2015). The OTU identities were checked against the NCBI nucleotide database using the BLASTN algorithm.

Effect of Bacteriophage Treatment on UF Membrane Fouling

A UF filtration system was set up as illustrated in **Figure S2**. Five UF cellulose acetate membranes of pore size 8 kDa (Sterilitech Corporation, Kent, WA) were aseptically cut into dimensions of 10 by 2.5 cm each, soaked in deionized water for 24 h, and then rinsed in 80% ethanol. Sterile membranes were then individually placed inside cassette modules. Subsequently, deionized water was circulated through the modules to reach a stable trans-membrane pressure (TMP_0). The modules were operated in cross-flow mode at room temperature with the concentrate recirculating into the feed tank. A constant flux of 12 $L/m^2/h$ (LMH) was maintained. Artificial seawater (26.29 g/L NaCl, 0.74 g/L KCl, 1.32 g/L $CaCl_2$ dehydrated, 6.09 g/L $MgCl_2{\cdot}7H_2O$, 1.92 g/L $MgSO_4$, pH 7.8) was used as feed solution. Nutrient broth (HiMedia, Mumbai, India) was added to the feed solution to obtain a nutrient concentration of 24 mg/L as described previously (Oh et al., 2017). Feed bottle was inoculated with *P. aeruginosa* culture at a final concentration of 5×10^7 CFU/mL and this feed was replaced every 3 d. Biofilm was established on each membrane for 6 d with a recording of the transmembrane pressure (TMP) every 8 h.

On the 7th day, the filtration system was kept in offline mode for four different cleaning treatments: (i) 5×10^8 PFU/mL phage cocktail application in SM buffer for 6 h followed by deionized water for 3 h, (ii) 0.1 M citric acid treatment alone for 3 h followed by deionized water for 6 h, (iii) 5×10^8 PFU/mL phage cocktail application in SM buffer for 6 h followed by 0.1 M citric acid treatment for 3 h, and (iv) 0.1 M citric acid treatment for 3 h followed by 5×10^8 PFU/mL phage cocktail application in SM buffer for 6 h. One membrane was used as non-treated control where deionized water was applied for the same 9 h duration as that of the treatments. All membranes were flushed for 10 min with deionized water at the end of the treatments, and the TMP monitoring was resumed after 1 h from the treatment. Cleaning cycles were repeated every 3 d for a total of three cycles.

At the end of the third cycle, membranes were removed from the modules and three 2×2 cm pieces were cut from each membrane sheet and placed in 2 mL 1× PBS to enumerate for the *Pseudomonas* colony counts and total cell counts. Cells were stained with SYBR® green (Thermo Fisher Scientific, Waltham, MA, US) and counted by BD Accuri C6 flow cytometer (BD, Bioscience, NJ, US). The cleaning experiment on the filtration membranes was performed in duplicate as run 1 and run 2.

Bacteriophages Morphology and Genome Size Characterization

Pure bacteriophages P1, P5, and P7 in cultures were fixed with 2.5% v/v glutaraldehyde. A 5 μL aliquot of each bacteriophage culture was deposited on carbon-coated copper grids and negatively stained with 1% w/v uranyl acetate (pH 4.5). Samples were washed with sterile water, air-dried, and visualized through transmission electron microscopy (TEM) (Tecnai Spirit TWIN, FEI) operated at 120 kV and equipped with an ORIUS SC1000 camera (Gaitan). Image analysis was carried out using ImageJ Software.

Direct phage plaques DNA was extracted for the three bacteriophages as described previously (Kot et al., 2014). Briefly, plaques were resuspended in DNase I buffer, filtered and treated for 30 min with DNase I; DNase was inactivated by 10 μL of 50 mM EDTA and further treated with Proteinase K (Thermo Scientific, Waltham, USA) before DNA extraction using UltraClean Soil DNA Isolation Kit (MoBio Laboratories, Carlsbad, USA) based on manufacturer's protocol. Bacterial DNA contamination was checked through 16S rRNA gene amplification and all plaque DNA samples showed no amplification for 16S rRNA genes. Extracted DNA was used to assess genome size through pulsed field gel electrophoresis (PFGE). DNA samples were run on 1% w/v agarose gel using the CHEF-DR III system (Bio-Rad, Hercules, CA, USA) (18 h, 6 V cm^{-1}, 14°C, angle 120°, switch time 0.1–1). *Lambda* DNA Ladder (New England, Biolabs, Ipswich, MA, USA) was used as size marker.

Statistical Analysis

One-way ANOVA was performed to evaluate for statistical differences between treatments. Statistical differences were considered significant at 95% confidence level ($p < 0.05$).

RESULTS

Bacteriophage Infectivity Against Planktonic *Pseudomonas aeruginosa*

Plaques were only observed when isolated bacteriophages were infected against *P. aeruginosa* but not against all other tested bacterial hosts (**Table 1**). Infectivity of the seven isolated bacteriophages against *P. aeruginosa* growing in planktonic phase was systematically analyzed at various MOIs, temperatures, pH values, and salinities based on lag phase duration and specific growth rates. Lag phase of non-infected control cultures ranged from 1 to 4 h (**Figures 1A–D**), while specific growth rates ranged from 0.21 to 0.40 h^{-1} (**Table 2**). In contrast, the lag phase duration of the infected bacterial culture was significantly longer compared to the control ($p < 0.0001$). The longer lag phase duration was observed regardless of the bacteriophage applied.

At a MOI of 10, the difference in the lag phase duration between bacteriophage-treated culture and control was the

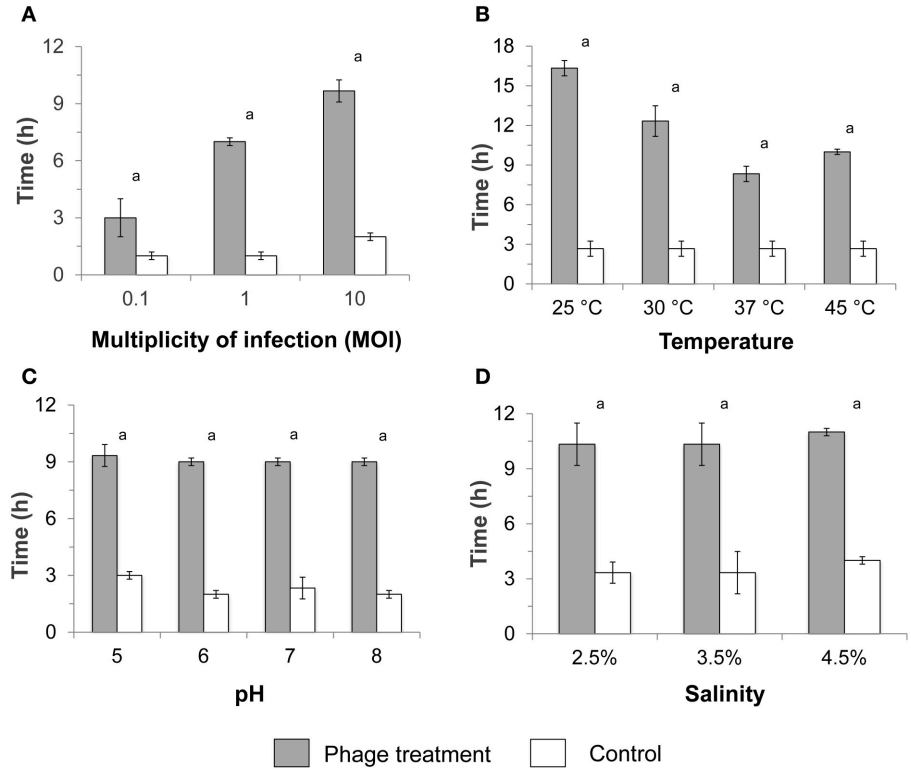

FIGURE 1 | Average duration of the lag phase in infected and non-infected (control) planktonic *Pseudomonas aeruginosa* culture after phage treatment at various **(A)** multiplicities of infection (MOIs), **(B)** temperatures, **(C)** pH values, and **(D)** salinities. The standard test conditions were MOI 10, 37°C, pH 7, and salinity 3.5% when these parameters were not varied. Bars indicate the standard deviation among the three biological replicates. Letter a indicates statistical difference between each treatment and the respective control at $p < 0.0006$.

highest (7.7 h; **Figure 1A**). Bacterial cultures infected with a MOI of 10 also showed significantly lower specific growth rates ($p < 0.0003$) compared with the control (**Table 2**). Infection at MOI 0.1 did not result in any specific growth rate reduction, while a MOI of 1 for phage P4 and P6 was able to reduce specific growth rates (**Table 2**). As such, subsequent experiments to test infectivity at various temperatures, pH values and salinities were conducted at a MOI value of 10.

Lag phase was at least 3 times longer in bacteriophage-treated cultures compared with the control over all temperatures tested ($p < 0.0001$) (MOI 10, pH 7, salinity 3.5%), with particularly longer lag phase at 25 and 30°C (**Figure 1B**). The lag phase was followed by a bacterial growth with lower specific rates compared with the control. Significant reductions in specific growth rates were observed at 25, 30, 37°C ($p < 0.0003$) and 45°C ($p < 0.03$) compared with the respective controls.

A longer lag phase of ca. 9 h was observed in the presence of bacteriophage regardless of the pH at a constant MOI of 10, 37°C, and 3.5% salinity ($p < 0.0001$; **Figure 1C**), compared to the ca. 3 h lag phase for controls. Specific growth rate reduction was also observed when *P. aeruginosa* was infected at various pH values, with a higher decrease at pH 5 and 6 ($p < 0.0005$) compared with infection at pH 7 and 8 ($p < 0.045$; **Table 2**). Similarly, the lag phase duration was significantly prolonged to ca. 10 h ($p < 0.0001$) at various salinities in the presence of bacteriophages (**Figure 1D**). One-way ANOVA test showed significant reduction in specific growth rates in the presence of bacteriophages compared to controls at all tested salinities ($p < 0.007$).

Bacteriophage Infectivity Against *P. aeruginosa*-Enriched Biofilm

Pseudomonas aeruginosa-enriched seawater biofilm was infected separately with three bacteriophages (P1, P5, and P7) at four different temperatures (25, 30, 37, and 45°C) and pH values (5, 6, 7, and 8) for 10 h. At all tested temperatures and upon infection with bacteriophages, the number of viable bacterial cells recovered from *Pseudomonas* isolation agar decreased significantly to an average of 2.8×10^5 CFU/cm^2 ($p < 0.0001$) compared with the initial number (1.37×10^6 CFU/cm^2) recovered from the membranes (**Figure 2A**). In contrast, the controls increased significantly to an average of 6.0×10^6 CFU/cm^2 and the number of bacterial colonies was significantly higher than the initial number ($p < 0.04$). Most of the bacteriophages, specifically P7, showed lower PFU recovery at high temperature of 45°C compared with the other temperatures (**Figure 2B**). Bacteriophage P7, in particular, had significantly lower PFU counts than the other bacteriophages at 45°C. The

TABLE 2 | Average specific bacterial growth rate (h^{-1}) for infected *Pseudomonas aeruginosa* culture in the presence of bacteriophages (P1–P7) and in non-infected culture (C).

Variable	Value	P1	P2	P3	P4	P5	P6	P7	C
MOI[a]	0.1	0.23	0.22	0.22	0.23	0.23	0.22	0.24	0.21
	1	0.28	0.24	0.27	0.23	0.25	0.24	0.25	0.29
	10	0.22	0.21	0.21	0.22	0.21	0.21	0.22	0.34
Temperature (°C)[b]	25	0.25	0.21	0.22	0.22	0.23	0.23	0.23	0.34
	30	0.30	0.28	0.28	0.26	0.27	0.26	0.28	0.38
	37	0.21	0.22	0.20	0.21	0.20	0.19	0.21	0.34
	45	0.20	0.19	0.19	0.20	0.22	0.21	0.22	0.29
pH[c]	5	0.20	0.21	0.18	0.19	0.22	0.23	0.22	0.34
	6	0.17	0.19	0.18	0.20	0.19	0.19	0.18	0.34
	7	0.21	0.26	0.22	0.22	0.23	0.26	0.20	0.33
	8	0.28	0.32	0.27	0.31	0.26	0.29	0.30	0.40
Salinity (%)[d]	2.5	0.25	0.23	0.24	0.23	0.24	0.24	0.24	0.38
	3.5	0.23	0.22	0.22	0.21	0.22	0.20	0.22	0.36
	4.5	0.24	0.24	0.22	0.20	0.21	0.20	0.24	0.32

Specific growth rates were determined at various MOIs (0.1, 1 and 10), temperatures (25, 30, 37, and 45 °C), pH values (5, 6, 7, and 8) and salinities (2.5, 3.5, and 4.5%). Gray shades indicate statistically lower growth rates ($p < 0.05$ green, $p < 0.007$ blue, and $p < 0.0006$ red) compared with the related control.

[a] *Temperature 37°C, pH 7, salinity 3.5%;*

[b] *MOI 10, pH 7, salinity 3.5%;*

[c] *MOI 10, temperature 37°C, salinity 3.5%;*

[d] *MOI 10, temperature 37°C, pH 7.*

number of PFU counts for P7 was also significantly different from the PFU counts obtained after infection at 25, 30, and 37°C ($p < 0.0001$ **Figure 2B**).

At all tested pH values, the number of bacterial colonies in infected biofilm decreased significantly to an average of 4.9×10^4 CFU/cm^2 compared with the initial spiked numbers of 1.7×10^6 CFU/cm^2 ($p < 0.001$; 1.5–2 logs reduction). This is in contrast with the bacterial cell count observed for the controls, where the number of bacterial colonies was significantly higher than the initial numbers ($p < 0.0001$; **Figure 2C**). Phages were able to replicate by 1.6–13 times of the initial number (1.7×10^7 PFU/cm^2) at all tested pH values ($p < 0.05$; **Figure 2D**).

The Effect of Phage Treatment on Biofilm Microbial Community Based on 16S rRNA Gene-Based Amplicon Sequencing Data Analysis

Overall *Proteobacteria* was the most abundant phylum with an average relative abundance of 95%. At genus level, *Vibrio* and unclassified *Vibrionaceae* together accounted for ca. 34.5–65% of the microbial community regardless of the tested condition. *Pseudoalteromonas* was found to be present at high relative abundance of up to 37.3% of total microbial community, while *Alteromonas*, *Arcobacter,* and *Thalassospira* showed a relative abundance lower than 10%. Unclassified *Pseudomonadaceae* and *Pseudomonas* spp. were present in all samples at an average relative abundance of 0.75 and 0.62%, respectively. The relative abundance of these unclassified *Pseudomonadaceae* and *Pseudomonas* spp. in infected biofilm ranged from 0.01 to 0.61% of the total community, while in the controls they ranged from 0.17 to 5.58% (**Table 3**). Specifically, at 25, 30, and 45°C, the relative abundance of both *Pseudomonas*-related taxa in bacteriophage-treated samples was significantly lower compared with the control ($p < 0.05$). Similarly, when the same experiment was carried out at various pH values, the average of relative abundance of both taxa was significantly lower in bacteriophage-infected samples compared with the controls at all tested pH values ($p < 0.03$).

From SIMPER analysis, the average dissimilarity between infected biofilm and control ranged from 13.8 to 17.4%. Unclassified *Pseudomonadaceae* and *Pseudomonas* accounted for the three main populations impacted by bacteriophages (**Table S1**). Other genera affected by bacteriophages were *Pseudoalteromonas*, unclassified *Alphaproteobacteria*, unclassified *Planococcaceae,* and unclassified *Rhodobacteraceae* (**Table S1**). An OTU-based analysis of biofilm infected at various temperatures and pH values further showed that the only OTU associated with genus *Pseudomonas* that was significantly impacted by the phage treatment shared at least 98% similarity with *P. aeruginosa* (**Table S2**). Finally, an OTU of at least 98% similarity with *Pseudoalteromonas shioyasakiensis* along with other OTUs related to *Thalassospira, Alcanivorax,* and *Aestuatiibacter* genera were also affected by bacteriophage application (**Table S2**).

Effects of Ultrafiltration (UF) Membrane Cleaning Treatments on Transmembrane Pressure (TMP)

Non-treated UF membrane showed a rapid increase in its TMP, and reached critical fouling after 130 h of operation. When the first cleaning cycle was implemented at 144 h, the membrane treated with citric acid alone showed a 30% reduction in TMP, while bacteriophage treatment alone resulted in 18% reduction. Bacteriophage in combination with citric acid, regardless of the sequence of treatment, resulted in a TMP decrease of ca. 49%. The same trend was observed for all subsequent cleaning cycles, albeit with decreasing efficacy toward TMP drop with every cycle (**Figure 3A**). The slopes of TMP increase exhibited by membranes subjected to bacteriophage cleaning alone for all cleaning cycles were significantly lower than those of other treatments (Paired *t*-test, $P < 0.01$, **Figure S3**). There was no statistical difference between the slopes of TMP increase for the respective treatment among the three cleaning cycles (**Figure S4**).

The lower TMP was due to a lower average number of bacterial cells attached on the membranes after the cleaning treatment. To exemplify, the average number of bacterial cells on non-treated membrane fragment was 8.3×10^6 CFU/cm^2. Instead, all treatments significantly reduced both the bacterial colony counts and total cell counts ($p < 0.0001$), with the highest log reduction of 1.1-logs observed when the combined cleaning was conducted (**Figures 3B,C**). Lower TMP and cell counts were also observed in the duplicate experiment (**Figure S5**).

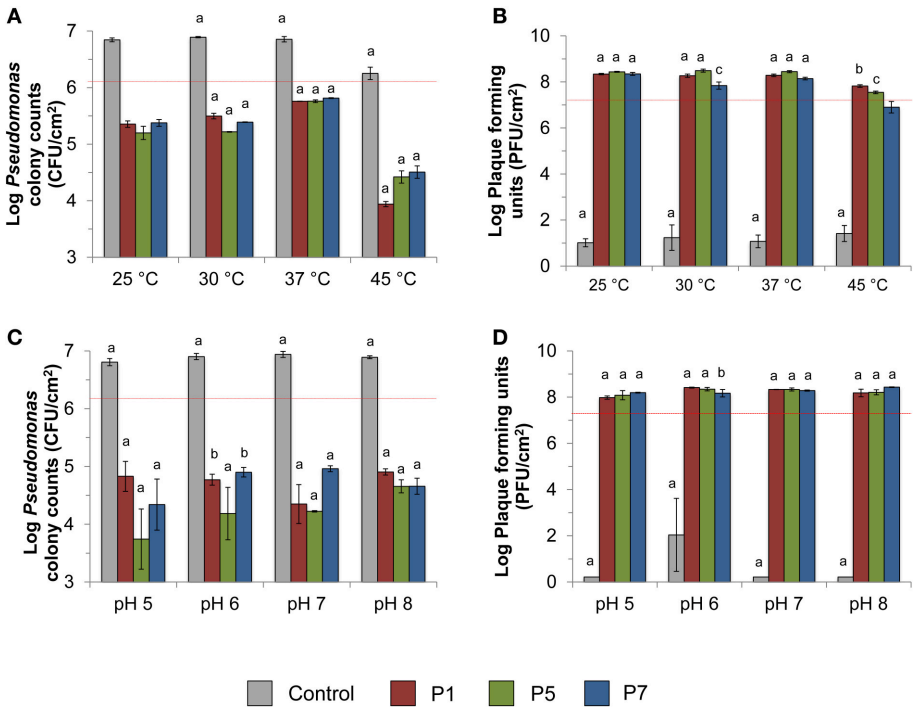

FIGURE 2 | Effect of phage treatment against *Pseudomonas aeruginosa* enriched biofilm. The effect was evaluated in terms of **(A)** viable colony counts on *Pseudomonas* isolation agar at various temperatures, **(B)** recovery of plaque counts after 10 h bacteriophage exposure at various temperatures, **(C)** viable colony counts on *Pseudomonas* isolation agar at various pH values, and **(D)** the recovery of plaque counts after 10 h bacteriophage exposure at various pH values. Dashed red lines indicate the number of CFU before infection or the number of PFU spiked for biofilm infection. The standard test conditions were MOI 10, 37°C, pH 7, and salinity 3.5% when these parameters were not varied. Bars indicate standard deviation among the three biological replicates. Letters indicate statistical difference between each treatment and the original spiked amount as indicated by red dash lines (a: $p < 0.0006$, b: $p < 0.007$, c: $p < 0.05$).

Bacteriophage Genome Size and Morphology

The genome sizes of bacteriophages P1, P5, and P7 were determined through pulse field gel electrophoresis (**Figure S6**), and were observed to share a similar genome size of approximately 48 kbp. This genome size fits in the reported range of both *Podoviridae* and *Siphoviridae* families (41.6–79.4 and 34.5–61.1 kbp, respectively; Pires et al., 2015).

Bacteriophages P1, P5, and P7 were further characterized for their morphology through transmission electron microscopy (TEM). Bacteriophages P1 and P5 had similar morphology, both had an icosahedral head of ∼55 and ∼47 nm, respectively, and short tail of ∼12 and ∼9 nm, respectively (**Figures S7**, **S8**). Phage P7 was often found in agglomerates (**Figure S9**) and showed ∼60 nm icosahedral head and with no easily identifiable tail (**Figure S10**). Following the Ackermann classification (Ackermann, 2006), these morphological traits suggest that the three bacteriophages could possibly belong to the order *Caudovirales*, family *Podoviridae*, as characterized by icosahedral head with short or no tail.

TABLE 3 | Average of the relative abundance in percentage among the three biological replicates of two *Pseudomonas*-related taxa (Unclassified *Pseudomonadaceae* and *Pseudomonas*).

Variable	Value	Unclassified *Pseudomonadaceae*				*Pseudomonas*			
		P1	P5	P7	C	P1	P5	P7	C
Temperature (°C)[a]	25°C	0.05	0.06	0.07	0.27	0.05	0.07	0.08	0.27
	30°C	0.01	0.04	0.01	0.29	0.02	0.07	0.02	0.27
	37°C	0.12	0.14	0.12	0.17	0.18	0.18	0.15	0.21
	45°C	0.61	0.43	0.32	2.50	0.59	0.38	0.29	2.78
pH[b]	5	0.13	0.07	0.13	5.58	0.10	0.06	0.11	4.26
	6	0.20	0.18	0.30	3.72	0.17	0.14	0.26	2.48
	7	0.1	0.08	0.23	3.23	0.07	0.08	0.18	2.46
	8	0.15	0.13	0.24	4.40	0.13	0.08	0.21	3.50

Gray shade indicates statistically higher average relative abundance of the related taxa in the control (C) compared with biofilm infected with bacteriophages P1, P5, or P7.
[a] *MOI 10, pH 7, salinity 3.5%;*
[b] *MOI 10, temperature 37°C, salinity 3.5%.*

DISCUSSION

In this study, the feasibility of applying bacteriophages to mitigate biofouling caused by *P. aeruginosa* in applications involving seawater is investigated. Infectivity against *P. aeruginosa* in both planktonic phase and biofilm were systematically studied under a range of salinity, temperature, and pH conditions that are representative of different stages of seawater desalination process. In addition, bacteriophages when applied in combination with

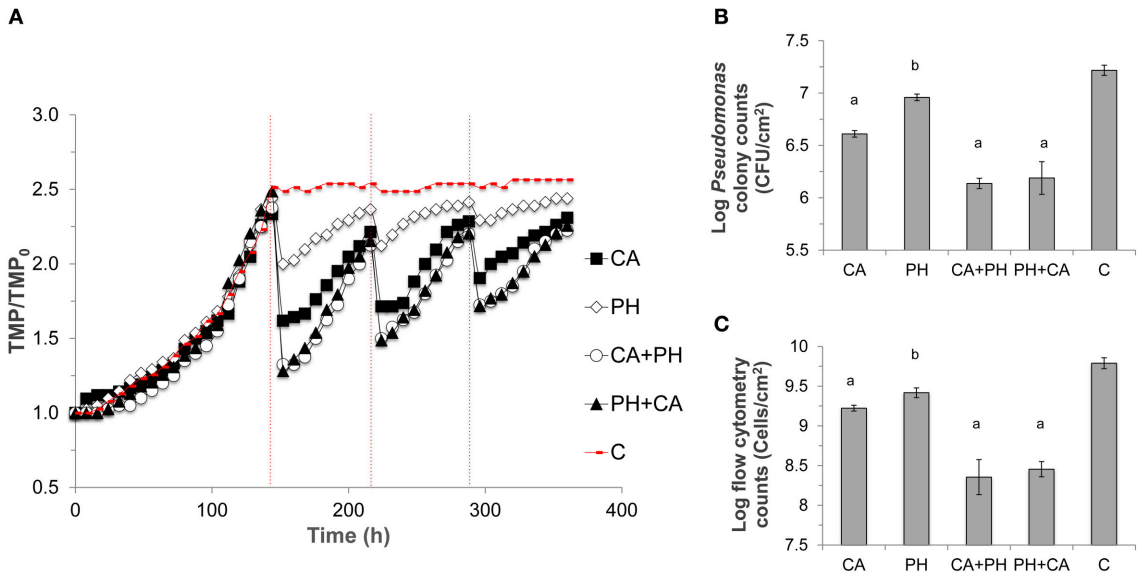

FIGURE 3 | Run 1 of the ultrafiltration membrane experiment. **(A)** Transmembrane pressure (TMP) profiles of ultrafiltration membranes. TMP was normalized against the initial TMP (TMP_0) for each membrane. Different treatments were applied, namely CA, Citric acid; PH, Phage; CA+PH, Citric acid followed by phage; PH+CA, Phage followed by citric acid; C, no treatment. Dashed red lines indicate the point at which treatment was applied over three different cycles. **(B)** Bacterial sell numbers from plate counts in terms of CFU/mL, **(C)** and from flow cytometry in terms of cell number/mL, were measured on three 2 × 2 cm pieces for each membrane at the end of the experiment. Bars indicate standard deviation among the three biological replicates. Letters indicate statistical difference compared with the control (a: $p < 0.0006$, b: $p < 0.007$).

conventional citric acid cleaning procedure were found to be effective in reducing the transmembrane pressure increment.

To infect bacterial hosts, bacteriophages first attach to host cells and integrate their DNA into the host genome without killing the hosts. Subsequently, in response to environmental or other signal cues from the bacterial hosts (Echols, 1972), bacteriophages then enter into lytic infection mode and result in the death of bacterial hosts through the induction of a suite of proteins including holins, endolysins, and spanins. These proteins collectively disrupt the cell membranes and achieve cell lysis (Young, 2013, 2014). Furthermore, bacteriophages possess enzymes that degrade the extracellular polymeric substances of biofilm matrix (Harper et al., 2014), in turn dispersing the biofilm structure to increase the susceptibility of bacterial cells to biocides or chemical cleaning. This is especially relevant for tackling membrane fouling issues in SWRO plants since traditional chemical cleaning and chlorination have limited effect in eradicating bacteria such as *Pseudomonas* spp. and SRB (Khan et al., 2015; Hong et al., 2016), both of which have been found to be associated with membrane fouling and production of corrosive hydrogen sulfide (Hong et al., 2016).

Most host-specific bacteriophages like the ones isolated in this study exhibit lytic actions that are specific against a limited number of hosts, and the use of host-specific bacteriophages can potentially minimize unintentional ecological impacts on the indigenous microbial community present within the ecosystem. However, to facilitate the use of bacteriophages as antifouling agent for seawater applications, parameters such as bacteriophage-host ratio, temperature, pH, and salinity need to be taken in consideration. In natural marine environments, bacteriophages distribution and proliferation are determined by the productivity and density of the specific host population. In our study, the highest lag phase extension and slowest specific growth rate were also observed for *P. aeruginosa* infected at a MOI of 10 (**Figure 1A** and **Table 2**) and in saline media (**Figure 1D** and **Table 2**). In natural marine environments, bacteriophages distribution and proliferation are determined by the productivity and density of the specific host population. In this study, a MOI value of 10 was the optimal for bacteriophage infection. It is likely that this MOI value maximized encounter rates between bacteriophage and bacterial cell, hence ensuring that nearly all host cells are infected by at least one bacteriophage particle.

Besides an optimal bacteriophage-host ratio, temperature plays a fundamental role in governing the attachment, proliferation, and cell lysis efficiencies. Attachment is dependent on capsid proteins of bacteriophages and surface proteins on bacterial hosts, both of which are sensitive to high temperatures. The findings of this work suggest that the isolated bacteriophages were able to infect within a broad temperature range of 25–45°C. However, the highest tested temperature resulted in a lower reduction in specific growth rates of *P. aeruginosa* compared to the other temperatures (**Table 2**). The lower lytic efficiency at 45°C can be accounted for by a lower bacterial growth and replication (**Figure 2A**), which may have provided lower surface area for bacteriophage adsorption (Sillankorva et al., 2004). Also, the high temperature of 45°C affected bacteriophage replication as evidenced from the lower PFU recovery compared to other

temperatures (**Figure 2B**). Among the isolated bacteriophages, P7 seemed to be particularly sensitive to high temperature of 45°C. The PFU recovery for this bacteriophage showed a complex trend in which it first decreased at 30°C compared with the one at 25°C ($p = 0.004$) and it subsequently increased again at 37°C ($p = 0.04$) before decreasing at 45°C ($p < 0.0001$). The exact reasons to account for this cyclical behavior are not known. However, it may be possible that this bacteriophage was more affected than P1 and P5 by the different host metabolic activity at different temperatures. Bacterial density and metabolic activities are, in fact, key factors for an efficient bacteriophage proliferation (Chibani-Chennoufi et al., 2004). High temperatures can also result in lower infection efficiency due to alteration made in the capsid proteins and bacterial surface receptors, hence inhibiting the initial phage attachment (Sillankorva et al., 2004). Similarly, Kwiatek and colleagues observed a 1 order of magnitude reduction in the virus particles concentration when bacteriophages from *Podoviridae* family were maintained at 50°C (Kwiatek et al., 2015).

In addition to temperature, pH is another important parameter that affects bacteriophage activity. Environmental pH can change the charge state of the amino acids in bacteriophage capsids, which in turn lead to modifications in the capsid structure (Nap et al., 2014). Moreover, at pH close to the isoelectric point, virus aggregation was observed in MS2 bacteriophage (Langlet et al., 2007), which can contribute to significant bias during PFU enumeration. Despite this, the pH range analyzed in this study exhibited no apparent effect on bacteriophage infectivity against both planktonic cells (**Figure 1C**, **Table 2**) and biofilm (**Figures 2C,D**), suggesting the applied pH was feasible for application in SWRO, which is generally operated within this pH range.

In an earlier study, bacteriophages were stored at a similar pH range and were determined to be stable (Kwiatek et al., 2015). Coincidentally, both in this and the earlier study, isolated lytic bacteriophages were possibly associated with the *Podoviridae* family. *Podoviridae* were shown to survive large temperature fluctuations compared to bacteriophages with smaller genome sizes (Jonczyk et al., 2011). A complete genome sequencing of the isolated bacteriophages is not done for this study and it was therefore not possible to provide better and definitive information about bacteriophage classification and infection mechanisms at different conditions. However, based on morphological traits, *Podoviridae* are generally characterized by a big icosahedral head and short tail, which were observed for the bacteriophages in this study. These phenotypic characteristics observed may have accounted for the stability of the bacteriophages observed over the wide range of temperatures and pH values. A complete genomic and taxonomical characterization for all bacteriophages used in this study would be necessary to confirm this hypothesis.

When evaluated for their host specificities, it was determined that the bacteriophages were not only able to delay the growth of planktonic cells, but were also able to statistically reduce the relative abundance of *Pseudomonas*-related taxa within the biofilm (**Table 3**). Specifically, OTU analysis showed that *P. aeruginosa* was detrimentally impacted by the bacteriophages (**Table S2**). However, it was also observed that other taxa such as unclassified *Alphaproteobacteria* and *Rhodobacteraceae* decreased in their relative abundance. Bacteriophages used in this study showed no infectivity against non-*P. aeruginosa* bacterial hosts. This means that the effect on other bacteria within the biofilm matrix was likely due to an indirect action rather than a direct virus infection. Indeed, these two taxa are within the most abundant *Proteobacteria* phylum, and the reduction may be due to the loss of bacterial cells upon bacteriophage-induced biofilm disruption. *Pseudoalteromonas* was also detrimentally impacted by bacteriophage application. This genus has been reported to play an important role in marine biofilm by contributing to the EPS production (Dheilly et al., 2010; Liu et al., 2016) and its decrease in relative abundance reiterate the effect of bacteriophages on biofilm matrix. Finally, the decrease in relative abundance of Gram-positive *Planococcaceae* could be due to a higher susceptibility to phage lysins since in the absence of outer membrane, those proteins can make direct contact with cell wall carbohydrates and peptidoglycans even if *Planococcaceae* is not the target host (Fischetti, 2005).

Developing resistance to bacteriophage remains to be of a concern. This was exemplified when bacteria eventually overcame the bacteriophage to grow albeit at a lower specific growth rate compared to the same host grown in absence of bacteriophage (**Table 2**). Similar trend was also observed in a separate study for *P. aeruginosa* infected with *Podoviridae* phages (Alves et al., 2016). The bacterial growth after a prolonged lag phase indicates the evolution of resistance to bacteriophage infection after a certain period of bacteria-virus interaction. Small gene mutation or change/loss of receptor proteins among a subpopulation of cells can result in the loss of bacteriophage infectivity (Ly-Chatain, 2014). Bacterial resistance to bacteriophage infection can also occur by the production of competitive inhibitors that bind to phage receptor or by preventing phage DNA entry (Labrie et al., 2010). It was observed that *P. aeruginosa* phage resistance can affect also the expression of virulence factors (Hosseinidoust et al., 2013a,b) but incurs a fitness cost for the bacteria in terms of specific growth rate and metabolic activity (Hall et al., 2012). This can potentially account for the lower specific bacterial growth rates observed in presence of bacteriophages (**Table 2**). Besides gaining resistance, bacterial regrowth could possibly be related to the establishment of phage lysogeny which leads to the presence of prophages in the bacterial cells instead of cell lysis, hence allowing bacterial regrowth. Further studies would have to be carried out to determine the cause of this bacterial regrowth observed in presence of bacteriophages.

Subsequently, when bacteriophages were applied to the *P. aeruginosa*-enriched biofilm attached on UF membranes, it was observed that the starting TMP at each initial point of cleaning cycle was higher than the previous cycle (**Figures S4**, **S5**). This suggests a slight loss in bacteriophage efficacy with each application. Since the slopes of TMP increase after each cleaning cycle were not significantly different, the increase of initial TMP at each cleaning cycle was most likely not due to changes in metabolic rates or infectivity rates. Instead, this can potentially be explained by an increased production of EPS that

would provide a physical barrier between bacteriophages and their receptors (Labrie et al., 2010). Earlier studies have reported a higher reduction in TMP decline compared to this study (i.e., ca. 18% decrease). For instance, Goldman and colleagues observed a 47% reduction in the UF permeability drop after phage application compared with the control (Goldman et al., 2009). However, bacteriophages were introduced in the feed solution and not directly on the formed biofilm, and the higher reduction may be due to a combined effect on both planktonic and biofilm-associated bacteria. In a full-scale SWRO, direct application of bacteriophage to a large volume of seawater would be impractical and costly as this means a large dose of bacteriophage would be required to maintain infectivity at an optimal MOI. In another study, Bhattacharjee et al. observed a 53 and 78% flux recovery after 1 and 2 days of phage application, respectively (Bhattacharjee et al., 2015). However, hollow-fiber membranes were conditioned with nutrient rich medium instead of environmental waters, and both bacteriophages and host may be more metabolically active to facilitate interactions.

Isolation of new bacteriophages or application of phages cocktail can be adopted to mitigate problems associated with phage resistance and lysogeny. However, isolating new bacteriophages can be challenging and time-consuming for long-term operations. Alternatively, this study demonstrated the feasibility of combining bacteriophages application with the common membrane cleaning procedure. Approximately 49% TMP recovery and 1.1 log biofilm removal was observed when UF membrane was treated with bacteriophages and citric acid, regardless of the order of application (**Figure 3**). This confirms that bacteriophages are not affected by the acidic pH and that they can be easily integrated with the common membrane treatment procedure to enhance the cleaning efficacy. Citric acid chelates inorganic minerals and disrupts the stability of biofilm matrix attached on the pretreatment UF membranes (Lee et al., 2001; Porcelli and Judd, 2010). Bacteriophages are able to further disrupt the biofilm structure, hence allowing for a better cleaning efficacy. Similarly, bacteriophages were applied successfully in combination with chlorine treatment against *P. aeruginosa* biofilm (Zhang and Hu, 2013). These findings suggest that bacteriophage can be applied synergistically with existing biocides or cleaning strategies to effectively mitigate biofouling associated with *P. aeruginosa*. Alternatively, other bacteriophages specific against other host targets, for example *Pseudoalteromonas* which is typically present in high abundance on a marine biofilm layer, can also be isolated and verified for their lytic efficiency against this new host based on the procedure described in this study. Finally, it could be interesting to analyze the effect of bacteriophages treatment in preventing biofilm formation rather than removing an established biofilm structure. In this context, the lower cell density could represent a limitation for bacteriophages activity and infectivity. A cocktail of bacteriophages from different taxonomical families targeting different bacterial host could also represent a better approach to maximize the impact of the infection and to further mitigate seawater membrane biofouling in the future for bigger scale operating systems.

CONCLUSION

This study demonstrated the ability of bacteriophages to infect planktonic *P. aeruginosa* and to reduce biofilm formation. Infectivity at different environmental conditions was systematically evaluated and bacteriophages showed great versatility to infect *P. aeruginosa* over a wide temperature and pH range. Although the bacteriophages were able to effectively reduce the relative abundance of *Pseudomonas*-related taxa, other taxa including *Pseudoalteromonas* and predominant *Proteobacteria* within a marine biofilm were also affected, suggesting that the bacteriophages lyse *P. aeruginosa* and disrupt the biofilm matrix. Finally, bacteriophages were demonstrated to be feasible for reducing *P. aeruginosa* biofouling on a lab-scale UF membrane. Specifically, the best reduction in transmembrane pressure was obtained when bacteriophage treatment was combined with citric acid cleaning. Collectively, the findings demonstrate that bacteriophages can be used as a biocidal agent to mitigate undesirable *P. aeruginosa*-associated problems in seawater applications.

AUTHOR CONTRIBUTIONS

GS and P-YH: Designed the experiment; GS and SY: Performed the experiments and analyzed the data; GS, P-YH, and AK: Wrote and revised the manuscript.

ACKNOWLEDGMENTS

The research reported in this publication was supported by CRG funding URF/1/2982-01-01 from King Abdullah University of Science and Technology (KAUST) awarded to P-YH. AK thanks KAUST and CSIRO Land and Water for financial support.

SUPPLEMENTARY MATERIAL

The Supplementary Material for this article can be found online at: https://www.frontiersin.org/articles/10.3389/fmicb.2018.00875/full#supplementary-material

Table S1 | Similarity percentages (SIMPER) analysis of the average composition of the microbial communities in phage infected and non-infected biofilms.

Table S2 | OTUs affected by bacteriophage infection are listed together with the closest match identified by the BLASTN algorithm.

Figure S1 | Phage forming units for each bacteriophage propagated with the double layer plate method. Bars indicate standard deviation.

Figure S2 | Cross-flow ultrafiltration membrane setup.

Figure S3 | Values of TMP/TMP_0 increment slopes, averaged from the three cycles of UF membrane cleaning. a, b represent homogenous subgroups by two-tailed *t*-test.

Figure S4 | Values of TMP/TMP_0 increment slopes for each cycle of membrane cleaning.

Figure S5 | Run 2 of the ultrafiltration membrane experiment. **(A)** Transmembrane pressure (TMP) profiles of ultrafiltration membranes. TMP was normalized against the initial TMP (TMP_0) for each membrane. Different treatments were applied, namely CA, Citric acid; PH, Phage; CA+PH, Citric acid followed by phage;

PH+CA, Phage followed by citric acid; C, no treatment. Dashed red lines indicate the point at which treatment was applied over three different cycles. **(B)** Cell numbers from plate counts in terms of CFU/mL, **(C)** and from flow cytometry in terms of cells number/mL, were measured on three 2 × 2 cm pieces for each membrane at the end of the experiment. Bars indicate standard deviation among the three biological replicates. Letters indicate statistical difference compared with the control (a: $p < 0.0006$, b: $p < 0.007$ and c: $p < 0.05$).

Figure S6 | Pulsed field gel electrophoresis images of P1, P5, and P7 genomes. **λ** and a indicate *lambda* and 1 kbp ladder respectively used as markers.

Figure S7 | Transmission electron microscopy images of the isolated bacteriophage P1.

Figure S8 | Transmission electron microscopy images of the isolated bacteriophage P5.

Figure S9 | Transmission electron microscopy images of the isolated bacteriophage P7 in aggregate.

Figure S10 | Transmission electron microscopy images of the isolated bacteriophage P7.

REFERENCES

Ackermann, H. W. (2006). "Classification of bacteriophages," in *The Bacteriophages*, ed R. Calendar (New York, NY: Oxford University Press), 8–16.

Adams, M. H. (1959). *Bacteriophages*. New York, NY: Interscience Publishers Inc.

Alemayehu, D., Casey, P. G., McAuliffe, O., Guinane, C. M., Martin, J. G., Shanahan, F., et al. (2012). Bacteriophages φMR299-2 and φNH-4 can eliminate *Pseudomonas aeruginosa* in the murine lung and on cystic fibrosis lung airway cells. *MBio* 3, e00029–e00012. doi: 10.1128/mBio.00029-12

Al-Jassim, N., Ansari, M. I., Harb, M., and Hong, P.-Y. (2015). Removal of bacterial contaminants and antibiotic resistance genes by conventional wastewater treatment processes in Saudi Arabia: is the treated wastewater safe to reuse for agricultural irrigation? *Water Res.* 73, 277–290. doi: 10.1016/j.watres.2015.01.036

Alves, D. R., Perez-Esteban, P., Kot, W., Bean, J., Arnot, T., Hansen, L. H., et al. (2016). A novel bacteriophage cocktail reduces and disperses *Pseudomonas aeruginosa* biofilms under static and flow conditions. *Microb. Biotechnol.* 9, 61–74. doi: 10.1111/1751-7915.12316

Bhattacharjee, A. S., Choi, J., Motlagh, A. M., Mukherji, S. T., and Goel, R. (2015). Bacteriophage therapy for membrane biofouling in membrane bioreactors and antibiotic-resistant bacterial biofilms. *Biotechnol. Bioeng.* 112, 1644–1654. doi: 10.1002/bit.25574

Chibani-Chennoufi, S., Bruttin, A., Dillmann, M.-L., and Brüssow, H. (2004). Phage-host interaction: an ecological perspective. *J. Bacteriol.* 186, 3677–3686. doi: 10.1128/JB.186.12.3677-3686.2004

Clarke, K. G. R. (2015). *PRIMER Version 7: User Manual/Tutorial*. Plymouth: PRIMER-E.

Dheilly, A., Soum-Soutéra, E., Klein, G. L., Bazire, A., Compère, C., Haras, D., et al. (2010). Antibiofilm activity of the marine bacterium *Pseudoalteromonas* sp. strain 3J6. *Appl. Environ. Microbiol.* 76, 3452–3461. doi: 10.1128/AEM.02632-09

Echols, H. (1972). Developmental pathways for the temperate phage: lysis vs lysogeny. *Annu. Rev. Genet.* 6, 157–190. doi: 10.1146/annurev.ge.06.120172.001105

Edgar, R. C., Haas, B. J., Clemente, J. C., Quince, C., and Knight, R. (2011). UCHIME improves sensitivity and speed of chimera detection. *Bioinformatics* 27, 2194–2200. doi: 10.1093/bioinformatics/btr381

Fischetti, V. A. (2005). Bacteriophage lytic enzymes: novel anti-infectives. *Trends Microbiol.* 13, 491–496. doi: 10.1016/j.tim.2005.08.007

Fritzmann, C., Löwenberg, J., Wintgens, T., and Melin, T. (2007). State-of-the-art of reverse osmosis desalination. *Desalination* 216, 1–76. doi: 10.1016/j.desal.2006.12.009

Fu, W., Forster, T., Mayer, O., Curtin, J. J., Lehman, S. M., and Donlan, R. M. (2010). Bacteriophage cocktail for the prevention of biofilm formation by *Pseudomonas aeruginosa* on catheters in an *in vitro* model system. *Antimicrob. Agents Chemother.* 54, 397–404. doi: 10.1128/AAC.00669-09

Gao, W., Liang, H., Ma, J., Han, M., Chen, Z.-L., Han, Z.-S., et al. (2011). Membrane fouling control in ultrafiltration technology for drinking water production: a review. *Desalination* 272, 1–8. doi: 10.1016/j.desal.2011.01.051

Goldman, G., Starosvetsky, J., and Armon, R. (2009). Inhibition of biofilm formation on UF membrane by use of specific bacteriophages. *J. Memb. Sci.* 342, 145–152. doi: 10.1016/j.memsci.2009.06.036

Goosen, M., Sablani, S., Al-Hinai, H., Al-Obeidani, S., Al-Belushi, R., and Jackson, D. (2005). Fouling of reverse osmosis and ultrafiltration membranes: a critical review. *Sep. Sci. Technol.* 39, 2261–2297. doi: 10.1081/SS-120039343

Greenlee, L. F., Lawler, D. F., Freeman, B. D., Marrot, B., and Moulin, P. (2009). Reverse osmosis desalination: water sources, technology, and today's challenges. *Water Res.* 43, 2317–2348. doi: 10.1016/j.watres.2009.03.010

Hall, A. R., De Vos, D., Friman, V.-P., Pirnay, J.-P., and Buckling, A. (2012). Effects of sequential and simultaneous applications of bacteriophages on populations of *Pseudomonas aeruginosa in vitro* and in wax moth larvae. *Appl. Environ. Microbiol.* 78, 5646–5652. doi: 10.1128/AEM.00757-12

Harper, D. R., Parracho, H. M., Walker, J., Sharp, R., Hughes, G., Werthén, M., et al. (2014). Bacteriophages and biofilms. *Antibiotics* 3, 270–284. doi: 10.3390/antibiotics3030270

Hong, P.-Y., Moosa, N., and Mink, J. (2016). Dynamics of microbial communities in an integrated ultrafiltration–reverse osmosis desalination pilot plant located at the Arabian Gulf. *Desalination Water Treat.* 57, 16310–16323. doi: 10.1080/19443994.2015.1083483

Hosseinidoust, Z., Tufenkji, N., and Van De Ven, T. G. (2013a). Predation in homogeneous and heterogeneous phage environments affects virulence determinants of *Pseudomonas aeruginosa*. *Appl. Environ. Microbiol.* 79, 2862–2871. doi: 10.1128/AEM.03817-12

Hosseinidoust, Z., Van De Ven, T. G., and Tufenkji, N. (2013b). Evolution of *Pseudomonas aeruginosa* virulence as a result of phage predation. *Appl. Environ. Microbiol.* 79, 6110–6116. doi: 10.1128/AEM.01421-13

Jonczyk, E., Kłak, M., Miedzybrodzki, R., and Górski, A. (2011). The influence of external factors on bacteriophages. *Folia Microbiol.* 56, 191–200. doi: 10.1007/s12223-011-0039-8

Khan, M. T., Hong, P.-Y., Nada, N., and Croue, J. P. (2015). Does chlorination of seawater reverse osmosis membranes control biofouling? *Water Res.* 78, 84–97. doi: 10.1016/j.watres.2015.03.029

Kot, W., Vogensen, F. K., Sørensen, S. J., and Hansen, L. H. (2014). DPS–a rapid method for genome sequencing of DNA-containing bacteriophages directly from a single plaque. *J. Virol. Methods* 196, 152–156. doi: 10.1016/j.jviromet.2013.10.040

Kwiatek, M., Mizak, L., Parasion, S., Gryko, R., Olender, A., and Niemcewicz, M. (2015). Characterization of five newly isolated bacteriophages active against *Pseudomonas aeruginosa* clinical strains. *Folia Microbiol.* 60, 7–14. doi: 10.1007/s12223-014-0333-3

Labrie, S. J., Samson, J. E., and Moineau, S. (2010). Bacteriophage resistance mechanisms. *Nat. Rev. Microbiol.* 8, 317–327. doi: 10.1038/nrmicro2315

Langlet, J., Gaboriaud, F., and Gantzer, C. (2007). Effects of pH on plaque forming unit counts and aggregation of MS2 bacteriophage. *J. Appl. Microbiol.* 103, 1632–1638. doi: 10.1111/j.1365-2672.2007.03396.x

Lee, H., Amy, G., Cho, J., Yoon, Y., Moon, S.-H., and Kim, I. S. (2001). Cleaning strategies for flux recovery of an ultrafiltration membrane fouled by natural organic matter. *Water Res.* 35, 3301–3308. doi: 10.1016/S0043-1354(01)00063-X

Le Roux, J., Nada, N., Khan, M. T., and Croué, J.-P. (2015). Tracing disinfection byproducts in full-scale desalination plants. *Desalination* 359, 141–148. doi: 10.1016/j.desal.2014.12.035

Liu, A., Mi, Z.-H., Zheng, X.-Y., Yu, Y., Su, H.-N., Chen, X.-L., et al. (2016). Exopolysaccharides play a role in the swarming of the benthic bacterium *Pseudoalteromonas* sp. SM9913. *Front. Microbiol.* 7:473. doi: 10.3389/fmicb.2016.00473

Ly-Chatain, M. H. (2014). The factors affecting effectiveness of treatment in phages therapy. *Front. Microbiol.* 5:51. doi: 10.3389/fmicb.2014.00051

Matin, A., Khan, Z., Zaidi, S., and Boyce, M. (2011). Biofouling in reverse osmosis membranes for seawater desalination: phenomena and prevention. *Desalination* 281, 1–16. doi: 10.1016/j.desal.2011.06.063

McVay, C. S., Velásquez, M., and Fralick, J. A. (2007). Phage therapy of *Pseudomonas aeruginosa* infection in a mouse burn wound model. *Antimicrob. Agents Chemother.* 51, 1934–1938. doi: 10.1128/AAC.01028-06

Nap, R. J., BoŽič, A. L., Szleifer, I., and Podgornik, R. (2014). The role of solution conditions in the bacteriophage PP7 capsid charge regulation. *Biophys. J.* 107, 1970–1979. doi: 10.1016/j.bpj.2014.08.032

Oh, H.-S., Tan, C. H., Low, J. H., Rzechowicz, M., Siddiqui, M. F., Winters, H., et al. (2017). Quorum quenching bacteria can be used to inhibit the biofouling of reverse osmosis membranes. *Water Res.* 112, 29–37. doi: 10.1016/j.watres.2017.01.028

Olszak, T., Zarnowiec, P., Kaca, W., Danis-Wlodarczyk, K., Augustyniak, D., Drevinek, P., et al. (2015). *In vitro* and *in vivo* antibacterial activity of environmental bacteriophages against *Pseudomonas aeruginosa* strains from cystic fibrosis patients. *Appl. Microbiol. Biotechnol.* 99, 6021–6033. doi: 10.1007/s00253-015-6492-6

Peñate, B., and García-Rodríguez, L. (2012). Current trends and future prospects in the design of seawater reverse osmosis desalination technology. *Desalination* 284, 1–8. doi: 10.1016/j.desal.2011.09.010

Pires, D. P., Boas, D. V., Sillankorva, S., and Azeredo, J. (2015). Phage therapy: a step forward in the treatment of *Pseudomonas aeruginosa* infections. *J. Virol.* 89, 7449–7456. doi: 10.1128/JVI.00385-15

Porcelli, N., and Judd, S. (2010). Chemical cleaning of potable water membranes: a review. *Sep. Purif. Technol.* 71, 137–143. doi: 10.1016/j.seppur.2009.12.007

Sanawar, H., Xiong, Y., Alam, A., Croue, J.-P., and Hong, P.-Y. (2017). Chlorination or monochloramination: balancing the regulated trihalomethane formation and microbial inactivation in marine aquaculture waters. *Aquaculture* 480, 94–102. doi: 10.1016/j.aquaculture.2017.08.014

Scarascia, G., Cheng, H., Harb, M., and Hong, P.-Y. (2017). Application of hierarchical oligonucleotide primer extension (HOPE) to assess relative abundances of ammonia-and nitrite-oxidizing bacteria. *BMC Microbiol.* 17:85. doi: 10.1186/s12866-017-0998-2

Sillankorva, S., Oliveira, R., Vieira, M. J., Sutherland, I., and Azeredo, J. (2004). Pseudomonas fluorescens infection by bacteriophage ΦS1: the influence of temperature, host growth phase and media. *FEMS Microbiol. Lett.* 241, 13–20. doi: 10.1016/j.femsle.2004.06.058

Wang, Q., Garrity, G. M., Tiedje, J. M., and Cole, J. R. (2007). Naive Bayesian classifier for rapid assignment of rRNA sequences into the new bacterial taxonomy. *Appl. Environ. Microbiol.* 73, 5261–5267. doi: 10.1128/AEM.00062-07

Young, R. (2013). Phage lysis: do we have the hole story yet? *Curr. Opin. Microbiol.* 16, 790–797. doi: 10.1016/j.mib.2013.08.008

Young, R. (2014). Phage lysis: three steps, three choices, one outcome. *J. Microbiol.* 52, 243–258. doi: 10.1007/s12275-014-4087-z

Zhang, Y., Hunt, H. K., and Hu, Z. (2013). Application of bacteriophages to selectively remove *Pseudomonas aeruginosa* in water and wastewater filtration systems. *Water Res.* 47, 4507–4518. doi: 10.1016/j.watres.2013.05.014

Zhang, Y., and Hu, Z. (2013). Combined treatment of *Pseudomonas aeruginosa* biofilms with bacteriophages and chlorine. *Biotechnol. Bioeng.* 110, 286–295. doi: 10.1002/bit.24630

Conflict of Interest Statement: The authors declare that the research was conducted in the absence of any commercial or financial relationships that could be construed as a potential conflict of interest.

frontiers in Microbiology

ORIGINAL RESEARCH
published: 05 December 2017
doi: 10.3389/fmicb.2017.02375

Thermal-Stability and Reconstitution Ability of *Listeria* Phages P100 and A511

*Hanie Ahmadi[1,2], Devon Radford[2], Andrew M. Kropinski[3], Loong-Tak Lim[1] and Sampathkumar Balamurugan[2]**

[1] Department of Food Science, University of Guelph, Guelph, ON, Canada, [2] Guelph Research and Development Centre, Agriculture and Agri-Food Canada, Guelph, ON, Canada, [3] Department of Pathobiology, Ontario Veterinary College, University of Guelph, Guelph, ON, Canada

The study evaluated the thermal-stability of *Listeria* phages P100 and A511 at temperatures simulating the preparation of ready-to-eat meats. The phage infectivity after heating to 71°C and holding for a minimum of 30 s, before eventually cooling to 4°C were examined. Higher temperatures of 75, 80, and 85°C were also tested to evaluate their effect on phages thermal-stability. This study found that despite minor differences in the amino acid sequences of their structural proteins, the two phages responded differently to high temperatures. P100 activity declined at least 10 log (PFU mL^{-1}) with exposure to 71°C (30 s) and falling below the limit of detection (1 log PFU mL^{-1}) while, A511 dropped from 10^8 to 10^5 PFU mL^{-1}. Cooling resulted in partial reconstitution of P100 phage particles to 10^3 PFU mL^{-1}. Exposure to 75°C (30 s) abolished A511 activity (8 log PFU mL^{-1}) and both phages showed reconstitution during cooling phase after exposure to 75°C. P100 exhibited reconstitution after treatment at 80°C (30 s), conversely A511 showed no reconstitution activity. Heating P100 to 85°C abolished the reconstitution potential. Substantial differences were found in thermal-stability and reconstitution of the examined phages showing A511 to be more thermo-stable than P100, while P100 exhibited reconstitution during cooling after treatment at 80°C which was absent in A511. The differences in predicted melting temperatures of structural proteins of P100 and A511 were consistent with the observed differences in thermal stability and morphological changes observed with transmission electron microscopy.

Keywords: Bacteriophage, *Listeria monocytogenes*, thermal-stability, transmission electron microscopy, ready-to eat meat, food safety

OPEN ACCESS

Edited by:
Robert Czajkowski, University of Gdańsk, Poland

Reviewed by:
Sanna Sillankorva, University of Minho, Portugal
Grzegorz Wegrzyn, University of Gdańsk, Poland

***Correspondence:**
Sampathkumar Balamurugan
balamurugans@agr.gc.ca

Specialty section:
This article was submitted to Virology, a section of the journal Frontiers in Microbiology

Received: *08 September 2017*
Accepted: *16 November 2017*
Published: *05 December 2017*

Citation:
Ahmadi H, Radford D, Kropinski AM, Lim L-T and Balamurugan S (2017) Thermal-Stability and Reconstitution Ability of Listeria Phages P100 and A511. Front. Microbiol. 8:2375. doi: 10.3389/fmicb.2017.02375

INTRODUCTION

Listeria monocytogenes continues to be a pathogen of concern in ready-to-eat (RTE) meat products causing listeriosis, a life threatening foodborne disease that primarily affects older adults, pregnant women, newborns, and adults with weakened immune systems. Due to high mortality rate of approximately 25–30%, the disease ranks among the most severe foodborne illnesses (Vazquez-Boland et al., 2001). Worldwide human listeriosis cases have been linked to the consumption of

Abbreviations: CFU, colony forming units; PBS, phosphate-buffered saline; PFU, plaque forming units; SM, Saline-Magnesium buffer; TEM, transmission electron microscopy; TSA, tryptic soy agar; TSB, tryptic soy broth.

contaminated meats, seafood, delicatessen (deli) meats, dairy and poultry products (Painter, 2007; Centers for Disease Control and Prevention, 2017; European Centre for Disease Prevention and Control, 2017). In Canada, a listeriosis outbreak associated with RTE meat products sickened a total of 57 Canadians and claimed 22 lives (Gilmour et al., 2010).

Food processors are advised to reduce or eliminate *L. monocytogenes* in RTE meat and poultry products by employing antimicrobial agents/processes and/or post-lethality procedure(s) (Canadian Food Inspection Agency, 2011). Antimicrobial agents are food additives which allow no more than 2 log CFU g^{-1} increase in *L. monocytogenes* throughout the stated shelf-life of the product. Chemical antimicrobials such as lactate and diacetate have been approved by Health Canada to control the growth of *L. monocytogenes* in RTE meat and poultry products (Health Canada, 2011).

In the last decade, several alternative processing and preservation technologies have been developed to enhance the safety of food. For example, bacteriophages have been investigated as antimicrobial agents in food systems, including meats, cut fruits, vegetables and milk (Leverentz et al., 2001; Whichard et al., 2003; Tabla et al., 2012; Chibeu et al., 2013; Ahmadi et al., 2015; Murray et al., 2015; Radford et al., 2017). Bacteriophage preparation such as LISTEX^{TM} P100 and LMP-102 are approved by regulatory agencies as processing aids, for use in raw and RTE foods to combat *L. monocytogenes* contamination (U.S. Food and Drug Administration, 2006; Health Canada, 2011). These commercial phage formulations are preservative-free and do not impact sensory and quality attributes of food (Brovko et al., 2012). As a processing aid, the bacteriophage suspension is sprayed on to the surface of products or added by dipping as a liquid prior to packaging (U.S. Food and Drug Administration, 2006). These methods may not be ideal, as they lead to the potential inactivation of the bacteriophages as a result of dilution of phages with other materials such as wash fluids (Anany et al., 2011). This problem may be overcome by incorporating the phage into the raw meat formulation as an additive to ensure phages are applied and distributed uniformly throughout the raw product matrix.

Stability of phages during heat pasteurization and cooking during industrial food production is a particular concern in their application as an additive. Considerable work has been focused on understanding thermal stability of lactic acid bacteria (LAB) phages which are the main cause of fermentation failure in the dairy industry (Wilkowske et al., 1954; Müller-Merbach et al., 2005; Buzrul et al., 2007). Buzrul et al. (2007) treated 10 *Lactococcal* bacteriophages in M17 broth at 72°C for 15 min and 90°C for 5 min. The former treatment resulted in total inactivation of just two phages while the latter inactivated half of the phages. Whitehead and Cox (1936) reported that one strain of lactic *Streptococcus* phage was not stable at 70°C for 30 min, and another strain was destroyed by 50°C for 30 min. While many of the LAB phages survived pasteurization treatments of 63°C for 30 min or 72°C for 15 s (Capra et al., 2004; Mercanti et al., 2012), thermal sensitivity of other phages was observed at 68°C and below (Duda et al., 2009; Brovko et al., 2012; Qiu, 2012) demonstrating the diversity in thermal stability of the phages. However, there is lack of information on thermal stability of phages against *L. monocytogenes,* particularly in the context of industrial heat pasteurization.

Here we examined the thermal stability of two broad host range, lytic *Listeria* phages P100 and A511 at temperatures simulating the preparation of RTE meats, which included heating to 71°C and holding for a minimum of 30 s, before eventually cooling to 4°C (Food Safety and Inspection Service, 1999; Canadian Food Inspection Agency, 2013). TEM analyses of the two *Listeria* phages were performed to understand structural changes under different thermal treatments. Relative estimates of minimum melting temperatures of structural proteins were also determined using Tm (melting temperature) predictor algorithm (Ku et al., 2009) to determine the differences between thermal-stability of P100 and A511 at protein sequence level.

MATERIALS AND METHODS

Establishment of *Listeria* Cultures

Listeria monocytogenes strain 08-5578 (serotype 1/2a) obtained from The National Microbiology Laboratory, Canadian Science Centre for Human and Animal Health (Winnipeg, MB, Canada) was used. Overnight cultures of *L. monocytogenes* were prepared by transferring a single colony of *L. monocytogenes* strain 08-5578 to 5.0 mL TSB (BD Diagnostics, San Jose, CA, United States) in a 15 mL screw cap, sterile Falcon tubes (Fisherbrand, Fisher Scientific International, Inc., Pittsburgh, PA, United States) in a rotary shaker and incubated for 18 h at 37°C and 120 rpm.

Bacteriophage Preparation

Listeria phage P100 was obtained from MICREOS Food safety, Inc. (Netherlands) in PBS at concentrations of 10^{10}–10^{11} PFU mL^{-1}. *Listeria* phage A511 was obtained from The Félix d'Hérelle Reference Center for Bacterial Viruses, University of Laval (Quebec, QC, Canada). Phage A511 was propagated as described by Radford et al. (2016) with some minor modifications. Briefly, 200 μL of *L. monocytogenes* subculture (10^9 CFU mL^{-1}) and 100 μL of phage A511 (10^9 PFU mL^{-1}) were added to 4 mL of top agar supplemented with $CaCl_2$ (TSB, 0.5% agar, 10 mM $CaCl_2$). The solution was uniformly mixed and poured onto sterile TSA plates (Fisherbrand). Plates were incubated at 30°C for 18 h to form a top agar layer of phage-host co-culture. After incubation, 5 mL of SM buffer (5.8 g NaCl, 2 g $MgSO_4.7H_2O$, 50 mL Tris-Cl at pH 7.5, 0.1 g gelatin) was added to the plates to cover the surface of top agar entirely and refrigerated at 4°C overnight. After refrigeration all the liquids were extracted using a micropipette and filtered through 0.22 μm membranes. The filtrate was retained and stored at 4°C until use (Radford et al., 2016). The titre of propagated phages was determined by adding serial dilutions to agar overlays and incubating as previously described by Kropinski et al. (2009).

Thermal Stability of P100 and A511 at Constant Temperature

The heating vessels used were standard 160 mL screw cap glass dilution bottles. Each bottle contained 90 mL of SM buffer

(pH 7.5) with a magnetic stir bar. Prior to inoculation, SM buffer was equilibrated to the test temperature of 45, 55, or 65°C in a circulating water bath (TW-2.03, Rose Scientific, Edmonton, AB, Canada). In the case of all experiments described in this manuscript the treatment temperatures were maintained within ± 0.5°C. During heating, the water level was maintained at least 2.0 cm above the level of the treatment solution at all times and the magnetic stirrer operated using a MS-01 four position magnetic stirrer (Rose Scientific). Phage P100 (commercially preparation) at 10^{10-11} PFU mL^{-1} and A511 at 10^9 PFU mL^{-1} (highest titre obtained by the propagation method indicated in the previous section) were used in the thermal stability experiment. An aliquot of 10 mL of P100 or A511 at 4°C was added to the heating solution and temperature monitored till the heating solution reached the respective treatment temperatures following which 1.0 mL sample was taken at $t = 0$ and then every 15 min for 75 min. Due to instability of phages in the 65°C treatment, samples were taken every 2.5 min for 20 min to assess thermal stability. Samples were immediately diluted in SM buffer and the phage titers determined with the phage overlay assay (Kropinski et al., 2009). All experiments were performed in triplicate and each sample plated in duplicate. A linear regression curve of the phage PFU mL^{-1} against time was constructed. Best fit regression lines for each plot were used to calculate the decimal reduction time (*D*-value; time required for one log reduction in plaque numbers at a given temperature).

Thermal Stability of P100 and A511 during Heating-Holding-Cooling Treatments

Treatments involved heating the phage suspensions from 4°C to 71, 75, 80, or 85°C, (referred to as heating) and holding for 30 s (referred to as holding) and then cooling back to 4°C (referred to as cooling) to check the stability of phages. The heating vessels used were standard 160 mL screw cap glass dilution bottles. Each bottle contained 90 mL of SM buffer (pH 7.5) with a magnetic stir bar. Prior to inoculation, the heating medium was equilibrated to 4°C. Then, 10 mL of P100 (10^{11} PFU mL^{-1}) or A511 (10^9 PFU mL^{-1}) at 4°C was added to the treatment solution and placed in a heated circulating water bath set at 72°C (temperature of the water bath was set to 1°C greater than the desired peak heating temperatures) and the temperature of the treatment solution monitored using a digital thermometer (Traceable Calibration Control, VWR International, Radnor, PA, United States). Aliquot of 1.0 mL samples were taken at $t = 0$ (4°C), 40°C and then at every 10°C increase in sample temperature from 40 to 70°C, and 71°C (heating). The heating vessel was then held at 71°C for 30 s (holding) and another sample was taken. Immediately after heating and holding, the heating vessel was transferred to circulating cooling water bath, cooled using a glycol circulating cooling jacket set at −3°C. Aliquots of 1.0 mL samples were taken at every 10°C reduction in sample temperature, until the treatment solution temperature reached 4°C (cooling). Samples were immediately diluted in SM buffer and the phage titers determined with the phage overlay assay (Kropinski et al., 2009). Based on preliminary results obtained, similar experiments were repeated at 75, 80, and 85°C peak heating temperatures for P100 while 75 and 80°C for phage A511. Time required for samples to reach peak temperature of 71, 75, 80, and 85°C were monitored and were consistently around 477 ± 14, 519 ± 38, 597 ± 74, and 711 ± 41 s respectively. Cooling time from peak temperatures to 4°C was approximately 1169 ± 46 s. P100 with initial concentration of 10^5 and 10^8 (PFU mL^{-1}) in treatment solutions were also examined at peak heating (71°C)-holding-cooling treatment and A511 with initial concentration of 10^5 PFU mL^{-1} in treatment solution was investigated at peak heating (75°C)-holding-cooling treatment. All experiments were performed in triplicate and each sample plated in duplicate.

Preparation and Visualization of Treated Phage

Transmission electron microscopy was performed on samples to visualize the effect of heat on phage morphology. Phage suspensions were concentrated by density gradient centrifugation (Cardarelli et al., 2010). The concentrated phages were diluted 1:20 with double–distilled water and directly negative stained for TEM. Copper–rhodium (400-mesh) grids were covered with a thin layer of amorphous carbon made hydrophilic by 45 s vacuum glow-discharge. Phage solution samples (4–6 μL) were placed on individual grids and left for 2 min to adsorb onto the carbon. Excess sample was gently removed by touching filter paper to the edge of the droplet after adsorption was stablished. Excess small molecule contaminants were washed from the grid with three rinses of water. Sample on the grids were stained with 2% (w/v) uranyl acetate (Cardarelli et al., 2010). A Tecnai G2 transmission electron microscope (FEI Company, Hillsboro, OR, United States) at Electron Microscopy Unit, University of Guelph (Guelph, ON, Canada) was used for visualization, operating at 200 kV under variable magnification. Images were acquired using the Gatan Ultascan 4K CCD (Pleasanton, CA, United States) and Gatan Digital Micrograph software imaging system.

Statistical Analysis

All experiments were carried out in triplicate and each sample plated in duplicate. Statistically analysis and analysis of variance (ANOVA) were conducted using the SAS Statistic Package (SAS Institute Inc., Cary, NC, United States), at a confidence interval of 95% to examine the variance in titre of the phage P100 and A511 at temperature points and between treatments. In cases where statistical differences between means were detected, Tukey's test was applied for multiple pair-wise comparisons between treatment means.

RESULTS AND DISCUSSION

Determination of Thermal Stability at Constant Temperature Treatments

Thermal stability of *Listeria* phages were examined at constant temperatures and heating-holding-cooling treatments. In order

to estimate the thermal stability of P100 and A511 at constant temperatures, both phages underwent heat treatments of 45, 55, and 65°C. P100 and A511 are well characterized and their genes sequenced (Carlton et al., 2005; Klumpp et al., 2008). These phages both are members of the *Myoviridae* family of bacteriophages, with small differences (3 genes) in their tail interfaces. While highly similar at the primary sequence level, these phages exhibited different thermal responses. P100 and A511 were stable at 45°C for 75 min (data not shown). However, unlike A511, P100 exhibited thermal sensitivity at 55°C and lost ∼2 log PFU mL^{-1} activity. At the end of 20 min heat treatment at 65°C, A511 activity was reduced by 1 log cycle (PFU mL^{-1}), while P100 was more sensitive with decreasing 4 log cycles in activity after 20 min (data are not shown). This is a significant ($P < 0.05$) decrease in *D*-value with the increase in treatment temperatures (**Table 1**). Increasing temperature to 65°C significantly ($P < 0.05$) decreased the *D*-values to 6.03 ± 0.47 and 16.80 ± 2.84 min for P100 and A511, respectively. Yamagishi and Ozeki (1972) suggested that thermal-sensitivity of phages may depend on their DNA content. A511 features a slightly smaller head diameter (87.36 nm) than P100 (89.55 nm). This feature along with the larger DNA molecule in the A511 head, with a unit genome 3.1 Kb larger than that of P100 (131,384 bp versus 134,494 bp) (Klumpp et al., 2008), indicating a denser head capsid content, which could explain the observed higher stability of A511.

The coefficient of determination R^2 was > 0.90 in all cases, indicating the data fits well with the linear regression model, except for A511 at 45°C (**Table 1**). At 45°C, A511 shows effectively no decline in titre, hence the near zero regression slope, and sensitivity to technical variation in measurements. Simple logarithmic inactivation of phages (Pollard and Reaume, 1951), as well as non-linear relationship inactivation model for thermal-resistant phages (a mixture of two virus population which are similar but have more different thermal-stability) has been previously reported (Wilkowske et al., 1954; Quiberoni et al., 2003). Linearity in P100 and A511 regression model affirmed rather homogenous population by virtue of thermal-stability in phage preparation. Unlike dairy phages which have been reported to be stable to 63°C (Quiberoni et al., 2003; Ebrecht et al., 2010; Chen et al., 2017), P100 and A511 exhibited sensitivity to heat and instability at 65°C (**Table 1**). Although both phages infect the same host species, they show significant differences in their thermal-stability. It suggested that the major lethal event during heat treatments was due to the release of DNA from the phage particles (Yamagishi et al., 1973; Atamer et al., 2010; Guglielmotti et al., 2012).

Determination of Thermal Stability at Heating-Holding-Cooling Treatments

In order to determine the thermal-stability of *Listeria* phages at temperatures simulating the preparation of RTE meats, P100 and A511 were treated by heating to 71°C-holding 30 s-cooling to 4°C. **Figures 1A**, **2A** show decline in P100 and A511 activity with increasing temperature during the heating phase. P100 reached below the limit of detection (1 log PFU mL^{-1}) after 30 s of exposure to 71°C. When the same treatment was applied to A511, phage activity declined by only 3 log cycles (PFU mL^{-1}), and retained activity even after 30 s of holding at 71°C, indicating that in spite of similar primary sequence of their structural proteins, A511 is more heat stable than P100. Release of phage DNA from viral capsids, as well as decomposition of the phages into head and tail structure and tail aggregation are known as common mechanisms observed for viruses thermal inactivation.

Unlike previous studies examining the effect of heat on LAB and enterobacterial phages (Kawai, 1999; Buzrul et al., 2007; Qiu, 2012), P100 exhibited partial reconstitution (3–4 log PFU mL^{-1} of activity) after heating (71°C, holding 30 s) followed by cooling to 4 ± 0.5°C (**Figure 1A**). Hereafter, the term reconstitution refers to the phenomenon when phage infectivity/activity reaches below the limit of detection during heating and/or holding, while exhibiting renewed infectivity during cooling phase. Since A511 did not exhibit a loss of the complete activity (below limit of detection) at 71°C, thermal-stability was tested to 75°C, a temperature which renders A511 inactive (**Figure 1A**), in order to examine if phage particles are capable of reconstitution. In addition, this approach enabled us to also examine if the phenomenon of reconstitution was observed in P100 at temperatures higher than 71°C. Raising the maximum temperature to 75°C yielded complete inactivation of P100 (**Figure 1B**), while complete inactivation of A511 was observed after 30 s of holding (**Figure 2B**). Cooling to 4.0°C after heating to 75°C resulted in partial reconstitution for both phages (**Figures 1B**, **2B**). This reconstitution activity was not observed when A511 was exposed to 80°C (**Figure 2C**), yet P100 particles reconstituted after 30 s of exposure to 80°C (**Figure 1C**). Despite the similarity of the two phages, A511 exhibited more thermo-stability compared to P100, but failed to show the same level of reconstitution. Raising the temperature to 85°C abolished

TABLE 1 | Thermal-stability (expressed as *D*-values in min) for P100 and A511 at 45, 55, and 65°C in SM buffer.

Phage	Temperature (°C)	*D*-value (min)	*Y*	R^2
P100	45	909.09 ± 174.09^{a}	$Y = -0.0011x + 10.394$	0.945
	55	42.01 ± 1.45^{b}	$Y = -0.0238x + 9.8568$	0.924
	65	6.03 ± 0.47^{c}	$Y = -0.0595x + 6.7825$	0.948
A511	45	$10{,}000.00 \pm 5{,}581.05^{d}$	$Y = -0.0001x + 8.14$	0.064
	55	312.50 ± 53.30^{e}	$Y = -0.0032x + 7.2086$	0.993
	65	16.80 ± 2.84^{f}	$Y = -0.1659x + 4.9238$	0.915

Different superscript letters associated with the numbers in the columns indicate statistical significance between two mean. Level of significance was 0.05.

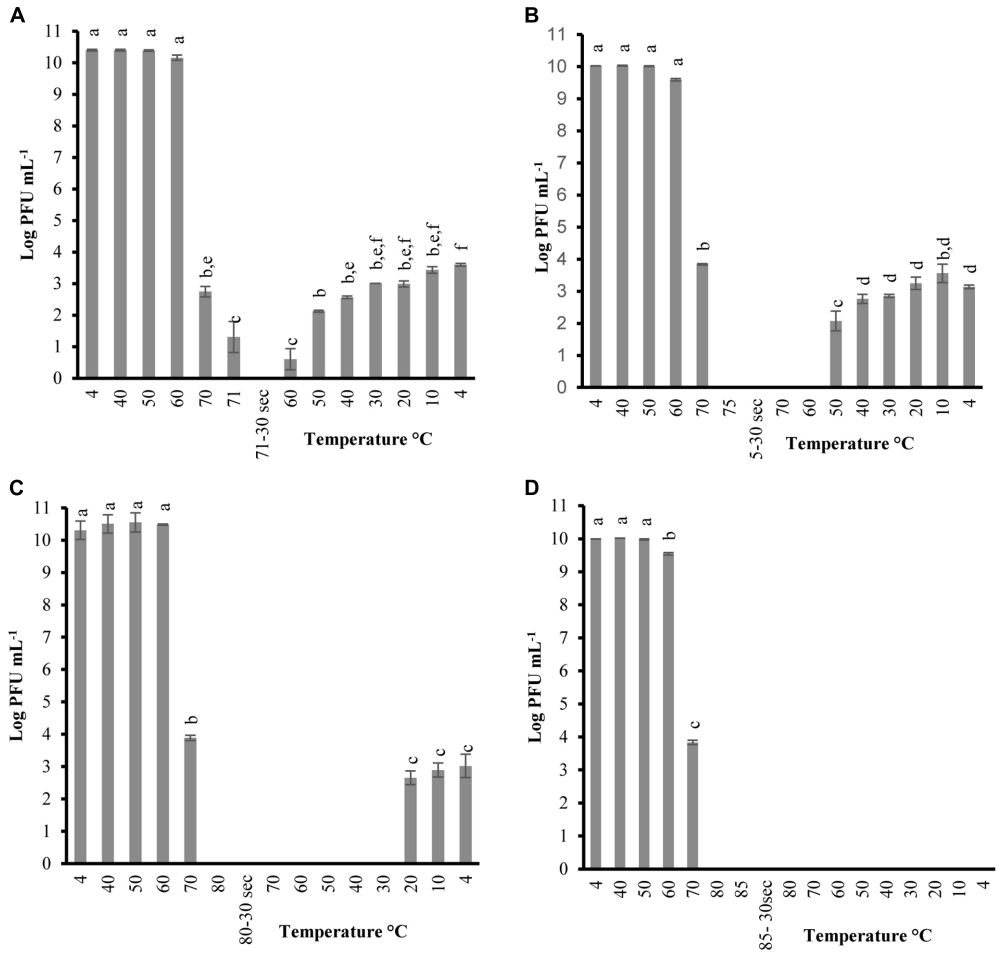

FIGURE 1 | Changes in phage P100 infectivity (in log PFU mL^{-1}) following the heating-holding-cooling trial in SM buffer at peak heating temperatures of 71°C **(A)**; 75°C **(B)**; 80°C **(C)**; 85°C **(D)**. Thirty seconds on the *x*-axis refers to holding time of 30 s at pertaining temperatures. Different superscript letters associated with the numbers on the bars indicate statistical significance between two means with the level of significance of 0.05. Error bars denote standard deviation.

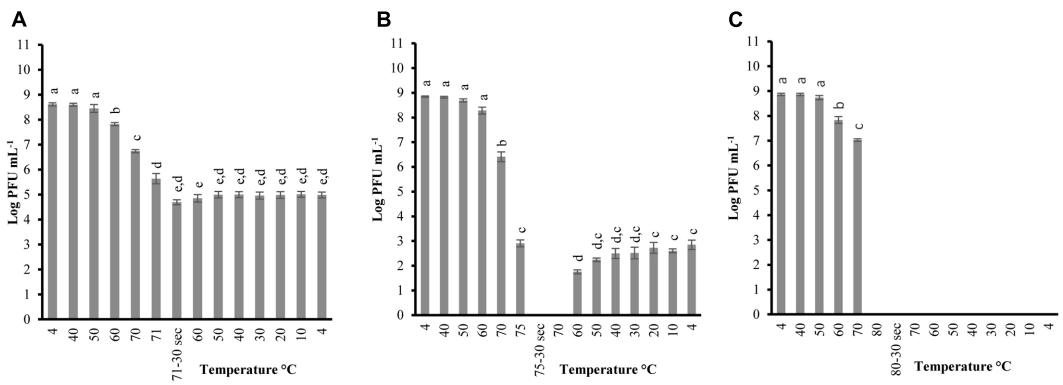

FIGURE 2 | Changes in phage A511 infectivity (in log PFU mL^{-1}) following the heating-holding-cooling trial in SM buffer at peak heating temperatures of 71°C **(A)**; 75°C **(B)**; 80°C **(C)**. Thirty seconds on the *x*-axis refers to holding time of 30 s at pertaining temperatures. Different superscript letters associated with the numbers on the bars indicate statistical significance between two means with the level of significance of 0.05. Error bars denote standard deviation.

the reconstitution ability for P100 (**Figure 1D**). Considering the thermal inactivation and reconstitution of these phages, it could be speculated that although A511 had higher thermal stability during the heating stage compared to P100 (**Figures 1**, **2**), lack of reconstitution in A511 during the cooling stage compared to P100 suggests that heating of A511 results in an irreversible damage to the phage particle compared to P100 where the damage was reversible.

Table 2 shows the temperature and phage population when reconstitution was observed, as well as phage population at the end of the heating-holding-cooling trial (4°C). There were an inverse relationship between peak heating temperature and the temperature at which reconstitution was observed. With an increase in peak heating temperature from 71 to 75 or 80°C, reconstitution was observed at 60, 50, and 20°C, respectively. The reconstitution of *Listeria* phages significantly ($P < 0.05$) decreased with an increase of temperature. P100 showed reduced reconstitution from 80°C (3.01 ± 0.36 log PFU mL^{-1}) compared to lower peak temperature of 71°C (3.59 ± 0.04 log PFU mL^{-1}). Similarly, A511 reconstitution of 2.84 ± 0.18 log PFU mL^{-1} was observed at 75°C, while no phage was detected after cooling following a peak heating temperature of 80°C (**Table 2**). In treatments with higher peak heating temperatures, cooling to lower temperatures was required to detect reconstitution (**Table 2**). It is possible that higher peak heating temperatures could result in irreversible damage/denaturation of the phage particles. This was evident from our results when phage suspension treated to higher peak temperatures, required cooling to lower temperatures to demonstrate the reconstitution phenomenon.

Viral inactivation by thermal treatment has been previously studied (Wilkowske et al., 1954; Caldentey et al., 1993; Moroni et al., 2002; Müller-Merbach et al., 2005; Buzrul et al., 2007; Atamer et al., 2013; Jurczak-Kurek et al., 2016; Chen et al., 2017), yet reconstitution during cooling phase after heating treatment has not been widely investigated. Zairi et al. (2014) investigated the effects of heating and cooling cycle (60°C and cooled to 10°C) on gp12 capsid fiber of *Bacillus* phage SPP1 in a buffer solution [500 mm NaCl and 50 mm Na_2HPO_4 (pH 8.0)] with a Fluorescence-based Thermal Shift Assay. They reported a loss of protein gp12 capsid fiber structure between 30 and 45°C and unfolding of polypeptide chains of gp12 was observed between 45 and 80°C. However, fast (<1 min) or progressive cooling of the sample back to 10°C led to complete reconstitution of the secondary, tertiary, and quaternary protein structures identical to that of the untreated proteins. Phenomenon of reconstitution for T4 phage tail particles previously was reported by Jayaraman et al. (1997). They observed the short tail fibers of bacteriophage T4 which are composed of gp12 was able to reconstitute after heating to 75°C. We believe that the underlying mechanisms involved phage reconstitution might be similar. Their results are consistent with the observations in this research. Although these researchers examined the capsid fiber protein of phage SPP1 and tail fiber protein of phage T4, our experiment was conducted with whole phage particles and focused on *Listeria* phages relevant to food protection. To date, no reconstitution of *Listeria* phages undergoing heating process has been reported. According to these results, it is possible to conclude that the P100 and A511 proteins have characteristic to retain a native folded state when exposed to denaturing conditions to some extent of temperature elevation. It was more evident for tail structural proteins, especially for P100. The irreversible inactivation of phages occurred at temperatures >80°C due to irreversible unfolding and dissociation of structural proteins.

Phages were tested with the same heating-holding-cooling protocol at different concentrations to evaluate the reconstitution activity. The lowest peak heating temperature at which complete inactivation and reconstitution was observed was picked to determine any correlation between phage concentrations and thermal-stability. Therefore, peak heating temperatures of 71°C and 75°C was used for P100 and A511, respectively. When P100 with initial concentrations of 10^5 and 10^8 (PFU mL^{-1}) were examined at heating 71°C-holding-cooling, phages could no longer be detected at 70°C (**Figures 3A,B**), while phage particles were still detected (10^{2-3} PFU mL^{-1}) at 70°C during the same treatment when initial concentration of phage was 10^{10} PFU mL^{-1} (**Figure 1A**). Reconstitution of P100 (10^8 PFU mL^{-1}) was observed during cooling starting at 50°C (**Figure 3B**), while the same treatment with initial concentration of 10^{10} PFU mL^{-1} resulted in reconstitution during cooling starting at 60°C (**Figure 1A**). P100 with initial concentration of 10^5 PFU mL^{-1} exhibited no reconstitution of phage particles with

TABLE 2 | Reconstitution temperature (°C) and population (Log PFU mL^{-1}) of P100 and A511 in heating-holding-cooling trials at different peak temperature treatments.

Bacteriophage	Heating peak temperature (°C)	Reconstitution		
		Temperature*(°C)	Population** (Log PFU ml^{-1})	Population*** (Log PFU ml^{-1})
P100	71	60	0.60 ± 0.30	3.59 ± 0.04[a]
	75	50	2.07 ± 0.30	3.13 ± 0.05[b]
	80	20	2.65 ± 0.21	3.01 ± 0.36[b]
	85	–	–	–
A511	71	–	–	4.98 ± 0.11
	75	60	1.75 ± 0.07	2.84 ± 0.18
	80	No reconstitution	–	–

*Different superscript letters associated with the numbers in the columns indicate statistical significance between two mean. The level of significance was 0.05. *Temperature at which reconstitution was observed; **Population when reconstitution was observed; ***Population at the end of heating-holding-cooling trails.*

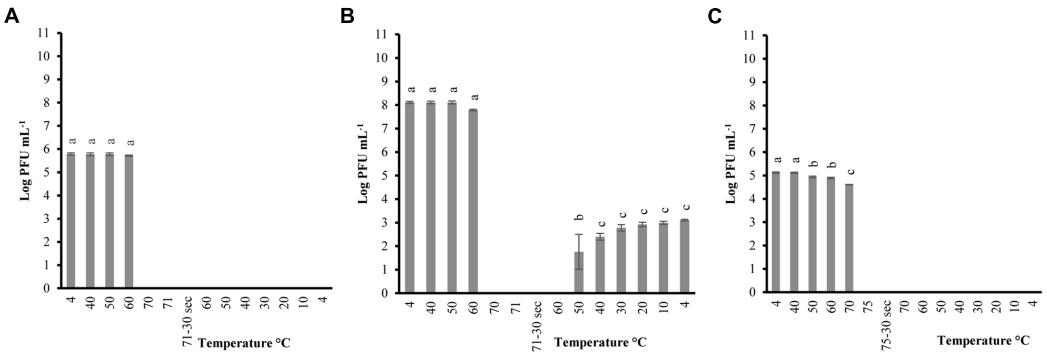

FIGURE 3 | Changes in phage P100 infectivity (in log PFU mL^{-1}) following the heating 71°C-holding-cooling trial in SM buffer with initial concentration of 10^5 PFU mL^{-1} **(A)**; 10^8 PFU mL^{-1} **(B)**; and phage A511 population following the heating 75°C-holding-cooling trial in SM buffer with initial concentration of 10^5 PFU mL^{-1} **(C)**. Thirty seconds on the *x*-axis refers to holding time of 30 s at pertaining temperatures Different superscript letters associated with the numbers on the bars indicate statistical significance between two means with the level of significance of 0.05. Error bars denote standard deviation.

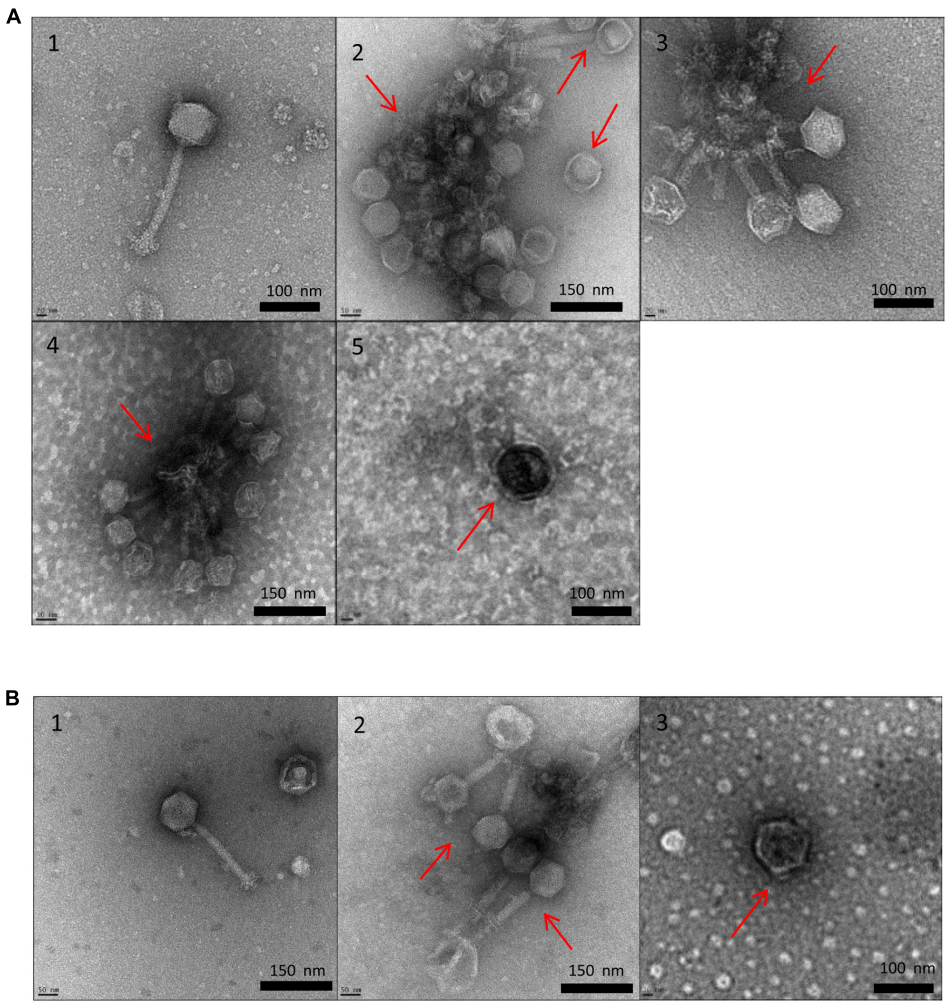

FIGURE 4 | Transmission electron micrographs of *Listeria* phages P100 **(A)** and A511 **(B)** exposed to different treatments. Untreated control (1); heating to 71°C (2); heating to 75°C (3); heating to 80°C (4); heating to 85°C (5).

TABLE 3 | Comparison between melting temperature of P100 and A511 proteins based on Tm predictor.

Structural Functional group	P100		A511		Descriptions (P100 relative to A511)
	Protein	Melting class (°C)	Protein	Melting class (°C)	
Putative head-tail connector	gp18	>65	gp87	>65	• 20aa shorter than A511 • Lower melting point than A511 • Plausible source of difference in tail disintegration
Predicted tail component protein related to side fibers	gp19	∼58	gp88	∼59	• Lower melting point than A511 • Plausible source of difference in tail aggregation
Hub and entry hydrolase	gp29	55–65	gp97	>65	• Lower melting point than A511 • Plausible source of difference in tail aggregation, and tail disintegration
Putative tail fiber protein	gp30	∼59	gp99	∼60	• Lower melting point than A511 • Plausible source of difference in tail aggregation
Predicted baseplate component	gp32	55–65	gp106	∼60	• Lower melting point than A511 • Plausible source of difference in tail aggregation
Receptor binding/fiber protein	gp39	55–65	gp108	55–60	• Lower melting point than A511 • 67aa shorter than A511 • Plausible source of difference in tail aggregation
Portal protein	gp14	55–60	gp83	∼55	• Higher melting point than A511 • Plausible source of difference in tail aggregation

the same treatment (**Figure 3A**). When phage A511 with 10^5 PFU mL^{-1} were examined at heating 75°C-holding-cooling, no reconstitution activity were observed (**Figure 3C**), while, partial reconstitution was observed with higher initial concentration of 10^8 PFU mL^{-1} (**Figure 2A**). It is possible that the lower reconstitution ability and thermal stability observed in less concentrated phage solutions might be due to a dilution effect on phage population.

TEM Analysis on P100 and A511 Structure

Transmission electron microscopy allowed us to visualize the physical effects of high temperature on P100 and A511. **Figures 4A1,B1** show untreated controls of P100 and A511, respectively, which feature long, contractile tails and isometric capsids that are characteristic of *Myoviridae* family in the order *Caudovirales* (Zink and Loessner, 1992). Heating P100 to 71°C (**Figure 4A2**) resulted in a mixed population of fully disrupted virions, aggregated tail (Supplementary Figure 2), empty head (dark color), and visually intact phages (white color indicating capsid containing nucleic acid) (**Figure 4A1**). Similar observations were made in treatment to 75 and 80°C (**Figures 4A3,A4**) with tail fibers and baseplates aggregation (Supplementary Figure 3). The tendency to clustering of empty head and aggregated phages particles of the P008 viral particles as a result of exposure to 70°C for 10 min was reported by Atamer et al. (2010). Exposure of P100 to 85°C (**Figure 4A5**) showed only dark isometric capsid structure indicating that they were empty of DNA. TEM images of phage A511 from heating to 75°C displayed less tail aggregation with more visually intact phages (**Figure 4B2**) suggesting higher thermal stability which is in agreement with results presented in **Table 1** and **Figure 2**. Samples treated to 80°C exhibited empty phage capsid without tails similar to that observed for P100 heated to 85°C (**Figure 4B3**).

Transmission electron microscopy observations suggested that tail component of the phage were more thermosensitive and denatured at lower temperatures compared to capsid. Similar observation were made by Qiu (2012) who reported that λ phage tail disrupted at 68°C, while capsid proteins disrupted later at 87°C. Unlike P100, heat-induced damages in A511 was more pronounced after heating to 80°C, while similar damages in P100 were observed when heated to 85°C. This explains the lack of observed reconstitution of A511 when heated to 85°C, while P100 heated to 80°C showed reconstitution (**Figures 1**, **2**).

Predicted Melting Temperature for Structural Proteins

In order to compare the differences between thermal-stability of P100 and A511 at the protein sequence level, relative estimate of minimum melting temperatures of structural proteins were determined using Tm predictor algorithm (Ku et al., 2009). Phage stability and functionality depends on both polar and hydrophobic interactions in their proteins. These interactions have different melting temperatures (Gorania et al., 2010), depending on the specific amino acids and geometry involved in formation of these interfaces. Predicting melting temperature (Tm, the temperature at which 50% of the protein is unfolded) from protein sequences can help with better understanding the molecular basis of thermal stability of proteins. The Tm predictor software determines the melting temperatures using primary sequence and correlative extrapolation of dipeptides interactions based on large representative dataset of thermally characterized proteins (Ku et al., 2009).

When comparing the primary sequence level between P100 and A511, 22 structural protein pairs were predicted as present in

both phages. Minimum melting temperatures of these structural proteins were estimated using the Tm predictor and are presented in **Table 3**. The P100 putative head-tail connector, predicted tail components such as tail fiber proteins, tail tip-collar, tail initiator, host recognition protein and baseplate hub, all were predicted to have lower melting temperatures than A511. The result is consistent with our observation of tail aggregation of P100 when exposed to heat. Portal proteins of A511 were predicted to melt at lower temperatures than P100 portal. Therefore, it is likely that heating A511 to 80°C caused the damage to the portal complex, disintegration of phage into head and tail and leakage of DNA (irreversible), while P100 retained the portal complex when exposed to 80°C (**Table 3**). This might be a plausible source of difference in ability of P100 and A511 to reconstitution after heating to 80°C and during cooling to 4°C.

CONCLUSION

The study evaluated the thermal-stability of *Listeria* phages P100 and A511 at temperatures simulating the preparation of RTE meats. P100 and A511 are very similar but not identical (98% identical over 95% of A511 genome), and they did not follow the same trend in thermal-stability and phage particle reconstitution, indicating thermal-stability is phage particle dependent. P100 showed more sensitivity to heat, being fully inactivated after exposure to 71°C and holding 30 s, yet was able to reconstitute even from heating to 80°C. However, phage A511 showed less sensitivity to heat and was not fully inactivated by exposure 71°C but didn't show reconstitution after heating to 80°C. TEM visualization showed the detrimental effect of heat on phage structure causing tail aggregation, detachment of phage head and tail and generation of empty capsid at higher temperature. While there are many similarities between melting temperature of functional proteins in P100 and A511, there are specific differences as well, notably among structural proteins based on Tm prediction, which would explain the plausible source of difference in ability of P100 compared to A511 in reconstitution after heating to 80°C and during cooling to 4°C. Further analysis by nuclear magnetic resonance spectroscopy (NMR) or circular dichroism (CD) measurements for protein structure determination and folding and unfolding of proteins would help to understand these differences. Evaluation of the thermal stability of these phages in food matrix and their efficacy to control *L. monocytogenes* is required to determine if phages can be used as an additive in foods.

AUTHOR CONTRIBUTIONS

HA performed all of the bacterial and phage assays presented, phage propagation, sampling, and data analysis. HA and DR both performed transmission electron microscopy and interpreted the resulting images. DR analyzed and interpreted the predicted protein melting temperature data. HA, DR, AK, SB, and L-TL contributed to experimental design for all assays presented. HA wrote the manuscript with input from SB, AK, DR, and L-TL. SB is the principle investigator of the project who was responsible for preparation of project proposal, procure funding, resource allocation and along with the AK and L-TL provided overall guidance and mentorship throughout the scope of this project.

ACKNOWLEDGMENTS

Financial support for the project and graduate stipend for HA came from Agriculture and Agri-Food Canada (Project ID: J-000232).

SUPPLEMENTARY MATERIAL

The Supplementary Material for this article can be found online at: https://www.frontiersin.org/articles/10.3389/fmicb.2017.02375/full#supplementary-material

REFERENCES

Ahmadi, H., Anany, H., Walkling-Ribeiro, M., and Griffiths, M. W. (2015). Biocontrol of *Shigella flexneri* in ground beef and *Vibrio cholerae* in seafood with bacteriophage-assisted high hydrostatic pressure (HHP) treatment. *Food Bioproc. Tech.* 8, 1160–1167. doi: 10.1007/s11947-015-1471-6

Anany, H., Chen, W., Pelton, R., and Griffiths, M. (2011). Biocontrol of *Listeria monocytogenes* and *Escherichia coli* O157: H7 in meat by using phages immobilized on modified cellulose membranes. *Appl. Environ. Microbiol.* 77, 6379–6387. doi: 10.1128/AEM.05493-11

Atamer, Z., Dietrich, J., Neve, H., Heller, K. J., and Hinrichs, J. (2010). Influence of the suspension media on the thermal treatment of mesophilic lactococcal bacteriophages. *Int. Dairy J.* 20, 408–414. doi: 10.1016/j.idairyj.2009.12.014

Atamer, Z., Samtlebe, M., Neve, H., Heller, K. J., and Hinrichs, J. (2013). Review: elimination of bacteriophages in whey and whey products. *Front. Microbiol.* 4:191. doi: 10.3389/fmicb.2013.00191

Brovko, L. Y., Anany, H., and Griffiths, M. W. (2012). "Bacteriophages for detection and control of bacterial pathogens in food and food-processing environment," in *Advances in Food and Nutrition Research*, ed. H. Jeyakumar Cambridge, MA: Academic Press), 241–288.

Buzrul, S., Ozturk, P., Alpas, H., and Akcelik, M. (2007). Thermal and chemical inactivation of lactococcal bacteriophages. *LWT Food Sci. Tech.* 40, 1671–1677. doi: 10.1016/j.lwt.2007.01.002

Caldentey, J., Luo, C., and Bamford, D. H. (1993). Dissociation of the lipid-containing bacteriophage PRD1: effects of heat, pH, and sodium dodecyl sulfate. *Virology* 194, 557–563. doi: 10.1006/viro.1993.1294

Canadian Food Inspection Agency (2011). *Annex H: policy on the Control of Listeria Monocytogenes in Ready-to-Eat (RTE) Meat and Poultry Product.* Available at: http://www.inspection.gc.ca/food/meat-and-poultry-products/manual-of-procedures/chapter-4/annex-h/eng/1370541840583/1370541911699 [accessed August, 2017].

Canadian Food Inspection Agency (2013). *Annex D: Cooking Time/Temperature Tables*. Available at: http://www.inspection.gc.ca/food/meat-and-poultry-products/manual-of-procedures/eng/1300125426052/1300125482318 [accessed October 30, 2017].

Capra, M. L., Quiberoni, A., and Reinheimer, J. A. (2004). Thermal and chemical resistance of *Lactobacillus casei* and *Lactobacillus paracasei* bacteriophages. *Lett. Appl. Microbiol.* 38, 499–504. doi: 10.1111/j.1472-765X.2004.01525.x

Cardarelli, L., Lam, R., Tuite, A., Baker, L. A., Sadowski, P. D., Radford, D. R., et al. (2010). The crystal structure of bacteriophage HK97 gp6: defining a large family of head-tail connector proteins. *J. Mol. Biol.* 395, 754–768. doi: 10.1016/j.jmb.2009.10.067

Carlton, R. M., Noordman, W. H., Biswas, B., De Meester, E. D., and Loessner, M. J. (2005). Bacteriophage P100 for control of *Listeria monocytogenes* in foods: genome sequence, bioinformatic analyses, oral toxicity study, and application. *Regul. Toxicol. Pharmacol.* 43, 301–312. doi: 10.1016/j.yrtph.2005.08.005

Centers for Disease Control and Prevention (2017). *Listeria Outbreaks*. Available at: https://www.cdc.gov/listeria/outbreaks/index.html [accessed October 30, 2017].

Chen, X., Liu, Y., Fan, M., Wang, Z., Wu, W., and Wang, J. (2017). Thermal and chemical inactivation of *Lactobacillus* virulent bacteriophage. *J. Dairy Sci.* 100, 7041–7050. doi: 10.3168/jds.2016-12451

Chibeu, A., Agius, L., Gao, A., Sabour, P. M., Kropinski, A. M., and Balamurugan, S. (2013). Efficacy of bacteriophage LISTEX^{TM}P100 combined with chemical antimicrobials in reducing *Listeria monocytogenes* in cooked turkey and roast beef. *Int. J. Food Microbiol.* 167, 208–214. doi: 10.1016/j.ijfoodmicro.2013.08.018

Duda, R. L., Ross, P. D., Cheng, N., Firek, B. A., Hendrix, R. W., Conway, J. F., et al. (2009). Structure and energetics of encapsidated DNA in bacteriophage HK97 studied by scanning calorimetry and cryo-electron microscopy. *J. Mol. Biol.* 391, 471–483. doi: 10.1016/j.jmb.2009.06.035

Ebrecht, A. C., Guglielmotti, D. M., Tremmel, G., Reinheimer, J. A., and Suarez, V. B. (2010). Temperate and virulent *Lactobacillus delbrueckii* bacteriophages: comparison of their thermal and chemical resistance. *Food Microbiol.* 27, 515–520. doi: 10.1016/j.fm.2009.12.012

European Centre for Disease Prevention and Control (2017). *Disease Data from ECDC Surveillance Atlas - Listeriosis. Surveillance and Disease Data.* Available at: https://ecdc.europa.eu/en/listeriosis/surveillance-and-disease-data/atlas [accessed October 30, 2017].

Food Safety and Inspection Service (1999). *Performance Standards for the Production of Certain Meat and Poultry Products, Requires a 6.5 Log Relative Reduction (6.5 log lethality) of Salmonella for Cooked Beef, Roast Beef and Corned Beef (9 cfr318.17)*. Available at: https://www.fsis.usda.gov/wps/wcm/connect/9ab2e062-7ac8-49b7-aea1-f070048a113a/RTE_Poultry_Tables.pdf?MOD=AJPERES

Gilmour, M. W., Graham, M., Van Domselaar, G., Tyler, S., Kent, H., Trout-Yakel, K. M., et al. (2010). High-throughput genome sequencing of two *Listeria monocytogenes* clinical isolates during a large foodborne outbreak. *BMC Genomics* 11:120. doi: 10.1186/1471-2164-11-120

Gorania, M., Seker, H., and Haris, P. I. (2010). Predicting a protein's melting temperature from its amino acid sequence. *Conf. Proc. IEEE Eng. Med. Biol. Soc.* 2010, 1820–1823. doi: 10.1109/IEMBS.2010.5626421

Guglielmotti, D. M., Mercanti, D. J., Reinheimer, J. A., and Quiberoni Adel, L. (2012). Review: efficiency of physical and chemical treatments on the inactivation of dairy bacteriophages. *Front. Microbiol.* 2:282. doi: 10.3389/fmicb.2011.00282

Health Canada (2011). *Policy on Listeria monocytogenes in Ready-to-Eat Foods, Identification, Number: FD-FSNP 0071*. Available at: http://www.hc-sc.gc.ca/fn-an/legislation/pol/policy_listeria_monocytogenes_2011-eng.php [accessed August, 2017].

Jayaraman, A., De Bernardez Clark, E., and Goldberg, E. (1997). Thermal unfolding of bacteriophage T4 short tail fibers. *Biotechnol. Prog.* 13, 837–843. doi: 10.1021/bp9701067

Jurczak-Kurek, A., Gąsior, T., Nejman-Faleńczyk, B., Bloch, S., Dydecka, A., Topka, G., et al. (2016). Biodiversity of bacteriophages: morphological and biological properties of a large group of phages isolated from urban sewage. *Sci. Rep.* 6:34338. doi: 10.1038/srep34338

Kawai, Y. (1999). Thermal transition profiles of bacteriophage T4 and its DNA. *J. Gen. Appl. Microbiol.* 45, 135–138. doi: 10.2323/jgam.45.135

Klumpp, J., Dorscht, J., Lurz, R., Bielmann, R., Wieland, M., Zimmer, M., et al. (2008). The terminally redundant, nonpermuted genome of *Listeria* bacteriophage A511: a model for the SPO1-like myoviruses of Gram-positive bacteria. *J. Bacteriol.* 190, 5753–5765. doi: 10.1128/JB.00461-08

Kropinski, A. M., Mazzocco, A., Waddell, T. E., Lingohr, E., and Johnson, R. P. (2009). Enumeration of bacteriophages by double agar overlay plaque assay. *Methods Mol. Biol.* 501, 69–76. doi: 10.1007/978-1-60327-164-6_7

Ku, T., Lu, P., Chan, C., Wang, T., Lai, S., Lyu, P., et al. (2009). Predicting melting temperature directly from protein sequences. *Comput. Biol. Chem.* 33, 445–450. doi: 10.1016/j.compbiolchem.2009.10.002

Leverentz, B., Conway, W. S., Alavidze, Z., Janisiewicz, W. J., Fuchs, Y., Camp, M. J., et al. (2001). Examination of bacteriophage as a biocontrol method for salmonella on fresh-cut fruit: a model study. *J. Food Prot.* 64, 1116–1121. doi: 10.4315/0362-028X-64.8.1116

Mercanti, D. J., Guglielmotti, D. M., Patrignani, F., Reinheimer, J. A., and Quiberoni, A. (2012). Resistance of two temperate *Lactobacillus paracasei* bacteriophages to high pressure homogenization, thermal treatments and chemical biocides of industrial application. *Food Microbiol.* 29, 99–104. doi: 10.1016/j.fm.2011.09.003

Moroni, O., Jean, J., Autret, J., and Fliss, I. L. (2002). Inactivation of lactococcal bacteriophages in liquid media using dynamic high pressure. *Int. Dairy J.* 12, 907–913. doi: 10.1016/S0958-6946(02)00118-8

Müller-Merbach, M., Rauscher, T., and Hinrichs, J. (2005). Inactivation of bacteriophages by thermal and high-pressure treatment. *Int. Dairy J.* 15, 777–784. doi: 10.1016/j.idairyj.2004.08.019

Murray, K., Wu, F., Aktar, R., Namvar, A., and Warriner, K. (2015). Comparative study on the efficacy of bacteriophages, sanitizers, and UV light treatments to control *Listeria monocytogenes* on sliced mushrooms (*Agaricus bisporus*). *J. Food Prot.* 78, 1147–1153. doi: 10.4315/0362-028X.JFP-14-389

Painter, J. S. (2007). Listeriosis in humans. *Food Sci. Technol.* 161, 85–110. doi: 10.1201/9781420015188.ch4

Pollard, E., and Reaume, M. (1951). Thermal inactivation of bacterial viruses. *Arch. Biochem. Biophys.* 32, 278–287. doi: 10.1016/0003-9861(51)90273-1

Qiu, X. (2012). Heat induced capsid disassembly and DNA release of bacteriophage lambda. *PLOS ONE* 7:e39793. doi: 10.1371/journal.pone.0039793

Quiberoni, A., Guglielmotti, D. M., and Reinheimer, J. A. (2003). Inactivation of *Lactobacillus delbrueckii* bacteriophages by heat and biocides. *Int. J. Food Microbiol.* 84, 51–62. doi: 10.1016/S0168-1605(02)00394-X

Radford, D., Guild, B., Strange, P., Ahmed, R., Lim, L. T., and Balamurugan, S. (2017). Characterization of antimicrobial properties of *Salmonella* phage Felix O1 and *Listeria* phage A511 embedded in xanthan coatings on poly (lactic acid) films. *Food Microbiol.* 66, 117–128. doi: 10.1016/j.fm.2017.04.015

Radford, D. R., Ahmadi, H., Leon-Velarde, C. G., and Balamurugan, S. (2016). Propagation method for persistent high yield of diverse *Listeria* phages on permissive hosts at refrigeration temperatures. *Res. Microbiol.* 167, 685–691. doi: 10.1016/j.resmic.2016.05.010

Tabla, R., Martínez, B., Rebollo, J. E., González, J., Ramírez, M. R., Roa, I., et al. (2012). Bacteriophage performance against *Staphylococcus aureus* in milk is improved by high hydrostatic pressure treatments. *Int. J. Food Microbiol.* 156, 209–213. doi: 10.1016/j.ijfoodmicro.2012.03.023

U.S. Food and Drug Administration (2006). *Food Additives Permitted for Direct Addition to Food for Human Consumption; Bacteriophage Preparation. 21 CFR Part 172*, 47729–47732. Available at: http://edocket.access.gpo.gov/2006/E6-13621.htm [accessed November, 2017].

Vazquez-Boland, J. A., Kuhn, M., Berche, P., Chakraborty, T., Dominguez-Bernal, G., Goebel, W., et al. (2001). *Listeria* pathogenesis and molecular virulence determinants. *Clin. Microbiol. Rev.* 14, 584–640. doi: 10.1128/CMR.14.3.584-640.2001

Whichard, J. M., Sriranganathan, N., and Pierson, F. W. (2003). Suppression of *Salmonella* growth by wild-type and large-plaque variants of bacteriophage felix O1 in liquid culture and on chicken frankfurters. *J. Food Prot.* 66, 220–225. doi: 10.4315/0362-028X-66.2.220

Whitehead, H. R., and Cox, G. A. (1936). Bacteriophage phenomena in cultures of lactic streptococci. *Dairy Res.* 7, 55–62. doi: 10.1017/S0022029900001655

Wilkowske, H. H., Nelson, F. E., and Parmelee, C. E. (1954). Heat inactivation of bacteriophage strains active against lactic streptococci. *Appl. Microbiol.* 2, 250–253.

Yamagishi, H., Eguchi, G., Matsuo, H., and Ozeki, H. (1973). Visualization of thermal inactivation in phages lambda and phi80. *Virology* 53, 277–282. doi: 10.1016/0042-6822(73)90486-8

Yamagishi, H., and Ozeki, H. (1972). Comparative study of thermal inactivation of phage φ80 and lambda. *Virology* 48, 316–322. doi: 10.1016/0042-6822(72)90042-6

Zairi, M., Stiege, A. C., Nhiri, N., Jacquet, E., and Tavares, P. (2014). The collagen-like protein gp12 is a temperature-dependent reversible binder of SPP1 viral capsid. *J. Biol. Chem.* 289, 27169–27181. doi: 10.1074/jbc.M114.590877

Zink, R., and Loessner, M. J. (1992). Classification of virulent and temperate bacteriophages of *Listeria* spp. on the basis of morphology and protein analysis. applied environmental microbiology. *J. Virol.* 58, 296–302.

Conflict of Interest Statement: The authors declare that the research was conducted in the absence of any commercial or financial relationships that could be construed as a potential conflict of interest.

The reviewer GW and handling Editor declared their shared affiliation.

Advantages of publishing in Frontiers

OPEN ACCESS
Articles are free to read for greatest visibility and readership

FAST PUBLICATION
Around 90 days from submission to decision

HIGH QUALITY PEER-REVIEW
Rigorous, collaborative, and constructive peer-review

TRANSPARENT PEER-REVIEW
Editors and reviewers acknowledged by name on published articles

Frontiers
Avenue du Tribunal-Fédéral 34
1005 Lausanne | Switzerland

Visit us: www.frontiersin.org
Contact us: info@frontiersin.org | +41 21 510 17 00

REPRODUCIBILITY OF RESEARCH
Support open data and methods to enhance research reproducibility

DIGITAL PUBLISHING
Articles designed for optimal readership across devices

FOLLOW US
@frontiersin

IMPACT METRICS
Advanced article metrics track visibility across digital media

EXTENSIVE PROMOTION
Marketing and promotion of impactful research

LOOP RESEARCH NETWORK
Our network increases your article's readership